

# **Expression and role of the human anti-apoptotic *bfl-1* gene in Hodgkin's Lymphoma**

A dissertation submitted for the degree of Ph.D.

By

**Sinéad T. Loughran B.Sc. (Hons) Biotechnology**

Under the supervision of Dr. Dermot Walls

July 2007

School of Biotechnology, Dublin City University, Dublin 9,  
Ireland

*For my Family*

## **Declaration**

'I hereby declare that this material, which I now submit for assessment on the programme of study leading to the award of Doctor of Philosophy is entirely my own work and has not been taken from the work of others save and to the extent that such work has been cited and acknowledged within the text of my work.'

Signed: Sinead Doughran

I.D. Number: 98355325

Date: 9<sup>th</sup> July 2007

William Rowan Hamilton (1805-1865)

Oh! Ambition hath its hour  
Of deep and spirit-stirring power;  
Not in the tented field alone,  
Nor peer-engirded court and throne;  
Nor the intrigues of busy life;  
But ardent Boyhood's generous strife,  
While yet the Enthusiast spirit turns  
Where'er the light of Glory burns,  
Thinks not how transient is the blaze,  
But longs to barter Life for Praise.  
Look round the arena, and ye spy  
Pallid cheek and faded eye;  
Among the bands of rivals, few  
Keep their native healthy hue:  
Night and thought have stolen away  
Their once elastic spirit's play.  
A few short hours and all is o'er,  
Some shall win one triumph more;  
Some from the place of contest go  
Again defeated, sad and slow.  
What shall reward the conqueror then  
For all his toil, for all his pain,  
For every midnight throb that stole  
So often o'er his fevered soul?  
Is it the applaudings loud  
Or wond'ring gazes of the crowd;  
Disappointed envy's shame,  
Or hollow voice of fickle Fame?  
These may extort the sudden smile,  
May swell the heart a little while;  
But they leave no joy behind,  
Breathe no pure transport o'er the mind,  
Nor will the thought of selfish gladness  
Expand the brow of secret sadness.  
Yet if Ambition hath its hour  
Of deep and spirit-stirring power,  
Some bright rewards are all its own,  
And bless its votaries alone:  
The anxious friend's approving eye;  
The generous rivals' sympathy;  
And that best and sweetest prize  
Given by silent Beauty's eyes!  
These are transports true and strong,  
Deeply felt, remembered long:  
Time and sorrow passing o'er  
Endear their memory but the more.

## Acknowledgements

To Dermot, thank you for all the guidance, support, direction and respect you have given me over the last several years. You have been my mentor since I arrived at DCU first at age 16, you inspired me to pursue science initially through the Biotechnology degree and since through this Ph.D. I am greatly indebted to you for the opportunity to carry out such interesting research and also for boundless encouragement and expertise. I have enormous respect for you as mentor and a friend.

To Eva, Sinéad, Susan, Pam and Brendan who have been and are my lab partners for the duration. I have been blessed with having you as great colleagues and exceptional friends. You have shared in the excitement, the disappointment, the good times and the struggles, thank you for all the help, all the troubleshooting, for all the laughs and for making it a pleasure working in the lab.

To all the friends I have made since I started out on the Ph.D. journey, Eva, Sinéad, Liz, Sharon, Susan, Caroline, Sue, Jen, Barry, Lynsey, Joanne, you are the reason I love this place. Thank you for the friendship, for all the fun, all the help, all the encouragement and all the tea breaks.

I am grateful to all the staff of the School of Biotechnology for all your contributions to my research for making it an enjoyable journey. To all the students who passed through the lab like hurricanes en route to completing their degree, it was a pleasure and a benefit working with you all and watching you learn.

I am grateful for suggestions, comments, and contributions from the following friends and colleagues to the research in my thesis; Dr. Brendan D'Souza, Dr. Sinead Smith, Eva Campion, Susan Phelan, Dr. Barry Ryan, Dr. Jonny Finlay, Sharon Stapleton, Liz Tully, Isobel O'Reilly, Dr. Aideen Long, Dr. Mike Freely, Dr. Pamela O'Brien, Dr. Ronan Murphy, Dr. Paul Murray, Dr. Joanne Flavell and Dr. Shihka Bose.  
This research would not have been possible without the financial assistance of Cancer Research Ireland (funded by the Irish Cancer Society), the Health Research Board and DCU Educational (Orla Benson Award). I express my gratitude to those agencies.

To the McDonald family, Sue, Brian and Don, for always having an interest in my thesis and for making me welcome in your home. I look forward to sharing my future with you all.

To Daddy, thank you for being so strong, for always doing the best for us and for encouraging and supporting us in every way. Thank you for being the foundation of our family, we have you to thank for everything. To Irene and Noeleen, I am so proud of you, thank you for being great sisters, for the constant phone calls, for the encouragement, for the laughs and the togetherness we share.

To Bernard, my best friend. Thank you for being my inspiration, my shoulder to cry on, my proof-reader, my counsellor and even sometimes my lab partner. Thank you for being so patient, kind and understanding. Thank you for the love we share and thank you for making me so happy.

To Mammy, for all the stardust from Heaven you dropped into my life. You have been an influence, an inspiration and a guiding light throughout my life.

## Abstract

Expression and role of the human anti-apoptotic *bfl-1* gene in Hodgkin's Lymphoma

Sinead Loughran

Hodgkin's Lymphoma (HL) is identified histologically by the presence of mononuclear Hodgkin (H) cells and multinucleated Reed-Sternberg (RS) cells surrounded by a background of lymphocytes, plasma cells, eosinophils, histiocytes and stromal cells in the affected lymph nodes. HL affects on average 2.5 per 100,000 of population and between 30 and 50 % of HL cases are Epstein-Barr virus associated (EBV positive HL). An important feature of HL is the constitutive activation of the NF-κB transcription factor, which has proliferative and anti-apoptotic roles in H/RS cells.

Bfl-1 is an anti-apoptotic protein of the Bcl-2 family, whose preferential expression in hematopoietic and endothelial cells is controlled by inflammatory stimuli. This thesis presents the novel finding that *bfl-1* is highly expressed in H/RS cells from primary tumour tissue from HL patients and cultured H/RS cells irrespective of their EBV status and that the short splice variant of *bfl-1*, designated *bfl-1S* is not expressed in these cell types or in type I Burkitt Lymphoma (BL), type III BL or lymphoblastoid cell lines. This thesis presents the novel discovery that *bfl-1* is a key NF-κB target gene in H/RS cells and death by apoptosis caused by inhibition of NF-κB is coincident with a loss of *bfl-1* expression. It is shown in this study for the first time that ectopic expression of Bfl-1 protected H/RS cells from apoptosis induced by NF-κB inhibition. The downregulation of *bfl-1* in a HL-derived cell line by RNA interference is reported in this study and shown to potentiate the effects of cytotoxic agents by decreasing the cellular apoptotic threshold. The novel finding that NF-κB regulates the *bfl-1* promoter, with a key role in this cell context for a novel NF-κB binding site in the upstream regulatory region of this gene is reported here. This study reports the mechanisms by which *bfl-1* expression is regulated in H/RS cells and serves to establish the contribution of *bfl-1* to the pathogenesis of HL.

Also as part of this thesis, as a means to generate an antibody to Bfl-1, a novel vector (pGSLink) was designed and constructed to permit high-level expression of a protein linked at the C- or N-terminal to a His-tag by a flexible, poorly immunogenic linker peptide of 21 amino acids; (Gly<sub>4</sub>Ser)<sub>4</sub>Gly (published in Analytical Biochemistry; Loughran *et al.*, 2006). The *bfl-1* coding fragment was successfully cloned into this novel vector to produce the fusion constructs from which His-Linker-Bfl-1 fusion

proteins were successfully overexpressed and purified using immobilised metal affinity chromatography. Sufficient protein was purified and used for the preparation of polyclonal antisera to Bfl-1.

In summary, the findings presented in this thesis are relevant to our understanding of the role of *bfl-1* as a crucial pro-survival NF-κB target in H/RS cells and the potential of Bfl-1 as a rational therapeutic target in HL is highlighted.

## Table of contents

Declaration.....	I
The Enthusiast- William Rowan Hamilton.....	II
Acknowledgements.....	III
Abstract.....	IV
Table of Contents.....	VI
List of Figures.....	XII
List of Tables.....	XVI
Abbreviations.....	XVII
Units.....	XXVIII
Publications.....	XXIX

<b><i>CHAPTER 1 Introduction .....</i></b>	<b>1</b>
<b>1.1 The Discovery of Hodgkin's Disease.....</b>	<b>2</b>
<b>1.2 From Hodgkin's Disease to Hodgkin's Lymphoma .....</b>	<b>3</b>
<b>1.3 Clinical Presentation, staging and therapy .....</b>	<b>4</b>
1.3.2 Recent advances in HL therapy.....	7
<b>1.4 Molecular origins of H/RS cells and immunopathogenesis .....</b>	<b>9</b>
1.4.2 H/RS cells evade apoptotic cell death and lead to systemic lymphoma.....	12
1.4.3 Neoplastic transformation of the progenitor .....	14
<b>1.5 Transcriptional control and aberrant activation of signaling pathways in HL .....</b>	<b>15</b>
1.5.2 Constitutive NF- $\kappa$ B activation in HL .....	16
1.5.3 STAT Family of transcription Factors.....	20
1.5.4 MAPK Signaling .....	20
1.5.5 AP-1 .....	22
1.5.6 PI3-K Signaling transduction.....	23
1.5.7 Notch Signaling Pathway.....	24
1.5.8 RTK signaling .....	27
<b>1.6 EBV and HL.....</b>	<b>27</b>

<b>1.7 Anti-apoptotic mechanisms in H/RS cells .....</b>	<b>30</b>
1.7.2 Bcl-2 Family: regulators of cell fate.....	32
1.7.3 Mechanism of action of Bcl-2 family members.....	34
1.7.4 Anti-apoptotic Bcl-2 member, Bfl-1 .....	35
1.7.5 <i>bfl-1</i> in malignant disease .....	37
1.7.6 <i>bcl-2</i> family member expression in HL .....	38
<b>1.8 Objectives of this study .....</b>	<b>39</b>
<b>CHAPTER 2 Materials and Methods.....</b>	<b>43</b>
<b>2.1 Biological Materials.....</b>	<b>44</b>
2.1.1 Cell lines .....	44
2.1.2 Antibodies used in the study .....	46
2.1.3 Bacterial strains.....	47
2.1.4 Bioinformatics software.....	48
2.1.5 Plasmids .....	49
2.1.6 Oligonucleotides.....	52
<b>2.2 Chemical Materials .....</b>	<b>53</b>
<b>2.3 DNA Manipulation.....</b>	<b>55</b>
2.3.1 Storage of DNA samples .....	55
2.3.2 Phenol/chloroform extraction and ethanol precipitation .....	55
2.3.3 Restriction digestion of DNA .....	56
2.3.4 Dephosphorylation of linearised plasmid DNA .....	56
2.3.5 Polymerase chain reaction .....	56
2.3.6 Purification of PCR products .....	58
2.3.7 Ligation of DNA molecules.....	58
2.3.8 Preparation of competent cells .....	59
2.3.9 Transformations .....	59
2.3.10 Small scale preparation of plasmid DNA (Miniprep) .....	59
2.3.11 DNA purification protocol (Maxiprep) .....	60
2.3.12 Spectrophotometric analysis of nucleic acids .....	60
2.3.13 Agarose gel electrophoresis of DNA.....	60
2.3.14 DNA Sequencing .....	61
<b>2.4 Cell Culture Methods.....</b>	<b>62</b>

2.4.1 Culture of cells in suspension .....	62
2.4.2 Culture of adherent cells.....	62
2.4.3 Co-culture of adherent and suspension cells.....	63
2.4.4 Cell Counts.....	63
2.4.5 Cell storage and recovery .....	63
2.4.6 Transient transfections.....	64
2.4.7 Stable Transfections .....	69
2.4.8 Measurement of Cell Proliferation.....	69
2.4.9 Acridine Orange/Ethidium Bromide staining .....	70
2.4.10 Flow cytometric analysis .....	70
2.4.11 Annexin V/vital dye staining .....	71
2.4.12 Statistics .....	72
<b>2.5 Tumour Tissue Methods .....</b>	<b>73</b>
2.5.1 Tissue sectioning .....	73
2.5.2 Laser Capture Microdissection .....	74
2.5.3 <i>In situ</i> hybridisation (ISH) .....	76
<b>2.6 RNA Analysis .....</b>	<b>80</b>
2.6.1 RNase-free environment.....	80
2.6.2 RNA analysis by gel electrophoresis.....	80
2.6.3 RNA extraction from cultured cells .....	80
2.6.4 Quantification of mRNA from cultured cells by RT-qPCR .....	82
2.6.5 RNA extraction from Laser Capture Microdissected Cells .....	85
2.6.6 Qualitative analysis of mRNA from microdissected cells.....	86
2.6.7 Quantitative analysis of mRNA from microdissected cells.....	87
<b>2.7 Protein Analysis.....</b>	<b>89</b>
2.7.1 Preparation of cellular protein.....	89
2.7.2 SDS-polyacrylamide gel electrophoresis of proteins .....	89
2.7.3 Coomassie Blue Staining .....	90
2.7.4 Western blotting .....	91
<b>2.8 Recombinant Protein Expression .....</b>	<b>94</b>
2.8.1 High-level expression of recombinant proteins .....	94
2.8.2 Determination of Protein Solubility .....	95
2.8.3 IMAC Purification of His-tagged recombinant proteins .....	95

2.8.4 Growth for preparative purification .....	96
2.8.5 Buffer exchange and concentration of purified protein.....	97
2.8.6 Antibody Preparation.....	97
<b>CHAPTER 3 <i>Bfl-1</i> is expressed in Hodgkin's Lymphoma tissue and cultured H/RS cells .....</b>	<b>98</b>
<b>3.1 Introduction.....</b>	<b>99</b>
3.1.1 Summary of results.....	99
<b>3.2 Results - Detection of <i>bfl-1</i> mRNA expression in HL.....</b>	<b>101</b>
3.2.1 Detection of <i>bfl-1</i> mRNA expression in H/RS cells of HD patients .....	101
3.2.2 Detection of <i>bfl-1</i> mRNA expression in cultured H/RS cells .....	114
<b>3.3 Discussion .....</b>	<b>118</b>
<b>CHAPTER 4 <i>Bfl-1</i> is a key NF-<math>\kappa</math>B target gene in H/RS-derived cell lines .....</b>	<b>121</b>
<b>4.1 Introduction.....</b>	<b>122</b>
4.1.1 Summary of results.....	123
<b>4.2 Results – NF-<math>\kappa</math>B pathway and regulation of <i>bfl-1</i> expression in HL .....</b>	<b>124</b>
4.2.1 Inhibition of NF- $\kappa$ B in H/RS cell lines and effect on <i>bfl-1</i> expression .....	124
4.2.2 The effect of maintenance of <i>bfl-1</i> expression during NF- $\kappa$ B inhibition. ...	136
<b>4.3 Discussion .....</b>	<b>156</b>
<b>CHAPTER 5 <i>Bfl-1</i> downregulation by RNAi.....</b>	<b>158</b>
<b>5.1 Introduction.....</b>	<b>159</b>
5.1.1 The RNAi pathway .....	159
5.1.2 Summary of Results .....	161
<b>5.2 Results.....</b>	<b>162</b>
5.2.1 Analysis of <i>bfl-1</i> -specific siRNAs.....	162
5.2.2 Efficiency of delivery of siRNA .....	163
5.2.3 Effect of anti- <i>bfl-1</i> siRNA on cell viability .....	168
5.2.4 Effect of anti- <i>bfl-1</i> siRNA during NF- $\kappa$ B inhibition.....	170
<b>5.3 Discussion .....</b>	<b>176</b>
<b>CHAPTER 6 Regulation of the <i>bfl-1</i> promoter in HL .....</b>	<b>177</b>
<b>6.1 Introduction.....</b>	<b>178</b>

6.1.1 Summary of results.....	178
<b>6.2 Results.....</b>	<b>180</b>
6.2.1 The <i>bfl-1</i> promoter is regulated by NF-κB in HL .....	180
6.2.2 Notch signaling .....	188
<b>6.3 Discussion .....</b>	<b>198</b>
<b><i>CHAPTER 7 Expression and Purification of recombinant Bfl-1 using a novel modified vector and generation of anti-Bfl-1 serum .....</i></b>	<b>202</b>
<b>7.1 Introduction.....</b>	<b>203</b>
7.1.1 The QIAexpress system.....	203
7.1.2 Polyhistidine-tag.....	205
7.1.3 Expression hosts .....	207
7.1.4 Summary of Results .....	209
<b>7.2 Results.....</b>	<b>210</b>
7.2.1 Cloning of pQE30-Bfl-1 and pQE60-Bfl-1 .....	210
7.2.2 Protein expression .....	214
7.2.3 Determination of protein solubility .....	220
7.2.4 Protein Purification.....	221
7.2.5 Design of Glycine-Serine Linker .....	224
7.2.6 Cloning and construction of pGSLink.....	226
7.2.7 Generation of pGSLink-N-Bfl-1 and pGSLink-C-Bfl-1 .....	229
7.2.8 Expression screening and purification of His-Linker-Bfl-1 and Bfl-1-Linker-His fusion proteins .....	230
7.2.9 Optimisation of purification.....	233
7.2.10 Antigen Preparation .....	236
7.2.11 Antibody preparation and analysis by ELISA and western blotting .....	237
<b>7.3 Discussion .....</b>	<b>239</b>
<b><i>CHAPTER 8 General Discussion .....</i></b>	<b>242</b>
<b><i>CHAPTER 9 Bibliography.....</i></b>	<b>252</b>
<b><i>CHAPTER 10 APPENDIX.....</i></b>	<b>a</b>
<b>10.1 Solutions for DNA Manipulation.....</b>	<b>b</b>
10.1.1 Storage of DNA.....	b

10.1.2 Solution for Bacterial Growth Media .....	b
10.1.3 Solutions for Preparation of Competent Cells .....	d
10.1.4 Solutions for DNA preparations.....	e
10.1.5 Solutions for Agarose Gel Electrophoresis.....	h
<b>10.2 Solutions for Cell Culture .....</b>	<b>i</b>
10.2.1 Media and Supplements.....	i
10.2.2 Solutions for DEAE-Dextran Tranfections Protocol.....	j
10.2.3 $\beta$ -Galactosidase Assay .....	j
<b>10.3 Solutions for Tumour Tissue Methods .....</b>	<b>l</b>
<b>10.4 Solutions for RNA Analysis .....</b>	<b>l</b>
<b>10.5 Solutions for Protein Analysis.....</b>	<b>m</b>
10.5.1 Solutions for Protein Isolation .....	m
10.5.2 Solutions for SDS-PAGE/ Western Blotting .....	n
<b>10.6 Solutions for Expression and Purification of Recombinant Proteins .....</b>	<b>q</b>
10.6.1 Denaturing solutions.....	q
10.6.2 Native solutions.....	r

## List of Figures

Figure 1.1 Typical morphology of a lymph-node affected by HD.....	2
Figure 1.2 Lymph node and cellular morphology of cHL disease types .....	4
Figure 1.3 The GC derivation of H/RS cells in cHL and L&H cells in LPHL .....	11
Figure 1.4 Cell-surface receptors and their respective intracellular mediators induce the proliferative and anti-apoptotic phenotype of H/RS cells.....	13
Figure 1.5 Activation and downstream effects of the canonical NF- $\kappa$ B pathway .....	17
Figure 1.6 Schematic view of CD30 signals and CD30 promoter induction by JunB in HL .....	23
Figure 1.7 Model and components of mammalian Notch signaling.....	26
Figure 1.8 A model for the evolution of EBV <sup>+</sup> HL .....	29
Figure 1.9 Anti-apoptotic mechanisms in H/RS cells.....	31
Figure 1.10 Schematic representation of Bcl-2 protein domain organisation.....	33
Figure 1.11 Mitochondrial pathway of apoptosis.....	35
Figure 2.1 Schematic representation of LCM .....	75
Figure 2.2 Principles of the TaqMan assay primers and probes .....	84
Figure 3.1 Detection of <i>bfl-1</i> mRNA expression in H/RS cells of HL patients .....	102
Figure 3.2 Detection of <i>bfl-1</i> mRNA expression in bystander/reactive cells of HL patients.....	103
Figure 3.3 The organisation of the <i>bfl-1</i> gene is compared with mRNAs encoding <i>bfl-1</i> and <i>bfl-1S</i> .....	104
Figure 3.4 Schematic of nested PCR approach to detect and resolve <i>bfl-1/bfl-1S</i> expression in H/RS cells.....	105
Figure 3.5 <i>bfl-1</i> mRNA detection in microdissected cells .....	106
Figure 3.6 Relative quantification of <i>bfl-1</i> mRNA level in H/RS and bystander/reactive cells from EBV +/- HL tumour tissue .....	108
Figure 3.7 Generation of pGEM- <i>bfl-1</i> -RP; a vector capable of synthesising sense/anti- sense <i>bfl-1</i> RNA transcripts for ISH .....	110
Figure 3.8 Analysis of the cloning steps in the construction of pGEM- <i>bfl-1</i> -RP .....	111
Figure 3.9 RNA gel electrophoresis of the <i>in vitro</i> transcribed sense/anti-sense <i>bfl-1</i> riboprobes .....	112
Figure 3.10 Detection of <i>bfl-1</i> mRNA expression in cultured H/RS cells.....	115

Figure 3.11 Real time qPCR analysis of <i>bfl-1</i> mRNA levels from HL-derived cell lines .....	116
Figure 3.12 Expression of <i>bfl-1/bfl-1S</i> mRNA in lymphoma cell lines.....	117
Figure 4.1 Determination of sodium arsenite IC <sub>50</sub> required to reduce viability of L428 cells. ....	126
Figure 4.2 Determination of sodium arsenite IC <sub>50</sub> required to reduce viability of L591 cells. ....	127
Figure 4.3 Acridine orange/ethidium bromide staining of L428 cells post treatment with sodium arsenite .....	128
Figure 4.4 Treatment of L428 cells with NF-κB inhibitor, sodium arsenite.....	129
Figure 4.5 Inhibition of NF-κB activity by sodium arsenite in HL.....	130
Figure 4.6 Effect of sodium arsenite inhibition of NF-κB activity on <i>bfl-1</i> mRNA expression in H/RS cell lines.....	131
Figure 4.7 Inhibition of NF-κB activity by BAY11 in HL .....	133
Figure 4.8 Treatment of L428 cells with NF-κB inhibitor, BAY11.....	134
Figure 4.9 Effect of BAY11 inhibition of NF-κB on <i>bfl-1</i> mRNA expression in H/RS cell lines.....	135
Figure 4.10 Cloning strategy .....	138
Figure 4.11 Construction of pRTS-1-HA- <i>bfl-1</i> .....	139
Figure 4.12 Ectopic expression of <i>bfl-1</i> mRNA and HA-tagged Bfl-1 and GFP proteins from DG75-pRTS-1-HA- <i>bfl-1</i> clones.....	141
Figure 4.13 Ectopic expression of <i>bfl-1</i> mRNA and HA-tagged Bfl-1 and GFP proteins from L428-pRTS-1-HA- <i>bfl-1</i> clones. ....	143
Figure 4.14 Cell proliferation of L428-pRTS-1-HA- <i>bfl-1</i> cells induced/non-induced to exogenously express HA-Bfl-1.....	145
Figure 4.15 Sodium arsenite treatment of L428-pRTS-1-HA- <i>bfl-1</i> .....	148
Figure 4.16 Effect of sodium arsenite treatment of L428-pRTS-1-HA- <i>bfl-1</i> .....	149
Figure 4.17 Sodium arsenite treatment of L428-pRTS-1-HA- <i>bfl-1</i> ; GFP expressing cells gated .....	150
Figure 4.18 BAY11 treatment of L428-pRTS-1-HA- <i>bfl-1</i> .....	151
Figure 4.19 Effect of BAY11 treatment of L428-pRTS-1-HA- <i>bfl-1</i> .....	152
Figure 4.20 BAY11 treatment of L428-pRTS-1-HA- <i>bfl-1</i> ; GFP expressing cells gated .....	153
Figure 4.21 Effect of serum deprivation on L428-pRTS-1-HA- <i>bfl-1</i> cells. ....	154

Figure 5.1 Three ways to trigger the RNAi pathway.....	160
Figure 5.2 Transfection of siRNA by electroporation .....	164
Figure 5.3 Transfection of siRNA using Riboforce transfection reagent.....	165
Figure 5.4 Transfection of siRNA by nucleofection .....	166
Figure 5.5 Knockdown of <i>bfl-1</i> mRNA expression by nucleofection of siRNA .....	167
Figure 5.6 Cell viability post nucleofection of siRNA .....	168
Figure 5.7 Effect of serum deprivation on anti- <i>bfl-1</i> siRNA-treated L428 cells. ....	169
Figure 5.8 Effect of sodium arsenite treatment on anti- <i>bfl-1</i> siRNA-treated L428 cells.	
.....	172
Figure 5.9 Effect of BAY11 treatment on anti- <i>bfl-1</i> siRNA-treated L428 cells.....	174
Figure 6.1 IκBα super-repressor IκBαDN blocks NF-κB activation in HL.....	181
Figure 6.2 IκBα DN inhibits the <i>bfl-1</i> promoter in HL.....	182
Figure 6.3 <i>bfl-1</i> promoter activation in HL-derived cell lines .....	184
Figure 6.4 IκBα DN blocks NF-κB activation of the <i>bfl-1</i> promoter in HL.....	186
Figure 6.5 Expression of Notch1/2 receptors, Jagged1 and EBNA2 expression in lymphoma cell lines .....	190
Figure 6.6 Presentation of the Notch ligand Jagged1 leads to increased proliferation of HL cells .....	192
Figure 6.7 Notch activation of CBF-1 expression in DG75, L428 and L591 cells.....	194
Figure 6.8 Jagged1 presentation effect on <i>bfl-1</i> promoter activation in H/RS cells....	195
Figure 6.9 <i>bfl-1</i> promoter activation in HL-derived cell lines. ....	197
Figure 7.1 pQE30 and pQE60 vector for N-terminal and C-terminal 6xHis tag constructs.....	205
Figure 7.2 Interaction between neighbouring residues in the 6xHis tag and Ni-NTA matrix. ....	207
Figure 7.3 Analysis of the cloning steps in the construction of the expression vector pQE60-Bfl-1 .....	211
Figure 7.4 Sequence verification of pQE30-Bfl-1 and pQE60-Bfl-1.....	213
Figure 7.5 Expression screening of His-Bfl-1 and Bfl-1-His in <i>E. coli</i> XL10 Gold ...	216
Figure 7.6 Expression screening of recombinant clones in <i>E. coli</i> RosettaBlue™ .....	218
Figure 7.7 Variation of growth parameters for optimal expression of pQE60-Bfl-1 in <i>E. coli</i> RosettaBlue™.....	219
Figure 7.8 Determination of protein solubility.....	220

Figure 7.9 Purification of His-Bfl-1 and Bfl-1-His under native and denaturing conditions .....	222
Figure 7.10 Western blot analysis of His-Bfl-1 and Bfl-1-His proteins .....	223
Figure 7.11 Design and construction of the Linker cassette fragment. ....	226
Figure 7.12 Generation of pGSLink .....	227
Figure 7.13 Analysis of the cloning steps in the construction of the expression vector pGSLink .....	228
Figure 7.14 Analysis of the cloning steps in the construction of the expression vector pGSLink-N-Bfl-1.....	230
Figure 7.15 Expression screening of recombinant pGSLink-N-Bfl-1 and pGSLink-C-Bfl-1 clones.....	231
Figure 7.16 Western blot analysis of His-Linker-Bfl-1 and Bfl-1-Linker-His proteins	232
Figure 7.17 Purification of His-Linker-Bfl-1 .....	233
Figure 7.18 Optimisation of purification of His-Linker-Bfl-1 and Bfl-1-Linker-His under native conditions. ....	234
Figure 7.19 Expression and purification of recombinant His-tagged Bfl-1 in.....	235
Figure 7.20 Purified concentrated Bfl-1 recombinant protein .....	236
Figure 7.21 ELISA to detect BFL-1-His in immune serum.....	237
Figure 7.22 Western blot using rabbit anti-sera .....	238

## List of Tables

Table 1-1 UICC-AJCC and the Ann Arbor staging classification for HL.....	5
Table 1-2 Long-terms toxic effects after treatment for HL.....	9
Table 1-3 Signaling pathways and transcription factors constitutively active in H/RS cells .....	15
Table 2-1 Cell lines used in the study.....	44
Table 2-2 Antibodies used in the study.....	46
Table 2-3 Bacterial Strains used in this study .....	47
Table 2-4 Web-based bioinformatics tools used in this study .....	48
Table 2-5 Expression and reporter constructs used in the study .....	49
Table 2-6 Oligonucleotides used in the study .....	52
Table 2-7 Suppliers of chemical and biological materials.....	53
Table 2-8 PCR Reactants .....	57
Table 2-9 PCR Thermocycling conditions.....	57
Table 2-10 Cycling conditions for PCR extension of Linker cassette.....	58
Table 2-11 <i>In vitro</i> transcription reactants .....	76
Table 2-12 MMLV RT reactants .....	83
Table 2-13 Real time qPCR reactants .....	85
Table 2-14 Sensiscript RT reactants .....	88
Table 2-15 Incubation Conditions for Antibodies Used in Western Blotting.....	92
Table 5-1 <i>bfl-1</i> specific siRNA specifications .....	162
Table 7-1 Predicted physico-chemical parameters of His-Bfl-1/Bfl-1-His .....	212
Table 7-2 Codon bias between <i>E. coli</i> genes and human <i>bfl-1</i> . ....	217
Table 10-1 10 % (v/v) resolving gels and 5 % (v/v) stacking polyacrylamide gels.....	n

## Abbreviations

A	Absorbance
aa	Amino acid
AAD	Amino-actinomycin D
ABI	Applied Biosystems
ABVD	Doxorubicin (adriamycin), bleomycin, vinblastine and dacarbazine
ADAM	A distintegrin and metalloprotease
Ago-2	Argonaute-2
AIDS	Acquired immuno-deficiency syndrome
AJCC	American Joint Committee on Cancer
Ank	Ankyrin
AO	Acridine orange
AP-1	Activator protein-1
AP	Alkaline phosphatase
Apaf	Apoptotic protease activating factor 1
APO2L	Apo 2 ligand
APS	Ammonium persulphate
Arg	Arginine
ATP	Adenosine tri-phosphate
B	BAY11
BART	<i>Bam</i> HI A rightward transcript
BATF	B cell specific transcription factor
BAY11	Bay 11-7082
BCA	Bicinchoninic acid
BCIP-NBT	5-Bromo-4-chloro-3-indolyl phosphate/nitro blue tetrazolium
BCR	B cell receptor
BEACOPP	Bleomycin      etoposide,      doxorubicin, cyclophosphamide, vincristine, procarbazine and prednisone
BH	Bcl-2 homology
BL	Burkitt's lymphoma

<i>Bla</i>	$\beta$ -lactamase gene
BSA	Bovine serum albumin
BTM	Basal transcription machinery
C	Cytosine
CAG	Chicken- $\beta$ -actin
CAT	Chloroamphenicol acetyl transferase
CBF	C promoter binding factor
CCL	Cleared cell lysate
CCR	Chemokine receptor
cdk	Cyclin dependent kinase
CDKI	Cyclin dependent kinase inhibitor
cDNA	Complementary DNA
cFLIP	Cellular FLICE inhibitory protein
ChIVPP/EVA	Chorambucil, vinblastine, procarbazine, prednisolone, etoposide, vincristine, and doxorubicin
cHL	Classical Hodgkin's lymphoma
chx	Cyclohexamide
c-IAP	Cellular inhibitor of apoptosis
CIP	Calf intestinal phosphatase
CIR	Co-repressor of CBF1
CK2	Casein kinase 2
CL	Cleared cell lysate
CMV	Cytomegalovirus
CO <sub>2</sub>	Carbon dioxide
COPP	Cyclophosphamide, vincristine, procarbazine and prednisone
Cp	C promoter
CR	Conserved region
CSL	CBF1/Su(H)/Lag-1/RBP-J $\kappa$ /KBF2
CST	Complementary-strand transcript
CTAR	C-terminal activating region
CtBP/CtIP	C-terminal-binding protein/ C-terminal-interacting protein

C-terminal	Carboxy terminal
Cys	Cysteine
Cyt c	Cytochrome c
DAB	Diaminobenzidine
DD	Death domain
DDR2	Discoidin receptor family, member 2
DEAE	Diethyl aminoethyl
DEPC	Diethylpyro-carbonate
dH <sub>2</sub> O	Distilled water
DIG	Digoxigenin
DLL	Delta-like
DMEM	Dulbecco's modified eagle medium
DMSO	Dimethylsulphoxide
DN	Dominant negative
DNA	Deoxyribonucleic acid
DNase	Deoxyribonuclease
dNTP	Deoxyribonucleotide
DS	Dyad symmetry
DS-DNA	Double stranded DNA
DS-RNA	Double stranded RNA
DSHB	Developmental Studies Hybridoma Bank
DSL	Delta, Serrate and LAG-2
DTT	Dithiothreitol
E	Elution
<i>E. coli</i>	<i>Escherichia coli</i>
EA	Early antigen
EA-D	Diffuse early antigen
EA-R	Restricted early antigen
EBER	Epstein-Barr virus encoded RNA
EBNA	Epstein-Barr virus nuclear antigen
EBNA-LP	Epstein-Barr virus nuclear antigen-leader protein
EBV	Epstein-Barr virus
EC	Extracellular
EDTA	Ethylenediamine tetraacetic acid

EGF	Epidermal growth factor
ELISA	Enzyme-linked Immunosorbent assay
EMSA	Electrophoretic mobility shift assay
EPHB1	Ephrin receptor B1
ER	Endoplasmic reticulum
ERE	EBNA2-responsive element
EREB	Estrogen-responsiv Epstein-Barr virus nuclear antigen
ERK	Extracellular signal-regulated kinase
est	Estrogen
EtBr	Ethidium bromide
FACS	Fluorescence activated cell sorting
FADD	Fas-associated death domain
FAM	6-carboxyfluorescein
FAS	Fatty acid synthase
FBS	Foetal bovine serum
FDA	Federal drug administration
FLICE	FADD-like IL-1 $\beta$ -converting enzyme
FR	Family of repeats
FSC	Forward light scatter
FT	Flow-through
G	Guanine
Gal	Galactosidase
GAPDH	Glyceraldehyde-3-phosphate dehydrogenase
GATA	Gene activator of TCR- $\alpha$
GC	Germinal centre
GFP	Green fluorescent protein
Gly	Glycine
GM-CSF	Granulocyte macrophage-colony stimulating factor
gp	Glycoprotein
GSLinker	Glycine/serine linker
H	Hodgkin
HA	Hemagglutinin

HAT	Histone acetyltransferase
HD	Hodgkin's disease
HDAC	Histone deacetylase
His	Histidine
HIV	Human immunodeficiency virus
HL	Hodgkin's lymphoma
HRP	Horseradish peroxidase
H/RS	Hodgkin/Reed-Sternberg
HRT	Hairy-related transcription factor
HSV	Herpes simplex virus
HTLV	Human T-cell leukaemia virus type
IC <sub>50</sub>	Inhibitory concentration 50
IC	Intracellular
ICAM	Intercellular cell adhesion molecule
IF-RT	Involved-field radiation therapy
Ig	Immunoglobulin
IgG	Immunoglobulin G
IgM	Immunoglobulin M
IκB	Inhibitor of κB
IKK	IκB kinase complex
IKAP	Inhibitor of kinase complex-associated protein
IL	Interleukin
Ile	Isoleucine
IM	Infectious mononucleosis
IMAC	Immobilised metal affinity chromatography
IP	Inducible protein
IP-CNS	Immunoblastic primary central nervous system
IPTG	Isopropyl thiogalactoside
IR	Internal repeat
IRAKs	IL-1-receptor-associated kinases
IRES	Internal ribosomal entry site
ISH	<i>In situ</i> hybridisation
ITAM	Immunoreceptor tyrosine-based activation motif
IVT	<i>In vitro</i> transcription

JAK	Janus kinase
JNK	c-Jun NH <sub>2</sub> terminal kinase
L	Ligand
L&H	Lymphocytic and histiocytic
<i>Lac</i>	<i>Lactose</i>
<i>Lac O</i>	<i>Lactose</i> operator
LB	Luria-Bertani broth
LCL	Lymphoblastoid cell line
LCM	Laser capture microdissection
LDHL	Lymphocyte-depleted Hodgkin's lymphoma
Leu	Leucine
LFA	Lymphocyte-function-associated antigen
LMP	Latent membrane protein
LPC	Laser Pressure Catapulting
LPHL	Lymphocyte predominant Hodgkin's lymphoma
LPS	Lipopolysaccharide
LRHL	Lymphocyte-rich Hodgkin's lymphoma
LT	Lymphotoxin
Luc	Luciferase
M	Molecular weight marker
MA	Membrane antigen
mAb	Monoclonal antibody
Mam	Mastermind
MAML	Mastermind in Drosophila
MAPK	Mitogen activated protein kinase
MAPKK	MAPK kinase
MAPKKK	MAPKK kinase
MCHL	Mixed cellularity hodgkin's lymphoma
MCS	Multiple cloning site
MDC	Macrophage-derived chemokine
MEK	MAP/ERK kinase
MEKK	MAPK/ERK kinase
MET	Methionine
MHC	Major histocompatibility complex

M-MLV RT	Moloney Murine leukemia virus reverse transcriptase
MMP	Matrix metalloproteinase
MOPP	Nitrogen mustard, vincristine, procarbazine and prednisone
mRNA	messenger RNA
MTS	3-(4,5-dimethylthiazol-2-yl)-5-(3-carboxymethoxyphenyl)-2-(4-sulfophenyl)-2H-tetrazolium salt
MUM	Multiple myeloma oncogene-1-protein
Mut	Mutant
NADH	Nicotinamide adenine dinucleotide
NADPH	Nicotinamide adenine dinucleotide phosphate
NC	Negative control
N-coR	Nuclear receptor corepressor
NEB	New England Biolabs
NEMO	NF-κB Essential MOdulator
NF-κB	Nuclear factor κB
NHL	Non-Hodgkin lymphomas
Ni <sup>2+</sup>	Nickel ion
NIK	NF-κB inducing kinase
NK	Natural killer cell
NLS	Nuclear localisation signal
NOD/Scid	Nonobese diabetic severe combined immunodeficient
NotchIC	Notch intracellular domain
NPC	Nasopharyngeal carcinoma
NS	Nodular sclerosis
NSHL	Nodular sclerosis Hodgkin's lymphoma
Nt	Nucleotide
NTA	NitriloTriacetic Acid
N-terminal	Amino terminal
O.D.	Optical density
ONPG	<i>o</i> -nitrophenyl-β-D-galactopuranoside

ORF	Open reading frame
ori	Origin of replication
p53	Protein 53
p38/MAPK	p38/mitogen activated protein kinase
PAGE	Polyacrylamide gel electrophoresis
PBS	Phosphate buffered saline
PCAF	p300/CBP-associated factor
PCR	Polymerase chain reaction
PDGFRA	Platelet-derived growth factor receptor A
PE	Phycoerythrin
PEN	Polyethylene naphthalate
PES	Phenazine ethosulphate
PEST	Proline-, glutamate, serine-, threonine-rich
pH	Power of the hydrogen ion
PI	Propidium Iodide
PI3-K	Phosphatidylinositol 3-kinase
PKC	Protein kinase C
PKR	RNA-dependent protein kinase
PMA	Phorbol-12-myristate 13-acetate
PMSF	Phenylmethanesulphonylfluoride
poly His	Polyhistidine
pRb	Retinoblastoma protein
PS	Phosphatidyl serine
PTK	Protein tyrosine kinase
PTLD	Post transplant lymphoproliferative disorder
Qp	Q promoter
qPCR	Quantitative PCR
R	Region
RAM	RBP-Jκ-associated molecule
RANK	Receptor activator of NF-κB
RbCl <sub>2</sub>	Rubidium chloride
RBP-Jκ	Jκ-recombinant-binding protein
RBS	Ribosome binding site
RHD	Rel homology domain

RIP	Receptor-interacting protein
RISC	RNA-inducing silencing complex
RNA	Ribonucleic acid
RNAi	RNA interference
Rnase	Ribonuclease
ROX	6-carboxyl-X-rhodamine
RPA	Ribonuclease protection assay
RPMI	Roswell Park Memorial Institute
RQ	Relative quantification
RS	Reed-Sternberg
RSK	Ribosomal S6 kinase
RT	Reverse transcriptase
RT-PCR	Reverse transcription polymerase chain reaction
RTK	Receptor tyrosine kinase
S	Subunit
SA	Sodium arsenite
SAPK	Stress-activated protein kinase
SCF $\beta$ -TrCP	Skp1, Cul1, F-box protein-type E3s
SDS	Sodium dodecyl sulphate
Ser	Serine
SHM	Somatic hypermutation
shRNA	short hairpin RNA
sIgG	Surface immunoglobulin G
siRNA	small-interfering RNA
SKIP	Ski-interacting protein
SMRT	Silencing mediator of retinoid and thyroid hormone receptors
SSC	Side light scatter
STAT	Signal transducers and activators of transcription
SuH	Suppressor of hairless
SV40	Simian virus 40
T	Time
+/- T	Plus/minus tetracycline
TACE	Tumour necrosis factor $\alpha$ -converting enzyme

TAD	Trans-activation domain
TAE	Tris acetate ethylenediamine tetraacetic acid
TAK	TGF- $\beta$ -activated kinase
TAMRA	Tetramethyl-6-carboxyrhodamine
TARC	Thymus- and activation-regulated chemokine
T-bet	T-box transcription factor
tBid	Truncated Bid
TBP	TATA box binding protein
TBS	Tris buffered saline
TBS-T	Tris buffered saline + Tween 20
TE	Tris EDTA
TEMED	N,N,N',N'-Tetramethylethylenediamine
TES	Transformation effector site
Tet	Tetracycline
TEY	Thr-Glu-Tyr
TFB	Transformation buffer
TGF	Transforming growth factor
Thr	Threonine
TLRs	Toll-like receptors
T <sub>m</sub>	Melting temperature
TMB	3,3',5,5'-tetramethylbenzidine
TNF	Tumour necrosis factor
TNFR	Tumour necrosis factor receptor
TR	Terminal repeat
TRADD	TNFR-associated death domain
TRAF	TNFR-associated factors
TRAIL	TNF-related apoptosis inducing ligand
TRAIL-R	TNF-related apoptosis inducing ligand receptor
TRKA	Tyrosine kinase receptor A
TRKB	Tyrosine kinase receptor B
tRNAs	Transfer RNAs
TT	Tranfusion transmitted
Tyr	Tyrosine
UICC	International Union Against Cancer

UL	Unique long
upH <sub>2</sub> O	Ultra pure water
US	Unique short
UV	Ultra violet
VAPEC-B	Vincristine, doxorubicin, prednisolone, etoposide, cyclophosphamide, and bleomycin
VCA	Viral capsid antigen
V <sub>H</sub>	Variable region of heavy chain
VHb	Bacterial hemoglobin
v/v	Volume per volume
W	Wash
Wp	W promoter
WHO	World Health Organisation
wt	Wild type
w/v	Weight per volume
XIAP	<i>X-linked mammalian inhibitor of apoptosis protein</i>
β-gal	Beta-galactosidase
λ <sub>max</sub>	Wavelength of maximum absorbance

## **Units**

%	Percentage
°C	Degrees Celsius
bp	Base pairs
cm	Centimetre
cpm	Counts per million
g	Grams
Gy	Gray
h	hours
Kb	Kilobase pairs
kDa	Kilo Dalton
Kg	Kilogram
L	Litres
lb/sq	Pounds per square inch
M	Molar
mA	Milliamperes
mg	Milligrams
ml	Millilitres
mM	Millimolar
ng	Nanograms
nm	Nanometres
nt	Nucleotides
pmole	Picomoles
rpm	Revolutions per minute
U	Enzyme units
V	Volts
x g	Relative centrifugal force
W	Watts
µF	Micro Faraday
µg	Micrograms
µl	Microlitre
µM	Micromolar
µm	Micrometer/ micron

## Publications

### Publications

- **Loughran, S.T.**, Campion, E.M., D'Souza, B., Murray, P., Bornkamm, G., Walls, D. *Bfl-1* is a crucial pro-survival Nuclear factor kappa B target gene in Hodgkin/Reed-Sternberg cells (Manuscript in preparation, September 2007).
- Campion, E.M., **Loughran, S.T.**, D'Souza, B.N., Phelan, S., Kempkes, B., Bornkamm, G., Hayward, D. and Walls, D. Downregulation of the Pro-apoptotic Nbk/Bik Gene During the EBV Growth Programme. (Manuscript in preparation, September 2007).
- **Loughran, S.T.**, Loughran, N.B., Ryan, B.J., D'Souza, B.N. and Walls, D. (2006). Modified His-tag fusion vector for enhanced protein purification by immobilized metal affinity chromatography. *Analytical Biochemistry.*, 355, 148-150.
- Pegman, P.M., Smith, S.M., D'Souza, B.N., **Loughran, S.T.**, Maier, S., Kempkes, B., Cahill, P.A., Simmons, M.J., Gelinas, C. and Walls, D. (2006). Epstein-Barr Virus Nuclear Antigen 2 trans-Activates the Cellular Anti-apoptotic bfl-1 Gene by a CBF1/RBPJ{kappa}-Dependent Pathway. *J. Virol.*, 80, 8133-8144.
- McMahon, K.J., Minihan, D., Campion, E.M., **Loughran, S.T.**, Allan, G., McNeilly, F. and Walls, D. (2006). Infection of pigs in Ireland with lymphotropic [gamma]-herpesviruses and relationship to postweaning multisystemic wasting syndrome. *Veterinary Microbiology.*, 116, 60-68.
- D'Souza, B.N., Edelstein, L.C., Pegman, P.M., Smith, S.M., **Loughran, S.T.**, Clarke, A., Mehl, A., Rowe, M., Gelinas, C. and Walls, D. (2004). Nuclear factor kappa B-dependent activation of the antiapoptotic bfl-1 gene by the Epstein-Barr virus latent membrane protein 1 and activated CD40 receptor. *J. Virol.*, 78, 1800-1816.

### Presentations: Posters

- **Loughran, S.T.**, Campion, E.M., D'Souza, B., Murray, P., Bornkamm, G., Walls, D. *Bfl-1* is a crucial pro-survival Nuclear factor kappa B target gene in Hodgkin/Reed-Sternberg cells. Irish Society for Immunology Annual Meeting, Dublin City University. Dublin 13<sup>th</sup> –14<sup>th</sup> September 2007.

- Campion, E.M., **Loughran, S.T.**, D'Souza, B.N., Phelan, S., Kempkes, B., Bornkamm, G., Hayward, D. and Walls, D. Downregulation of the Pro-apoptotic NbK/Bik Gene During the EBV Growth Programme. Royal Academy of Medicine in Ireland, Winter Meeting, Dublin City University. Dublin, January 11<sup>th</sup> 2007.
- Campion, E.M., **Loughran, S.T.**, D'Souza, B.N., Phelan, S., Kempkes, B., Bornkamm, G., Hayward, D. and Walls, D. Downregulation of the Pro-apoptotic NbK/Bik Gene During the EBV Growth Programme. Tumour Associated Herpes Viruses 13<sup>th</sup> International Symposium on Epstein Barr Virus and associated malignant Disease. Boston, USA, 8<sup>th</sup> – 12<sup>th</sup> July 2006.
- **Loughran, S.T.**, Loughran, N.B., Ryan, B.J., D'Souza, B.N. and Walls, D. Expression and purification of His-tagged recombinant human Bfl-1: use of a modified *E. coli* expression vector enables purification by Immobilised Metal Affinity Chromatography. GE Healthcare Challenging Proteins European Contest for Young Scientists 2005. Paris, 16<sup>th</sup>-18<sup>th</sup> October 2005.
- **Loughran, S.T.**, D'Souza, B.N., Smith, S.M., Campion, E.M., McGee, S., Tam, L., and Walls, D. The cellular anti-apoptotic *bfl-1* gene is highly expressed in cultured Hodgkin/Reed Sternberg cells from Hodgkin's Lymphoma and is regulated by NF-κB. Irish Association for Cancer Research Conference 2005. Kilkenny, 11<sup>th</sup>-12<sup>th</sup> March 2005.
- Pegman, P., Smith, S., D'Souza, B., **Loughran, S.T.**, Rowe, M., Kempkes, B., Gelinas, C. and Walls, D. The Epstein-Barr virus nuclear antigen 2 transcriptionally activates the cellular anti-apoptotic bfl-1 gene by an RBPJκ/CBF1 dependent pathway. Irish Association for Cancer Research Conference 2005. Kilkenny, 11<sup>th</sup>-12<sup>th</sup> March 2005.
- Pegman, P.M., Smith, S.M., D'Souza, B.N., **Loughran, S.T.**, Rowe, M., Kempkes, B., Gelinas, C. and Walls, D. The Epstein-Barr virus nuclear antigen 2 transcriptionally activates the cellular anti-apoptotic bfl-1 gene by an RBPJκ/CBF1 dependent pathway. Tumour Associated Herpes Viruses 11<sup>th</sup> International Symposium on Epstein Barr Virus and associated malignant Disease. Regensburg, Germany, 20<sup>th</sup> – 25<sup>th</sup> September 2004.
- D'Souza, B.N., Pegman, P.M., Smith, S.M., **Loughran, S.T.**, Clarke, A., Mehl, A., Floettmann, E., Edelstein, L., Gelinas, C., Rowe, M. and Walls, D. Transcriptional Activation of the cellular anti-apoptotic BFL-1/A1 gene by the Epstein-Barr virus Latent Membrane Protein 1. Society for General Microbiology- Irish Branch Meeting "Microbial Diseases in the Immunocompromised patient" Department of Biology, National University of Ireland, Maynooth, 24<sup>th</sup> -25<sup>th</sup> April 2003.

- D'Souza, B.N., Pegman, P.M., Smith, S.M., **Loughran, S.T.**, Clarke, A., Mehl, A., Floettmann, E., Edelstein, L., Gelinas, C., Rowe, M. and Walls, D. Transcription Activation of the Bfl-1 gene by the EBV Latent Membrane Protein 1. Irish Association for Cancer Research Meeting 2003. Kilkenny, 10<sup>th</sup> –11<sup>th</sup> April 2003.
- D'Souza, B.N., Mehl, A., Pegman, P.M., Clarke, A., **Loughran, S.T.**, Edelstein, L., Brennan, P., Rowe, M., Gelinas, C., and Walls, D. Transcription Activation of the Bfl-1 gene by the EBV Latent Membrane Protein 1. Tumour Associated Herpes Viruses 10<sup>th</sup> International Symposium on Epstein Barr Virus and associated malignant Disease. Cairns, Australia. July 16<sup>th</sup> –21<sup>st</sup> 2002.

#### **Presentations: Oral**

- **S.T. Loughran.** Cellular/Viral Pathways regulating expression of the Human anti-apoptotic *bfl-1* gene in Hodgkin's Disease. Transfer from MSc to PhD presentation, 25<sup>th</sup> August 2005.
- **S.T. Loughran,** D. Walls. Epstein-Barr virus and Associated Diseases, part of the Infectious Agents; Biology & Clinical Implications Module for MSc In Molecular Medicine. Trinity Centre for Molecular Medicine, St. James Hospital, 26<sup>th</sup> January 2006 and 1<sup>st</sup> March 2007.
- Smith, S.M., Pegman, P.M., D'Souza, B.N., **Loughran, S.T.** and Walls, D. Epstein-Barr virus latent genes regulate expression of the anti-apoptotic cellular *bfl-1* gene. Biological seminar series, DCU, Glasnevin, Dublin 9. April 20<sup>th</sup> 2004.
- D'Souza, B.N., Pegman, P.M., Smith, S.M., **Loughran, S.T.**, Mehl, A., Clarke, A., Brennan, P., Edelstein, L., Floettmann, E., Gelinas, C., Kempkes, B., Rowe, M. and Walls, D. The anti-apoptotic *bfl-1/A1* gene is a transcriptional target of the Epstein -Barr Virus latent proteins LMP1 and EBNA2. Irish society of Immunology Conference. St Vincent's Hospital, 2002.
- D'Souza, B.N., Pegman, P.M., Smith, S.M., **Loughran, S.T.**, Clarke, A., Mehl, A., Brennan, P., Edelstein, L., Floettmann, E., Gelinas, C., Kempkes, B., Rowe, M. and Walls, D. Mechanisms of Transcriptional Upregulation of the Anti-Apoptotic *bfl-1/A1* Gene by Epstein-Barr Virus Latent Proteins. Joint European Association of Cancer Research/British Association of Cancer Research Conference. Dublin, March 1<sup>st</sup>-4<sup>th</sup> 2003. Abstract accepted but conference subsequently cancelled.

### **Training courses attended during this study**

- Production and Application of Antibodies and Other Immunological Reagents Incorporating Web-based and Practical Approaches. National Centre for Sensor Research, DCU. 12<sup>th</sup> Feb 2002.
- Clinical Applications of Laser Capture Microdissection in the protein analysis of colonic tumours. Institute of Molecular Medicine, Trinity centre for Health sciences, St. James' Hospital. 23<sup>rd</sup> October 2003.
- Society for General Microbiology/ MWG Biotech workshop on Production and Application of Microarrays. Dublin City University, 3<sup>rd</sup> - 4<sup>th</sup> June 2004.
- SiRNA Training Course: siRNA User Workshop presented by Ambion Inc at the NICB, Dublin City University, 20<sup>th</sup> –22<sup>nd</sup> April 2005.
- Refworks Training Course; web based bibliographic manager, 13<sup>th</sup> December 2005.
- Applied Biosystems Real Time PCR training, Dublin City University, 13<sup>th</sup> –14<sup>th</sup> June 2005

### **Awards, achievements and positions held during this study**

- Recipient of DCU Postgraduate Accommodation Scholarship 2002-2003
- Chairperson of Biological Research Society 2002-2003. Involved promotion of Science during science week, organising scientific seminars, social events and away trips.
- Recipient of Orla Benson Award for Postgraduate Travel 2004
- Recipient of DCU Postgraduate Travel Bursary 2004
- Postgraduate Representative for the School of Biotechnology 2005.
- Selected as a contestant (44 contestants from 13 countries) for GE Healthcare European Workshop on Challenging Proteins in conjunction with the 3<sup>rd</sup> European Contest for Young Scientists, Paris, 17<sup>th</sup> –18<sup>th</sup> October 2005.

# **CHAPTER 1 Introduction**

## 1.1 The Discovery of Hodgkin's Disease

Hodgkin's disease (HD) was first described by Thomas Hodgkin more than a century ago, who reported 7 patients in 1832, based solely on gross examination of the enormous nodal and splenic expansions caused by the disease (Hodgkin, 1832). Advancements in microscopic examination and histological techniques in the subsequent years led to the description of giant cells with abundant protoplasm, multiple bizarre nuclei and prominent nucleoli (Taylor and Riley, 2001). In 1898, Carl Sternberg described the microscopic features of these cells in detail but attributed the giant cells and lymphocytic background to an unusual form of tuberculosis, as many patients at the time were stricken by both diseases (Sternberg, 1898). However, in 1902, Dorothy Reed published eight cases of non-tuberculosis-associated HD that proved instrumental in separating tuberculosis from the etiology of this malignant process (Reed, 1902).

Hodgkin, Reed and Sternberg described a characteristic feature of HD which distinguishes this disease from other cancers; the extraordinary and unexplained scarcity of its neoplastic cells in involved tissue, identified histologically as mononuclear Hodgkin (H) cells and multinucleated Reed-Sternberg (RS) cells (Figure 1.1), surrounded by a background of lymphocytes, plasma cells, eosinophils, histiocytes and stromal cells in the affected lymph nodes.

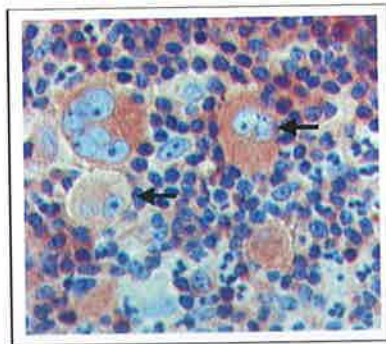


**Figure 1.1 Typical morphology of a lymph-node affected by HD.**

The use of a specific antibody to stain for H/RS cells (indicated by black arrows) shows them to be morphologically abnormal mononucleated and multinucleated giant cells surrounded by a characteristic infiltrate of rosetting T-cells, granulocytes, and histiocytes. Adapted from Thomas *et al.*, 2004a.

## 1.2 From Hodgkin's Disease to Hodgkin's Lymphoma

The discovery, in 1994 by Kuppers *et al.*, that the malignant cells of HD were B-cell derived led to the World Health organisation (WHO) reclassification of HD as Hodgkin's lymphoma (HL). HL, which is one of the most frequent lymphomas in the Western world (accounting for 30 % of all lymphomas), often affecting young adults, is composed of two different entities: the rare lymphocyte predominant HL (LPHL) and the more frequent classical HL representing 95 % of all HL (Pileri *et al.*, 2002). LPHL is characterised by detection of lymphocytic and histiocytic (L&H) cells embedded in a reactive infiltrate. Classical Hodgkin's lymphoma (cHL), a separate clinicopathologic entity from LPHL, characterised by the presence of H/RS cells surrounded by a reactive infiltrate, can be divided into four morphological subtypes: nodular sclerosis cHL, mixed cellularity cHL, lymphocyte-rich cHL and lymphocyte-depleted cHL. LPHL differs from cHL in terms of immunophenotype (presence versus absence of B-cell markers, respectively), mutational status of the heavy chain immunoglobulin (Ig) gene (ongoing somatic mutations versus crippling mutations, respectively), signaling pathways involved in malignant transformation (e.g., presence versus absence of *BCL6* expression, respectively) and presence of Epstein-Barr virus (EBV) (detected in H/RS cells of cHL mostly in the mixed cellularity variant (80 %) but rarely in L&H cells of LPHL [< 1%]) (Re *et al.*, 2005).

The most frequent subtype of cHL is nodular sclerosis (NSHL) (Figure 1.2A), accounting for 70 to 80 % of cases and is the only subtype without a male predominance. Mixed cellularity subtype (MCHL) (Figure 1.2B) represents 10 to 15 % of cases, 70 to 80 % are male and is more common in developing countries and in patients infected with the human immunodeficiency virus (HIV). The lymphocyte-rich subtype (LRHL) (Figure 1.2C) represents approximately 5 % of HL, and the clinical features are similar to LPHL. The least common subtype, lymphocyte-depleted (LDHL) (Figure 1.2D), is very rarely seen in primary presentation and is less well characterised because of its rarity. LDHL usually affects males presenting in advanced stages with the worst prognosis among all the subtypes.

The focus of the research in this study was cHL, particularly NSHL, the most prevalent disease type, due to the availability of cell lines and tissue biopsies.

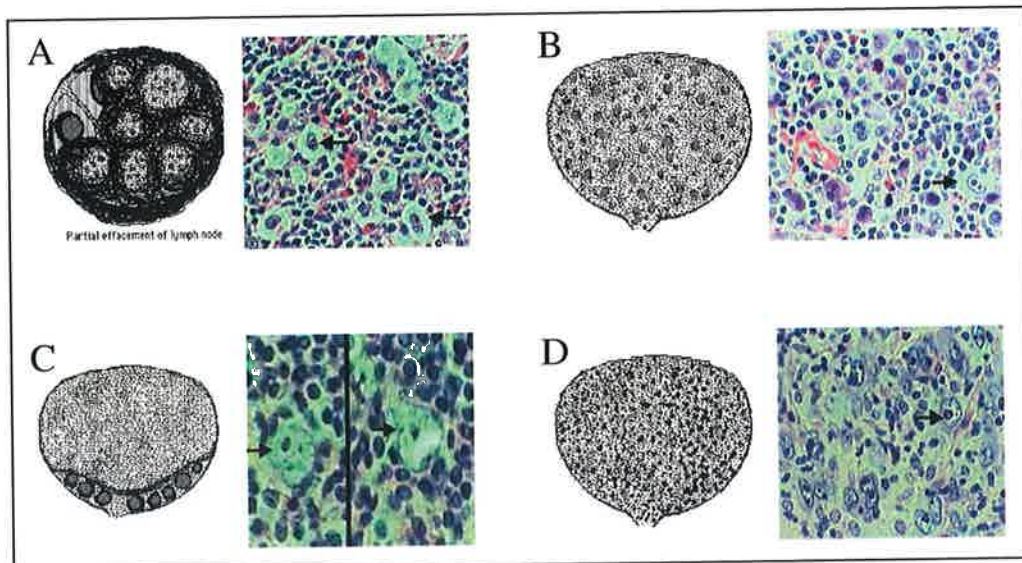


**Figure 1.2 Lymph node and cellular morphology of cHL disease types**

(A) NS disease type lymph node characteristic appearance (left) displaying numerous "lacunar" RS variants and sclerosing bands of collagenous fibrosis forming a nodular pattern. The fibrosis thickens the capsule and divides the proliferating process into "nodules" or islands. Cellular morphology of affected lymph node (right) showing H/RS cells indicated by black arrows. Predominant morphology of the H/RS cells is the lacunar cell, characterised by lobulated nucleus, prominent eosinophilic nucleolus and abundant clear cytoplasm. (B) MC disease type lymph node characteristic appearance (left) displaying numerous RS cells in a mixed inflammatory background that obliterates the normal architecture. Plasma cells and eosinophils are frequent. Only small amounts of fibrosis and occasional necrosis may be present. Cellular morphology of affected lymph node (right) showing H/RS cell indicated by black arrow. (C) LR disease type lymph node characteristic appearance (left), classic RS cells are rare and difficult to find, but mononuclear "L&H" Hodgkin's cells with "popcorn" shaped nuclei and inconspicuous nucleoli are present against a background of small lymphocytes. Cellular morphology of affected lymph node (right) showing H/RS cells indicated by black arrows. (D) LDHL node characteristic appearance (left) is characterised by many RS cells and variants (small lymphocytes are virtually absent) or by extensive fibrosis. Cellular morphology of affected lymph node (right) showing H/RS cell indicated by black arrow. Adapted from <http://www.med-ed.virginia.edu/courses/path/innes/wcd/hodgkin1.cfm>.

### 1.3 Clinical Presentation, staging and therapy

HL patients usually present with an asymptomatic lymph node enlargement in supradiaphragmatic areas, usually in the neck, which may increase and decrease over a period of a few months. Staging upon clinical presentation allows for the determination

of most relevant treatment choice. The extent of disease is assessed with the four-stage International Union Against Cancer (UICC, 2002)- American Joint Committee on Cancer (AJCC) Cancer Staging Manual (Greene *et al.*, 2002) and Ann Arbor classification (Carbone *et al.*, 1971) (Table 1-1). Patients are classified as having early-stage favourable, unfavourable (intermediate), or advanced-stage disease according to anatomic stage and B-symptoms (and possibly prognostic factors, such sex and age). Approximately 70 % of patients present with stage I or II disease but fortunately, due to the successes of modern cancer therapy, in excess of 90 % for early stages and 80 to 85 % for advanced stages, of all patients treated for HL reach complete remission after initial treatment, depending on stage and risk factor profile.

**Table 1-1 UICC-AJCC and the Ann Arbor staging classification for HL**

Clinical Stage	Description
Stage I	Involvement of a single lymph node region.
Stage I <sub>E</sub>	Localised involvement of a single extralymphatic organ or site.
Stage II	Involvement of two or more lymph node regions on the same side of the diaphragm.
Stage II <sub>E</sub>	Localised involvement of a single extralymphatic organ or site and its regional lymph node(s) with or without involvement of other lymph nodes regions on the same side of the diaphragm.
Stage III	Involvement of lymph node regions on both sides of the diaphragm.
Stage III <sub>E</sub>	Localised involvement of an associated extralymphatic organ/site.
Stage III <sub>S</sub>	Involvement of the spleen.
Stage III <sub>E+S</sub>	Involvement of both extralymphatic organ/site and spleen.
Stage IV	Disseminated (multifocal) involvement of one or more extralymphatic organs, with or without associated lymph node involvement; or isolated extralymphatic organ involvement with distant (nonregional) nodal involvement.
All stages divided	
A	Without weight loss/fever/night sweats.
B*	With weight loss (> 10 % of body weight within previous 6 months)/fever (>38 °C)/drenching night sweats.

\* Systemic symptoms of night sweats, fever, and weight loss are reported in approximately 30 % of patients. Adapted from Diehl, Thomas and Re, 2004.

In the 1950s to 1960s, the management of HL was based on the use of radiation therapy alone as the main treatment modality. Chemotherapy was introduced as a treatment in the 1960s, with the multiagent therapy; MOPP (nitrogen mustard, vincristine,

procarbazine, and prednisone), used chiefly in patients with advanced stage disease. In the intervening years, improved survival rates have been obtained with polychemotherapy such as ABVD [doxorubicin (adriamycin), bleomycin, vinblastine, dacarbazine] and BEACOPP (bleomycin etoposide, doxorubicin, cyclophosphamide, vincristine, procarbazine, prednisone) (Devita *et al.*, 1970; Bonadonna *et al.*, 1982; Kaplan, 1980; Diehl *et al.*, 1998). At present, it is internationally accepted that the “gold standard” for early-stage HL therapy consists of a combined modality treatment comprising a short-duration chemotherapy (two to four cycles of ABVD) followed by involved-field radiation therapy (IF-RT) (low-dose of 20–30 Gy). Treatment by IF-RT includes the clinically involved lymph node region, with or without limited coverage of the adjacent uninvolved lymph node region.

Intermediate disease indicated by the presence of one or more of the following adverse factors; systemic symptoms (Table 1-1; Stage IB or Stage IIB), bulky mediastinal disease, extranodal extension (Table 1-1; Stage IE or Stage IIE) or unexplained anemia places the patient in the ‘unfavourable’ group. Patients presenting with early unfavourable or intermediate disease receive four cycles of ABVD followed by IF-RT (20–30 Gy).

Those patients presenting with advanced-stage disease are treated with escalated chemotherapy (with six to eight cycles of ABVD). However, there are cardiotoxicity and pulmonary side effects with six to eight courses of ABVD, which are exacerbated with the addition of radiotherapy. Unfortunately, advanced stage HL is associated with a poor prognosis, particularly in patients presenting with B symptoms or relapsed/refractory status. One-third to 40 % of patients in stage IV will relapse after first-line therapy, and the majority of these will ultimately have a fatal outcome (Balzarotti *et al.*, 2003).

For patients with progressive or relapsing disease, depending on previous treatment, therapeutic options include radiotherapy, chemotherapy, and high-dose chemotherapy followed by autologous stem-cell transplantation (Canellos, 1998; Josting *et al.*, 1998; Brice *et al.*, 1999), which has been shown to be superior to standard chemotherapy in two clinical trials (Diehl, Thomas and Re, 2004). Disease status is the most important factor in predicting outcome of patients scheduled to receive high-dose chemotherapy and autologous stem cell transplantation (Sweetenham *et al.*, 1997; Crump *et al.*, 1993).

### **1.3.2 Recent advances in HL therapy**

Bartlett *et al.*, (1995) developed a seven-drug regimen, Stanford V (mechlorethamine, doxorubicin, vinblastine, vincristine, bleomycin, etoposide, prednisone, and granulocyte colony-stimulating factor) that was given on a weekly alternating basis for a total of 12 weeks in combination with radiotherapy for advanced stage disease. The alternation and extended time frame was such that the cumulative total dose for each drug was minimised, therefore resulting in a low toxicity profile but yet maintaining optimal efficacy for chemotherapy. A phase II clinical trial showed the 5-year freedom from progression was 89 % and the overall survival was 96 % (Horning *et al.*, 2002). Importantly, few mid-term toxic effects were reported and fertility could be preserved in both men and women (Horning *et al.*, 2002).

An increased dose of the BEACOPP regimen, developed by the German Hodgkin's Study group, is considerably superior to COPP/ABVD for primary progression and freedom from treatment failure (Diehl *et al.*, 2003). This therapy results in a 10–20 % higher freedom-from-progression rate and an overall survival benefit of about 8 % over ABVD or C(M)OPP/ABVD at 5 years. However, increased short-term and long-term toxicities were documented in the group undergoing increased dose BEACOPP regimen (secondary leukemia/infertility). Presently, whether BEACOPP when given with partial increased doses is superior to ABVD is the subject of an ongoing international trial.

A marginally less intense hybrid than the BEACOPP regimen comprising chlorambucil, vinblastine, procarbazine, and prednisolone with etoposide, vincristine, and doxorubicin (ChIVPP/EVA) has been used in the United Kingdom. It seems to provide similar levels of disease control to BEACOPP but without the same leukemia incidence (Radford *et al.*, 2002) but does result in permanent azoospermia in a high proportion of men (Clark *et al.*, 1995).

Radford *et al.*, (2002), compared the abbreviated, 11-week chemotherapy regimen vincristine, doxorubicin, prednisolone, etoposide, cyclophosphamide, and bleomycin (VAPEC-B) with ChIVPP/EVA plus radiotherapy for previous bulky disease or residual disease. Freedom from progression, event-free survival, and overall survival were significantly superior with ChIVPP/EVA than with VAPEC-B.

Tumour immunotherapy has been the focus of intense research into more targeted HL therapy in recent times. H/RS cells specifically express CD30 antigen and experimental therapeutics with antibody-based regimens targeting malignant cells are currently being

investigated. SGN-30, a monoclonal antibody (mAb) with activity against CD30+ malignancies (Wahl *et al.*, 2002), is currently in phase II clinical evaluation for treatment of HL. Cerveny *et al.*, 2005, have shown that signaling via the anti-CD30 mAb SGN-30 sensitises HL cells to conventional chemotherapeutics. A fully human monoclonal anti-CD30 antibody (5F11, also known as MDX-060), developed by Borchmann *et al.*, (2003), has been shown in combination with conventional chemotoxic agents to enhance efficacy in killing a variety of lymphoma cell lines (Heuck *et al.*, 2004). A phase I/II clinical trial with 5F11 in patients with relapsed HL is underway and is showing promising results (Ansell *et al.*, 2003).

Bortezomib (PS-341), is a reversible inhibitor of the 26S proteasome, one of a novel class of chemotherapeutic agents that has been FDA-approved for the treatment of multiple myeloma in adults (Voorhees *et al.*, 2003) and is being tested as a chemosensitiser in a variety of adult solid tumor and hematologic malignancies. It interferes with the degradation of a variety of proteins including  $\text{I}\kappa\text{B}\alpha$ , leading to less nuclear factor- $\kappa\text{B}$  (NF- $\kappa\text{B}$ ) and increased apoptosis. Clinical trials have recently been proposed to explore the use of bortezomib as a chemosensitising agent in HL.

Potential therapies meriting further study include, the anti-CD25 ricin A-chain immunotoxin (Engert *et al.*, 1997), anti-CD16/CD30 bispecific antibodies (Hartmann *et al.*, 1997) and infusion of cytotoxic T cells specific for EBV (Heslop *et al.*, 1996). These emerging experimental strategies may be used in combination with chemotherapy as future treatment and could be effective in a setting of minimum residual disease induced by high-dose chemotherapy.

Thanks to the advances in effective treatment, HL has become a highly curable disease over the last few decades because of the introduction of efficient polychemotherapy and the use of risk-adapted reduced (dose and field size) radiotherapy. In summary, ABVD remains the standard treatment for advanced HL, given the event free survival and overall survival results, and the better toxicity profile, including late effects. An improvement in overall survival is unlikely to show in future study generations because of already excellent long-term results obtained with combined modality treatment (i.e., a 10-year overall survival of about 95 %) (Diehl, Thomas and Re, 2004).

However, long-term toxic effects are a major concern in HL-cured patients, who are usually very young at diagnosis and show a high probability of cure of their disease (Table 1-2). The main challenge in the near future will be the development of strategies

that decrease late morbidity and mortality but retain the same efficacy of current regimens (Diehl, Thomas and Re, 2004).

The anti-apoptotic phenotype is one of the hallmarks of H/RS cells of cHL. It might, therefore, be promising to target molecules that mediate apoptotic resistance using small molecules or antisense molecules. More targeted treatment of deregulated genes may permit the use of reduced-dose chemotherapy with less adverse treatment sequelae. The expression and role of the anti-apoptotic *bfl-1* gene has been examined in H/RS cells of cHL in this study, with a view to establishing the therapeutic potential of this gene and addressing the aforementioned therapeutic challenge.

**Table 1-2 Long-terms toxic effects after treatment for HL**

Effects	Description
Minor	Endocrine dysfunctions (hypothyroidism, hypo-amenorrhea, decreased libido). Long-term immunosuppression. Viral Infections (Herpes simplex, Varziella zoster, papillomaviruses, warts viruses).
Serious	Lung fibrosis from radiation plus bleomycin. Myocardial damage from anthracyclines and radiation. Sterility in men and women. Growth abnormalities in children and adolescents. Opportunistic infections. Psychological problems. Psychosocial disturbances. Fatigue.
Potentially fatal	Acute myeloid leukaemia/myelodysplastic syndrome. Non-Hodgkin lymphomas. Solid tumours (lung, breast, and colon cancer, sarcomas). Overwhelming bacterial sepsis after splenectomy or spleen irradiation (OPSI).

Adapted from Diehl, Thomas and Re, 2004.

#### 1.4 Molecular origins of H/RS cells and immunopathogenesis

The normal cellular counterpart of the H/RS cell has long been enigmatic due to the promiscuous expression in H/RS cells of markers that are normally expressed in distinct

hematopoietic lineages (Staudt, 2000). H/RS cells can variably express T cell markers (CD2, CD4, granzyme B), B cell markers (CD19, CD20), and myeloid markers (CD15, c-fms) (Staudt, 2000).

Single-cell PCR studies have shown that in the vast majority of cHL cases and in all cases of LPHL subtype, the neoplastic cells (H/RS cells and L&H cells respectively) carry clonal Ig heavy and light chain gene rearrangements, providing strong evidence for both the clonal nature and the B-lymphoid derivation of the malignant population. Analysis of this DNA also demonstrated that rearranged Ig genes in HL L&H and H/RS cells have been targets of the somatic hypermutation (SHM) process, implying that HL originates from neoplastic transformation of a germinal centre (GC) B cell because mutations are introduced into Ig genes during this particular developmental stage of the B-cell (Figure 1.3) (Kanzler *et al.*, 1996). The data presented by Marafioti *et al.*, (2000), indicate that HL is in nearly all cases<sup>1</sup>, irrespective of phenotype and EBV infection, a B-cell-derived lymphoproliferative disorder and that the H/RS cells with rearranged Ig genes represent without any exception a clonal outgrowth of a single transformed B cell. Recent findings of Bai *et al.*, (2006), indicate that H/RS cells in most cHL (82 %) display bcl6/CD10/MUM1/CD138 immunophenotypes consistent with late GC/early post-GC or post-GC B-cell differentiation.

Although H/RS cells are usually transformed B cells, global gene expression analysis of H/RS cell lines using microarrays revealed that these cells have lost the expression of most B-cell markers to an extent that is unique among B-cell lymphomas (Schwering *et al.*, 2003). H/RS cells do not express functional B cell receptor (BCR) (Figure 1.3) either because of non-functional V<sub>H</sub> gene re-arrangements or because of loss of transcription factors necessary for Ig transcription (Kanzler *et al.*, 1996; Marafioti *et al.*, 2000; Re *et al.*, 2001a and b) but have acquired the capacity to survive loss of BCR expression, an event that would otherwise invariably lead to death by apoptosis of a GC B cell (Jungnickel *et al.*, 2000).

In EBV-positive cases of HL, the latent membrane protein LMP2a is expressed, which harbours a cytoplasmatic motif that is also found in the coreceptors of the BCR and that mediates signaling of cross-linked BCR. It has been speculated that LMP2a may replace the survival signal of the BCR in GC B cells acquiring destructive Ig V gene mutations. Bechtel *et al.*, (2005), tested the capability of EBV to rescue BCR-deficient human GC B cells from apoptosis. GC B cells were infected *in vitro* with EBV to establish

---

<sup>1</sup> In rare cases (about 2%) H/RS cells originate from T cells (Muschen *et al.*, 2000; Seitz *et al.*, 2000).

lymphoblastoid cell lines, several of which carried destructive mutations rendering originally functional Ig V gene rearrangements non-functional. Normally, these destructive mutations would have caused rapid cell death but EBV rescued these BCR-deficient GC B cells from apoptosis.

Surprisingly, L&H cells differed markedly from H/RS cells in that they consistently expressed typical B-lineage markers, such as CD20 or the BCR, placing LPHL disease in this distinct stage of B-cell maturation (Figure 1.3).

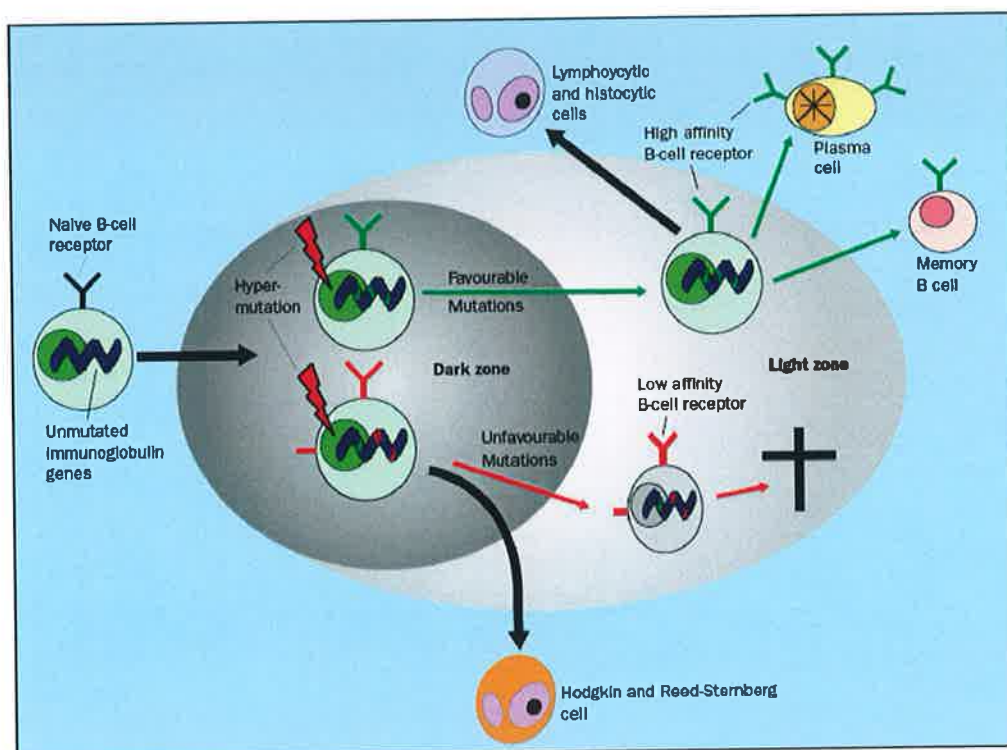


**Figure 1.3 The GC derivation of H/RS cells in cHL and L&H cells in LPHL**

Clonal rearranged Ig genes were amplified from single H/RS cells that had been micromanipulated from primary HL biopsy specimens (Kuppers *et al.*, 1994). The detection of somatic mutations within the rearranged Ig genes implied a GC or post-GC B cell to be the precursor of H/RS cells, because mutations are introduced into Ig genes during this particular developmental stage of the B-cell (Kanzler *et al.*, 1996). Because selection for antigen is a hallmark of the GC, the precursor of the H/RS cells was defined as a pre-apoptotic GC B cell that by acquiring selection advantages by yet undetermined mechanisms, had escaped the negative selection. LPHL showed clonal Ig gene rearrangements with ongoing mutations, defining a mutating GC B-cell clone with signs of selection for antigen as the putative precursor of L&H cells (Kuppers *et al.*, 1994; Braeuninger *et al.*, 1997; Marafioti *et al.*, 1997). A hallmark of the GC reaction is the process of hypermutation resulting in a large number of somatic mutations in the

rearranged Ig genes of B cells in the dark zone of the GC in order to increase antibody affinity (Rajewsky, 1996). The hypermutation process precedes negative selection of B cells in the light zone of the GC that have acquired unfavourable mutations in their Ig genes leading to the expression of a low-affinity, truncated, or autoreactive BCR. In a physiological immune reaction, B cells that display such unfavourable features are efficiently eliminated by fatty acid synthase (FAS)-mediated apoptosis. Adapted from Thomas *et al.*, 2004a.

#### **1.4.2 H/RS cells evade apoptotic cell death and lead to systemic lymphoma**

H/RS cells express CD95 (Fas) and other tumour necrosis factor receptor (TNFR) family members such as TNFR1, TRAIL-R1 and TRAIL-R2, which carry death domains (DDs) and can induce apoptosis by caspase activation (Maggio *et al.*, 2003; Xerri *et al.*, 1995). In the B-cell lineage, *FAS* gene expression peaks at the GC stage (Martinez-Valdez *et al.*, 1996). B cells with self reactive or low affinity antibody die by Fas-mediated apoptosis, whereas cells that express Ig with increased affinity for the corresponding antigen are stimulated to proliferate and exit the GC as memory B cells or plasma cells (Figure 1.3) (Rajewsky, 1996).

H/RS cells have been shown to be resistant to cell death-induction via CD95 activation *in vitro* (Re *et al.*, 2000), evidence that the CD95 death-signaling pathway must be interrupted in H/RS cells. In the GC, cellular FAS associated DD-like IL-1 $\beta$ -converting enzyme (FLICE) inhibitory protein (c-FLIP), a proximal negative regulator of the CD95-induced death program, is normally restricted to B cells that display high-affinity and non-self reactive BCRs. However, c-FLIP is expressed at high levels in H/RS cells (Maggio *et al.*, 2003; Dutton *et al.*, 2004) and its knockdown results in a sensitisation of HL-derived cell lines to CD95-induced apoptosis, implying that c-FLIP plays a central role in preventing CD95-mediated apoptosis of H/RS cells (illustrated in Figure 1.4 and Figure 1.9) (Dutton *et al.*, 2004; Mathas *et al.*, 2004). Thus, c-FLIP expression by H/RS cells represents the illegitimate use of an anti-apoptotic gene (Thomas *et al.*, 2004a).

Lineage promiscuity may also prevent killing of the H/RS cell in the hostile environment of the GC. H/RS cells hide from immunological surveillance by displaying many non-GC B-lineage features specific for various other cell types, such as CD15 (granulocytes), CD30, perforin (T cells), syndecan (post-GC B cells), fascin, restin, and

TARC (dendritic cells) (Foss *et al.*, 1996; Carbone *et al.*, 1997; Pinkus *et al.*, 1997; Delabie *et al.*, 1992; van den Berg *et al.*, 1999). Bai *et al.*, (2006), showed that the typical GC B-cell-like immunophenotype, which is characterised by the coexpression of bcl6 and CD10 proteins, was not detected in a study of 101 cHL cases.

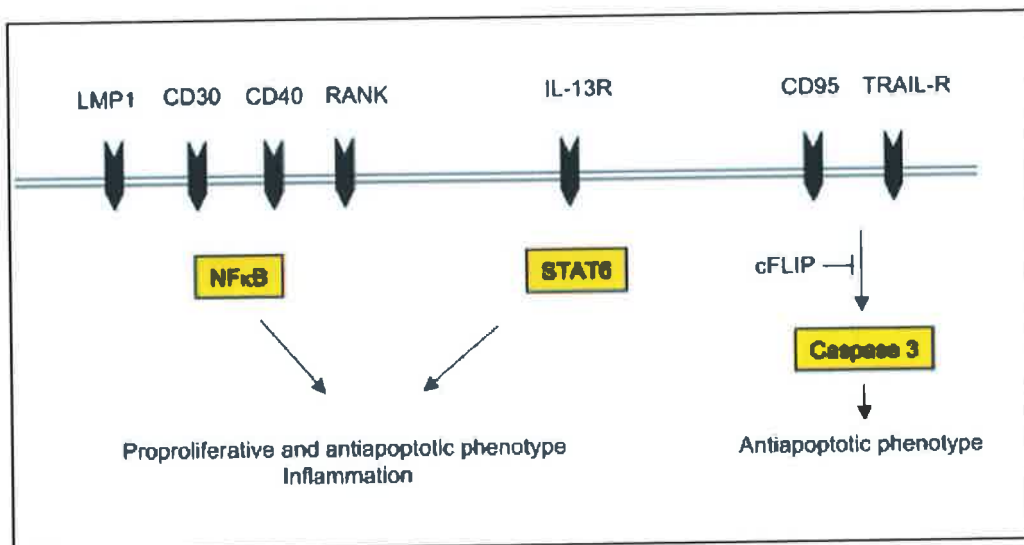


**Figure 1.4 Cell-surface receptors and their respective intracellular mediators induce the proproliferative and anti-apoptotic phenotype of H/RS cells.**

Up to 99 % of the cells in the involved HL tissue are immune cells. Attracted immune cells influence the H/RS cell phenotype as they provide survival signals, examples are endothelial smooth muscle cells, eosinophils, and T cells that engage CD30, RANK and CD40 receptors on H/RS cells, respectively. Binding of members of the TNF receptor (TNFR) family results in NF- $\kappa$ B activation by signaling via TRAF molecules, TRAF1 (Rodig *et al.*, 2005) and TRAF2 (Horie *et al.*, 2002a) being expressed and cytoplasmatically aggregated in H/RS cells, and also via the mitogen activated protein kinase (MAPK) pathway (Zheng *et al.*, 2003). In contrast to TNFR signaling, cytokine signaling, such as that stimulated via IL-13R is mediated by signal transducer and activator of transcription (STAT) molecules. Transcriptional deregulation and aberrant signaling via cell-surface receptors contribute to the proproliferative and anti-apoptotic phenotype of H/RS cells. H/RS cells lack expression of functional BCRs on the cell surface (Marafioti *et al.*, 2000) and thus are supposed to die within the GC reaction of the lymph node by induction of the CD95 pathway (Rajewsky *et al.*, 1996). Nevertheless, H/RS cells are resistant to CD95-mediated cell death (Re *et al.*, 2000), probably due to the constitutive expression of the anti-apoptotic protein cFLIP (Thomas *et al.*, 2002a). Besides CD95, other TNFR family members such as tumour necrosis factor receptor 1 (TNFR1) and TNF-related apoptosis inducing ligand receptor 1 (TRAIL-R1) and TRAIL-R2 are also expressed in H/RS cells (Mathas *et al.*, 2004). TNFR1 activation induces the extrinsic pathway, while binding of TRAIL receptors induces both the extrinsic and the intrinsic apoptotic pathway under physiologic circumstances. In H/RS cells, cFLIP expression inhibits proper TRAIL-induced signal

transduction similar to the inhibition of CD95, and TRAIL sensitivity could be restored by downregulation of cFLIP (Mathas *et al.*, 2004). Adapted from Re *et al.*, 2005.

### 1.4.3 Neoplastic transformation of the progenitor

As discussed above, H/RS cells would normally have died by apoptosis within the GC but seem to have been rescued by a neoplastic transformation event. Several reports suggest the transcription factor NF- $\kappa$ B is a central effector of malignant transformation in cHL. Genetic alterations have been described that may lead to constitutive NF- $\kappa$ B activity in H/RS cells (Cabannes *et al.*, 1999; Emmerich *et al.*, 1999; Emmerich *et al.*, 2003; Jungnickel *et al.*, 2000), the consequences of which are discussed in detail in Section 1.5.2.

Several recurrent chromosomal aberrations have been described (e.g. gains of 2p and 9p). Recurrent imbalances were also shown on 6q25 in about 79 % primary cases of cHL (Re *et al.*, 2003). Joos *et al.*, (2000), used comparative genomic hybridisation to reveal recurrent gains on chromosomes 2p, 9p, and 12q in primary H/RS cells substantiating the opinion that chromosomal instability is a typical feature of cHL. Specifically, 2p turned out to be recurrently affected by genomic imbalances, involving the *REL* and *BCL11a* loci on 2p13-16 (Joos *et al.*, 2002; Martin-Subero *et al.*, 2002), providing mechanistic explanations for the constitutive activation of both STATs (Section 1.5.3) and NF- $\kappa$ B.

Aberrant activation of other signaling pathways is a feature of H/RS cells and is discussed in detail in Section 1.5. As outlined above, events inactivating the FAS pathway allow the H/RS cell to evade an apoptotic destiny such as cFLIP or inherited *FAS* gene mutations that seem to be specific for this cancer entity (Straus *et al.*, 2001).

Also, for a large fraction of cases, infection of H/RS-cell precursors with EBV is an important pathogenetic event (30-50 % of cHL cases are EBV-positive). EBV has been shown to have an important role in HL tumourigenesis, at least in part by leading to NF- $\kappa$ B activation (discussed in more detail in Section 1.6). There are also recent indications that the tranfusion transmitted (TT) virus may be involved in HL pathogenesis. zur Hausen *et al.*, (2005), found that persistent infections with TT virus-like agents increased the risk for specific chromosomal translocations contributing to the conversion to a malignant phenotype.

## 1.5 Transcriptional control and aberrant activation of signaling pathways in HL

In cHL, DNA sequence changes include mainly  $I\kappa B\alpha$  mutations found in at least one third of cases, whereas mutations affecting *n-ras*, protein 53 (*p53*), or *CD95* were not detected in a significant proportion (Thomas *et al.*, 2004a). NF- $\kappa$ B, first described to be constitutively upregulated in HL in 1996 (Bargou *et al.*, 1996), is tightly regulated by binding to inhibitory  $I\kappa B\alpha$  molecules. Mechanistic explanations of NF $\kappa$ B up-regulation in H/RS cells are listed in Table 1-3.

Activator protein 1 (AP-1) has been shown to be aberrantly up-regulated in H/RS cells, mediating some of the proproliferative and anti-apoptotic characteristics of H/RS cells partly in concert with NF- $\kappa$ B (Mathas *et al.*, 2002) (Table 1-3). In contrast, typical Ig specific transcription factors such as Oct2, Bob1, and PU.1 (Re *et al.*, 2001a; Stein *et al.*, 2001b; Torlakovic *et al.*, 2001) are down-regulated in H/RS cells.

In normal cells the activation of most signaling pathways is transient and tightly regulated. However, in H/RS cells several signaling molecules and pathways, listed in Table 1-3, are aberrantly activated and experimental inhibition of several of these signaling modules revealed the importance of such constitutive activation for H/RS-cell survival and proliferation. The principal transduction pathways will now be discussed in turn.

**Table 1-3 Signaling pathways and transcription factors constitutively active in H/RS cells**

Pathway	Proposed effect of activation	Mechanisms of activation
NF- $\kappa$ B Section 1.5.2	Inhibits apoptosis; supports proliferation; recruits T cells to lymphoma; promotes dissemination.	Mutations in $I\kappa B\alpha$ ; mutations in $I\kappa B\epsilon$ genomic c-Rel amplifications; CD40 stimulation by CD40 ligand expressing T cells; CD30 stimulation; ligand independent or via CD30 ligand expressing T cells; LMP1 <sup>1</sup> mimicry of active CD40 in EBV-positive cases (Figure 1.4).
JAK-STAT Section 1.5.3	Supports proliferation; promotes survival.	Autocrine stimulation via IL-13/IL-13R (Figure 1.4).
MAPK/ERK Section 1.5.4	Supports proliferation; inhibits apoptosis.	CD30-, CD40-, RANK-signaling; RTK signaling?

AP-1	Supports proliferation.	Autoregulation of c-Jun; NF-κB activation of JunB.
Section 1.5.5		
PI3K/AKT	Promotes survival.	CD40 signaling?; LMP1 and LMP2a in EBV-positive cases; RTK signaling?
Section 1.5.6		
Notch1	Induces proliferation; inhibits apoptosis; downregulates B-cell phenotype?	Expression of ligand Jagged1 in H/RS cells and surrounding cells.
Section 1.5.7		
Receptor tyrosine kinases <sup>2</sup>	Supports proliferation; others?	Autocrine or paracrine stimulation through ligands; no indication for mutations.
Section 1.5.8		

<sup>1</sup>LMP1 (EBV latent membrane protein 1), <sup>2</sup>PDGFRA (platelet-derived growth factor receptor A), DDR2 (discoidin receptor family, member 2), EPHB1 (ephrin receptor EphB1), RON, TRKB (tyrosine kinase receptor B), TRKA (tyrosine kinase receptor A) and MET. Adapted from Brauninger *et al.*, 2006.

### 1.5.2 Constitutive NF-κB activation in HL

NF-κB/Rel is a structurally and evolutionary conserved family of transcription factors sharing a 300 amino acid domain named the Rel homology domain (RHD) which is required for DNA-binding, dimerisation, nuclear translocation and binding to the so called inhibitory IκB proteins (Hayden and Ghosh, 2004). The term NF-κB collectively refers to the class of dimeric transcription factors comprising p65 (RelA), c-Rel (Rel), RelB, p50 and p52 and since its discovery nearly 20 years ago, NF-κB has emerged as one of the most studied transcription factors in mammals. Transcription factors of the NF-κB family are crucial for the control of the immune response to viral/bacterial infection and stress-inducing agents, exposure to pro-inflammatory cytokines, mitogens and growth factors, and are involved in the regulation of cell proliferation and survival (Figure 1.5) (Foo and Nolan, 1999; Karin and Ben-Neriah, 2000). Different stimuli for NF-κB activation initiate different signal transduction pathways that involve distinct scaffolding and signaling proteins which include NF-κB-inducing kinase (NIK), mitogen-activated protein kinase/extracellular signal regulated kinase kinase 1 (MEKK1), interleukin (IL)-1-receptor-associated kinases (IRAKs), TNFR-associated factors (TRAFs), double-stranded (ds) RNA-dependent protein kinase (PKR), protein

kinase C (PKC) and transforming growth factor- $\beta$  (TGF- $\beta$ )-activated kinase (TAK1) (Silverman and Maniatis, 2001).

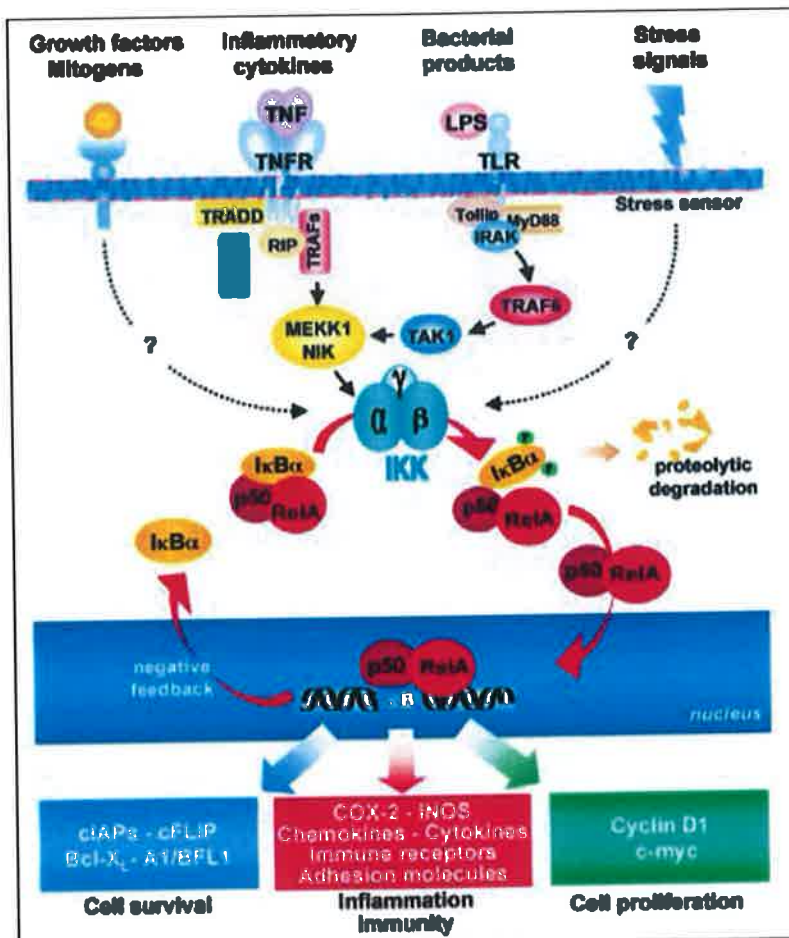


**Figure 1.5 Activation and downstream effects of the canonical NF-κB pathway**

NF-κB heterodimers (p50/RelA) are sequestered in the cytoplasm by I $\kappa$ B inhibitory proteins (I $\kappa$ B $\alpha$ ). Stimulation by stress-inducing agents, or exposure to inflammatory cytokines, mitogens or a diverse array of bacterial and viral pathogens leads to the activation of signaling cascades converging on the IKK complex. Phosphorylation of I $\kappa$ B $\alpha$  by activated IKK is a signal for its ubiquitylation and proteasome-dependent degradation. Freed NF-κB dimers translocate to the nucleus where they bind to κB elements and activate the transcription of a variety of genes involved in the control of cell proliferation and survival, in the inflammatory and immune response, as well as autoregulatory genes, including I $\kappa$ B $\alpha$  itself. In the non-canonical pathway (not shown), the p100-RelB complex is activated by phosphorylation of the C-terminal region of p100 by an IKK $\alpha$  homodimer (lacking IKK $\gamma$ ), which leads to ubiquitination followed by degradation of the p100 I $\kappa$ B-like C-terminal sequences to generate p52-RelB. Adapted from Santoro, Rossi and Amici, 2003.

The rapid and transient activation of NF-κB complexes (e.g. p50/p65), in response to the wide range of stimuli mentioned above including pro-inflammatory cytokines (TNF $\alpha$ , IL-1 $\beta$ , IL-6, CD40L), DNA damaging agents (camptothecin, daunomycin) and Toll-like receptors (TLRs) agonists or viruses (HTLV1, EBV) is generally regulated by the classical NF-κB pathway (or canonical pathway) (Pahl, 1999).

IκB proteins (IκB $\alpha$ , IκB $\beta$ , IκB $\epsilon$ , p105, and p100) retain NF-κB in an inactive form in the cytoplasm. Following stimulation by activating agents, IκB $\alpha$  is rapidly phosphorylated at two serine residues (Ser-32 and Ser-36) by the IκB kinase (IKK) complex. IKK $\alpha$  and IKK $\beta$  are the two catalytic subunits of the IKK complex and two additional molecules, IKK $\gamma$ /NEMO and IKAP, have been described as further integral members (Krappmann *et al.*, 2000). Phosphorylated IκB $\alpha$  is then a substrate for ubiquitin ligases that catalyse the addition of ubiquitin groups to IκB $\alpha$ ; this modification then targets IκB $\alpha$  for degradation by the 26-S proteasome. Degradation of IκB $\alpha$  releases active NF-κB, which translocates to the nucleus where it binds to its target DNA sequence (GGGRNNYYCC) and activates the transcription of a vast number and wide range of gene target promoters. However, this activation is only short-lived as NF-κB stimulates transcription of the IκB $\alpha$  gene leading to a rapid replenishment of the inhibitor, which enters the nucleus and binds to NF-κB dimers causing their disassociation from target gene promoters. The cytoplasmic pool of inducible NF-κB is restored and NF-κB-dependent transcription returns to basal levels.

When NF-κB is found persistently in the nucleus, it is referred to as constitutive activation. Constitutively activated NF-κB has been associated with increased cell proliferation and survival in several cancers of lymphoid or myeloid origin, including multiple myeloma, HL and some non-Hodgkin lymphomas (NHL) and may be linked to drug resistance in these cells (Bargou *et al.*, 1997; Nakshatri *et al.*, 1997; Giri and Aggarwal, 1998). HL was the first hematopoietic tumour from which an aberrant constitutive NF-κB activation was described (Hinz *et al.*, 2002). Constitutive NF-κB is almost universal in HL, has proliferative and anti-apoptotic roles in H/RS cells and can be caused by multiple defects in this system.

High levels of IκB $\alpha$  are also a highly characteristic feature of cultured and primary H/RS cells. Because NF-κB activates transcription of its own inhibitor, this finding reflects the high transcriptional activity of NF-κB in this lymphoid malignancy (Emmerich *et al.*, 1999). The paradoxical finding of high NF-κB activity despite the strong expression of its inhibitor indicates that the NF-κB/IκB $\alpha$  system is severely

deregulated in H/RS cells (Emmerich *et al.*, 1999). Point mutations in the I $\kappa$ B $\alpha$  gene, producing non-functional or unstable I $\kappa$ B $\alpha$  proteins are recurrent molecular abnormalities of H/RS cell lines (Hinz *et al.*, 2002). The analysis of 7 HL-derived cell lines showed mutations in the I $\kappa$ B $\alpha$  gene in 2 cell lines: L428 and KMH2, which lead to C-terminally truncated proteins (Emmerich *et al.*, 1999). In both cases the mutant I $\kappa$ B $\alpha$  proteins are too small to contain the complete ankyrin repeat domain, neither form of I $\kappa$ B $\alpha$  is able to block translocation and DNA binding activity of NF- $\kappa$ B (Krappmann *et al.*, 1999). The 5 remaining HD-derived cell lines (L540, L591, L1236, HD-LM2, and HD-MyZ) showed expression of full-length I $\kappa$ B $\alpha$  proteins of 38 kDa (Emmerich *et al.*, 1999). In other cells it is thought that a soluble factor secreted by H/RS cells can trigger NF- $\kappa$ B activation. H/RS cells produce and secrete inflammatory cytokines that are potentially able to activate NF- $\kappa$ B. This was seen when growth medium of H/RS cells, when added to Reh cells (which lack constitutive NF- $\kappa$ B) transiently activated NF- $\kappa$ B (Krappmann *et al.*, 1999).

As illustrated in Figure 1.4, other mechanistic explanations of NF- $\kappa$ B up-regulation in H/RS cells include gene amplification of c-rel (Joos *et al.*, 2002); ligand-mediated and ligand-independent activation of cell-surface receptors such as CD30 (Horie *et al.*, 2002b), CD40 (Annunziata *et al.*, 2000; Gruss *et al.*, 1997), receptor activator of NF- $\kappa$ B (RANK) (Fiumara *et al.*, 2001), or Notch1 (Jundt *et al.*, 2002) or EBV-encoded LMP1 (Gires *et al.*, 1997) or LMP2A (Caldwell *et al.*, 1998) expression in EBV-positive cases.

Using a dominant negative inhibitor of NF- $\kappa$ B stably introduced into H/RS cell lines, constitutive NF- $\kappa$ B-RelA activation has been shown to be essential for both proliferation and survival of HL tumour cells (Bargou *et al.*, 1997). This dominant negative inhibitor, I $\kappa$ B $\alpha\Delta N$ , is able to bind to NF- $\kappa$ B upon cellular stimulation since it lacks serine and tyrosine residues required for signal-dependent activation (Bargou *et al.*, 1997), thereby blocking NF- $\kappa$ B nuclear activity.

Constitutive NF- $\kappa$ B activity regulates the expression of genes typically overexpressed by H/RS cells, including the cell cycle regulatory protein cyclin D2, anti-apoptotic proteins c-IAP2, TRAF1 and Bcl-xL and the cell surface receptors CD40 and CD86 (Hinz *et al.*, 2002).

### **1.5.3 STAT Family of transcription Factors**

STATs are key mediators of cytokine signaling and their perturbation contributes to various human diseases (Cochet *et al.*, 2006). Cytokine-receptor binding leads to activation of JAK and a subsequent activation of STATs by tyrosine phosphorylation. Upon phosphorylation, STATs translocate to the nucleus as homo- and hetero-dimers where they bind to specific DNA elements within the promoter region of target genes, thereby activating transcription. Seven STAT family members have been identified to date (STAT 1-4, 5a/b and 6).

STAT 6 is an important autocrine growth factor in cHL, activated primarily by IL-4 and IL-13 (reviewed in Wurster, Tanaka and Grusby, 2000), its expression has been detected in all H/RS cell lines and 78 % of primary H/RS cells (95 % in NSHL) (Skinnider *et al.*, 2002b). A wide range of cytokines activate STAT 3, including the IL-6 family of cytokines, IL-10, IL-2, IL-7, IL-9 and IL-15 (Leonard and O'Shea, 1998). Also, EBV LMP-1 and CD40 engagement can lead to STAT 3 activation (Hanessian and Geha, 1997; Gires *et al.*, 1999). Several of these activators are commonly expressed in cHL and constitutive activation of STAT3 has been demonstrated in 5 out of 6 H/RS cell lines and 87 % of primary H/RS cells (Kube *et al.*, 2001). STAT 5a is activated by several cytokines including IL-2, IL-3, IL-4, IL-7, IL-9 and IL-15. Hinz *et al.*, (2002), reported high-level STAT 5a expression as a feature of all H/RS cell lines.

Kube *et al.*, (2001), have shown that constitutively activated STAT3 in the HL cell line L428 could be inhibited by the tryphostin AG490 and inhibited spontaneous growth of HL tumour cells. AG490 is a tyrosine kinase inhibitor that inhibits Jak2 and perhaps other kinases. Cochet *et al.*, (2006), demonstrated constitutive activation of STAT1 proteins in the HDLM-2 and L540 HL-derived cell lines. Interestingly, *bfl-1* was shown in the Cochet study to be one of a number of target genes of STAT proteins, and inhibition of constitutive STAT activation led to apoptosis in HL-derived cell lines (Cochet *et al.*, 2006).

### **1.5.4 MAPK Signaling**

The mitogen activated protein kinase (MAPK) family, consisting of the extracellular signal regulated protein kinase (Section 1.5.4.1), c-Jun amino terminal MAPK (Section 1.5.4.2) and p38 subfamilies, is implicated in diverse cellular processes including cell

growth, migration, proliferation, differentiation, survival and development (Johnson *et al.*, 2005; Bogoyevitch and Court, 2004; Roux and Blenis, 2004). MAPKs transmit signals in the form of sequential phosphorylation events. The phospho-relay system is composed of three kinases: a MAPK kinase kinase (MAPKKK), a MAPK kinase (MAPKK) and a MAPK. Phosphorylation of the MAPKs occurs at a conserved dual-phosphorylation domain (Thr-Xxx-Tyr) and leads to activation of the protein and the subsequent formation of dimers, which translocate to the nucleus to activate downstream targets (Krens, Spaink and Snaar-Jagalska, 2006). Extensive work by several groups has established that MAP kinase pathways play critical roles in the pathogenesis of various hematological malignancies (Staber *et al.*, 2004; Kerr *et al.*, 2003; James *et al.*, 2003).

#### 1.5.4.1 ERK1/2 MAP kinase

Extracellular signal regulated kinase (ERK) MAP kinase signaling pathway is among the key mechanisms that transmit signals from the cell surface to the nucleus (Torii *et al.*, 2006). ERK1, also known as MAPK3 or p44MAPK was the first identified MAPK (Boulton *et al.*, 1990) while ERK2 is also known as MAPK1 or p42MAPK. After stimulation by a variety of mitogens including peptide growth factors, MAP/ERK kinase 1 (MEK1) and MEK2 (referred to as MEK1/2) is activated by MAPKKK-mediated phosphorylation. MEK1/2 then phosphorylates threonine and tyrosine residues in the Thr–Glu–Tyr (TEY) sequence of ERK1/2, resulting in the activation of ERK1/2. MAPK/ERK kinase (MEKK) 1, 2 and 3 are involved in NF- $\kappa$ B activation initiation (Yang *et al.*, 2001; Zhao and Lee 1999; Mercurio *et al.*, 1997).

The ERK1/2 pathway is implicated in the proliferation of tumour cells (Chang *et al.*, 2003; Dent and Grant, 2001). Zheng *et al.*, (2003), reported that MEK/ERK pathway is aberrantly active in cultured and primary HL cells. They showed that inhibition of the MEK/ERK lead to decreased levels of Bcl-2 and Mcl-1 and induced G<sub>2</sub>M cell-cycle arrest or apoptosis in HL cell lines, pointing to an important role in the regulation of H/RS-cell survival and proliferation. They also showed that activating CD30, CD40 and RANK by their respective ligands activates MEK/ERK pathways in H/RS cells and inhibition of this pathway by the small molecule UO126 induces cell death or cell-cycle arrest and potentiates the killing effect of APO2L/TRAIL and chemotherapy. Watanabe

*et al.*, 2005, also showed that ERK1/2 MAPK pathway is involved in CD30 promoter regulation in H/RS cells as highlighted in Figure 1.6.

#### 1.5.4.2 JNK signal transduction

Jun N-terminal kinase (JNK; also known as stress-activated protein kinase, SAPK) is activated in response to certain growth factors or stresses such as ultraviolet radiation. JNK, activated by upstream MAPK kinases, MKK7 and MKK4 (Weston and Davis, 2002; Tournier *et al.*, 2001; Davis, 2000) phosphorylates and activates its major substrate c-Jun as well as several other transcription factors and proteins required for cell survival, proliferation, transformation and cell death (Shaulian and Karin, 2002). Both JNK activation and c-Jun phosphorylation regulate cell growth, whereas sustained JNK and c-Jun activation following stress induces cell apoptosis, indicating that the role of JNK in cell survival and death is complex (Ip and Davis, 1998). A major target of the JNK signaling pathway is activation of the AP-1 transcriptional factor that is mediated in part by the phosphorylation of c-Jun and related molecules (Weston and Davis, 2002). In HL, Knecht *et al.*, 1999, reported that the JNK pathway is critically involved in the formation of RS cell morphology. CD30, a member of TNFR superfamily, which is overexpressed in H/RS cells (Al-Shamkhani, 2004) has been shown to activate JNK in H/RS cells (Zheng *et al.*, 2003) (Figure 1.6).

#### 1.5.5 AP-1

Transcription factor activator protein-1 (AP-1) is composed of homo- or heterodimers formed by related Jun (c-Jun, JunB, JunD), Fos (c-Fos, FosB, Fra-1, Fra-2) and ATF, CREB family proteins (Wagner, 2001). These proteins are rapidly and transiently transcribed in response to a number of extracellular signals, which trigger activation of JNK, ERK or p38 MAP kinase pathways (Karin *et al.*, 1997; Leppa and Bohmann, 1999). Expression of c-Fos, c-Jun, JunB and JunD in H/RS cell lines has been documented previously (Hsu *et al.*, 1992a; Gruss *et al.*, 1992; Cossman *et al.*, 1999). Mathas *et al.*, 2002, showed that constitutively activated AP-1 with robust c-Jun and JunB overexpression was found in all tumour cells of cHL. They demonstrated that AP-1 cooperates with NF-κB and stimulates the expression of the cell-cycle regulator cyclin

D2, proto-oncogene c-met and the lymphocyte homing receptor CCR7, which are all strongly expressed in H/RS cells. The results of Watanabe *et al.*, 2003, suggest that constitutively active JunB causes overexpression of the hallmark CD30 in H/RS cells through acting on the AP-1 site of the CD30 microsatellite sequence and relieving its suppressive activity on the Sp-1-derived core promoter. In a subsequent report, Watanabe *et al.*, 2005, suggest an autoregulatory mechanism by which levels of CD30 promoter activity are controlled by CD30-ERK1/2 MAPK signaling. CD30-ERK1/2 MAPK signals induce JunB expression that maintains high levels of the CD30 promoter in H/RS cells as illustrated in Figure 1.6.

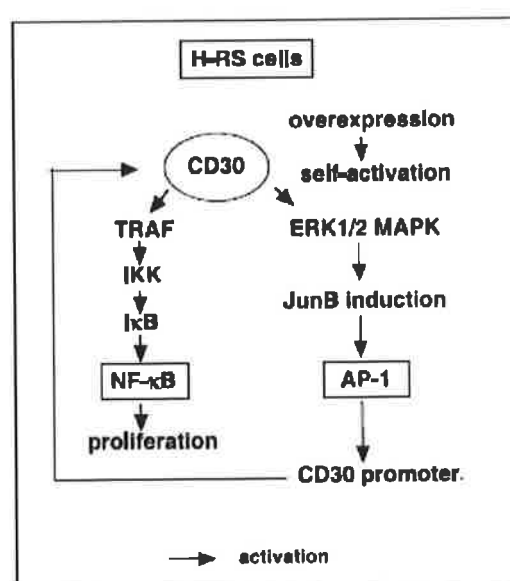


**Figure 1.6 Schematic view of CD30 signals and CD30 promoter induction by JunB in HL**

In H/RS cells, overexpressed CD30 activates the TRAF-I $\kappa$ B kinase (IKK)-I $\kappa$ B-NF- $\kappa$ B pathway. CD30-ERK1/2 MAPK-JunB-AP-1 is a TRAF-independent common pathway that stabilises overexpression of CD30 in H/RS cells. Adapted from Watanabe *et al.*, 2005.

### 1.5.6 PI3-K Signaling transduction

Phosphatidyl-inositide 3-kinase (PI3-K) plays an important role in a variety of biological processes, is involved in lymphocyte survival (Pogue *et al.*, 2000; Carey and Scott, 2001) and proliferation (Brennan *et al.*, 1997; Craddock *et al.*, 1999) and can be

activated by oncogenic Ras (Vanhaesebroeck and Alessi, 2000). In B cells, PI3-K is involved in several key signal transduction pathways such as CD40 and BCR signaling (Andjelic *et al.*, 2000; Aagaard-Tillery and Jelinek, 1996). PI3-K is constitutively activated in HL and contributes to the survival of HL cells (Dutton *et al.*, 2005) and inhibition of the PI3-K/Akt promotes G<sub>1</sub> cell cycle arrest and apoptosis in HL (Georgakis *et al.*, 2006).

### 1.5.7 Notch Signaling Pathway

The Notch family of transmembrane receptors control cell proliferation and differentiation in response to extracellular ligands expressed on neighbouring cells. The ligands that bind and activate Notch receptor belong to the DSL family, defined by the invertebrate ligands Delta, Serrate and LAG-2 (Henderson *et al.*, 1994; Mello *et al.*, 1994; Tax *et al.*, 1994). Four Notch genes, designated Notch1-Notch4 and five ligands, Jagged1 and Jagged2 and Delta-like 1 (DLL1), DLL3 and DLL4 have been identified in mammals to date. Although Notch and its ligands are often expressed on the same cell, it has been shown that Notch is activated primarily through binding to its ligands on adjacent cells (Jundt *et al.*, 2002).

Both the Notch receptor and its ligands have large extracellular domains that consist primarily of epidermal growth factor (EGF)-like repeats and Notch signaling activation, depicted in Figure 1.7, is mediated through interactions between the ligand DSL domain and the EGF repeats located in the extracellular portion of the Notch receptor. Ligand binding promotes two proteolytic cleavage events in the Notch receptor, firstly cleavage is catalysed by ADAM-family metalloproteases and the second event is mediated by a  $\gamma$ -secretase enzyme complex (Mumm and Kopan, 2000; Fortini, 2002; Selkoe and Kopan, 2003). The second cleavage releases the Notch intracellular domain (NotchIC), which then translocates to the nucleus and forms a trimeric complex with the DNA-binding protein CBF1/RBP-J $\kappa$  and its coactivator Mastermind (Mam). CBF-1/RBP-J $\kappa$  in the absence of NotchIC, binds the sequence CGTGGGAA and acts as a constitutive repressor by recruiting a corepressor complex, including SMRT or N-coR, SKIP, CIR, and class I or II histone deacetylases (Lai, 2002), as well as SHARP (Oswald *et al.*, 2002) and CtBP/CtIP (Oswald *et al.*, 2005). Notch binding to CBF-1/RBP-J $\kappa$  replaces the SMRT corepressor complex with a coactivator complex including SKIP, MAML1,

and histone acetyltransferases PCAF, GCN5, or p300 activating transcription of target genes (Miele, 2006).

Notch signaling is likely to regulate multiple aspects of lymphoid development and function (He and Pear, 2003). Bertrand *et al.*, (2000), found that Notch1 is expressed throughout human B cell development, Notch2 in the late pre-B cell compartment and Notch ligands Delta, in pro-B, early pre-B and late pre-B cells and Jagged-1, in bone marrow stromal cells. Notch activity emerges as a contributory factor to many cancers (Radtke and Raj, 2003). HL, anaplastic large-cell non-HL, some acute myeloid leukemias, B-cell chronic lymphoid leukemias, and multiple myeloma all show deregulated expression of Notch receptors or ligands (Tohda and Nara, 2001; Hubmann *et al.*, 2002; Jundt *et al.*, 2002; Nefedova *et al.*, 2004). Notch1 is aberrantly expressed in primary H/RS cells and H/RS cell lines and experimental activation of Notch1 showed that its signaling could contribute to proliferation and apoptosis resistance of H/RS cells (Jundt *et al.*, 2002).

Notch signaling has been implicated in the regulation of NF- $\kappa$ B (Guan *et al.*, 1996; Bash *et al.*, 1999 and Bellavia *et al.*, 2000). Antagonistic or synergistic connections between NF- $\kappa$ B and CBF1-mediated Notch signal transduction pathways have been reported (Guan *et al.*, 1996; Bash *et al.*, 1999; Wang *et al.*, 2001). Furthermore, it has been shown that basal expression of I $\kappa$ B $\alpha$  as a consequence NF- $\kappa$ B activity is under CBF1 control (Oakley *et al.*, 2003).

#### **1.5.7.1 EBNA2 and Notch-IC overlap in their functions and in their target genes**

Like NotchIC, EBV nuclear antigen 2 (EBNA2) trans-activates genes by interacting with RBP-J $\kappa$ /CBF1. Although there is no obvious sequence homology between these two proteins, they interact with similar regions of RBP-J $\kappa$ /CBF1 and replace repressor proteins with their trans-activation domains and also overlap in the range of functional activities and in the genes that they regulate. Both proteins have the ability to activate (i) the same RBP-J $\kappa$ /CBF1-regulated genes in reporter assays (Hofelmayr *et al.*, 1999), (ii) EBV latency promoters (with the exception of LMP1) (Strobl *et al.*, 2000) and (iii) effect expression of the same cellular genes such as BATF (Johansen *et al.*, 2003), CD21 (Strobl *et al.*, 2000) and Ig enhancer (Strobl *et al.*, 2000; Morimura *et al.*, 2001).

It has previously been shown in our laboratory and by others (Hsieh *et al.*, 1996) that EBNA2 is a more potent transactivator than NotchIC.

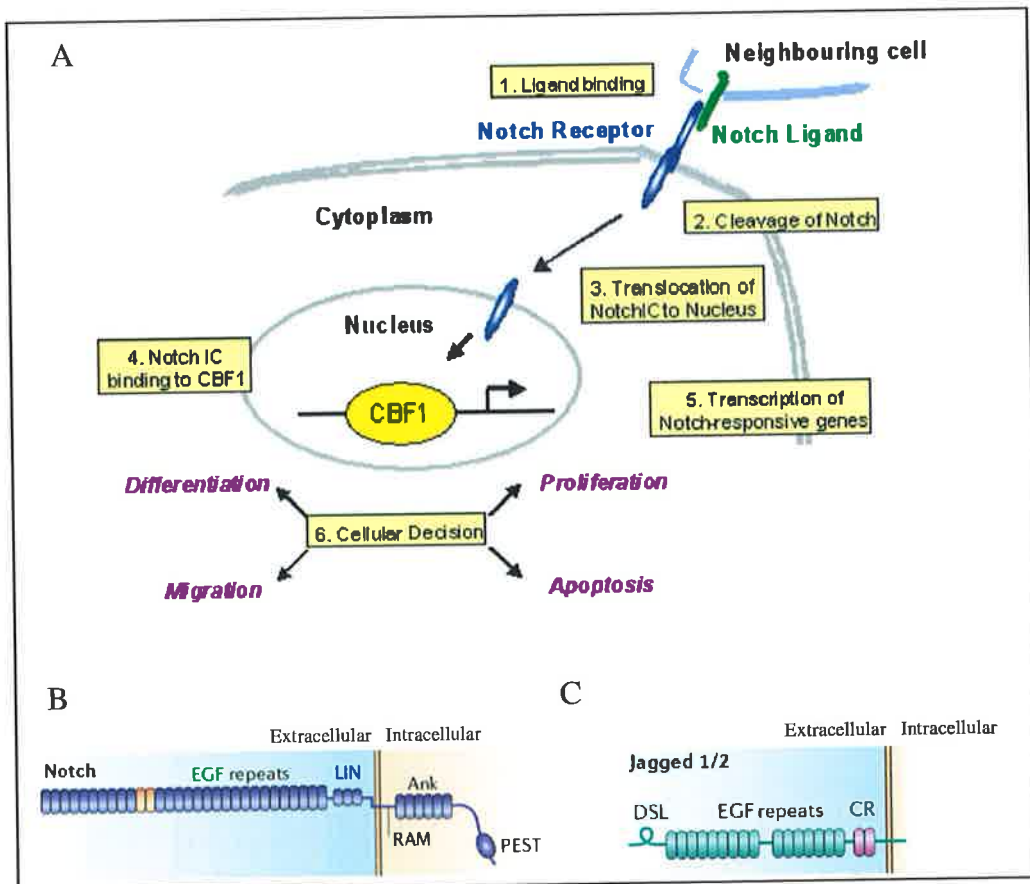


**Figure 1.7 Model and components of mammalian Notch signaling**

(A) (1) Notch ligands Jagged1, -2, Delta-like-1, -3 or -4 bind to Notch receptors 1, -2, -3 or -4 on adjacent cells. (2) Receptor-ligand binding leads to two cleavage events: an S2 cleavage immediately outside the transmembrane domain by tumour necrosis factor  $\alpha$  converting enzyme (TACE), which cleaves the extracellular domain from the intracellular domain; followed by an S3 cleavage event within the transmembrane domain by a multiprotein  $\gamma$ -secretase complex that liberates the Notch receptor's entire intracellular domain (NotchIC) from the membrane. (3) As a result of S3 cleavage, NotchIC is translocated to the nucleus, where it interacts via the RAM domain and ankyrin repeats with RBP-J $\kappa$ /CBF1 (4). (5) Binding of NotchIC to RBP-J $\kappa$ /CBF1 displaces the co-repressor complex, allowing transcriptional activation of Notch responsive genes. (6) Expression of Notch responsive genes determines the fate of the cell. (B) Notch extracellular domains contain 29–36 epidermal growth factor (EGF) repeats, 3 cysteine rich LIN repeats and a region that links to the transmembrane and intracellular fragment. EGF-repeats 11 and 12 (orange) are essential for ligand binding. The intracellular portion consists of a RAM domain, six ankyrin (Ank) repeats and a C-

terminal PEST domain. It also contains nuclear localisation signals. (C) Notch ligands are transmembrane proteins that are characterised by an N-terminal DSL (Delta, Serrate and LAG-2) domain that is essential for interactions with the Notch receptor. The extracellular domains of the ligands contain varying numbers of EGF -repeats. The ligands are subdivided into two classes, Delta or Delta-like (Dll) and Serrate (Jagged in mammals), depending on the presence or absence of a cysteine rich domain. A; adapted from Smith (2005) and B-C; adapted from Bray, 2006.

### 1.5.8 RTK signaling

Aberrant receptor tyrosine kinase (RTK) activities are commonly involved in cellular transformation. RTKs usually activate the PI3K/AKT and MEK1/2/ERK1/2 pathways and can also activate STATs (Schlessinger, 2000). As listed in Table 1-3, six RTKs, PDGFRA, DDR2, EPHB1, RON, TRKB and TRKA, are aberrantly expressed in H/RS cells from a considerable fraction of cHL cases (Renné *et al.*, 2005), most pronounced in NSHL, where the vast majority of cases coexpressed 2–6 of the RTKs. In the study by Renné *et al.*, treatment of H/RS cells with the PDGFRA inhibitor, Imatinib, lead to growth inhibition indicating that aberrant RTK activities may have important functions in H/RS-cell pathogenesis. The aberrant expression of RTKs in HL is a recent discovery and establishing a role for RTK signaling is the subject of ongoing investigation.

## 1.6 EBV and HL

Viruses have also been found to be involved in the development of some cancers and contribute to tumourigenesis by different mechanisms, indirectly by inducing immunosuppression or by modifying the host cell genome without persistence of viral DNA, or directly by expressing oncoproteins or by altering the expression of host cell proteins. The oncogenic viruses that are implicated in cancer are diverse and vary greatly in the complexity of their genomes, their target tissues and their requirements for additional co-factors during tumour progression. Some members of the human herpes viruses, most notably EBV, have been linked by experimental and clinical evidence to a number of cancers of both lymphoid and epithelial origin including Burkitt's lymphoma (BL), HL, lymphomas in immuno-compromised individuals and certain T cell lymphomas.

EBV is classified as a gamma-herpes virus and is transmitted from host to host through saliva, although blood transfusion and bone marrow and organ transplantation also have

been implicated. Primary infection begins at the oropharyngeal epithelium and B-lymphocytes are infected as they traffic in close proximity to these cells (Thompson and Kurzrock, 2004). Seroepidemiologic studies indicate that >90 % of adults worldwide are infected with EBV (Hsu and Glaser, 2000) and primary infection usually occurs in the first few years of life and does not result in any recognised disease. However, the dramatic immune response that can occur when primary infection is delayed until adolescence or adulthood frequently results in Infectious Mononucleosis (IM) (Wensing and Farrell, 2000). IM is characterised by a variety of symptoms, including fever, malaise, lymphadenopathy (marked swelling of peripheral lymphoid tissues) and the presence of atypical dividing lymphocytes in the peripheral blood (Eliopoulos and Young, 2001). Long-term EBV co-exists with most human hosts without overt serious consequences. However, in a small percentage of individuals, the virus may be implicated in the development of malignancy.

To date, three main types of EBV latent infection have been described, these are referred to as latency I, II and III. Latency III is found in all lymphoblastoid cell lines (LCLs), B cell lymphomas of immunosuppressed individuals, and some B cell blasts in patients with infectious mononucleosis (Wensing and Farrell, 2000). The full range of latency genes are expressed in latency III. In latency I, which is characteristic of Burkitt's lymphoma (BL), only EBNA1, the EBERs and the *Bam*HI A transcripts are regularly detected (Murray and Young, 2001). Latency II type gene expression is found in EBV-associated HL, undifferentiated nasopharyngeal carcinoma (NPC) and T-cell lymphomas, with expression limited to the EBERs, EBNA1, LMP1, LMP2 and the *Bam*HI A transcripts.

As mentioned previously, EBV is found in significant proportions of HL cases (30-50 %) with geographical variation and represents the most common genetic abnormality detectable in HL. If present, EBV is found in all tumour cells with a usually monoclonal composition of episomes, indicating that EBV infection occurs prior to clonal expansion of the tumour cells (Herbst, 1996). The existence of EBV-negative disease raises the question of whether EBV, when present, is simply a 'passenger'. Although this remains formally possible, the likelihood of HL having arisen in an EBV-positive target cell by chance seems remote, given that infected cells normally make up a tiny fraction (1-100 cells per million) of the total B-cell pool (Young and Rickinson, 2004). Furthermore, in EBV-positive tumours, the viral genome is present in every H/RS cell. Gulley *et al.*, (1994), demonstrated the monoclonality of EBV DNA in HL implying that the RS cells

were infected before malignant transformation suggesting that HL could develop as a consequence of malignant transformation of an EBV-infected cell. EBV-specific DNA sequences were detected from frozen and/or paraffin embedded tissues of 58 % of HL cases while only 10 % of control lymph nodes with normal histology were EBV positive (Herbst *et al.*, 1993). The relative risk of developing HL in individuals with a history of IM, relative to those with no prior history was shown to range between 2.0 to 5.0. As observed with BL and NPC, elevated titres to EBV antigens are seen prior to and at the onset of tumour development (Griffin, 2000). EBV-positive tumours express the viral genes EBNA-1, LMP-1 and LMP-2 of the default transcription program, which is the program that is used by latently infected GC B cells, further supporting the idea that HL arises from an EBV-infected GC B cell (Thorley-Lawson and Gross, 2004). The identification of H/RS cells as failed products of GC reactions by Ig genotyping does indeed indicate a plausible pathogenetic role for the virus, based on rescuing such tumour progenitors from apoptosis. LMP1 is capable of constitutively activating the CD40 pathway, thereby replacing a signal that is normally provided by cognate T cells during memory-cell selection, and LMP2A can mimic signalling from surface Ig, replacing the usual requirement for high-affinity binding to cognate antigen (Young and Rickinson, 2004) as detailed in Section 1.4 and Figure 1.8.

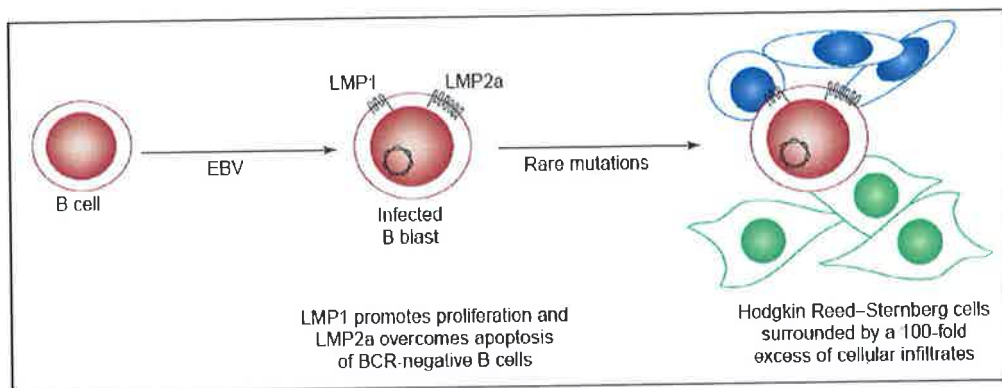


**Figure 1.8** A model for the evolution of EBV<sup>+</sup> HL

EBV infects a resting immature B cell before it has participated in a GC reaction (Crawford, 2001; Portis *et al.*, 2002). The virus expresses multiple genes, including EBV-encoded RNAs (EBERs), Epstein–Barr nuclear antigen (EBNA)-1, EBNA2, LMP1 and LMP2a. LMP2a enables the survival of the infected cell that fails to support the maturation and expression of Ig (Caldwell *et al.*, 1998; Casola *et al.*, 2004). LMP1 might promote its proliferation. Additional mutations enable the cell to evolve into a H/RS cell. Adapted from Hammerschmidt and Sugden, 2004.

The association of EBV with HL varies with country of residence, histological subtype, sex, ethnicity and age. EBV-positive HL is more frequent in childhood, in older adults (>45 years) and in mixed cellularity cases. Other consistent findings are that, among EBV-positive HL, there is a male predominance (Gandhi, 2004). The true contribution of EBV to the pathogenesis of HL remains unknown. Several reports have presented conflicting evidence regarding the influence of EBV on the outcome of patients with HL. Some studies have found no effect of the EBV status on outcome (Herling *et al.*, 2003; Axdorph *et al.*, 1999), but there are also contradictory reports suggesting both a survival disadvantage (Stark *et al.*, 2002) and a survival advantage (Morente *et al.*, 1997) in EBV-associated HL patients. Population-based studies on the influence of EBV on relapse and survival after HL found a marked survival disadvantage in older EBV-positive HL patients as compared to EBV-negative HL cases (Gandhi, 2004). Cases of HL in patients with human immunodeficiency virus (HIV) or from developing countries are more likely to contain EBV genomes than persons without HIV or from developed countries. EBV-positive HL is the most frequent non- AIDS defining cancer diagnosed in HIV patients (Gandhi, 2004).

Although the incidence of HL is relatively low (2-3/100,000 per year) this tumour is not genetically restricted, making its association with EBV significant in worldwide health terms.

## 1.7 Anti-apoptotic mechanisms in H/RS cells

Two alternative convergent pathways can initiate apoptotic cell death: the extrinsic pathway (the death receptor pathway), which is mediated by cell surface death receptors (members of TNFR superfamily, e.g. CD95 as discussed in Section 1.4.2), and the intrinsic pathway, which is mediated by mitochondria, both of which are illustrated in Figure 1.9. The intrinsic pathway of apoptosis triggers the release of proapoptotic proteins (primarily Bcl-2 family members) from mitochondria, which form a multi-protein complex, the apoptosome, where caspase-9 is activated by dimerisation, leading to proteolytic cell destruction (Brauninger *et al.*, 2006).

Apart from the capacity to evade the extrinsic apoptosis pathway as described in Section 1.4.2, H/RS cells also show malfunctions in the intrinsic apoptosis pathway. As seen in Figure 1.9, caspase activities are modulated by a group of proteins, the inhibitors of

apoptosis, such as the X-linked inhibitor of apoptosis (XIAP), which binds to caspases and inhibits their proteolytic activity. Kashkar *et al.*, 2003, reported expression of XIAP in HL cell lines and H/RS cells in biopsy samples and showed that inhibition of XIAP restored sensitivity of HL cells to caspase-3-mediated apoptosis. The anti-apoptotic protein cFLIP (Figure 1.9) is constitutively expressed in HL (Thomas *et al.*, 2002a) and inhibits proper TRAIL-induced signal transduction similar to the inhibition of the CD95 as TRAIL sensitivity could be restored by downregulation of cFLIP (Mathas *et al.*, 2004). Kreuz *et al.*, 2001, suggested that strong expression of c-FLIP in H/RS cells could be due to constitutive NF- $\kappa$ B activity.

Constitutive NF- $\kappa$ B activity as illuminated in Section 1.5.2 and illustrated in Figure 1.9 contributes significantly to the survival phenotype of H/RS cells. NF- $\kappa$ B target genes in H/RS cells, identified by experimental NF- $\kappa$ B inhibition, include transcription factors and anti-apoptotic molecules (Hinz *et al.*, 2002).

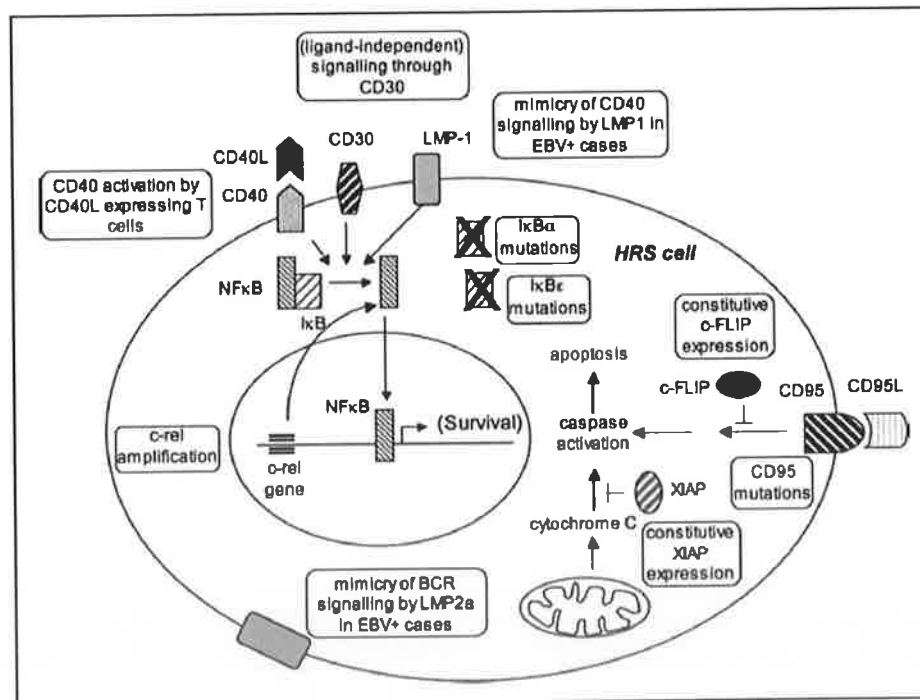


**Figure 1.9 Anti-apoptotic mechanisms in H/RS cells.**

Several factors may contribute to the constitutive activity of the transcription factor NF- $\kappa$ B, which is an important anti-apoptotic factor in H/RS cells: somatic mutations in the genes of the NF- $\kappa$ B inhibitors I $\kappa$ B $\alpha$  and I $\kappa$ B $\beta$  in some cases, LMP1 expression in EBV-positive cases, CD40 ligand-CD40 interaction and (ligand-independent) signaling through CD30. CD95 signaling is inhibited in rare cases by mutation in the CD95 gene,

and presumably frequently by cFLIP expression. Downstream caspase activation is likely inhibited by XIAP expression. Adapted from Brauninger *et al.*, 2006.

### 1.7.2 Bcl-2 Family: regulators of cell fate

Apoptosis or programmed cell death plays a vital role in normal development, tissue homeostasis, and the removal of damaged and infected cells, ensuring a proper balance of cell production and cell loss. Necrosis is a passive, catabolic process, always pathological, that represents a cell's response to extreme accidental or toxic insults. Apoptosis, in contrast, occurs under normal physiological conditions and is an active process requiring energy (Renvoizé *et al.*, 1998) is genetically controlled and tumourigenesis involves its inhibition. The Bcl-2 family of proteins contains key regulators of the mitochondrial (intrinsic) pathway of apoptosis (Danial and Korsmeyer, 2004). Bcl-2 family members reside upstream of irreversible cellular damage and focus much of their efforts at mitochondrial level, where they act as key regulators of apoptosis (Gross *et al.*, 1999). The Bcl-2 family comprises 17 or more members in mammalian cells (Cory and Adams, 2002). The members share homology, clustered within four conserved regions, Bcl-2 homology (BH) 1-4 domains, which control the ability of these proteins to dimerise and function as regulators of apoptosis (Figure 1.10). The proapoptotic members are Bax, Bcl-x<sub>S</sub>, Bak, and Bad, whereas the anti-apoptotic members comprise Bcl-2, Bfl-1, Bcl-x<sub>L</sub>, Bcl-W, Bcl-B, NR-13 (human homolog nrh), Bcl2-L-10 and Mcl-1. The family may be subdivided into three main groups based on BH domains and function:

1. multidomain anti-apoptotic (BCL-2, BCL-X<sub>L</sub>, BCL-w, MCL-1, BFL-1/A1)
2. multidomain proapoptotic (BAX, BAK, BOK), and
3. BH3-only proapoptotic (BID, BIM, BAD, BIK, NOXA, PUMA, BMF, HRK).

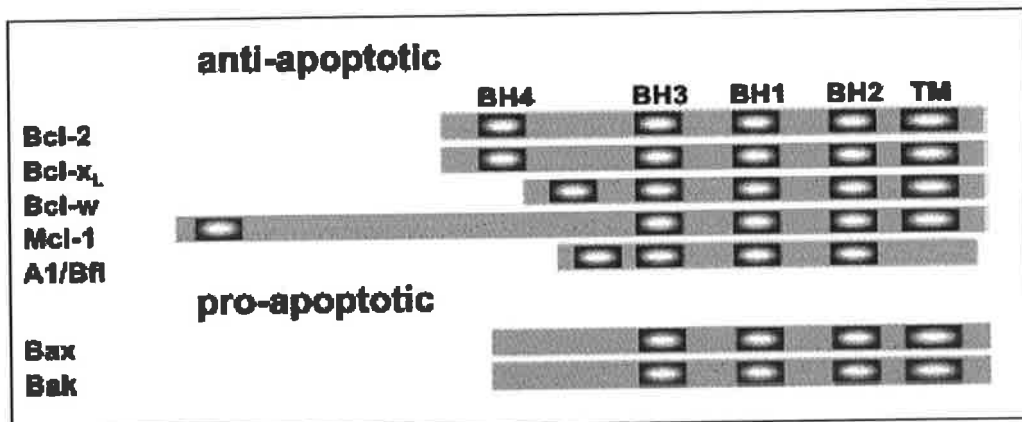


**Figure 1.10 Schematic representation of Bcl-2 protein domain organisation**

The domain structure of pro- and anti-apoptotic bcl-2 family members. Bcl-2 contains four conserved bcl-2 homology domains (BH1–4), which can be found in other family members. Some of the family members also have a carboxy-terminal hydrophobic transmembrane domain (TM). Adapted from Sorenson, 2004.

The first group consists of the anti-apoptotic Bcl-2 type proteins, which contain three to four BH domains that are required for their anti-apoptotic function. The BH domains mediate interactions between the Bcl-2 like proteins and other members of the Bcl-2 family. Over-expression of anti-apoptotic Bcl-2-family proteins, such as Bcl-2, Bcl-xL, Mcl-1, Bfl-1, Bcl-W and Bcl-B, occurs during the pathogenesis or progression of most cancers and leukemias (Adams and Cory, 1998; Gross, McDonnell and Korsmeyer, 1999; Reed 1998). The second group of the Bcl-2 family consists of the Bax-like pro-apoptotic proteins, including Bax, Bak and Bok (Kirkin *et al.*, 2004). While Bax and Bak are widely expressed (Krajewski *et al.*, 1994; Krajewski *et al.*, 1996), Bok appears to be restricted to the reproductive tissues (Hsu *et al.*, 1997). The third group of Bcl-2 proteins is the pro-apoptotic BH3 domain-only group. This group has many members, which differ strikingly in their responsiveness to stimuli and thereby in the pathways they regulate (Huang and Strasser, 2000). The BH3 domain-only family members share only the short BH3 domain with the other Bcl-2 family members (and with each other), which is essential for their killing function (Huang and Strasser, 2000; Willis and Adams, 2005).

Several family members contain a hydrophobic region that is responsible for targeting these proteins to intracellular membranes, including the outer mitochondrial membrane, the endoplasmic reticulum and the nuclear envelope (Adams and Cory, 1998).

### **1.7.3 Mechanism of action of Bcl-2 family members**

Most anti-apoptotic Bcl-2 family members localise to the mitochondria and other intracellular membranes while the pro-apoptotic members are localised in the cytosol or the cytoskeleton. Upon cellular exposure to a death signal, pro-apoptotic members (Bim, Bax and Bak) are targeted and integrate into membranes, mainly the mitochondrial outer membrane. The targeting of Bax and/or Bak to the mitochondrial membranes results in their oligomerisation and subsequently in pore formation in the mitochondrial membranes (reviewed in Gross McDonnell and Korsmeyer, 1999; Korsmeyer *et al.*, 2000).

Studies using Bak and Bax knockout mice have provided evidence into how pro-apoptotic Bcl-2 family members induce cell death. Cells lacking both Bax and Bak did not die upon expression of BH3 domain-only proteins, in contrast to cells expressing either one of these molecules. This indicated that BH3 domain-only proteins require at least one Bax-type partner to induce cell death (Zong *et al.*, 2001; Wei *et al.*, 2001). Both Bax and Bak undergo a conformational change in response to apoptotic stimuli (Werner *et al.*, 2002) and assemble into homo-multimers in the mitochondrial membrane. Upon oligomerisation, they actively induce cytochrome c (Cyt c) release (Borner, 2003), possibly by (i) forming a new channel (Schlesinger *et al.*, 1997); (ii) by enlarging an existing permeability transition pore (Tsujimoto and Shimizu, 2000; Zamzami and Kroemer, 2001) or (iii) forming supramolecular openings in the outer membrane which are different from discrete protein channels (Kuwana *et al.*, 2002).

Anti-apoptotic family members like Bcl-2 and Bcl-xL, hold Bax and Bak in check, possibly forming heterodimers, thereby preserving mitochondrial integrity (Borner, 2003). The conformational change and multimerisation of Bax or Bak is inhibitable by Bcl-2 (Antonsson *et al.*, 2001; Mikhailov *et al.*, 2001) and inducible by the BH3 domain-only protein Bid (Wei *et al.*, 2000; Antonsson *et al.*, 2001). In healthy cells, BH3-only proteins are kept inactive (Cory and Adams, 2002). In response to pro-apoptotic signals, they become transcriptionally up-regulated and/or post-translationally modified to gain their full apoptotic potential (Kirkin *et al.*, 2004). The Bid protein is cleaved by caspase 8 in response to death receptor activation (Li *et al.*, 1998; Luo *et al.*, 1998). Cleavage results in exposure of the Bid BH3 domain, which is normally buried within the full-length protein (Chou *et al.*, 1999; McDonnell *et al.*, 1999). The cleaved C-terminus complex, truncated Bid (tBid), is then myristoylated and translocated to the mitochondria (Zha *et al.*, 2000). Bid seems to form hetero-trimers in the mitochondrial

membrane, which then may induce mitochondrial Bax or Bak to oligomerise (Wei *et al.*, 2000), promoting Cyt c release (Luo *et al.*, 1998; Li *et al.*, 1998). Cyt c binds to apoptotic protease activating factor-1 (Apaf-1) to form the apoptosome, which, in turn activates caspase 9 to initiate apoptosis (Hengartner, 2000) (Figure 1.11). The ultimate balance between the expression levels and the subcellular localisation of pro-and anti-apoptotic proteins determines whether a cell will live or die.

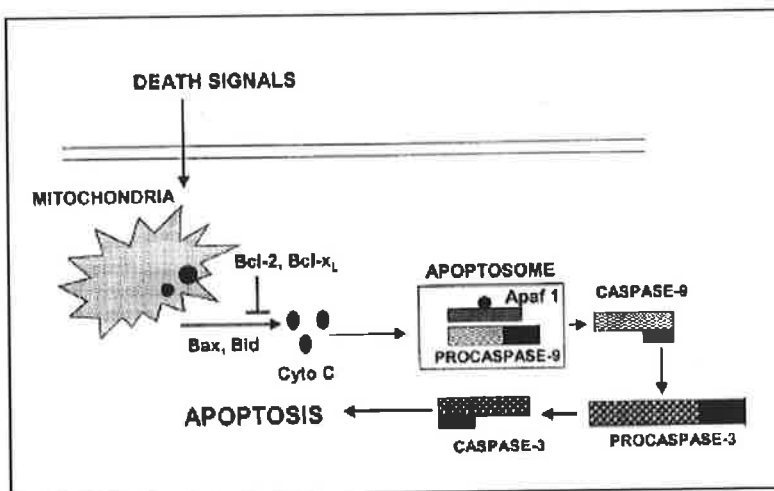


**Figure 1.11 Mitochondrial pathway of apoptosis**

A number of signals cause changes in mitochondrial membrane potentials and mitochondrial permeability transition resulting in the release of Cyt c. Bax and Bid facilitate the release of Cyt c from the mitochondria, whereas the release of Cyt c is blocked by Bcl-2 and Bcl-x<sub>L</sub>. Cyt c binds to Apaf-1 and recruits procaspase-9 to form an ‘apoptosome’. Caspase-9 activates effector caspases to induce apoptosis. Adapted from Gupta, 2003.

#### 1.7.4 Anti-apoptotic Bcl-2 member, Bfl-1

Bfl-1 was originally identified from granulocytes macrophage-colony stimulating factor (GM-CSF)-induced mouse bone marrow as a novel hematopoietic specific early response gene with sequence similarity to Bcl-2 (Lin *et al.*, 1993) and was subsequently cloned and characterised by Choi *et al.* (1995). Human Bfl-1/A1 and mouse A1 share about 72 % amino acid identity (Choi *et al.*, 1995).

Bfl-1 has a similar core structure to Bcl-xL (seven alpha helices present) and consists of highly conserved BH1 and BH2 domains and the limitedly conserved BH3 and BH4 (Figure 1.10) but does not, however, have a well-defined C-terminal transmembrane domain, which is characteristic of most Bcl-2 family proteins (Choi *et al.*, 1995; D'Sa-Eipper and Chinnadurai, 1998; Zhang *et al.*, 2000). Functional dissection of the Bfl-1 protein has revealed that (D'Sa-Eipper and Chinnadurai, 1998) the BH1, 2 and 4 domains are essential in conferring the anti-apoptotic and transforming properties of this protein. The fact that mutations, which abolish the anti-apoptotic function, also abolish the oncogene co-operating function suggests that both of these functions are linked (D'Sa-Eipper and Chinnadurai, 1998; D'Sa-Eipper *et al.*, 1996). Bfl-1/A1 can interact with Bax to neutralise its lethality and suppress apoptosis by inhibiting the release of Cyt c and caspase-3 activation (Sedlak *et al.*, 1995; Zhang *et al.*, 2000; Duriez *et al.*, 2000). Bfl-1 has also been shown to exert its anti-apoptotic activity by inhibiting the collaboration between the BH3 domain-only protein Bid and its pro-apoptotic partners Bax or Bak in the induction of Cyt c release (Werner *et al.*, 2002). Bfl-1 does this by binding to the full length Bid via the Bid BH3 domain. It does not interfere with the proteolytic activation of Bid, nor with its mitochondrial insertion, but remains selectively complexed to tBid in the mitochondrial membrane, where it prevents the activity of a pro-apoptotic complex (Werner *et al.*, 2002).

In 2005, Chen *et al.*, reported that Bfl-1/A1, bound PUMA among the sensitiser BH3 peptides and BIK, HRK, and NOXA among the activator peptides. Certo *et al.*, (2006), also showed by fluorescence polarisation binding assays that Bfl-1 selectively binds the sensitiser, PUMA, but in contrast reported that Bfl-1 binds only Bid and Bim among that anti-apoptotic activators.

Bfl-1, is early response gene and its expression is rapidly and transiently induced by inflammatory cytokines, TNF and IL-1 (Karsan *et al.*, 1996a and b; Pang, Hershman and Karsan, 1997), phorbol ester (Karsan *et al.*, 1996b), lipopolysaccharide (Chuang *et al.*, 1998; Hu *et al.*, 1998), pathogens (Orlofsky *et al.*, 1999; Gross *et al.*, 2000), vascular endothelial growth factor (VEGF) (Gerber, Dixit and Ferrara, 1998), GM-CSF (Feldman *et al.*, 1997), granulocyte-colony stimulating factor (G-CSF) (Chuang *et al.*, 1998; Feldman *et al.*, 1997), CD40 ligand (Lee *et al.*, 1999; Kuss *et al.*, 1999), oxidative stress (Kim *et al.*, 2005), and the anti-cancer drugs etoposide (Wang *et al.*, 1999) and cisplatin (Kim *et al.*, 2004).

Bfl-1/A1 is expressed abundantly in bone marrow and at low levels in the spleen and lung and in cancer cell lines (Choi *et al.*, 1995; Park *et al.*, 1997 and Jung-Ha *et al.*, 1998). Expression is generally confined to immune cells and tissues, in a pattern similar to that of NF-κB and many studies have shown Bfl-1/A1 to be a direct transcriptional target of NF-κB (Zong *et al.*, 1999; Lee *et al.*, 1999; Wang *et al.*, 1999; Grumont *et al.*, 1999; Cheng *et al.*, 2000; Pagliari *et al.*, 2000).

Unlike some other Bcl-2 family members, no role in cell cycle has been identified for Bfl-1. In fact, Bfl-1 was shown specifically not to have a cell cycle inhibitory effect when expressed as a transgene driven by the lck distal promoter, in that more A1-expressing T cells accumulated in culture after activation than Bcl-2-expressing T cells (Gonzalez, Orlofsky and Prystowsky, 2003). It was suggested that this is because A1 rescued T cells from activation-induced cell death and allowed them to cycle, whereas Bcl-2 saved the cells from apoptosis but also inhibited their proliferation.

### **1.7.5 *bfl-1* in malignant disease**

Bfl-1 is expressed in several epithelial and hematopoietic malignancies and numerous reports suggest that Bfl-1 expression may be important in controlling resistance to chemotherapeutic responses in tumour cells. Several studies have found that Bfl-1 transfected cells are less sensitive to apoptosis (Tarte *et al.*, 2004; Zong *et al.*, 1999; D'Sa-Eipper, Subramanian and Chinnadurai, 1996; Carrio *et al.*, 1996; Shim *et al.*, 2000; Cheng *et al.*, 2000). Wang *et al.*, (1999), reported that Bfl-1/A1 was induced in fibrosarcoma cells by etoposide and overexpression of Bfl-1/A1 in NF-κB-deficient HT1080 cells strongly suppresses etoposide-induced cell death. Tarte *et al.*, (2004), found that constitutive Bfl-1 expression rescued myeloma cells from apoptosis induced by IL-6 withdrawal and dexamethasone (chemotherapeutic agent). Bfl-1 was found to be upregulated in cisplatin-resistant human bladder cell lines (Kim *et al.*, 2004). Cheng *et al.*, (2000), reported that NF-κB inhibition sensitises A549 lung adenocarcinoma cells to death by chemotoxins and Bfl-1 expression inhibits death of these cells. Ectopic expression of Bcl-x and Bfl-1 in NF-κB activation-deficient A549 cells was sufficient for protection against death from chemotherapy or TNF. Xia *et al.*, (2006), showed that increased expression of Bfl-1/A1 in leukemia cells undergoing differentiation has an important role in attenuating cytotoxic chemotherapeutic agent induced apoptosis.

Several studies suggest that *bfl-1* expression is a key factor in lymphomas. In B cell chronic lymphocytic leukaemia, high expression of *bfl-1* contributes to the apoptosis resistant phenotype (Morales *et al.*, 2005) and engagement of surface IgM elicits a survival programme that is associated with upregulation of Bcl-2, Mcl-1 and Bfl-1 anti-apoptotic proteins (Bernal *et al.*, 2001). Overexpression of the murine homologue of Bfl-1, A1, protects murine B lymphoma cells from anti-IgM-induced apoptosis (Craxton *et al.*, 2000). Also, in mantle cell lymphomas, inhibition of constitutively activated NF-κB pathway leads to tumour cell apoptosis in association with the down-regulation of *bfl-1* expression (Pham *et al.*, 2003).

Despite these studies, which have elucidated a role for this gene in other malignancies, the role of *bfl-1* in HL has not so far been investigated.

### **1.7.6 *bcl-2* family member expression in HL**

The expression of *bcl-2* family members has been extensively studied in H/RS cells of HL (Stetler-Stevenson *et al.*, 1990; Hell *et al.*, 1995; Schlaifer *et al.*, 1996; Brink *et al.*, 1998; Messineo *et al.*, 1998; Chu *et al.*, 1999; Brousset *et al.*, 1999; Kanavaros *et al.*, 2000; Dukers *et al.*, 2002; Kashkar *et al.*, 2002; Rassidakis *et al.*, 2002a, b and c; Montalban *et al.*, 2004; Kim *et al.*, 2004; Bai *et al.*, 2006). The interplay between these proteins is thought to be important in the survival of H/RS cells in cHL and may influence chemosensitivity in some cases. Bai *et al.*, (2006), hypothesised that the anti-apoptotic proteins Bcl2, Bcl-x<sub>L</sub>, and Mcl-1 may counteract the expression of the pro-apoptotic proteins Bax, Bad, and Bim, thereby contributing to the survival of H/RS cells. The involvement of Bcl-x<sub>L</sub> and Bax in the survival of H/RS cells can be highlighted by the findings that ectopic expression of Bcl-x<sub>L</sub> restored viability in H/RS cells lacking NF-κB activity (Hinz *et al.*, 2001) and that defective Bax activation in HL cell lines confers resistance to staurosporine-induced apoptosis (Kashkar *et al.*, 2002).

The H/RS cell expression patterns of Bad, Bim, Bid, Bcl-2, Bcl-x, Bcl-x<sub>L</sub>, Mcl-1, Bax, and Bak have all been reported to date. However, despite the many studies on *bcl-2* family member expression in HL, information on the status of *bfl-1* expression is limited to an observation in Hinz *et al.*, (2002), that *bfl-1* mRNA expression was downregulated in a H/RS cell line following NF-κB inhibition by microarray analysis.

Investigating the expression of *bfl-1* in primary tissue and cultured H/RS cells was, therefore, necessary to gain full insight into the apoptosis profile of HL.

## 1.8 Objectives of this study

Previous work in our laboratory has shown that the cellular *bfl-1* gene plays an important role in regulating the survival of EBV-infected B cells (D’Souza *et al.*, 2000) and is regulated by EBV via two different pathways with roles for NF-κB (D’Souza *et al.*, 2004) and Notch nuclear proteins (Pegman *et al.*, 2006). Establishing a role for *bfl-1* in HL and elucidating the mechanisms by which this anti-apoptotic gene is regulated by some of the major signaling pathways outlined in this chapter, is the primary focus of this study. These experiments will permit us to establish if *bfl-1* expression can serve as a prognostic marker for HL and will also validate *bfl-1* as a potential target for the design of rational therapeutic strategies for the treatment of HL.

Over the last years several aberrantly expressed proteins and inappropriately activated signaling pathways have been identified, which are important for H/RS cell phenotype, survival and proliferation. Constitutive NF-κB signaling is a universal hallmark of HL and proliferative and anti-apoptotic roles. The *bfl-1* gene is a recognised direct transcriptional target of transcription factor NF-κB and has been linked to apoptosis-resistant phenotype in several malignancies as highlighted in Section 1.7.5. Expression of Bcl-2 family members in HL has been the focus of rigorous study in the past but to date no study of the expression or role of Bfl-1 in HL has been carried out. As discussed in Section 1.3, HL has become a highly curable disease thanks to advances in polychemotherapy regimens in recent years but long-term toxic effects in often-young patients is a major concern and can frequently be fatal. Targeting deregulated genes that mediate apoptotic resistance in H/RS cells in tandem with low-dose polychemotherapy is now the therapeutic challenge and holds significant future promise for disease management with reduction in adverse treatment sequelae.

Mechanistic studies of the contribution of *bfl-1* to H/RS cell survival will provide important information about potential routes to this B cell malignancy. The main objectives of the current study were to investigate the expression, role and molecular basis of *bfl-1* regulation in H/RS cells of HL.

The absence of a good quality antibody for Bfl-1 protein detection has been a limitation in investigating the contribution of this protein to various malignancies for many years

now. The generation of anti-Bfl-1 antibody preparations using overexpressed and purified recombinant Bfl-1 protein as antigen for rabbit immunisation was also an aim of this study to overcome the difficulty of having no such reagent available.

In summary, the following conclusions may be drawn from the experiments below:

*Bfl-1* is expressed in Hodgkin's lymphoma tissue and cultured H/RS cells;

- These results show for the first time that *Bfl-1* mRNA is expressed in H/RS and reactive cells of tumour tissue from HL patients, irrespective of EBV status, with high mRNA expression levels observed in all cases of EBV+/- HL primary cases tested.
- High-level *bfl-1* mRNA expression was observed in cultured H/RS cell lines relative to BL type I cells.
- The novel *bfl-1* splice variant designated *bfl-1S*, was not expressed in H/RS or reactive cells of HL tumour tissue, cultured H/RS cells, tonsillar germinal center B cells, Burkitt's lymphoma or lymphoblastoid cell lines.
- Previously unreported mRNA levels of Bcl-2 family members, *bcl-w* and *bik* were observed in cultured H/RS cells by RPA.

*Bfl-1* is a key NF-κB target gene in H/RS cells

- Inhibition of NF-κB by sodium arsenite or Bay11 chemical inhibitors resulted in apoptosis of H/RS cells.
- Apoptosis, associated with NF-κB inhibition, was coincident with a significant decline in *bfl-1* mRNA expression levels.
- The pRTS-1-HA-*bfl-1* vector, constructed in this study was validated for capability to inducibly express Bfl-1 protein fused to the hemagglutinin tag in DG75 cells.
- Stable cell clones of H/RS-derived cell line, L428, were generated by transfection of pRTS-1-HA-*bfl-1* for ectopic expression of Bfl-1.
- Ectopic expression of Bfl-1 had no effect on proliferation of L428 cells under normal physiological conditions.
- It is shown in this study for the first time that ectopic expression of Bfl-1 protected H/RS cells from apoptosis induced by NF-κB inhibition.
- Cells induced to express Bfl-1 from pRTS-1-HA-*bfl-1* proliferated to a greater extent than non-induced cells during serum deprivation.

### *Bfl-1* downregulation by RNAi

- Downregulation of *bfl-1* mRNA in H/RS-derived cell line, L428, by 90 % was achieved by nucleofection of siRNA.
- Knockdown of *bfl-1* mRNA did not significantly reduce the apoptotic threshold of L428 cells during serum deprivation.
- The novel finding that downregulation of *bfl-1* mRNA expression sensitises L428 cells to apoptosis induced by sodium arsenite and Bay11, potentiating the effect of these chemotoxic NF-κB inhibitors is presented in this study.

### Regulation of the *bfl-1* promoter in HL

- The *bfl-1* promoter is regulated by NF-κB in H/RS-derived cell lines of EBV negative (L428) and positive (L591) status.
- Inhibition of NF-κB in L428 and L591 cell lines by inhibitory-gene transfer blocks NF-κB activation of the *bfl-1* promoter.
- NF-κB trans-activates the *bfl-1* promoter in the EBV-negative HL-derived cell line L428, and an NF-κB-like binding site at position -52 to -42 relative to the transcription start site is essential for this effect.
- Notch 1 and 2 receptors are abundantly expressed in cultured H/RS cells and Notch ligand, Jagged1, is expressed in the EBV-positive cell line, L591.
- Presentation of Notch ligand Jagged1 leads to increased proliferation of cultured H/RS cells.
- The requirement of the putative CBF1 site (at position -243 to -249) on the *bfl-1* promoter was not essential for conferring responsiveness on the *bfl-1* promoter in this cell context; the *bfl-1* gene is not a downstream target for transcriptional activation by Notch signaling in this cell milieu.

Expression and purification of recombinant Bfl-1 using a novel modified vector and generation of anti-Bfl-1 serum.

- A novel vector, pGSLink, was designed and constructed to permit high-level expression of a protein linked at the N- or C-terminal to a His-tag by a flexible linker (published in Analytical Biochemistry; Loughran *et al.*, 2006).
- The *bfl-1* coding fragment was cloned into this vector to produce the fusion constructs; pGSLink-N-Bfl-1 and pGSLink-C-Bfl-1, from which the His-Linker-Bfl-1 and Bfl-1-Linker-His fusion proteins were overexpressed and purified

using IMAC. Purified recombinant Bfl-1 was used to immunise a rabbit for the generation of polyclonal antibodies to Bfl-1.

Ultimately, it is hoped that this investigation will enable better characterisation of the molecular pathways of apoptosis and of the defects in such pathways that HL cancer cells exhibit and therefore lead to efficient and specific anti-cancer therapies.

## **CHAPTER 2 Materials and Methods**

## 2.1 Biological Materials

### 2.1.1 Cell lines

**Table 2-1 Cell lines used in the study**

Cell Lines	EBV Status	Cell Classification	Description
AG876	+	Type III BL	Type III BL expressing all of the EBV latent genes.
BL41	-	EBV negative BL Type I	EBV negative BL cell line (Calender <i>et al.</i> , 1987).
BL41 B95-8	+	EBV positive BL type III	BL41 cell line stably transformed with the EBV strain B95.8 expressing all the EBV latent genes (Calender <i>et al.</i> , 1987).
BL74	+	Type I BL	BL74 is a group I BL cell line established from an EBV-positive tumour biopsy (Lenoir, Vuillaume and Bonnardel, 1985).
Daudi	+	EBV positive BL Type III	Daudi, described by Klein <i>et al.</i> , 1968, is deleted for EBNA-2 and does not express LMP1, expresses only EBNA1 and LMP2A. The EB virus genome in Daudi cells has a deletion similar to that observed in a non-transforming strain (P3HR-1) of the virus (Jones <i>et al.</i> , 1984).
DG75	-	EBV negative BL	Lymphoid B cell line derived from an Israeli Burkitt's-like lymphoma case (Ben-Bassat <i>et al.</i> , 1977).
DG75-pRTS-1-HA-bfl-1	-	HA-tagged bfl-1 expressing cell line	DG75 cell line stably transfected with pRTS-1-HA-bfl-1, capable of expressing hemagglutinin (HA)-tagged BFL-1 protein under tetracycline control (This study).
HtTA-jagged1	-	Jagged1 presenting HeLa derived cell line.	HeLa-derived cell line expressing Jagged1 under tetracycline control (Bash <i>et al.</i> , 1999)
IARC 171	+	LCL	IARC 171 is a spontaneously transformed LCL from the same patient from whom the BL41 cell line was derived (Andersson <i>et al.</i> , 1991).

IARC 290B	+	LCL	A spontaneously transformed LCL from the same patient from whom the BL74 cell line was derived (Nilsson and Ponten, 1975).
Jurkat T	-	T cell	Acute T-lymphocytic leukemic cell line (Brattsand <i>et al.</i> , 1990).
KMH2	-	EBV negative HL	Established from the pleural effusion of a 37-year-old man with Hodgkin lymphoma (mixed cellularity progressing to lymphocyte depletion; stage IV at relapse) in 1974 (Kamesaki <i>et al.</i> , 1986).
KMH2 EBV	+	EBV positive HL	The parental EBV-negative KMH2 cells were infected with recombinant EBV to produce an EBV-positive clone (Baumforth <i>et al.</i> , 2005).
L1236	-	EBV negative HL	Established from the peripheral blood of a 34-year-old man with HL (mixed cellularity, stage IV, refractory, terminal, third relapse) in 1994 (Wolf <i>et al.</i> , 1996).
L428	-	EBV negative HL	Established from the pleural effusion of a 37-year-old woman with HL (stage IVB, nodular sclerosis, refractory, terminal) in 1978 (Schaadt <i>et al.</i> , 1979).
L428-pRTS-1-HA-bfl-1	-	EBV negative HL	L428 cell line stably transfected with pRTS-1-HA-bfl-, capable of expressing HA-tagged BFL-1 protein under tetracycline control (This study).
L591	+	EBV positive HL	EBV positive cell line established from pleural effusion of a female patient with nodular sclerosis HL (Diehl <i>et al.</i> , 1982)
L591-SD3	-	EBV negative HL	The parental EBV-positive L591 cells were serially diluted to generate an EBV-negative clone (Baumforth <i>et al.</i> , 2005).
Mutu I	+	EBV positive TypeI BL	EBV positive early passage BL cell line expressing EBNA1 as the sole viral latent gene (Gregory <i>et al.</i> , 1990)
Mutu III	+	EBV positive Type III BL	EBV positive MUTU I clone, which has drifted to express full complement of EBV latent genes, but no longer expresses LMP-1 (Gregory <i>et al.</i> , 1990).
OKU BL	+	Type I	OKU BL is a group I BL cell line expressing only EBNA1 (Kelly, Bell and Rickinson, 2002).
X50-7	+	LCL	A spontaneously transformed LCL (Wilson and Miller, 1979).

All HL cell lines were obtained from Dr. Paul Murray, University of Birmingham, England. All BL, LCLs and Jurkat cell lines were obtained from Professor Martin Rowe, University of Wales, Cardiff, Wales. HtTA-jag10 cell line was obtained from Dr. Celine Gelinas, University of Medicine and Dentistry of New Jersey, U.S.A.

### 2.1.2 Antibodies used in the study

**Table 2-2 Antibodies used in the study**

Antibody	Name	Description	Supplier
Rabbit anti-Bfl-1	Anti-Bfl-1 SL	Rabbit polyclonal anti-sera directed against His-Bfl-1 antigen.	This study.
Mouse Anti-DIG	Anti-digoxigenin Clone D1-22	A monoclonal antibody that recognises digoxigenin; small organic molecule rather than amino acids.	Sigma-Aldrich.
Horse Biotinylated universal secondary	Biotinylated universal secondary	Biotinylated antibody, made in horse, which recognises rabbit, mouse and goat IgG.	Vector Laboratories.
Mouse Anti-β-actin	Anti-β-actin AC-15	An IgG purified monoclonal that recognises an N-terminal peptide of actin protein.	Sigma-Aldrich.
Rat Anti-HA-HRP	Anti-HA-peroxidase high affinity	HRP-conjugated rat monoclonal antibody that recognises the HA peptide sequence (YPYDVPDYA) derived from the influenza HA protein.	Roche.
Rat Anti-Jagged1	TS1.15H	A monoclonal antibody that is specific for the intracellular domain of human Jagged1.	Developmental Studies Hybridoma Bank (DSHB), USA.
Rat Anti-Notch1	bTAN20	A monoclonal antibody that is specific for the intracellular domain of human Notch1.	DSHB.
Rat Anti-Notch2	C651.6 DbHN	A monoclonal antibody that is specific for the intracellular domain of human Notch2.	DSHB.
Rabbit anti-rat biotinylated	Anti-rat biotinylated	A polyclonal antibody that reacts with rat-IgG and is Biotinylated.	DAKO.

Goat anti-mouse IgG,	Anti-mouse	A goat anti-mouse antibody that reacts with mouse IgG, and is conjugated to AP.	Promega.
Alkaline Phosphatase (AP) Conjugate	IgG, AP conjugate		
Mouse anti-EBNA2	PE2	A monoclonal antibody that reacts with the latent gene product EBNA2.	Professor Rowe, University of Cardiff, Wales.
Mouse anti-His-HRP	Anti-His-HRP	A monoclonal antibody that reacts with polyHistidine residues, and is conjugated to horseradish peroxidase.	Sigma-Aldrich.
Mouse anti-LMP1	CS1-4	An affinity purified monoclonal antibody that reacts with EBV-encoded latent gene product LMP1.	Professor Rowe, University of Cardiff, Wales.

### 2.1.3 Bacterial strains

**Table 2-3 Bacterial Strains used in this study**

Bacterial Strain	Genotype
<i>E. coli</i> JM109	<i>e14</i> <sup>-</sup> ( <i>mcrA</i> <sup>-</sup> ), <i>recA1</i> , <i>endA1</i> , <i>gyrA96</i> , <i>thi-1</i> , <i>hsdR17(r<sub>K</sub><sup>-</sup>m<sub>K</sub><sup>-</sup>)</i> , <i>supE44</i> , <i>relA1</i> , $\lambda$ <sup>-</sup> , $\Delta$ (lac-proAB), [F' <i>traD36</i> , <i>proAB</i> , <i>lacI</i> <sup>R</sup> ZΔ M15].
<i>E. coli</i> M15 [pREP4]	<i>Nal</i> <sup>S</sup> , <i>Str</i> <sup>S</sup> , <i>Rif</i> <sup>S</sup> , <i>Thi</i> <sup>-</sup> , <i>Lac</i> <sup>-</sup> , <i>Ara</i> <sup>+</sup> , <i>Gal</i> <sup>+</sup> , <i>Mtl</i> <sup>-</sup> , <i>F</i> <sup>-</sup> , <i>RecA</i> <sup>+</sup> , <i>Uvr</i> <sup>+</sup> , <i>Lon</i> <sup>+</sup> pREP4 ( <i>lacI</i> <sup>R</sup> ) (Kan <sup>R</sup> )
<i>E. coli</i> RosettaBlue	<i>endA1</i> , <i>hsdR17(r<sub>K12</sub><sup>-</sup>,m<sub>K12</sub><sup>+</sup>)</i> , <i>supE44</i> , <i>thi-1</i> , <i>recA1</i> , <i>gyrA96</i> , <i>relA1</i> , <i>lac</i> [F' <i>proA</i> <sup>+</sup> <i>B</i> <sup>+</sup> <i>lacI</i> <sup>R</sup> ZΔM15 ::Tn10(tet <sup>R</sup> )] pRARE(argU, argW, ileX, glyT, leuW, proL) (Cm <sup>R</sup> ).
<i>E. coli</i> XL10-Gold	Tet <sup>R</sup> , $\Delta(\mu\chi\beta\alpha)$ 183 $\Delta(mcrCB-hsdSMR-mrr)173$ , <i>endA1</i> , <i>supE44</i> , <i>thi-1</i> , <i>recA1</i> , <i>gyrA96</i> , <i>relA1</i> , <i>lac</i> Hte[F' <i>proAB</i> <i>lacI</i> <sup>R</sup> ZΔM15 Tn10(tet <sup>R</sup> ) Amy Cam <sup>R</sup> ].

## 2.1.4 Bioinformatics software

A number of web-based bioinformatics tools listed in Table 2-4 were used routinely in this study.

**Table 2-4 Web-based bioinformatics tools used in this study**

Tool	Source	Use
BLAST	<a href="http://www.ncbi.nlm.nih.gov/">http://www.ncbi.nlm.nih.gov/</a> BLAST	Comparison of nucleotide or protein sequences to sequence databases and statistical significance of matches calculated.
ClustalW	<a href="http://www.ebi.ac.uk/clustalw/">http://www.ebi.ac.uk/clustalw/</a>	Sequence alignment.
Format converter	<a href="http://bioinformatics.org/JaM/BW/1/2/index.html">http://bioinformatics.org/JaM/BW/1/2/index.html</a>	Conversion of nucleotide sequences to Fasta and other formats.
NEB Cutter	<a href="http://tools.neb.com/NEBCutter2/index.php">http://tools.neb.com/NEBCutter2/index.php</a>	Identification of restriction enzymes sites along a DNA sequence.
NetPrimerLaunch	<a href="http://www.premierbiosoft.com/netprimer/netprlaunch/netprlaunch.html">http://www.premierbiosoft.com/netprimer/netprlaunch/netprlaunch.html</a>	Primer analysis software for prediction of primer properties such as $T_m$ , GC content, likelihood of forming primer-dimers/hairpins.
PlasMapper	<a href="http://wishart.biology.ualberta.ca/PlasMapper/jsp/format.jsp">http://wishart.biology.ualberta.ca/PlasMapper/jsp/format.jsp</a>	Plasmid draw programme.
ProtParam	<a href="http://www.expasy.org/tools/protparam.html">http://www.expasy.org/tools/protparam.html</a>	Prediction of protein parameters such as molecular weight and extinction coefficients.
Translate tool	<a href="http://www.expasy.org/tools/translate.html">http://www.expasy.org/tools/translate.html</a>	Translation of a nucleotide (DNA/RNA) sequence to a protein sequence.

## 2.1.5 Plasmids

**Table 2-5 Expression and reporter constructs used in the study**

Plasmid	Source	Description
pSG5	Lindsey Spender, Ludwig Institute for Cancer Research, Imperial College School of Medicine, London.	pSG5-EBNA2 expresses the wild type B95.8 EBNA2 gene that has been cloned into pSG5 (Stratagene).
pGEM-3ZF	Promega.	This plasmid serves as a standard cloning vector and as a template for <i>in vitro</i> transcription with SP6 and T7 RNA polymerase promoters flanking a region of multiple cloning sites.
pGEM- <i>bfl-1</i> -RP	This study.	pGEM- <i>bfl-1</i> -RP is capable of <i>in vitro</i> transcription of sense and antisense riboprobes to <i>bfl-1</i> .
pCDNA3 HA- <i>bfl-1</i>	Dr. G. Chinnadurai, Saint Louis University School of Medicine, Missouri, U.S.A.	Expresses Bfl-1 protein tagged to the influenza virus HA epitope (D'Sa Eipper <i>et al.</i> , 1996).
pEFBOSneo	Professor Kenji Tanigaki, Department of Medical Chemistry, Kyoto University, Kyoto, Japan.	pEFBOSneo-R218H expresses a mutant RBP-Jκ/CBF1 where an arginine residue at position 218 has been replaced with a histidine residue (Chung <i>et al.</i> , 1994) cloned into the empty vector pEFBOSneo (Kato <i>et al.</i> , 1997).
pRTS-1	Professor Dr. med. Georg W. Bornkamm, GSF-Research Centre for Environment and Health, Institute of Clinical Molecular Biology and Tumour Genetics, Munich, Germany.	Novel tetracycline-inducible vector carrying all the elements for conditional gene expression including the gene of interest on one EBV-derived episomally replicating plasmid (Bornkamm <i>et al.</i> , 2005).

---

pRTS-1-HA- <i>bfl-1</i>	This study.	Generated by insertion of HA- <i>bfl-1</i> ORF into pRTS-1, capable of conditional expression of HA-tagged Bfl-1 protein.
pSG5-LMP1 pSG5-LMP1 <sup>AAAG</sup>	Professor Martin Rowe, University of Wales, College of Medicine, Cardiff, UK.	pSG5-LMP1 expresses wild type B95.8 LMP1, which has been cloned in front of the SV40 promoter, contained in pSG5 (Stratagene). pSG5 LMP1 <sup>AAAG</sup> expresses LMP1 with amino acids proline 204, glutamine 206 and threonine 208 mutated to alanine and amino acid 384 changed from tyrosine to glycine (Floettmann <i>et al.</i> , 1998).
pEFCX pEFCX-I $\kappa$ B $\alpha$ DN	Dr. Peter Brodin, Umea University, Sweden.	pEFCX-I $\kappa$ B $\alpha$ DN expresses a super-repressor mutant form of I $\kappa$ B $\alpha$ in which the serine residues at positions 32 and 36 have been replaced with alanines. pEFCX is the empty vector (Liljeholm <i>et al.</i> , 1998).
pCMV-LacZ	Clontech.	pCMV-LacZ contains <i>E.coli</i> $\beta$ -galactosidase gene under the control of the CMV promoter-enhancer.
-1374/+81-Luc -1374/+81 m $\kappa$ B (-52) -1374/+81 m $\kappa$ B (-833)	Dr. Brendan D'Souza, School of Biotechnology, Dublin City University.	-1374/+81-Luc was generated by sub-cloning the <i>bfl-1</i> promoter sequence from a corresponding CAT reporter construct (Zong <i>et al.</i> , 1999) into pGL2-Basic. -1374/+81 m $\kappa$ B (-52) contains a mutation at the NF- $\kappa$ B-like binding site at position -52 to -43 (D'Souza <i>et al.</i> , 2004). -1374/+81 m $\kappa$ B (-833) contains a mutation at the NF- $\kappa$ B-like binding site at position -833.

---

---

(D'Souza *et al.*, 2004).

-1374/+81 (mCBF1 -249)	Dr. Pamela Pegman, School of Biotechnology, DCU, Dublin, Ireland.	A luciferase reporter construct where the putative RBP-Jκ binding site at -243 to -249 on the wt <i>bfl-1</i> promoter has been mutated to an <i>Xba</i> I restriction site (Pegman <i>et al.</i> , 2006).
3x enh κB luc	Professor Martin Rowe, University of Wales College of Medicine, Cardiff, U.K.	This reporter construct contains 3 κB elements upstream of a minimal conalbumin promoter linked to the firefly luciferase gene (Floettmann and Rowe, 1997).
pGA50-7 pGA981-6	Dr. Bettina Kempkes, Institute of Clinical Molecular Biology and Tumour Genetics, GSF, Munich, Germany.	The pGa981-6 reporter construct (Minoguchi <i>et al.</i> , 1997) was generated using a 50 bp oligonucleotide harbouring both CBF1 binding sites of the EBV <i>TPI</i> promoter, which was then ligated as a hexamer into plasmid pGa50-7 (Laux <i>et al.</i> , 1994a).
pQE60/pQE30	QIAgen.	High-copy number expression vectors for expression of C- or N-terminal 6xHis-tagged fusion proteins respectively.
pGSLink	This study.	High-level expression vector for expression of N- or C-terminal 6xHis-tagged fusion proteins linked to protein of interest via a flexible peptide linker (Loughran <i>et al.</i> , 2006).
pGSLink-N-Bfl-1 pGSLink-C-Bfl-1	This study.	High-level expression vector for expression of N- or C-terminal 6xHis-tagged fusion protein linked to Bfl-1 via a flexible peptide linker (Loughran <i>et al.</i> , 2006).

## 2.1.6 Oligonucleotides

**Table 2-6 Oligonucleotides used in the study**

All oligonucleotides were synthesised by and obtained from MWG-Biotech, Ebersberg, Germany.

Target	Primer Sequence
bfl(30)F	5'- <u>CGCGGATCC</u> CACAGACTGTGAATTGG-3'
bfl(30)R	5'- CCC <u>AAGCTT</u> ACAGTATTGCTTCAGGAG-3'
bfl(60)F	5'-CATGCC <u>ATGG</u> CAACAGACTGTGAATTGG-3'
bfl(60)R	5'-CGCG <u>GATCC</u> CACAGTATTGCTTCAGGAG-3'
BFL-1 EXT F	5'-ATATATTACAGGCTGGCTCA-3'
BFL-1 EXT R	5'-AGCATTACAGATCTTCCT-3'
BFL-1 INT F	5'-CTGGGGAAAGAATTGTAACCAT-3'
BFL-1 INT R	5'-CTTCTAGAAAAGTCATCCAGC-3'
Bfl1F	5'-TTCATATTTGTTGCGGAGTTC-3'
Bfl1R	5'-AGCATTACAGATCTTCCT-3'
Bfl-1RevSfiI	5'-AATT <u>CGCGGGCCTCACTGGCCT</u> CAACAGTATTGCTTCAG-3'
GAPDH F	5'-TGCACCACCAACTGCTTA-3'
GAPDH R	5'-GATGATGTTCTGGAGAGC-3'
GS-C-bflF	5'-CATGCC <u>ATGG</u> CAACAGACTGTGAATTGG-3'
GS-C-bflR	5'-CTCCCC <u>CCGG</u> ACAGTATTGCTTCAGGAG-3'
GSLinkF	5'-CATGCC <u>ATGG</u> CGCATCACCACCACTCACCA CCC <u>GGGTGGCG</u> g <sub>gg</sub> g <sub>cc</sub> g <sub>gg</sub> g <sub>cc</sub> g <sub>gg</sub> g <sub>cc</sub> g <sub>gg</sub> -3'
GSLinkR	5'-CGGG <u>GATCC</u> AACACCACCAACCAGAAC CACCAACCAGAAC <sub>gg</sub> cc <sub>cc</sub> g <sub>cc</sub> g <sub>gg</sub> g <sub>cc</sub> g <sub>cc</sub> g <sub>gg</sub> -3'
GS-N-bflF	5'-CGCG <u>GATCC</u> CACAGACTGTGAATTGG-3'
GS-N-bflR	5'-CCC <u>AAGCTT</u> ACAGTATTGCTTCAGGAG-3'
HABf1ForSfiI	5'-TCT <u>ATGGGCCTCACTGGC</u> ATGGTTACCCATACGATGT-3'
pEBNAseqFor	5'-CAAGCTTT <u>CGGCCTCACTGGCC</u> -3'
pQE For	5'-GTATCACGAGGCC <u>TTTCGTCT</u> -3'
pQE Rev	5'-CATTACTGGATCTATCACAGGAG-3'
RiboFor	5'-CCC <u>AAGCTT</u> CAGGCTGGCTCAGGACTATCTGCA-3'
RiboRev	5'-CCGG <u>ATTCTCGT</u> AGAACGTTCTTGATGAGAAT-3'
RT Primer1	5'-AGCTCAAGACTTTGCTCTCCACC-3'
RT Primer2	5'-TGGAGTGCCTTCTGGTCAACAG-3'
T7 primer	5' -TAATACGACTCACTATAAGGG-3'

Restriction enzymes sites are underlined. GSLinkF/GSLinkR homology in lowercase. The sequences of all primers were designed so as to avoid primer-dimer/hairpin

loop/cross-dimer formation and to have similar G/C content/T<sub>m</sub> as predicted using the NetPrimerLaunch bioinformatics tool (Table 2-4).

## 2.2 Chemical Materials

**Table 2-7 Suppliers of chemical and biological materials**

Supplier	Product (Code)
<b>Advanced Biotechnologies</b>	ISH Geneframes and coverslips (AB0576/7/8)
<b>Amaxa GmbH</b>	Cell Line Nucleofector Kit L (VCA-1005).
<b>Ambion</b>	Anti-bfl-1 ID#120800 siRNA (16708A), anti-bfl-1 ID#120801 siRNA (16708A), anti-bfl-1 ID#120802 siRNA (16708A), GAPDH silencer siRNA including anti-scrambled RNA negative control siRNA (4624), siPORT transfection buffer (8991).
<b>Amersham</b>	Rainbow full range molecular weight marker (RPN800).
<b>Applied Biosystems</b>	β-Actin Endogenous control TaqMan assay (Hs_99999903m1), Bfl-1(Bcl2A1) TaqMan assay (Hs_00187845m1), GAPDH Endogenous control TaqMan assay (Hs_99999905m1), TaqMan universal PCR master mix (4364341).
<b>BDH</b>	Bromophenol blue (44385), EDTA (280254D), Eosin (CB350844K), Glycine (444495D), Haemalum (CB350604T), Hydrochloric acid (28507BF), Isopropanol (296946H), Magnesium sulphate (29117), Mayer's haematoxylin (CC36048), Methanol (29192BL), Nitrocellulose membrane (436107E), Paraformaldehyde (CB294474L), Potassium acetate (295814P), Sodium dihydrogen orthophosphate (30716), Sucrose (102745C), Tris base (271195Y).
<b>Becton-Dickinson</b>	FACS flow (342003).
<b>DAKO</b>	Biotinylated rabbit antirat IgG (E0468).
<b>DSHB</b>	Anti-Jagged1 antibody (TS1.15H), Anti-Notch1 (bTAN20), Anti-Notch2 (C651.6 DbHN).
<b>Invitrogen</b>	100 bp DNA ladder (15628-019), 1 kb DNA ladder (15615-016), DMEM high glucose (10938-025), Foetal calf serum (10270-106), Non-essential amino acids 100 X (11140-035), RPMI 1640 (31870-025), Trypan blue (15250-061), Trypsin (25090-028), Versene (15040-033), Vitamin solution 100 X (11120-037), Yeast tRNA (15401011). Vybrant apoptosis assay Kit (V13241).
<b>Labscan</b>	Chloroform (A3505E).
<b>Merck</b>	BAY11(7082) (196870), Calcium chloride (23821000), Glacial acetic acid (100632511), Magnesium chloride (1058321000), Potassium Hydroxide (50321000), Sodium carbonate (A654792), Ribojuice (7115-3), di-Sodium hydrogen phosphate (1065860500).
<b>Millipore</b>	Amicon Ultrafilter (UFC8 00508)

<b>National</b>	Acrylagel (EC810), Bis-acrylagel (EC820).
<b>Diagnostics</b>	
<b>New England</b>	Calf Intestinal Phosphatase & 10 X dephosphorylation buffer (M0290L),
<b>Biolabs</b>	Restriction enzymes, 10 X buffers and 100 X BSA, T4 DNA Ligase (M0202L).
<b>Oxoid</b>	Agar (L13), PBS tablets (BR14), Tryptone (L42), Yeast extract (L21).
<b>PALM</b>	1 mm PALM membrane slides (1440-1600).
<b>Microlaser</b>	
<b>Promega</b>	Anti-Mouse IgG-AP conjugated (S3721), dNTPs (U1330), Cell Proliferation Assay Kit (TB245), <i>E. coli</i> JM109 cells (P9751), Luciferase Assay System (E1501), Magnesium chloride 25 mM (A3511), M-MLV reverse transcriptase & RT buffer (M1701), 5 X Reporter lysis buffer (E3971), RNasin (N2111), Wizard® PCR Preps DNA purification system (A7170).
<b>QIAgen</b>	Ni-NTA resin (30210), Ni-NTA spin columns (31314), Omniscript and Sensiscript RT Kits (205211), QIAgen® Plasmid Purification Kit (12143), SYBR Green Kit (204143), RNeasy Purification Kit (74104).
<b>Roche</b>	Anti-HA-peroxidase High affinity (12013819001), Hygromycin B (843555), Leupeptin (1017128), DIG-labelling kit (SP6 RNA polymerase, T7 RNA polymerase) (11 175 025 910).
<b>Sigma-Aldrich</b>	3 M sodium acetate, pH5.2 (S7899), Anti-DIG antibody (D8156), Anti-HIS-HRP (A7058), Agarose (A5093), Ampicillin (A9518), Anti-β-actin antibody (A1978), Aprotinin (A4529), APS (215589), BCIP-NBT (B3679), Bovine serum albumin (A9647), Chelating resin (C7901), Chloroform: isoamyl alcohol (24:1) (C0549), Colorburst electrophoresis markers (C4105), Coomassie Brilliant Blue R (B0149), DEAE-dextran (D9855), DEPC (D5758), DMEM: F12 Hams (D6421), DMSO (D8779), DNase I and DNase I digestion buffer (AMPD1), Ethanol ACS grade 100 % proof (459844), β-estradiol (E8875), Ethidium bromide (E4391), Formamide (F7503), G418 (A1720), Glucose (G7528), Glycerol (G5516), Hydrocortisone (H4001), Hydrogen peroxide (H1009), <i>In situ</i> hybridisation solution (H7782), Insulin (I5500), L-glutamine (G7513), Manganese chloride (M3634), Molecular grade/Nuclease-free water (W4502), MOPS (M3183), ONPG (N1127), PAP pen (Z377821), Penicillin/streptomycin (P0781), Phenol:chloroform:isoamyl alcohol (25:24:1) (P3803), PMSF (P7626), Ponceau S (P7170), Potassium chloride (P4504), Propidium iodide (P4170), Puromycin (P8833), RedTaq Polymerase (D4309), RNase A (R6513), RNase-ZAP (R2020), Rubidium chloride (R2252), SDS (L6026), Sigmafast DAB reagent (D0426), Sodium Arsenite (35000), Sodium chloride (S3014), Sodium hydroxide (S5881), Tetracycline (T7660), TEMED (T7024), TMB substrate (T0565), Tri reagent (T9424), Tween 20 (P1379), Xylene cyanol FF (33594).
<b>Stratagene</b>	Absolute RNA Nanoprep Kit (400753), <i>E. coli</i> XL-10Gold ultracompetent cells (200314).
<b>Surgipath</b>	DPX mounting reagent (01705), Scott's tap water (02900).
<b>Europe</b>	

## 2.3 DNA Manipulation

### 2.3.1 Storage of DNA samples

DNA samples were stored in Tris-EDTA (TE; 10 mM Tris-Cl, 1 mM EDTA) buffer (pH 8.0) (Appendix) at 4 °C. EDTA was used to chelate heavy metal ions that are needed for DNase activity while storage at pH 8.0 minimises de-amidation.

### 2.3.2 Phenol/chloroform extraction and ethanol precipitation

Phenol/chloroform extraction and ethanol precipitation were carried out to concentrate nucleic acid samples or change the buffers in which a sample was dissolved. An equal volume of phenol:chloroform:isoamyl alcohol (25:24:1) was added to the DNA solution, mixed by vortexing and centrifuged for 10 minutes at 13,000 x g. The upper aqueous phase was removed, avoiding any material at the interphase, and placed in a sterile microfuge tube. An equal volume of chloroform:isoamyl alcohol (24:1) was added to the aqueous phase, vortexed as before, and centrifuged for 5 minutes at 13,000 x g. Again the upper aqueous phase was removed to a fresh tube. One-tenth volume of 3 M sodium acetate (pH 5.2) (Sigma-Aldrich) was added to the solution of DNA, mixed and followed by addition of 2 volumes of 100 % (v/v) ethanol. This mixture was vortexed and incubated at -80 °C for >5 minutes. The DNA samples were then centrifuged for 30 minutes at 12,000 x g at 4 °C, the supernatant was removed and pellets were washed with 1 ml 70 % (v/v) ethanol to remove excess salts. The samples were then centrifuged for 5 minutes at 10,000 x g, the supernatant was removed and pellets were air dried for approximately 10 minutes at room-temperature. Pellets were re-suspended in an appropriate volume of sterile TE (pH 8.0) or dH<sub>2</sub>O.

### **2.3.3 Restriction digestion of DNA**

Restriction digestion of DNA was carried out for identification purposes, for plasmid linearisation or to cut particular fragments from a plasmid. Restriction enzymes specifically bind and cleave double-stranded DNA at specific sites within or adjacent to a particular sequence, which is known as the recognition site. Restriction digestion patterns were predicted for DNA sequences using the NEBCutter bioinformatics tool (Table 2-4). All restriction enzymes used were supplied with incubation buffers at a concentration of 10 X (working concentration 1 X). DNA digestion reactions were set up according to manufacturer's instructions (New England Biolabs) and incubated for 2.5 h at the optimum enzyme temperature (between 37 °C and 50 °C, usually 37 °C).

### **2.3.4 Dephosphorylation of linearised plasmid DNA**

To minimise re-circularisation of linearised DNA required for ligation, treatment with calf intestinal phosphatase (CIP) is required. This dimeric glycoprotein prevents re-circularisation by removing the 5' phosphate groups on the linearised DNA molecule. Digested DNA (<100 ng/μl) was de-phosphorylated using CIP in a 100 μl volume (1 unit/100 pmoles for cohesive termini) according to the manufacturer's protocol (New England Biolabs) and incubated for 30 minutes at 37 °C. This was followed by an enzyme denaturation step achieved by heating to 75 °C for 10 minutes. Where appropriate, the DNA was then purified by phenol:chloroform extraction and ethanol precipitation as described in Section 2.3.2. The purified linearised, CIP-treated DNA was stored at 4 °C until required for ligation.

### **2.3.5 Polymerase chain reaction**

The polymerase chain reaction (PCR) was used to amplify target sequences of DNA for sub-cloning into linearised vectors, or for identification purposes. PCR involves the amplification of specific DNA sequences using DNA primers, which anneal to the DNA of interest. The primers are designed so that one anneals to the forward DNA strand and the other anneals to the reverse strand thus allowing polymerisation of both strands by the enzyme *Taq* DNA polymerase. This results in exponential amplification of the

sequence of interest. PCR reactions were set up by addition of reagents in the order listed in Table 2-8.

**Table 2-8 PCR Reactants**

Component	Volume
dH <sub>2</sub> O	37 µl
Template DNA (~500 ng)	1 µl
Forward primer (40 pmole)	2.5 µl
Reverse primer (40 pmole)	2.5 µl
10 X enzyme buffer (+15 mM MgCl <sub>2</sub> )	5 µl
dNTP mix (each at 5 mM)	2 µl
Taq polymerase (5 U/µl)	1 µl

All PCR reactions were carried out in a Hybaid thermocycler using the conditions listed in Table 2-9.

**Table 2-9 PCR Thermocycling conditions**

Stage	Step	Number of cycles
<u>Denaturation</u>	95 °C, 5 minutes	} 1 Cycle
<u>Denaturation</u>	95 °C, 45 seconds	
<u>Annealing</u>	X °C, 45 seconds	30 Cycles
<u>Extension</u>	72 °C, 1 minute	} 1 Cycle
<u>Extension</u>	72 °C, 8 minutes	

X = Annealing temperature was calculated by subtracting 5 °C from the melting temperature ( $T_m$ ) of a primer pair. Primers are listed in Table 2-6.  $T_m = [2*(A/T content) + 4*(G/C content)]$ .

### 2.3.5.2 Cassette extension by PCR

A glycine-serine linker was introduced into the pQE60 vector (Table 2-5) to allow production of a protein of interest (namely the Bfl-1 protein) spatially separated from the His-tag moiety by a flexible linker (Chapter 7). First, a DNA fragment was designed so as to encode a 6XHis-tag domain followed by the chosen linker peptide, which consisted of 21 glycine and serine residues [(Gly4Ser)4Gly; GS Linker]. This sequence

was generated by annealing two partially overlapping oligonucleotides, GSLinkF and GSLinkR (Table 2-6), followed by extension and amplification by PCR using the conditions listed in Table 2-10.

**Table 2-10 Cycling conditions for PCR extension of Linker cassette**

Cycle	Temperature	Duration	Cycles
Denature	95 °C	2.5 min	1
Cycling	95 °C	50 sec	15
	56 °C	50 sec	
	72 °C	30 sec	
Extension	72 °C	5 min	1

### 2.3.6 Purification of PCR products

PCR products were purified from contaminants (including primer-dimers and amplification primers) using the Promega Wizard® PCR Preps DNA Purification System according to the manufacturers instructions. The purified DNA was stored at 4 °C until required for further use.

### 2.3.7 Ligation of DNA molecules

Cohesive end ligations of equimolar amounts of vector and insert DNA (1 µg) were carried out overnight at 16 °C or for 3 h at 22 °C in a commercial ligation buffer (containing 5 mM ATP) with 10 units of T4 DNA ligase/ml in a total volume of 10 µl. After ligation, the samples were heated at 70 °C for 10 minutes to inactivate the ligase and were transformed immediately or stored at –20 °C until required for transformation.

### **2.3.8 Preparation of competent cells**

XL10-Gold *E. coli* ultracompetent cells were purchased from Stratagene. A modified Rubidium chloride ( $\text{RbCl}_2$ ) method was employed to prepare competent cells of *E. coli* strains; JM109 and RosettaBlue<sup>TM</sup> (as described in Hanahan, 1985). All buffers were as described in the Appendix. *E. coli* JM109 and RosettaBlue<sup>TM</sup> competent cells prepared by this method and stored at  $-70^{\circ}\text{C}$  were stable for 1 year.

### **2.3.9 Transformations**

Competent cells were transformed with DNA by heat shock as described in Sambrook *et al.*, 1989. All buffers were as described in the Appendix. Transformed cells were plated on LB plates containing the appropriate antibiotic (Appendix; usually ampicillin at a concentration of 100  $\mu\text{g/ml}$ ) and incubated overnight at  $37^{\circ}\text{C}$ . Transformed cells were resistant to the antibiotic and cells yielded colonies. These colonies were subsequently used to prepare broth cultures for DNA mini-preparations.

### **2.3.10 Small scale preparation of plasmid DNA (Miniprep)**

A single bacterial colony was used to inoculate 5 ml of LB broth (with appropriate antibiotic) and incubated overnight at  $37^{\circ}\text{C}$ . An aliquot (1.5 ml) of this culture was transferred to a sterile microfuge tube and centrifuged for 30 seconds at room temperature; the remainder was stored at  $4^{\circ}\text{C}$ . The supernatant was removed from the tube, leaving the pellet as dry as possible. Plasmid DNA was purified according to the manufacturer's instructions (QIAGEN Plasmid Purification Handbook, 2005). All buffers were as described in the Appendix. Glycerol stocks of all bacterial cultures were prepared at this stage by the addition of 0.5 ml of a 50 % (v/v) glycerol solution (Appendix) to 0.5 ml of the overnight bacterial culture of interest and stored at  $-80^{\circ}\text{C}$ .

### **2.3.11 DNA purification protocol (Maxiprep)**

Plasmid DNA was purified using the QIAgen Plasmid Midi Kit according to the manufacturer's instructions (QIAGEN Plasmid Purification Handbook, 2005). Purified DNA was quantified by spectrophotometric analysis.

### **2.3.12 Spectrophotometric analysis of nucleic acids**

DNA/RNA concentration was determined by measuring the absorbance at 260 nm, which is the wavelength at which nucleic acids absorb maximally ( $\lambda_{max}$ ). A 50 µg/ml preparation of pure DNA has an absorbance of 1 unit at 260 nm, while 40 µg/ml of pure RNA has an absorbance reading of 1 at this wavelength. The purity of a RNA or DNA preparation was determined by reading absorbance at 260 nm (the  $\lambda_{max}$  for nucleic acids) and at 280 nm (the  $\lambda_{max}$  for proteins) and obtaining the ratio for these absorbances. Pure DNA and RNA have  $A_{260}/A_{280}$  ratios of 1.8 and 2.0 respectively. Lower ratios indicate the presence of protein while higher ratios often indicate residues of organic reagents. Absorbances were read on the Shimadzu UV-160A spectrophotometer using a quartz cuvette or using a Nanodrop spectrophotometer by direct aliquoting onto the measuring platform. Nucleic acid concentrations were determined according to the following equations:

$$\text{DNA } (\mu\text{g}/\mu\text{l}) = \frac{\text{Absorbance (260 nm)} \times 50 \times \text{dilution factor}}{1000}$$

$$\text{RNA } (\mu\text{g}/\mu\text{l}) = \frac{\text{Absorbance (260 nm)} \times 40 \times \text{dilution factor}}{1000}$$

### **2.3.13 Agarose gel electrophoresis of DNA**

Electrophoresis through agarose gel is the standard method used to separate, identify, and in some cases purify DNA fragments. Agarose gels were prepared as detailed in Sambrook *et al.*, 1989. The Hybaid horizontal gel electrophoresis system was used for

electrophoresis at constant voltage (5 V/cm), for 1 to 2 h. After completion, the gel was stained in ethidium bromide (0.5 mg/ml; Appendix) for 30 minutes, destained in dH<sub>2</sub>O for 15 minutes, viewed under UV illumination and photographed using a UV image analyser.

### **2.3.14 DNA Sequencing**

Sequencing of plasmid DNA was performed to ensure the nucleic acid fidelity and ‘in-frame’ insertion of DNA fragments following cloning. Plasmid DNA as prepared in Section 2.3.11 was quantified (Section 2.3.12) and 1-2 µg (typically 1-2 µl) was transferred to a sterile 1.5 ml eppendorf. The DNA was lyophilised in a Savant DNA110 speed vac on the low heat setting for 15-20 minutes or until the solvent had evaporated. The lyophilised DNA was sent to MWG-Biotech, Ebersberg, Germany for sequencing. Sequencing forward and reverse primers were supplied by MWG-Biotech for most commercially available cloning systems. In the absence of existing sequencing primers (as in the case of the pRTS-1 vectors), a forward and/or reverse primer was designed and purchased and 100 pmol of primer was transferred to a sterile eppendorf and sent with each sequencing reaction to MWG-Biotech.

## **2.4 Cell Culture Methods**

All cell culture techniques were performed in a sterile environment using a Holten laminar flow cabinet. Cells were visualised with an Olympus CK2 inverted phase contrast microscope. All media compositions and media supplements are given in the Appendix.

### **2.4.1 Culture of cells in suspension**

Suspension cell lines (all detailed in Table 2-1) were maintained in RPMI 1640 supplemented with 10 % (v/v) foetal bovine serum (FBS), 2 mM L-glutamine, 100 µg/ml streptomycin and 100 U/ml penicillin. Cultures were seeded at a density of 2 x 10<sup>5</sup> to 5 x 10<sup>5</sup> cells per ml in 25 cm<sup>2</sup> flasks and expanded in 75 cm<sup>2</sup> flasks. Cells were sub-cultured two or three times per week by harvesting into a sterile centrifuge tube and pelleting at 100 x g for 5 minutes at room temperature. The cell pellet was re-suspended gently in an appropriate volume of fresh supplemented media and replaced into the tissue culture flask. All cell lines were incubated in a humidified 5 % CO<sub>2</sub> atmosphere at 37 °C in a Heraeus cell culture incubator.

### **2.4.2 Culture of adherent cells**

The HtTA-jag10 cell line (Table 2-1; HeLa-derived cell line expressing Jagged1 under tetracycline control) was maintained in high glucose Dulbecco modified Eagle medium (DMEM) supplemented with 10 % (v/v) FBS, 1 % (v/v) non-essential amino acids and 1 % (v/v) MEM vitamins, 2 mM L-glutamine, 100 µg/ml streptomycin, 100 U/ml penicillin, 125 µg/ml G418, 225 U/ml Hygromycin and 2µg/ml tetracycline. HtTA-jag10 cells were seeded into 25 cm<sup>2</sup> and 75 cm<sup>2</sup> tissue culture flasks. Adherent cells were detached by treatment with Versene solution (Invitrogen). For versenisation the medium was decanted and the cells were washed with 2 ml of sterile 1X PBS to remove any residual serum. A volume of 2 ml of 1X versene solution was added to each flask and the flasks incubated at 37 °C for 5 minutes or until all the cells could be visualised as having detached from the flask surface. The cell suspension was then decanted into a sterile centrifuge tube containing 5 ml of sterile supplemented media and centrifuged at

100 x g for 5 minutes. Cells were resuspended in supplemented media at 2 to 5 x 10<sup>5</sup> cells/ml, using 5 ml per 25 cm<sup>2</sup> flask and 15 ml per 75 cm<sup>2</sup> flask and incubated in a humidified 5 % CO<sub>2</sub> atmosphere at 37 °C in a Heraeus cell culture incubator.

#### **2.4.3 Co-culture of adherent and suspension cells**

HtTA-jag10 cells were plated in duplicate in 10 cm dishes in the presence of tetracycline. Jagged1 expression was induced by washing HtTA-jag10 cells three times in medium lacking tetracycline 24 h and 48 h after plating. After 72 h, the cells were overlaid with L428 or L591 cells in suspension (2.5 x 10<sup>6</sup> cells/dish). The co-cultures were incubated for 48 h. Firm tapping was used to dislodge the lymphoid cells that aggregated onto the adherent cell monolayer, prior to lysis of co-cultivated lymphoid cells.

#### **2.4.4 Cell Counts**

Cell counts were performed using an improved Neubauer haemocytometer slide. Trypan blue exclusion dye was routinely used to determine cell viability. A volume of 10 µl of trypan blue was added to 90 µl of a cell suspension and mixed. A volume of 10 µl of this mixture was added to the counting chamber of the haemocytometer and cells were visualised by light microscopy. Viable cells excluded the dye and remained clear while dead cells stained blue. Cell numbers were ascertained by multiplying the average cell count (of 3 individual counts) by the dilution factor (usually 1.1) and again by the volume of the haemocytometer chamber (1 x 10<sup>4</sup> cells/ml). Thus, cell counts were expressed as the number of cells per ml.

#### **2.4.5 Cell storage and recovery**

In order to prepare stocks of suspension cells for long-term storage, 1 x 10<sup>7</sup> cells in exponential phase were pelleted and re-suspended in 750 µl of supplemented RPMI to which 150 µl of FBS was added, and then placed on ice for 10 minutes. DMSO was added to a final concentration of 10 % (v/v), mixed gently and transferred to a sterile

cryotube. In the case of adherent cells, one confluent 75 cm<sup>2</sup> flask of cells was used per cell stock. Adherent cells were washed with 1 X PBS followed by trypsinisation and re-suspended in 900 µl of FBS and 100 µl of DMSO. The cells were mixed gently and added to a sterile cryotube.

The cryotubes were slowly lowered into the gas phase of liquid nitrogen and then immersed in liquid nitrogen in a cryofreezer (Cooper Cryoservices).

Cells were recovered from liquid nitrogen by thawing rapidly at 37 °C and transferring to a sterile centrifuge tube containing 5 ml of pre-warmed supplemented media. The cells were centrifuged at 100 x g for 5 minutes, the pellet was re-suspended in 5-10 ml of fresh supplemented media, transferred to a culture flask and incubated at 37 °C in 5 % CO<sub>2</sub>.

## 2.4.6 Transient transfections

Transient transfection of cells was performed by electroporation, nucleofection, using the propriety formulation; Ribojuice or using the DEAE-dextran method. In all cases, cells were seeded at a density of 2.5 x 10<sup>5</sup> per ml of media 24 h prior to transfection. After 24 h in culture, cells were counted again, it was essential for cell numbers to have almost doubled before beginning the transfection, thus ensuring that cell growth was in logarithmic phase, allowing for optimal DNA/RNA uptake during transfection. The same quantity of total DNA/RNA was used per transfection.

### 2.4.6.1 Electroporation of B lymphocytes

Transfection of L428 and L591 cell lines (Table 2-1) was carried out by electroporation. During the electroporation method of transfection, the application of brief high voltage electric pulses to the cells leads to the formation of nanometer-sized pores in the plasma membrane. DNA is taken directly into the cell cytoplasm either through these pores or as a consequence of redistribution of membrane components that accompanies the closure of the pores.

Total DNA (10-20 µg per transfection) dissolved in 30 µl TE buffer (pH 8.0) was transferred into a sterile electroporation cuvette. A total of 1 x 10<sup>7</sup> cells were used per

transfection. Cells were centrifuged at 100 x g for 5 minutes and the supernatant discarded. The cells were then washed in PBS, centrifuged at 100 x g for 5 minutes and the supernatant again discarded. For each  $1 \times 10^7$  cells, 220  $\mu$ l of serum-free media was used for re-suspension and the cells transferred to the DNA-containing electroporation cuvettes. The cell/DNA mix was incubated at room temperature for 5 minutes. Each cell/DNA mix was then pulsed at 250 V with a capacitance of 960  $\mu$ F (using a capacitance extender) and resistance set to infinity using a Biorad Gene Pulser. Immediately after electroporation the cuvettes were placed on ice until the cell/DNA mix was transferred into 5 ml supplemented media in a 6 well dish. Transfected cells were harvested 48 h later.

#### **2.4.6.2 Nucleofection of B lymphocytes**

The Nucleofector technology is based on electroporation. It consists of the Nucleofector device II (Amaxa), which delivers a cell-specific combination of electrical parameters, and Nucleofector Solutions, in which the cells are contained while the unique electrical program is executed. Optimised conditions for nucleofection of L428 cells were pre-determined and yielded 80 % transfection efficiency.

The cell line nucleofector solution L was pre-warmed to room temperature and 50 ml of supplemented media was pre-warmed to 37 °C. Supplemented medium (2 ml) was aliquoted into the appropriate numbers of wells of a 6 well plate and pre-incubated at 37 °C/5 % CO<sub>2</sub>/humidified atmosphere. A total of 2  $\mu$ g DNA was prepared in sterile 1.5 ml eppendorfs for each sample. For each transfection,  $1 \times 10^6$  cells were pelleted by centrifugation at 90 x g for 10 minutes and the supernatant was discarded completely so that no residual medium remained. The pellet was resuspended in room-temperature solution L to a final concentration of  $1 \times 10^6$  cells/100  $\mu$ l. Care was taken to ensure cells were stored in nucleofector solution no longer than 15 minutes to avoid reduction in cell viability/gene transfer efficiency. A volume of 100  $\mu$ l of cell suspension was mixed with the DNA and the nucleofection sample was transferred to an Amaxa-certified cuvette, taking care to avoid bubbles. The cuvette was placed in the nucleofection chamber and pulsed on program X-01. The sample was then incubated for 10 minutes at room temperature, after which time, 500  $\mu$ l of pre-warmed medium was added to the cuvette. The contents were gently transferred to the prepared 6-well plates and incubated at 37 °C/5 % CO<sub>2</sub>/humidified atmosphere until cells were harvested.

#### **2.4.6.3 RiboJuice-mediated transfection**

RiboJuice™ siRNA transfection reagent (Novagen), composed of a nontoxic cellular protein and a small amount of a novel polyamine, is used to deliver small interfering RNA (siRNA) into a wide range of mammalian cell lines for targeted gene suppression. L428 cells were diluted with medium to a density of  $1 \times 10^6$  cells per 250 µl in 6-well plates. A volume of 6 µl of transfection reagent was added to 244 µl of serum-free medium for each sample. After gentle vortexing, these samples were incubated for 5 minutes at room temperature. siRNAs (various concentrations) were then added to this solution and after a further 15-minute incubation the mixture was added dropwise to the cell suspension. Plates were left overnight at 37 °C under a 5 % CO<sub>2</sub>/humidified atmosphere.

#### **2.4.6.4 DEAE-Dextran-mediated transfection**

Transfection of DG75 cells was performed using this method of transfection. During transfection, positively charged DEAE-dextran binds to the negatively charged phosphate groups of the DNA, forming aggregates. These complexes, when applied to cells, subsequently bind to the negatively charged plasma membrane. It is believed that cellular uptake of DNA is mediated by endocytosis, further assisted by osmotic shock.

A total of up to 25 µg of DNA dissolved in dH<sub>2</sub>O was used per transfection. Total DNA was prepared in a sterile microfuge tube and brought to a volume of 600 µl with TBS (Appendix). Then, 600 µl of 1 mg/ml DEAE-dextran solution (Appendix) was mixed with the DNA solution. On the day of transfection,  $1 \times 10^7$  cells/transfection were centrifuged at 100 x g for 5 minutes and the supernatant was discarded. The cells were washed in PBS, centrifuged at 100 x g for 5 minutes and the supernatant again discarded. The cell pellet was gently re-suspended in the DNA/DEAE-dextran mix. The transfection cocktails were incubated at 37 °C for 30 minutes with gentle swirling every 5-10 minutes to allow homogenisation. Transfections were terminated by addition of 10 ml supplemented medium. The cells were pelleted by centrifugation at 100 x g for 5 minutes, washed in PBS as before and transferred to 25 cm<sup>2</sup> cell culture flasks

containing 10 ml supplemented media for incubation. Cells were harvested 48 h post transfection.

#### **2.4.6.5 Microscopic analysis following gene transfer**

Following some transfections gene transfer efficiency was monitored by fluorescence microscopy for green fluorescent protein (GFP)-expressing cells at 4–72 h post transfection. A volume of 600 µl of suspension cells was removed to a 1.5 ml sterile eppendorf and centrifuged at 100 × g for 5 minutes. The supernatant was discarded and the cell pellet was resuspended in 20 µl of PBS/0.5 % BSA and applied to a glass microscope slide. A coverslip was applied with care taken to avoid air bubbles and the slide was examined under bright field and fluorescent field microscopy using an Olympus DP-50 fluorescent microscope [excitation 450–500 nm, emission 515–565 nm] with a camera and StudioLife software (Olympus Optical Company).

#### **2.4.6.6 Harvesting cells post-transfection for luciferase/β-gal assays**

Cells were pelleted by centrifugation at 100 × g for 5 minutes at room temperature. The cells were washed once in sterile PBS and centrifuged again at 100 × g for 5 minutes. The supernatant was discarded, insuring all traces of PBS were removed from the pellet. The pellet was re-suspended in 50 µl of 1 X reporter lysis buffer (diluted with dH<sub>2</sub>O from a 5 X stock, Promega) and the cell suspension transferred to a microfuge tube. The tubes were vortexed for 10–15 seconds. The lysates were clarified by centrifugation at 13,000 × g for 5 minutes and the supernatant saved in a fresh tube. Samples were stored at –80 °C until luciferase/β-galactosidase assays were performed.

#### **2.4.6.7 Luciferase assay**

During transfections, promoter activity was determined by means of the luciferase assay. Firefly luciferase, a monomeric 61 kDa protein, catalyses luciferin oxidation using ATP-Mg<sup>++</sup> as a co-substrate. Light is produced by converting the chemical energy of luciferin oxidation through an electron transition, forming the product molecule oxyluciferin. In the conventional assay for luciferase, a flash of light is generated that decays rapidly after the enzyme and substrates are combined.

Luciferase assay reagent was prepared by reconstituting luciferase assay substrate with luciferase assay buffer (Promega) and stored in aliquots in the dark at -70 °C. At the time of assay, it was important to allow sufficient time for the luciferase detection reagent to equilibrate to room temperature. A volume of 20 µl of cell lysate was dispensed into individual wells in a white 96 well plate, along with 20 µl of 1 X lysis buffer to act as a blank. Subsequently, 100 µl of detection reagent was added to the lysate to initiate enzyme activity, mixed by repetitive pipetting (3 times) and light emission integrated over a period of 60 seconds, after lag period of 10 seconds, was measured on a luminometer (Labsystems Luminoskan 391A). Luciferase activity levels were adjusted for transfection efficiencies, estimated using  $\beta$ -galactosidase assay.

#### 2.4.6.8 $\beta$ -Galactosidase assay

When measuring the effect of promoters or enhancers on gene expression, it is essential to include an internal control that will distinguish differences in the level of transcription from differences in the efficiency of transfection or in the preparation of extracts. This is best achieved by co-transfected the cells with two plasmids: one that carries the construct under investigation, and another that constitutively expresses an activity that can be assayed in a separate experiment. An enzyme frequently used for this is *E. coli*  $\beta$ -galactosidase. The  $\beta$ -galactosidase ( $\beta$ -gal) assay is a convenient method for assaying  $\beta$ -gal activity in lysates prepared from cells transfected with  $\beta$ -gal reporter vectors, in this case pCMV-LacZ.

The  $\beta$ -gal assay was performed using a sample from the same lysates assayed for luciferase activity. Cell extract (30 µl) was added to 3 µl 100 X Mg solution, 66 µl 1 X *o*-nitrophenyl- $\beta$ -D-galactopuranoside (ONPG) and 201 µl 0.1 M sodium phosphate (all described in Appendix) and incubated at 37 °C for >30 minutes or until a faint yellow colour developed. This yellow colour development is the result of hydrolysis of ONPG by  $\beta$ -gal to form *o*-nitrophenyl. A reaction tube was included containing 1 X lysis buffer instead of cell lysate in order to obtain a background reading. Reactions were terminated by addition of 500 µl 1 M Na<sub>2</sub>CO<sub>3</sub> (Appendix). Optical densities were read at 420 nm using a Shimadzu spectrophotometer over a linear range of 0.2-0.8.

## **2.4.7 Stable Transfections**

Stable cells lines were established by transfection (as in Section 2.4.6) followed by selection with the appropriate drug 48 h later. Within 2-4 weeks drug resistant cells grew out. In some cases, specific drug concentrations for selection in individual cell lines were known from previous publications/projects, otherwise drug curves were prepared in advance of transfection to determine the minimum drug concentration to cause cell death. For the L428-pRTS-1-HA-bfl-1 cell line, stable clones were selected with hygromycin at 600 µg/ml, for the DG75-pRTS-1-HA-bfl-1, stable clones were selected with hygromycin at 400 µg/ml.

## **2.4.8 Measurement of Cell Proliferation**

The CellTiter 96 Aqueous One Solution cell proliferation assay is a colorimetric method for determining the number of viable cells in proliferation or cytotoxicity assays. The assay is based on the addition of a reagent containing a novel tetrazolium compound<sup>2</sup> (MTS) and an electron-coupling reagent<sup>3</sup> (PES) to cells in culture. The MTS tetrazolium compound is bioreduced by cells into a coloured formazon product that is soluble in cell culture media. This conversion is thought to be facilitated by NADPH or NADH produced by dehydrogenase enzymes in metabolically active cells (Berridge and Tan, 1993). The quantity of formazon product as measured by the amount of absorbance at a wavelength of 490 nm, is directly proportional to the number of living cells in culture.

To perform the assay, the CellTiter 96 Aqueous One Solution was thawed from frozen in a 37 °C water bath. Subsequently, 20 µl of reagent was added directly to 100 µl of cells in culture media (in triplicate) in 96-well plates. The plates were incubated at 37 °C/5 % CO<sub>2</sub> for 4 h and absorbance at 495 nm was measured using a Tecan Saffire II 96-well plate reader. Triplicate control wells containing media alone were prepared to correct for background absorbance.

---

<sup>2</sup> 3-(4,5-dimethylthiazol-2-yl)-5-(3-carboxymethoxyphenyl)-2-(4-sulfophenyl)-2H-tetrazolium, (MTS)

<sup>3</sup> phenazine ethosulphate, (PES)

#### **2.4.9 Acridine Orange/Ethidium Bromide staining**

Acridine orange is used to determine how many cells within a given population have undergone apoptosis, but it cannot differentiate between viable and nonviable cells. For this, a mixture of acridine orange and ethidium bromide is used. The differential uptake of these two dyes allows for the identification of viable and nonviable cells.

Early apoptotic cells have nuclei with apoptotic morphology and generally appear brighter than nonapoptotic nuclei due to chromatin condensation, but do not stain with ethidium bromide due to an intact plasma membrane. Late apoptotic and necrotic cells are diffusely red due to ethidium bromide staining of DNA and RNA. Live interphase cell nuclei fluoresce green and have variations in fluorescent intensity reflecting the distribution of euchromatin and heterochromatin. Apoptotic nuclei, in contrast, have highly condensed crescents around the periphery of the nucleus or the entire nucleus can be present as one or a group of featureless bright spherical beads.

The cells were pelleted by centrifugation at 100 x g for 5 minutes, washed with 5 ml of PBS (Appendix) and centrifuged at 100 x g for 5 minutes. The cell pellet was resuspended in 20 µl of PBS and applied to a glass microscope slide, then fixed in ice-cold 100 % (v/v) isopropanol for 5 minutes, and subsequently rehydrated in PBS for 10 minutes. The cells were stained with 10 µg/ml acridine orange/ethidium bromide (Appendix) for 5 min, rinsed with PBS, and visualised using an Olympus DP-50 fluorescent camera with StudioLife software (Olympus Optical Co.).

#### **2.4.10 Flow cytometric analysis**

Flow cytometry may be defined as a technology to measure properties of cells as they move, or flow, in liquid suspension. Most flow cytometers can measure two kinds of light from cells, light scatter and fluorescence. Light scatter is the interaction of light and matter. All materials, including cells, will scatter light. In the flow cytometer, light scatter detectors are located opposite the laser (relative to the cell), and to one side of the laser, in-line with the fluid-flow/laser beam intersection. The measurements made by these detectors are called forward light scatter and side light scatter, respectively. Forward light scatter provides information on the relative size of individual cells, whereas side light scatter provides information on the relative granularity of individual

cells. Fluorescence is the property of a molecule to absorb light of a particular wavelength and re-emit light of a longer wavelength. The wavelength change relates to an energy loss that takes place in the process.

### **2.4.11 Annexin V/vital dye staining**

In normal live cells, phosphatidyl serine (PS) is located on the cytoplasmic surface of the cell membrane. However, in apoptotic cells, PS is translocated from the inner to the outer leaflet of the plasma membrane, thus exposing PS to the external cellular environment. The human anticoagulant, annexin V, is a 35–36 kDa Ca<sup>2+</sup>-dependent phospholipid-binding protein that has a high affinity for PS and can be used to identify apoptotic cells by binding to PS. Fluorescent dyes that bind to nucleotides and penetrate only damaged cellular membranes were used (vital dyes). Intercalation complexes are formed by propidium iodide (PI) or 7-Amino-actinomycin (7-AAD) with double-stranded DNA, which effect an amplification of the fluorescence.

#### **2.4.11.1 Annexin V-Alexa Fluor 488/PI**

The Vybrant® Apoptosis Assay Kit (Invitrogen) contains recombinant annexin V conjugated to Alexa Fluor® 488 dye and PI nucleic acid binding dye. After staining a cell population with Alexa Fluor® 488 annexin V and PI in the provided binding buffer, apoptotic cells show green fluorescence, dead cells show red and green fluorescence, and live cells show little or no fluorescence.

To perform the assay, cells were harvested and washed in ice-cold PBS. The cell pellet was resuspended in 1X annexin-binding buffer, cell density was determined and cells were diluted in 1X annexin-binding buffer to ~1 x 10<sup>6</sup> cells/ml. A volume of 5 µl of alexa fluor 488 annexin V solution and 1 µl of 100 µg/ml PI solution was added to 100 µl of cell suspension. The cells were incubated at room temperature for 15 minutes and 400 µl of 1X annexin-binding buffer was then added and the samples were kept on ice and analysed as soon as possible by flow cytometry.

#### **2.4.11.2 Annexin V-PE/7-AAD**

The Annexin-PE Apoptosis Detection Kit (Becton Dickinson) contains recombinant annexin V conjugated to the fluorochrome, phycoerythrin (PE) and the vital dye 7-AAD. Viable cells with intact membranes exclude 7-AAD, whereas the membranes of dead and damaged cells are permeable to 7-AAD. Cells that stain positive for Annexin V-PE and negative for 7-AAD are undergoing apoptosis. Cells that stain positive for both Annexin V-PE and 7-AAD are either in the end stage of apoptosis, are undergoing necrosis, or are already dead. Cells that stain negative for both Annexin V-PE and 7-AAD are alive and not undergoing measurable apoptosis.

To perform the assay, cells were harvested and washed twice in ice-cold PBS. The cell pellet was resuspended in 1X annexin-binding buffer at a concentration of  $\sim 1 \times 10^6$  cells/ml. A volume of 5  $\mu$ l of Annexin V-PE solution and 5  $\mu$ l of 7-AAD solution were added to 100  $\mu$ l of cell suspension. The cells were incubated at room temperature for 15 minutes in the dark and 400  $\mu$ l of 1X annexin-binding buffer was then added and the samples were analysed within one hour by flow cytometry.

#### **2.4.12 Statistics**

The parametric paired *t*-test was used to assess differences between two related samples (as described by Hawkins, 2005, p. 153). The four steps of the hypothesis-testing procedure were followed. These were as follows; The null hypothesis was stated, a critical significance level ( $\alpha$ ) of 5 % (0.05) was chosen, the test statistic was calculated using SPSS software and the null hypothesis was accepted or rejected using *P* values generated on the computer output.

$$\begin{aligned} P \text{ value } < \alpha(0.05) &= \text{reject null hypothesis} &\rightarrow && \text{significant result} \\ P \text{ value } > \alpha(0.05) &= \text{accept null hypothesis} &\rightarrow && \text{non-significant result.} \end{aligned}$$

## **2.5 Tumour Tissue Methods**

Tumour biopsies from patients with EBV positive and EBV negative HL were investigated for *bfl-1* expression in conjunction with a leading HL research laboratory at the University of Birmingham, UK. The laboratory visited was that of Dr. Paul Murray, at the Institute for Cancer Studies. Tissue sections from these biopsies were prepared for laser capture microdissection (LCM) of H/RS cells and for *in situ* hybridisation (ISH) using anti-*bfl-1* riboprobes (Section 3.2.1.3).

### **2.5.1 Tissue sectioning**

For the successful preservation of RNA, special procedures were essential both during tissue preparation and in subsequent LCM and ISH techniques. RNase-free reagents and equipment were used throughout. All glassware was washed, dried and covered in aluminium foil and baked in a dry oven at 240 °C for a minimum of 4 h. Filter pipette tips were bought as certified DNase/RNase-free. All pipettes/micropipettes were wiped down with absolute alcohol and exposed to ultraviolet light for 1 h. Gloves were worn at all times. RNase-ZAP (Sigma-Aldrich), a spray containing an RNase-inhibitor was repeatedly applied to materials and surfaces used throughout tissue sectioning and LCM/ISH.

#### **2.5.1.1 Tissue sectioning for LCM**

Tissue sections for LCM were cut onto PEN (polyethylene naphthalate) membrane slides (PALM Microlaser). PEN membrane is highly absorptive in the UV-A range, which facilitates laser cutting. Prior to section cutting, slides were sprayed on both sides with RNase-ZAP, rinsed twice in nuclease-free H<sub>2</sub>O (Sigma-Aldrich) and dried at 37 °C for 30 minutes. The slides were UV-irradiated for 30 minutes. Apart from sterilising and eradicating any remaining nucleases, this irradiation step served to increase the hydrophilicity of the membrane for increased tissue adherence.

A microtome was used to cut 7 µm sections from frozen tumour tissues in a cryostat (Leica CMI900). The microtome blade and cutting area were cleaned and sterilised with absolute alcohol between each tissue block to avoid cross-contamination of tissue. Tissue sections were immediately fixed in 100 % (v/v) ethanol for 15 minutes.

For laser capture prior staining was necessary to visualise cell and tissue morphology. Haematoxylin staining is routinely used as it does not interfere with RNA and stains the nuclei blue. The glass slides were immersed in Mayer's Haemalum (BDH) (a solution of haematoxylin and alum) for 30 seconds in an RNase-free staining tray, then washed in nuclease-free water for 2 minutes and dehydrated by immersion twice in 100 % (v/v) ethanol for 10 minutes. The slides were allowed to air-dry. Ideally, LCM was performed immediately after sectioning but if this was not possible, frozen sections were stored at –70 °C. Prior to use, sections were slowly brought to room temperature.

#### **2.5.1.2 Tissue sectioning for *in situ* hybridisation**

Prior to tissue cutting, all slides were coated with Vectabond™ Reagent (Vector Laboratories, UK), prepared by adding 7 ml of Vectabond™ Reagent to 350 ml of acetone (BDH). DNase/RNase-free Snowcoat™ microscope slides (Surgipath Europe) were washed in slide racks in acetone for 5 minutes. The slides were then soaked in the Vectabond™ solution for 5 minutes, before being rinsed with nuclease-free water for 30 seconds. Slides were covered and allowed to dry overnight at room temperature before use.

A microtome was used to cut 7 µm sections onto the slides in a cryostat at –20 °C from frozen tissues, sections were briefly allowed to dry onto the Vectabond™-coated slides and fixed in 4 % (v/v) paraformaldehyde (Appendix). The microtome blade and cutting area were cleaned and sterilised with absolute alcohol between each tissue block to avoid cross-contamination of tissue. All tissue sections were stored at room temperature in DNase/RNase-free conditions until further use in ISH techniques.

#### **2.5.2 Laser Capture Microdissection**

LCM is a novel technique that permits a one-step procurement of pure cells from tissue and cell preparations by using the precision of lasers to selectively adhere target cells to a thermoplastic transfer membrane. The laser system used in this study was PALM® MicroBeam system from PALM Microlaser Technologies with a Zeiss microscope and PALM RoboSoftware. This system permits microdissection and microablation using laser pressure catapulting (LPC) technology, which allows non-contact capture of large, homogeneous cell areas, small cell clusters, single cells or chromosomes.

The tissue sections (Section 2.5.1.1) cut on PEN-LPC membrane slides were examined using the inverted microscope. A volume of 30 µl of cell lysis buffer (Absolutely RNA Nanoprep kit) was added to the detached cap of a 0.5 ml microfuge tube, which was then mounted upside down in the cap holder (Figure 2.1). The cells of interest were identified and predefined by outlining with a graphic tool using the RoboSoftware, which automatically performed the laser activation and catapulting. The PEN-LPC membrane was easily cut with the sample and acted like a stabilising backbone during catapulting of microdissected tissue to the lysis buffer-containing cap.

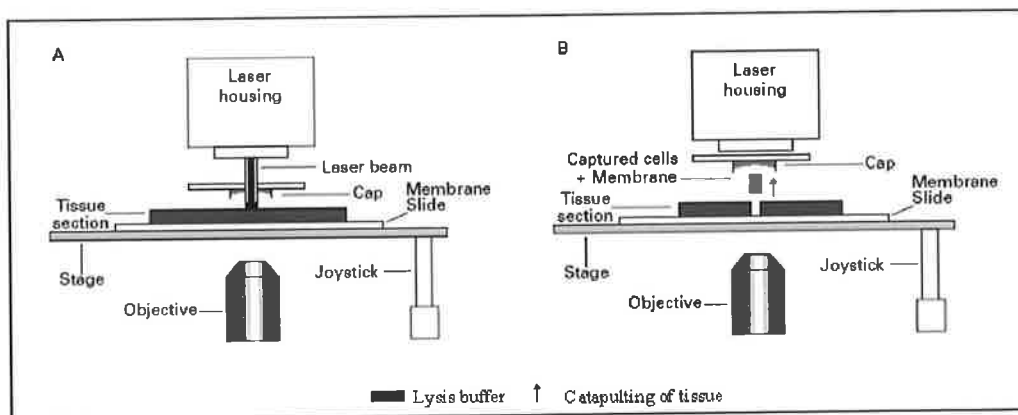


**Figure 2.1 Schematic representation of LCM**

The system consists of an inverted microscope, a solid state near infrared laser diode, a laser control unit, a joy stick controlled microscope stage, a CCD camera, and a colour monitor. (A) Activation of the laser leads to focal melting of the polymer membrane. (B) Cells or tissue section adherent to the activated membrane are catapulted into lysis buffer-containing cap. Adapted from Fend and Raffeld, 2000.

Following microdissection, the cap containing the cells in 30 µl of lysis buffer fitted directly onto a standard 0.5 ml microfuge tube to which a further 70 µl of lysis buffer was added (to give total volume of 100 µl lysis buffer). Although the transferred tissue was firmly bound to the transfer film, it was completely accessible to aqueous solutions and extraction of cell components. RNA was extracted using the Absolutely RNA Nanoprep Kit (Section 2.6.4).

## **2.5.3 *In situ* hybridisation (ISH)**

RNA-RNA ISH using anti-*bfl-1* riboprobes was carried out on EBV+/- HL cases in an attempt to detect *bfl-1* mRNA in identified cells of HL tissue. Digoxigenin-labelled probes were prepared by *in vitro* transcription of recombinant plasmid pGEM-*bfl-1*-RP (Table 2-5) in the presence of digoxigenin-labelled nucleotides. Hybridisation of probes to tissue and subsequent detection of DIG-labelled probes were performed (Section 3.2.1.3).

### **2.5.3.1 Synthesis of digoxigenin-labeled RNA probes**

Sense and anti-sense riboprobes were synthesised as ‘run-off’ transcripts from linearised template DNA. pGEM-*bfl-1*-RP was linearised by restriction digestion (Section 2.3.3) using *Hind*III or *Eco*RI enzymes and antisense or sense transcripts were transcribed by SP6 and T7 RNA polymerases (Roche) respectively in the presence of a digoxigenin (DIG)-labelled ribonucleotide (Roche).

For *in vitro* transcription, the reagents in Table 2-11 were mixed in the order listed and incubated for 2 h at 37 °C. A volume of 10 µl of yeast tRNA (Invitrogen) and 2 µl RNase-free DNase I (Sigma-Aldrich) was added to the reaction mix and incubated for 15 minutes at 37 °C.

**Table 2-11 *In vitro* transcription reactants**

\*400 mM TrisCl (pH 8.25), 60 mM MgCl<sub>2</sub>, 20 mM spermidine (Roche)

\*\*10 mM GTP, 10 mM ATP, 10 mM CTP, 6.5 mM UTP, 3.5 mM digoxigenin UTP; pH 8.0 (Roche)

Reactant	Volume
Sterile, nuclease-free H <sub>2</sub> O	13 µl
10 X transcription buffer*	2 µl
0.2 M Dithiothreitol	1 µl
Nucleotide mix**	2 µl
Linearised plasmid DNA (1 µg/ml)	1 µl
RNasin (100 U/ml)	1 µl
RNA polymerase (SP6 or T7, 10 U/µl)	1 µl
Total	21 µl

To precipitate the RNA transcripts, 20 µl of 3 M sodium acetate (Sigma-Aldrich) and 148 µl of nuclease-free H<sub>2</sub>O (Sigma-Aldrich) were added to each tube. The tubes were vortexed and 200 µl of phenol-chloroform was added and followed by vortexing and centrifugation at 13,000 x g for 5 minutes at room temperature. The top aqueous layer was removed to a new 0.5 ml microfuge tube and 20 µl of 3 M sodium acetate was added to each sample followed by 400 µl of ice-cold 100 % (v/v) ethanol. The samples were vortexed and allowed to precipitate at -80 °C for 1-24 h. The RNA was then pelleted at 13,000 x g for 30 minutes at 4 °C and the supernatant carefully aspirated. The RNA pellet was washed with 250 µl of 70 % (v/v) ethanol and centrifuged at 13,000 x g for 30 minutes at 4 °C. The supernatant was carefully aspirated and the RNA pellet was allowed to dry at room temperature. A volume of 13 µl of 100 mM DTT and 12 µl of nuclease-free H<sub>2</sub>O were added to each sample, followed by 1 h refrigeration at 4 °C. Finally 15 µl of formamide (Sigma-Aldrich) was added to each tube and the probes were stored at -20 °C until required.

### 2.5.3.2 Hybridisation

Tissue sections on coated slides were dehydrated in xylene twice for 5 minutes and 100 % (v/v) ethanol twice for 5 minutes. The ethanol was washed off with PBS and slides were left in PBS for 5 minutes. Endogenous peroxidase activity was blocked by 10-minute incubation in 3 % (v/v) hydrogen peroxide (Sigma-Aldrich) in methanol, and then washed in PBS for 10 minutes. Pronase E solution (0.6 µg/ml) was prepared by diluting stock solution (10 mg/ml) in DEPC H<sub>2</sub>O, allowing 100 µl per slide. Sections were incubated in 100 µl of pronase E for 5 minutes, rinsed in PBS for 5 minutes, then dehydrated in ethanol for 5 minutes and air-dried.

An appropriately sized Geneframe (25 µl, 65 µl, or 125 µl; Advanced Biotechnologies) was placed onto the slide so that it surrounded the tissue section. The DIG-labelled sense and anti-sense probes (Section 2.5.3.1) were thawed, pulse centrifuged and heated to 80 °C for 30 seconds before being plunged straight into ice. The probes were then mixed and diluted 1:200 with *in situ* hybridisation solution (Sigma-Aldrich). The appropriate volume of 25 µl, 65 µl, or 125 µl of sense/anti-sense probe solution was then added inside the Geneframe to the tissue sections. A Geneframe polyester cover slip was slowly pressed over the gene frame, applying pressure from one end, spreading the probe mixture evenly over the tissue section without trapping air bubbles. This created a complete seal around the tissue section, preventing evaporation of the probe

mixture during the high temperature incubation period. The slides were then incubated at 50 °C overnight.

#### **2.5.3.3 Detection of DIG-labeled probes**

Following incubation, Geneframes and coverslips were carefully removed and slides were placed in a staining tray (a lid was used during all incubations to minimise evaporation), washed once in 2 X SSC (Appendix) for 5 minutes, washed twice 0.1 X SSC (Appendix) for 5 minutes each time and washed once in PBS for 5 minutes. The PBS solution was tipped off, the area of the slide around the cells/tissue was carefully dried, and a ring of wax was applied (PAP pen; Sigma-Aldrich) to keep subsequent reagent application contained to the cells/tissue area. Following a 10-minute incubation with 100 µl of horse blocking serum (diluted 1:40 in PBS, from the Vectastain Universal Quick kit, Vector Labs) to prevent non-specific immunoreactivity, detection of DIG-labelled probes was performed by incubation with 50 µl mouse monoclonal anti-digoxigenin antibody (Sigma-Aldrich) diluted 1:1000 with PBS for 1 h. Secondary detection reagents were supplied in the Vectastain Universal Quick Kit. A volume of 100 µl of biotinylated universal secondary antibody (diluted 1:20 in PBS with 10 % (v/v) blocking serum) was added to each tissue section for 10 minutes. Sections were washed in PBS for 5 minutes, followed by a 10-minute incubation in 100 µl of the streptavidin/peroxidase pre-formed complex antibody (diluted 1:40 with PBS), and a final 5-minute wash in PBS.

Detection of antigen-bound peroxidases was achieved using the Sigmafast DAB substrate system (Sigma-Aldrich). One DAB tablet and one urea/hydrogen peroxide tablet was dissolved in 5 ml PBS. A minimum of 200 µl of this substrate solution was applied to each tissue section for 10 minutes, during which time the substrate was converted to an insoluble brown product by the antigen-bound peroxidases.

Haematoxylin (stained nuclei blue) and eosin counter-staining (stained cytoplasm red/pink) of tissue sections was performed to facilitate pathological review. Slides were immersed in Mayer's haematoxylin (BDH) for 10 seconds before washing thoroughly in tap water. Scott's tap water (Surgipath Europe) was then used to 'blue' the haematoxylin for 1 minute, before washing thoroughly again in tap water. The slides were immersed in Eosin (BDH) for 10 seconds before being rinsed off with tap water. Tissue sections were then dehydrated through ethanol twice, for 5 minutes followed by

xylene twice for 5 minutes, before being mounted with one drop of DPX mounting medium (Surgipath Europe) and coverslips (Surgipath Europe). Slides were dried flat overnight before microscopic analysis.

## **2.6 RNA Analysis**

### **2.6.1 RNase-free environment**

Because RNA is easily degraded by ubiquitous RNases, standard procedures were employed to avoid this potential hazard (Sambrook *et al.*, 1989).

Prior to running an RNA gel, the electrophoresis apparatus was treated to remove any RNase. The tank, gel tray, comb and lid were washed in detergent and rinsed well in DEPC-treated H<sub>2</sub>O, then in 100 % (v/v) ethanol and finally allowed to air dry. The tank, gel tray and comb were immersed in a 3 % (v/v) solution of hydrogen peroxide (Sigma-Aldrich) for 15 minutes. The apparatus was then rinsed thoroughly in DEPC treated upH<sub>2</sub>O and allowed to dry. Because hands are a major source of RNase contamination, gloves were used at all times and changed frequently.

### **2.6.2 RNA analysis by gel electrophoresis**

In order to examine RNA transcripts/ascertain the integrity of RNA, isolated samples were run on 1.5 % (w/v) agarose gels. The appropriate amount of agarose was dissolved in DEPC-treated H<sub>2</sub>O and prepared according to Section 2.3.13. The RNA samples (1 µl) were prepared for electrophoresis by adding 3 µl of RNA sample buffer (Appendix) and made up to 15 µl in DEPC-treated H<sub>2</sub>O. The samples were heated to 65 °C for 10 minutes prior to loading on the gel. The gel was run in 1 X TAE as described in Section 2.3.13. As ethidium bromide is included in the RNA sample buffer the gels did not require further staining and could be visualised directly on a UV trans-illuminator.

### **2.6.3 RNA extraction from cultured cells**

Prior to RNA isolation the condition of cells was reviewed by phase contrast microscopy. A cell count was performed as described in Section 2.4.4.

### **2.6.3.1 RNA extraction using Tri reagent**

Cells grown in suspension were pelleted at 100 x g for 5 minutes, washed once in PBS and the cell pellet lysed by repeat pipetting in Tri Reagent (Sigma-Aldrich). A volume of 1 ml of Tri reagent was used per  $1 \times 10^7$  cultured cells. The lysate was left at room temperature for five minutes after which time the procedure could be halted by storing samples at –80 °C.

Phase separation was achieved by adding 200 µl of chloroform per 1 ml of lysate. The samples were covered and shaken gently but thoroughly for 15 seconds or until completely emulsified. Samples were incubated at room temperature for 15 minutes. The resulting mixture was centrifuged at 13,000 x g for 20 minutes at 4 °C. During centrifugation the mixture separated into a lower red, phenol-chloroform phase, an interphase and a colourless upper aqueous phase. The aqueous phase, which contained the RNA, was removed to a fresh tube and RNA was precipitated by addition of 500 µl of ice-cold isopropanol per ml of Tri reagent used initially. The samples were incubated for 10 minutes on ice and then centrifuged at 13,000 x g for 15 minutes at 4 °C. The resulting RNA pellet was washed using 1 ml of 75 % (v/v) ethanol by inverting the tube 5 times. The pellets were then centrifuged at 13,000 x g for 5 minutes at 4 °C, and the 75 % (v/v) ethanol was aspirated. Pellets were air dried and dissolved in DEPC treated upH<sub>2</sub>O. The resulting RNA preparation was heated at 60 °C and mixed gently to ensure a homogeneous solution prior to aliquoting. An aliquot was removed for spectrophotometric (Section 2.3.12) and gel electrophoretic analysis (Section 2.3.13) and the remainder of the purified RNA was stored at –80 °C.

### **2.6.3.2 Total RNA isolation from cells using QIAgen RNeasy™ kit**

RNA was extracted from small numbers of cultured cells ( $<5 \times 10^5$ ) using an RNeasy kit (QIAgen) according to the manufacturer's protocol (RNeasy Mini Handbook, 2006). An aliquot of purified RNA was removed for spectrophotometric (Section 2.3.12) and gel electrophoretic analysis (Section 2.6.2) prior to RT-PCR.

## **2.6.4 Quantification of mRNA from cultured cells by RT-qPCR**

The quantification of mRNA purified from cultured cells was performed in a two-step procedure. In the first step, cDNA was prepared from RNA by reverse transcription (RT) with random hexamers serving as primers. During the second step, cDNA was amplified by real time quantitative PCR (qPCR). Real-time qPCR is increasingly being adopted for RNA quantification based on its ability to detect the amount of PCR product present at every cycle (i.e. in real time), as opposed to the endpoint detection by conventional PCR methods, thus allowing the real-time progress of the reaction, especially its exponential phase, to be viewed. The real-time PCR approach is based on the detection and quantification of a fluorescent reporter, where the signal increases in direct proportion to the amount of PCR product in a reaction. TaqMan gene expression assays were used in this study for comparative gene expression analysis, normalising with *gapdh* or  $\beta$ -*actin* endogenous control mRNA levels.

### **2.6.4.1 Moloney Murine Leukemia Virus (M-MLV) reverse transcriptase**

In this process mRNA was transcribed into cDNA using Moloney Murine Leukemia Virus (M-MLV) reverse transcriptase. Initially, 2  $\mu$ l of random hexamers was added to 2  $\mu$ g RNA and the volume brought up to 10  $\mu$ l with DEPC H<sub>2</sub>O. The mixture was heated to 70 °C for 5 minutes, to destabilise secondary mRNA structures, and then placed on ice. Then, the RT reactants were added in the order listed in Table 2-12.

**Table 2-12 MMLV RT reactants**

Component	Volume
Reverse Transcriptase buffer (5 X)	8 µl
dNTP mix (20 mM)	1 µl
MgCl <sub>2</sub> (25 mM)	4 µl
BSA (4 µg/µl)	1 µl
DEPC H <sub>2</sub> O	13 µl
RNasin ribonuclease inhibitor	2 µl
M-MLV reverse transcriptase (200 U/µl)	1 µl
Total	40 µl

The reactions were placed in a Hybaid thermocycler at 37 °C for 1 h and 95 °C for 2 minutes followed by storage at 4 °C.

#### 2.6.4.2 Real time relative PCR (q-PCR)

cDNA generated by RT was quantified by real time PCR using the TaqMan gene expression assays (Applied Biosystems), which consisted of two unlabeled primers for amplifying the sequence of interest (final concentration of 900 nM each) and one dual-labeled TaqMan MGB probe (6-FAM dye- and TAMRA-labeled) for detecting the sequence of interest (final concentration of 250 nM). The PCR reaction exploits the 5'-3' nuclease activity of the DNA polymerase system to cleave a TaqMan probe during PCR as illustrated in Figure 2.2.

Quantification of a cDNA target was normalised for differences across experiments/samples using an endogenous control as an active reference (*gapdh* or  $\beta$ -*actin*). The PCR reaction mix was prepared for each sample (in triplicate) by addition of the reagents listed in Table 2-13 to the individual wells of a 96-well reaction plate (Applied Biosystems) followed by the addition of 2 µl of cDNA to give a total reaction volume of 25 µl.

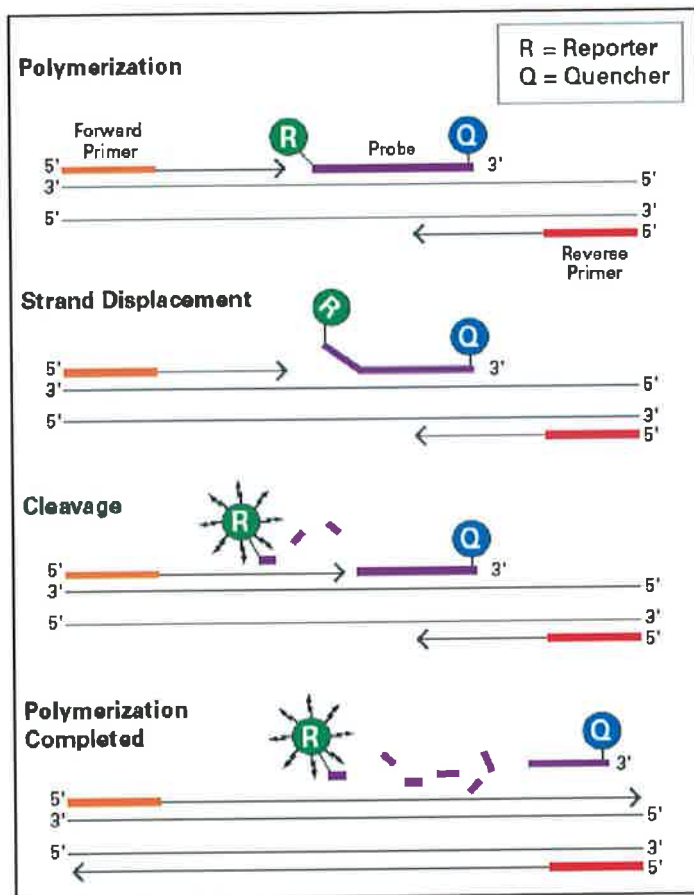


**Figure 2.2 Principles of the TaqMan assay primers and probes**

When the probe is intact, the proximity of the reporter dye to the quencher dye results in suppression of the reporter fluorescence primarily by Förster-type energy transfer (Förster, 1948; Lakowicz, 1983). During PCR, if the target of interest is present, the probe specifically anneals between the forward and reverse primer sites. The 5'-3' nucleolytic activity of the DNA polymerase system cleaves the probe between the reporter and the quencher only if the probe hybridises to the target. The probe fragments are then displaced from the target, and polymerisation of the strand continues. The 3' end of the probe is blocked to prevent extension of the probe during PCR. This process occurs in every cycle and does not interfere with the exponential accumulation of product. The increase in fluorescence signal is detected only if the target sequence is complementary to the probe and is amplified during PCR. Because of these requirements, any non-specific amplification is not detected (Adapted from Applied Biosystems White Paper on TaqMan gene expression assays <http://docs.appliedbiosystems.com/pebiomedocs/00106737.pdf>).

**Table 2-13 Real time qPCR reactants**

Component	Volume/Reaction
Assay	1.25 µl
20 x TaqMan PCR master mix*	12.5 µl
Nuclease Free H <sub>2</sub> O	9.25 µl
Total	23 µl

\*TaqMan universal PCR Master mix contained AmpliTaq gold polymerase, dNTPs and the passive reference, ROX.

The plate was covered with an optical adhesive cover and centrifuged at 2,000 x g for 2 minutes to eliminate air bubbles and the reaction plate was placed in the instrument. Amplification and detection were performed with an ABI Prism 7500 sequence detection system under the following conditions: 10 minutes at 95 °C to activate AmpliTaq Gold DNA polymerase, and 45 cycles of 15 seconds at 95 °C and 1 minute at 60 °C.

During amplification, the ABI Prism sequence detector monitored real-time PCR amplification by quantitatively analysing fluorescence emissions. The reporter dye (FAM) signal was measured against the internal reference dye (ROX) signal to normalise for non-PCR-related fluorescence fluctuations occurring from well to well. The threshold cycle represented the refraction cycle number at which a positive amplification reaction was measured and was set at 10 times the standard deviation of the mean baseline emission calculated for PCR cycles 3 to 15. The results were analysed according to the Comparative C<sub>T</sub> method ( $\Delta\Delta C_T$ ) as described by Livak and Schmittgen, 2001.

## 2.6.5 RNA extraction from Laser Capture Microdissected Cells

The Absolute RNA (Stratagene) Nanoprep kit allowed rapid purification of high quality total RNA from cells harvested by LCM (small number of cells [1 cell to  $5 \times 10^5$  cells]). Cells were disrupted in 100 µl lysis buffer containing a strong protein denaturant (the chaotropic salt guanidine thiocyanate) and 0.7 µl β-mercaptoethanol, permitting effective cell lysis and preventing degradation of the RNA by RNases. Following cell lysis, each sample was then mixed with an equal volume of 70 % (v/v) ethanol and

applied to a spin cup where the RNA bound to a silica-based fiber matrix. After centrifugation at 13,000 x g for 2 minutes and disposal of the flow-through, the fibre matrix was washed with 600 µl low-salt wash buffer and then dried by centrifugation at 13,000 x g for 2 minutes. DNase treatment, to remove contaminating DNA, was performed by addition of 50 U DNase (Sigma-Aldrich) and 25 µl DNase digestion buffer in a 15-minute incubation at 37 °C. The fibre matrix was washed with 500 µl high-salt wash, followed by 600 and 300 µl low-salt washes to remove DNase and other contaminants. The spin cup was centrifuged at 13,000 x g for 2 minutes to dry the fiber matrix. RNA was eluted from the fibre matrix with 30 µl elution buffer (10 mM Tris, pH 7.5). The purified RNA was subsequently used in qualitative and quantitative RT-PCR reactions.

## **2.6.6 Qualitative analysis of mRNA from microdissected cells**

RNA from microdissected cells was analysed for *bfl-1* mRNA expression using the OneStep RT-PCR kit (QIAgen) and *bfl-1*-specific internal and external (BFL-1 INT F/R and BFL-1 EXT F/R) primers listed in Table 2-6.

### **2.6.6.1 OneStep RT-PCR**

The OneStep RT-PCR Kit contains optimised components that allow both RT and PCR amplification to take place in what is commonly referred to as a “one-step” reaction. The OneStep RT-PCR Enzyme Mix provides highly efficient and specific RT using two reverse transcriptases; Omniscript and Sensiscript reverse transcriptases. Omniscript reverse transcriptase is specially designed for RT of RNA amounts greater than 50 ng, and Sensiscript reverse transcriptase is optimised for use with very small amounts of RNA (<50 ng). HotStarTaq DNA Polymerase included in the OneStep RT-PCR enzyme mix provides hot-start PCR for highly specific amplification. During RT, HotStarTaq DNA Polymerase is completely inactive and does not interfere with the reverse-transcriptase reaction. After reverse transcription by Omniscript and Sensiscript Reverse Transcriptases, reactions are heated to 95 °C for 15 minutes to activate HotStarTaq DNA Polymerase and to simultaneously inactivate the reverse transcriptases. This hot-start procedure using HotStarTaq DNA Polymerase eliminates extension from nonspecifically annealed primers and primer-dimers in the first cycle ensuring highly

specific and reproducible PCR. OneStep RT-PCR was performed according to the manufacturer's instructions (QIAGEN OneStep RT-PCR Handbook, 2002).

## 2.6.7 Quantitative analysis of mRNA from microdissected cells

The relative level of *bfl-1* mRNA from microdissected cells was quantified by RT-qPCR using the Sensiscript RT-PCR kit (QIAgen) (Section 2.6.7.1) followed by quantitative PCR using TaqMan assays for *bfl-1* and *gapdh*; endogenous control (Section 2.6.4.2).

### 2.6.7.1 Sensiscript RT

Sensiscript reverse transcriptase, which has a high affinity for RNA, enables efficient and sensitive RT of <50 ng RNA.

Initially the template RNA, primer solutions, 10 X buffer RT, dNTP mix and RNase-free water were thawed on ice at room temperature and stored on ice immediately after thawing. RNase inhibitor (RNasin; 40 units/ $\mu$ l) was diluted to a final concentration of 10 units/ $\mu$ l in ice-cold 1x Buffer RT (an aliquot of the 10 X Buffer RT was diluted accordingly using the RNase-free water supplied). A fresh dilution of RNase inhibitor was prepared each time. A fresh master mix was prepared on ice according to Table 2-14. The master mix was mixed thoroughly and carefully by vortexing for no more than 5 seconds, then centrifuged briefly to collect residual liquid from the walls of the tube, and stored on ice. The master mix contained all components required for first-strand synthesis except the template RNA.

The appropriate volume of master mix was distributed into individual reaction tubes, kept on ice. Template RNA was added to the individual tubes containing the master mix. The reaction was incubated for 60 minutes at 37 °C. An aliquot of the finished RT reaction was added to the real time qPCR mix (Section 2.6.4.2) or for long-term storage; RT reactions were stored at -20 °C.

**Table 2-14 Sensiscript RT reactants**

Component	Volume/reaction	Final concentration
<b><u>Master Mix</u></b>		
10x Buffer RT	2.0 $\mu$ l	1x
dNTP Mix (5 mM each dNTP)	2.0 $\mu$ l	0.5 mM each dNTP
Oligo-dT primer (10 $\mu$ M)*	2.0 $\mu$ l	1 $\mu$ M*
RNase inhibitor (10 units/ $\mu$ l)	1.0 $\mu$ l	10 units (per reaction)
Sensiscript reverse transcriptase	1.0 $\mu$ l	
RNase-free water	Variable –	
<b><u>Template RNA</u></b>		
Template RNA	Variable –	<50 ng (per reaction)
<b>Total volume</b>	20 $\mu$ l –	

## **2.7 Protein Analysis**

### **2.7.1 Preparation of cellular protein**

Proteins were isolated from both suspension and adherent cells for analysis by SDS-polyacrylamide gel electrophoresis (SDS-PAGE) and by western blotting. Prior to isolation, cells were washed in PBS. Suspension cells were pelleted at 100 x g for 5 minutes and the supernatant removed. Ice-cold PBS (10 ml) was added; the cells were centrifuged again at 100 x g and all of the supernatant removed. Adherent cells were washed twice with 10 ml of ice-cold PBS, and the cells were scraped into 1 ml of PBS. The crude cell suspension was pelleted at 100 x g for 5 minutes. For both suspension and adherent cells, the cell pellet was re-suspended in ice-cold suspension buffer (Appendix) using 200 µl of suspension buffer for every  $1 \times 10^7$  cells and the cell suspension transferred to a microfuge tube. An equal volume of 2 X SDS gel loading buffer (Appendix) was immediately added to the cell suspension, after which the sample became extremely viscous. The sample was then subjected to sonication for 1 minute on full power (using a Vibra Cell Sonicator) to shear the DNA. The lysate was clarified by centrifugation at 12,000 x g for 10 minutes at room temperature. The supernatant was aliquoted and stored at –20 °C until required for analysis.

### **2.7.2 SDS-polyacrylamide gel electrophoresis of proteins**

During polyacrylamide gel electrophoresis (PAGE), proteins are driven by an applied current through a gel composed of polyacrylamide that is cross-linked to form a molecular sieve. PAGE is usually carried out in the presence of the negatively charged detergent sodium dodecylsulphate (SDS), which binds in large numbers to all types of protein molecules. The electrostatic repulsion between the bound SDS molecules causes the proteins to unfold into a similar rod-like shape, thus eliminating differences in shape as a factor in separation. As the amount of SDS bound is proportional to the molecular weight of the polypeptide and is sequence independent, SDS-polypeptide complexes migrate through polyacrylamide gels in accordance with the size of the polypeptide.

#### **2.7.2.1 Preparation of SDS-polyacrylamide gels**

SDS-PAGE was performed using 10 % (v/v) resolving gels and 5 % (v/v) stacking polyacrylamide gels prepared as detailed in Appendix.

An ATTO protein gel electrophoresis system was used in this study. Glass plates were washed with detergent, rinsed first with tap water, then with dH<sub>2</sub>O and finally wiped in one direction with tissue soaked in 100 % (v/v) ethanol. The gasket was placed around the ridged plate; the plates were assembled and secured with clamps. The resolving gel was then poured to within 2 cm of the top of the larger plate and overlaid with 100 % (v/v) ethanol. When set, the ethanol was removed and the stacking gel was poured. A clean comb that had been wiped in 100 % (v/v) ethanol was inserted and the gel was allowed to polymerise for at least 20 minutes. The electrophoresis tank was filled with 1 X Tris-glycine running buffer (Appendix) to a level of about 5 cm deep. After polymerisation, the gaskets and clamps were removed and the pre-poured gels were lowered into the buffer at an angle to exclude air bubbles from the gel-buffer interface. The tank was completely filled with 1 X running buffer and the comb removed from the gel. Un-polymerised gel was removed by gently rinsing the wells with 1 X running buffer and the wells were then straightened using a loading tip. The gel plates were fixed firmly in place with the pressure plates. The chamber formed by the inner plates (notched plate facing inwards) was filled with 1 X running Buffer, the samples were loaded and the electrodes attached. The gels were electrophoresed at a constant current of 30 mA per gel until the blue dye front had reached the bottom of the gel. When complete the plates were removed, separated and the gel was either placed in transfer buffer prior to western blotting (Section 2.7.4) or stained in Coomassie blue (Section 2.7.3).

#### **2.7.3 Coomassie Blue Staining**

The gel was placed in Coomassie stain (Appendix) for 30 minutes with gentle agitation. The gel was then placed in destain (Appendix) with constant agitation, and destain was changed 4 or 5 times at 1 h intervals until all background staining was removed from the gel. An image of the gel in black and white was captured using the UV trans-illuminator switched to white light only and using a white tray.

## **2.7.4 Western blotting**

During western blotting, electrophoretically separated proteins were transferred from the polyacrylamide gel to a solid support, usually a nitrocellulose membrane, and probed with antibodies that reacted specifically with antigenic epitopes displayed by the target protein attached to the solid support. The bound antibody, unless conjugated, was detected by a secondary immunological reagent, conjugated to either the alkaline phosphatase or horseradish peroxidase enzyme for detection.

### **2.7.4.1 Transfer of protein to nitrocellulose filters**

Following gel electrophoresis, gels were equilibrated in transfer buffer (Appendix) for at least 15 minutes. Equilibration facilitated the removal of electrophoresis salts and detergents. Salts if not removed, increase the conductivity of the transfer and the amount of heat generated during transfer. Nitrocellulose membrane was cut to the dimensions of the gel, along with 6 pieces of 3 MM filter paper that were required for the gel/membrane sandwich. Protein transfer was carried out on the Bio-Rad Trans-Blot<sup>®</sup> SD semi-dry electrophoretic transfer cell. A pre-soaked sheet of filter paper was placed onto the platinum anode. A pipette was rolled over the surface of the filter paper to exclude all air bubbles. This step was repeated with two more sheets of filter paper. Then, the pre-wetted blotting membrane was placed on top of the filter paper and all bubbles rolled out. The equilibrated gel was carefully placed on top of the nitrocellulose membrane, aligning the gel on the centre of the membrane. Any air bubbles were again rolled out. Another 3 sheets of pre-wetted filter were placed on top of the gel, with care taken to remove air bubbles. The cathode was placed on top of the stack and the safety cover replaced on the transfer unit. Gels were transferred for 22 minutes at 15 V.

### **2.7.4.2 Staining of proteins immobilised on nitrocellulose filters**

Ponceau S staining was employed to determine whether uniform transfer of proteins to the nitrocellulose membrane had taken place. Transferred protein were detected as red bands on a white background. This staining technique is reversible to allow further immunological analysis. Ponceau S is a negative stain, which binds to positively charged amino acid groups of proteins. It also binds non-covalently to non-polar regions of proteins. Following electrophoretic transfer, the nitrocellulose membrane was

immersed in 20 ml Ponceau S solution (Sigma-Aldrich) and stained for 5 minutes with constant agitation. After proteins were visualised, the membrane was washed in several changes of dH<sub>2</sub>O until all the stain had been washed away. The membrane was then used for immunological probing.

#### **2.7.4.3 Immunological probing**

Following Ponceau S staining, the membrane was incubated in blocking buffer (Appendix) for 2 h at room temperature followed by incubation with the appropriate primary antibody (diluted in blocking buffer, see Table 2-15) at 4 °C overnight. Sodium azide was added to each antibody solution to a final concentration of 0.02 % (w/v) as a preservative thus permitting reuse of the antibody.

**Table 2-15 Incubation Conditions for Antibodies Used in Western Blotting**

<b>Primary Antibody</b>	<b>Name</b>	<b>Dilution</b>		<b>Secondary Antibody</b>		<b>Dilution</b>	
		<b>In Buffer</b>	<b>Blocking</b>	<b>In Buffer</b>	<b>Blocking</b>	<b>In Buffer</b>	<b>Blocking</b>
Anti-β-actin	Anti-actin AC-15	1/10,000		AP-conjugated mouse IgG		Anti-	1/20,000
Anti-BFL-1	Anti-BFL-1 SL	Various		AP-conjugated anti-rabbit IgG		1/10,000	
Anti-HA-peroxidase	Anti-HA-peroxidase, high affinity	1/1000		None		-	
Anti-Jagged1	TS1.15H	1/1000		Biotinylated rabbit Anti- rat and Streptavidin-HRP tertiary		1/1000	
Anti-Notch1	bTAN20	1/1000		As above			
Anti-Notch2	C651.6 DbHN			As above			
Anti-His-HRP	Anti-His- HRP	1/1000		None		-	
Anti-EBNA2	PE2	1/100		AP-Conjugated Mouse IgG		Anti	1/5000
Anti -LMP1	CS1-4	1/1000		AP-Conjugated Mouse IgG		Anti	1/5000

After overnight incubation, the membrane was washed three times in TBS-T (0.1 % (v/v) Tween-20 in TBS [Appendix]) for 15 minutes. The filter was then incubated with

the appropriate secondary antibody (Table 2-15) for 1 h 30 minutes at room temperature, followed by three 15-minute washes in TBS-T. All of the above incubations were carried out with constant agitation. The membrane was then placed in a clean container and covered with 5-Bromo-4-chloro-3-indolyl phosphate/Nitro Blue Tetrazolium (BCIP/NBT, Sigma) or 3,3',5,5'-tetramethylbenzidine (TMB, Sigma), which are used for the colourimetric detection of alkaline phosphatase- or hydrogen peroxidase-conjugated molecules respectively. When incubated with alkaline phosphatase or hydrogen peroxidase, bound enzyme catalysed the production of a coloured product that was easily observable. The membrane was then rinsed in distilled water to stop the reaction and photographed.

## **2.8 Recombinant Protein Expression**

### **2.8.1 High-level expression of recombinant proteins**

High-level expression of recombinant proteins was achieved by induction with isopropyl thiogalactoside (IPTG). All buffers used are described in the Appendix.

Single colonies of transformants were used to inoculate 1.5 ml of LB broth supplemented with antibiotics and grown overnight at 37 °C in an orbital shaker at 200 rpm. A volume of 500 µl of these cultures was used to inoculate 10 ml cultures of supplemented LB broth, which were grown for 3-4 h until logarithmic phase [Optical Density at 600 nm wavelength ( $OD_{600\text{ nm}}$ ) of 0.5] was reached. The cultures were induced to express fusion proteins by the addition of IPTG at a final concentration of 1.0 mM followed by growth for a further 5 h as above. Cells were then collected by centrifugation at 15,339 x g for 5 minutes. The supernatant was discarded and cell pellets were lysed in 8 M urea lysis buffer (Buffer B), sonicated for 20 seconds with 1 second pulses at an amplitude: 40/output, 200 W using a Vibra Cell Sonicator. Cell debris was removed by centrifugation at 15,339 x g for 15 minutes and the supernatant was analysed by SDS-PAGE (Section 2.7.2) (15 % separating gel, 5 % stacking gel) to confirm protein expression at the predicted protein molecular weight.

To optimise the expression of a given protein construct, a time-course analysis of the level of protein expression was performed by harvesting cells from expression cultures at time zero and at time intervals of 1 h for 5 h and at a final timepoint of 12 h post induction. The level of recombinant protein expression was optimised by performing small scale expression cultures with variation of the following relevant growth parameters; IPTG concentration for induction (varied over the range 0.0025 mM- 1.5 mM), optical density measured at 600 nm at the time of induction (varied over the range 0.3-1.0 absorbance units), growth temperature before and after induction (varied over the range 25 °C- 37 °C). The solubility of recombinant proteins was also determined as described in Section 6.2.3.

Western blotting of His-fusion proteins was performed as in Section 2.7.4. Immunoreactivity with the anti-His HRP-conjugated monoclonal antibody was evident with chromogenic development following addition of TMB substrate to the probed nitrocellulose membrane.

## **2.8.2 Determination of Protein Solubility**

Expression cultures (Section 2.8.1) were pelleted cells and resuspended in 5 ml of native lysis buffer. Lysozyme (1 mg/ml) was added and the sample was incubated for 30 minutes on ice followed by sonication on ice for 6 x 10 seconds with 10 seconds pauses at 200 W. The lysate was centrifuged at 10,000 x g at 4 °C for 20 minutes and the supernatant aspirated and kept on ice (Soluble extract). The remaining pellet was resuspended in 5 ml lysis buffer and kept on ice (Insoluble matter). The soluble and insoluble extracts were examined by SDS-PAGE analysis (Section 2.7.2).

## **2.8.3 IMAC Purification of His-tagged recombinant proteins**

Purification of His-tagged recombinant proteins was performed in batch and column procedure under native and denaturing conditions.

### **2.8.3.1 Batch purification**

Under denaturing conditions, 1 ml of 50 % Ni-NTA resin was equilibrated by addition of 10 ml of Buffer B. The resin-buffer mixture was centrifuged at 1,252 x g for 1 minute and the supernatant removed. A volume of 4 ml of cleared lysate (Section 2.8.1) was added to the equilibrated resin and mixed gently for 60 minutes at room temperature with rotation at 200 rpm on a rotary shaker. The lysate-resin mixture was centrifuged at 1,252 x g for 1 minute and the supernatant removed. Wash buffer (Buffer C, D) was added to the resin, mixed thoroughly and centrifuged at 1,252 x g for 1 minute. The wash step was repeated twice more followed by addition of elution buffer (Buffer E; pH 5.5/5.0/4.8/4.5/4.2) to the resin and centrifuged at 1,252 x g for 1 minute. During the process of purification all eluates and fractions were collected and analysed by SDS-PAGE (15 % separating gel, 5 % stacking gel).

Under native conditions, cells collected as in Section 2.8.1 were lysed in native lysis buffer and sonicated for 20 seconds with 1-second pulses (40/output, 200W). Cell debris was removed by centrifugation at 15,000 x g for 15 minutes. A volume of 1 ml of 50 % Ni-NTA resin was equilibrated by addition of 10 ml of native lysis buffer, centrifuged at 1,252 x g for 1 minute and the supernatant removed. A volume of 4 ml of cleared lysate was added to the equilibrated resin and mixed gently for 60 minutes at

room temperature with rotation at 200 rpm on a rotary shaker. The lysate-resin mixture was centrifuged at 1,252 x g for 1 minute and the supernatant removed. Native wash buffer was added to the resin, mixed thoroughly and centrifuged at 1,252 x g for 1 minute. The wash step was repeated once more followed by addition of native elution buffer to the resin and centrifuged at 1,252 x g for 1 minute. During the process of purification all eluates and fractions were collected and analysed by SDS-PAGE (15 % separating gel, 5 % stacking gel).

#### **2.8.3.2 Column purification**

Under denaturing conditions; cell lysates were loaded onto Ni-NTA IMAC minicolumns pre-equilibrated with Buffer B. Following two wash steps with wash buffer (Buffer C), the column was eluted with elution buffer (Buffer E; pH 4.5). During the process of purification all eluates and fractions were collected and analysed by SDS-PAGE (15 % separating gel, 5 % stacking gel).

Under native conditions, cell lysates were loaded onto Ni-NTA IMAC minicolumns that had been pre-equilibrated with native lysis buffer. Following two wash steps with native wash buffer, purified proteins were eluted with native elution buffer. Samples from purification stages were analysed by SDS-PAGE (15 % separating gel, 5 % stacking gel) followed by staining with Coomassie blue.

#### **2.8.4 Growth for preparative purification**

A single colony of *E. coli* RosettaBlue<sup>TM</sup> harbouring expression plasmids encoding His-Linker-Bfl-1 (pGSLink-N-Bfl-1) and Bfl-1-Linker-His (pGSLink-C-Bfl-1) fusion proteins was used to inoculate 1.5 ml of LB broth supplemented with antibiotics and grown overnight at 37 °C in an orbital shaker at 200 rpm. A volume of 500 µl of these cultures was used to inoculate 20 ml cultures of supplemented LB broth, which were grown overnight at 37 °C in an orbital shaker at 200 rpm. LB broth (1L) was inoculated 1/50 with these cultures and grown for 3-4 h until logarithmic phase [OD<sub>600 nm</sub> of 0.8] was reached. The cultures were induced to express fusion proteins by the addition IPTG at a final concentration of 0.1 mM followed by growth for a further 5 h at 37 °C in an orbital shaker at 200 rpm. Cells were then collected by centrifugation at 4,000 x g for 20

minutes. The supernatant was discarded and cell pellets were lysed in native lysis buffer (5 ml per gram wet weight), incubated in lysozyme (1 mg/ml for 30 minutes) and sonicated on ice for six 10 second pulses with 10 second breaks between pulses at an amplitude: 40/output, 200 W. Cell debris was removed by centrifugation at 15,339 x g for 25 minutes at 4 °C. The supernatant was applied to 2 ml Ni-NTA matrix that had been packed into a column and pre-equilibrated with native lysis buffer. The flow through collected was reapplied to the resin a further three times, then washed twice with wash buffer. Purified proteins were eluted twice using 5 ml volumes of elution buffer. All fractions were analysed by SDS-PAGE to monitor purification performance.

#### **2.8.5 Buffer exchange and concentration of purified protein**

The eluates from preparative purification were pooled and applied to an Amicon ultrafilter (Millipore; with 10 kDa molecular weight cut-off). The 10 ml preparation was buffer exchanged to PBS (Appendix; the desired buffer for immunisation) and simultaneously concentrated (by reducing volume from 10 ml to 500 µl three times) by centrifugation at 1,252 x g and 4 °C.

#### **2.8.6 Antibody Preparation**

Concentrated purified antigen was quantified using a Nanodrop<sup>TM</sup> spectrophotometer by direct aliquoting of 1.2 µl onto the measuring platform and measurement of absorbance at 280 nm. Protein concentration was a factor of the protein molecular weight and extinction co-efficient predicted using ProtParam software (Table 2-4). A total of 2 mg of concentrated purified protein was used for rabbit immunisation. Immunisation, blood collection and sera recovery were performed by Custom Hybridoma laboratories (The Netherlands).

**CHAPTER 3 *Bfl-1* is expressed in  
Hodgkin's Lymphoma tissue and  
cultured H/RS cells**

### **3.1 Introduction**

Classical Hodgkin's lymphoma (cHL) is a lymphoid malignancy with characteristic features that distinguish it from nodular lymphocyte-predominant HL (NLPHL) and non-Hodgkin lymphomas (NHLs) (Harris *et al.*, 1994 and Stein *et al.*, 2001a). The malignant cells in cHL, termed the Hodgkin's/Reed-Sternberg (H/RS) cells, constitute only a minor component of the tumour, whereas the majority of the tumour mass is composed of a mixed inflammatory infiltrate including lymphocytes, eosinophils, fibroblasts, macrophages, and plasma cells. This chapter set out to investigate the expression of the anti-apoptotic Bcl-2 family member, *bfl-1*, in H/RS cells of cHL by examination of H/RS primary tumour tissue using methods, which enabled examination of malignant cells in a complex reactive background. The expression of *bfl-1* was subsequently examined in established cultured H/RS cell lines in order to validate the cell culture model of the malignant H/RS cell for future experiments.

#### **3.1.1 Summary of results**

In this study, tumour tissue from HL patients was examined for expression of *bfl-1* mRNA. Laser capture microdissection was used to procure H/RS cells and RT-PCR analysis was performed to detect *bfl-1* specific mRNA transcripts. High mRNA expression levels of *bfl-1* were observed in all cases of EBV+/- HL primary cases tested. All cases were tested and found negative for expression of a novel *bfl-1* splice variant designated *bfl-1S*. Relative quantification of the level of *bfl-1* mRNA in H/RS and reactive/bystander cells revealed high mRNA expression levels in both malignant H/RS and reactive/bystander cells in EBV+/- HL primary cases. *bfl-1* mRNA levels in H/RS cells varied between 0.01 to 2 times that seen in selected bystander cells or between 0.02 and 2 times that seen in activated tonsillar GC cells. In an additional attempt to analyse *bfl-1* mRNA expression, a vector was designed and constructed in this study to produce sense and antisense *bfl-1* transcripts by *in vitro* transcription, for detection of *bfl-1* mRNA in tumour tissues by *in situ* hybridisation. Sense and antisense probes were tested on HL tumour biopsy but no signal was detected for *bfl-1* mRNA. No subsequent attempts at *bfl-1* mRNA detection were made with the sense and antisense *bfl-1* transcripts due to time constraints.

A panel of HL-derived cell lines was tested for the expression of *bfl-1* mRNA. High-level *bfl-1* mRNA expression was observed in all cultured H/RS cell lines tested relative to the type I EBV positive Burkitt's lymphoma (BL) cell line, MUTU I, and the housekeeping genes *gapdh* and *L32* by RNase protection assay (RPA) and relative to the EBV negative BL cell lines, DG75 and OKU BL by realtime quantitative PCR. RNA from a panel of lymphoma cell lines was also tested for expression of a novel *bfl-1* splice variant designated *bfl-IS*. *Bfl-1* but not *bfl-IS* mRNA expression was detected in Type I/III BL cell lines, lymphoblastoid cell lines (LCLs) and HL-derived cell lines.

## **3.2 Results - Detection of *bfl-1* mRNA expression in HL**

The expression of Bcl-2 family members has been extensively studied in cultured/primary H/RS cells with the exception of *bfl-1*, *bik* and *bcl-w* (Section 1.7.6). Based on this need to complete the apoptosis profile in this cell context and on previous findings in our laboratory establishing a role for *bfl-1* in regulating the survival of EBV-infected B cells (*bfl-1* is regulated by EBV proteins LMP1 and EBNA2), and in other laboratories suggesting that *bfl-1* expression is a key factor in other B-cell neoplasias (Section 1.7.5), it was a primary aim of this study to evaluate the expression of *bfl-1* in H/RS cells of EBV positive/negative HL.

### **3.2.1 Detection of *bfl-1* mRNA expression in H/RS cells of HD patients**

Examination of *bfl-1* mRNA expression status in HL tumour tissue was carried out in collaboration with a leading HL/EBV research laboratory at the University of Birmingham, U.K. Unfortunately, immunohistochemistry was not an available option due to the lack of a suitable anti-Bfl-1 antibody. Two RNA-based techniques were chosen to detect *bfl-1* expression in primary tumour tissue; laser capture microdissection (LCM) followed by one-step nested RT-PCR and *in situ* hybridisation (ISH) using an anti-sense riboprobe to *bfl-1* synthesised by *in vitro* transcription from a dedicated plasmid (pGEM-*bfl-1*-RP) designed and constructed prior to the Birmingham visit. The analysis was restricted to cases of nodular sclerosis (NS) disease type, the main histotype of cHL (Section 1.2) due to the availability of tissues.

#### **3.2.1.1 Laser Capture Microdissection**

Since HL tumours are comprised of heterogeneous populations of cells, with only 1-2 % malignant cells, a technique that enabled the analysis of pure H/RS cell populations was necessary. LCM is a powerful technique that permits procurement of single/multiple cells from tissue using the precision of lasers. Frozen primary tumour tissue from HD patients diagnosed with NS disease type was prepared at 7 µm on RNase-free glass slides, fixed in 100 % (v/v) ethanol and stained with Haemalum (blue nuclear stain) for pathological review (Section 2.5.1.1). LCM was used to procure a pure population of

H/RS or reactive/bystander cells under direct microscopic visualisation (Section 2.5.2). Cells were chosen on the basis of their morphology. H/RS cells (Figure 3.1) from three EBV negative HL cases (referred to as Case 1, 2 and 3) and three EBV positive HL cases (referred to as Case 4, 5 and 6) were collected. Reactive/bystander cells (Figure 3.2) were collected from EBV negative Case 2 and EBV positive Case 6. Germinal centre (GC) B cells from tonsil were also collected by LCM to act as a positive control as *bfl-1* transcript has been detected in the GC cells of lymphoid follicles (Jung-Ha *et al.*, 1998).

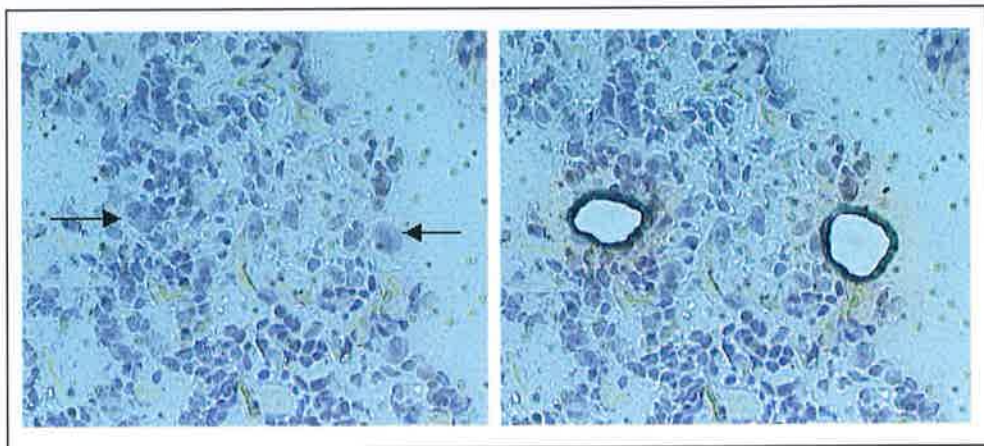


**Figure 3.1 Detection of *bfl-1* mRNA expression in H/RS cells of HL patients.**

LCM of H/RS cells from frozen primary tumour tissue sections prepared at 7 µm on RNase-free glass slides and stained with haemalum. H/RS cells (arrows) identified by their characteristic morphology were microdissected (left; before, right; after).

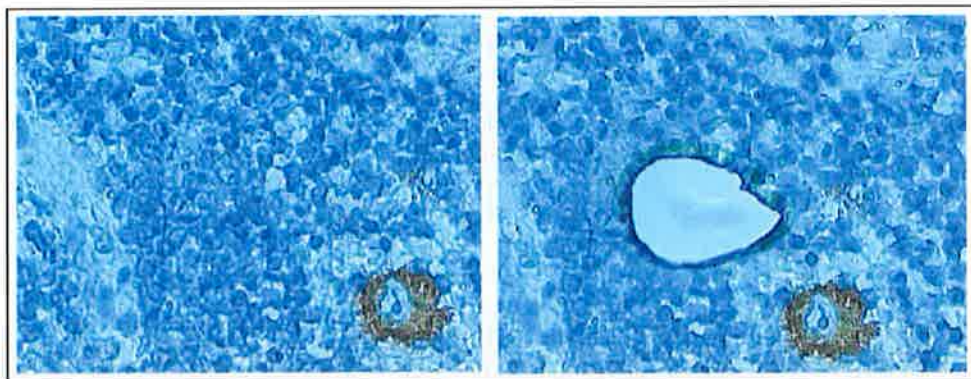


**Figure 3.2 Detection of *bfl-1* mRNA expression in bystander/reactive cells of HL patients.**

Frozen primary tumour tissue sections from two NSHL patients (1 EBV positive, 1 EBV negative, all nodular sclerosis disease type) were prepared at 7 µm on RNase-free glass slides and were stained with hematoxylin. H/RS cells (arrows) identified by their characteristic morphology and CD30-positive staining are shown. Cells were collected by LCM. Bystander/reactive cells (within circle) identified by their characteristic morphology (left; before, right; after).

RNA was extracted from microdissected cells and reverse-transcribed to DNA in a manner that facilitated detection of the two isoforms of the *bfl-1* gene.

### 3.2.1.2 *Bfl-1* isoforms

Several proteins of the Bcl-2 family, including Bcl-2, Bcl-x and Bax, have membrane-bound and soluble isoforms, which are generated by alternative splicing (Hockenberry *et al.*, 1990, Boise *et al.*, 1993 and Shi *et al.*, 1999). Isoforms of the Bcl-2 family can either cooperate or antagonise each other (reviewed in Akgul, Moulding and Edwards, 2004). Alternative splicing forms of Bcl-x give rise to two transcripts coding for either a long (Bcl-x<sub>L</sub>) or a short (Bcl-x<sub>S</sub>) form of the protein. Bcl-x<sub>L</sub> inhibits cell death, whereas Bcl-x<sub>S</sub> antagonises the anti-apoptotic action of both Bcl-2 and Bcl-x<sub>L</sub>. It has been demonstrated that mice have three functional variants of A1, the mouse homologue of Bfl-1 (Hatakeyama *et al.*, 1998), and recently two isoforms of human Bfl-1 have been reported by Ko *et al.*, (2003b), designated Bfl-1 and Bfl-1S (Figure 3.3).

The *bfl-1S* primary sequence contains four conserved Bcl-2 homology (BH) domains and a positive-charged C-terminus containing KKRK amino acids. Bfl-1 localises to the

mitochondrial membrane while Bfl-1S has been shown to localise in the nucleus. Although currently the biological role for Bfl-1S is not fully understood it is postulated that Bfl-1S delays the activation of mitochondrial apoptosis by sequestering Bid at the nucleus and by interfering with cleavage of Bid. Cleavage of Bid to produce truncated Bid (tBid) subsequently promotes Cytochrome c (Cyt c) release and apoptosis upon translocation to the mitochondria. The expression of *bfl-1S* mRNA was detected predominantly in normal lymph nodes and in B-lymphoid leukemia cells. However, the expression of Bfl-1S in HL was not investigated by Ko *et al.*, 2003b.

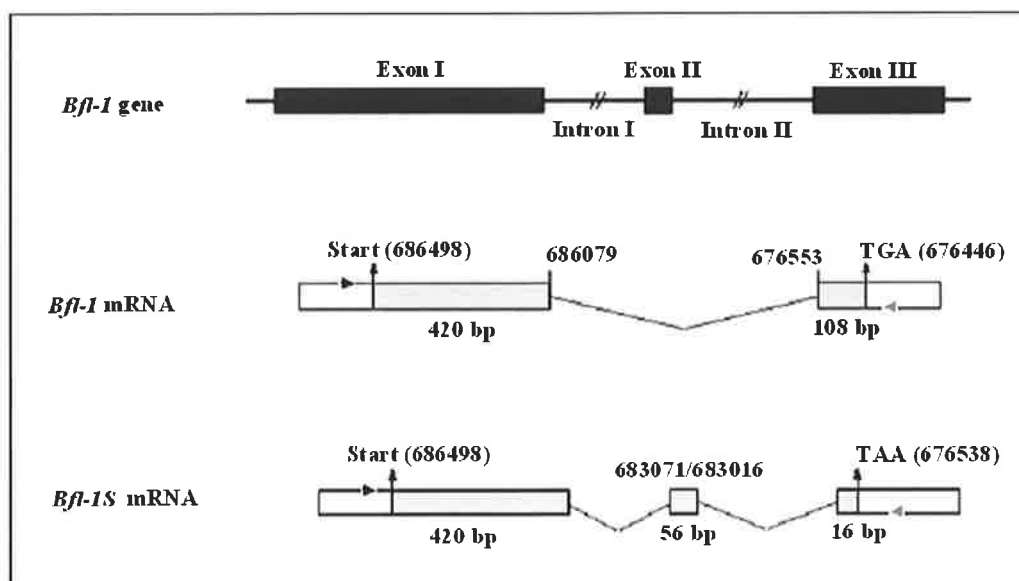


**Figure 3.3 The organisation of the *bfl-1* gene is compared with mRNAs encoding *bfl-1* and *bfl-1S*.**

The *bfl-1* gene located on chromosome 15 was identified from 1688 kb of the Working Draft Sequence of Human Chromosome 15 (the GenBank/EBI database no. NT\_010360). Splicing sites and start and stop positions are indicated as upper numbers at their respective genomic nucleotide positions. Ligation of exons I and III produces *bfl-1* mRNA (U27467), whereas the inclusion of the 56-bp exon II produces *bfl-1S* mRNA, which encodes a 163 amino-acid protein by an open reading frame (ORF) shift, and causes an early translation termination. Positions of the RT-PCR primers are indicated by a black arrowhead for RT-primer1 and a grey arrowhead for RT-Primer2. Adapted from Ko *et al.*, 2003b.

To test for *bfl-1* mRNA expression, RNA was extracted from microdissected cells (Section 2.6.5), reverse-transcribed and PCR amplified in a nested PCR assay (Figure

3.4) designed to detect *bfl-1* mRNA in a single-step RT-PCR approach (Section 2.6.6) using *bfl-1*-specific internal and external primers (BFL-1 INT F/R and BFL-1 EXT F/R; sequences listed in Table 2-6). This assay was also designed to resolve the *bfl-1* mRNA splice variants discussed in Section 3.2.1.2 in the manner outlined in Figure 3.4.

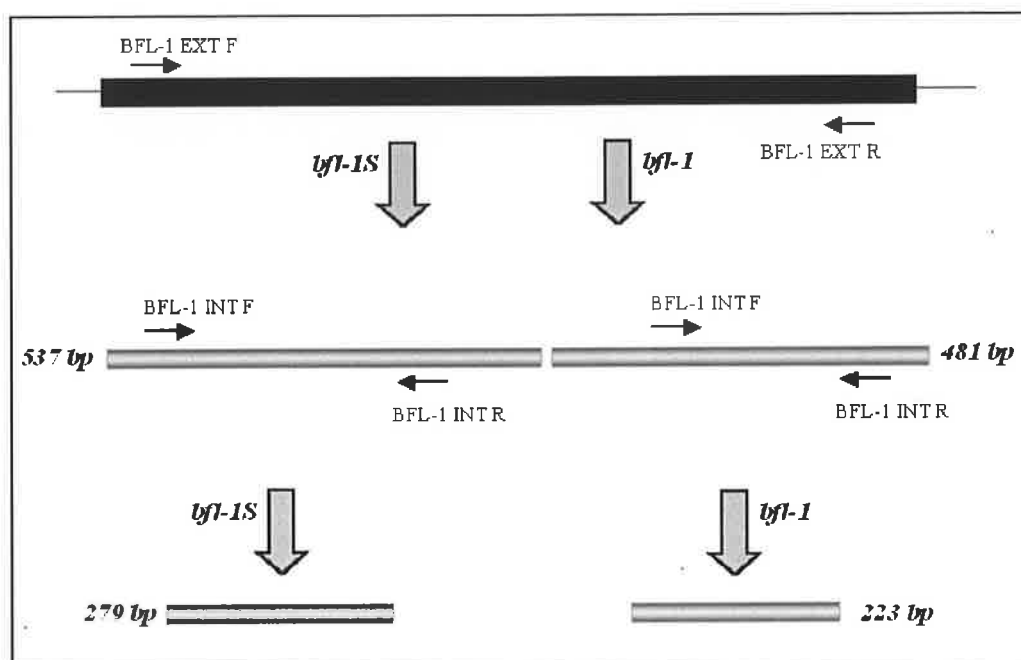


**Figure 3.4 Schematic of nested PCR approach to detect and resolve *bfl-1/bfl-1S* expression in H/RS cells.**

PCR amplification with Bfl-1 INT F/R primers would generate a fragment of size 223/279 bp indicating the presence of *bfl-1/bfl-1S*. Similarly amplification with BFL-1 EXT F/R would generate a fragment of size 481/537 bp indicating the presence of *bfl-1/bfl-1S* respectively.

From these results, it can be seen that *bfl-1* mRNA expression (without *bfl-1S* expression) was detected in primary tumour H/RS cells (Figure 3.5). Similarly, *bfl-1* expression (without *bfl-1S* expression) was detected in reactive cells from primary tumour tissue and in GC B cells. While *bfl-1* mRNA expression was previously detected in GC B cells (Jung-Ha *et al.*, 1998), the profile of the *bfl-1S* splice variant expression was not investigated. The detection of expression of *bfl-1* mRNA only in primary tumour H/RS cells and GC B cells is a novel observation.

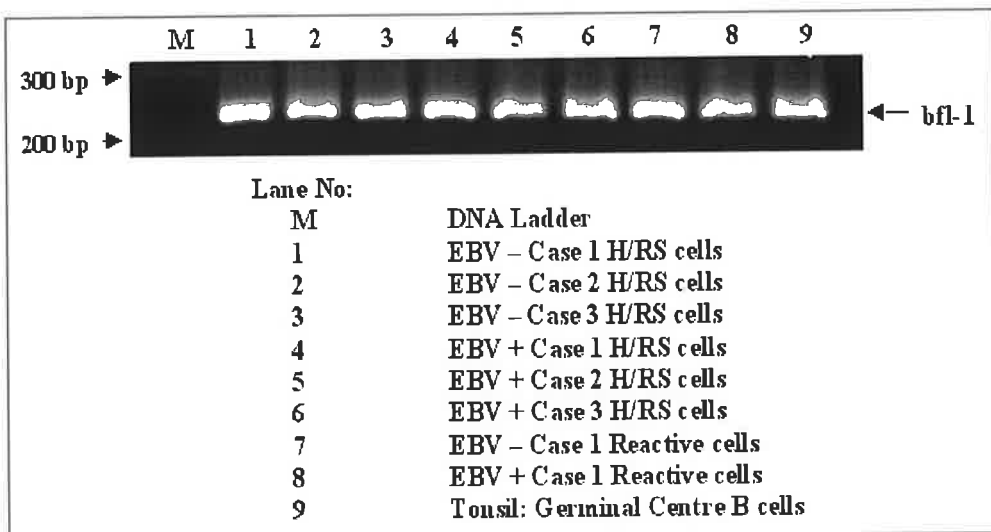


**Figure 3.5 *bfl-1* mRNA detection in microdissected cells.**

RT-PCR analysis using a nested PCR approach was used to detect *bfl-1/bfl-1S* mRNA expression. *Bfl-1* mRNA expression was detected as a 232 bp product in all HL cases irrespective of EBV status, in bystander cells/reactive lymphoid tissue of both EBV positive and negative cases and in GC B cells from tonsil.

Detection of the presence of *bfl-1* mRNA in reactive cells of tumour tissue was not surprising. H/RS cells of HL represent <1 % of cells in an involved lymph node. These malignant cells are embedded in a background of non-neoplastic cells, which are believed to be recruited and activated by H/RS-derived cytokines (Pinto *et al.*, 1998). The reactive background, constituting the majority of the malignancy, is composed of a mixed inflammatory infiltrate variably composed of lymphocytes, eosinophils, fibroblasts, macrophages and plasma cells (Skinnider and Mak, 2002). Lymphocytes making up the inflammatory background of HL are not innocent bystanders, but can interact with neoplastic RS cells, and have the potential to affect tumour genesis and progression (Poppema and van den Berg, 2000). Jung-Ha *et al.*, (1998), observed prominent *bfl-1* mRNA expression signals by ISH in the lymphatic tissue, including tonsil, lymph nodes and lymphoid nodules of the gastrointestinal tract.

These results confirm the expression of *bfl-1* mRNA in H/RS and bystander cells of HL but do not indicate the relative level of expression. To make a comparative quantitative analysis, RNA extracted from H/RS cells and reactive/bystander cells procured by LCM was reverse-transcribed to cDNA using random primers and the Sensiscript reverse

transcriptase (enables RT of <50 ng RNA) (Section 2.6.7.1). The relative level of *bfl-1* mRNA was quantified in H/RS cells and reactive/bystander cells (Figure 3.6) by real-time q-PCR using TaqMan assays (Section 2.6.4.2) for *bfl-1* and *gapdh* (endogenous control). RNA from H/RS cells of two EBV negative (Case 1 and Case 2) and two EBV positive (Case 4 and Case 5) HL cases and RNA from reactive/bystander cells in two cases (Case 2; EBV negative and Case 6; EBV positive) was quantified for *bfl-1* level by q-PCR. Unfortunately RNA from H/RS cells from Case 3 and Case 5 was not of sufficient integrity or quantity for quantification by q-PCR.

Specifically, it was found that the level of *bfl-1* mRNA in reactive/bystander cells from lymphoid tissue of EBV negative HL (Bystander Case 2) was ~50-fold greater relative to H/RS cells from the same Case (EBV negative 2). However, H/RS cells from EBV negative Case 1 expressed ~2 fold greater level of *bfl-1* mRNA relative to reactive/bystander cells of EBV negative Case 2. In the EBV positive cases, direct comparison of *bfl-1* level in H/RS cells from Case 6 was not possible but the level of *bfl-1* mRNA in reactive/bystander cells (Bystander Case 6) was found to be ~100-fold greater relative to H/RS cells from EBV negative Cases 4 and 5.

In the cases examined, therefore, *bfl-1* mRNA was expressed to a greater extent in bystander cells than in H/RS cells in Case 2 (EBV+), Case 4 and Case 5 (EBV-) and expressed to a greater extent in H/RS cells than in bystander cells in Case 1 (EBV+).

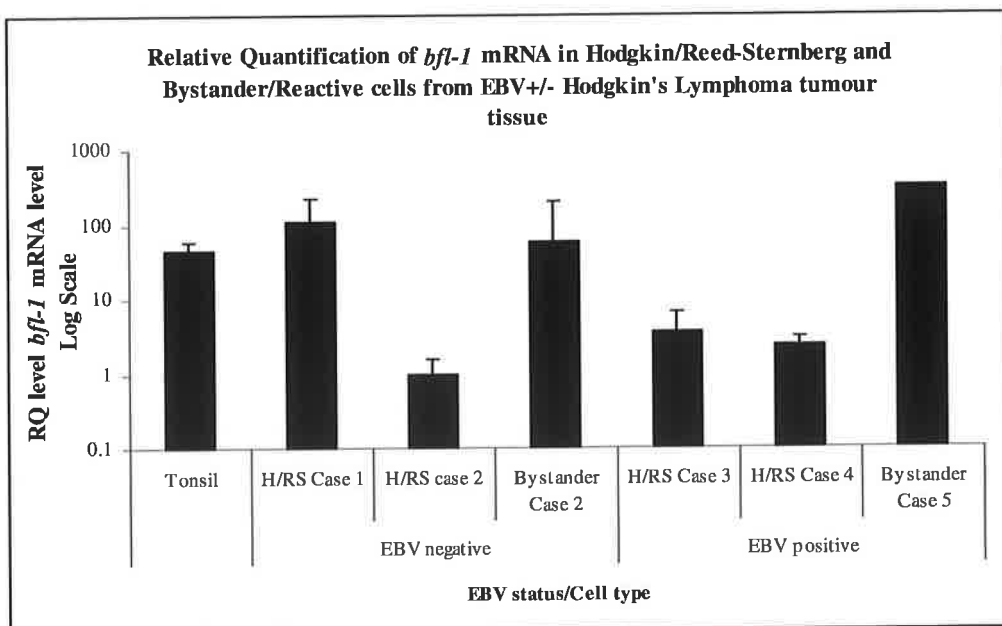


**Figure 3.6 Relative quantification of *bfl-1* mRNA level in H/RS and bystander/reactive cells from EBV +/- HL tumour tissue.**

H/RS and bystander/reactive cells were procured by LCM under strict RNase-free conditions. RNA was extracted and reverse transcribed using random primers and Sensiscript reverse transcriptase. Amplification of DNA was monitored in real-time by detection of fluorescence intensity using a FAM-labeled TaqMan probe for *bfl-1* and a FAM-labeled TaqMan probe for *gapdh*. Fluorescent signals were detected using an ABI Prism 7500 Sequence Detection System. Log<sub>10</sub> *bfl-1* mRNA expression levels were plotted following normalisation for *gapdh*.

### **3.2.1.3 *In situ* hybridisation using sense/anti-sense *bfl-1* riboprobes**

*In situ* RNA-RNA hybridisation (ISH) is a technique that enables the visualisation of specific mRNAs in identified cells using a targeted anti-sense probe. To analyse *bfl-1* mRNA expression in tumour tissues by ISH, a vector was designed and constructed to produce sense and antisense *bfl-1* transcripts by *in vitro* transcription (IVT). These probes were subsequently synthesised to incorporate the digoxigenin (DIG)-label and were used in attempts to detect *bfl-1* mRNA in malignant HL tissue by ISH experiments.

In order to generate a vector capable of expression of sense/anti-sense *bfl-1* RNA transcripts, a portion of the *bfl-1* ORF was amplified by PCR and inserted into the expression vector pGEM 3ZF (Table 2-5) to produce pGEM-*bfl-1*-RP (Figure 3.7). The pGEM 3ZF (Promega) expression vector (Figure 3.8A) was firstly linearised by restriction digestion with *Eco*RI/*Hind*III restriction enzymes (Figure 3.8B), followed by dephosphorylation using calf intestinal phosphatase (CIP) (Section 2.3.4) to prevent recircularisation of the linearised DNA. The linearised, CIP-treated DNA was then purified by phenol: chloroform extraction followed by ethanol precipitation (Section 2.3.2).

pCDNA3-HA-*bfl-1* (Table 2-5) was used as template DNA. This construct contains the full length *bfl-1* ORF sub-cloned downstream of a hemagglutinin (HA) peptide (derived from the human influenza HA protein) in pCDNA3 (D'Sa-Eipper *et al.*, 1996). A portion of the *bfl-1* ORF was amplified by PCR using RiboFor/RiboRev primers (sequences are given in Table 2-6) which led to the incorporation of *Eco*RI/*Hind*III restriction sites (underlined in primers) at the 5'/3' end of the PCR products. Following PCR, the products were analysed by agarose gel electrophoresis (Section 2.3.13) (Figure 3.8C). The PCR products were subsequently purified using the Wizard® DNA purification system (Section 2.3.6), digested with *Eco*RI/*Hind*III and purified by phenol: chloroform extraction followed by ethanol precipitation. The digested, purified PCR products were then sub-cloned into the *Eco*RI/*Hind*III sites of pGEM 3ZF. Ligation (Section 2.3.7) of vector and insert DNA was carried out at 22 °C for 3 h.

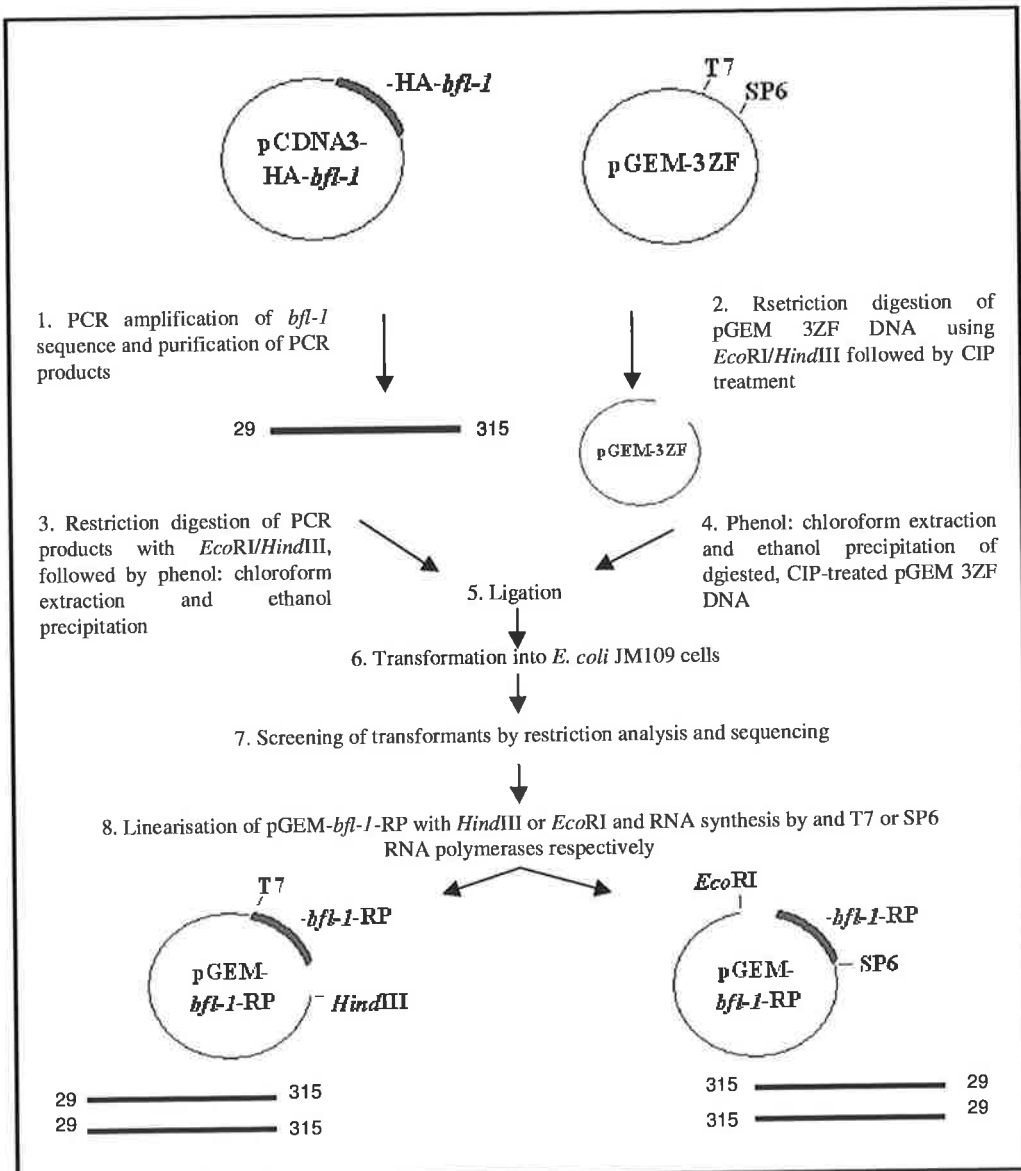


**Figure 3.7 Generation of pGEM-bfl-1-RP; a vector capable of synthesising sense/anti-sense *bfl-1* RNA transcripts for ISH.**

Flow diagram detailing the steps involved in generating the pGEM-bfl-1-RP construct. Briefly, a portion of the *bfl-1* ORF was amplified by PCR using pCDNA3-HA-bfl-1 as template DNA, digested with EcoRI/HindIII and sub-cloned into the EcoRI/HindIII sites of pGEM 3ZF. Competent *E. coli* JM109 cells were transformed with the recombinant plasmid and a number of independently transformed colonies were selected for growth of small-scale cultures. Plasmid DNA isolated from each culture was then analysed by restriction digestion and sequencing. pGEM-bfl-1-RP DNA was linearised with HindIII or EcoRI and run-off transcripts were *in vitro* transcribed using T7 or SP6 RNA polymerases respectively.

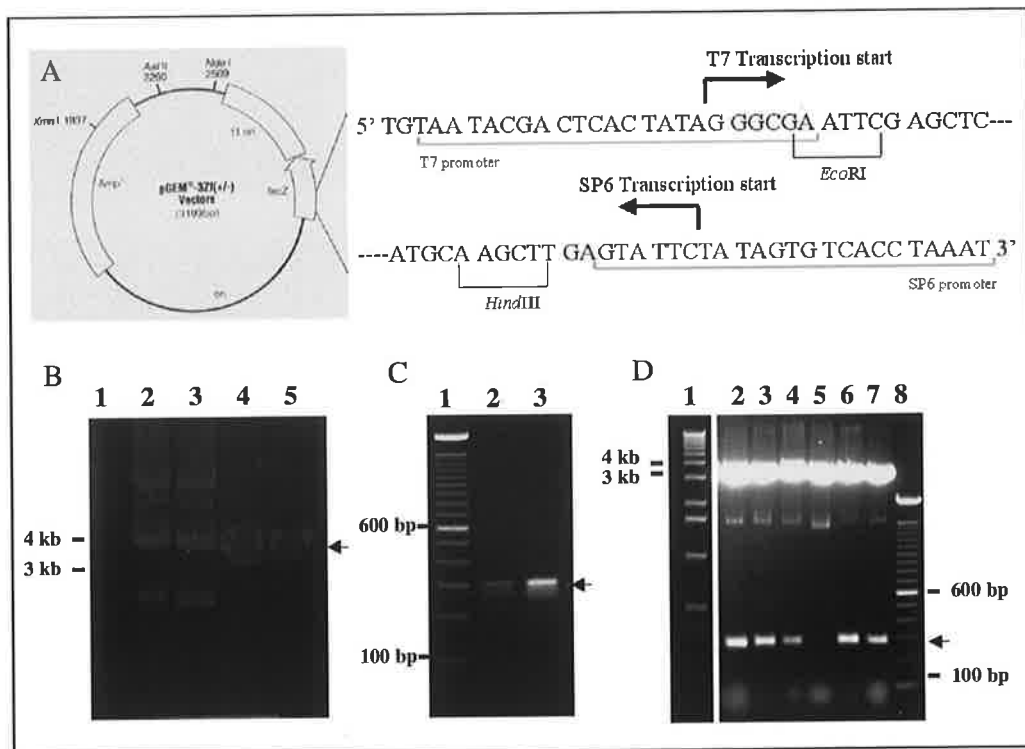


**Figure 3.8 Analysis of the cloning steps in the construction of pGEM-*bfl-1*-RP**

The pGEM-*bfl-1*-RP mRNA expression plasmid was constructed by cloning a portion of the *bfl-1* gene into the plasmid pGEM 3ZF (A; left) between the *Eco*RI and *Hind*III sites of the multiple cloning site, flanked by transcription start sites for T7 and SP6 RNA polymerases (A; right). Agarose gel electrophoresis [0.7 % (B), 2 % (C) and 1 % (D) agarose-1 X TAE gel electrophoresed at 100 V for 1 h in 1 X TAE] was used to monitor cloning steps. (B) Lane 1; 1 kb ladder (Invitrogen), lane 2, 3; pGEM 3ZF DNA, lane 4, 5; pGEM 3ZF DNA linearised with *Eco*RI/*Hind*III to reveal ~3.2 kb fragment, indicated by black arrow. (C) Lane 1; 100 bp ladder, lane 2/3; *bfl-1* PCR product of ~300 bp before/after purification, indicated by black arrow. (D) *Eco*RI/*Hind*III restriction analysis of transformant DNA. Lane 1/8; 1 kb/100 bp ladder, lane 2-7; transformant DNA, positive clones (lanes 2-4, 6-7) revealed ~300 bp fragment upon digestion, designated by black arrow.

Following the ligation reaction, competent *E. coli* JM109 (Section 2.3.8) cells were transformed (Section 2.3.9) with the recombinant plasmid DNA. Transformants were selected for ampicillin (100 µg/ml) resistance. Following overnight incubation at 37 °C, a number of colonies were randomly selected and individually sub-cultured into fresh 5 ml volumes of LB broth. The selected clones were grown overnight at 37 °C with shaking at 200 rpm, reaching stationary growth phase. Cells were pelleted by centrifugation at 6,000 x g. Plasmid isolation (Section 2.3.10) was performed on the

resulting cell pellet. Restriction analysis was carried out on the resultant DNA to detect the presence of the *bfl-1* insert at the expected size (Figure 3.8D). Integrity of plasmid DNA was verified by sequencing (Section 2.3.14) using a T7 primer (Table 2-6). The pGEM-*bfl-1*-RP-derived plasmid DNA, demonstrated 100 % homology with the *bfl-1* gene as derived from the GenBank coding sequence; accession number U27467 (data not shown).

For synthesis of sense/anti-sense transcripts, the pGEM-*bfl-1*-RP plasmid was linearised in two independent reactions by restriction digestion using *Eco*RI or *Hind*III enzymes, extracted by phenol: chloroform, ethanol precipitated and dissolved in DEPC H<sub>2</sub>O. Sense and anti-sense run-off transcripts were synthesised by *in vitro* transcription (IVT) using SP6 (*Eco*RI linearised DNA) or T7 (*Hind*III linearised DNA) RNA polymerases (Section 2.5.3.1) respectively. The resultant ~300 nt transcripts were analysed by RNA gel electrophoresis (Section 2.6.2) (Figure 3.9).

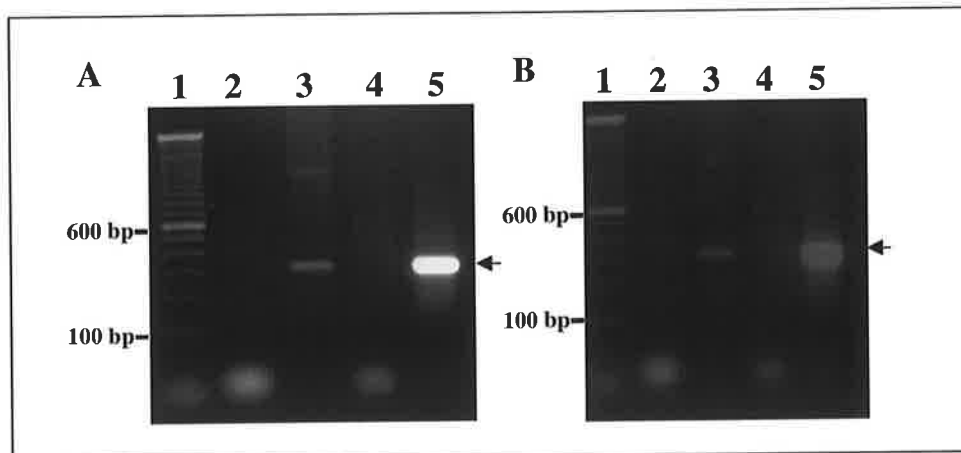


**Figure 3.9 RNA gel electrophoresis of the *in vitro* transcribed sense/anti-sense *bfl-1* riboprobes.**

(A) T7 *in vitro* transcription from linearised pGEM-*bfl-1*-RP. Lane 1: 100 bp DNA ladder (denatured by boiling), Lane 2: pGEM-*bfl-1*-RP antisense (maxiprep in UpH<sub>2</sub>O) digested with *Eco*RI (negative control), Lane 3: pGEM-*bfl-1*-RP antisense (maxiprep in UpH<sub>2</sub>O) digested with *Hind*III (anti-sense riboprobe), Lane 4: pGEM-*bfl-1*-RP antisense (maxiprep in DEPC H<sub>2</sub>O) digested with *Eco*RI (negative control), Lane 5: pGEM-*bfl-1*-RP antisense (maxiprep in DEPC H<sub>2</sub>O) digested with *Hind*III (anti-sense riboprobe). (B) SP6 *in vitro* transcription from linearised pGEM-*bfl-1*-RP. Lane 1: 100 bp DNA ladder (denatured by boiling), Lane 2: pGEM-*bfl-1*-RP antisense (maxiprep in

UpH<sub>2</sub>O) digested with *Hind*III (negative control), Lane 3: pGEM-*bfl-1*-RP antisense (maxiprep in UpH<sub>2</sub>O) digested with *Eco*RI (sense riboprobe), Lane 4: pGEM-*bfl-1*-RP antisense (maxiprep in DEPC H<sub>2</sub>O) digested with *Hind*III (negative control), Lane 5: pGEM-*bfl-1*-RP antisense (maxiprep in DEPC H<sub>2</sub>O) digested with *Eco*RI (sense riboprobe).

The sense/anti-sense *bfl-1* riboprobes were then used in an attempt to detect *bfl-1* mRNA expression in NS tumour biopsies by ISH. Cryosections for ISH of 7 µm thickness were cut at -20 °C, collected on Vectabond slides and fixed in 4 % paraformaldehyde (Section 2.5.1.2). RNA transcripts were transcribed using digoxigenin (DIG)-labelled nucleotides in anti-sense and sense orientation using T7 and SP6 polymerases (Section 2.5.3.1). DIG-probes were hybridised with tissue sections overnight (Section 2.5.3.2) and immunodetected using an anti-DIG antibody (Section 2.5.3.3). However, no signal was detected for *bfl-1* mRNA. Optimisation of ISH conditions to determine favourable parameters for probe hybridisation and signal amplification would have been necessary but were not carried out due to time constraints. As *bfl-1* mRNA was simultaneously detected by LCM followed by RT-PCR, no further ISH experimentation was performed.

### **3.2.2 Detection of *bfl-1* mRNA expression in cultured H/RS cells**

Cell lines derived from human tumours have been extensively used as experimental models of neoplastic disease (Ross *et al.*, 2000). Physiological or experimental adaptation for growth in culture can overwrite the gene expression programmes established during differentiation *in vivo*. In order to ensure that the high-level expression of *bfl-1* mRNA observed in H/RS cells from primary tumour tissue was reflected in cultured H/RS cells subject to the tissue culture environment of synthetic growth media and fetal bovine serum, an attempt was made to confirm *bfl-1* mRNA expression in H/RS cell lines to validate the cell culture model.

The mRNA expression levels of nine members of the Bcl-2 family in cultured H/RS cells were analysed by RNase protection assay (RPA) (Figure 3.10; in collaboration with Dr. Brendan D'Souza). For relative quantification of mRNA, EBV positive BL isogenic cell lines with type I latency (MUTU I) and type III latency (MUTU III) phenotypes were included in the analysis. The MUTU I cell line is a type I BL cell line and is thought to be the *in vitro* equivalent of a GC B cell (MacLennan *et al.*, 1988). MUTU III cell line was previously shown in the laboratory to express ~20-fold greater level of *bfl-1* mRNA relative to MUTU I (D'Souza, Rowe and Walls, 2000).

Consistent with previous reports, the expression of *bcl-2*, *bcl-x<sub>L</sub>*, *bcl-x<sub>S</sub>*, *bad*, *bak*, *bax* and *mcl-1* can be seen to be a feature of cultured H/RS cells (Figure 3.10). High levels of *bfl-1* mRNA are present in all H/RS cell lines irrespective of EBV status relative to the type I BL cell line, MUTU I. In addition, previously unreported expression levels of two other members of the bcl-2 family (*bcl-w* and *bik*) are seen here. The expression of *bcl-w* mRNA is a feature of all the H/RS and BL cell lines tested. The absence of *bik* mRNA expression in all H/RS cell lines is distinctly evident in contrast to the expression of *bik* mRNA in the BL cell lines tested and the role of *bik* expression in EBV-associated B-cell malignancies is the subject of ongoing investigation in the laboratory.

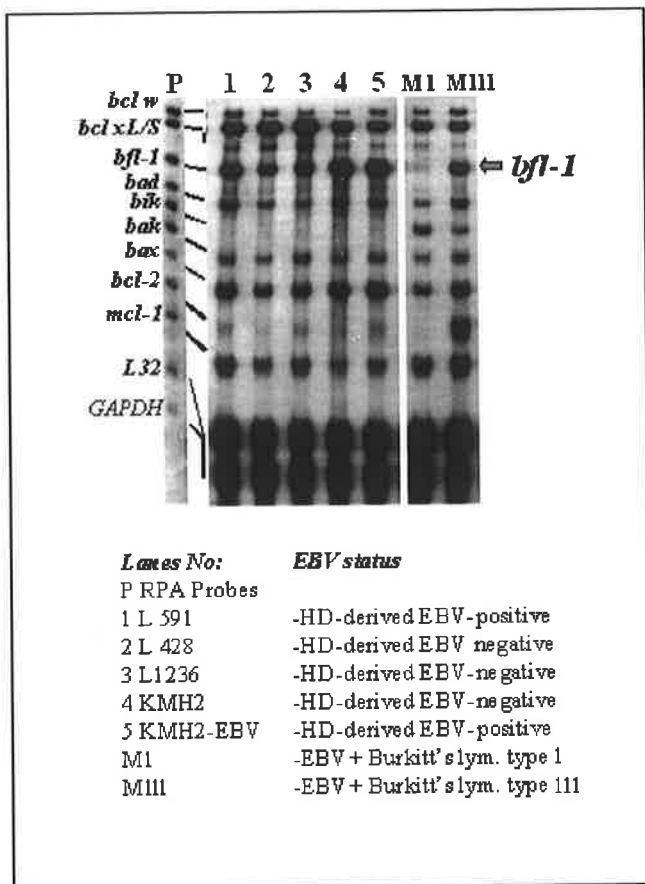


**Figure 3.10 Detection of *bfl-1* mRNA expression in cultured H/RS cells.**

Ribonuclease protection assay in which mRNA levels from the apoptosis-related genes *bcl-x<sub>L</sub>*, *bcl-x<sub>S</sub>*, *bfl-1*, *bik*, *bak*, *bax*, *bcl-2* and *mcl-1* were analysed in a range of HL-derived cell lines, a type I BL cell line and a type III BL cell line. Unprotected  $\text{P}^{32}$ -labeled antisense riboprobes (P) were loaded alongside RPA-processed samples and are shown linked to their smaller RNase-protected fragments, which correspond to the steady-state levels of mRNA in the sample. The location of the protected fragment derived from *bfl-1* mRNA is indicated by the arrow. *bfl-1* mRNA levels are elevated in HD-derived cell lines irrespective of EBV status.

Further to this experiment, it was shown that *bfl-1* is highly expressed in cultured H/RS cells by RT-qPCR (Section 2.6.4.2) (Figure 3.11) relative to EBV negative BL cell lines (DG75 and OKU BL) after normalising with *gapdh* levels. The DG75 cell line was chosen as the calibrator as it expresses very low levels of *bfl-1* mRNA (D'Souza *et al.*, 2000). The relative level of *bfl-1* mRNA (calculated using the Comparative  $C_T$  method [ $\Delta\Delta C_T$ ] as described by Livak and Schmittgen, 2001) as seen in Figure 3.11 is 165-,

2,711-, 10,111-, 1,211- and 1,800,000- fold in L591, L428, L1236, KMH2 and KMH2-EBV cell lines respectively.

Efforts were also made to detect Bfl-1 protein in H/RS cell lines using many different batches of commercially available antibodies in western blot analysis without success (data not shown). Many authors studying Bfl-1 expression have described this difficulty (Moreb and Zucali, 2001).

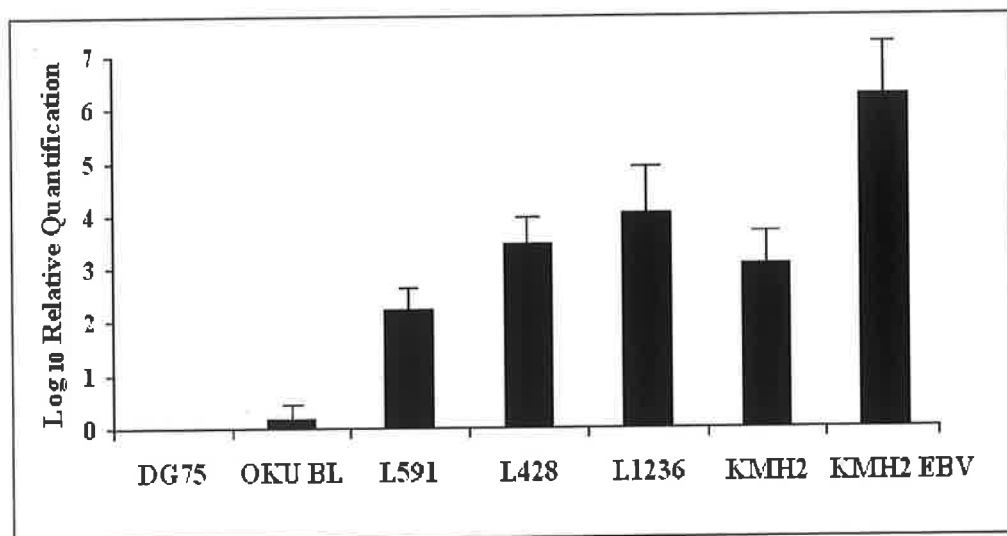


**Figure 3.11 Real time qPCR analysis of *bfl-1* mRNA levels from HL-derived cell lines**

RNA isolated from cell lines was reverse transcribed using random primers and amplification of DNA was monitored in real-time by detection of fluorescence intensity using a FAM-labeled TaqMan probe for *bfl-1* and a FAM-labeled TaqMan probe for *gapdh*. Fluorescent signals were detected using an ABI Prism 7500 Sequence Detection System. After normalisation for *gapdh*, Log<sub>10</sub> *bfl-1* mRNA expression levels in HL-derived cell lines were plotted relative to *bfl-1* mRNA expression level in the EBV-negative BL cell lines DG75 and OKU BL.

RPA analysis showed the presence of high levels of *bfl-1* mRNA in the HL-derived cell lines (Figure 3.10) but failed to resolve the mRNAs encoding *bfl-1* and *bfl-1S* due to probe location along *bfl-1* transcript. To this end, RNA from a panel of HL (L428, L592, L1236, KMH2, KMH2-EBV), BL and LCLs was examined for splice variant expression by RT (Section 2.6.4.1), followed by endpoint PCR (Section 2.3.5) using RT-primers 1 and 2 (Table 2-6), which annealed upstream/downstream of the *bfl-1*

start/stop codons, indicated as black and grey arrowheads (Figure 3.3) respectively. It was clear from this experiment that only the longer of the two known splice variants of *bfl-1* mRNA was expressed in cultured H/RS, type I BL, type III BL cells and in LCLs (Figure 3.12).

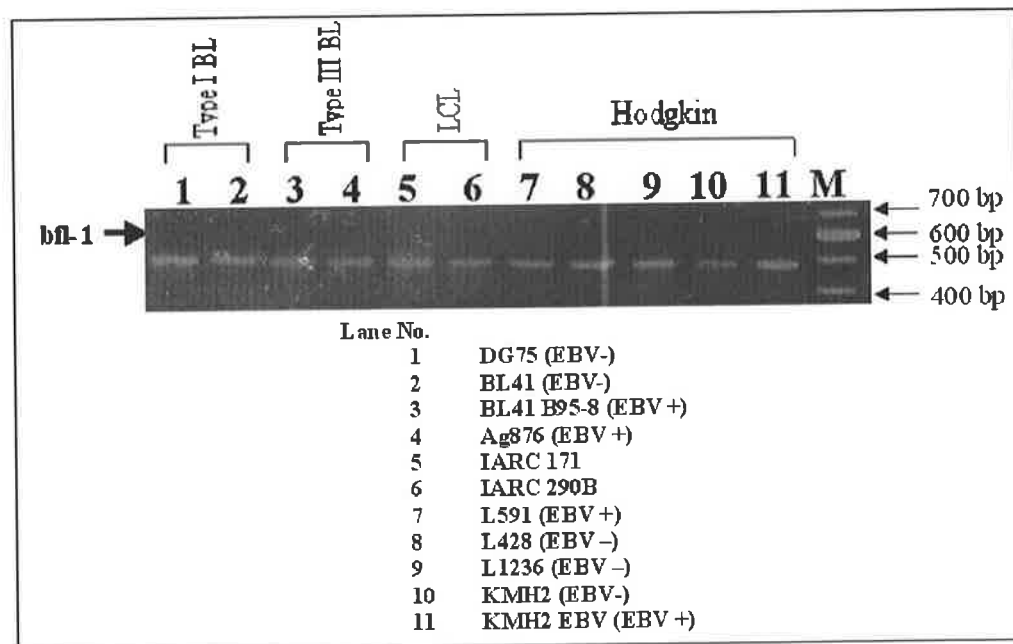


**Figure 3.12 Expression of *bfl-1/bfl-1S* mRNA in lymphoma cell lines.**

RT-PCR was performed with RT-primers 1 and 2 to amplify simultaneously *bfl-1* and *bfl-1S* cDNA as 481 and 537 bp products. *Bfl-1* mRNA expression was detected in Type I BL cell lines, Type III BL cell lines, LCLs and HL-derived cell lines. In contrast, *bfl-1S* mRNA expression was not detected in any of the cell lines tested.

In agreement with the finding in Section 3.2.1.2 that *bfl-1* mRNA only (and not *bfl-1S* mRNA) was expressed in H/RS cells from primary tumour tissue (Figure 3.5), *bfl-1* mRNA only was expressed in cultured H/RS cells (Figure 3.12).

Together these data, showing the high level expression of *bfl-1* in primary tissue mRNA and in cultured H/RS cells (Figure 3.5 and Figure 3.11) might suggest an active role for this anti-apoptotic gene in the pathogenesis of HL.

### 3.3 Discussion

The cell composition of the tumoural microenvironment plays a role in tumour genesis and progression, although its relevance is generally poorly understood, and varies among tumour types (Poppema and van den Berg, 2000). HL, with its characteristically rich inflammatory background, is a prototypical disease that lends itself to the study of the interplay between the tumour and its microenvironment.

Cytokines produced by H/RS cells are thought to contribute to the pathogenesis of this disease both by acting as autocrine (affecting the H/RS cell itself) and paracrine growth factors by initiating and sustaining the reactive infiltrate (Skinnider and Mak, 2002) and may be responsible for the expression of *bfl-1* in neighbouring cells by activation of various signaling pathways. Similarly, cytokines produced by surrounding reactive cells may be contributing to H/RS cell proliferation and survival.

Interleukin (IL)-13 regulates the humoral immune response by stimulating the proliferation and survival of B cells and triggering Ig class switching (Zurawski and de Vries, 1994). IL-13 is expressed by 4 of 5 H/RS cell lines (Skinnider *et al.*, 2002b; Kapp *et al.*, 1999) and in 100 % of primary H/RS cells tested (Ohshima *et al.*, 2001). IL-13 has been shown to activate STAT 6 signaling (Wurster *et al.*, 2000). Preventing constitutive STAT activation induced apoptosis of HL cell lines (HDLM2 and L540) and was associated with a strong decrease in the expression of anti-apoptotic genes including *bfl-1* (Cochet *et al.*, 2006).

IL-5 is essential for the growth and differentiation of eosinophils and is expressed by 2 of 6 H/RS cell lines tested (Klein *et al.*, 1992 and Kapp *et al.*, 1999) and in 95 % of primary H/RS cells from cHL tumours (Samoszuk and Nansen, 1990). The proliferation of 2 IL-5 positive H/RS cell lines (L428, KMH2) was not affected by antibody-mediated neutralisation of IL-5, suggesting that IL-5 is not an autocrine growth factor for cHL (Kapp *et al.*, 1999). Guthridge *et al.*, (2004), found that the IL-5 receptor mediates hematopoietic cell survival through activation of NF- $\kappa$ B and induction of Bcl-2.

IL-6 expression has been confirmed in 5 out of 7 H/RS cell lines (Wolf *et al.*, 1996, Klein *et al.*, 1992, Hsu *et al.*, 1992b; Jucker *et al.*, 1991) and in RS cells from 65 % to 100 % of cHL cases (Hsu *et al.*, 1992b, Merz *et al.*, 1991, Jucker *et al.*, 1991, Foss *et al.*, 1993, Herbst *et al.*, 1997; Beck *et al.*, 2001). IL-6 inhibits apoptosis in human gastric cancer AGS cells through up-regulation of anti-apoptotic bcl-2 family member

genes (Ming-Tsan *et al.*, 2001). Tarte *et al.*, (2004) demonstrated that constitutive Bfl-1/A1 expression rescued myeloma cells from apoptosis induced by IL-6 withdrawal.

Several chemokines (chemoattractant cytokines) are produced by H/RS cells, which regulate the selective migration of leukocytes through binding to specific chemokine receptors (Skinnider and Mak, 2002). Thymus- and activation-regulated chemokine (TARC) was expressed by 4 out of 4 H/RS cell lines examined, and by H/RS cells in 88 % of cHL cases (van den Berg *et al.*, 1999; Peh *et al.*, 2001). Macrophage-derived chemokine (MDC) expression was demonstrated in 87 % of cHL cases primarily in the H/RS cells (Hedvat *et al.*, 2001). Other chemokines expressed in both H/RS cell lines and primary cHL tissues include Eotaxin, inducible protein (IP)-10 and IL-8.

Several members of the tumour necrosis factor (TNF) family are expressed in cHL, primarily by H/RS cells, including TNF- $\alpha$  and lymphotoxin (LT)- $\alpha$  (Kretschmer *et al.*, 1990; Xerri *et al.*, 1992; Benharroch *et al.*, 1996; Ryffel *et al.*, 1991a and b; Ruco *et al.*, 1990). CD40L is absent on cultured and primary H/RS cells, but is present on CD4+ T cells within cHL tissues (Gruss *et al.*, 1994; O'Grady *et al.*, 1994; Carbone *et al.*, 1995a and b; Murray *et al.*, 1995). CD30L is expressed on eosinophils and mast cells adjacent to CD30+ H/RS cells (Pinto *et al.*, 1996; Molin *et al.*, 2001). RANK ligand (RANKL), another member of the TNF family is expressed in H/RS cell lines and primary H/RS cells (Fiumara *et al.*, 2001). Bfl-1 was identified as a TNF-inducible transcript (Karsan *et al.*, 1996a) and was shown to protect endothelial cells against TNF-induced cell death (Karsan *et al.*, 1996b).

The production of various chemokines and cytokines by the malignant H/RS cell may be responsible for the high-level *bfl-1* expression seen in surrounding reactive cells. High-level *bfl-1* expression has been observed in reactive cells of stomach and colon carcinoma. Jung-Ha *et al.*, (1998), showed that the mRNA ISH signal for *bfl-1* was localised within the inflammatory cells of tumour tissues of stomach and colon cancers, including neutrophils, eosinophils and lymphocytes.

The high ratio of *bcl-x<sub>L</sub>*/*bcl-2* mRNA expression seen here in cultured H/RS cells (Figure 3.10) is in agreement with the high ratio of Bcl-x<sub>L</sub>/Bcl-2 protein expression described by Kim *et al.*, (2004). Double immunohistochemical staining of primary H/RS cells for Bcl-x<sub>L</sub>/Bcl-2 revealed greater intensity staining for Bcl-x<sub>L</sub> relative to Bcl-2 and the authors hence suggested a more dominant role for Bcl-x<sub>L</sub> in ensuring survival of H/RS cells than Bcl-2. From Figure 3.10, it is possible to discern greater level expression of *bfl-1* compared to *bcl-x<sub>L</sub>* in some H/RS cell lines (L591, KMH2 and

KMH2-EBV). Furthermore, examination of microarray data presented by Hinz *et al.*, (2002), reveals *bfl-1* mRNA was expressed at 1.4 and 1.8-fold greater level than *bcl-xL* in H/RS cell lines, L428 and HDLM2. Given the high levels of *bfl-1* mRNA, it was reasonable to suggest a role for Bfl-1 in ensuring survival of H/RS cells.

Werner *et al.*, (2002), showed that Bfl-1 acts by inhibiting the collaboration between the BH3 domain-only protein Bid (by binding to full length Bid via the Bid BH3 domain) and its pro-apoptotic partners Bax or Bak in the induction of Cyt c release. The ratio of anti-and pro-apoptotic molecules determines the response to a death signal. The ratio of *bfl-1/bid* may indicate the degree to which the pro-apoptotic action of Bid may be counteracted by Bfl-1 but cannot be extrapolated from these results due to the absence of a *bid* RPA probe. However, high-level/equilevel *bfl-1* mRNA expression in all H/RS cell lines tested relative to Bid's pro-apoptotic partners *bak/bax*, respectively, is evident (Figure 3.10) and it could be hypothesised that expression of the anti-apoptotic Bfl-1 protein may counteract the expression of the pro-apoptotic proteins Bax, Bak, and Bid, thereby contributing to the survival of H/RS cells.

In summary, *bfl-1* mRNA is expressed in HL primary tumour tissue and cultured H/RS cells but a conclusion on the level of expression in H/RS cells relative to reactive cells in biopsies of NSHL cannot be drawn from these results given the high-level expression observed in some bystander cells. *Bfl-1* mRNA is expressed in all cases of primary tissue and cultured H/RS cells irrespective of EBV status. The novel *bfl-1* splice variant designated *bfl-1S*, was not expressed in H/RS or reactive cells of HL tumour tissue, cultured H/RS cells, tonsillar GC B cells, BL cell lines or LCLs.

## **CHAPTER 4 *Bfl-1* is a key NF-κB target gene in H/RS-derived cell lines**

## 4.1 Introduction

The interaction of cytokines with their specific cell surface receptors triggers the activation of intracellular signaling cascades that ultimately have effects on multiple cellular functions. The clinical and pathologic features of cHL reflect an abnormal immune response that is thought to be due to the elaboration of a variety of cytokines by the malignant H/RS cells or surrounding tissues (Skinnider and Mak, 2002). Several signal transduction pathways are involved in the manifestation of clinical and pathological features of this disease (discussed in Section 1.5). These signaling pathways have been shown to play a role in lymphocyte growth and transformation. Cell survival is an important feature of malignancy and transformation. The NF- $\kappa$ B family of transcription factors mediate the expression of numerous genes involved in diverse functions such as inflammation, immune response, apoptosis and cell proliferation. Constitutive NF- $\kappa$ B activity is a feature of H/RS cells of HL. Activated NF- $\kappa$ B in H/RS cells induces expression of anti-apoptotic genes (e.g., bcl-xL, c-IAP2, TRAF1 and c-FLIP) [Bargou *et al.*, 1997, Hinz *et al.*, 2001, Hinz *et al.*, 2002, Mathas *et al.*, 2002, Mathas *et al.*, 2004]).

The Bcl-2 family of proteins are central components of the cellular apoptotic programme and of primary interest in this study is the Bcl-2 anti-apoptotic member Bfl-1. As affirmed in Section 1.7.4, *bfl-1* was found to be a direct transcriptional target of NF- $\kappa$ B and has been linked to chemoresistance through NF- $\kappa$ B activation in some cancers. Previous work in our laboratory has shown that the *bfl-1* gene plays an important role in regulating the survival of EBV-infected B cells (D'Souza *et al.*, 2000) and is regulated by EBV with a role for NF- $\kappa$ B (D'Souza *et al.*, 2004). In a related study in our laboratory, it was observed that expression of EBNA2 as the sole EBV protein in an EBV-negative BL-derived cell line (DG75-tTA-EBNA2, Floettmann *et al.*, 1996) also led to an increase in *bfl-1* mRNA levels (Pegman *et al.*, 2006), demonstrating for the first time that a second EBV protein activates transcription of the *bfl-1* gene. EBNA2 expression was also subsequently found to trans-activate the *bfl-1* promoter in EBV-negative BL-derived cell lines (Pegman *et al.*, 2006).

This chapter set out to investigate the regulation of the *bfl-1* gene by the NF- $\kappa$ B signaling pathway in HL-derived cell lines. Understanding fully the precise apoptotic pathways abrogated in HL will be essential for devising targeted pro-apoptotic therapies.

#### **4.1.1 Summary of results**

The data presented here shows that inhibition of NF-κB activity by sodium arsenite or BAY11 chemical inhibitors resulted in apoptosis of H/RS cells. Apoptosis associated with inhibition of NF-κB activity by these chemical inhibitors lead to down-regulation of the expression of the anti-apoptotic gene, *bfl-1*. It was next tested if ectopic expression of Bfl-1 could protect these cells from NF-κB-inhibitor-induced apoptosis. In order to do this a vector (pRTS-1-HA-*bfl-1*) capable of inducible expression of Bfl-1 protein fused to the hemagglutinin tag was constructed and subsequently validated in the EBV-negative B cell line, DG75. Next, stable cell clones of the H/RS-derived cell line, L428, were generated by transfection of pRTS-1-HA-*bfl-1*. Ectopic expression of Bfl-1 had no effect on proliferation of L428 cells in agreement with previously reported data relating to A1, the mouse homolog of Bfl-1. Importantly, during NF-κB inhibition, ectopic expression of *bfl-1*, from the pRTS-1-HA-*bfl-1* vector, dramatically rescued L428 cells from an apoptotic fate. These results indicate that *bfl-1* is a key NF-κB target gene in H/RS cells and show for the first time that ectopic expression of Bfl-1 protects H/RS cells from apoptosis induced by chemotoxic NF-κB inhibitors.

## **4.2 Results – NF-κB pathway and regulation of *bfl-1* expression in HL**

### **4.2.1 Inhibition of NF-κB in H/RS cell lines and effect on *bfl-1* expression**

NF-κB inhibition may be achieved by targeting either the apical signaling proteins responsible for its activation, the downstream kinases (IKK and CK2) at which NF-κB activating signaling pathways converge, the proteasome-mediated degradation of IκB proteins or the transcriptional function of Rel proteins (Ravi and Bedi, 2004). Several strategies have been employed to block the activation of NF-κB, including blocking of IκB phosphorylation or proteasome degradation, blocking of nuclear translocation or up-regulation of the inhibitory IκB subunit. Numerous compounds have been described as inhibitors of the NF-κB pathway (reviewed in Yamamoto and Gaynor, 2001). These compounds block NF-κB activation through multiple mechanisms by intercepting various steps leading to NF-κB activation.

#### **Sodium Arsenite**

Kapahi *et al.*, (2000), reported that one such compound, sodium arsenite ( $\text{NaAsO}_2$ ), potently inhibited NF-κB and IKK activation by binding to cysteine-179 in the activation loop of the IKK catalytic subunits, IKK $\alpha/\beta$ . Mathas *et al.*, (2003), showed that sodium arsenite strongly inhibited constitutive IKK and NF-κB activity in H/RS cells and down-regulated NF-κB-dependent target genes, among these TNF- $\alpha$  receptor associated factor 1 (TRAF1), c-IAP2, interleukin-13 (IL-13) and CCR7. The effect of NF-κB inhibition on *bfl-1* levels in H/RS cell lines was not investigated in the study by Mathas *et al.*, (2003).

Abrogation of NF-κB activity in H/RS-derived cell lines by chemical treatment with sodium arsenite was chosen to directly investigate the effect of NF-κB inhibition on *bfl-1* expression in this cell context. Initially, to determine an inhibitory concentration 50 ( $\text{IC}_{50}$ ) of sodium arsenite, L428 (EBV negative NS disease type) and L591 (EBV positive NS disease type) cells were treated with a range of concentrations of this chemical inhibitor and cell viability was monitored by trypan blue dye exclusion (Section 2.4.4). A dramatic decrease in cell viability was observed upon treatment of

L428 and L591 cells with sodium arsenite in a time-dependent and dose-dependent manner (data not shown), further evidence in support of the findings of Mathas *et al.*, (2003) that cell death protection is a key function of constitutive NF- $\kappa$ B activity in H/RS cells.

From treatment of cells with a range of concentrations (1  $\mu$ M to 2 mM), the minimum concentration ( $IC_{50}$ ) of sodium arsenite required to reduce cell viability by 50 % in 48 h of L428 and L591 cells was determined by propidium iodide (PI) staining and fluorescence activated cell-sorting (FACS) analysis (Section 2.4.10). Initially measurements were made using forward light scatter (FSC) and side light scatter (SSC). A population of lymphocytes was gated on region 1 (R1) using forward (FSC) and side scatter (SSC). The nucleic acid stain, PI, stained cells that did not have an intact plasma membrane red and was detected on the FL3 parameter. The apoptotic cells were gated on region 3 (R3) while cells with intact plasma membrane (live cells) were gated on region 2 (R2). As can be seen in Figure 4.1 (L428) and Figure 4.2 (L591), within the untreated population of cells, ~ 6 % of cells were non-viable, appearing in R3. The  $IC_{50}$  of sodium arsenite was determined to be 10  $\mu$ M as approximately 50 % of cells appeared in R3 at 48 h post treatment for L428 (Figure 4.1) and L591 cells (Figure 4.2).

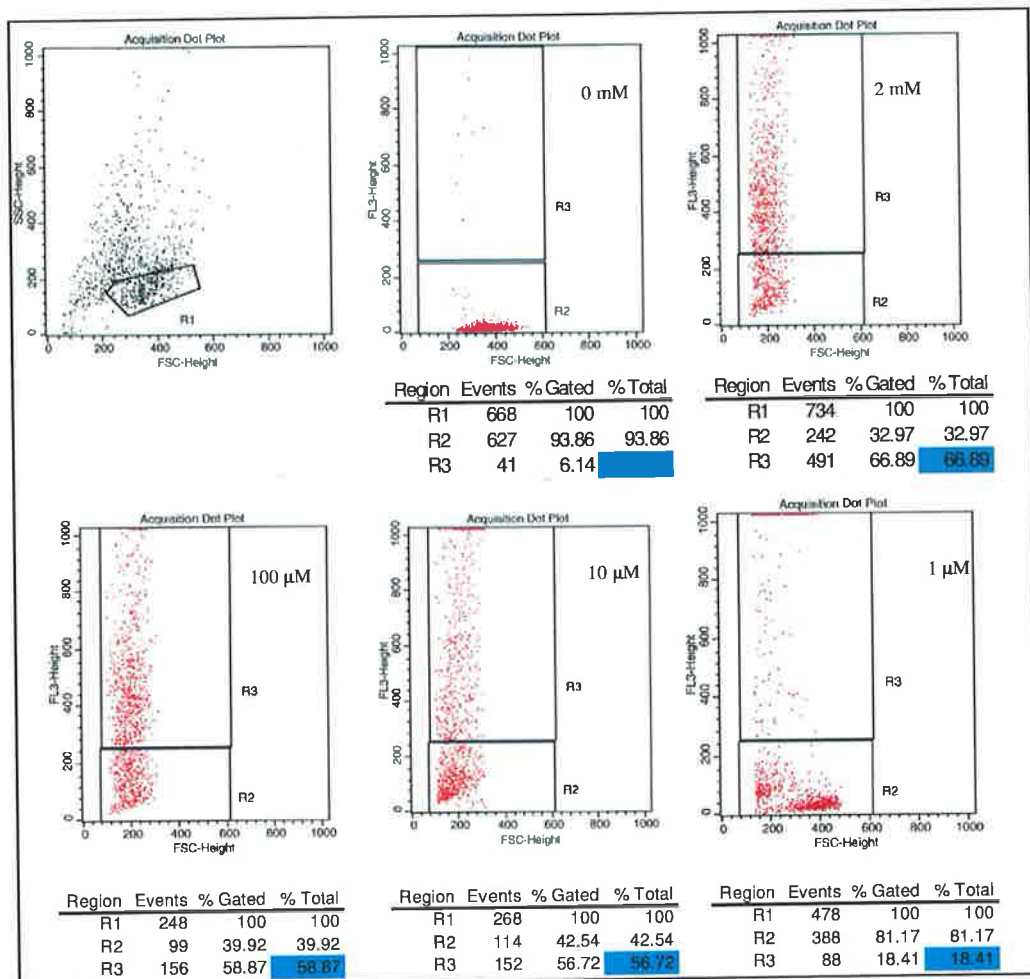


**Figure 4.1 Determination of sodium arsenite IC<sub>50</sub> required to reduce viability of L428 cells.**

Viability of L428 cells is reduced upon treatment with sodium-arsenite. Minimum concentration (IC<sub>50</sub>) of sodium arsenite required to reduce viability by 50 % at 48 h was determined by PI staining and FACS analysis using a FACS Caliber flow cytometer. Region markers were based on stained and unstained controls and values reflect the percentages of cells in each region and are given for each event below the graph. Cells in region 2 (R2) are viable cells (PI -), while cells in R3 are non-viable (PI +). Percentages of non-viable cells in R3 are highlighted in blue.

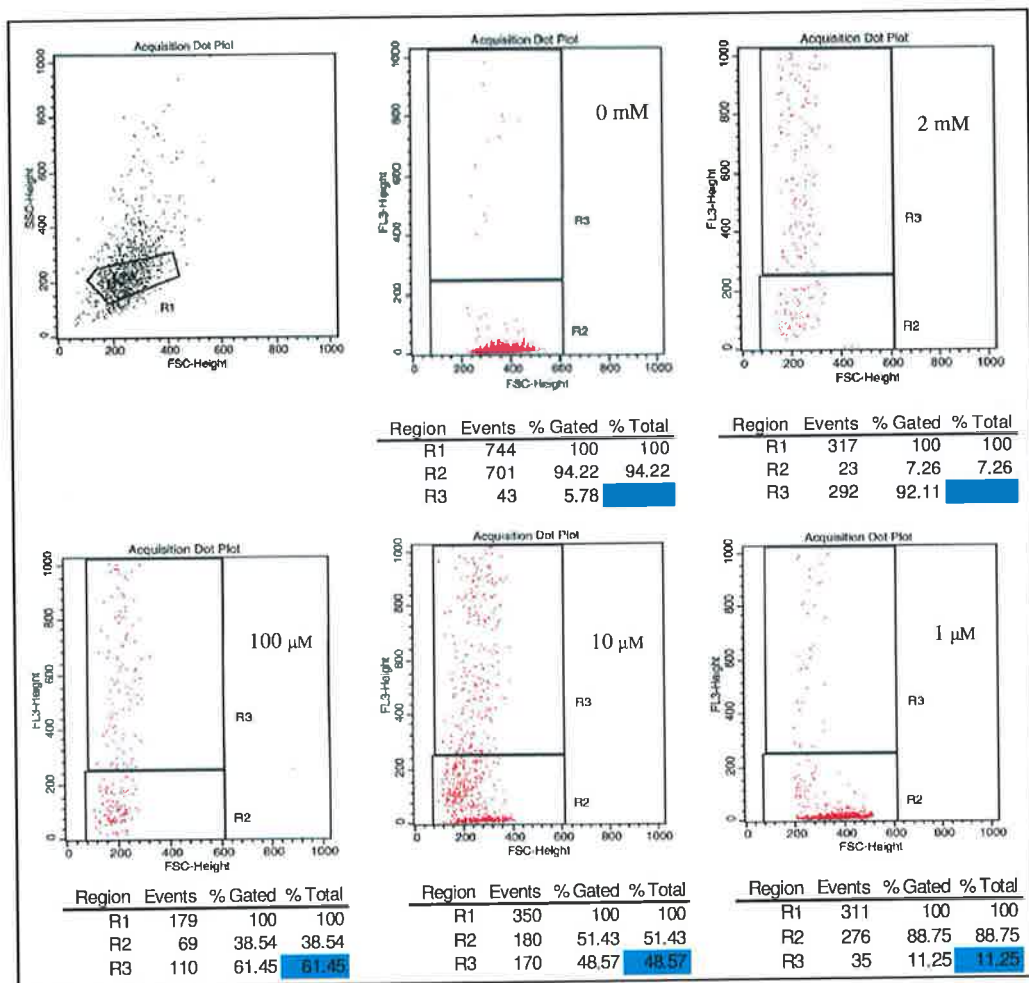


**Figure 4.2 Determination of sodium arsenite IC<sub>50</sub> required to reduce viability of L591 cells.**

Viability of L591 cells is reduced upon treatment with sodium-arsenite. Minimum concentration (IC<sub>50</sub>) of sodium arsenite required to reduce viability by 50 % at 48 h was determined by PI staining and FACS analysis using a FACS Caliber flow cytometer. Region markers were based on stained and unstained controls and values reflect the percentages of cells in each region and are given for each event below the graph. Cells in region 2 (R2) are viable cells (PI -), while cells in R3 are non-viable (PI +). Percentages of non-viable cells in R3 are highlighted in blue.

As PI penetrates compromised cell membranes but does not distinguish necrotic from apoptotic cells, it was next tested if cell death following sodium arsenite treatment was by apoptosis. As outlined in Section 2.4.9, acridine orange is used to determine how many cells within a given population have undergone apoptosis, but it cannot differentiate between viable and nonviable cells. For this, a mixture of acridine orange

and ethidium bromide is used. The differential uptake of these two dyes allows for the identification of viable and nonviable cells. Using acridine orange/ethidium bromide staining followed by fluorescence microscopy, L428 and L591 cells were observed to die by apoptosis (Figure 4.3; shown for L428 cells treated with sodium arsenite).

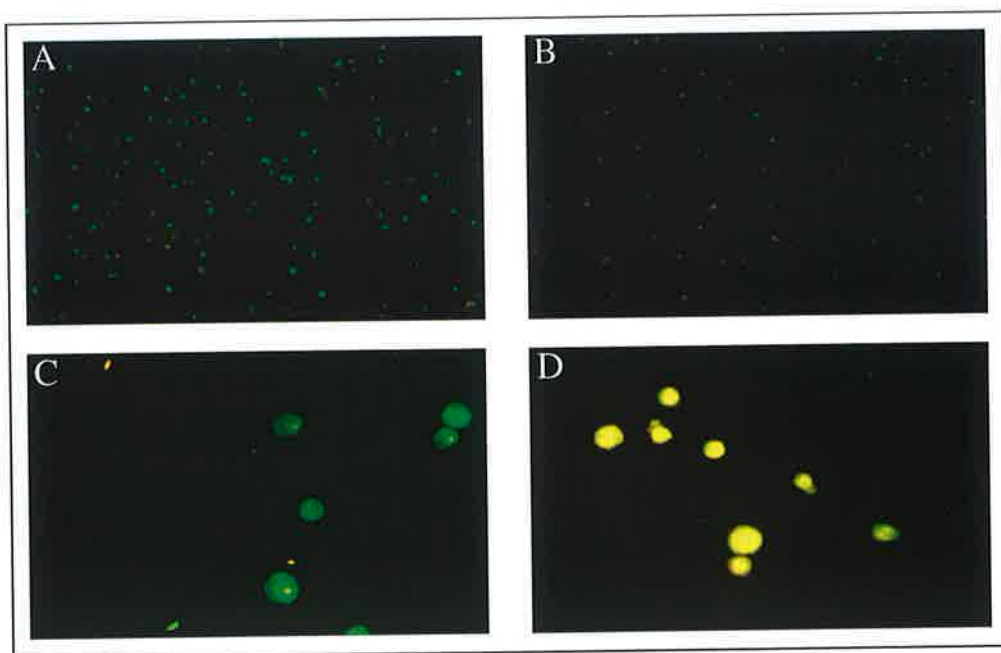


**Figure 4.3 Acridine orange/ethidium bromide staining of L428 cells post treatment with sodium arsenite**

L428 cells were treated with 10 µM sodium arsenite or vehicle (A and C or B and D respectively). At 48 h post-treatment, cells were stained with 10 µg/ml acridine orange/ethidium bromide and visualised using an Olympus DP-50 fluorescent camera under 10-X (A and B) or 40-X (C and D) magnification. Live interphase cell nuclei fluoresce green and have variations in fluorescent intensity reflecting the distribution of euchromatin and heterochromatin. Early apoptotic cells have nuclei with apoptotic morphology and generally appear brighter than non-apoptotic nuclei due to chromatin condensation, but do not stain with ethidium bromide due to an intact plasma membrane. Late apoptotic cells are diffusely red due to ethidium bromide staining of DNA and RNA.

Apoptotic cells exhibit phosphatidyl serine (PS) translocation from the inner to the outer leaflet of the plasma membrane, thus exposing PS to the external cellular environment (Section 2.4.11). Annexin V is commonly used for PS detection and in tandem with a vital dye, such as PI, early/late apoptotic, necrotic and viable cells are easily differentiated by FACS analysis. L428 cells treated with 10 µM sodium arsenite were

shown to die by apoptosis using an annexin V/PI dual stain followed FACS analysis as seen in Figure 4.4.

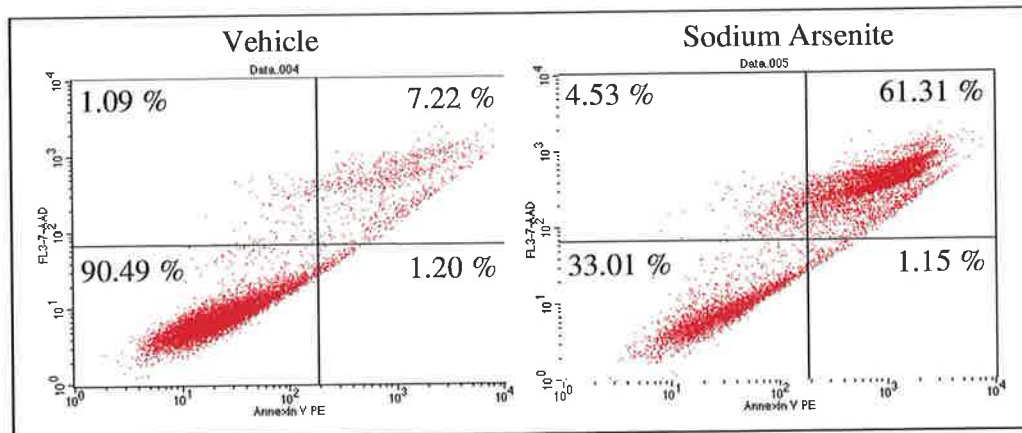


**Figure 4.4 Treatment of L428 cells with NF-κB inhibitor, sodium arsenite**

L428 cells were treated with or without 10 μM sodium arsenite and cell viability/apoptosis profile was analysed at 48 h post treatment by PI/annexin V staining and subsequent flow cytometric analysis. Quadrant markers were based on stained/unstained controls and values reflect the percentage of cells in each quadrant. Cells in the lower left quadrant are viable cells (PI/Annexin V), cells in the lower right quadrant are early apoptotic cells (PI/Annexin V<sup>+</sup>), cells in the upper right quadrant are late apoptotic cells (PI<sup>+</sup>/Annexin V<sup>+</sup>) and cells in the upper left quadrant are necrotic cells (PI<sup>+</sup>/Annexin V).

To monitor the effect of sodium arsenite treatment on levels of activated NF-κB, co-transfections were carried out using a known NF-κB-dependent reporter construct, 3x enh-κB luc (Floettmann and Rowe, 1997), which contains 3 NF-κB binding sites upstream of a minimal conalbumin promoter, linked to the luciferase gene. In a control experiment to demonstrate inhibition of NF-κB by sodium arsenite, cells of L428 and L591 cell lines were co-transfected with 3x enh-κB luc and pCMV LacZ reporter constructs. Transfected cells were treated with sodium-arsenite and the effect on activated NF-κB levels was monitored by luciferase assay and β-gal normalisation at 48 h and 72 h post treatment (Section 2.4.6.6-8) (Figure 4.5). Treatment with sodium arsenite almost completely abolished the level of activated NF-κB at 48 and 72 h when compared to controls.

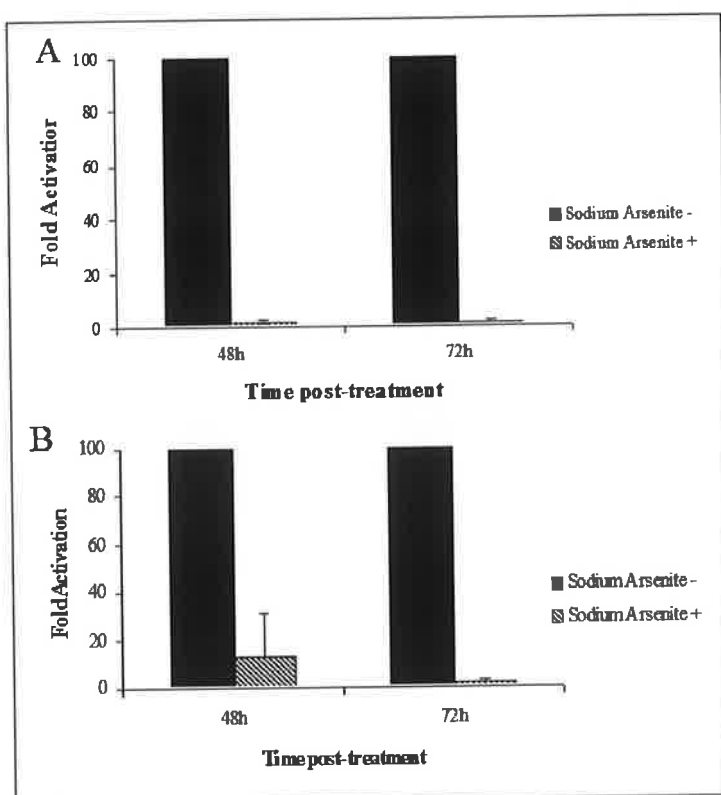


**Figure 4.5 Inhibition of NF-κB activity by sodium arsenite in HL**

L428 (A) and L591 (B) cells were co-transfected with 3xenh-κB Luc and pCMV LacZ. Transfected cells were treated post-transfection with sodium arsenite (10 μM). The effect on levels of activated NF-κB was monitored by luciferase assay and β-gal normalisation at 48 h and 72 h post treatment.

Having established that NF-κB activity was abrogated by sodium arsenite treatment, L428 and L591 cells were then incubated with 10 μM sodium arsenite and analysed by RT-qPCR to determine *bfl-1* mRNA expression levels at various intervals over a 72 h period. Inhibition of NF-κB by sodium arsenite treatment is associated with a decrease in *bfl-1* mRNA expression levels in both L428 (Figure 4.6A) and L591 (Figure 4.6B).

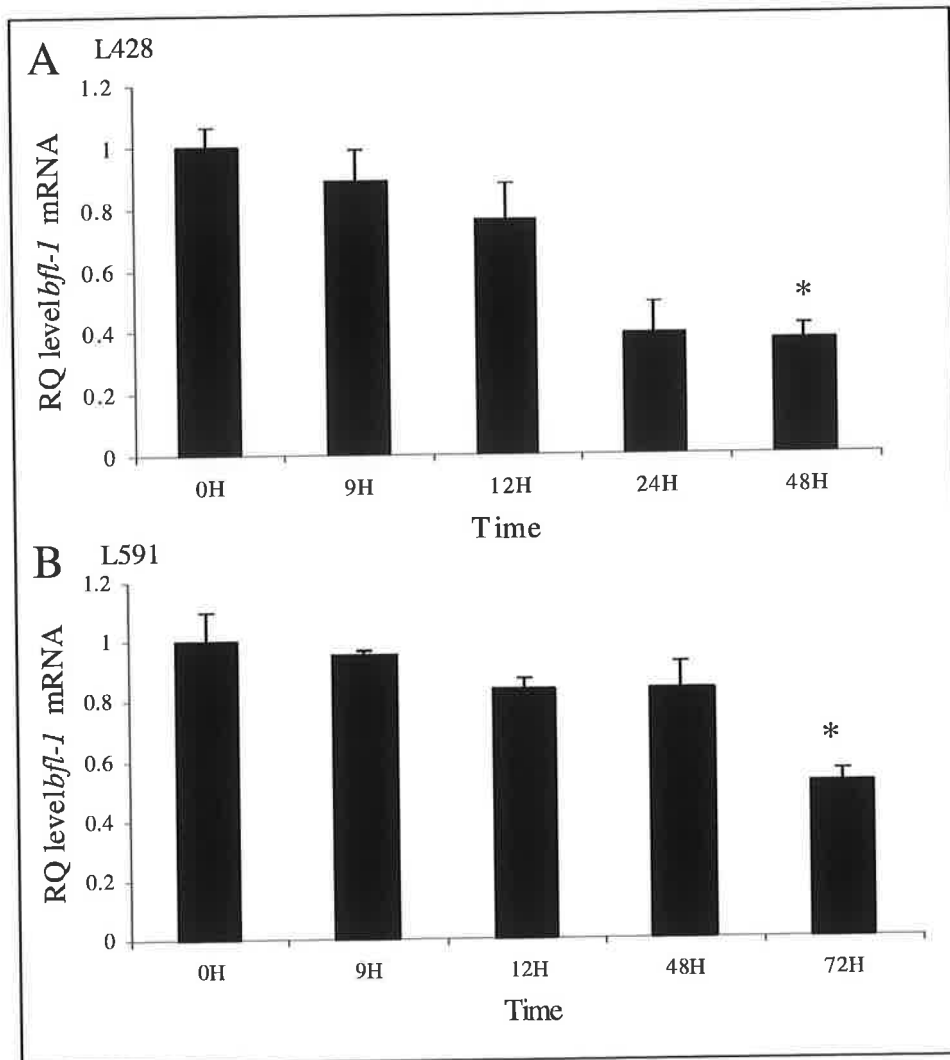


**Figure 4.6 Effect of sodium arsenite inhibition of NF- $\kappa$ B activity on *bfl-1* mRNA expression in H/RS cell lines**

L428 (A) and L591 (B) cells were incubated in 10  $\mu$ M sodium arsenite. RNA extracts were prepared at various timepoints over a 72-h period. The amount of *bfl-1* mRNA was quantified by reverse transcription followed by real time PCR using an ABI 7500 detection system. *Bfl-1* levels were assayed in triplicate (using a TaqMan gene expression assay for *bfl-1*) and normalised by *gapdh* levels (assayed using a TaqMan gene expression assay for *gapdh*). Fold differences were calculated relative to *bfl-1* levels at time zero (assigned a value of 1). Data are mean  $\pm$  SD, \* $P \leq 0.038$ .

The level of *bfl-1* mRNA was reduced by 60 % in L428 cells at 48 h post treatment with 10  $\mu$ M sodium arsenite. This decrease is concomitant with a 50 % reduction in viability of cells as observed in Figure 4.1. In L591 cells, the decrease in *bfl-1* mRNA expression

is less pronounced but nonetheless significant with a 50 % decrease in expression levels at 72 h post treatment.

### BAY11 Treatment

A similar compound to sodium arsenite, also a cell-permeable inhibitor of NF- $\kappa$ B, known as Bay 11-7082 (BAY11), has been shown by Pierce *et al.*, (1997) to decrease TNF- $\alpha$ -induced nuclear translocation of NF- $\kappa$ B through inhibition of the TNF- $\alpha$ -inducible phosphorylation of I $\kappa$ B $\alpha$  in endothelial cells. The specificity of BAY11 to the NF- $\kappa$ B pathway has been extensively characterised (Keller, Schattner and Cesarman, 2000).

H/RS-derived cell lines, L428 and L591 were thus treated with the I $\kappa$ B-phosphorylation inhibitor BAY11 in the present study. The IC<sub>50</sub> for BAY11, determined as previously for sodium arsenite, was found to be 10  $\mu$ M (data not shown). It was then shown that NF- $\kappa$ B activity was abrogated by treatment of L428 and L591 cells with 10  $\mu$ M BAY11 (Figure 4.7A; shown for L428 only). As previously, L428 and L591 cell lines were co-transfected with 3x enh- $\kappa$ B luc and pCMV LacZ reporter constructs. Transfected cells were treated with 10  $\mu$ M BAY11 and the effect on activated NF- $\kappa$ B levels was monitored by luciferase assay and  $\beta$ -gal normalisation at 48 h post treatment. Activated NF- $\kappa$ B levels were reduced by ~90 % upon treatment with BAY11. NF- $\kappa$ B inhibition using this compound led to cell death by apoptosis (Figure 4.7B) as determined by analysis of cells stained with acridine orange/ethidium bromide (Section 2.4.9) using fluorescence microscopy and by annexin V/PI staining followed by FACS analysis (Figure 4.8). Next, the effect of inhibition of NF- $\kappa$ B activity in H/RS cells using this chemotoxic agent on *bfl-1* mRNA expression levels was investigated. RNA extracted from L428 and L591 cells incubated with 10  $\mu$ M BAY11 were analysed by RT-qPCR to determine *bfl-1* mRNA expression levels at various intervals over a 48 h period. A decrease in *bfl-1* mRNA levels of 50 % was seen in both L428 and L591 cell lines at 48 h post-treatment with BAY11 (Figure 4.9).

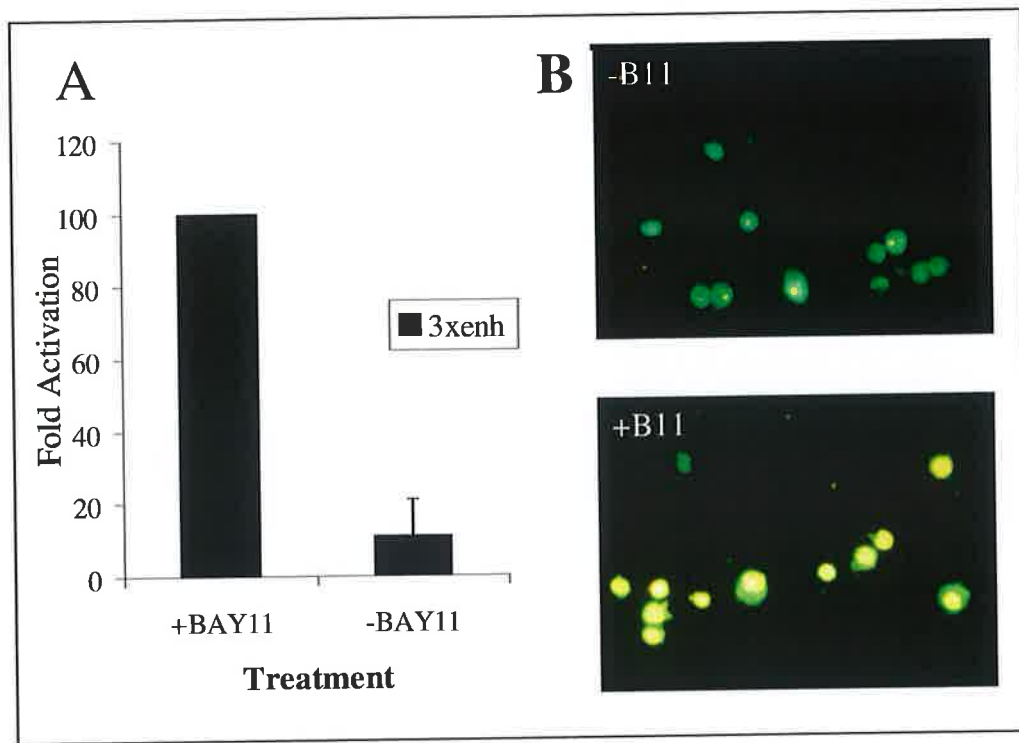


**Figure 4.7 Inhibition of NF- $\kappa$ B activity by BAY11 in HL**

(A) L428 cells were co-transfected with 3xenh- $\kappa$ B Luc and pCMV LacZ. Transfected cells were treated with BAY11. The effect on NF- $\kappa$ B was monitored by luciferase assay and  $\beta$ -gal normalisation at 48 h post treatment. (B) L428 cells were treated with 10  $\mu$ M BAY11 (+B) or vehicle (-B). At 48 h post-treatment, cells were stained with 10  $\mu$ g/ml acridine orange/ethidium bromide and visualised using an Olympus DP-50 fluorescent camera under 40-X magnification

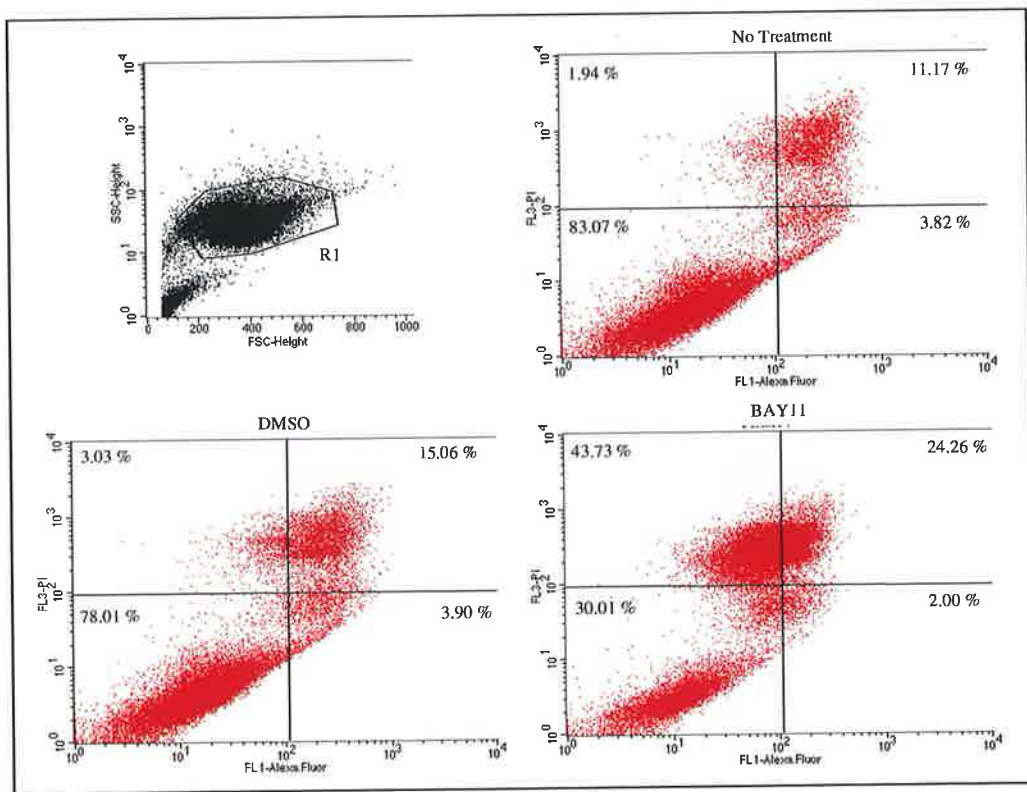


**Figure 4.8 Treatment of L428 cells with NF- $\kappa$ B inhibitor, BAY11**

L428 cells were treated with or without 10  $\mu$ M BAY11 or DMSO (vehicle) and cell viability/apoptosis profile was analysed at 48 h post treatment by PI/annexin V staining and subsequent flow cytometric analysis. Quadrant markers were based on stained/unstained controls and values reflect the percentage of cells in each quadrant. Cells in the lower left quadrant are viable cells (PI/Annexin V $^-$ ), cells in the lower right quadrant are early apoptotic cells (PI/Annexin V $^+$ ), cells in the upper right quadrant are late apoptotic cells (PI $^+$ /Annexin V $^+$ ) and cells in the upper left quadrant are necrotic cells (PI $^+$ /Annexin V $^-$ ).

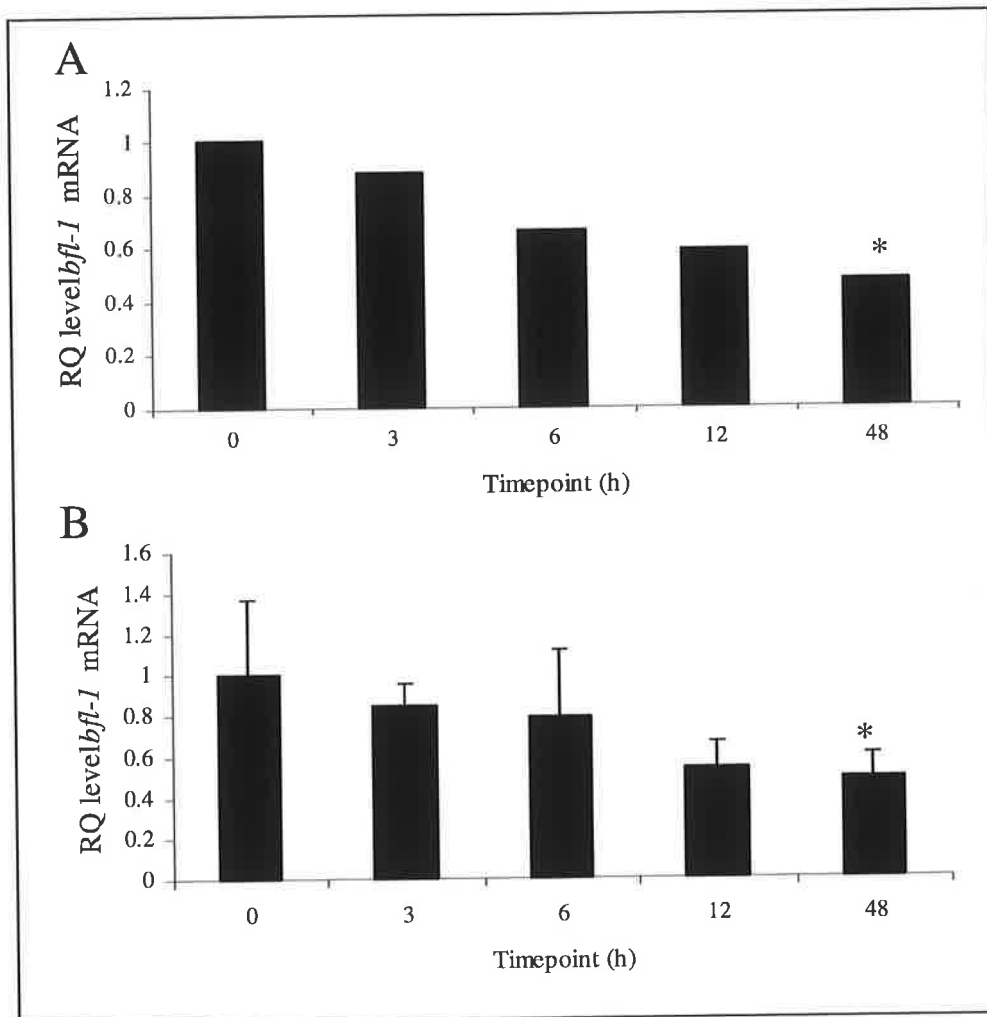


**Figure 4.9 Effect of BAY11 inhibition of NF-κB on *bfl-1* mRNA expression in H/RS cell lines**

L428 (A) and L591 (B) cells were incubated in 10 µM BAY11. RNA extracts were prepared at various timepoints. The amount of *bfl-1* mRNA was quantified by reverse transcription followed by real time PCR using an ABI 7500 detection system. *Bfl-1* levels were assayed in triplicate (using a TaqMan gene expression assay for *bfl-1*) and normalised by *gapdh* levels (assayed using a TaqMan gene expression assay for *gapdh*). Fold differences were calculated relative to *bfl-1* levels at time zero (assigned a value of 1). Data are mean ±SD, \* $P \leq 0.05$ .

Taken together these results demonstrate that NF-κB inhibition of H/RS cells results in death by apoptosis, which is coincident with a significant decline in *bfl-1* mRNA expression. The effect is seen with two independent NF-κB inhibitors, which abrogate NF-κB activity by different mechanisms and is evidence to suggest that *bfl-1* is a key

NF-κB target gene in cultured H/RS cells. Further substantiation of this finding is later presented in Chapter 6, where it is shown that the *bfl-1* promoter is regulated by NF-κB in H/RS-derived cell lines of EBV negative (L428) and positive (L591) status.

#### **4.2.2 The effect of maintenance of *bfl-1* expression during NF-κB inhibition.**

In order to investigate how crucial the loss of *bfl-1* expression is in arriving at the apoptotic outcome seen upon NF-κB inhibition, it was decided to examine the effect of substituting for the loss by exogenous expression of Bfl-1 during NF-κB inhibition. In order to do this, a plasmid capable of inducibly expressing *bfl-1* was first constructed using the tetracycline-regulatable plasmid pRTS-1 (Table 2-5; Bornkamm *et al.*, 2005). pRTS-1 is a novel EBV-derived episomally replicating plasmid that carries all the elements for conditional expression of a gene of interest via tetracycline regulation (Bornkamm *et al.*, 2005). The gene of interest is expressed from the bidirectional promoter P<sub>tet</sub>bi-1 (Figure 4.11A) that allows simultaneous expression of two genes, of which one may be used as surrogate marker for the expression of the gene of interest. Tight down regulation is achieved through binding of the silencer tTS<sub>KRAB</sub> to P<sub>tet</sub>bi-1 in the absence of tetracycline (or doxycycline). Addition of tetracycline releases repression and via binding of rtTA2s-M2 activates P<sub>tet</sub>bi-1. The expression cassette contained on the plasmid conferring tetracycline responsiveness is composed of the chicken-β-actin promoter (CAG) flanked by the mouse Ig heavy chain intron enhancer (E<sub>μ</sub>) and drives expression of the two genes encoding rtTA2s-M2 and tTS<sub>KRAB</sub> separated by an internal ribosomal entry site (IRES). The E<sub>μ</sub> intron enhancer was included for efficient expression of tetracycline-controlled regulators in B cells and makes this plasmid especially suited to the study of B cell lymphomagenesis.

##### **Cloning of pRTS-1-HA-bfl-1**

The sub-cloning strategy is summarised in Figure 4.10. A circular map of pRTS-1 is shown in Figure 4.11A. The plasmid was firstly characterised by restriction digestion (Section 2.3.3) using *Sac* I and *Sal* I restriction enzymes (Figure 4.11B). Prior to ligation, the plasmid was linearised by digestion with *Sfi* I to excise the luciferase gene (Figure 4.11C), followed by dephosphorylation using CIP to prevent recircularisation of

the linearised DNA (Section 2.3.4). The linearised, CIP-treated DNA was then purified by phenol: chloroform extraction followed by ethanol precipitation (Section 2.3.2).

The *bfl-1* ORF fused to a hemagglutinin (HA) tag was amplified using the construct pCDNA3-HA-bfl-1 as template DNA (Table 2-5). This construct contains the full length *bfl-1* ORF sub-cloned downstream of a HA peptide (derived from the human influenza hemagglutinin protein) in pCDNA3 (D'Sa-Eipper *et al.*, 1996). HA is a short epitope tag, commonly used for detection of fusion proteins mediated by highly specific anti-HA antibodies. pCDNA3-HA-bfl-1 DNA was first characterised by restriction digestion (Section 2.3.3) prior to PCR (not shown).

The HA-*bfl-1* ORF was amplified by PCR (Section 2.3.5) with a forward primer (HABfl1ForSfiI) with HA tag sequence homology and a reverse primer (Bfl-1RevSfiI) from the region downstream of the *bfl-1* termination codon (sequences in Table 2-6). The primers included *Sfi I* restriction sites for cloning. Following PCR, the products were analysed by agarose gel electrophoresis (Section 2.3.13) to check for migration of fragments at the expected size (Figure 4.11D). The PCR products were subsequently purified (Section 2.3.6), digested with *Sfi I* and purified by phenol: chloroform extraction followed by ethanol precipitation. Ligation of vector and insert DNA were carried out overnight at 16 °C (Section 2.3.7).

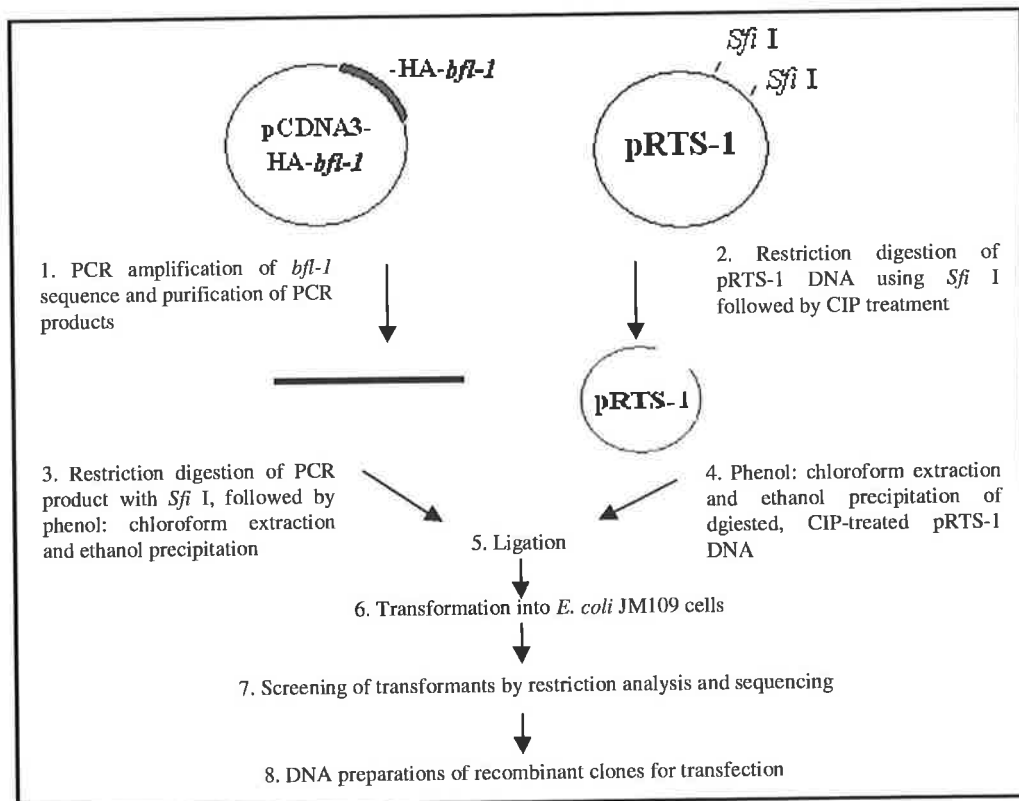


**Figure 4.10 Cloning strategy**

Flow diagram detailing the steps involved in generating the pRTS-1-HA-bfl-1 construct. Briefly, the *bfl-1* ORF was amplified by PCR using pCDNA3-HA-bfl-1 as template DNA, digested with *Sfi* I and sub-cloned into the *Sfi* I sites created when the luciferase gene was excised from pRTS-1. Competent *E.coli* JM109 cells were transformed with the recombinant plasmid and a number of independently transformed colonies were selected for growth of small-scale cultures. Plasmid DNA isolated from each culture was then analysed by digestion with restriction enzymes and PCR. Large-scale DNA preparations of the recombinant plasmids were performed and the pRTS-1-HA-bfl-1 construct was used in transfections with DG75 and L428 cell lines.

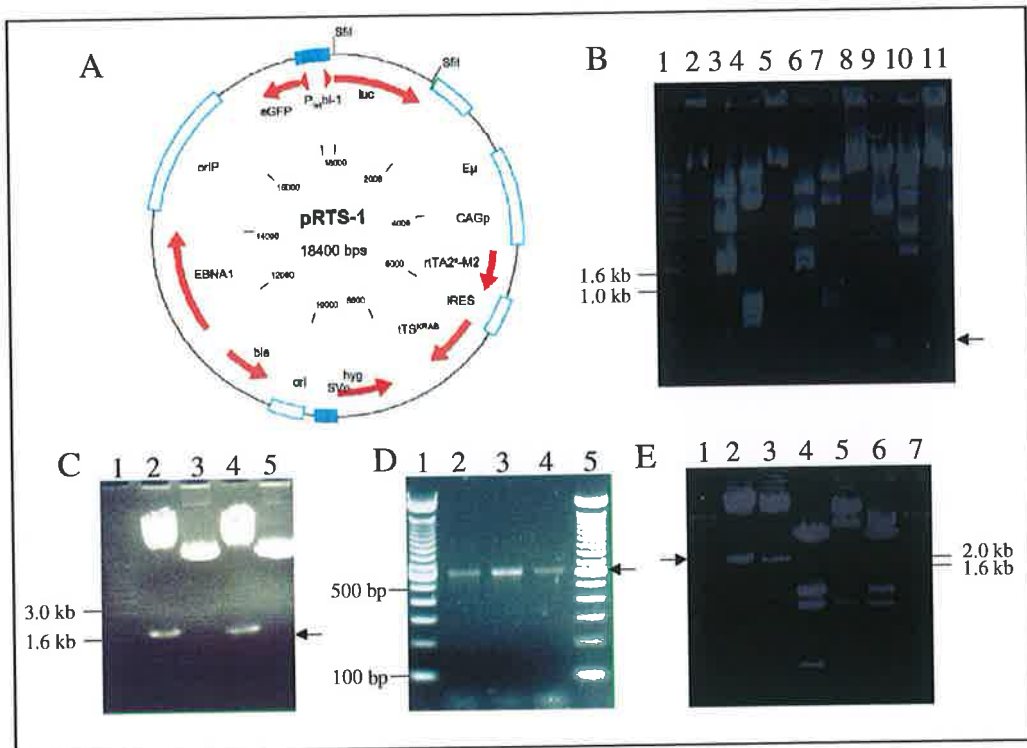


**Figure 4.11 Construction of pRTS-1-HA-bfl-1.**

(A) Schematic circular map of pRTS-1 vector adapted from Bornkamm *et al.*, 2005. The luciferase gene is designated luc. The bicistronic expression cassette driving expression of rTAs-M2 and tTSKRAB, separated by an internal ribosomal entry site (IRES), is placed behind the chicken β-actin intron and transcribed from a promoter/enhancer consisting of the mouse heavy chain intron enhancer (Em) and the chicken β-actin promoter (CAGp). Ptetbi-1 denotes the bidirectional tetracycline-regulated promoter and oriP the EBV episomal origin of replication. EBNA1, the EBV gene EBNA1; bla, β-lactamase; SVp, the SV40 early promoter; ori, the bacterial origin of replication derived from pMB1; and hyg, the hygromycin phosphotransferase gene. (B) The 18,400 bp pRTS-1 plasmid was characterised prior to cloning by restriction digestion using *Sac* I and *Sal* I enzymes followed by agarose gel electrophoresis (0.7 % agarose-1X TAE gel). Restriction digestion patterns were predicted using NEBcutter software (Table 2-4). A 1 kb DNA ladder (Invitrogen) is shown in lane 1. Undigested DNA can be seen in lane 11. Restriction digestion with *Sac* I resulted in five fragments at 13,496 bp, 4,483 bp, 314 bp, 104 bp and 53 bp as expected (lane 9; bands at 104 bp and 53 bp too faint to discern). Restriction digestion with *Sal* I yielded four fragments of 10,060 bp, 3,182 bp, 3070 bp and 2088 bp (lane 10). Electrophoresis was carried out at 100 V for 1 h using a 1 % agarose-1X TAE gel. (C) Restriction digestion of pRTS-1 with *Sfi* I excised luciferase gene (1.6 kb), designated by black arrow. A 1 kb ladder is seen in lane 1. Undigested (lane 3/5) and *Sfi* I-digested plasmid DNA (lane 1/4) was analysed using a 0.7 % agarose-1X TAE gel. (D) PCR products amplified from the pCDNA3-HA-bfl-1 using forward and reverse primers; HABfl1ForSfiI and Bfl-1RevSfiI, were analysed by agarose gel electrophoresis on a 2 % agarose-1 X TAE gel and electrophoresis was carried out at 100 V for 1 h in 1 X TAE. Amplification of the HA-bfl-1 fragment resulted in a band at 610 bp (lane 2-4), designated by black arrow. A 100 bp DNA ladder (Invitrogen) is shown in lanes 1 and 5. (E) Restriction analysis of

recombinant pRTS-1-HA-*bfl-1* clones to determine correct insert orientation by digestion using *Bgl* II enzyme followed by agarose gel electrophoresis (0.7 % agarose-1X TAE gel). Correct insert orientation would yield two fragments of 1,923 bp and 15,399 bp while incorrect orientation would produce two fragments of 1471 bp and 15,851 bp upon digestion. A 1 kb ladder is seen in lanes 1 and 7. pRTS-1-HA-*bfl-1* clones harboured the HA-*bfl-1* fragment in the correct orientation as discerned by the presence of a digested fragment at ~1.9 kb (lanes 2 and 3), indicated by a black arrow.

Following the ligation reaction, competent *E. coli* JM109 cells were transformed with the recombinant plasmid DNA. Single colonies were used to inoculate cultures from which DNA mini-preparations were generated. Restriction analysis was performed on the DNA to detect the presence of insert DNA. Uniquely, even though both *Sfi* I sites used for cloning were different in base-pair composition it was possible for the insert DNA to ligate into the vector in either the forward or reverse orientation as the overhangs produced are palindromes. To determine whether insert DNA had ligated in the forward orientation, a PCR based strategy was first employed using the pEBNAseqFor forward primer (homologous to region upstream of start codon of pRTS-1) and the Bfl-1RevSfiI reverse primer used in PCR amplification of the HA-*bfl-1* fragment (sequences in Table 2-6). A PCR product was generated if the insert DNA had ligated in the forward orientation (not shown). Correct/incorrect insert orientation was also differentiated by restriction analysis using *Bgl* II restriction enzyme (Figure 4.11E). Once it was established that the HA-*bfl-1* sequence had ligated into pRTS-1 in the correct orientation, DNA maxi-preparations were carried out (Section 2.3.11) and the fidelity of the cloned sequence was verified by sequencing (Section 2.3.14) using the pEBNAseqFor primer (Table 2-6). The pRTS-1-HA-*bfl-1*-derived plasmid DNA, demonstrated 100 % homology with the predicted sequence as derived from the known HA tag and BFL1 (GenBank accession number U27467) coding sequences (not shown).

In order to test expression of HA-tagged Bfl-1, stable transfection of the pRTS-1-HA-*bfl-1* construct and the corresponding empty vector (pRTS-1) was performed in the BL DG75 cell line (Table 2-1) by electroporation (Section 2.4.6.1) followed by selection of positive clones using hygromycin (400 µg/ml). DG75 is a readily transfectable, EBV-negative BL cell line with a low basal level of *bfl-1* expression (D'Souza *et al.*, 2004) and was, therefore, a suitable cell line to test exogenous expression of *bfl-1* from pRTS-1-HA-*bfl-1*. DG75-pRTS-1-HA-*bfl-1* and DG75-pRTS-1 clones were induced or non-induced to express their respective proteins by addition of tetracycline (1 µg/ml) or an

equal volume of vehicle (100 % ethanol) to the culture media. Total protein from these cells was prepared at 72 h and the presence of HA-tagged Bfl-1 was confirmed by western blotting (Section 2.7.4) using an anti-HA antibody (Table 2-2) (Figure 4.12A). Co-expression of GFP from the bi-directional promoters of pRTS-1-HA-*bfl-1* and pRTS-1 upon induction with tetracycline was also confirmed using fluorescence microscopy (Section 2.4.6.5) (Figure 4.12B). RNA from these cells was prepared (Section 2.6.3.1) at 72 h post-addition of tetracycline and was reverse transcribed to cDNA (Section 2.6.4.1). Relative quantification of *bfl-1* mRNA expression levels was performed by realtime q-PCR (Section 2.6.4.2) (Figure 4.12C).

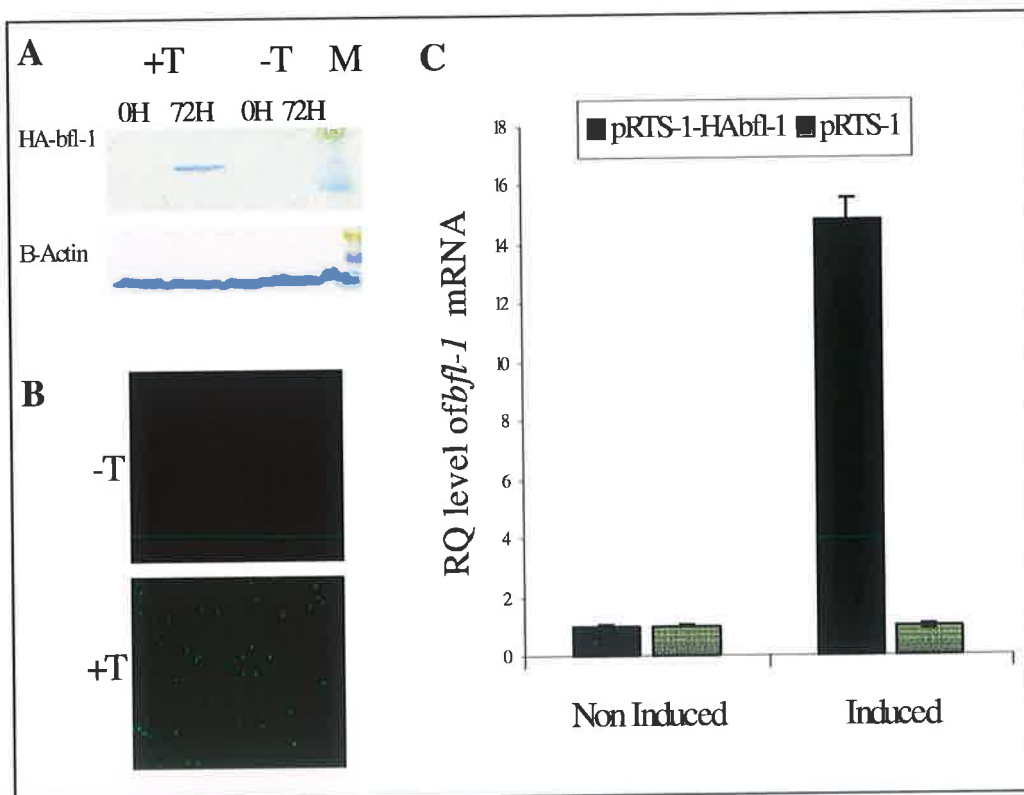


**Figure 4.12 Ectopic expression of *bfl-1* mRNA and HA-tagged Bfl-1 and GFP proteins from DG75-pRTS-1-HA-*bfl-1* clones.**

DG75-pRTS-1-HA-*bfl-1* and DG75-pRTS-1 clones were induced or non-induced by addition of tetracycline to express HA-Bfl-1 and GFP proteins or GFP and Luciferase proteins respectively. (A) The expression of HA-tagged Bfl-1 was confirmed by western blotting at 72 h post addition of tetracycline using an anti-HA antibody (upper panel) and normalised for  $\beta$ -actin levels (lower panel) using an anti-actin antibody. (B) The induction of GFP protein expression was monitored at 72 h by using an Olympus

DP-50 fluorescent microscope. (C) RNA was extracted at 72 h and reverse transcribed using random primers. The induction of *bfl-1* mRNA was monitored in real-time by detection of fluorescence intensity using a FAM-labeled TaqMan probe for *bfl-1* and a FAM-labeled TaqMan probe for β-actin using an ABI Prism 7500 Sequence Detection System. After normalisation for β-actin, Relative Quantification (RQ) level of *bfl-1* mRNA was plotted a function of the empty vector control (arbitrarily assigned a value of 1).

These results, together, confirmed the expression of HA-tagged Bfl-1 protein from pRTS-1-HA-*bfl-1* construct in DG75 cells and completed validation of the vector for use in subsequent experiments investigating the effect of expression of exogenous Bfl-1 in HL cell lines.

In preparation for stable transfection of L428 cells with pRTS-HA-*bfl-1*, a hygromycin drug curve (not shown) was performed to establish the minimum concentration of drug to cause cell death in this cell line, determined to be 500 µg/ml. L428 cells were thus transfected with pRTS-1-HA-*bfl-1* by electroporation (Section 2.4.6.1) and positive clones were selected for hygromycin resistance. Despite several attempts stable positive clones of pRTS-1-HA-*bfl-1* in L428 were not established, this was most likely due to the poor uptake of plasmid DNA during electroporation. However, stable cell lines were established when nucleofection (Section 2.4.6.2) of L428 with pRTS-1-HA-*bfl-1* and subsequent hygromycin resistance selection was performed.

L428-pRTS-1-HA-*bfl-1* clones were then induced or non-induced to express their respective proteins by addition of tetracycline (1 µg/ml) or an equal volume of vehicle (100 % ethanol) to the culture media. Total protein from these cells was prepared at 48 h and the presence of HA-tagged Bfl-1 was confirmed by western blotting (Section 2.7.4) using an anti-HA antibody (Table 2-2) (Figure 4.13A). Co-expression of the GFP protein from the bi-directional promoter of pRTS-1-HA-*bfl-1* upon induction with tetracycline was also confirmed using fluorescence microscopy (Section 2.4.6.5) (Figure 4.13B). RNA from these cells was prepared (Section 2.6.3.1) at 48 h post-addition of tetracycline and was reverse transcribed to cDNA (Section 2.6.4.1). Quantification of *bfl-1* mRNA expression levels was performed by realtime q-PCR (Section 2.6.4.2) (Figure 4.13C).

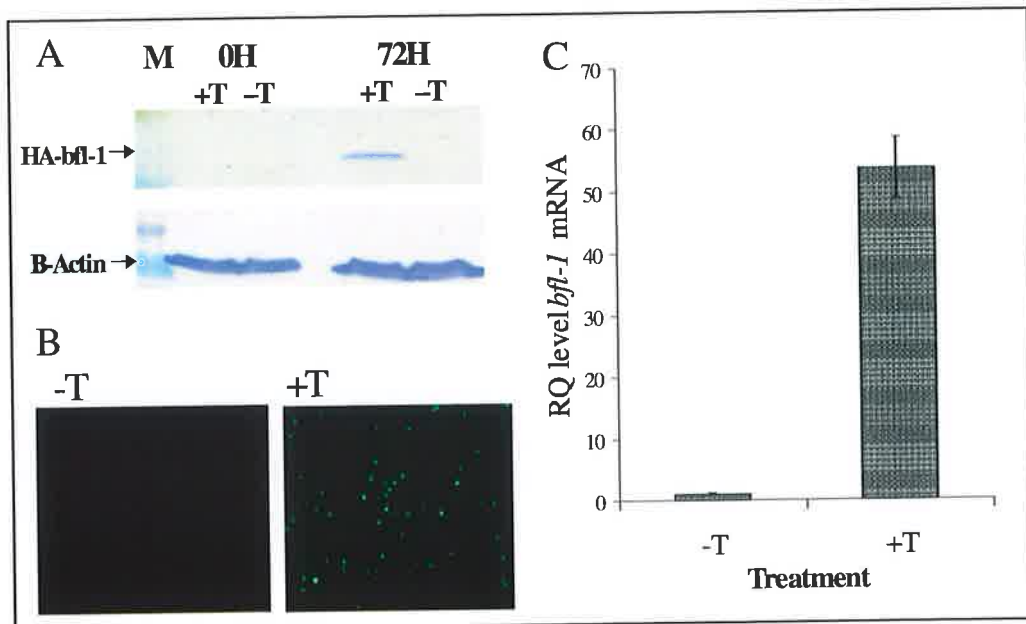


**Figure 4.13 Ectopic expression of *bfl-1* mRNA and HA-tagged Bfl-1 and GFP proteins from L428-pRTS-1-HA-*bfl-1* clones.**

L428 pRTS-1-HA-*bfl-1* clones were induced or non-induced by addition of tetracycline to express HA-Bfl-1 and GFP proteins. (A) The expression of HA-tagged Bfl-1 was confirmed by western blotting at 72 h post addition of tetracycline using an anti-HA antibody (upper panel) and normalised for  $\beta$ -actin levels (lower panel) using an anti-actin antibody. (B) The induction of GFP protein expression was monitored at 48 h by using an Olympus DP-50 fluorescent microscope. (C) RNA was extracted at 48 h and reverse transcribed using random primers. The induction of *bfl-1* mRNA was monitored in real-time by detection of fluorescence intensity using a FAM-labeled TaqMan probe for *bfl-1* and a FAM-labeled TaqMan probe for  $\beta$ -actin using an ABI Prism 7500 Sequence Detection System. After normalisation for  $\beta$ -actin, Relative Quantification (RQ) level of *bfl-1* mRNA was plotted a function of the non-induced sample (arbitrarily assigned a value of 1).

Once the L428-pRTS-1-HA-*bfl-1* cell clones were validated as capable of simultaneously expressing HA-tagged Bfl-1 and GFP proteins, experiments to test the effect of ectopic expression of Bfl-1 during conditions of cellular stress were initiated.

There is evidence that Bcl-2 family proteins such as the anti-apoptotic proteins Bcl-x<sub>L</sub>, Bcl-w, Bcl-2, and Mcl-1 have anti-proliferative effects in *in vitro* systems (O'Reilly *et al.*, 1996, Huang *et al.*, 1997, Rathmell *et al.*, 2000, Craig, 2002, Janumyan *et al.*, 2003, Gil-Gomez *et al.*, 1998, Fujise *et al.*, 2000 and Winter *et al.*, 1998). For example, bcl-x<sub>L</sub> and bcl-2 enhance G0 arrest and delay G0- to G1 transition in fibroblasts (Janumyan *et*

*al.*, 2003). Furthermore, Bcl-2 protein expression correlates with lower proliferative activity (S-phase fraction measured by flow cytometry) in intermediate and high-grade non-HL (Winter *et al.*, 1998). Unlike other anti-apoptotic members of the Bcl-2 family, expression of Bfl-1 was shown to facilitate proliferation (D'Sa-Eipper and Chinnadurai, 1998). Furthermore, expression of the mouse homologue, A1, did not affect cell cycle entry when overexpressed in primary T cells (Gonzalez *et al.*, 2003).

Inhibition of NF- $\kappa$ B in earlier experiments led to a decrease in proliferation due to cell death. As phenotypic analysis of the effect of exogenous Bfl-1 expression from pRTS-1-HA-*bfl-1* during NF- $\kappa$ B inhibition in HL cell lines included examination of cell proliferation, it was important to exclude the possibility that exogenous Bfl-1 expression could result in decreased/increased cell proliferation due to cell cycle arrest/acceleration. In a control experiment, a proliferation assay (Section 2.4.8) was performed on induced and non-induced L428-pRTS-1-HA-*bfl-1* cells in order to determine if the expression of exogenous HA-Bfl-1 could affect proliferation. It can be seen from Figure 4.14 that ectopic expression of Bfl-1 does not significantly affect cell proliferation over a 72 h period post induction under normal physiological conditions.

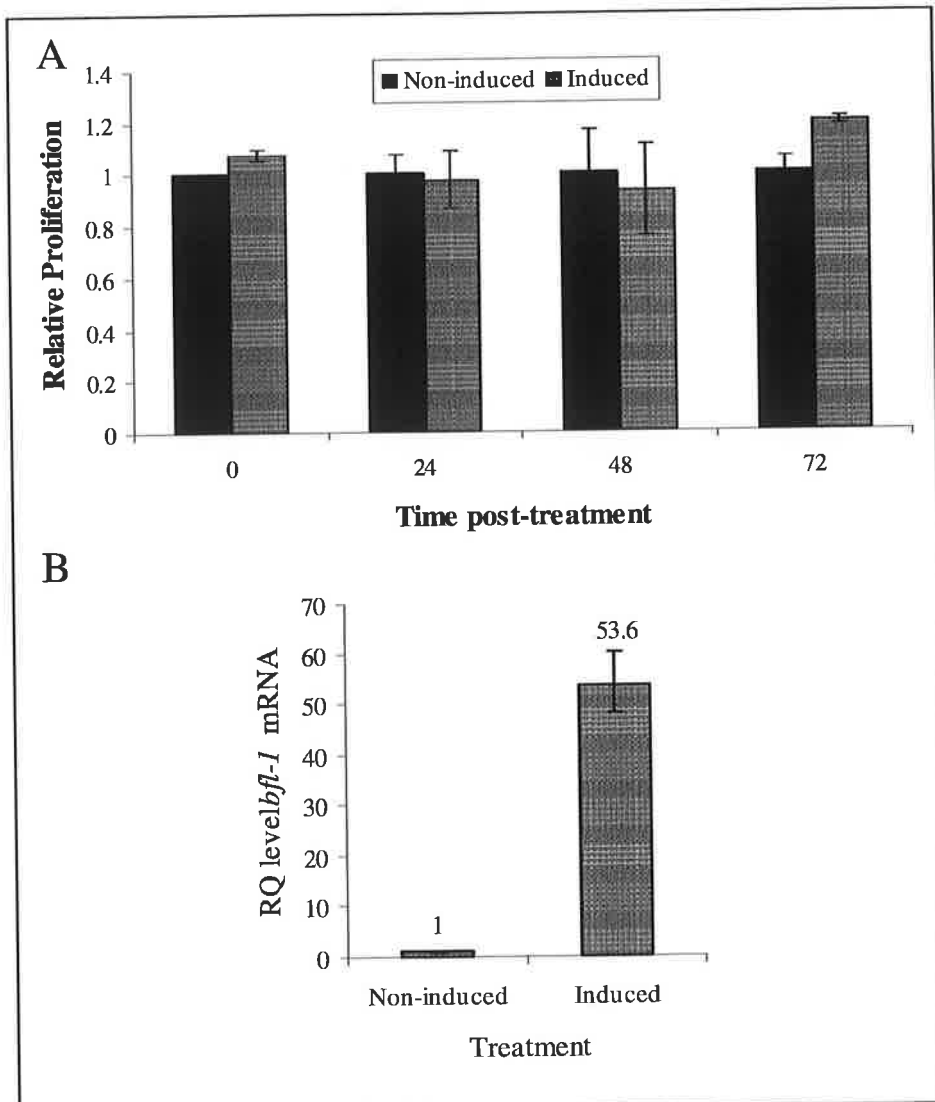


**Figure 4.14 Cell proliferation of L428-pRTS-1-HA-*bfl-1* cells induced/non-induced to exogenously express HA-Bfl-1.**

L428 pRTS-1-HA-*bfl-1* clones were induced or non-induced to express HA-Bfl-1 by addition of tetracycline or 100 % ethanol. Cell proliferation was monitored at 0-72 h timepoints (A-D) post addition of tetracycline by addition of 20 µl of CellTiter 96 Aqueous One Solution to 100 µl of cells in culture medium (in triplicate) in 96-well plates. The plates were incubated at 37 °C/5 % CO<sub>2</sub> for 4 h and absorbance at 495 nm was measured using a Tecan Saffire II 96-well plate reader. Proliferation of induced samples was relative to non-induced samples (arbitrarily assigned a value of 1). (B) RNA was extracted at 48 h and reverse transcribed using random primers. The induction of *bfl-1* mRNA was monitored in real-time by detection of fluorescence intensity using a FAM-labeled TaqMan probe for *bfl-1* and a FAM-labeled TaqMan probe for β-actin using an ABI Prism 7500 Sequence Detection System. After normalisation for β-actin, RQ level of *bfl-1* mRNA was plotted a function of the non-induced sample (arbitrarily assigned a value of 1).

Previous experiments in this project using the NF-κB inhibitors sodium arsenite and BAY11 demonstrated that death by apoptosis was coincident with a loss in *bfl-1* mRNA levels over a 48 h/72 h period in HL cell lines (Figure 4.6 and Figure 4.9). It was possible that the abolition of activated NF-κB levels following inhibition resulted in decreased transcriptional upregulation of the *bfl-1* promoter, resulting in the loss of *bfl-1* expression seen. It was an important aim, therefore, to determine if a loss of *bfl-1* expression was a critical factor in the apoptotic outcome observed and if exogenous expression of Bfl-1 could protect these cells from sodium arsenite and BAY11-induced death by apoptosis.

This hypothesis that ectopic expression of Bfl-1 could protect cells from apoptosis induced by NF-κB inhibition was tested here. L428-pRTS-1-HA-*bfl-1* cells were induced or non-induced to express HA-Bfl-1. At 24 h post addition of tetracycline or vehicle, the cells were treated with sodium arsenite. The number of viable cells was monitored over a 48/72 h period by MTS assay.

From the results, it can be discerned that sodium arsenite treatment of non-induced L428-pRTS-1-HA-*bfl-1* cells (-T+SA) caused a time-dependent decrease in proliferation by 50 % in 48 h relative to the control (-T-SA) (Figure 4.15). This is consistent with the finding seen in Figure 4.1 that cell viability of the parent cell line, L428, was reduced by 50 % at 48 h post sodium arsenite treatment. In striking contrast, proliferation of L428-pRTS-1-HA-*bfl-1* cells induced to ectopically express Bfl-1 during NF-κB inhibition by sodium arsenite (+T+SA) remained constant with no reduction in proliferation relative to the control (+T-SA).

The effect of sodium arsenite treatment of L428-pRTS-1-HA-*bfl-1* cells was also examined by Annexin V/7-AAD staining (Section 2.4.11.12and FACS analysis. The number of cells expressing GFP (M2; Figure 4.16, left panel of graphs) in the non-induced (-T-SA and -T+SA) samples was negligible (< 0.5 %), while in the induced samples was almost half of the total population (+T-SA; ~ 45 % and +T+SA; ~ 48 %). M1 denotes the non-GFP expressing population. Cell viability in this experiment was monitored by annexin V/7-AAD staining (Figure 4.16, right panel of graphs). It is evident from these results that sodium arsenite treatment of non-induced L428-pRTS-1-HA-*bfl-1* cells (-T+SA) caused an ~10 % increase in the number of apoptotic cells relative to the control (-T-SA) (Figure 4.16). In contrast, cells induced to ectopically express Bfl-1 were protected from this apoptotic outcome (+T+SA). The differential sensitivity of induced and non-induced cells to sodium arsenite, indicates that the

presence of Bfl-1 is sufficient to ensure survival of cultured H/RS cells during chemotoxic agent-induced cell death. Strikingly, when the GFP-expressing cells treated with sodium arsenite were examined in isolation (by analysing cells in R2; Figure 4.17A left panel), this population of cells exhibited complete protection from apoptosis with uncompromised viability as seen in Figure 4.17A, right panel. Distinctly, examination of the non-GFP expressing population treated with BAY11 (cells in R2; Figure 4.20B left panel) revealed that only 65 % of this population of cells were viable.

These experiments were also performed using BAY11, to test the effect of another NF- $\kappa$ B inhibitor. L428-pRTS-1-HA-*bfl-1* cells were induced and non-induced to express HA-Bfl-1. At 24 h post addition of tetracycline or vehicle, the cells were treated with BAY11. The number of viable cells was monitored over a 48/72 h period by MTS assay. The results seen in Figure 4.18 show that BAY11 treatment of non-induced L428-pRTS-1-HA-*bfl-1* cells (-T+B) caused a time-dependent decrease in proliferation by 50 % in 48 h relative to the control (-T-B) (Figure 4.18A). In striking contrast, proliferation of L428-pRTS-1-HA-*bfl-1* cells induced to ectopically express Bfl-1 during NF- $\kappa$ B inhibition by BAY11 (+T+B) remained constant with no reduction in proliferation relative to the control (+T-B). RNA from these cells was prepared (Section 2.6.3.2) at 48 h and reverse transcribed to cDNA (Section 2.6.4.1). *Bfl-1* mRNA expression levels were measured using realtime q-PCR (2.6.4.2) (Figure 4.18B; shown for BAY11 only). A ~50 % decrease in *bfl-1* mRNA expression level in the non-induced BAY11 treated samples was observed at 48 h consistent with earlier findings in this project (Figure 4.9).

Using annexin V/7-AAD staining, the effect of BAY11 treatment on viability of L428-pRTS-1-HA-*bfl-1* cells was also examined. The number of cells expressing GFP (M2; Figure 4.19, left panel of graphs) in the non-induced (-T-B and -T+B) samples was negligible (< 0.2 %), while in the induced samples was almost half of the total population (+T-B; ~ 49 % and +T+B; ~ 31 %). M1 denotes non-GFP expressing population. It is evident from these results that BAY11 treatment of non-induced L428-pRTS-1-HA-*bfl-1* cells (-T+B) caused a 54 % decrease in cell viability relative to the control (-T-B) (Figure 4.19, right panels). In contrast, cells induced to ectopically express Bfl-1 were protected from this apoptotic outcome (+T+B) and exhibited a 31 % decrease in cell viability of the total cell population. Moreover, when the GFP-expressing cells treated with BAY11 were examined in isolation (by analysing cells in R2; Figure 4.20A left panel), this population of cells exhibited complete protection from

apoptosis with uncompromised viability as seen in Figure 4.20A, right panel. Distinctly, examination of the non-GFP expressing population treated with BAY11 (cells in R2; Figure 4.20B left panel) revealed that only 35 % of this population of cells were viable.

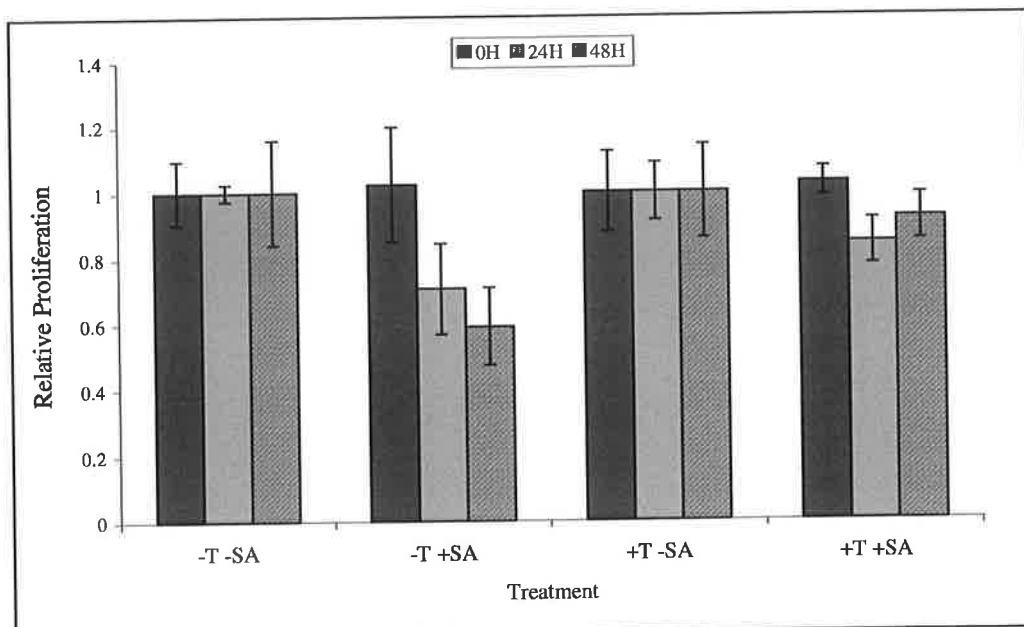


**Figure 4.15 Sodium arsenite treatment of L428-pRTS-1-HA-*bfl-1***

L428 pRTS-1-HA-*bfl-1* clones were induced or non-induced to express HA-Bfl-1 by addition of tetracycline or 100 % ethanol. At 24 h post addition of tetracycline or vehicle, the cells were treated with or without 10  $\mu$ M sodium arsenite and cell proliferation was monitored at 0-48 h timepoints post addition of tetracycline by addition of 20  $\mu$ l of CellTiter 96 Aqueous One Solution to 100  $\mu$ l of cells in culture medium (in triplicate) in 96-well plates. The plates were incubated at 37 °C/5 % CO<sub>2</sub> for 4 h and absorbance at 495 nm was measured using a Tecan Saffire II 96-well plate reader. Proliferation of samples was relative to sodium arsenite-treated samples (arbitrarily assigned a value of 1).

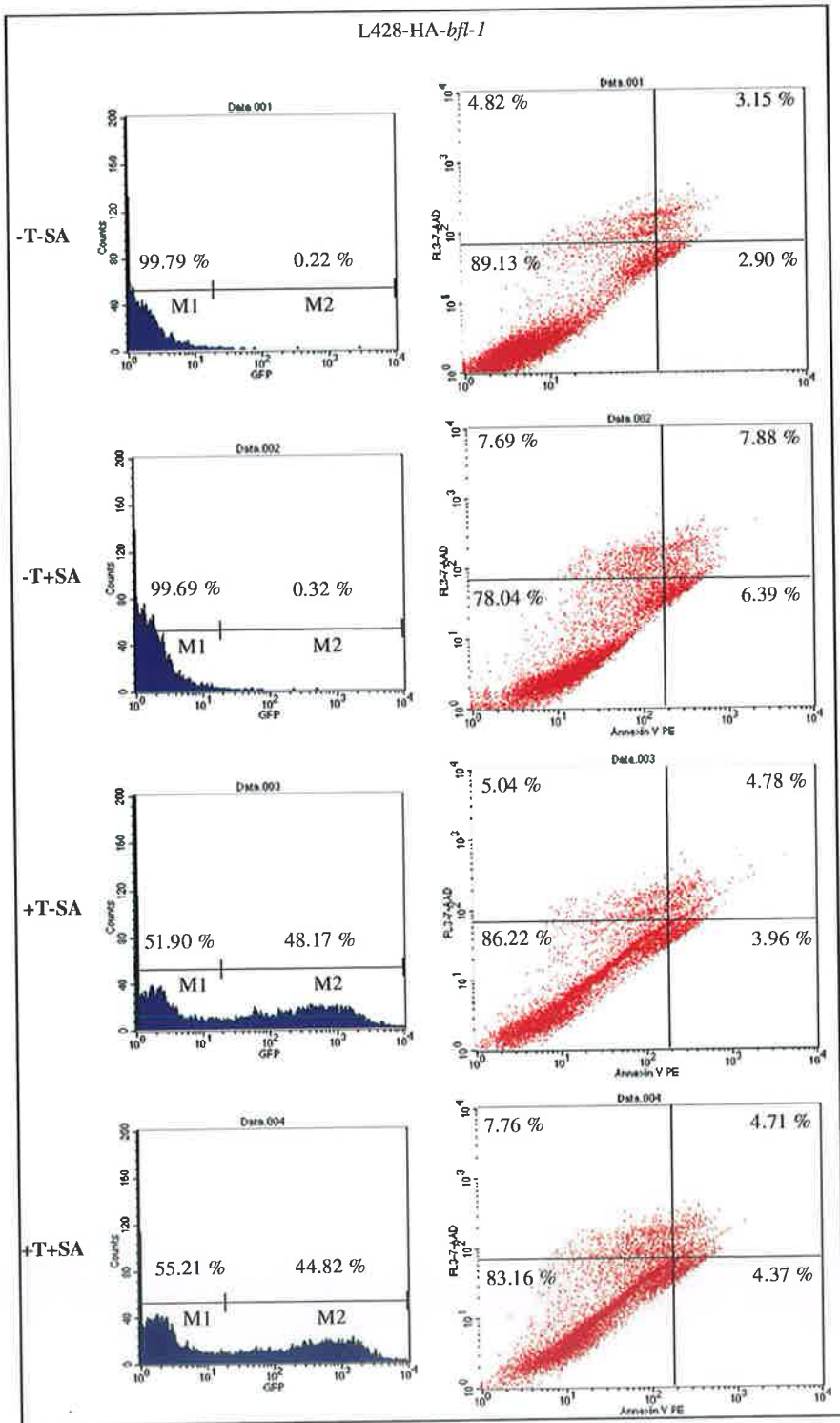


**Figure 4.16 Effect of sodium arsenite treatment of L428-pRTS-1-HA-*bfl-1***

L428 pRTS-1-HA-*bfl-1* clones were induced or non-induced to express HA-Bfl-1 by addition of tetracycline or 100 % ethanol. At 24 h post addition of tetracycline or vehicle, the cells were treated with or without 10  $\mu$ M sodium arsenite and cell

viability/apoptosis profile was analysed at 48 h post treatment by PI/annexin V staining and subsequent flow cytometric analysis. Quadrant markers were based on stained/unstained controls and values reflect the percentage of cells in each quadrant. Cells in the lower left quadrant are viable cells ( $\text{PI}^-/\text{Annexin V}^-$ ), cells in the lower right quadrant are early apoptotic cells ( $\text{PI}^-/\text{Annexin V}^+$ ), cells in the upper right quadrant are late apoptotic cells ( $\text{PI}^+/\text{Annexin V}^+$ ) and cells in the upper left quadrant are necrotic cells ( $\text{PI}^+/\text{Annexin V}^-$ ).

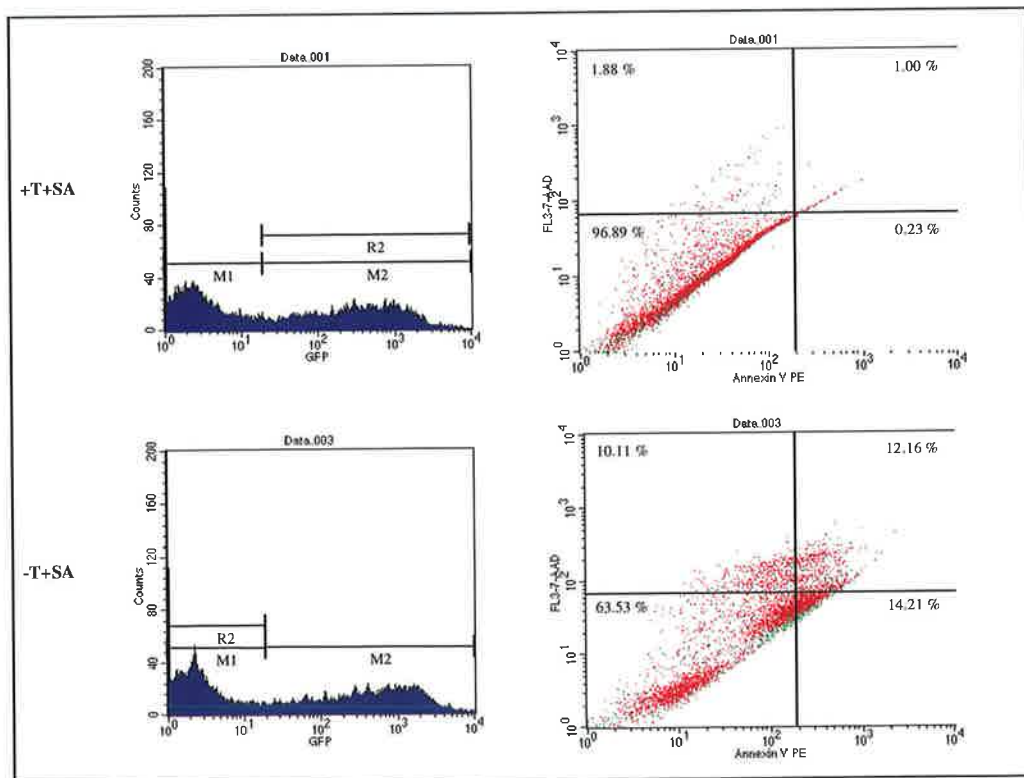


**Figure 4.17 Sodium arsenite treatment of L428-pRTS-1-HA-*bfl-1*; GFP expressing cells gated**

L428 pRTS-1-HA-*bfl-1* clones were induced or non-induced to express HA-Bfl-1 by addition of tetracycline or 100 % ethanol. At 24 h post addition of tetracycline or vehicle, the cells were treated with or without 10  $\mu\text{M}$  sodium arsenite and cell viability/apoptosis profile was analysed at 48 h post treatment by PI/annexin V staining and subsequent flow cytometric analysis. Quadrant markers were based on stained/unstained controls and values reflect the percentage of cells in each quadrant. Cells in the lower left quadrant are viable cells ( $\text{PI}^-/\text{Annexin V}^-$ ), cells in the lower right quadrant are early apoptotic cells ( $\text{PI}^-/\text{Annexin V}^+$ ), cells in the upper right quadrant are late apoptotic cells ( $\text{PI}^+/\text{Annexin V}^+$ ) and cells in the upper left quadrant are necrotic cells ( $\text{PI}^+/\text{Annexin V}^-$ ).

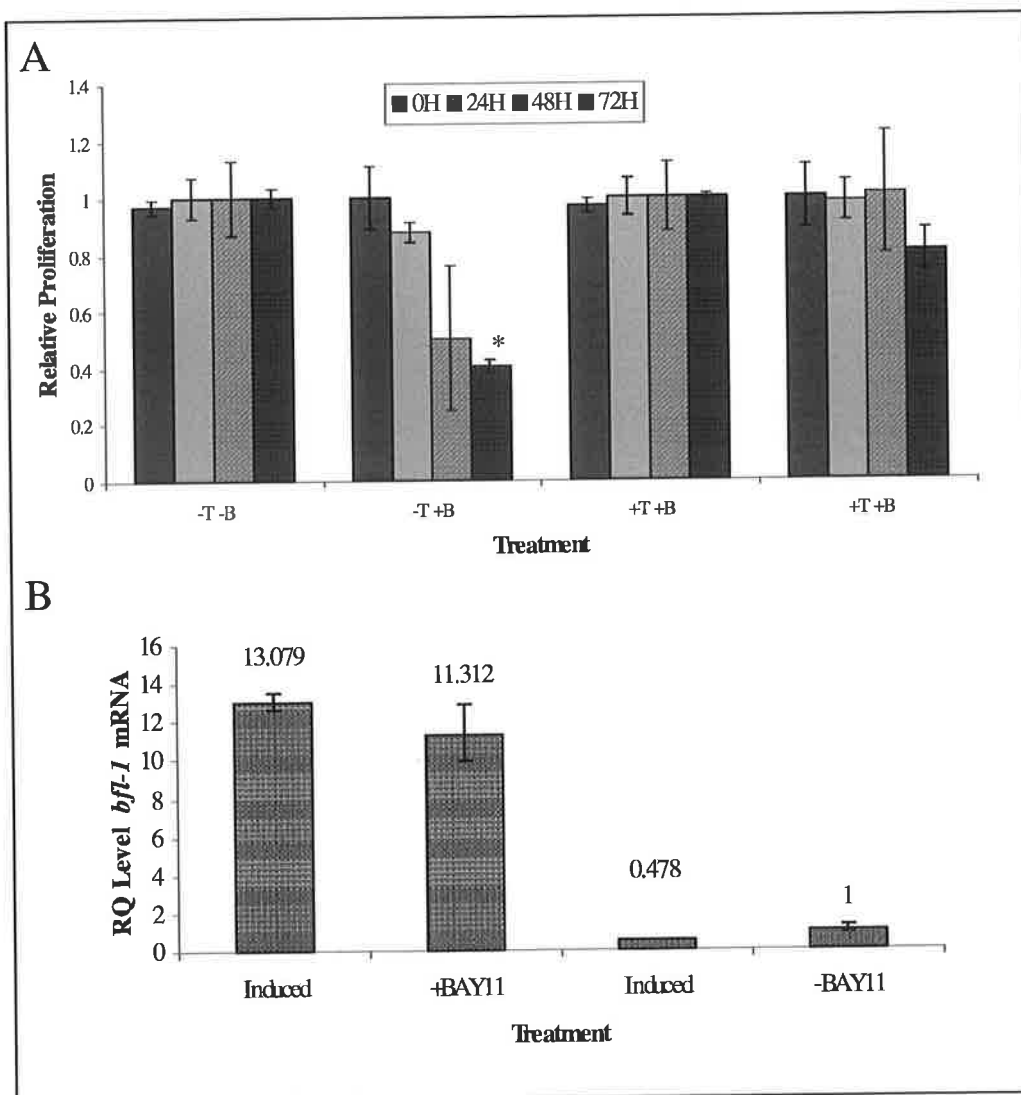


**Figure 4.18 BAY11 treatment of L428-pRTS-1-HA-*bfl-1***

(A) L428 pRTS-1-HA-*bfl-1* clones were induced or non-induced to express HA-Bfl-1 by addition of tetracycline or 100 % ethanol. At 24 h post addition of tetracycline or vehicle, the cells were treated with or without 10  $\mu$ M BAY11 and cell proliferation was monitored at 0-72 h timepoints post addition of tetracycline by addition of 20  $\mu$ l of CellTiter 96 Aqueous One Solution to 100  $\mu$ l of cells in culture medium (in triplicate) in 96-well plates. The plates were incubated at 37 °C/5 % CO<sub>2</sub> for 4 h and absorbance at 495 nm was measured using a Tecan Saffire II 96-well plate reader. Proliferation of samples was relative to BAY11-treated samples (arbitrarily assigned a value of 1). (B) RNA was extracted at 48 h and reverse transcribed using random primers. The induction of *bfl-1* mRNA was monitored in real-time by detection of fluorescence intensity using a FAM-labeled TaqMan probe for *bfl-1* and a FAM-labeled TaqMan probe for  $\beta$ -actin using an ABI Prism 7500 Sequence Detection System. After normalisation for  $\beta$ -actin, RQ level of *bfl-1* mRNA was plotted a function of the non-induced control sample (arbitrarily assigned a value of 1). Data are mean  $\pm$ SD, \*P≤0.01.

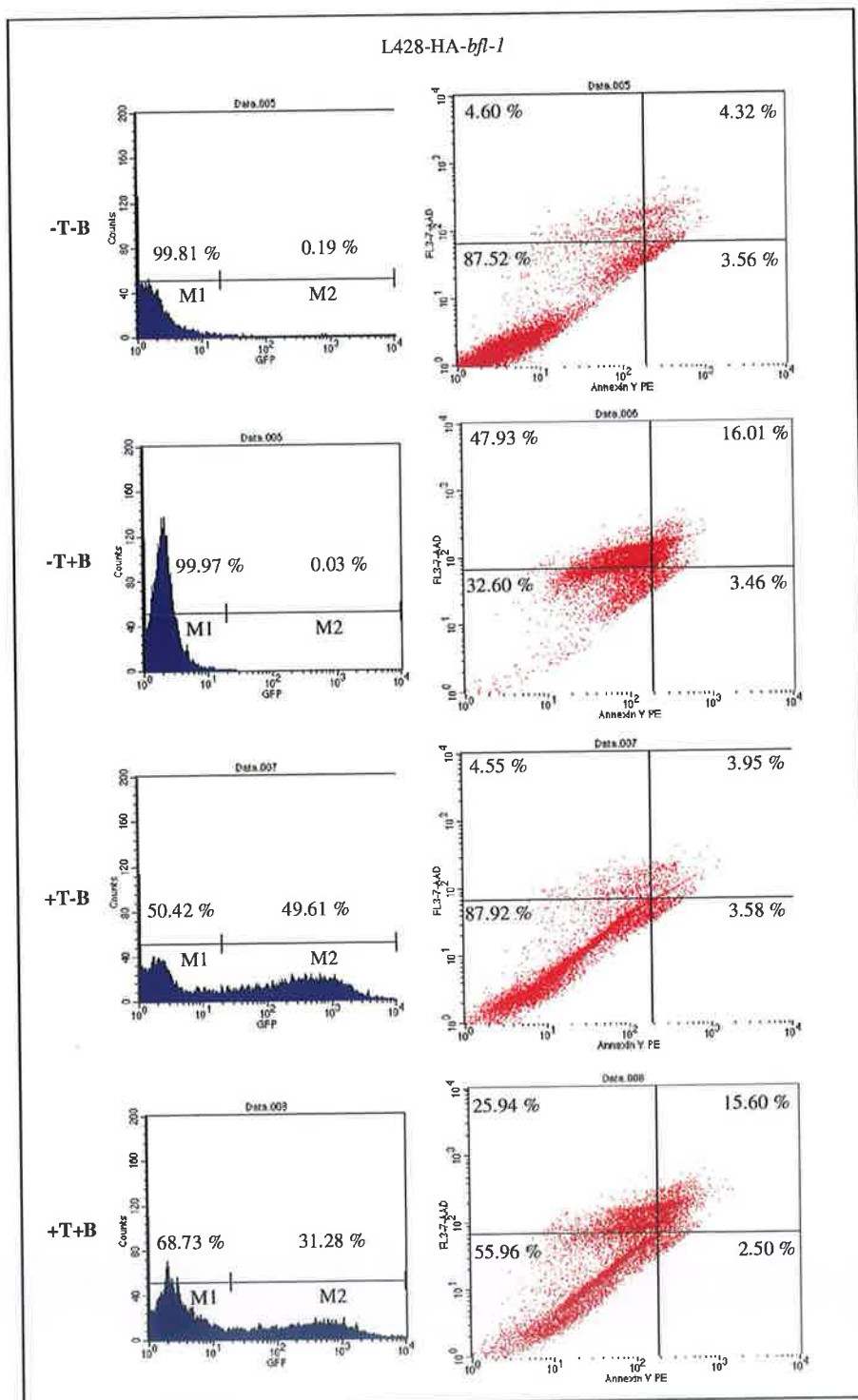


**Figure 4.19 Effect of BAY11 treatment of L428-pRTS-1-HA-*bfl-1***

L428 pRTS-1-HA-*bfl-1* clones were induced or non-induced to express HA-Bfl-1 by addition of tetracycline or 100 % ethanol. At 24 h post addition of tetracycline or vehicle, the cells were treated with or without 10  $\mu$ M BAY11 and cell

viability/apoptosis profile was analysed at 48 h post treatment by PI/annexin V staining and subsequent flow cytometric analysis. Quadrant markers were based on stained/unstained controls and values reflect the percentage of cells in each quadrant. Cells in the lower left quadrant are viable cells (PI/Annexin V<sup>-</sup>), cells in the lower right quadrant are early apoptotic cells (PI/Annexin V<sup>+</sup>), cells in the upper right quadrant are late apoptotic cells (PI<sup>+</sup>/Annexin V<sup>+</sup>) and cells in the upper left quadrant are necrotic cells (PI<sup>+</sup>/Annexin V<sup>-</sup>).

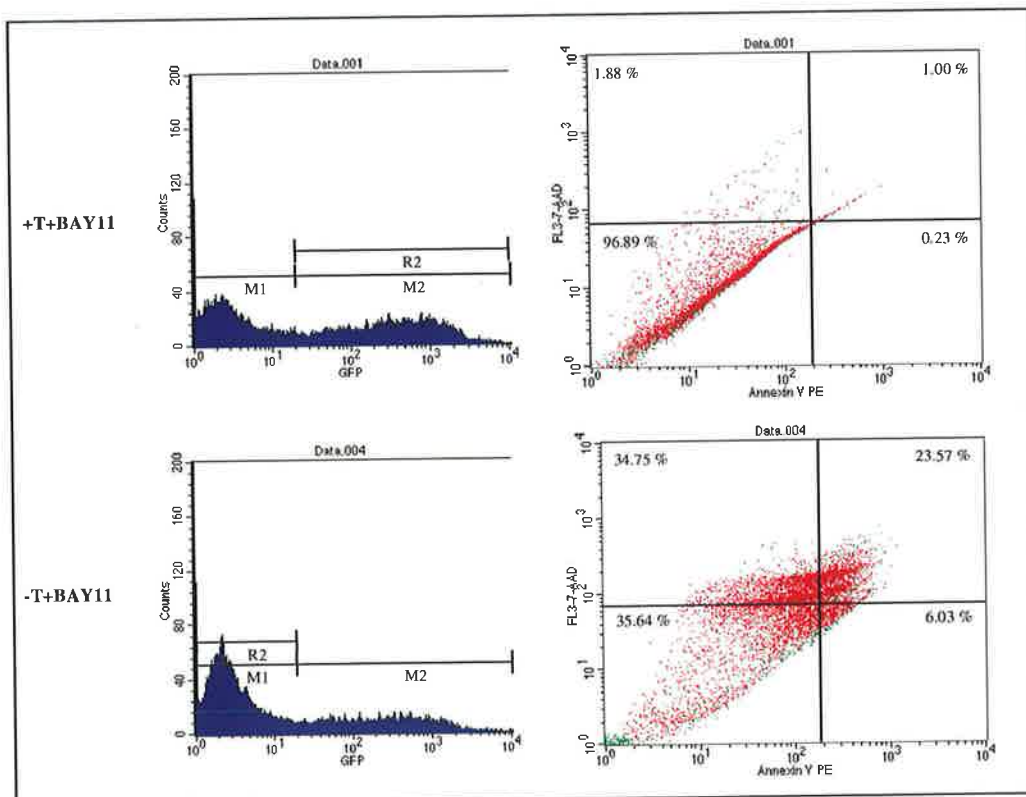


**Figure 4.20 BAY11 treatment of L428-pRTS-1-HA-*bfl-1*; GFP expressing cells gated**

L428 pRTS-1-HA-*bfl-1* clones were induced or non-induced to express HA-Bfl-1 by addition of tetracycline or 100 % ethanol. At 24 h post addition of tetracycline or vehicle, the cells were treated with or without 10  $\mu$ M BAY11 and cell viability/apoptosis profile was analysed at 48 h post treatment by PI/annexin V staining and subsequent flow cytometric analysis. Quadrant markers were based on stained/unstained controls and values reflect the percentage of cells in each quadrant. Cells in the lower left quadrant are viable cells (PI/Annexin V<sup>-</sup>), cells in the lower right quadrant are early apoptotic cells (PI/Annexin V<sup>+</sup>), cells in the upper right quadrant are late apoptotic cells (PI<sup>+</sup>/Annexin V<sup>+</sup>) and cells in the upper left quadrant are necrotic cells (PI<sup>+</sup>/Annexin V<sup>-</sup>).

In summary, in cells induced to express exogenous Bfl-1, apoptotic death was almost completely inhibited at the same inhibitor concentrations used in the controls. In this dual expression system, the amount of GFP in a given cell is proportional to the level of exogenous Bfl-1, and it is clearly to be seen in these experiments that even those cells expressing the lowest levels of GFP were rescued from apoptosis induced using the NF- $\kappa$ B inhibitors.

In a similar experiment, L428-pRTS-1-HA-bfl-1 cells were exposed to an apoptotic stimulus by means of serum deprivation to test if ectopic expression of Bfl-1 conferred protection against this cellular insult. Induced or non-induced cells were cultured in media supplemented with 10 %, 5 %, 1 % and 0.1 % serum concentrations. Viable cell number/proliferation was monitored over a 72 h period by MTS assay in order to determine the affect of overexpression of Bfl-1 under these conditions.

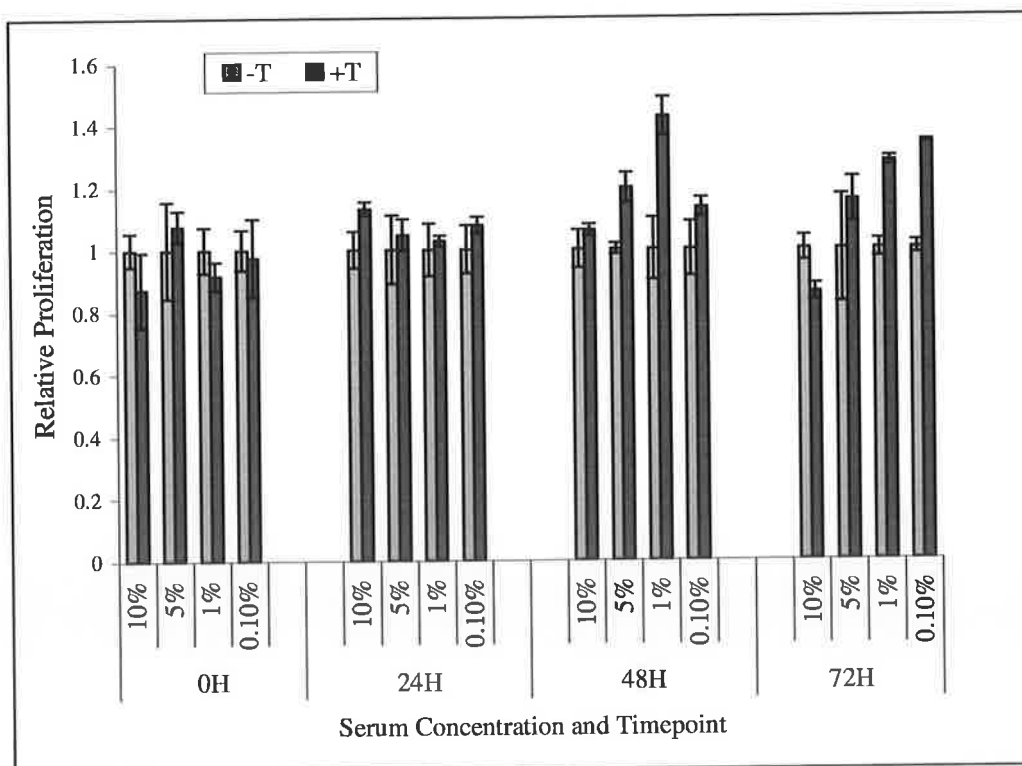


**Figure 4.21 Effect of serum deprivation on L428-pRTS-1-HA-bfl-1 cells.**

L428 pRTS-1-HA-bfl-1 clones were induced or non-induced to express HA-Bfl-1 by addition of tetracycline or 100 % ethanol and placed in media with various serum

concentrations (10 %, 5 %, 1 % and 0.1 %). Cell proliferation was monitored at 0-72 h timepoints post addition of tetracycline by addition of 20  $\mu$ l of CellTiter 96 Aqueous One Solution to 100  $\mu$ l of cells in culture medium (in triplicate) in 96-well plates. The plates were incubated at 37 °C/5 % CO<sub>2</sub> for 4 h and absorbance at 495 nm was measured using a Tecan Saffire II 96-well plate reader. Proliferation of samples was relative to uninduced samples maintained in 10 % serum (arbitrarily assigned a value of 1).

Figure 4.14 demonstrated that ectopic expression of Bfl-1 did not interrupt or drive cell proliferation under physiological conditions. However, it can be seen from Figure 4.21 that ectopic Bfl-1 expression corresponds to improved relative proliferation (~1.3-fold) compared to controls at lower serum concentrations of 1 and 0.1 % serum at 48 and 72 h post serum deprivation. No alteration in relative proliferation was observed under normal physiological conditions of 10 % serum, consistent with the findings in Figure 4.14.

### **4.3 Discussion**

A major concern about the use of anti-NF-κB agents for the treatment of cancer comes from the heterogeneous NF-κB function in cancer progression and in the apoptotic response to DNA-damaging agents. The NF-κB pathway is required for the normal functioning of the body. For example, the turnover of the outer layers of skin requires the function of a specific ubiquitin ligase complex, SCFβ-TrCP, which is also part of the traditional activation cascade for NF-κB (Maniatis, 1999). Ironically, oncogenesis could be a consequence of its inhibition. Complete inhibition of NF-κB via genetic knockout may produce severe toxicity as evidenced from mice studies using dominant-negative Rel A, which die during embryogenesis due to pathologic apoptosis of the liver (Beg *et al.*, 1995 a and b). Specific targeting of the phenotypic effector genes could therefore prove more effective than transcription factor targeting.

A number of recent reports have shown that inhibition of NF-κB with various compounds leads to decreased Bfl-1 expression and results in decreased resistance to apoptosis induced by chemotoxins and cytokines. Lee *et al.*, (2003), identified two structurally related compounds, manassantin A and B as specific inhibitors of NF-κB activation and treatment of HT-1080 cells with these compounds prevented the TNF-α-induced expression of Bfl-1/A1 and sensitised cells to TNF-α-induced cell death. The NF-κB inhibitor, celastrol, inhibited TNF-α-induced Bfl-1/A1 expression, in LPS-stimulated macrophage RAW264.7 cells (Lee *et al.*, 2006). The anti-inflammatory agent, curcumin, was found to be an NF-κB inhibitor and inhibited TNF-α-induced Bfl-1/A1 expression in human myeloid leukemia, U937 cells (Aggarwal *et al.*, 2005). Shishodia and Aggarwal, (2006), reported that NF-κB-dependent reporter gene expression was abrogated by diosgenin, a steroid saponin and TNF-induced expression of NF-κB-regulated gene products, including Bfl-1, was inhibited by diosgenin treatment of human myeloid KBM-5 cells. Also, plumbagin, a plant derivative, suppressed NF-κB activation and NF-κB-regulated gene products, including Bfl-1 and lead to potentiation of apoptosis induced by cytokine and chemotherapeutic agents (Sandur *et al.*, 2006).

Ectopic expression of Bcl-2 family members has been shown previously to protect malignant cells from apoptosis. Alam *et al.*, (1997), demonstrated that overexpression of Bcl-xL or Bcl-2, protected the BL cell line, Ramos, from apoptosis induction in response to calcium ionophore, anti-Ig and macromolecular synthesis inhibition. However, in contrast to Bcl-2 in that study, ectopic overexpression of Bcl-xL did not rescue Ramos cells from Fas-mediated apoptosis. Wagner *et al.*, (1993), showed that Bcl-2 effectively inhibited Myc-induced apoptosis in serum-deprived Rat 1a fibroblasts without blocking entry into the cell cycle. Elsewhere, high-level expression of an exogenous *bcl-2* gene, introduced into IL-6-dependent B9 myeloma cells via retroviral or bovine papilloma virus-based vectors, was shown to suppress apoptotic death following cytokine deprivation (Schwarze and Hawley, 1995).

Indeed, infection of the L428 cell line with a recombinant adenoviral vector expressing the super-repressor IκBαDN, which inhibits NF-κB activation, induced an apoptotic response that was rescued by ectopic expression of Bcl-xL (Hinz *et al.*, 2001).

In this study the effect of NF-κB inhibition by treatment with sodium arsenite and BAY11 inhibitors on H/RS-derived cell lines and the consequences for *bfl-1* expression were examined. Evidence is presented that *bfl-1* is an NF-κB target gene in HL cells and that exogenous expression of Bfl-1 in the presence of NF-κB inhibitors can rescue these cells from apoptosis.

## **CHAPTER 5 *Bfl-1* downregulation by RNAl**

## 5.1 Introduction

RNA interference (RNAi) is a ubiquitous mechanism in eukaryotic cells to suppress the expression of genes that determine fundamental cell fate decisions of differentiation and survival (Abrahante *et al.*, 2003; Brennecke *et al.*, 2003). Recently, RNAi mediated by small interfering RNAs (siRNA) has emerged as a powerful tool to target specific knockdown of gene expression in gene-function studies. The disruption of gene expression by RNAi involves sequence-specific degradation of mRNA induced by a double-stranded RNA homologous to the target sequence. It was reasoned that this strategy of knockdown would be used to investigate the role of *bfl-1* mRNA in H/RS cell lines.

### 5.1.1 The RNAi pathway

Long double-stranded RNAs (dsRNAs; typically >200 nucleotides [nt]) can be used to silence the expression of target genes. Upon entry to the cell, the long dsRNAs enter a cellular pathway that is commonly referred to as the RNAi pathway (Figure 5.1). First, an RNase III-like enzyme called Dicer processes the dsRNAs, yielding 21- to 23-bp RNA fragments with 2-nt 3' overhangs (Bernstein *et al.*, 2001a and b), which have symmetric 2–3 nt 3' overhangs and 5' phosphate and 3' hydroxyl groups (Tuschl *et al.*, 1999). These RNA duplexes, referred to as siRNA, associate with a multiprotein RNA-inducing silencing complex (RISC), guiding RISC to a homologous target mRNA and triggering its endonucleolytic cleavage by Slicer (Argonaute-2, Ago-2), an enzyme residing within the RISC complex. The end result is the cleavage and degradation by cellular exonucleases of cognate RNA resulting in shutdown of gene expression in a sequence-specific manner.

In mammalian cells, introduction of long dsRNA (>30 nt) initiates a potent antiviral response, exemplified by non-specific inhibition of protein synthesis and RNA degradation. As a consequence, in eukaryotes long dsRNA is not useful for sequence-specific silencing of target gene expression. The mammalian antiviral response can be bypassed, however, by the introduction or expression of siRNAs (~21 nt in length). These 21-mer siRNA molecules were short enough to bypass mechanisms that lead to a general shutdown of protein synthesis due to long double-strand RNA recognition yet

sufficient to direct RISC (containing the RNA endonuclease Ago2) to cleave target mRNA bearing a complementary sequence (Figure 5.1).

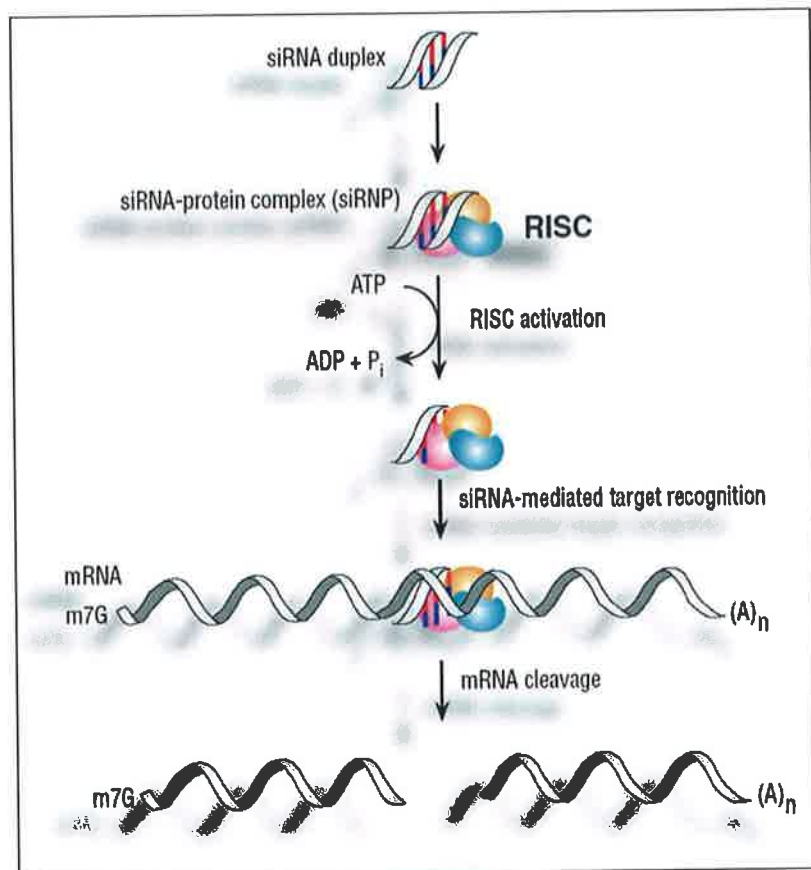


**Figure 5.1 Three ways to trigger the RNAi pathway.**

In mammalian systems, RNAi can be triggered by synthetic siRNA molecules. The mechanism of activation of RISC by joining of siRNA, unwinding and removal of sense strand of the siRNA is shown. Gene silencing results in the destruction of mRNA that is complementary to the input siRNA. Adapted from [www.cellsignal.com](http://www.cellsignal.com).

### **5.1.2 Summary of Results**

To fully elucidate the contribution of *bfl-1* gene expression to the survival/persistence of the malignant H/RS cell, a strategy was chosen to directly target the *bfl-1* mRNA transcripts for degradation. For this purpose the common technique of downregulation using *bfl-1*-specific siRNAs was employed in this cell context to monitor the effects of *bfl-1* downregulation on cell phenotype, proliferation, apoptotic threshold and relevant malignant properties. A major bottleneck in achieving RNAi in this study was the delivery of these molecules to the desired cells. A variety of strategies were used to deliver siRNAs to cells. Efficient delivery was eventually achieved by nucleofection and the phenotypic effect of knockdown was subsequently evaluated. Knockdown of *bfl-1* mRNA did not significantly reduce the apoptotic threshold of L428 cells during serum deprivation. However, downregulation of *bfl-1* mRNA correlated with an increase in apoptosis upon treatment with the chemotoxic agents, sodium arsenite and BAY11 implying a crucial role for Bfl-1 in setting the elevated threshold of resistance of these malignant cells.

## 5.2 Results

siRNAs must be efficiently delivered into the cytoplasm of cells, the site of precursor RNA processing by the enzyme Dicer and uptake of the siRNA guide strand into RISC (Hutvagner and Zamore, 2002). RNAs do not readily cross the cell membrane on their own because of their large molecular mass and their high negative charge. Efficiency of RNAi varies between cell types and conditions must be optimised empirically. The main challenges in this chapter were the identification of efficient siRNAs directed against *bfl-1* mRNA that led to a shutdown of gene expression in a sequence-specific manner and the identification of an efficient method of nucleic acid delivery to facilitate RISC–siRNA complex targeting of complementary mRNA.

### 5.2.1 Analysis of *bfl-1*-specific siRNAs

In order to test the affect of knockdown of *bfl-1* mRNA, three independent anti-*bfl-1* specific siRNAs (Table 5-1) were purchased (Ambion) and tested for efficacy of knockdown following transfection. The siRNAs were selected based on the Tuschl and co-workers' design guidelines (Elbashir *et al.*, 2002) and several other criteria including specificity and position of siRNA within the transcript. The anti-*bfl-1* specific siRNAs were pre-designed but not previously validated.

**Table 5-1 *bfl-1* specific siRNA specifications**

ID	Properties	Sense	Antisense
#80	Sequence	GUGCUACAAAUGUUGCGUtt	ACGCAACAUUUUGUAGCACtc
	Length	21	21
	% G/C	38	43
#81	Sequence	GUUUGAAGACGGCAUCAUtt	AAUGAUGCUCUUCAAAActc
	Length	21	21
	% G/C	38	43
#82	Sequence	GAUUUCAUAUUUUGUUGCGtt	CGCAACAAAAUAUGAAAUCtc
	Length	21	21
	% G/C	29	33

### 5.2.2 Efficiency of delivery of siRNA

The glyceraldehydes-3-phosphate dehydrogenase (*gapdh*) gene is widely recognised as an ideal target for positive control siRNAs as GAPDH is expressed ubiquitously in virtually all mammalian cells. In this study *gapdh* positive control siRNA was used to optimise transfection efficiency and to identify conditions for the maximum knockdown of *gapdh* mRNA. Silenced experimental samples were compared with cells transfected with a non-targeting, negative control siRNA rather than to non-transfected cell samples. The use of negative control siRNA eliminated the possibility that phenotypic effects observed upon knockdown were due to an immune response to siRNA transfection.

Initially, the H/RS cell line, L428, was transfected by electroporation (Section 2.4.6.1) with the anti-*bfl-1* siRNAs described in Table 5-1, a non-targeting siRNA and a pre-validated anti-*gapdh* siRNA. Transfected cells were analysed by realtime qPCR for *bfl-1*, *gapdh* and  $\beta$ -*actin* (endogenous control) levels at 48 h post transfection (Figure 5.2). No knockdown was observed upon transfection of L428 cells with anti-*bfl-1* specific siRNAs (Figure 5.2A) or using pre-validated anti-*gapdh* siRNA as compared to non-targeting siRNA (Figure 5.2B). This experiment was repeated with varying concentrations of siRNA (0.1 – 400 nM) but yielded similar results to those observed in Figure 5.2 (data not shown). Electroporation parameters [voltage conditions (200 – 250 V), volume and solvent in which cells were electroporated (200 – 300  $\mu$ l and supplemented serum/serum-free media/siPORT electroporation buffer)] were also varied but cells remained refractory to siRNA uptake by electroporation as the positive control pre-validated anti-*gapdh* siRNA failed to knockdown *gapdh* mRNA levels as expected (data not shown).

Next, lipid-mediated transfection using the Riboforce reagent (Novagen) was used in an attempt to efficiently deliver siRNA to L428 cells. Again, the extent of mRNA degradation was determined by realtime qPCR following transfection with anti-*bfl-1* siRNAs (Figure 5.3A) and anti-*gapdh* siRNA (Figure 5.3B) as compared to non-targeting siRNA. A degree of efficiency of knockdown was observed using this reagent with anti-*bfl-1* siRNAs, as seen in Figure 5.3A (~40 %; anti-*bfl-1* #81) and with anti-*gapdh* siRNA, as seen in Figure 5.3B (~30 %). Transfection conditions such as the total siRNA concentration, the siRNA:lipid ratio and the duration of transfection were modified in an attempt to improve knockdown efficacy but no amelioration was achieved.

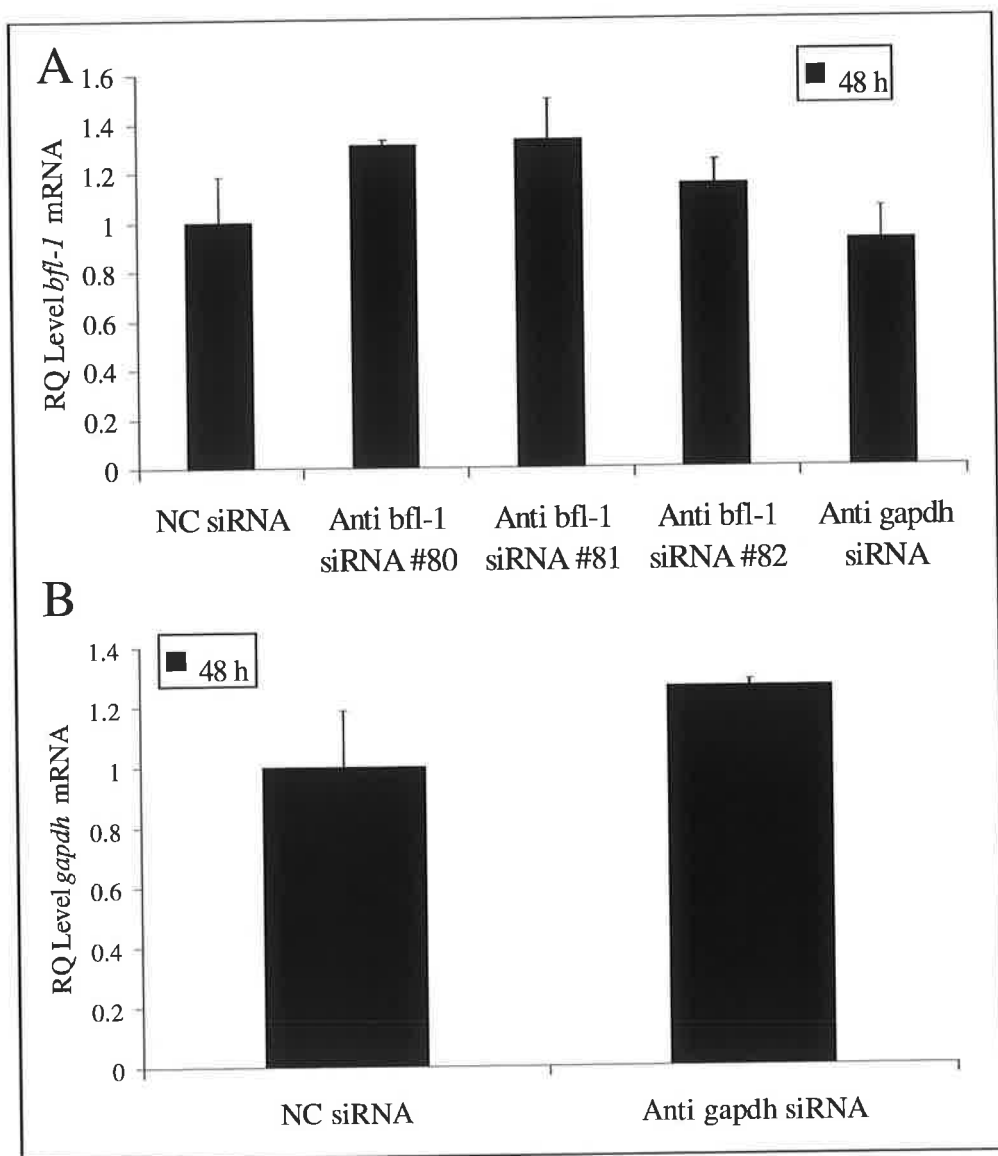


**Figure 5.2 Transfection of siRNA by electroporation**

L428 cells were transfected by electroporation with (A) 40 nM anti-*bfl-1* siRNA #80, #81 or #82 and (B) 40 nM of anti-*gapdh* siRNA or negative control non-targeting siRNA. RNA was extracted at 48 h using the RNeasy mini kit (Qiagen). Isolated RNA was reverse transcribed using random primers and amplification of DNA was monitored in real-time by detection of fluorescence intensity using a FAM-labeled TaqMan probe for *bfl-1* or *gapdh* and a FAM-labeled TaqMan probe for  $\beta$ -actin. Fluorescent signals were detected using an ABI Prism 7500 Sequence Detection System. After normalisation for  $\beta$ -actin, relative quantification (RQ) level of *bfl-1* or *gapdh* mRNA was plotted as a function of the control (NC; arbitrarily assigned a value of 1).

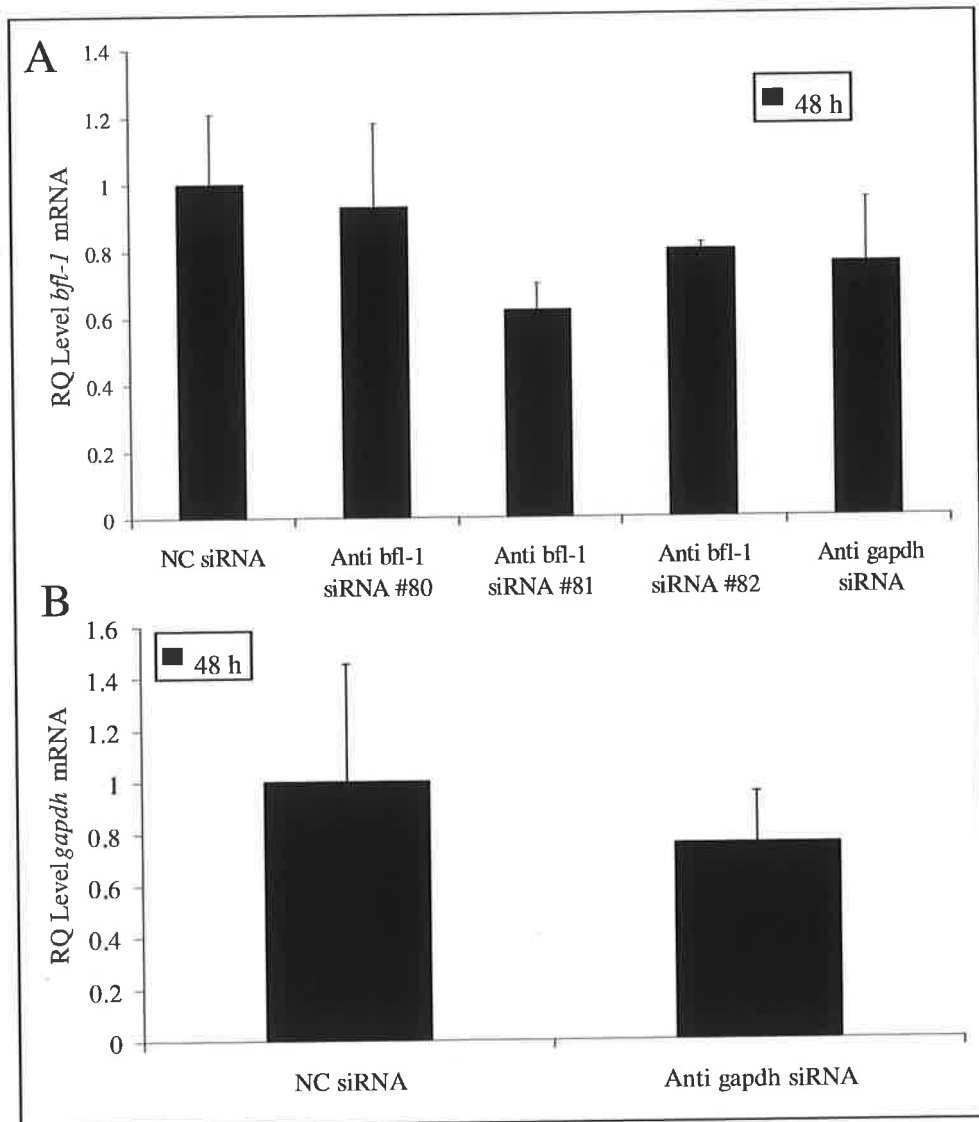


**Figure 5.3 Transfection of siRNA using Ribojuice transfection reagent**

L428 cells were transfected using Ribojuice with (A) 40 nM anti-*bfl-1* siRNA #80, #81 or #82 and (B) 40 nM of anti-*gapdh* siRNA or negative control non-targeting siRNA. RNA was extracted at 48 h using the RNeasy mini kit (Qiagen). Isolated RNA was reverse transcribed using random primers and amplification of DNA was monitored in real-time by detection of fluorescence intensity using a FAM-labeled TaqMan probe for *bfl-1* or *gapdh* and a FAM-labeled TaqMan probe for  $\beta$ -actin. Fluorescent signals were detected using an ABI Prism 7500 Sequence Detection System. After normalisation for  $\beta$ -actin, relative quantification (RQ) level of *bfl-1* or *gapdh* mRNA was plotted as a function of the control (NC; arbitrarily assigned a value of 1).

The level of knockdown achieved using the Ribojuice transfection agent was not sufficient given the anticipation of the pre-validated 90 % knockdown associated with

the anti-*gapdh* siRNA. Realising an efficient delivery method for the siRNA molecules was, therefore, the subject of further experimentation.

A modified electroporation technique known as nucleofection (Section 2.4.6.2), which benefited from cell line-specific electroporation parameters in tandem with a cell line-specific buffer, was next employed with the pre-validated anti-*gapdh* siRNA to determine efficiency of siRNA transfection. Expression of *gapdh* mRNA in L428 cells as evaluated by realtime qPCR was reduced by ~90 % and ~75 % at 12 and 24 h post nucleofection respectively relative to a negative control siRNA transfection as seen in Figure 5.4. In a parallel experiment, nucleofection with the GFP-reporter plasmid, pmaxGFP revealed a transfection efficiency of 80 % when transfected cells were analysed for GFP expression by fluorescence microscopy (data not shown), indicating the efficacy of knockdown seen in this experiment using anti-*gapdh* siRNA was primarily due to efficient delivery.

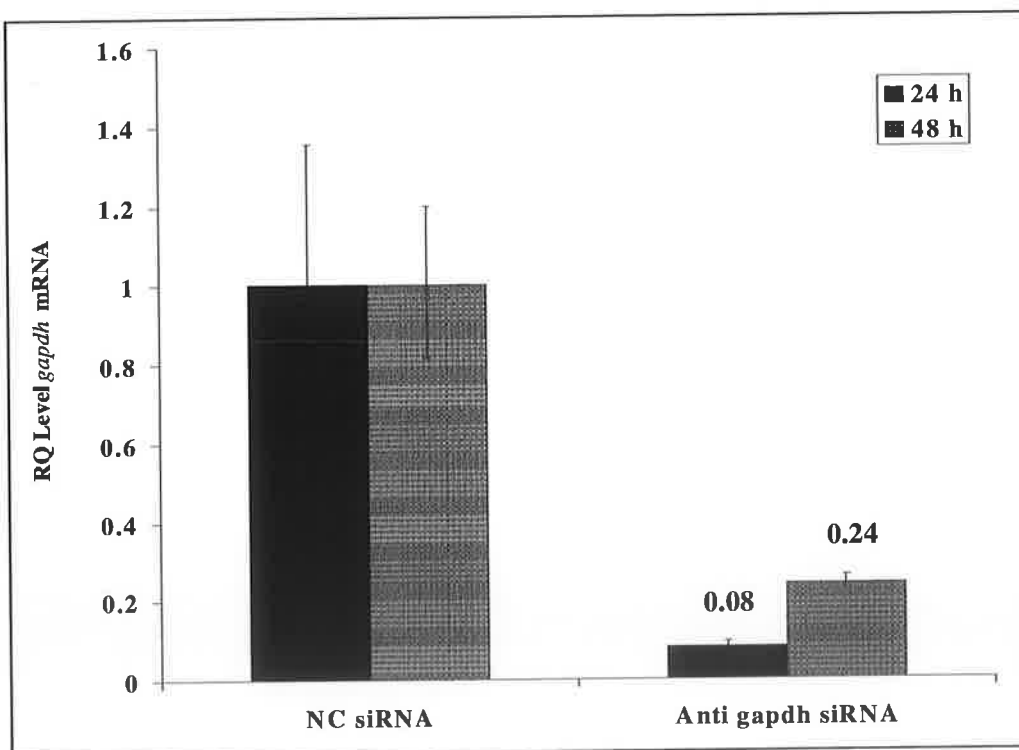


**Figure 5.4 Transfection of siRNA by nucleofection**

L428 cells were nucleofected with 30 nM of anti-*gapdh* siRNA or negative control scrambled siRNA. RNA was extracted at 12 or 24 h post nucleofection using the

RNeasy mini kit (Qiagen). Isolated RNA was reverse transcribed using random primers and amplification of DNA was monitored in real-time by detection of fluorescence intensity using a FAM-labeled TaqMan probe for *gapdh* and a FAM-labeled TaqMan probe for  $\beta$ -*actin*. Fluorescent signals were detected using an ABI Prism 7500 Sequence Detection System. After normalisation for  $\beta$ -*actin*, relative quantification (RQ) level of *gapdh* mRNA was plotted as a function of the control (NC; arbitrarily assigned a value of 1).

Transfection of anti-*bfl-1* siRNAs by nucleofection was next attempted and resulted in a 90 % knockout of *bfl-1* mRNA using the anti-*bfl-1* siRNA designated #81 and a 40 % knockout of *bfl-1* siRNA using the anti-*bfl-1* siRNA designated #80 relative to a negative control siRNA transfected at 12 h in L428 (Figure 5.5). No reduction in *bfl-1* mRNA expression was detected in L428 using the anti-*bfl-1* siRNA designated #82.

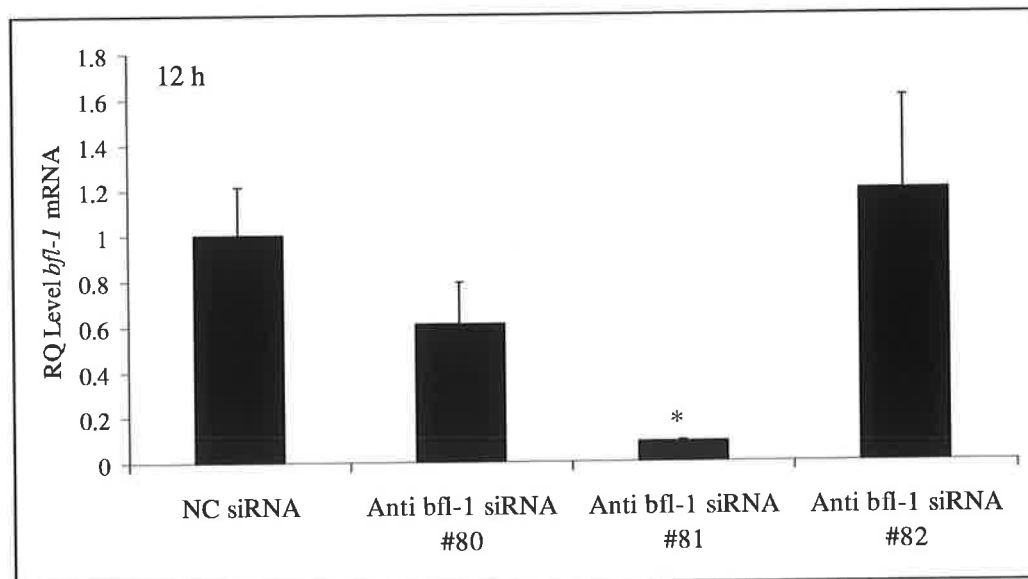


**Figure 5.5 Knockdown of *bfl-1* mRNA expression by nucleofection of siRNA**

L428 cells were nucleofected with 30 nM anti-*bfl-1* siRNA or negative control scrambled siRNA. RNA was extracted at 12 h using the RNeasy mini kit (Qiagen). Isolated RNA was reverse transcribed using random primers and amplification of DNA was monitored in real-time by detection of fluorescence intensity using a FAM-labeled TaqMan probe for *bfl-1* and a FAM-labeled TaqMan probe for  $\beta$ -*actin*. Fluorescent signals were detected using an ABI Prism 7500 Sequence Detection System. After normalisation for  $\beta$ -*actin*, relative quantification (RQ) level of *bfl-1* mRNA was plotted as a function of the control (NC; arbitrarily assigned a value of 1). Data are mean  $\pm$  SD, \*P=0.019.

### 5.2.3 Effect of anti-*bfl-1* siRNA on cell viability

It was important to determine the impact of siRNA nucleofection on cell viability to evaluate the toxicity of these molecules. L428 cells were nucleofected with anti-*bfl-1* and non-targeting siRNAs and cell viability was measured at 72 h post-nucleofection by MTS assay (Section 2.4.8) and plotted as a function of non-nucleofected cells (Figure 5.6). Nucleofection of L428 cells resulted in ~25 % reduction in cell viability relative to non-nucleofected control. No decrease in cell viability greater than that induced by nucleofection alone was observed when L428 cells were nucleofected with anti-*bfl-1* or non-targeting siRNAs.

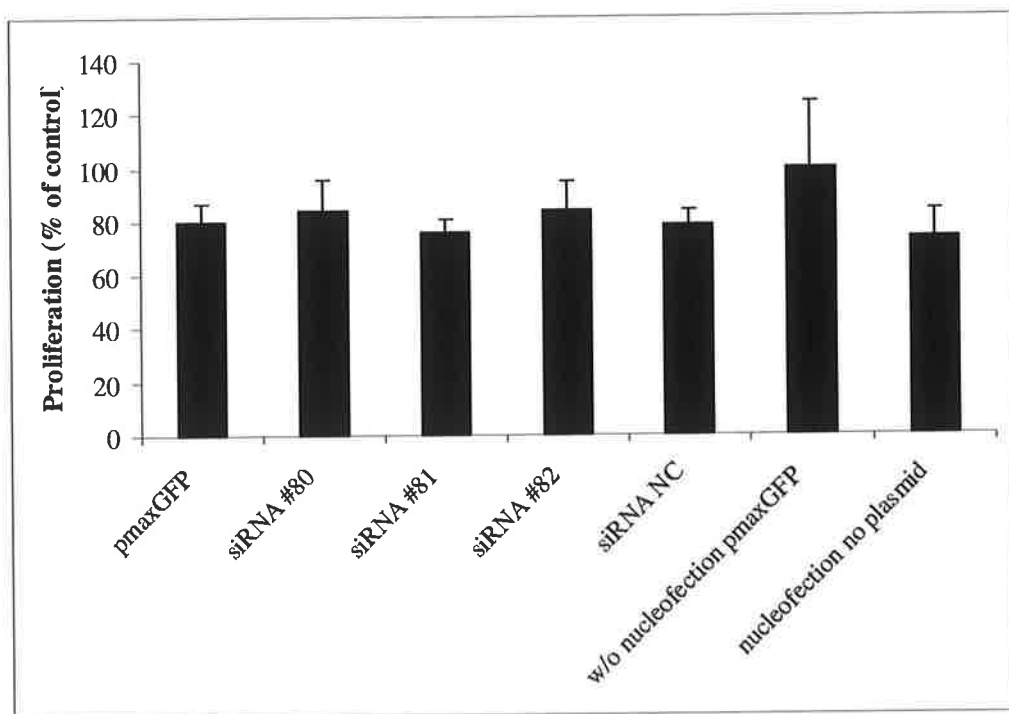


**Figure 5.6 Cell viability post nucleofection of siRNA**

L428 cells were nucleofected with pmax GFP, 30 nM of anti-*bfl-1* siRNA, 30 nM of negative control (NC) scrambled siRNA or no DNA/RNA. A replicate sample was also incubated with DNA but not nucleofected. Cell viability was monitored at 72 h post nucleofection by addition of 20 µl of CellTiter 96 Aqueous One Solution to 100 µl of cells in culture medium (in triplicate) in 96-well plates. The plates were incubated at 37 °C/5 % CO<sub>2</sub> for 4 h and absorbance at 495 nm was measured using a Tecan Saffire II 96-well plate reader. Cell viability was relative to ‘no nucleofection’ sample (arbitrarily assigned a value of 100 %).

Treatment with anti-*bfl-1* siRNA did not directly impact cell viability so loss of mRNA expression of this anti-apoptotic gene was not detrimental to the cell in normal physiological conditions. To determine whether knockdown of *bfl-1* mRNA expression in conditions of physiological stress could decrease the apoptotic threshold of H/RS cells, L428 cells were nucleofected with anti-*bfl-1* and non-targeting siRNAs and subjected to degrees of serum deprivation (10 %; normal and low-serum concentrations of 1 % and 0.1 % serum). The cell viability/apoptosis profile was evaluated by flow cytometric analysis of annexin V/propidium iodide stained cells.

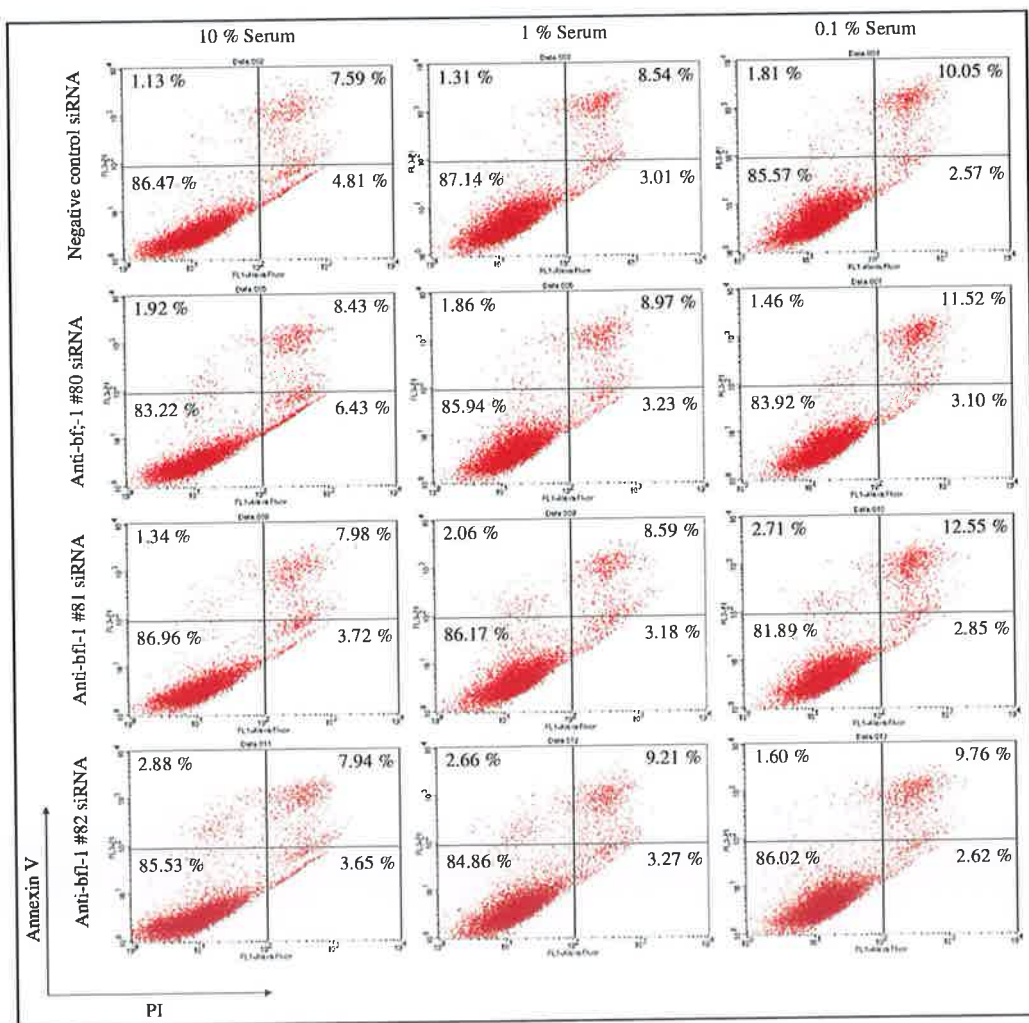


**Figure 5.7 Effect of serum deprivation on anti-*bfl-1* siRNA-treated L428 cells.**

L428 cells were nucleofected with anti-*bfl-1* siRNA or negative control non-targeting siRNA and placed in media with various serum concentrations (10 %, 1 % and 0.1 %).

The cell viability/apoptosis profile was analysed at 48 h post treatment by PI/annexin V staining and subsequent flow cytometric analysis. Quadrant markers were based on stained/unstained controls and values reflect the percentage of cells in each quadrant. Cells in the lower left quadrant are viable cells (PI/Annexin V<sup>-</sup>), cells in the lower right quadrant are early apoptotic cells (PI/Annexin V<sup>+</sup>), cells in the upper right quadrant are late apoptotic cells (PI<sup>+</sup>/Annexin V<sup>+</sup>) and cells in the upper left quadrant are necrotic cells (PI<sup>+</sup>/Annexin V<sup>-</sup>).

From Figure 5.7, it can be seen that there is no significant difference in viability of anti-*bfl-1* siRNA-treated and non-targeting siRNA-treated cells undergoing serum starvation. The percentage of apoptotic cells (early apoptotic cells in the lower right quadrant and late apoptotic cells in the upper right quadrant) under 0.1 % serum conditions is greatest in the sample treated with the most potent anti-*bfl-1* siRNA (#81) but is not significant.

#### 5.2.4 Effect of anti-*bfl-1* siRNA during NF-κB inhibition

In Chapter 4, it was shown that inhibition of NF-κB by sodium arsenite or BAY11 chemical inhibitors resulted in apoptosis of H/RS cells, which was coincident with a significant decline in *bfl-1* mRNA expression levels. Furthermore, it was shown in this study for the first time that ectopic expression of Bfl-1 protected H/RS cells from apoptosis induced by NF-κB inhibition.

It was next tested whether Bfl-1 silencing would affect chemotoxic agent-induced apoptosis. siRNA transfected cells were left untreated or treated with suboptimal levels of sodium arsenite (Figure 5.8) or BAY11 (Figure 5.9) and cell viability/apoptotic profile was examined by annexin V/7-AAD staining and flow cytometry.

Examination of the siRNA/sodium arsenite-treated population in Figure 5.8, reveals a significant difference in the percentage of apoptotic<sup>4</sup> cells in the anti-*bfl-1* siRNA-treated sample when compared to the non-targeting siRNA-treated population (56.21 % for anti-*bfl-1* siRNA; #81 versus 32.77 % for non-targeting siRNA). This effect is also seen in the sodium arsenite-treated population nucleofected with anti-*bfl-1* siRNA; #80, but to a lesser extent (53.66 % for anti-*bfl-1* siRNA; #80 versus 32.77 % for non-targeting siRNA). The most potent anti-*bfl-1* siRNA elicits the more dramatic effect on apoptotic outcome following sodium arsenite treatment and conversely, the least

---

<sup>4</sup> Early apoptotic cells in the lower right quadrant and late apoptotic cells in the upper right quadrant.

effective anti-*bfl-1* siRNA (#82), does not induce a significant effect (41.54 % for anti-*bfl-1* siRNA; #82 versus 32.77 % for non-targeting siRNA).

Similarly, using the NF-κB inhibitor, BAY11, a significant difference in the percentage of apoptotic cells in the anti-*bfl-1* siRNA-treated sample is evident when compared to the non-targeting siRNA-treated population (47.26 % for anti-*bfl-1* siRNA; #81 versus 26.26 % for non-targeting siRNA) (Figure 5.9).

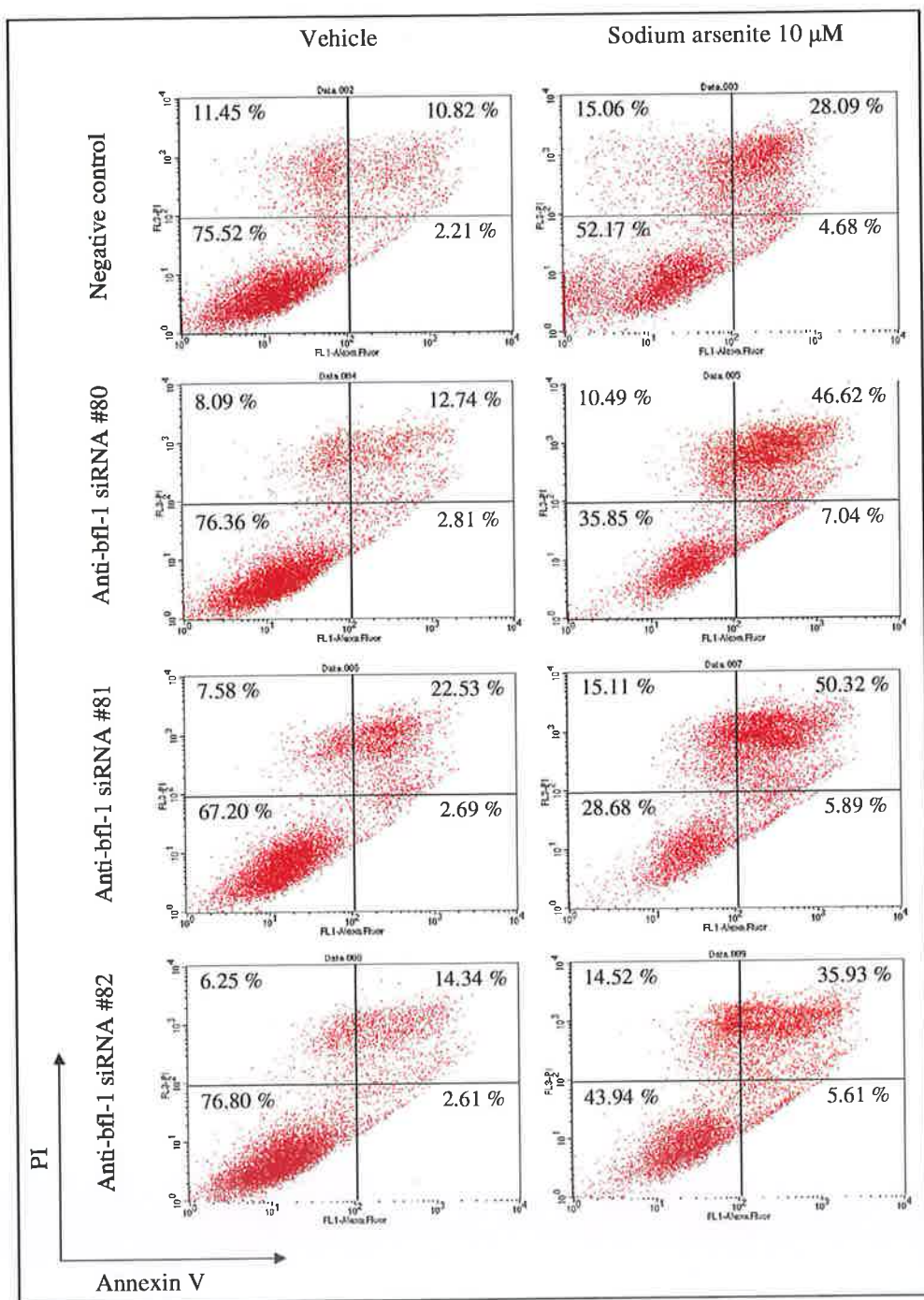


**Figure 5.8 Effect of sodium arsenite treatment on anti-*bfl-1* siRNA-treated L428 cells.**

L428 cells were nucleofected with anti-*bfl-1* siRNA or negative control anti-scrambled siRNA and treated with sodium arsenite or vehicle. The cell viability/apoptosis profile was analysed at 48 h post treatment by PI/annexin V staining and subsequent flow

cytometric analysis. Quadrant markers were based on stained/unstained controls and values reflect the percentage of cells in each quadrant. Cells in the lower left quadrant are viable cells ( $\text{PI}^-/\text{Annexin V}^-$ ), cells in the lower right quadrant are early apoptotic cells ( $\text{PI}^-/\text{Annexin V}^+$ ), cells in the upper right quadrant are late apoptotic cells ( $\text{PI}^-/ \text{Annexin V}^+$ ) and cells in the upper left quadrant are necrotic cells ( $\text{PI}^+/\text{Annexin V}^-$ ).

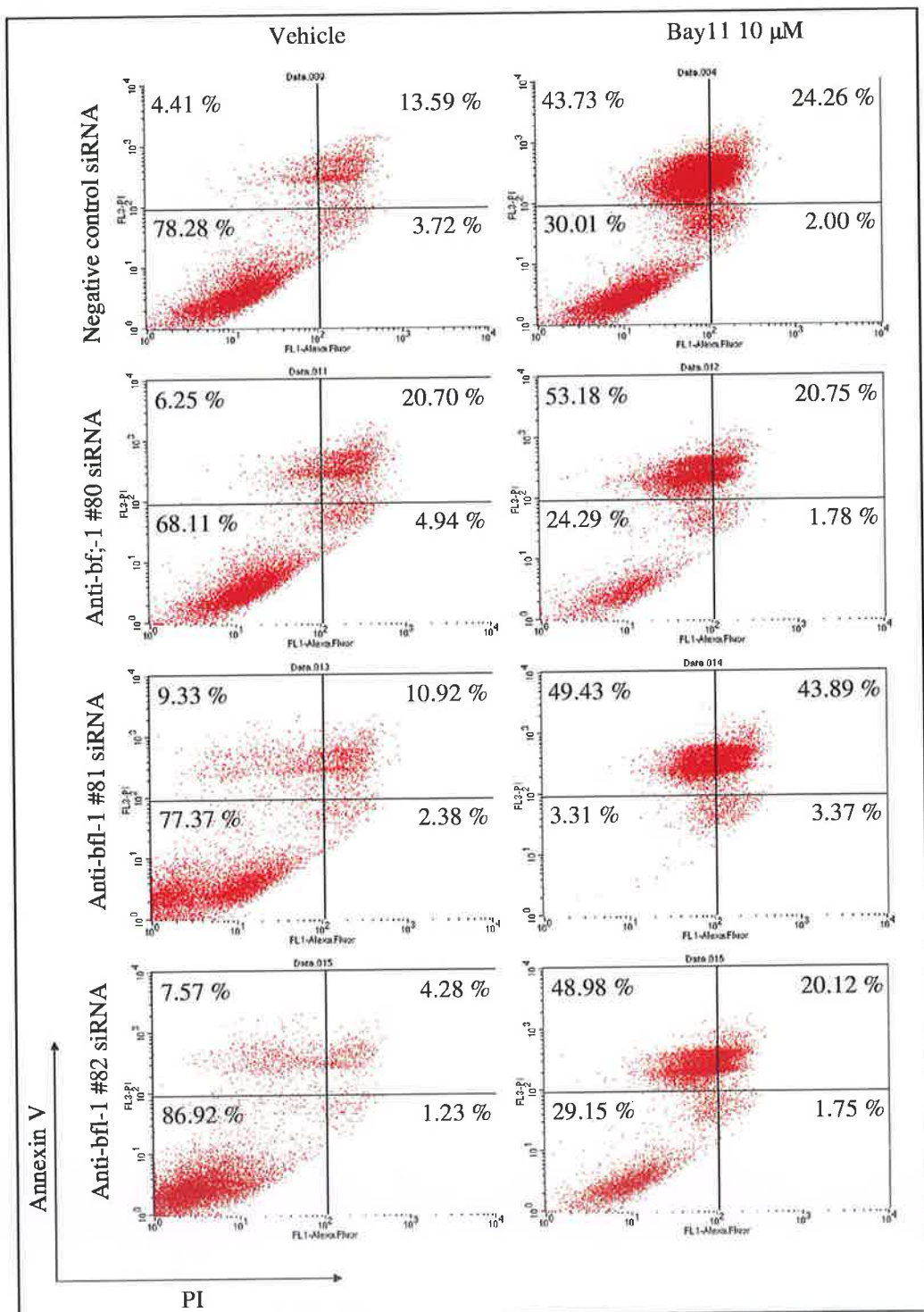


**Figure 5.9 Effect of BAY11 treatment on anti-*bfl-1* siRNA-treated L428 cells.**

L428 cells were nucleofected with anti-*bfl-1* siRNA or negative control anti-scrambled siRNA and treated with BAY11 or vehicle. The cell viability/apoptosis profile was analysed at 48 h post treatment by PI/annexin V staining and subsequent flow

cytometric analysis. Quadrant markers were based on stained/unstained controls and values reflect the percentage of cells in each quadrant. Cells in the lower left quadrant are viable cells ( $\text{PI}^-/\text{Annexin V}^-$ ), cells in the lower right quadrant are early apoptotic cells ( $\text{PI}^-/\text{Annexin V}^+$ ), cells in the upper right quadrant are late apoptotic cells ( $\text{PI}^+/\text{Annexin V}^+$ ) and cells in the upper left quadrant are necrotic cells ( $\text{PI}^+/\text{Annexin V}^-$ ).

### 5.3 Discussion

Numerous reports have now demonstrated the successful application of RNAi as a tool for posttranscriptional gene silencing in mammalian cells (reviewed in Shi, 2003). siRNAs have been exploited in cancer research to downregulate misappropriately expressed genes, such as K-RAS transcripts carrying the valine-112 oncogenic mutation which constitutively activates RAS leading to pancreatic and colon cancer. Knockdown of mutated K-RAS using specific siRNAs resulted in inhibition of colony growth in soft agar (Brummelkamp *et al.*, 2002). Other authors have shown that bcl-2 antisense and RNAi treatments can inhibit tumour growth and induce apoptosis activity in various tumour cells (Cioca *et al.*, 2003; Lima *et al.*, 2004; Fu *et al.*, 2005). siRNA has also been shown to be extremely specific *in vitro*. Studies have demonstrated effective silencing of a wide variety of mutated oncogenes such as *K-Ras* (Brummelkamp *et al.*, 2002), mutated *p53* (Martinez *et al.*, 2002), *Her2/neu* (Choudhury *et al.*, 2004) and *bcr-abl* (Scherr *et al.*, 2003).

Here, the technique of siRNA was employed to suppress the expression of *bfl-1* mRNA in the H/RS cell line, L428 and its effect on apoptotic phenotype was evaluated. Knockdown of *bfl-1* mRNA did not significantly reduce the apoptotic threshold of L428 cells during serum deprivation. However, anti-*bfl-1* siRNA potentiated the apoptosis induced by NF-κB inhibitors validated as chemotoxic agents in Chapter 4. Furthermore, it can be seen that knockdown of *bfl-1* expression significantly contributed to the pro-apoptotic effect of both inhibitors to an extent commensurate with the degree of knockdown achieved with each siRNA.

Since downregulation served to greatly increase the sensitivity of cells to chemotoxic agent-induced apoptosis, silencing of Bfl-1 in this cell context might be of considerable interest for the treatment of HL in tandem with low-dose polychemotherapy. Targeting of Bfl-1 in H/RS cells by means of its functional blockade or inhibition of its expression, could possibly restore the apoptotic machinery in these cells and sensitise HL tumours to chemo- and radiotherapies.

## **CHAPTER 6 Regulation of the *bfl-1* promoter in HL**

## 6.1 Introduction

The objective was set in this Chapter to ascertain the regulation of the *bfl-1* gene at its promoter level in H/RS-derived cell lines. Previous work in our laboratory has shown that the *bfl-1* gene plays an important role in regulating the survival of EBV-infected B cells (D’Souza *et al.*, 2000) and is regulated by EBV LMP1 with a role for NF- $\kappa$ B (D’Souza *et al.*, 2004). It was shown in Chapter 4, that inhibition of transcription factor NF- $\kappa$ B in H/RS-derived cell lines led to death by apoptosis, concomitant with the loss of *bfl-1* mRNA levels. The *bfl-1* gene contains functional NF- $\kappa$ B-binding sites in its upstream transcriptional regulatory region (Zong *et al.*, 1999; D’Souza *et al.*, 2004) and it was therefore investigated here whether dysregulated NF- $\kappa$ B in HL might drive *bfl-1* promoter activity through one of these elements.

In a related study in our laboratory, it was observed that expression of EBNA2 as the sole EBV protein in an EBV-negative BL-derived cell line (DG75-tTA-EBNA2, Floettmann *et al.*, 1996) also led to an increase in *bfl-1* mRNA levels (Pegman *et al.*, 2006), demonstrating for the first time that a second EBV protein activates transcription of the *bfl-1* gene. EBNA2 expression was subsequently found to trans-activate the *bfl-1* promoter in EBV-negative BL-derived cell lines, and the ability of EBNA2 to bind RBP-J $\kappa$ /CBF1 is central for this effect (Pegman *et al.*, 2006).

Notch is considered cellular functional homologue of EBNA2 and both proteins interact with RBP-J $\kappa$ /CBF1 to modulate gene expression (reviewed in Chapter 1). Bearing in mind that the *bfl-1* promoter was trans-activated by EBNA2 via RBP-J $\kappa$ /CBF1 (Pegman *et al.*, 2006) and that aberrant expression of Notch receptors and ligands is a feature of H/RS cells (Kapp *et al.*, 1999; Jundt *et al.*, 2002), this study set out to investigate if the *bfl-1* gene was a target of NotchIC.

### 6.1.1 Summary of results

It was shown in this study that the *bfl-1* promoter is regulated by NF- $\kappa$ B in H/RS-derived cell lines of EBV negative (L428) and positive (L591) status. Inhibition of NF- $\kappa$ B in L428 and L591 cell lines by inhibitory-gene transfer blocks NF- $\kappa$ B activation of the *bfl-1* promoter. It was shown that the *bfl-1* promoter was trans-activated by NF- $\kappa$ B, primarily through the  $\kappa$ B-binding site at position -52 on the promoter.

Also in this study, the levels of Notch 1 and 2 receptors were investigated and found to be abundantly expressed in cultured H/RS cells. The Notch ligand, Jagged1, expressed in the EBV-positive cell line, L591 and presentation of Notch ligand Jagged1 led to increased proliferation of cultured H/RS cells.

Transient transfection studies with the paired promoter reporter constructs demonstrated the requirement of the putative CBF1 site (at position -243 to -249) on the *bfl-1* promoter was not essential for conferring responsiveness on the *bfl-1* promoter.

## 6.2 Results

### 6.2.1 The *bfl-1* promoter is regulated by NF-κB in HL

In order to directly investigate if the *bfl-1* promoter was regulated by NF-κB in this cell context, it was necessary to first inhibit NF-κB signaling in H/RS cell lines and examine the consequence of abrogation of this transcription factor pathway on the *trans*-activation of the *bfl-1* promoter. Suppression by gene transfer was the method adopted at the outset of this investigation to inhibit NF-κB for promoter examination.

In a control experiment, to monitor NF-κB activity in these cells, co-transfections were carried out using a known NF-κB-dependent reporter construct, 3x enh-κB luc (Table 2-5) (Floettmann and Rowe, 1997), which contains 3 NF-κB binding sites upstream of a minimal conalbumin promoter, linked to the luciferase gene. High basal level of activated NF-κB was apparent upon transfection of L428 and L591 (EBV positive) cell lines with 3 x enh κB luc reporter construct (Figure 6.1, actual normalised luciferase values were 536.8 and 982.9 respectively).

Co-transfections of L428 and L591 cell lines were carried out using an expression vector for a mutant form of IκBα (pEFCX-IκBαDN; Table 2-5), in which serine residues at positions 32 and 36 have been replaced with alanines (Liljeholm *et al.*, 1998) and the NF-κB-responsive vector; 3x enh-κB luc. Activation of NF-κB is initiated by phosphorylation of the inhibitory subunit, IκB, which targets IκB for degradation and leads to the release of active NF-κB. The mutant IκBα cannot be phosphorylated and subsequently proteolysed as a result of the amino acid replacements. NF-κB is thus retained in the cytoplasm by IκBαDN and NF-κB translocation to the nucleus and target gene activation is blocked.

To demonstrate the functionality of the IκBαDN, co-transfections were performed using the NF-κB-responsive reporter construct, 3x enh-κB luc together with increasing amounts of the super-repressor pEFCX-IκBαDN. In the absence of the mutant, transfection of the NF-κB-responsive vector, 3x enh-κB luc, in both cell lines resulted in a high level of luciferase activity, arbitrarily assigned a value of 100 %. In the presence of the IκBα super-repressor, a dramatic decrease in luciferase activity was

observed in L428 (80 % using 5  $\mu$ g I $\kappa$ B $\alpha$ DN DNA) (Figure 6.1A) and in L591 (60 % and 80 % using 5  $\mu$ g and 10  $\mu$ g I $\kappa$ B $\alpha$ DN DNA; respectively) (Figure 6.1B).

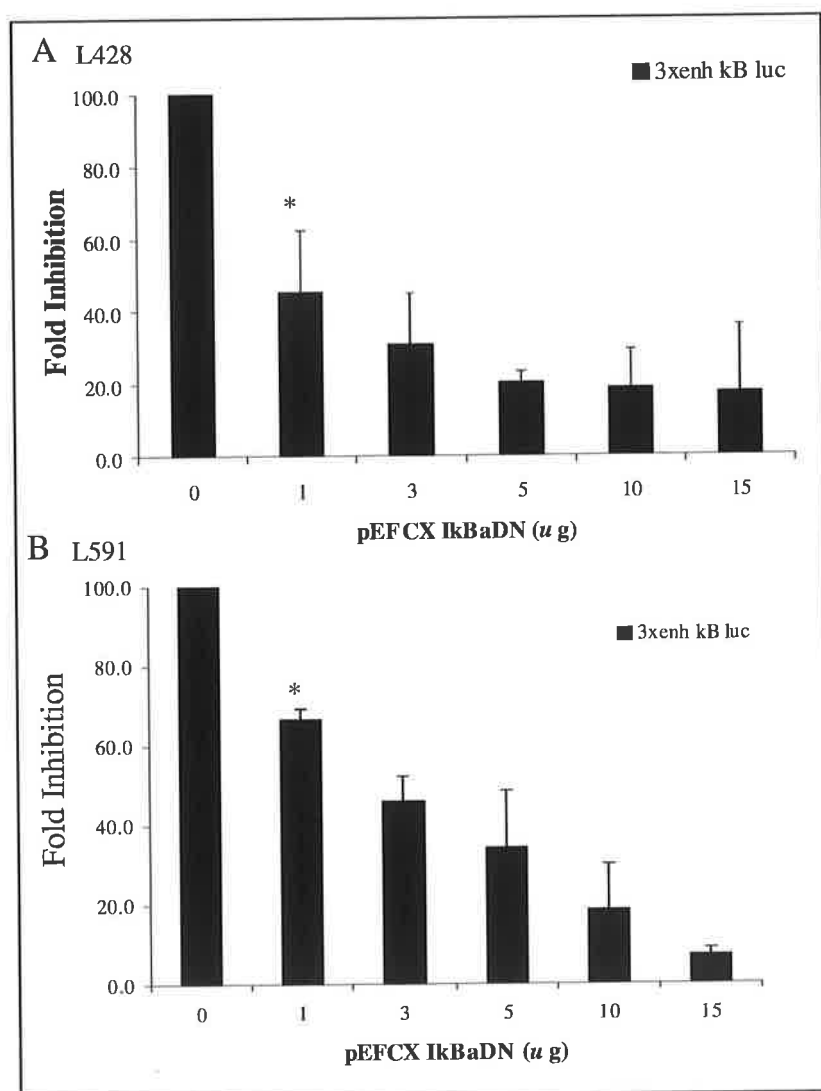


**Figure 6.1 I $\kappa$ B $\alpha$  super-repressor I $\kappa$ B $\alpha$ DN blocks NF- $\kappa$ B activation in HL**

NF- $\kappa$ B activation was determined by transfection using the 3x enh- $\kappa$ B luc reporter construct which has three  $\kappa$ B elements upstream of a minimal conalburnin promoter linked to luciferase. L428 (A) and L591 (B) cells were co-transfected by electroporation with 3x enh- $\kappa$ B luc, pCMV LacZ and increasing quantities of the I $\kappa$ B $\alpha$  super-repressor expression vector pEFCX-I $\kappa$ B $\alpha$ DN. Cells were harvested 48 h post-transfection and luciferase and  $\beta$ -galactosidase ( $\beta$ -gal) assays performed. Cells transfected without pEFCX-I $\kappa$ B $\alpha$ DN were assigned a value of 100 %. Data are  $\pm$ SD, \*P $\leq$ 0.032.

It was next tested if inhibition of NF- $\kappa$ B activation in L428 and L591 would affect the *trans*-activation of the *bfl-1* promoter. To this end, co-transfections were performed using various amounts of the mutant I $\kappa$ B $\alpha$ , along with the full length *bfl-1* promoter reporter construct -1374/+81-Luc (Table 2-5) (D'Souza *et al.*, 2004). Over-expression of the I $\kappa$ B $\alpha$  super-repressor resulted in a significant decrease (> 40 %) in luciferase activity, when up to 5  $\mu$ g of expression vector was used in L428 and L591 cell lines (Figure 6.2).

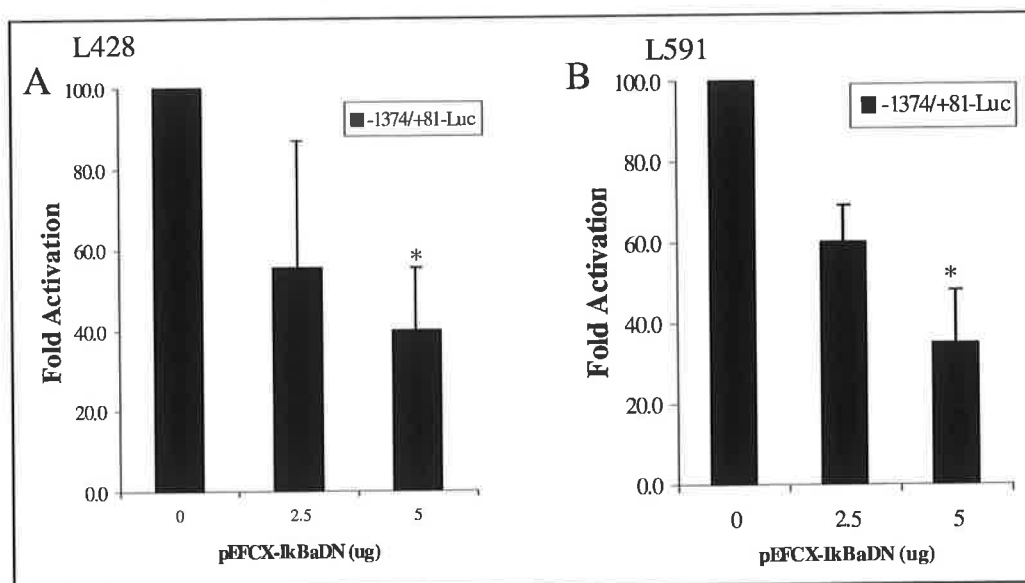


**Figure 6.2 I $\kappa$ B $\alpha$  DN inhibits the *bfl-1* promoter in HL.**

L428 (**A**) and L591 (**B**) cells were co-transfected by electroporation with wild type *bfl-1* promoter (-1374/+81 -luc) reporter construct, pCMV LacZ and increasing quantities of the I $\kappa$ B $\alpha$  super-repressor expression vector pEFCX-I $\kappa$ B $\alpha$ DN. Cells were harvested 48 h post-transfection and luciferase and  $\beta$ -gal assays were performed. Cells transfected without pEFCX-I $\kappa$ B $\alpha$ DN were assigned a value of 100 %. Data are  $\pm$ SD, \* $P \leq 0.011$ .

These results suggested that the activation of NF- $\kappa$ B plays a major role in *trans*-activation of the *bfl-1* promoter in L428 and L591 cells, based on evidence that *bfl-1* promoter activity is affected when NF- $\kappa$ B is inhibited by over-expression of an I $\kappa$ B $\alpha$  mutant in this cell context.

A previously identified NF- $\kappa$ B binding site at position -833 to -823 relative to the transcription initiation site of the *bfl-1* promoter was shown to be essential for activation

by the NF-κB sub-unit c-Rel in HeLa cells (Zong *et al.*, 1999). However, experiments performed in our laboratory demonstrated that elimination of this binding site by site directed mutagenesis did not affect the level of LMP1-mediated promoter activity in EBV-negative BL-derived cell lines (D’Souza *et al.* 2004). Subsequently it was found that a 210 bp *bfl-1* promoter fragment (-129/+81-Luc) containing a deletion from the 5' end of the full-length *bfl-1* promoter (-1374/+81-Luc) mediated NF-κB-dependent trans-activation by both LMP1 and phorbol-12-myristate 13-acetate (PMA). Using transcription element search software, an NF-κB binding site at position -52 to -43 was previously identified in our laboratory in the region 5' to the transcription initiation site. When base substitutions were introduced into the core of this binding motif, complete loss of trans-activation by LMP1 was observed, thus demonstrating a direct role for the NF-κB-like binding site at position -52 to -43 in LMP1-mediated activation of the *bfl-1* promoter (D’Souza *et al.* 2004).

In order to identify elements along the *bfl-1* promoter that confer NF-κB responsiveness in HL, co-transfection of *bfl-1* promoter reporter constructs (-1374/+81-Luc, -1374/+81mκB(-52)-Luc and -1374/+81mκB(-833)-Luc; Table 2-5) outlined in Figure 6.3A in L428 and L591 cell lines were performed.

This data demonstrates that NF-κB regulates the *bfl-1* promoter and evidence of a key role for a novel NF-κB-like binding site in the upstream regulatory region of this gene in this cell context is presented (Figure 6.3B; L428 and C; L591). Mutation of the NF-κB-like binding site at position -52 reduces *bfl-1* promoter transcriptional activation by ~85% in the L428 cell line and by ~65% in the L591 cell line. This data shows that the mutation at position -52 effectively blocks activation of the *bfl-1* promoter and suggests a crucial role for the transcription factor NF-κB in regulating *bfl-1* in L428. The mutation at position -52 blocks activation of the *bfl-1* promoter to a lesser extent in the EBV-positive HL cell line, while also suggesting a role for the transcription factor NF-κB in regulating *bfl-1* here, it is possible that the presence of EBNA2 is responsible for maintaining the level of *bfl-1* promoter activity by signaling independently through the CBF1/Notch pathway. *bfl-1* promoter activity is not significantly affected by mutation of the NF-κB binding site at position -833 to -823 in L428 and L591 cell lines with only a 20 % decrease in promoter activation associated with the -833 mutation (Figure 6.3).

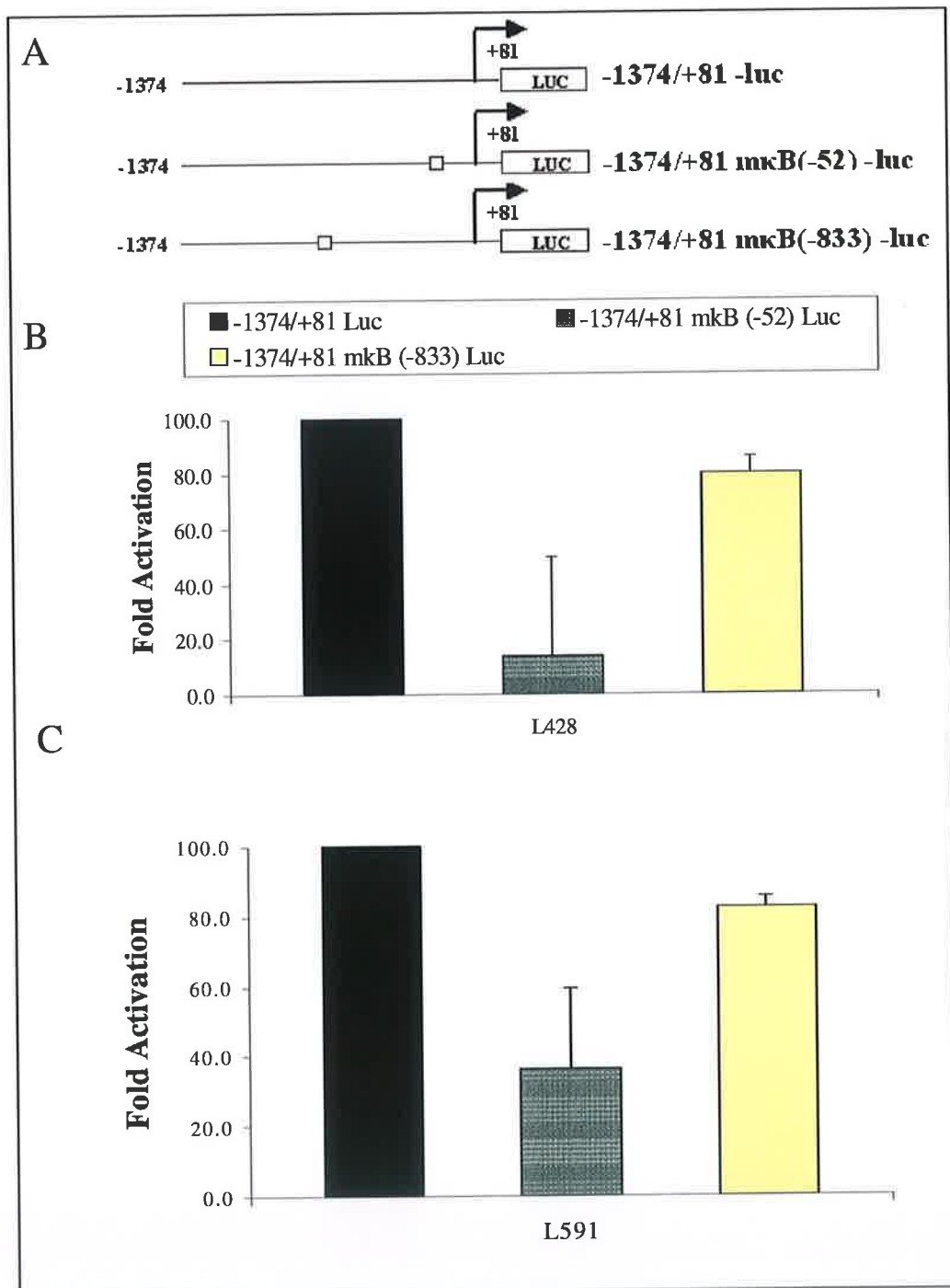


**Figure 6.3 *bfl-1* promoter activation in HL-derived cell lines**

(A) Schematic representation of the full-length wild type and κB-site-mutated *bfl-1* promoter-reporter constructs. These constructs share a common 3' terminus 81 bp downstream from the transcription initiation site (designated by a bent arrow), at which point they are joined to the luciferase gene (luc). The position of the NF-κB site at position -52 is indicated on the plasmid -1374/+81 mκB(-52) -luc as an open box.

Similarly, the position of a previously identified NF- $\kappa$ B site at position -833 is indicated on the plasmid -1374/+81 m $\kappa$ B(-833) -luc as an open box. L428 (B) and L591 (C) cells were co-transfected by electroporation with wild type (-1374/+81 -luc) or mutated promoter (-1374/+81 m $\kappa$ B(-52) -luc, -1374/+81 m $\kappa$ B(-833) -luc) reporter constructs and pCMV LacZ. Cells were harvested 48 h post-transfection and luciferase and  $\beta$ -gal assays were performed. Cells transfected with full-length promoter constructs were assigned a value of 100 %.

Once it was established that the dominant negative I $\kappa$ B $\alpha$  mutant effectively blocked activation of NF- $\kappa$ B in L428 and L591 cells and that the novel NF- $\kappa$ B binding site (-52) on the *bfl-1* promoter mediates *trans*-activation by NF- $\kappa$ B, co-transfections were performed to investigate if this mutant (I $\kappa$ B $\alpha$ DN) could further block *bfl-1* promoter activation in these cell lines. In order to determine if additional activation of the *bfl-1* promoter was occurring through NF- $\kappa$ B-like binding sites on the promoter, other than the -52 site, co-transfections were performed using the I $\kappa$ B $\alpha$  mutant and the '-52 mutated' *bfl-1* promoter construct.

Various amounts of the expression vector for the I $\kappa$ B $\alpha$  mutant were co-transfected into L428 and L591 cells (Figure 6.4A and B; respectively) along with the wild type *bfl-1* promoter reporter -1374/+81-Luc or -1374/+81 m $\kappa$ B(-52)-Luc mutated construct. In the absence of I $\kappa$ B $\alpha$ DN, transfection of the *bfl-1* promoter reporter construct (-1374/+81-Luc) in both cell lines resulted in a high level of luciferase activity and was assigned a value of 100 %. This data showed that the mutant form of I $\kappa$ B $\alpha$  effectively blocks activation of the full-length *bfl-1* promoter in L428 and L591 and that no significant further blocking of NF- $\kappa$ B activation of the '-52-mutated' *bfl-1* promoter occurs in either cell line. This data corroborates the findings illustrated in Figure 6.3, that NF- $\kappa$ B-like binding site at position -52 on the *bfl-1* promoter mediates *trans*-activation by NF- $\kappa$ B.

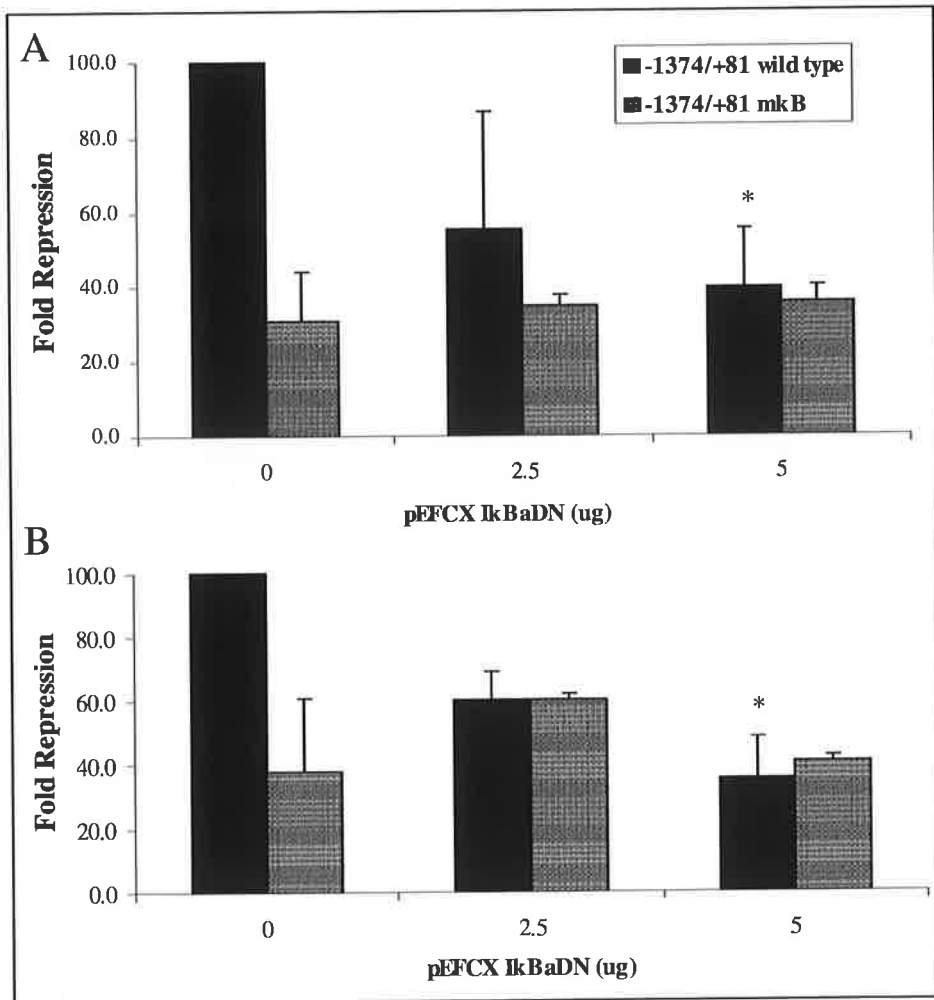


**Figure 6.4 I $\kappa$ B $\alpha$  DN blocks NF- $\kappa$ B activation of the *bfl-1* promoter in HL.**

L428 (A) and L591 (B) cells were co-transfected by electroporation with wild type (-1374/+81 -luc) or mutated promoter (-1374/+81 mkB(-52) -luc) reporter constructs, pCMV LacZ and increasing quantities of the I $\kappa$ B $\alpha$  super-repressor expression vector pEFCX-I $\kappa$ B $\alpha$ DN. Cells were harvested 48 h post-transfection and luciferase and  $\beta$ -gal assays were performed. Cells transfected with full-length promoter constructs were assigned a value of 100 %. Data are  $\pm$ SD, \*P<0.011.

As previously discussed, NF- $\kappa$ B is constitutively expressed in HL and has been shown to be involved in the pathogenesis of HL. A key role for the transcription factor NF- $\kappa$ B in the regulation of the anti-apoptotic cellular gene *bfl-1* was established when it was shown that treatment of a variety of cell lines with the chemical agent PMA, a well-known activator of NF- $\kappa$ B, up-regulated *bfl-1* mRNA levels in BL cell lines (Moreb and Schweder, 1997). A study carried out in our laboratory demonstrated that EBV LMP1

trans-activated the *bfl-1* promoter in EBV-negative BL-derived cell lines by a mechanism that is dependent upon NF-κB (D'Souza *et al.*, 2004).

In summary, the data presented here is evidence that the *bfl-1* promoter is regulated by NF-κB in H/RS-derived cell lines of EBV negative (L428) and positive (L591) status, that inhibition of NF-κB in L428 and L591 cell lines by inhibitory-gene transfer blocks NF-κB activation of the *bfl-1* promoter and implies that the element located at -52/-43 in the transcriptional regulatory region of *bfl-1* is the key site through which NF-κB drives *bfl-1* in HL cells.

## **6.2.2 Notch signaling**

The Notch family of transmembrane receptors (Notch1-4) control cell proliferation and differentiation in response to extracellular ligands expressed on neighbouring cells. Although the role of Notch receptors and downstream effectors in HL is currently being characterised the potential influence on regulation of the anti-apoptotic *bfl-1* gene remained to be defined. This study tested the hypothesis that the *bfl-1* gene was regulated by Notch signals in HL.

Potentially oncogenic targets of Notch-1 include PI3K/AKT (Rangarajan *et al.*, 2001; Sade *et al.*, 2004), NF- $\kappa$ B (Bash *et al.*, 1999; Jang *et al.*, 2004; Cheng *et al.*, 2001), NF- $\kappa$ B2 (Oswald *et al.*, 1998) and STAT-3 (Kamakura *et al.*, 2004). Given the constitutive activation of these signal transduction pathways in HL, it is possible that Notch1 functions upstream of some of these pathways in this malignant context and it proved interesting to determine whether Notch1IC could trans-activated the *bfl-1* promoter in this cell context.

### **6.2.2.1 Expression of Notch1/2 receptors and the Notch ligand Jagged1 in cultured H/RS cells**

It was previously shown in our laboratory by Dr. Brendan D'Souza that Notch1 and 2 receptors are abundantly expressed in H/RS cell lines by western blotting (Section 2.7.4) (Figure 6.5A) using monoclonal antibodies specific for the intracellular domains of human Notch1/2. For relative quantification of protein levels, EBV-/+ cell lines with type I latency (DG75 and BL41)/ (BL74, MUTU I and OKU BL), EBV+ cell lines with type III latency (BL41/B95-8, MUTU III, AG876 and DAUDI) and lymphoblastoid cell lines (IARC 171 and X50-7) were included in the analysis (Figure 6.5B). High-level Notch1 expression was detected in all HL cell lines (with the exception of L1236) and was more pronounced than in all type I EBV+/- and type III cell lines and LCLs tested. High-level Notch2 was detected in all HL cell lines tested in contrast with absence of Notch2 expression in all type I EBV+/- and type III cell lines and LCLs tested. These findings complement previous studies that have documented the expression of Notch1 (Jundt *et al.*, 2002) and Notch 2 (Kapp *et al.*, 1999) in H/RS cell lines.

Jundt *et al.*, (2002), found abundant Jagged1 protein and mRNA expression in H/RS cells of primary tumour tissue, in endothelial and smooth muscle cells and in epithelioid cells neighbouring H/RS cells suggesting that Jagged1-induced Notch1 signaling might contribute to the pathobiology of cHL. Jagged1 is a 135 kDa transmembrane DSL-family protein, which is highly expressed in B cells raising the possibility of a role for Jagged1 mediated signaling through Notch in the pathways that control the later stages of B-lymphocyte activation and differentiation. NF- $\kappa$ B can trigger the Notch signaling pathway by inducing the expression of Jagged1, an NF- $\kappa$ B responsive gene (Bash *et al.*, 1999).

H/RS cell lines were examined in this study for the expression of the Notch ligand, Jagged1, using a monoclonal antibody specific for the intracellular domain of human Jagged1 (Figure 6.5C) but showed low to undetectable levels of Jagged1. The EBV-positive H/RS cell line, L591, was found to express low-level Jagged1 ligand relative to controls while Jagged1 expression was not detected in other H/RS cell lines tested or in all type I EBV+/- and type III cell lines and LCLs tested (Figure 6.5D). The absence of detectable levels of Jagged1 expression in H/RS cell lines was in contrast to the detection of abundant Jagged1 expression in H/RS cells of primary tumour tissue indicating that Notch activation induced by Jagged1 ligation may be absent in the *in vitro* cell culture system. In order to study the effect of Jagged1-induced Notch activation in this cell context, the Jagged1 ligand was presented to H/RS cell lines using Jagged1-presenting feeder cells to mimic the *in vivo* scenario. The HtTA-jag10 cell line is a HeLa-derived adherent cell line (Bash *et al.*, 1999; Table 2-1), which expresses human Jagged1 under tetracycline control and was used in co-cultivation experiments to activate Notch signaling in H/RS cell lines by Jundt *et al.*, (2002), leading to the promotion of cell proliferation in the L428 cell line.

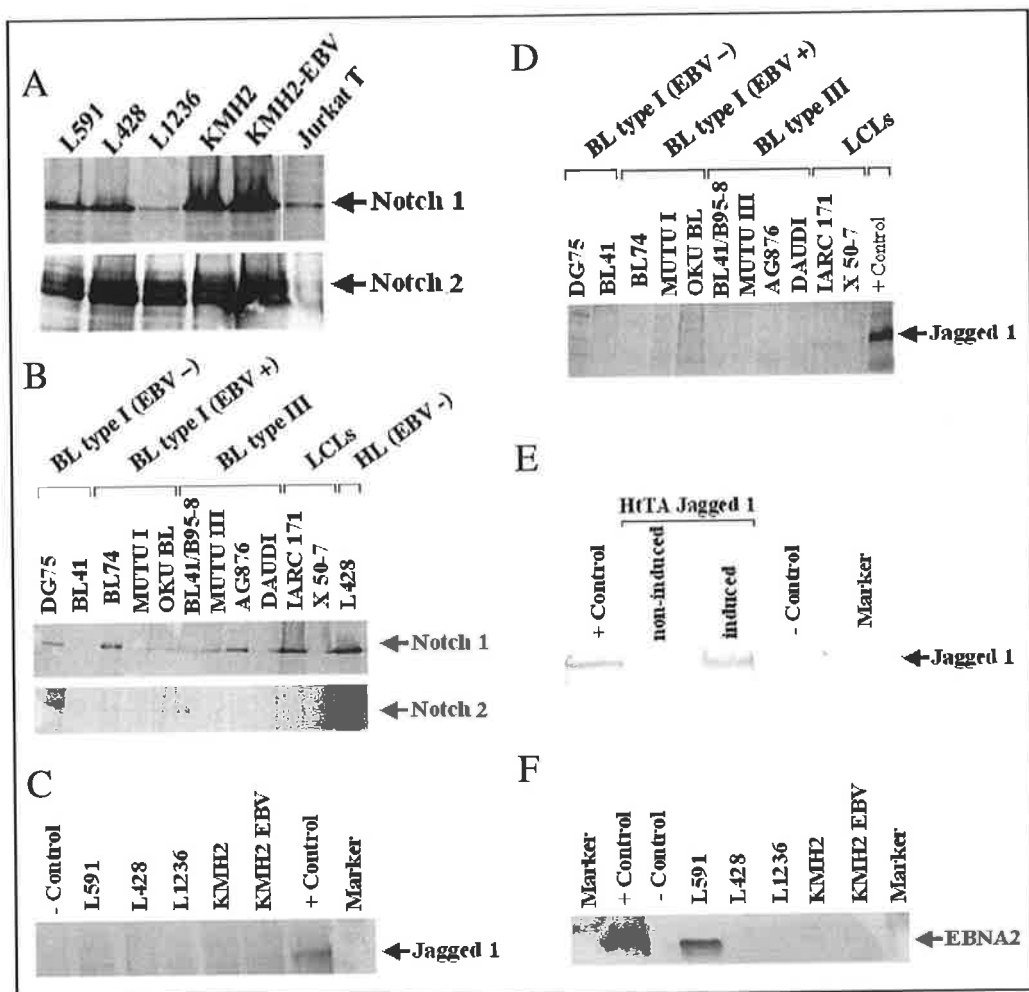


**Figure 6.5 Expression of Notch1/2 receptors, Jagged1 and EBNA2 expression in lymphoma cell lines**

Notch1 (A; upper panel) and Notch2 (A; lower panel) receptors are strongly expressed in B-cell derived HL cells relative to type I, type II, type III cell lines and LCLs (B; upper and lower panels). High level Notch1 and Notch2 expression is seen by western blotting in all HL cell lines with the exception of low level expression of Notch1 in the cell line L1236. (C) Western blot analysis for Notch ligand Jagged1 reveals low-level Jagged1 (135 kDa) expression in L591 (EBV positive) cell line relative to type I, type II, type III and LCLs (D). (E) The effect of Jagged1 presentation to cells of HL and BL origin was carried out by co-culture with a tetracycline inducible Jagged1-expressing HeLa-derived cell line HtTA-jag10. Western blot analysis of Jagged1 was performed on protein from HtTA-jag10 cells induced or non-induced to express Jagged1 to confirm presence of Jagged1 upon induction with tetracycline. (F) Expression of EBNA2 in cultured H/RS cells; western blot analysis of HL cell lines for EBV latent protein EBNA2 (functional homologue of activated Notch1/2 receptors) reveals EBNA2 (83 kDa) expression only in the EBV positive L591 cell line.

It was first examined whether in cultured H/RS cells, Notch signaling could be activated by stimulation with exogenous Jagged1 by co-cultivation with HtTA-jag10 cells to induce the accelerated growth response observed by Jundt *et al.*, (2002) for the L428 cell line. L428 and L591 cells were thus cultured in the presence of Jagged1-expressing feeder cells and number of viable cells was measured at 24 h post-cultivation by MTS assay (Section 2.4.8). HtTA-jag10 cells expressed Jagged1 upon withdrawal of tetracycline from media. Stimulation by Jagged1 increased proliferation of L428 and L591 cells by 2.5- and ~3-fold respectively (Figure 6.6) at 24 h post co-cultivation relative to unstimulated controls. In contrast no additional proliferative response was observed in the DG75 BL type I cell line also co-cultivated with HtTA-jag10 cells. These findings complement the observations of Jundt *et al.*, (2002), that Jagged1 activation of Notch signaling in H/RS cells accelerated growth of L428 cells by 1.6 - 1.9-fold, using thymidine incorporation to measure proliferative response.

Jundt *et al.*, (2002), addressed the possibility that increased growth observed upon Jagged1 presentation was not due to increased Notch activation in feeder cells by presenting Jagged1 in the form of a soluble ligand to the culture medium. Similarly, soluble Jagged1 ligand presentation behaved as a potent growth factor for H/RS cells.

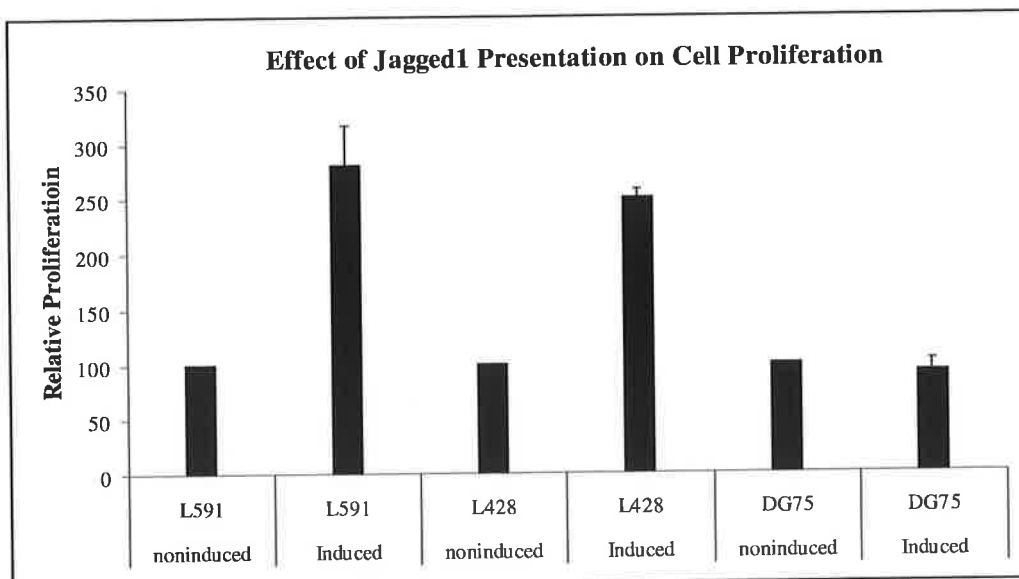


**Figure 6.6 Presentation of the Notch ligand Jagged1 leads to increased proliferation of HL cells**

The impact of Jagged1 activation of Notch signaling on the proliferation of cells of HL (L428 and L591) and BL (DG75) origin. The rate of proliferation of cells co-cultured in the presence/absence of Jagged1 was measured by MTS assay at 24 h post co-culture. Proliferation of activated cells (induced) is given relative to proliferation of non-activated cells (non-induced), which is arbitrarily set at 100 % for each cell line. Stimulation by Jagged1 increased the proliferation of HL cells up to 2.7 (L591) and 2.5 (L428) -fold in 24 h compared with unstimulated controls, unlike the BL-derived cell line DG75.

It was next tested if presentation of the Notch ligand Jagged1 effected target gene expression through RBP-J $\kappa$ /CBF1 in cultured H/RS cells. To demonstrate NotchIC-mediated promoter activation via RBP-J $\kappa$ /CBF1, transient transfections using L428, L591 and DG75 cells with the luciferase reporter construct pGa981-6 (Table 2-5) were performed. This construct contains a 50 bp oligonucleotide harbouring both RBP-J $\kappa$ /CBF1 binding sites of the EBV *TPI* promoter sub-cloned as a hexamer into the plasmid pGa50-7 (Minoguchi *et al.*, 1997; Table 2-5). Using this RBP-J $\kappa$ /CBF1 promoter-reporter assay system, it was defined that signal transduction following Jagged1-Notch activation induced RBP-J $\kappa$ /CBF1 activity (Figure 6.7A) could be inhibited by dominant-negative RBP-J $\kappa$  (Figure 6.7B and C). Co-transfections by electroporation using DG75 (Figure 6.7 upper panel), L428 (Figure 6.7 middle panel) and L591 (Figure 6.7 lower panel) cells were carried out using the RBP-J $\kappa$ /CBF1-

regulated luciferase reporter construct pGa981-6 or pGa50-7 and CMV LacZ, followed by co-cultivation with HtTA-jag10 cells induced or non-induced to express Jagged1. Lymphoma cells aggregated onto the HtTA-jag10 monolayer were harvested by firm tapping at 48 h post-transfection followed by luciferase and  $\beta$ -gal assays. In BL-derived cell line, DG75, a 1.2-fold increase in CBF-1 binding activity upon Jagged1 activation of Notch1 was observed when compared to control samples. In L428, a 3-fold increase in CBF-1 binding activity was observed when cells co-cultured with Jagged1 presenting cells were compared to controls. A 3-fold increase in CBF-1 binding activity with Jagged1 presentation was also observed in the EBV positive cell line L591 when compared to control samples (Figure 6.7). A high level of CBF-1 binding activity was observed in the transfections of L591 cells not co-cultured with Jagged1 presenting cells, possibly due to the presence of the EBNA2 in this cell line as detected by western blot, shown in Figure 6.5F. EBNA2 is considered to be the viral functional homologue of Notch1.

The role of RBP-J $\kappa$ /CBF1 in mediating EBNA2/NotchIC-mediated responsiveness was further investigated using an expression vector for a non-DNA binding mutant of RBP-J $\kappa$ /CBF1 (pEFBOSneo-R218H, Chung *et al.*, 1994; Table 2-5). This protein has been shown to act as a dominant-negative suppressor of activation of the cellular *HES-1* promoter by NotchIC, and is likely to exert such an effect by competing with NotchIC, (or EBNA2) or unknown co-factors, for binding to CBF1 (Kato *et al.*, 1996; Kato *et al.*, 1997). To investigate if pEFBOSneo-R218H could inhibit trans-activation of the luciferase reporter construct pGa981-6, co-transfections were performed in L428 and L591 cells with increasing amounts of pEFBOSneo-R218H. It can be seen from this experiment that expression of the mutant RBP-J $\kappa$ /CBF1 inhibited trans-activation of pGa981-6 in L428 by approximately 50 % when 10  $\mu$ g of pEFBOSneo-R218H was used (Figure 6.7B). This non-DNA binding mutant of CBF1 inhibits CBF1-driven promoter activity in the EBV-positive L591 to a greater extent (Figure 6.7C) in a dose-dependent manner, with maximum inhibition of approximately 80 % when 10  $\mu$ g of pEFBOSneo-R218H was used.

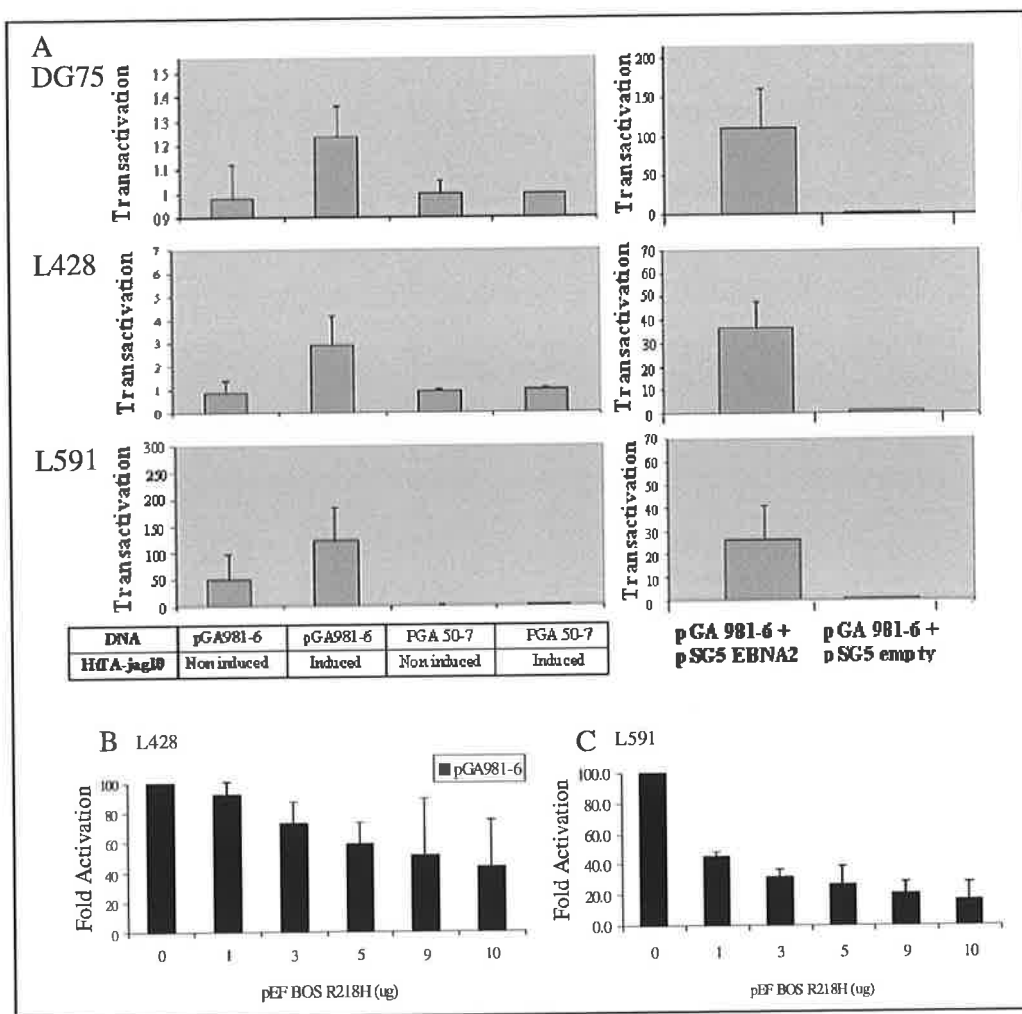


**Figure 6.7 Notch activation of CBF-1 expression in DG75, L428 and L591 cells**

(A) DG75 (upper left), L428 (middle left) and L591 (lower left) cells were co-transfected with pCMVlacZ and pGA981-6 or pGA50.7 (empty plasmid) and subsequently co-cultured with HtTA-jag10 cells induced or non-induced to express Jagged1. pGA981-6 contains a 50 bp oligonucleotide harbouring both RBP-J $\kappa$ /CBF1 binding sites of the EBV *TPI* promoter sub-cloned as a hexamer into the plasmid pGA50.7. To verify that the pGA981-6 construct is EBNA2-responsive and act as a transfection control; DG75, L428 and L591 cells were co-transfected with pCMVlacZ, pGA981-6 and pSG5EBNA2 or pSG5 (empty vector) (upper, middle and lower right panels respectively). Cells were harvested 48 h post-transfection/co-culture and luciferase and  $\beta$ -gal assays were performed. Normalised luciferase values were expressed as fold activation relative to the corresponding value obtained upon co-transfection with empty vector (arbitrarily assigned a value of 1). A dominant negative suppressor of CBF1 binding, R218H, was used to block CBF1 promoter activity in L428 (B) and L591 (C) cells. Cells were co-transfected with pCMVlacZ, pGA981-6 and pEF-BOS R218H or pEF-BOS (empty vector). Cells were harvested 48 h post-transfection and luciferase and  $\beta$ -gal assays were performed. Normalised luciferase values were expressed as % activation relative to the corresponding value obtained upon co-transfection without pEF-BOS R218H (arbitrarily assigned a value of 100 %).

Taken together, the data presented here indicates that the critical elements of the Notch receptor signal transduction pathway are present within the H/RS cell and suggest that L428 and L591 are Jagged1-responsive cells lines.

A similar experimental strategy was used to determine the effect of Jagged1-induced Notch activation on *bfl-1* promoter *trans*-activation in this cell context. L428 and L591 cells were co-transfected with the full-length *bfl-1* promoter construct (-1374/+81 -luc; Table 2-5) and CMV-LacZ. Transfected cells were co-cultured with Jagged1 induced/non-induced HtTA-jag10 cells and lymphoma cells were harvested at 48 h. Promoter activation was quantified by measurement of luciferase activity normalised for  $\beta$ -galactosidase levels. Activation of Notch signaling by Jagged1 had no effect on the *bfl-1* promoter in the L428 cell line (Figure 6.8A) with promoter activation remaining unchanged in cells co-cultured with HtTA-jag10 cells induced to express Jagged1, compared to non-induced control. In the EBV-positive L591 cell line, promoter activation in cells co-cultured with non-induced HtTA-jag10 cells, was assigned a value of 100 %. Strikingly, in this cell line, activation of Notch signaling by Jagged1 ligation resulted in a decrease in *bfl-1* promoter activation to 50 % when compared to the non-induced control.

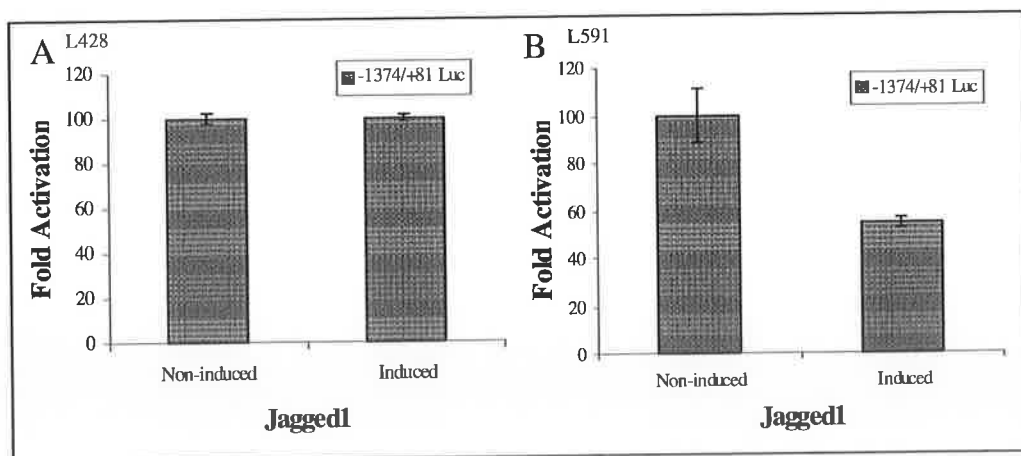


**Figure 6.8 Jagged1 presentation effect on *bfl-1* promoter activation in H/RS cells**

L428 and L591 cells were co-transfected with wild type and mutated *bfl-1* promoter reporter constructs and pCMVlacZ. Transfected cells were subsequently co-cultured with HtTA cells induced/non-induced to express Jagged1. Luciferase and  $\beta$ -gal assays

were performed 48 h post-transfection/co-culture. Cells transfected with full-length promoter constructs were assigned a value of 100 %.

Ideally, examination of the levels of *bfl-1* mRNA (by realtime PCR) in H/RS-derived cell lines presented with Jagged1 would have been desired to determine the effect of Jagged1 induced-Notch1 activation on *bfl-1* expression levels. However, due to the heterogeneous nature of the co-cultivation assay it was not possible to isolate lymphocytes from feeder cells for RNA extraction. An alternative strategy would have been to present Jagged1 to these cells in the form of a soluble ligand, thereby effecting Notch1 activation yet removing possible RNA contamination from co-cultivated cells. Unfortunately, the only commercially available soluble ligand was Rat Jagged1 and 'in-house' production of Human Jagged1 was beyond the remit of this project.

It is known that NotchIC does not bind to DNA directly, but is tethered to responsive promoters by the DNA binding repressor protein RBP-J $\kappa$ /CBF1 (reviewed in Chapter 1). It has previously been shown in our laboratory using *bfl-1* promoter deletion reporter constructs, that the sequence from position -367 to -129 is essential in mediating EBNA2-responsiveness on the *bfl-1* promoter (Pegman *et al.*, 2006). Analysis of this region of the promoter using transcription element search software and the Alibaba transcription factor prediction database revealed one copy of the sequence motif 5'-GGTGGGAA-3' at position -243 to -250 on the inverse strand. This element is part of the consensus binding sequence for CBF1 (CGTGGGAA), and site-directed mutagenesis was used to introduce base substitutions into the core of this motif in the reporter plasmid -1374/+81-luc so as to eliminate potential binding by CBF1 (Figure 6.9A). The contribution of this site in facilitating EBNA2-mediated trans-activation of the *bfl-1* promoter was then investigated. Mutation of this binding site resulted in a dramatic reduction in EBNA2-mediated activation of the *bfl-1* promoter (Pegman *et al.*, 2006).

In order to investigate if *bfl-1* promoter activity in H/RS-derived cell lines could be inhibited by blocking NotchIC-mediated activation, experiments were performed using a *bfl-1* promoter construct containing a mutation in the putative RBP-J $\kappa$ /CBF1 binding site at position -343 to -249 relative to the transcription start site (-1374/+81 (mCBF1), Pegman *et al.*, 2006).

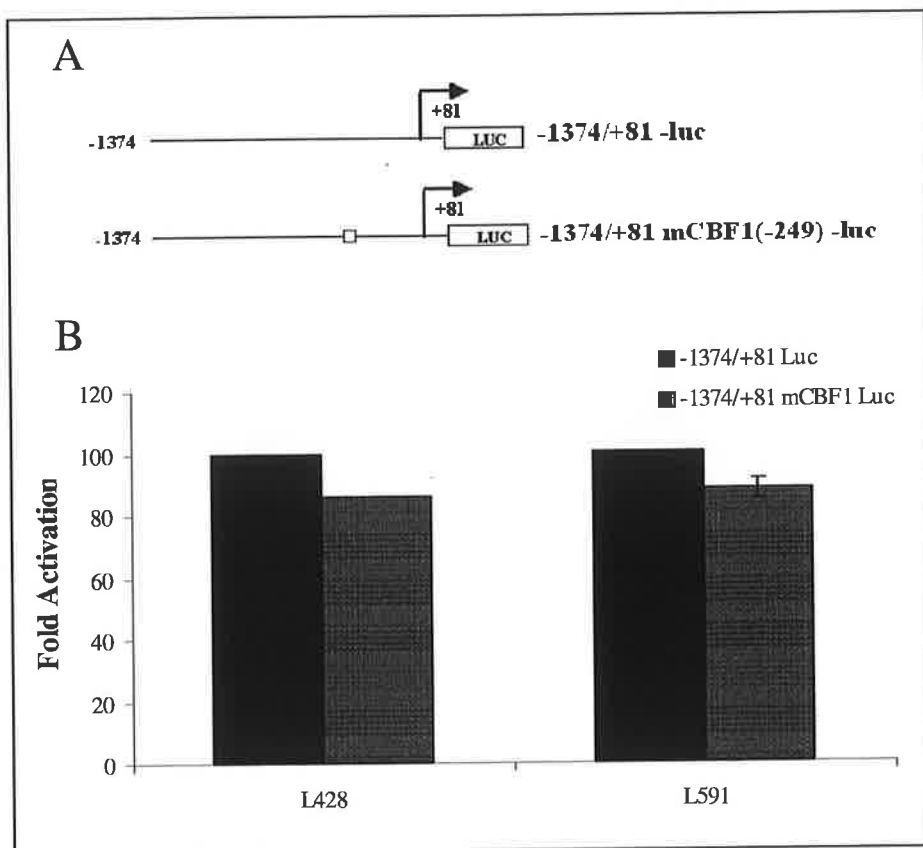


**Figure 6.9 *bfl-1* promoter activation in HL-derived cell lines.**

(A) Schematic representation of the full-length wild type and CBF1-mutated *bfl-1* promoter-reporter constructs. These constructs share a common 3' terminus 81 bp downstream from the transcription initiation site (designated by a bent arrow), at which point they are joined to the luciferase gene (luc). The position of a previously identified binding site for the Notch nuclear protein CBF1 at position -249 is indicated on the plasmid -1374/+81 mCBF1(-249) -luc as an open box. (B) L428 (left) and L591 (right) cells were co-transfected by electroporation with wild type (-1374/+81 -luc) or mutated promoter (-1374/+81 mCBF1(-249) -luc) reporter constructs and pCMV LacZ. Cells were harvested 48 h post-transfection and luciferase and  $\beta$ -gal assays were performed. Cells transfected with full-length promoter constructs were assigned a value of 100 %.

The results seen in Figure 6.9B, suggest that the CBF1 binding site at position -249 is not an important site for *bfl-1* promoter activation in L428 or L591 cells as only a marginal decrease in promoter activity of -1374/+81 mCBF1(-249) -luc was observed relative to the full-length wild-type promoter (-1374/+81 -luc).

In summary, the data presented here demonstrates that the *bfl-1* gene is not a downstream target for transcriptional activation by Notch signaling in this cell context.

### 6.3 Discussion

A key role for the transcription factor NF-κB in the regulation of the anti-apoptotic cellular gene *bfl-1* was established when it was shown that treatment of a variety of cell lines with the chemical agent PMA, a well-known activator of NF-κB, up-regulated *bfl-1* mRNA levels in BL cell lines (Moreb and Schweber, 1997).

Previously in our laboratory, an important role for NF-κB was implied in the LMP1-mediated regulation of the *bfl-1* promoter. Firstly, co-expression of a super-repressor IκBαDN mutant inhibited LMP1-mediated trans-activation of the *bfl-1* promoter. Secondly, treatment with PMA, a well-known activator of NF-κB in many cell types, stimulated *bfl-1* promoter activity (D’Souza *et al.*, 2004). The implication of a role for NF-κB is in keeping with other studies, where increases in *bfl-1* mRNA levels have been demonstrated in response to agents such as LPS, TNFα or etoposide, all of which are known to lead to activation of NF-κB (Hu *et al.*, 1998; Wang *et al.*, 1999; Zong *et al.*, 1999). In addition, mitogen stimulation of primary B cells was shown to induce expression of mouse A1 (the murine *bfl-1* homologue) in a c-Rel-dependent fashion (Grumont *et al.*, 1999). Elsewhere, ectopic expression of the NF-κB subunits c-Rel and p65 (but not p50) was also shown to independently up-regulate *bfl-1* mRNA levels in the epithelial cell line HeLa (Zong *et al.*, 1999). In the same study, it was shown that c-Rel trans-activated the *bfl-1* promoter through its interaction with a consensus NF-κB binding site at position -833 to -823 relative to the transcription start site of the *bfl-1* gene. However, experiments performed in our laboratory demonstrated that removal of this binding site did not affect the level of LMP1-mediated *bfl-1* promoter activity in EBV-negative BL-derived cell lines (D’Souza *et al.*, 2004). Subsequently it was found that a 210 bp *bfl-1* promoter fragment (-129 to +81) mediated NF-κB-dependent trans-activation by both LMP1 and PMA in this cell context. Furthermore, it was demonstrated that an NF-κB-like binding site at position -52 to -43 relative to the transcription start site of the *bfl-1* gene, is essential for LMP1-mediated trans-activation of the *bfl-1* promoter (D’Souza *et al.*, 2004).

In Chapter 4, it was shown that inhibition of transcription factor NF-κB in H/RS-derived cell lines led to death by apoptosis, which was associated with a loss of *bfl-1* mRNA expression. It was therefore investigated here whether dysregulated NF-κB in HL might drive *bfl-1* promoter activity through one of the functional NF-κB-binding sites (described by Zong *et al.*, 1999; D’Souza *et al.*, 2004) in its upstream transcriptional regulatory region. Initially, it was shown that co-expression of a super-

repressor I $\kappa$ B $\alpha$ DN mutant inhibited NF- $\kappa$ B activity in H/RS cell lines, L428 and L591. This dominant negative super-repressor was next shown to block NF- $\kappa$ B-mediated trans-activation of the *bfl-1* promoter by ~60 % in these cell lines. The previously identified NF- $\kappa$ B binding site at position -833 to -823 relative to the transcription start site of the *bfl-1* gene was shown not to be an important promoter element in this cell context. This site was shown previously in our laboratory to be non-essential for *bfl-1* promoter trans-activation in EBV negative BL-derived cell lines. However, in keeping with previous findings in our laboratory regarding the NF- $\kappa$ B binding site at position -52 to -43 (relative to the transcription start site of the *bfl-1* gene), it was demonstrated that the NF- $\kappa$ B binding site at this position is the key site through which NF- $\kappa$ B drives *bfl-1* in HL.

The subunit composition of NF- $\kappa$ B can greatly influence not only its ability to bind a particular DNA sequence motif, but also the extent of promoter activation (Perkins *et al.* 1992). The ability of Rel family members to drive transcription from the *bfl-1* promoter was directly investigated in a previous study in our laboratory by transient co-transfections of DG75 cells with vectors that express individual NF- $\kappa$ B subunit proteins and *bfl-1* promoter reporter constructs. It was demonstrated that homo-dimers of p65 directly trans-activated the *bfl-1* promoter and that the NF- $\kappa$ B-like binding site at -52 to -43 was essential both for this effect, and for conferring p65-responsiveness on a heterologous minimal promoter. Classic NF- $\kappa$ B (p65/p50) binds the sequence 5'-GGGRNNYYCC-3', whereas the p65/c-Rel dimer binds to the sequence 5'-HGGARNYYCC-3' [H indicates A, C or T; R is purine (A or G); and Y is pyrimidine (T or C)] (Baldwin, 1996). The NF- $\kappa$ B site at position -52 to -43 on the *bfl-1* promoter differs from the p65/p50 and p65/c-Rel consensus binding sites at nucleotide positions 3 and 2 respectively. NF- $\kappa$ B-like sites that diverge from the consensus sequence have been identified in the promoters of several apoptosis-related genes, such as *bcl-xL*, *c-IAP1*, *c-IAP2* and mouse *A1*, as well as cytokine genes such as *IL-8*, and the functionality of these sites in the promoter activation has been demonstrated in several of these cases (Chen *et al.*, 1999a and b; Grumont *et al.*, 1999; Hong *et al.*, 2000; Okamoto *et al.*, 1994). Significantly, the -52 to -43 site on the *bfl-1* promoter is 100 % complimentary to a CD28-responsive  $\kappa$ B site in the IL-2 promoter (Civil *et al.*, 1996; Civil *et al.*, 1999; Verweij *et al.*, 1991) and both c-Rel and p65 have been shown to play roles in mediating this process (Ghosh *et al.*, 1993).

Notch1 activity emerged as a contributory factor in HL when Jundt *et al.*, (2002), reported that Notch1 was aberrantly expressed in primary H/RS cells and H/RS cell lines and that experimental activation of Notch1 showed that its signaling could contribute to proliferation and apoptosis resistance of H/RS cells.

Like EBNA2, NotchIC does not bind DNA directly, but is recruited to its sites of action through interactions with cellular proteins including RBP-Jκ/CBF1 (Henkel *et al.*, 1994; Ling *et al.*, 1994; Waltzer *et al.*, 1994; Grossman *et al.*, 1994; Zimber-Strobl *et al.*, 1994). Although no cellular homologue of the EBNA2 protein has been identified, the intracellular domain of the Notch receptor is considered to be a cellular equivalent from a mechanistic and functional point of view (Hsieh *et al.*, 1996). There is no obvious sequence homology between EBNA2 and NotchIC, however both EBNA2 and NotchIC interact with similar regions of RBP-Jκ/CBF1 and displace repressor proteins by their trans-activation domains (Zimber-Strobl and Strobl, 2001). The set of promoters, which is regulated by EBNA2 and NotchIC is overlapping but not identical.

In this Chapter, the expression of Notch1 and 2 receptors and the Notch ligand Jagged1 was investigated in HL. Notch 1 and 2 receptors were found to be abundantly expressed in cultured H/RS cells irrespective of EBV status and Notch ligand, Jagged1, was expressed in the EBV-positive cell line, L591. Presentation of Notch1 ligand Jagged1 by co-cultivation with feeder cells led to increased proliferation of cultured H/RS cells. Jagged1 presentation effected Notch1 target gene expression via RBP-Jκ/CBF1 in L428, L591 and DG75 cells and this Notch1 activation of CBF-1 expression could be inhibited by a dominant negative RBP-Jκ.

It has already been observed in our laboratory that EBNA2 trans-activates the *bfl-1* promoter in an RBP-Jκ/CBF1 dependent manner with an essential role for a core consensus CBF1 binding site on the *bfl-1* promoter (Pegman *et al.*, 2006). An essential role for this novel consensus CBF1 binding site was demonstrated in our laboratory when it was found that the sequence between -367 and -129 of the *bfl-1* promoter contained DNA sequence element(s) that mediated a high proportion of the observed EBNA2/CBF1-dependent *trans*-activation. A search of the available *bfl-1* upstream transcriptional regulatory region led to the identification of one copy of the sequence motif 5'-GGTGGGAA-3' at position -243 to -250 on the inverse strand. This element is part of the consensus binding sequence for CBF1 (CGTGGGAA) and site-directed mutagenesis was used to introduce base substitutions into the core of this motif in the reporter plasmid -1374/+81-luc so as to eliminate potential binding by CBF1 (Ling *et*

*al.*, 1994; Tun *et al.*, 1994). This mutation led to the near complete loss of *trans*-activation by EBNA2. It was shown that *trans*-activation was dependent both on the presence of CBF1 and the ability of EBNA2 to interact with this cellular protein. It was investigated whether EBNA2 could activate *bfl-1* in DG75 cells in which the CBF1 gene had been inactivated by somatic knockout (Maier *et al.*, 2005). *Bfl-1* mRNA levels were examined by reverse transcription real-time PCR in DG75 clones that had been stably transfected with ER-EBNA2 and in which the CBF1 gene had (SM296 D3) or had not (SM295 D6) been inactivated. Addition of estrogen to SM296 cells led to a significant transient increase in the level of *bfl-1* mRNA (peaking at 8.7 fold after 6 h), an effect that was not seen upon knockout of the CBF1 gene, demonstrating that CBF1 was required for transcriptional activation of *bfl-1* by EBNA2.

This study set out to investigate if the *bfl-1* gene is a target of NotchIC. In a related study in our laboratory, it was shown that like EBNA2, Notch1IC trans-activated the RBP-Jκ/CBF1-regulated control promoter pGa981-6 with an essential role for RBP-Jκ/CBF1. However, unlike EBNA2, mNotch1IC did not trans-activate the *bfl-1* promoter reporter construct -1374/+81-Luc in DG75 cells and the failure of Notch1IC to trans-activate the *bfl-1* promoter was not due to a weak trans-activation domain. The effect of Jagged1 induced Notch1 activation on *bfl-1* promoter activity was examined in H/RS cell lines in this study. In the EBV negative L428 cell line, promoter activation remained unchanged when feeder cells were induced or non-induced to express Jagged1 ligand. In the EBV positive L591 cell line, activation of Notch1 signaling by Jagged1 ligation resulted in a decrease in *bfl-1* promoter activation to 50 % when compared to the non-induced control. The obvious difference in promoter activation seen in L428 and L591 cell lines may be due to the fact that the L591 cell line has been shown to express EBNA2 (Figure 6.5F), which is in contrast to the EBV-positive H/RS cells of primary HL tumour where EBNA2 is not expressed. It was therefore decided not to further investigate the exact mechanisms by which the *bfl-1* promoter was activated in L591 as this cell line may not be a good model of the H/RS cell due to its deviance from EBV positive primary tumour tissue. The requirement of the putative CBF1 site (at position -243 to -249) on the *bfl-1* promoter was not essential for conferring responsiveness on the *bfl-1* promoter in this cell context. Together, these data indicate that the *bfl-1* gene is not a downstream target for transcriptional activation by Notch signaling in this cell milieu.

# **CHAPTER 7 Expression and Purification of recombinant Bfl-1 using a novel modified vector and generation of anti-Bfl-1 serum**

## 7.1 Introduction

Due to the unavailability of robust anti-Bfl-1 antibody preparations for several years now, many studies on the role of this gene have been limited to RNA-based analyses, and conclusions drawn from these cannot be confirmed at the protein level (Park *et al.*, 1997; Kenny *et al.*, 1997; Moreb and Zucali, 2001; Tarte *et al.*, 2004; Yoon *et al.*, 2003; Edelstein *et al.*, 2003; D'Souza *et al.*, 2000; D'Souza *et al.*, 2004; Ko *et al.*, 2003b; Wang *et al.*, 1999).

The expression of affinity-tagged recombinant proteins is an established method of generating antigen for raising antibodies. Affinity tags are highly efficient tools for purifying recombinant proteins from crude extracts (reviewed in Waugh, 2005; Terpe, 2003). The use of genetically engineered affinity tags for improved protein purification has increased greatly in recent years and affinity tags have become indispensable tools for structural and functional proteomics initiatives. The most commonly employed method utilises immobilised metal affinity chromatography (IMAC) to purify recombinant proteins containing a short affinity-tag consisting of polyhistidine (poly His) residues (Porath *et al.*, 1975).

In the absence of suitable reagents, the objective was set to clone the *bfl-1* gene into a appropriate expression vector and optimise its expression and purification from a compatible expression host. Once purified, the recombinant protein was used as antigen to generate polyclonal antibodies specific for Bfl-1.

### 7.1.1 The QIAexpress system

IMAC-purified recombinant Bfl-1 was prepared from an *Escherichia coli* (*E. coli*) host by exploiting elements of the QIAexpress system from QIAGen. This system provides a complete system for the cloning, expression, purification and detection of heterologous proteins. High-level expression of 6xHis-tagged proteins in *E. coli* is achieved using the pQE range of vectors which contain an optimised promoter-operator element consisting of the T5 promoter and two *lac* operator sequences that increase *lac* repressor binding and ensure efficient repression of the powerful T5 promoter (recognised by the *E. coli* RNA polymerase).

The *lac* operon promoter system is the most widely used bacterial expression system and encodes proteins that facilitate the uptake and metabolism of β-galactosides and is subject to both negative regulation (by binding of the *lac* repressor protein to the *lac* operator and preventing transcription) and positive regulation (by binding of an activator to the *lac* promoter and stimulating transcription). IPTG (an allolactose analogue) is a gratuitous inducer of the *lac* operon, insofar as it competes strongly with the *lac* operator for binding to the *lac* repressor, yet is itself is not metabolised in the process and can, thus, be used to induce expression.

#### 7.1.1.1 N/C-Terminal tagging

Recombinant constructs based on the pQE vectors can be produced by placing the 6xHis tag at the N-terminus or the C-terminus of the protein of interest. When incorporating C-terminal His tags, the cloned insert must be in-frame both with the ATG start codon and the 3' 6xHis coding sequence. The C-terminal placement of the 6xHis tag ensures only full-length proteins are purified. The pQE30 vector (Figure 7.1A) allows for the incorporation of a N-terminal 6xHis tag, while the pQE60 vector (Figure 7.1B) facilitates C-terminal tagging with 6xHis.

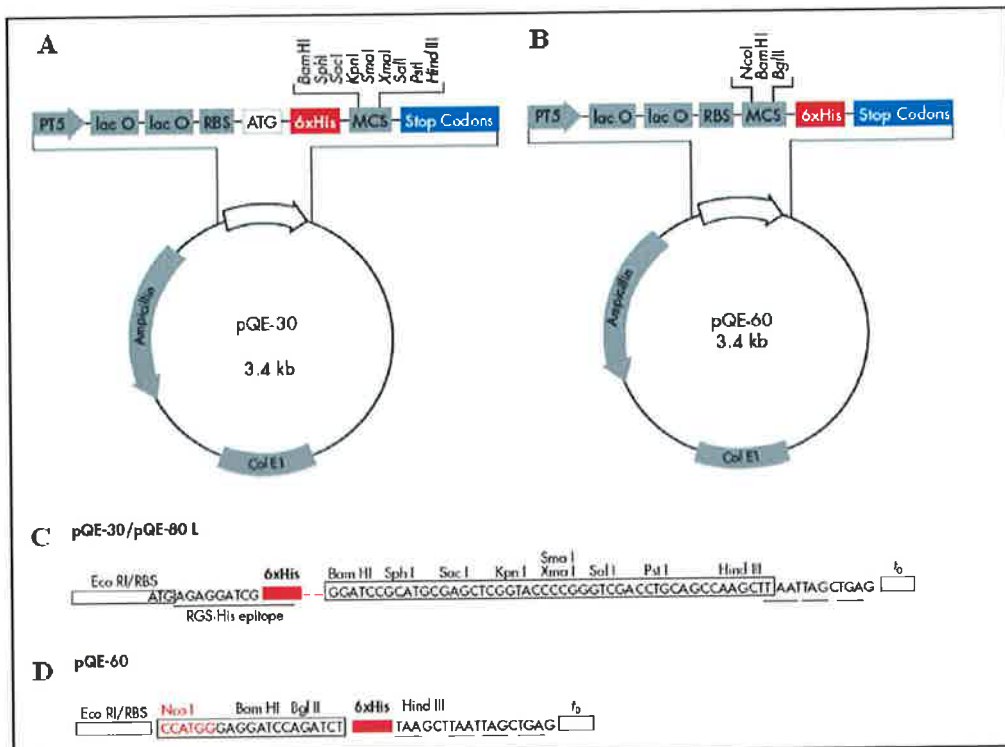


**Figure 7.1 pQE30 and pQE60 vector for N-terminal and C-terminal 6xHis tag constructs.**

The 3.4 kb pQE30 (A) and pQE60 (B) vectors allow for the incorporation of a N-terminal or C-terminal 6xHis tag respectively. Plasmid features include an optimised promoter-operator element consisting of phage T5 promoter and two *lac* operator sequences (lac O), which increase *lac* repressor binding and ensure efficient repression of the powerful T5 promoter. The plasmids also feature a synthetic ribosomal binding site, RBS, for high translation rates, a multiple cloning site (MCS) (C for pQE30 and D for pQE60) to enable fragment insertion and a 6xHis tag coding sequence 5' or 3' to the cloning region. In pQE30, the MCS is followed by translational stop codons in all reading frames, while in pQE60, the 6xHis tag is followed by translational stop codons in all reading frames. Two transcriptional terminators:  $t_0$  from phage lambda (Schwarz *et al.*, 1987), and T1 from the *rrnB* operon of *E. coli*, are present to prevent read-through transcription and ensure stability of the expression construct. The plasmids harbour the  $\beta$ -lactamase gene (*bla*) conferring resistance to ampicillin and the ColE1 origin of replication (adapted from QIAexpressionist manual, 2003).

### 7.1.2 Polyhistidine-tag

The small peptide polyhistidine tag utilises IMAC to purify recombinant proteins containing an affinity-tag of polyhistidine residues. IMAC is based on the interaction between a transition metal ion (in this study the Nickel ion,  $Ni^{2+}$ ) immobilised on a

matrix and specific amino acid side chains (in this study 6xHistidine residues). Hochuli *et al.*, (1987) developed a tetradentate chelating adsorbent, nitrilotriacetic acid (NTA), for metal-chelate affinity chromatography. NTA occupies four of the six ligand binding sites in the coordination sphere of the nickel ion, leaving two sites free to interact with the 6xHis tag (QIAexpressionist, 2003). The complexing of the chelators and metal ions is illustrated in Figure 7.2. Histidine is the amino acid that exhibits the strongest interaction with immobilised metal ion matrices, as electron donor groups on the histidine imidazole ring readily form coordination bonds with the immobilised transition metal (Terpe, 2003).

Histidine residues are infrequent amino acids in globular proteins, amounting to approximately 2 % of the amino acid content. The 6xHis affinity tag is poorly immunogenic, therefore it is usually not necessary to remove the tag for the purposes of antibody generation. At pH 8.0 the tag is small (0.84 kDa), uncharged, and therefore does not generally affect secretion, compartmentalisation, or folding of the fusion protein within the cell (QIAexpressionist, 2003). Additionally, in most cases, the 6xHis tag does not interfere with the structure or function of the purified protein as demonstrated for a wide variety of proteins, including enzymes, transcription factors, and vaccines. An additional advantage of this system is that anti-His Antibodies can be used for detection of tagged recombinant proteins during expression and purification steps.

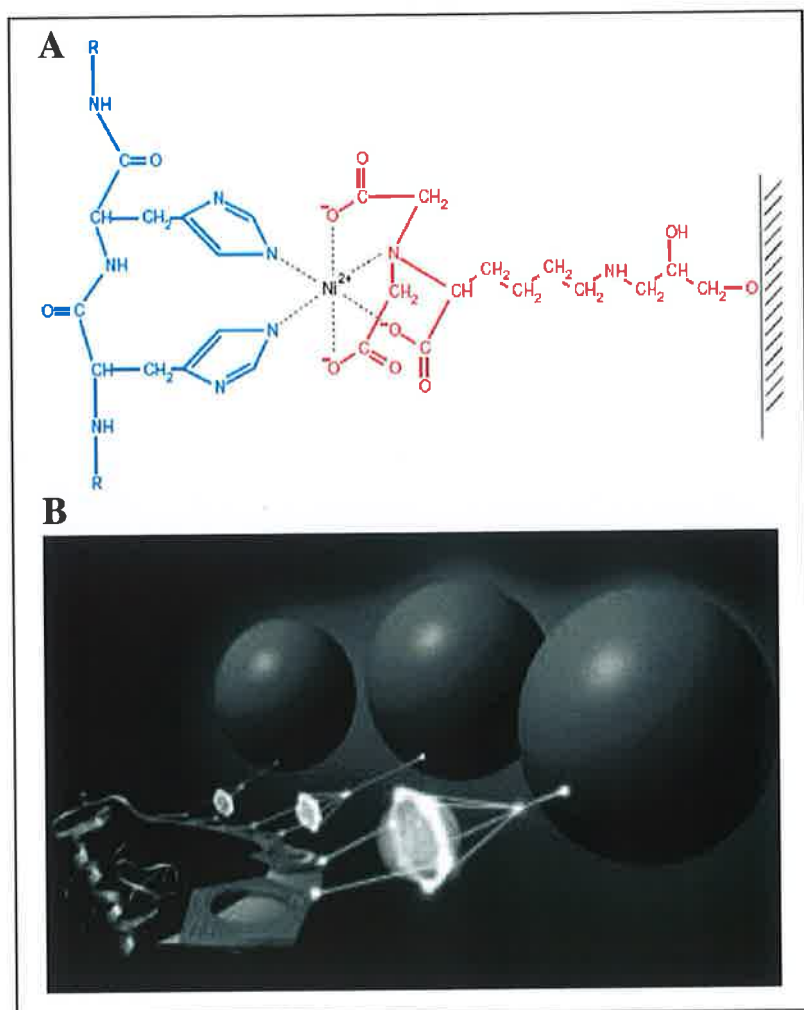


**Figure 7.2 Interaction between neighbouring residues in the 6xHis tag and Ni-NTA matrix.**

(A) NTA occupies four of the six ligand binding sites in the coordination sphere of the nickel ion, leaving two sites free to interact with the 6xHis tag. NTA binds metal ions far more stably than other available chelating resins (Hochuli, 1989) and retains the ions under a wide variety of conditions, especially under stringent wash conditions. (B) The interaction between the 6xHis tag and the Ni-NTA resin is presented in a 3D format (adapted from QIAexpressionist Manual, 2003).

### 7.1.3 Expression hosts

A variety of expression hosts are available for recombinant protein expression including bacteria, mammalian cells, insect cells (using baculovirus vectors), yeast and plants. Generally, most recombinant proteins can be cloned and expressed at high levels in *E.*

*coli*. However many polypeptide gene products expressed in *E. coli* accumulate as insoluble aggregates that lack functional activity. Furthermore, the use of *E. coli* as an expression host can present problems with cell toxicity, protein instability, improper processing or post-translational modification and inefficient translation (QIAexpressionist, 2003). The use of *E. coli* strain M15 [pREP4] (Table 2-3) is recommended by QIAgen for high-level recombinant protein expression using the range of pQE vectors. The M15 strain is derived from *E. coli* K12 and contains a low copy number of the pREP4 plasmid, which confers kanamycin resistance and constitutively expresses the *lac* repressor protein encoded by the *lac I* gene. Similarly, *E. coli* strains that harbour the *lacI<sup>q</sup>* mutation also produce enough *lac* repressor to efficiently regulate and repress the T5 promoter. Strains harbouring the *lacI<sup>q</sup>* mutation include JM109, SURE 2, XL-1 Blue, NovaBlue, RosettaBlue and XL 10-Gold.

One limitation of the use of *E. coli* strains for recombinant heterologous protein expression is the deviant codon usage from the *E. coli* gene repertoire. Most amino acids are encoded by more than one codon, and each organism carries its own bias in the usage of the 61 available amino acid codons. In each cell, the tRNA population closely reflects the codon bias of the mRNA population (Ikemura, 1981; Dong *et al.*, 1996). A subset of codons, namely AGG/AGA, CGA/CGG, AUA, CUA, GGA and CCC are rarely expressed in *E. coli* and appear to cause problems from a translational point of view. If the recombinant protein being expressed contains several of these rare codons the protein may not be expressed due to this translational limitation. *E. coli* RosettaBlue<sup>TM</sup> (Table 2-3) and *E. coli* Rosetta<sup>TM</sup> (Novagen) strains have been engineered to provide the tRNAs for rarely expressed codons on a chloramphenicol resistant plasmid, pRARE. The use of *E. coli* RosettaBlue<sup>TM</sup> or *E. coli* Rosetta<sup>TM</sup> strains as expression hosts facilitates the expression of proteins that would otherwise be limited by codon bias in *E. coli*.

### 7.1.4 Summary of Results

The above technologies were exploited for subcloning of the *bfl-1* open reading frame (ORF) and heterologous expression and purification of a recombinant Bfl-1 protein in the manner outlined below.

Directional cloning of the *bfl-1* ORF and the N-terminal (pQE30) or C-terminal (pQE60) His-tag vectors (Qiagen, West Sussex, UK) successfully generated recombinant plasmids capable of high level expression of the Bfl-1 protein fused to a 6xhistidine tag (His-Bfl-1 for pQE30-Bfl-1 or Bfl-1-His for pQE60-Bfl-1). Initial attempts at protein expression failed in some *E. coli* strains probably due to a major codon bias between the *bfl-1* gene and *E. coli* genes. High-level expression was achieved in an *E. coli* strain equipped with the transfer RNAs (tRNAs) for rare codons. Purification of His-Bfl-1 or Bfl-1-His from small-scale expression cultures was attempted under native and denaturing conditions using commercially available NTA resin in a batch IMAC procedure but was not achieved.

For the reasons outlined in Section 7.2.5 and to overcome this challenge, a novel vector (pGSLink) was designed and constructed to permit high-level expression of a protein linked at the N- or C-terminal to a His-tag by a flexible, poorly immunogenic linker peptide of 21 glycine and serine amino acids; (Gly<sub>4</sub>Ser)<sub>4</sub>Gly. The *bfl-1* coding fragment was directionally cloned into this novel vector to produce the fusion constructs; pGSLink-N-Bfl-1 and pGSLink-C-Bfl-1, from which the His-Linker-Bfl-1 and Bfl-1-Linker-His fusion proteins were successfully overexpressed and purified using IMAC. A manuscript arising from this work was recently published in Analytical Biochemistry (Loughran *et al.*, 2006). Purified recombinant Bfl-1 was then used to immunise a rabbit (Custom Hybridoma Laboratories) for the generation of polyclonal antibodies to Bfl-1. Anti-sera was collected and tested by ELISA for reactivity with the His-tagged Bfl-1 antigen over a range of dilutions. Antibodies specific for His-tagged Bfl-1 in the rabbit serum was shown to detect the antigen over the serum dilution range of 1/300 and 1/19,200. The anti-sera was subsequently tested for reactivity with the antigen by western blot and was shown to detect His-tagged Bfl-1 protein over a range of antibody dilutions but did not react with an unrelated His-tagged protein indicating that antibodies were specific for the Bfl-1 portion of the fusion protein. The anti-sera is currently being tested for its ability to detect endogenous Bfl-1 protein in human cell lines.

## 7.2 Results

To express recombinant His-tagged human Bfl-1 in *E. coli* the *bfl-1* ORF was initially inserted into the expression vector pQE30 of the QIAexpress system (Section 7.1.1) to produce pQE30-Bfl-1 capable of expression of N-terminal His-tagged Bfl-1 fusion protein. pQE30 was the initial vector of choice as the optimised translation initiation region in the pQE expression vectors enables the expression of proteins in N-terminal tag constructs 2-4 times more efficiently than proteins with a C-terminal affinity tag (QIAexpressionist, 2003). Also only the 5' end of the ORF must be ligated in frame as the N-terminal constructs contain termination codons in all three reading frames.

However, for the reasons outlined in Section 7.2.2, the *bfl-1* insert was subsequently cloned into the pQE60 vector (to produce the C-terminal tagged construct pQE60-Bfl-1). In the interest of succinctness, the cloning of pQE30-Bfl-1 and pQE60-Bfl-1 are described together below.

### 7.2.1 Cloning of pQE30-Bfl-1 and pQE60-Bfl-1

Firstly the *bfl-1* ORF was amplified by polymerase chain reaction (PCR) (Section 2.3.5) using the construct pCDNA3-HA-Bfl-1 (Table 2-5) as template DNA. This construct contains the full length *bfl-1* ORF sub-cloned downstream of a hemagglutinin (HA) peptide (derived from the human influenza HA protein) in pCDNA3 (D'Sa-Eipper *et al.*, 1996). pCDNA3-HA-Bfl-1 DNA was first characterised by restriction digestion (Section 2.3.3) prior to PCR (not shown). The *bfl-1* ORF was amplified by PCR in two separate PCR reactions with primer pairs bfl(30)F/bfl(30)R and bfl(60)F/bfl(60)R (sequences are given in Table 2-6) which led to the incorporation of *Bam*HI/*Hind*III and *Nco*I/*Bam*HI restriction sites (underlined in primers) at the 5'/3' end of the respective PCR products.

Following PCR, the products were analysed by agarose gel electrophoresis (Section 2.3.13) to check for migration of fragments at the expected size (Figure 7.3A; shown for bfl(60) product, bfl(30) product not shown). The PCR products were subsequently purified using the Wizard® DNA purification system (Section 2.3.6), digested with *Bam*HI/*Hind*III (bfl(30) product) or *Nco*I/*Bam*HI (bfl(60) product) and purified by phenol:chloroform extraction followed by ethanol precipitation (Section 2.3.2).

The pQE30 and pQE60 expression vectors (Figure 7.1) were firstly characterised by restriction digestion (Figure 7.3B shown for pQE60 only). Prior to ligation, the plasmids were linearised by restriction digestion with *Bam*HI/*Hind*III or *Nco*I/*Bam*HI restriction enzymes respectively, followed by dephosphorylation using calf intestinal phosphatase (CIP) (Section 2.3.4) to prevent recircularisation of the linearised DNA. The linearised, CIP-treated DNA was then purified by phenol:chloroform extraction followed by ethanol precipitation. The digested, purified PCR products were then sub-cloned into the *Bam*HI/*Hind*III sites of pQE30 or the *Nco*I/*Bam*HI sites of pQE60. Ligations (Section 2.3.7) of vectors and insert DNA were carried out overnight at 16 °C.

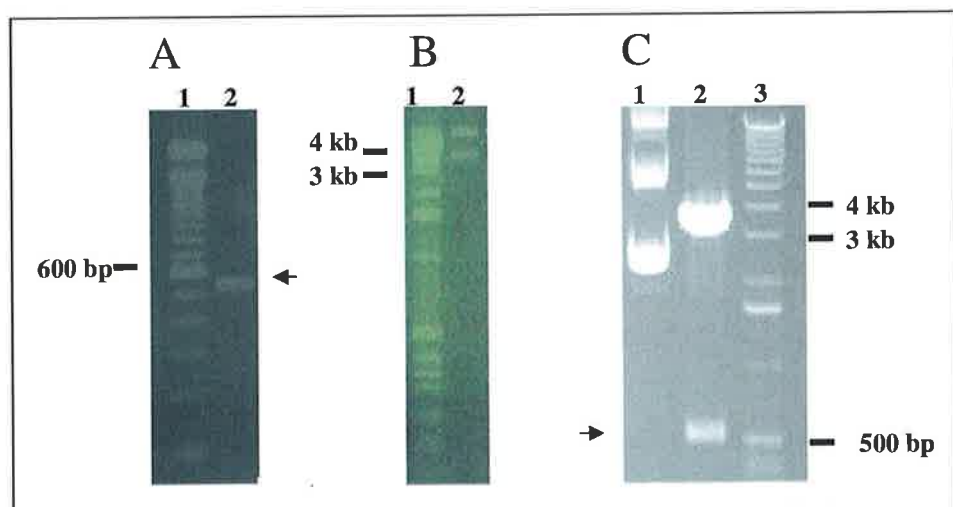


**Figure 7.3 Analysis of the cloning steps in the construction of the expression vector pQE60-Bfl-1**

The pQE60-Bfl-1 expression plasmid was constructed by cloning the *bfl-1* gene into the plasmid pQE60. Agarose gel electrophoresis (2 % (A), 0.7 % (B) and 1 % (C) agarose-1 X TAE gel electrophoresed at 100 V for 1 h in 1 X TAE) was used to monitor cloning steps. (A) Lane 1; 100 bp ladder (Invitrogen), Lane 2; The amplified DNA fragment encoding *bfl-1* following digestion with the appropriate restriction enzymes was about 0.53 kb, indicated by black arrow. (B) Plasmid vector pQE60, Lane 1; 1 kb ladder, Lane 2; pQE60 plasmid at 3.4 kb. (C) Restriction analysis of selected transformants of pQE60-Bfl-1 with *Nco*I/*Bam*HI revealed the predicted bands of ~0.53 kb indicating that the fusion constructs had been successfully generated. Lane 1; Undigested pQE60-Bfl-1 plasmid DNA, Lane 2; pQE60-Bfl-1 digested with *Nco*I and *Bam*HI, the excised *bfl-1* fragment is indicated by a black arrow, Lane 3; 1 kb ladder.

Following the ligation reaction, competent *E. coli* JM109 (Section 2.3.8) cells were transformed (Section 2.3.9) with the recombinant plasmid. Transformants were selected for ampicillin (100 µg/ml) resistance. Following overnight incubation at 37 °C, colonies were evident only on the plates that had been inoculated with cells transformed with digested CIP-treated plasmid plus corresponding digested PCR product and not on control (vector only or insert only) plates. A number of colonies were randomly selected and individually sub-cultured into fresh 5 ml volumes of LB broth. The selected clones were grown overnight at 37 °C with shaking at 200 rpm, reaching stationary growth phase. Cells were pelleted by centrifugation at 6,000 x g. Plasmid isolation (Section 2.3.10) was performed on the resulting cell pellet. Restriction analysis was carried out on the resultant DNA to detect the presence of the *bfl-1* insert at the expected size (Figure 7.3C shown for pQE60-Bfl-1 only).

In order to verify that the *bfl-1* insert had been faithfully cloned in terms of nucleotide content and was ‘in-frame’, plasmid DNA was sequenced (Section 2.3.14) using pQE For and pQE Rev primers (Table 2-6). Sequencing results, received as linear nucleotide sequences, were aligned with the known nucleic acid sequence of the *bfl-1* gene using the ClustalW multiple alignment program (Table 2-4). The pQE30-Bfl-1- and pQE60-Bfl-1-derived plasmid DNA, demonstrated 100 % homology with the native *bfl-1* gene as derived from the Bfl-1 coding sequence with GenBank accession number U27467 (Figure 7.4). The nucleotide sequences of the His-tagged Bfl-1 clones were translated to amino acid sequences using the ‘Translate’ bioinformatics tool (Table 2-4). The physico-chemical parameters (Table 7-1) of the protein sequences were then calculated using the ‘ProtParam’ bioinformatics tool (Table 2-4).

**Table 7-1 Predicted physico-chemical parameters of His-Bfl-1/Bfl-1-His**

Parameter	His-Bfl-1	Bfl-1-His
Number of amino acids	189	186
Molecular weight: kDa	21.75	21.41
Theoretical pI	7.00	6.59
Extinction coefficients M <sup>-1</sup> cm <sup>-1</sup> , at 280 nm	31190	31190

A					
	Start	Oligo	6xHis Tag	Aligned sequences	STOP
pQE30Bfl-1 U27467	-	AGAGGATCC	<b>ATCACCACTACCCATRC</b>	GGATCCACAGACTGTGAATTGGATATAT	59
				<b>ACAGACTGTGAATTGGATATAT</b>	26
pQE30Bfl-1 U27467	TTACAGGCTGGCTCAGGACTATCTGCAGTGCCTACAGATACCACAACTGGATCAGG	119			
	TTACAGGCTGGCTCAGGACTATCTGCAGTGCCTACAGATACCACAACTGGATCAGG	86			
pQE30Bfl-1 U27467	TCCAAGCAAAACGTCCAGAGTGCACAAATGTTGCGTCTCAGTCAGTCAGTCAGTCAGG	179			
	TCCAAGCAAAACGTCCAGAGTGCACAAATGTTGCGTCTCAGTCAGTCAGTCAGTCAGG	146			
pQE30Bfl-1 U27467	AAAAGAATCTGAAGTCATGCTGGACAATGTTAATGTTGTCGGTAGACACTGCCAGAAC	239			
	AAAAGAATCTGAAGTCATGCTGGACAATGTTAATGTTGTCGGTAGACACTGCCAGAAC	206			
pQE30Bfl-1 U27467	ACTATTCAACCAAGTGATGGAAAAGGAGTTGAAGACGGCATCATTAACTGGGAAGAAAT	299			
	ACTATTCAACCAAGTGATGGAAAAGGAGTTGAAGACGGCATCATTAACTGGGAAGAAAT	266			
pQE30Bfl-1 U27467	TGTAACCACATTTGCATTGAGGTATTCTCATCAAGAAACTCTACGACAGCAAATTGC	359			
	TGTAACCACATTTGCATTGAGGTATTCTCATCAAGAAACTCTACGACAGCAAATTGC	326			
pQE30Bfl-1 U27467	CCCGGATGTGGATACCTATAAGGAGATTCTATTTGTTGCGGAGTTCTATAATGAATAA	419			
	CCCGGATGTGGATACCTATAAGGAGATTCTATTTGTTGCGGAGTTCTATAATGAATAA	386			
pQE30Bfl-1 U27467	CACAGGAGAATGGTAAGGCAAAACGGAGCTGGGAAATGGCTTGTAAAGAAGTTGAA	479			
	CACAGGAGAATGGTAAGGCAAAACGGAGCTGGGAAATGGCTTGTAAAGAAGTTGAA	446			
pQE30Bfl-1 U27467	ACCTAAATCTGGCTGGATGACTTTCTAGAAGTTACAGGAAAGATCTGTGAATGCTATC	539			
	ACCTAAATCTGGCTGGATGACTTTCTAGAAGTTACAGGAAAGATCTGTGAATGCTATC	506			
pQE30Bfl-1 U27467	TCTCCTGAAGCAAACTGTAAAGCTTAATTAG-	570			
	TCTCCTGAAGCAAACTGTAAAGCTTAATTAG-	528			
B					
	Start	Oligo	6xHis Tag	Aligned sequences	STOP
pQE60Bfl-1 U27467	-	ACAGACTGTGAATTGGATATTTACAGGCTGGCTCAGGACTATCTGCAGTGCCTC	57		
		<b>ACAGACTGTGAATTGGATATTTACAGGCTGGCTCAGGACTATCTGCAGTGCCTC</b>	60		
pQE60Bfl-1 U27467	CTACAGATAACACAACTGGATCAGGCTCAAGCAAAACGTCCAGAGTGCACAAATGTT	117			
	CTACAGATAACACAACTGGATCAGGCTCAAGCAAAACGTCCAGAGTGCACAAATGTT	120			
pQE60Bfl-1 U27467	GCGTTCTCAGTCCAAAAAGAAGTGGAAAAGAATCTGAAGTCATGCTTGGACAATGTTAAT	177			
	GCGTTCTCAGTCCAAAAAGAAGTGGAAAAGAATCTGAAGTCATGCTTGGACAATGTTAAT	180			
pQE60Bfl-1 U27467	GTTGTTCCGTAGACACTGCCAGAACACTATTCAACCAAGTGATGGAAAAGGAGTTGAA	237			
	GTTGTTCCGTAGACACTGCCAGAACACTATTCAACCAAGTGATGGAAAAGGAGTTGAA	240			
pQE60Bfl-1 U27467	GACGGCATCATAACTGGGAAAGAATTGTAACCATATTGCTTGAAGGTATTCTCATC	297			
	GACGGCATCATAACTGGGAAAGAATTGTAACCATATTGCTTGAAGGTATTCTCATC	300			
pQE60Bfl-1 U27467	AAGAAAATTCTACGACAGCAATTGCCCGGATGTGGATACCTATAAGGAGATTCTCATAT	357			
	AAGAAAATTCTACGACAGCAATTGCCCGGATGTGGATACCTATAAGGAGATTCTCATAT	360			
pQE60Bfl-1 U27467	TTTGTGCGGAGTTCTATAATGAATAACAGGAGAATGGATAAGGCAACGGAGGCTGG	417			
	TTTGTGCGGAGTTCTATAATGAATAACAGGAGAATGGATAAGGCAACGGAGGCTGG	420			
pQE60Bfl-1 U27467	AAAAATGGCTTGTAAAGAAGTTGAAACCTAACTGGCTGGATGACTTTCTAGAAGTT	477			
	AAAAATGGCTTGTAAAGAAGTTGAAACCTAACTGGCTGGATGACTTTCTAGAAGTT	480			
pQE60Bfl-1 U27467	ACAGGAAAAGATCTGTGAATGCTATCTCTCTGAAGCAAACTGTGGATCCAGATCT	537			
	ACAGGAAAAGATCTGTGAATGCTATCTCTCTGAAGCAAACTGTGGATCCAGATCT	525			
pQE60Bfl-1 U27467	<b>CACCATCACCATCACAA</b>	555			

**Figure 7.4 Sequence verification of pQE30-Bfl-1 and pQE60-Bfl-1.**

The nucleotide sequence of the inserted fragments was verified by sequencing using pQE vector specific forward and reverse primers and pQE30-Bfl-1 (A) or pQE60-Bfl-1 (B) as template. Sequence results were aligned with the published *bfl-1* sequence (GenBank Accession number: U27467) using ClustalW. Sequences highlighted in grey demonstrated 100 % homology. It was apparent from these results that the cloned gene

was 100 % homologous with the native nucleic acid sequence of *bfl-1*. The only areas of non-homology (unhighlighted) were the N- and C-terminal 6xHis coding sequences (pQE30- and pQE60-Bfl-1 respectively), the remaining restriction sites of the MCS of pQE30-Bfl-1 and pQE60-Bfl-1) and the RGS peptide at the 5' end of the 6xHis tag in pQE30-Bfl-1.

Once it was established that the *bfl-1* ORF had ligated correctly with pQE30 or pQE60 in the correct reading frame relative to the His-tag, stop/start codons, plasmid DNA from selected transformants was then used to transform *E. coli* strains M15[pREP4] and XL10-Gold (capable of inducible expression of the recombinant protein). Transformants were selected for antibiotic resistance (M15[pREP4]: ampicillin; 100 µg/ml, kanamycin; 50 µg/ml and XL-10 Gold: ampicillin; 100 µg/ml, tetracycline; 10 µg/ml, chloramphenicol; 25 µg/ml) and subsequently screened for protein expression.

### 7.2.2 Protein expression

Several single colonies from *E. coli* strains M15[pREP4] and XL10-Gold harbouring expression plasmids encoding His-Bfl-1 (pQE30-Bfl-1) and Bfl-1-His (pQE60-Bfl-1) fusion proteins were screened for protein expression as described in Section 2.8.1. SDS-PAGE analysis (Section 2.7.2) (15 % separating gel, 5 % stacking gel) was used to confirm protein expression at the predicated molecular weight (His-Bfl-1/Bfl-1-His; ~21 KDa) (Table 7-1).

As stated in Section 7.2, the first His-tagged Bfl-1 construct to be cloned was the N-terminal tag construct; pQE30-Bfl-1. This construct was first transformed into the M15[pREP4] *E. coli* strain, however, despite several attempts, recombinant His-tagged Bfl-1 (in M15[pREP4] cells harbouring pQE30-Bfl-1) was not detected following induction of expression with IPTG and SDS-PAGE analysis (data not shown).

A re-assessment of the design of the system (vector and host choices) was performed in order to determine the possible cause of the failure to detect His-tagged Bfl-1. One possibility was that an undetected frame shift or translational stop codon would lead to premature termination of translation (switching the tag to the C-terminus would ensure only full-length fusion protein would be purified). In some cases the 5' end of the inserted DNA sequence may encode elements that interfere with transcription or

translation by masking of the Shine-Dalgarno sequence by stem-loop structures resulting from inverted repeats. Switching the tag to the opposite terminus, modifications of growth media and the use of different host strains may correct this problem (QIAexpressionist, 2003). Also, low level or no expression can occur because the protein is toxic or unstable, recombinant protein with hydrophobic regions often have a toxic effect on host cells, most likely due to the association of the protein with or incorporation into vital membrane systems. Lowering the growth temperature before and after induction is recommended (QIAexpressionist, 2003). Furthermore, insufficient tRNA pools can lead to translational stalling, premature translation termination, translation frameshifting and amino acid misincorporation (Kane, 1995).

Steps were therefore taken to address these possibilities and overcome the failure to detect expression by variation of growth parameters. The growth temperature before and after induction was reduced to 25 °C and 30 °C, and a time-course analysis was performed to determine if induction over a shorter period of time at lower growth temperatures would reveal that the protein was unstable. All buffers and manipulations for harvesting cells following induction were kept at or performed at 4 °C. Protease inhibitors were also included in the cell lysis buffers to eliminate the possibility that the recombinant protein was subject to degradation by proteases. The *bfl-1* gene was also cloned into the pQE60 expression vector to generate a C-terminal tag construct; pQE60-Bfl-1 (Section 7.2.1) to eliminate the possibility of 5' end interference or premature termination due to undetected frame shift or translational stop codon as discussed above.

A different host strain was also tested by transformation of pQE30-Bfl-1 and pQE60-Bfl-1 into the *E. coli* strain, XL10-Gold, followed by induction of expression and SDS-PAGE analysis. However, the use of these variations of the growth conditions, host strain, tag placement and harvesting parameters did not resolve the failure to detect recombinant protein expression in M15[pREP4] or XL-10 Gold *E. coli* strains harbouring pQE30-Bfl-1 or pQE60-Bfl-1 (Figure 7.5A and B; shown for XL10-Gold harbouring pQE30-Bfl-1 or pQE60-Bfl-1 respectively).

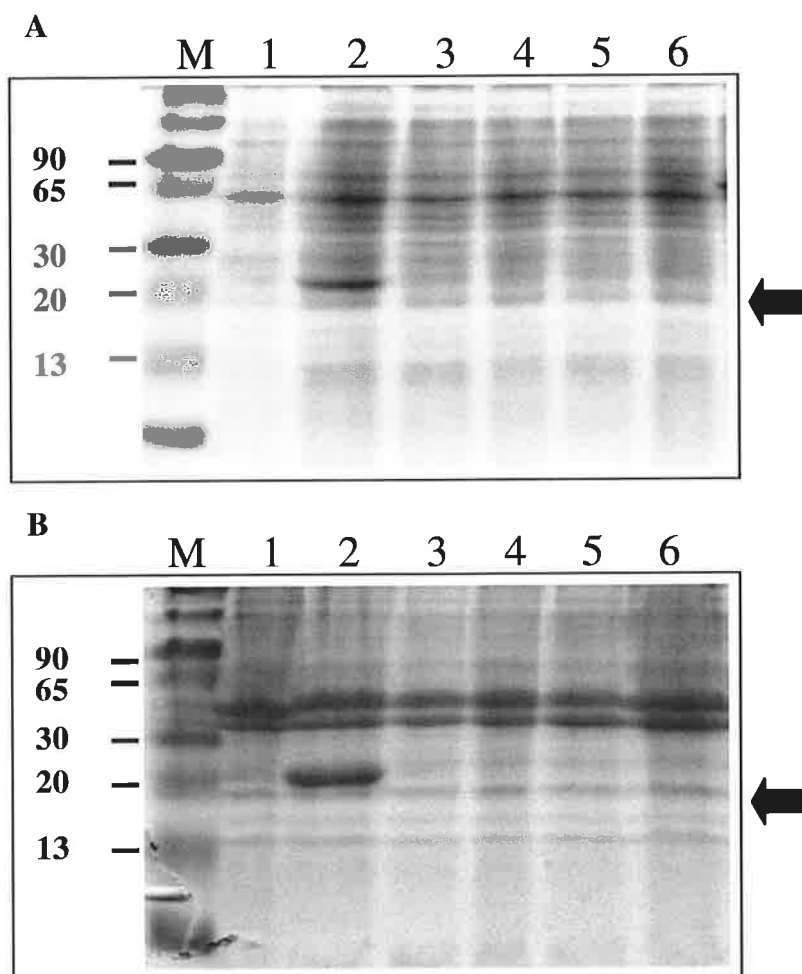


**Figure 7.5 Expression screening of His-Bfl-1 and Bfl-1-His in *E. coli* XL10 Gold.**

Recombinant clones (A; pQE30-Bfl-1 and B; pQE60-Bfl-1) were screened for expression of the His-tagged Bfl-1 protein by preparation of small-scale expression cultures of *E. coli* XL10-Gold, harvested at 5 h post induction/non induction followed by cell lysis and SDS-PAGE analysis. Expression of His-tagged Bfl-1 protein was not detected at predicted molecular weight of ~21.5 kDa. Lane 1: Colour marker (Sigma-Aldrich), Lane 2: noninduced control sample, Lane 3: Induced control fusion construct expressing a recombinant protein of 23 kDa molecular weight, Lane 3-6: Induced pQE30-Bfl-1 (A) or pQE60-Bfl-1 (B) clones. The molecular weight markers are indicated on the left and black arrowheads designate the location of the expected recombinant Bfl-1.

Sequencing of pQE30- and pQE60-Bfl-1 constructs (Figure 7.4) confirmed that the problem was not at the DNA level and prompted a fundamental re-assessment of the Bfl-1 protein with respect to its amino acid content and associated physicochemical

properties. As the difficulties apparent in the failure of expression were not rectified by variation of the growth parameters they were then most likely related to intrinsic complications when expressed in the heterologous host species, *E. coli*. More specifically, an analysis of the human *bfl-1* ORF revealed that this was likely to be due to the presence of a significant number of codons (12 %) that were rarely used in *E. coli* (Table 7-2). It was concluded that this represented the most probable cause of the undetectable expression levels.

**Table 7-2 Codon bias between *E. coli* genes and human *bfl-1*.**

“All genes” is the fraction represented in all 4,290 coding sequences in the *E. coli* genome (fractions adapted from Novy *et al.*, 2001).

Amino Acid	Codon	Occurrence in <i>bfl-1</i> gene	Fraction in all <i>E. coli</i> genes
Gly	GGA	6	0.109
Arg	AGG	2	0.022
Leu	CTA	6	0.037
Ile	ATA	4	0.073
Arg	AGA	3	0.039
Total		21 rare codons (12 % of <i>bfl-1</i> codons are rare codons in <i>E. coli</i> )	

In order to overcome this, the *E. coli* RosettaBlue™ strain (Table 2-3) was chosen as host as it has been engineered to expresses tRNAs for many codons that are rarely to be found in *E. coli* genes as discussed in Section 7.1.3.

*E. coli* RosettaBlue™ cells were thus transformed (Section 2.3.9) with pQE30-Bfl-1 and pQE60-Bfl-1 constructs. Single colonies of selected transformants (selected for ampicillin (100 µg/ml), tetracycline (12.5 µg/ml) and chloramphenicol (34 µg/ml) resistance) were used to inoculate overnight cultures and were screened for over-expression of the recombinant fusion proteins as in Section 7.2.2. SDS-PAGE analysis of cell lysates from some clones showed induction of a single major protein band of the expected ~21.5 KDa (Figure 7.6) for *E. coli* RosettaBlue™ cells harbouring pQE30-Bfl-1 (A) and pQE60-Bfl-1 (B).

A timecourse analysis of protein expression was performed to establish the optimal induction period (Figure 7.7A for pQE60-Bfl-1), which was found to be 5 h. The level of expression of recombinant His-tagged protein was optimised following induction by varying IPTG concentration (data not shown), incubation temperature (Figure 7.7B) and OD<sub>600 nm</sub> at induction (Figure 7.7B) in *E. coli* RosettaBlue™ cells harbouring pQE60-Bfl-1 (determined to be 0.1 mM, 37 °C and 0.8 respectively).

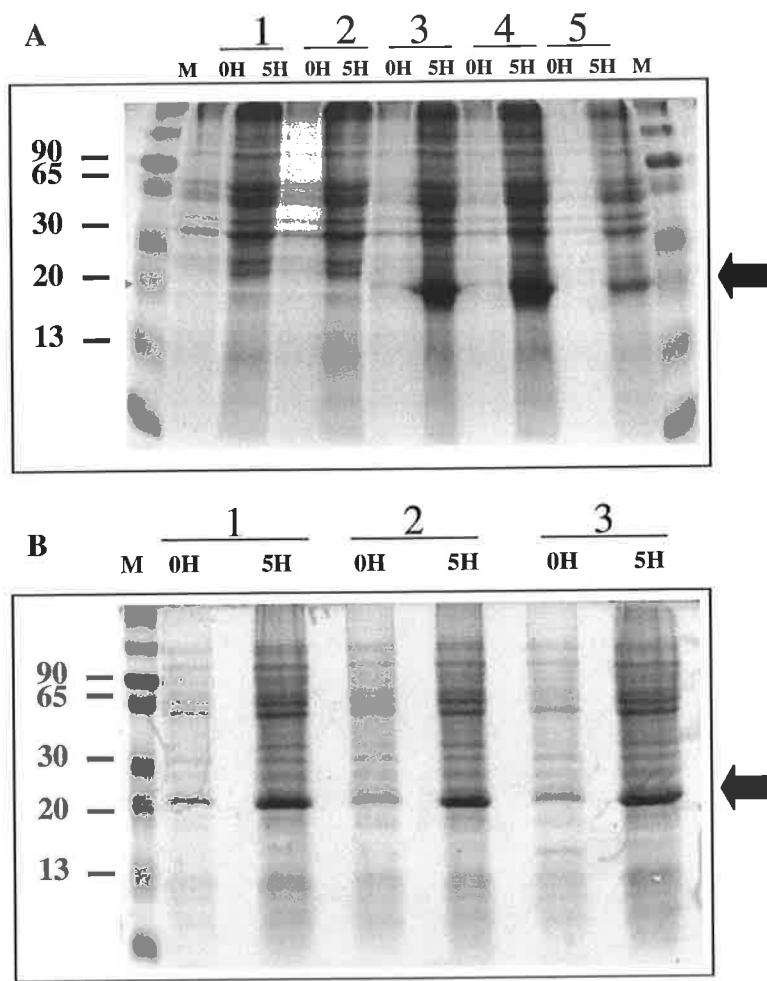


**Figure 7.6 Expression screening of recombinant clones in *E. coli* RosettaBlue™**

Selected transformants of (A) pQE30- and (B) pQE60-Bfl-1 were screened for expression of the His-tagged Bfl-1 protein by preparation of small-scale expression cultures followed by cell lysis at 5 h post induction with IPTG and SDS-PAGE analysis. Expression of His-tagged Bfl-1 protein was detected at predicted molecular weight of ~21.5 kDa, M: Colour marker (Sigma-Aldrich), numbers 1-5 (A) denotes clones of pQE30-Bfl-1 and numbers 1-3 (B) denotes clones of pQE60-Bfl-1. 0 h is time of induction and lysates were prepared at 5 h post-induction. pQE30-Bfl-1 clones 3, 4 and

5 and pQE60-Bfl-1 clones 1-3 overexpressed a recombinant protein at the predicted molecular weight of His-tagged Bfl-1 upon induction. The molecular weight markers are indicated on the left and black arrowheads designate the predicted location of recombinant Bfl-1.

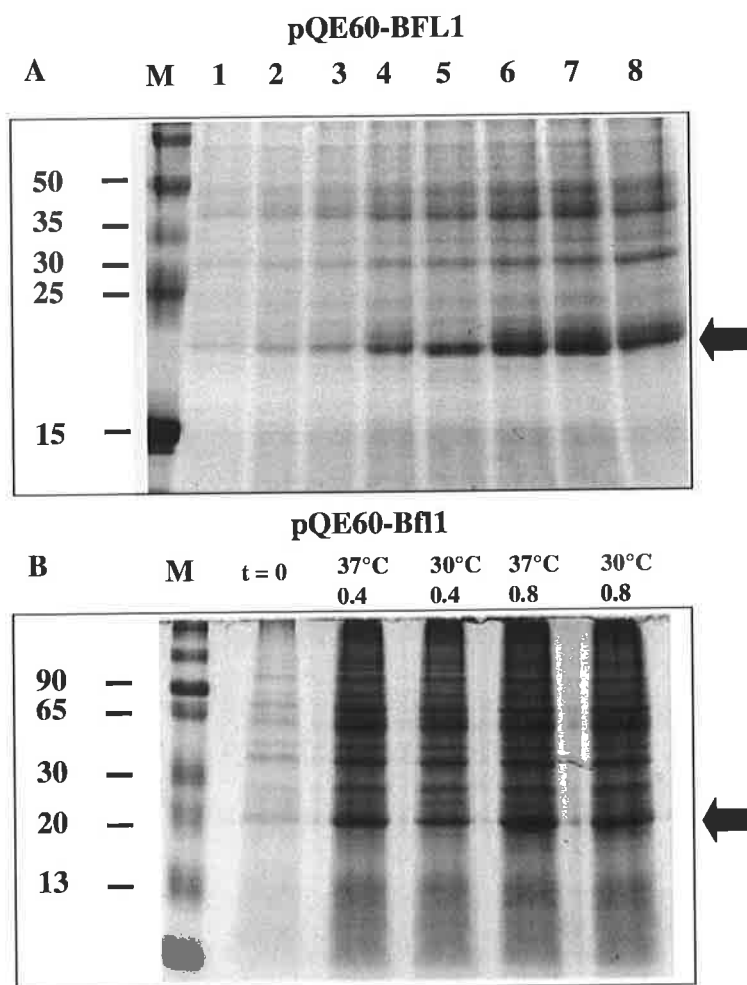


**Figure 7.7 Variation of growth parameters for optimal expression of pQE60-Bfl-1 in *E. coli* RosettaBlue<sup>TM</sup>.**

(A) Time course analysis of recombinant Bfl-1 protein expression. M; Marker, 0-8; 0,1, 2, 3, 4, 5, and 12 h post induction with 1 mM IPTG. (B) Effect of variation of incubation temperature and OD<sub>600 nm</sub> at induction point on Bfl-1 protein expression. Protein lysates prepared at 5 h post-induction. M: Marker (Sigma-Aldrich), t = 0: sample at time zero, 0.4/0.8: OD<sub>600nm</sub> at t=0, 37 °C/30 °C: Incubation temperature prior to and during induction of expression. The molecular weight markers are indicated on the left and black arrowheads designate the predicted location of recombinant Bfl-1.

### 7.2.3 Determination of protein solubility

Many polypeptide gene products expressed in *E. coli* accumulate as insoluble aggregates. Eukaryotic proteins expressed intracellularly in *E. coli* are frequently sequestered into insoluble inclusion bodies. Since the interaction between Ni-NTA and the 6xHis tag of the recombinant protein does not depend on tertiary structure, proteins can be purified either under native or denaturing conditions (QIAexpressionist, 2003). For antigen production, the protein can be expressed either in native or denatured form. In order to determine if the protein was soluble in the cytoplasm and therefore purifiable under native conditions, the soluble and insoluble fractions (Section 2.8.2) of expression lysates were examined by SDS-PAGE analysis (Figure 7.8). The Bfl-1-His protein was resolved in the soluble fraction as can be seen by comparing the soluble and insoluble extracts in lanes 4 and 6 respectively, indicating that the protein was therefore purifiable under native conditions.

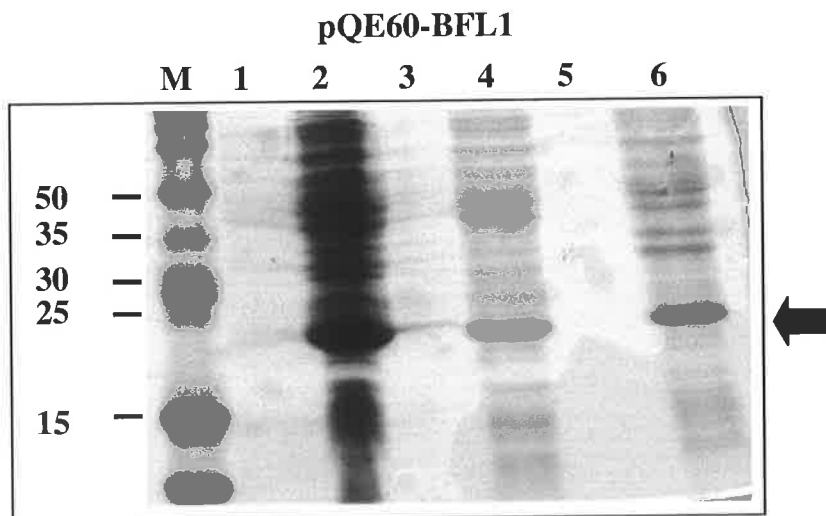


**Figure 7.8 Determination of protein solubility.**

Expression cultures harvested at 5 h post induction were lysed in native lysis buffer followed by incubation with lysozyme and sonication. Soluble and insoluble extracts were prepared and analysed by SDS-PAGE. Lanes: M; Marker (Amersham), 1 & 2; unrelated experiment, 3 & 5; blank, 4; Extract A, soluble extract, 6; Extract B, insoluble extract. The molecular weight markers are indicated on the left and black arrowheads designate the predicted location of recombinant Bfl-1.

#### **7.2.4 Protein Purification**

Batch IMAC purification of His-Bfl-1 and Bfl-1-His was performed with the use of Ni-NTA resin (Qiagen, West Sussex, UK) under native and denaturing conditions (Section 2.8.3).

Purification of His-Bfl-1 and Bfl-1-His was not achieved by IMAC under native (Figure 7.9 A and C) or denaturing conditions (Figure 7.9 B and D). Imidazole concentrations/pH conditions were adjusted in an attempt to achieve purification under native/denaturing conditions respectively in a series of small-scale batch purifications (not shown). As the 6xHis-tagged proteins appeared to elute along with endogenous *E. coli* proteins in the FT fractions (Figure 7.9), the amount of Ni-NTA resin used was increased in an effort to eliminate the possibility that the binding capacity was too low. The lysate was incubated with the resin for prolonged periods with rotation to increase resin-binding opportunity. Lysis and purification steps were performed at 4 °C and a cocktail of protease inhibitors (PMSF, Aprotinin and Leupeptin; (Appendix)) were added to the lysis/wash and elution buffers to prevent protein degradation. Cells were also lysed in 6 M guanidine hydrochloride, a more efficient solubilisation and cell lysis reagent used to solubilise very hydrophobic receptor or membrane proteins, before purification. Despite repeated attempts the difficulties apparent in the purification failure were not resolved by variation of the purification parameters.

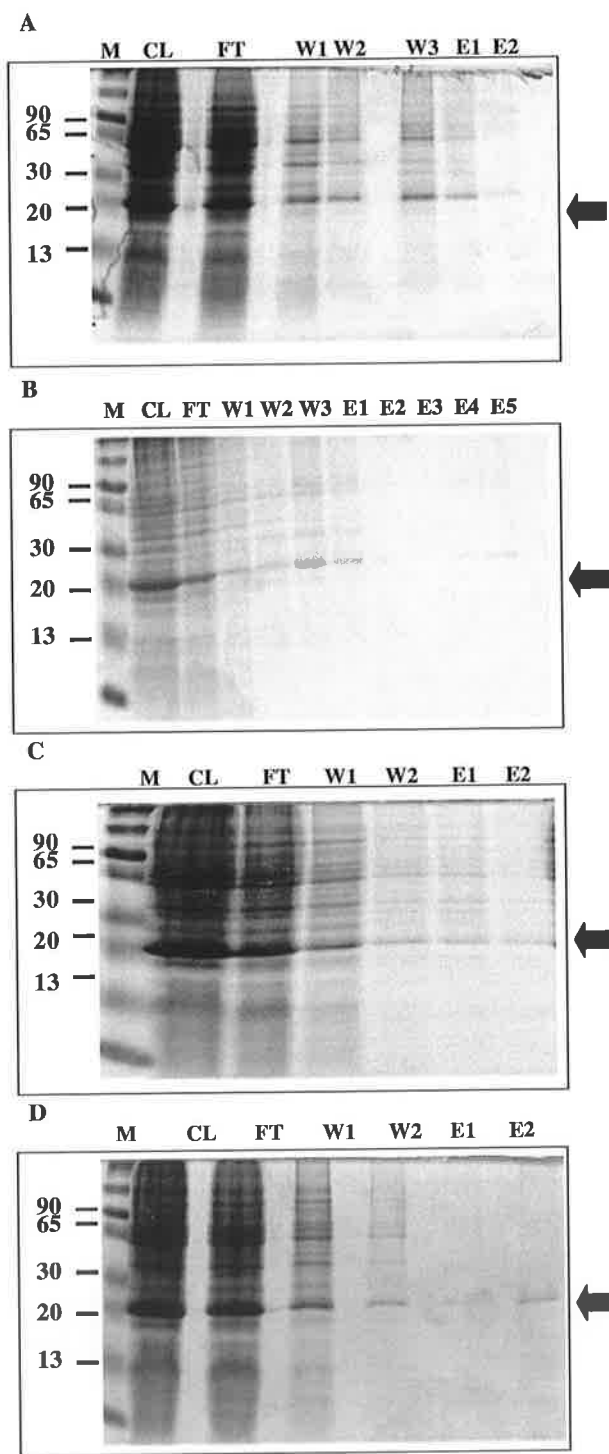


**Figure 7.9 Purification of His-Bfl-1 and Bfl-1-His under native and denaturing conditions.**

Attempted protein purification of His-Bfl-1 (A) and Bfl-1-His (C) under native conditions using Ni-NTA resin. M: Marker (Sigma-Aldrich), CL: Cleared cell lysate,

FT: Flow through, W1-2/3: Wash with 10 mM imidazole, E1-2: Elution with 250 mM imidazole. (B and D) Attempted protein purification under denaturing conditions of His-Bfl-1 and Bfl-1-His respectively using Ni-NTA resin. M: Marker, CL: Cleared cell lysate, FT: Flow through, W12/3: Wash with buffer pH 6.3/6.1/5.9, E1-5: Elution with buffer pH 5.5, 5.0, 4.8, 4.5, 4.2. The molecular weight markers are indicated on the left and black arrowheads designate the predicted location of recombinant Bfl-1.

Western blot analysis (Section 2.7.4) of expression lysates was performed to certify the integrity of the His tag element of the fusion proteins (Figure 7.10 shown for pQE60-Bfl-1/ Bfl-1-His only). Nitrocellulose membrane with transferred electrophoresed proteins from expression lysates was probed with an anti-His monoclonal antibody which had been conjugated with HRP.

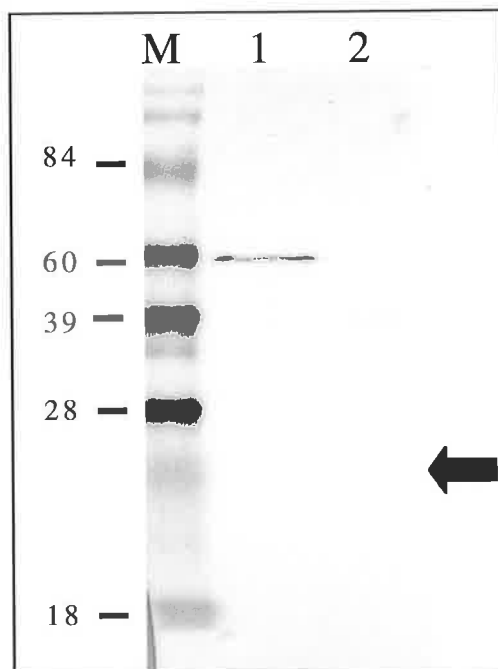


**Figure 7.10** Western blot analysis of His-Bfl-1 and Bfl-1-His proteins

Immunoreactivity of HRP-labeled anti-His monoclonal antibody (Sigma-Aldrich) with expression lysates of *E. coli* RosettaBlue<sup>TM</sup> expressing positive control his-tagged protein procured from the Applied Biochemistry group, DCU (Lane 1; ~60 kDa) and Bfl-1-His (Lane 2) protein. Bfl-1-His was not detected at predicted molecular weight of ~21.5 kDa. The molecular weight markers (Lane M (Pierce BlueRange marker)) are indicated on the left and a black arrowhead designates the predicted location of recombinant Bfl-1.

Chromogenic detection of HRP and consequently the presence of His tag moieties was evident only for the positive control sample (procured from the Applied Biochemistry group, DCU; ~60 kDa) as can be seen in Lane 1 (Figure 7.10). The presence/accessibility of the His-tag of the Bfl-1-His protein (Lane 2) was not confirmed by the anti-His antibody. As sequencing results and SDS-PAGE analysis revealed coding sequence fidelity for full-length His-tagged Bfl-1 protein and high-level expression of a protein at the correct size following induction respectively, it was concluded that somehow the His-tag was unavailable for interaction with the anti-His antibody or the Ni-NTA matrix during purification.

One relatively common reason for the failure to purify His-tagged proteins by IMAC is the inaccessibility of the His-tag due it being buried as a result of protein folding or tightly bound via interaction with adjacent residues on the protein's surface. It was reasoned that a novel approach to solving this problem would be to distance the His-tag from the rest of the protein by inserting a spacer or linker peptide between the two domains. To this end it was decided to engineer a linker between the His-tag and the *bfl-1* primary sequences so as to spatially elongate them from one another.

### 7.2.5 Design of Glycine-Serine Linker

In design of the linker, consideration was given to several important factors that would ensure optimal functionality. The composite residues of the linker had to be poorly immunogenic, flexible, stable, non-toxic and should not cause a codon bias in the host organism. Also the linker length had to offer sufficient separation of fusion partners and at the same time be short enough to avoid affects on secretion or protein function.

Linkers are commonly used in recombinant antibody research to separate antibody fragments and allow correct chain-chain binding and proper folding. A review of the literature revealed that functional designed linkers are usually glycine-based peptides with lengths calculated to span the minimum distance between the C terminus of one subunit or domain and the N terminus of the next. Lengths ranged from 8 amino acid residues to 30, with linker length of about 21 amino acids occurring most commonly (allowing sufficient separation for flexibility without affecting protein solubility).

Glycine (Gly or G) is the smallest amino acid with the simplest structure, is hydrophobic and has a hydrogen atom in the side-chain position. Glycine is generally

used in designed linkers because the absence of a  $\beta$ -carbon permits the polypeptide backbone to access dihedral angles that are energetically forbidden for other amino acids (Ramachandran and Sasisekharan, 1968). Thus, a glycine-rich linker is more flexible than a linker of comparable length composed of non-glycine residues. Serine (Ser or S) is a polar uncharged amino acid due to the reactive hydroxyl group in the side-chain and can participate in hydrogen bonding. It is thought that the ability of serine to form hydrogen bonds allows formation of new stabilising interactions in the native state (Robinson and Sauer, 1998). Overall, the rationale for this choice was that serine residues would enhance the hydrophilicity of the peptide backbone to allow hydrogen bonding to solvent molecules, and the glycyl residues would provide the linker with flexibility to adopt a range of conformations (Argos, 1990). These properties would also serve to prevent interaction of the linker peptide with hydrophobic interfaces on the individual domains (Guo *et al.*, 2000).

Given the difficulties encountered in Section 7.2.2, namely failure to detect recombinant protein expression due to a significant codon bias between the *bfl-1* gene and *E. coli* genes, consideration was given to the codon choice for the Gly/Ser linker and how this could influence the level of protein expression. Codon use preferences reflect the amounts of corresponding cellular tRNA levels suggesting that recombinant genes containing rare codons may be subject to slower translation due to non-saturating amounts of corresponding tRNAs in the host cell (Grosjean and Fiers, 1982; Sorensen *et al.*, 1989). While alternative codons can be used for the same amino acid due to the degeneracy of the genetic code, certain codons tend to be favored over others in different organisms (Grantham *et al.*, 1980). Codon optimisation (to correct for the host organism's specific codon usage bias) was important to ensure optimal expression of the Gly/Ser linker. None of the codons for Ser are rare codons but the GGA codon, which codes for Gly is an *E. coli* rare codon (Table 7-2). Also an analysis of codon pairs used in two glycine-rich linkers by Trinh *et al.*, (2004) found within each of the linkers the presence of one pair (GGA GGC) that is significantly over-represented in mammalian genes. According to their prediction of the codon pair theory described in Gutman and Hatfield, (1989), such over represented codon pairs may introduce bottlenecks to translational speed and affect the amount of protein synthesised. Trinh *et al.*, found that changing the two "slow" codon pairs within the flexible linker, dramatically improved expression levels. The nucleotide choices for the codons selected to comprise the linker were therefore based on commonly used codons in *E. coli* and mammalian genes for glycine and serine; GGT, GGC and TCT, TCC respectively.

### 7.2.6 Cloning and construction of pGSLink

The pGSLink plasmid was constructed to allow for N- or C-terminal positioning of the 6xHis tag linked to the protein of interest by a 21 amino acid linker peptide comprising Gly and Ser residues; (Gly<sub>4</sub>Ser)<sub>4</sub>Gly. The DNA fragment encoding the Linker was prepared in collaboration with Mr. Barry Ryan at DCU by annealing of sense (GSLinkF) and antisense (GSLinkR) oligonucleotides (Table 2-6) followed by PCR extension (Figure 7.11 and Table 2-10). Oligonucleotides were designed and synthesised to code for the 6xHis followed by the GlySer Linker, with an 18 bp overlap for annealing and *NcoI* and *BamHI* restriction sites at the 5' and 3' ends respectively to allow for insertion into pQE60 (Figure 7.12A). An *XmaI* site was included between the 6xHis and the GS Linker (Figure 7.12B) and together with the *NcoI*, *BamHI* and *HindIII* restriction sites of pQE60 would facilitate directional cloning of the fragment of interest with a C-terminal or N-terminal Linker-6xHis (Figure 7.12C).

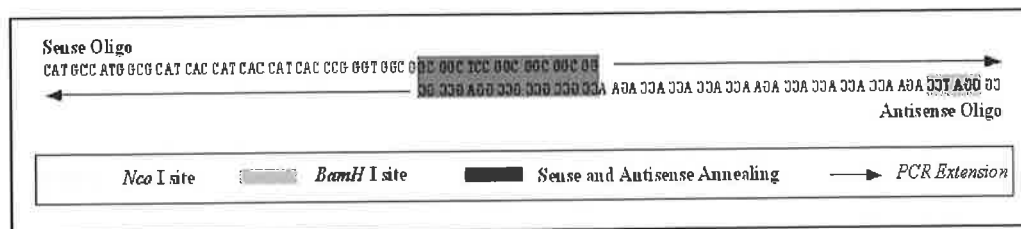


**Figure 7.11 Design and construction of the Linker cassette fragment.**

Oligonucleotides were designed and synthesised to code for the 6xHis followed by the GlySer Linker, with an 18 bp overlap for annealing (shaded grey) and *Nco*I (shaded yellow) and *Bam*HI (shaded green) restriction sites at the 5' and 3' ends respectively. The Linker cassette was constructed by annealing of sense and antisense oligonucleotides followed by extension by 15 cycles of PCR.

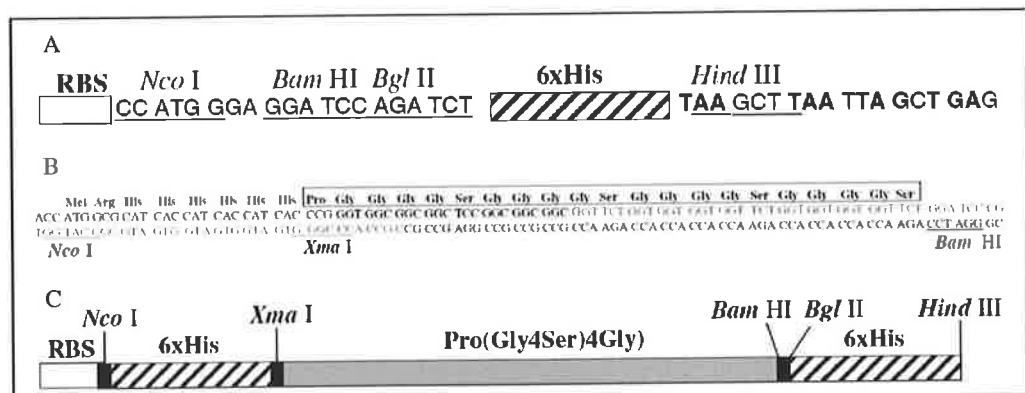


**Figure 7.12 Generation of pGSLink**

(A) Partial sequence and features of the polylinker region of the *E. coli* expression plasmid pQE60. RBS indicates the ribosome-binding site. Restriction enzyme sites are underlined; the location of the coding sequence for the 6xHis-tag is indicated as a striped box; stop codons are shown in boldface. (B) Sequence and features of the PCR product generated using the primers GSLinkF and GSLinkR. The primer sequences are shown in black and bases inserted by *Taq* polymerase are in gray; restriction enzyme sites are underlined. The corresponding amino acid sequences are indicated above the DNA sequence. The GS linker peptide is boxed. (C) Schematic illustration of the pGSLink polylinker region showing relative locations of the sequences encoding the His-tags (striped boxes), GS linker (grey box), and DNA features [RBS (open box) and unique restriction sites (black boxes)].

Following PCR amplification, the double stranded Linker fragments were purified from any remaining PCR reactants using the Wizard PCR Preps DNA purification system, the purified fragments were then digested with *Nco*I and *Bam*HI to produce cohesive ends for ligation into the pQE60 plasmid. Agarose gel electrophoresis of the digested PCR product revealed the expected 0.1 kb DNA band (Figure 7.13A). Purification of digested linker fragments was by phenol-chloroform extraction and ethanol precipitation. Restriction digestion of plasmid DNA (pQE60) was performed using *Nco*I and *Bam*HI followed by dephosphorylation using CIP and purification by phenol-chloroform extraction and ethanol precipitation. The GS Linker fragment was cloned into the *Nco*I/*Bam*HI sites of pQE60. The ligated products were transformed into competent *E. coli* JM109 cells and the positive transformants were selected for ampicillin (100 µg/ml) resistance.

Following overnight incubation at 37 °C, several colonies were randomly selected and individually sub-cultured into fresh 5 ml volumes of LB broth. The selected clones were grown overnight at 37 °C with shaking at 200 rpm, reaching stationary growth phase.

Plasmid isolation was performed on the resulting cell pellet and a sample of each plasmid preparation was then analysed by restriction enzyme mapping.

Digestion of pGSLink with *Nco*I and *Bam*HI revealed the predicted bands of ~0.1 kb respectively indicating that the fusion construct had been successfully generated (Figure 7.13B). In order to determine that the *bfl-1* insert had been faithfully cloned in terms of nucleotide content and was ‘in-frame’, plasmid DNA was sequenced using pQE vector specific forward and reverse primers (Table 2-6) and pGSLink as template DNA and identified as pGSLink (Figure 7.12B). Sequencing results, received as linear nucleotide sequences, were subsequently translated to amino acid sequences and aligned with the expected amino acid sequence of GS linker as described in Section 7.2.1 to reveal 100 % homology.

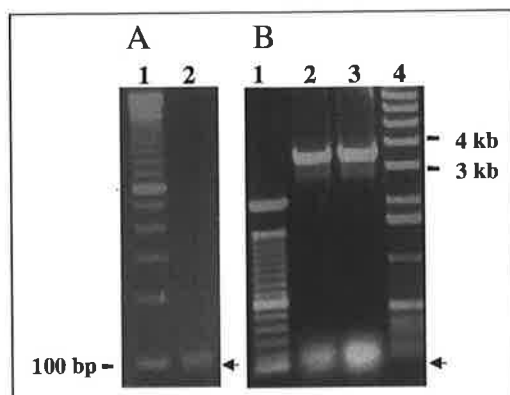


**Figure 7.13 Analysis of the cloning steps in the construction of the expression vector pGSLink**

The amplified DNA fragments encoding His-Linker were about 0.1 kb. Agarose gel electrophoresis (on a 2 % (A), and 0.7 % (B) agarose-1 X TAE gel and electrophoresis was carried out at 100 V for 1 h in 1 X TAE) of the PCR product revealed the expected 0.1 kb DNA bands following digestion with the appropriate restriction enzymes. Lane 1: 100 bp ladder (Invitrogen), Lane 2 His-Linker PCR product 100 bp. (B) Digestion of pGSLink with *Nco*I and *Bam*HI revealed the predicted bands of ~0.1 kb indicating that the fusion construct had been successfully generated. Lane 1: 100 bp ladder (Invitrogen), Lane 2 and 3: pGSLink digested with *Nco*I and *Bam*HI, Lane 4: 1 kb ladder (Invitrogen).

### 7.2.7 Generation of pGSLink-N-Bfl-1 and pGSLink-C-Bfl-1

Human *bfl-1* cDNA was cloned into pGSLink *BamHI/HindIII* sites using PCR with forward and reverse oligonucleotides; GS-N-bflF and GS-N-bflR (Table 2-6) and pCDNA3-HA-Bfl-1 as template (to generate N-terminal tagged construct). The primers were synthesised with terminal ends designed to incorporate dedicated *BamHI* and *HindIII* restriction sequences at the respective 5' and 3' termini of the amplified *bfl-1* gene. Similarly, *bfl-1* cDNA was cloned into pGSLink *NcoI/XmaI* sites using PCR with forward and reverse oligonucleotides; GS-C-bflF and GS-C-bflR (Table 2-6) and pCDNA3-HA-bfl-1 as template (to generate C-terminal tagged construct). The PCR products were purified, double digested with *BamHI/HindIII* or *NcoI/XmaI* to produce cohesive ends, phenol chloroform extracted and ethanol precipitated (Figure 7.14 A shown for GS-N-bfl product only). The pGSLink plasmid DNA was double digested with *BamHI/HindIII* or *NcoI/XmaI*, CIP-treated, phenol chloroform extracted and ethanol precipitated (Figure 7.14 B shown for *BamHI/HindIII* digest only).

Ligation of plasmid and insert was performed using the enzyme T4 DNA ligase for 3 h at 22 °C. The ligated products were transformed into competent *E. coli* RosettaBlue™ cells, the positive transformants were selected and transformed clones were screened by PCR. Amplification of a short fragment of the *bfl-1* gene using *bfl-1* specific primers (*bfl-1F/bfl-1R* Table 2-6) and pGSLink-N-Bfl-1 or pGSLink-C-Bfl-1 transformant DNA as template revealed a 100 bp band indicating that the fusion construct had been successfully generated (Figure 7.14 C shown for pGSLink-N-Bfl-1 only). In order to determine that the *bfl-1* insert had been faithfully cloned in terms of nucleotide content and was ‘in-frame’, plasmid DNA was sequenced (data not shown) using pQE vector specific forward and reverse primers (Table 2-6). Sequencing results, received as linear nucleotide sequences, were subsequently translated in amino acid sequences as described in Section 7.2.1 and aligned with the known amino acid sequence of the Bfl-1 protein using the ClustalW multiple alignment program. The pGS-N-Bfl-1- and pGS-C-Bfl-1-derived plasmid DNA, when translated, demonstrated 100 % homology with the native Bfl-1 protein as derived from the Bfl-1 coding sequence with GenBank accession number U27467 (data not shown). The physico-chemical parameters of the protein sequences were calculated using the ProtParam tool (parameters deviated only slightly from those predicted in Table 7-1 for His-Bfl-1 and Bfl-1-His, apart from molecular

weight, predicted to be 22.8 kDa, the small increase being due to the presence of the linker).

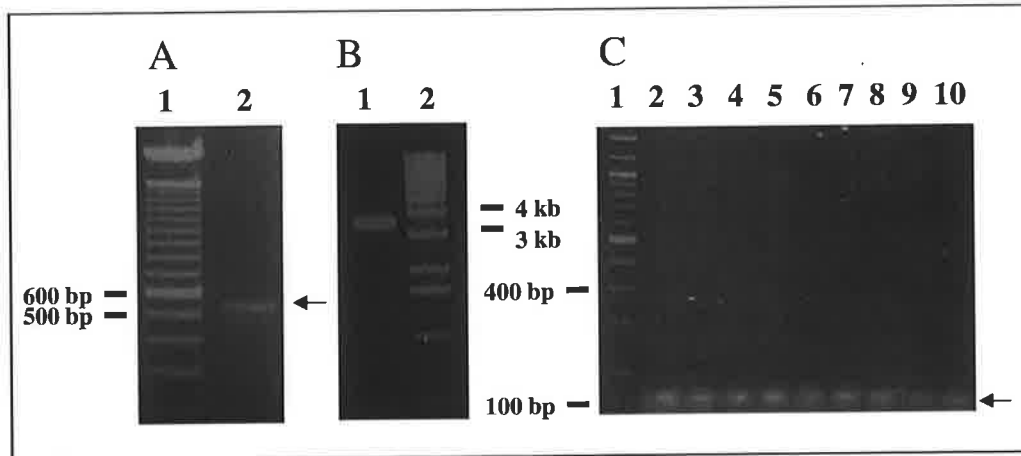


**Figure 7.14 Analysis of the cloning steps in the construction of the expression vector pGSLink-N-Bfl-1.**

The amplified DNA fragments encoding *bfl-1* was about 0.53 kb. Agarose gel electrophoresis (on a 2 % (A and C), and 0.7 % (B) agarose-1 X TAE gel carried out at 100 V for 1 h in 1 X TAE) of the PCR product revealed the expected 0.53 kb DNA bands following digestion with *Bam*HI and *Hind*III restriction enzymes (A). Lane 1: 100 bp ladder (Invitrogen), Lane 2 *bfl-1* PCR product 532 bp indicated by a black arrow. (B) Digestion of pGSLink with *Bam*HI and *Hind*III revealed a single band of ~3.4 kb indicating that the plasmid DNA was completely linearised. Lane 1: pGSLink digested with *Bam*HI and *Hind*III, Lane 2: 1 kb ladder (Invitrogen). (C) A PCR assay was used to verify the presence of the *bfl-1* insert in potential pGSLink-N-Bfl-1 clones. The amplified DNA fragments encoding *bfl-1* was about 0.1 kb, indicated by a black arrow. Lane 1: 100 bp ladder (Invitrogen), Lane 2-10: PCR products (pGSLink-N-Bfl-1 clones as template DNA).

## 7.2.8 Expression screening and purification of His-Linker-Bfl-1 and Bfl-1-Linker-His fusion proteins

Several single colonies of selected transformant clones were used to inoculate overnight cultures to screen for the expression of His-Linker-Bfl-1 and Bfl-1-Linker-His. Expression cultures were induced to express recombinant proteins by addition of IPTG to logarithmic phase cultures (Section 7.2.2). SDS-PAGE analysis of cell lysates revealed a single major protein band of the expected ~23 kDa size (Figure 7.15).

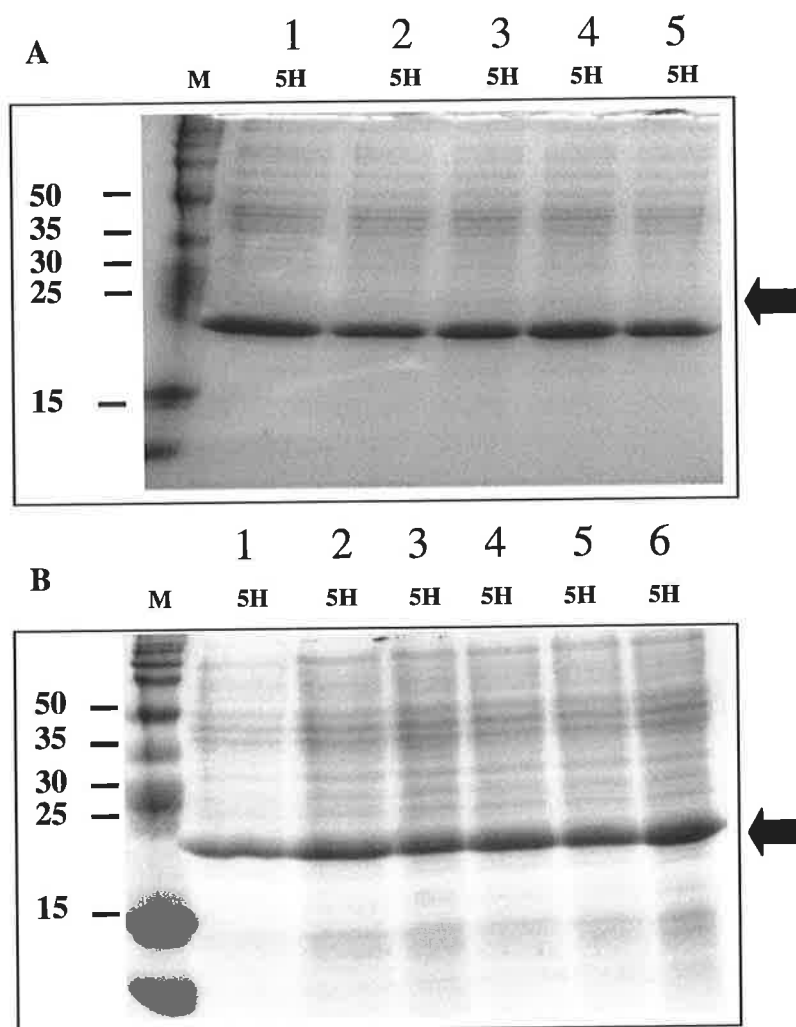


**Figure 7.15 Expression screening of recombinant pGSLink-N-Bfl-1 and pGSLink-C-Bfl-1 clones**

Selected transformants were screened for expression of the His-Linker-Bfl-1 (A) and Bfl-1-Linker-His (B) proteins by preparation of small-scale expression cultures followed by cell lysis at 5 h post induction and SDS-PAGE analysis. Expression of His-Linker-Bfl-1 and Bfl-1-Linker-His proteins were detected at predicted molecular weight of ~23 kDa. Lane M: Marker (Amersham), lane 1-5/1-6: pGSLink-N-Bfl-1(A)/pGSLink-C-Bfl-1(B) recombinant clones. The molecular weight markers are indicated on the left and black arrowheads designate the location of recombinant Bfl-1.

Western blot analysis (Section 2.7.4) of expression lysates was performed to certify the integrity of the His tag prior to purification (Figure 7.16). Nitrocellulose membrane with transferred electrophoresed proteins from expression lysates were probed with an anti-

His monoclonal antibody which had been conjugated with HRP. Chromogenic detection of HRP and consequently the presence of His tag moieties of the fusion proteins was evident as can be seen in Lanes 1 and 2 for His-Linker-Bfl-1 and Bfl-1-Linker-His proteins respectively.

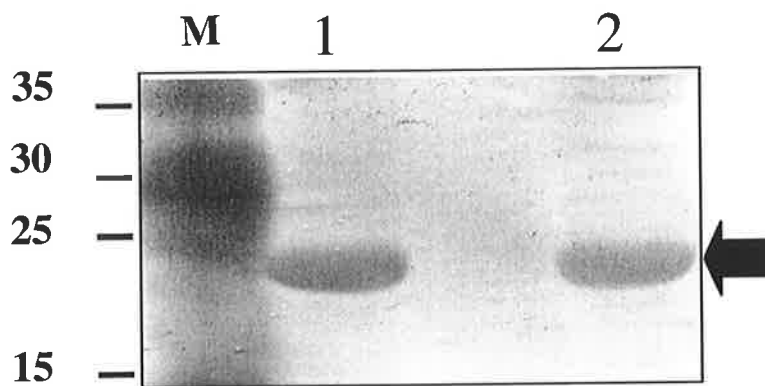


**Figure 7.16 Western blot analysis of His-Linker-Bfl-1 and Bfl-1-Linker-His proteins**

Immunoreactivity of HRP-labeled anti-His monoclonal antibody (Sigma-Aldrich) with expression lysates of *E. coli* RosettaBlue™ harbouring pGSLink-N-Bfl-1 and pGSLink-C-Bfl-1. His-Linker-Bfl-1 (Lane 1) and Bfl-1-Linker-His (Lane 2) proteins were detected at predicted molecular weight of ~23 kDa. The molecular weight markers (Lane M (Amersham)) are indicated on the left and black arrowheads designate the location of recombinant Bfl-1.

Purification of His-Linker-Bfl-1 and Bfl-1-Linker-His was achieved in a column procedure (Section 2.8.3.2) under native and denaturing conditions (Figure 7.17; shown for His-Linker-Bfl-1 under native conditions only).

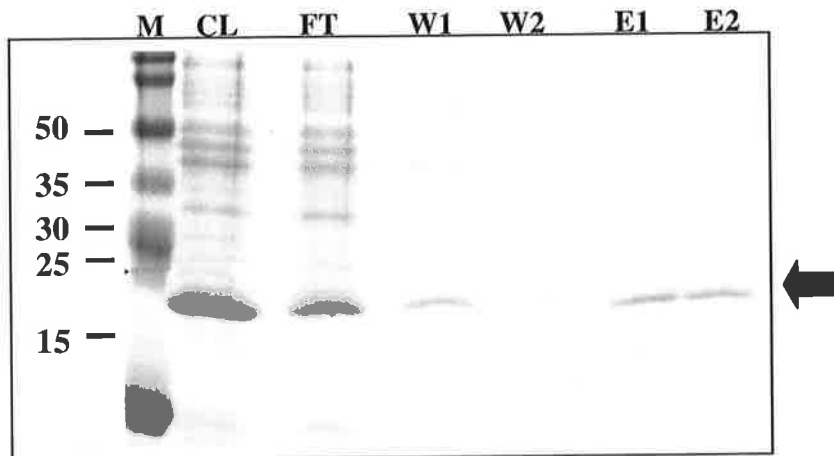


**Figure 7.17 Purification of His-Linker-Bfl-1**

Recombinant protein purification of His-Linker-Bfl-1 under native conditions using Ni-NTA resin. M: Marker (Amersham), CL: Cleared cell lysate, FT: Flow through, W1 and W2: Wash with 10 mM imidazole buffer, E1-2: Elution with 250 mM imidazole buffer. The molecular weight markers are indicated on the left and black arrowheads designate the location of recombinant Bfl-1.

### 7.2.9 Optimisation of purification

Once purification was achieved, the optimal conditions for purification were determined empirically. Purification of His-Linker-Bfl-1 and Bfl-1-Linker-His was optimised by performing a series of minicolumn native purifications (Section 7.2.8) with variation of imidazole concentrations in the lysis, wash and elution buffers to achieve optimal binding levels for the recombinant fusion proteins yet minimise non-specific binding of contaminant proteins (Figure 7.18). Optimal binding of recombinant protein with minimum non-specific binding to the Ni-NTA matrix was achieved when the imidazole concentration was reduced to 2 mM and when the lysate was passed over the column a further three times. The improved level of binding can be seen by comparing the CL and FT fractions of Figure 7.17 and Figure 7.18. The high level of His-Linker-Bfl-1 protein in the FT fraction of Figure 7.17 indicates sub-optimal binding and ‘run-through’ of the desired protein. The yield of purified protein in E1/E2 fractions is therefore detrimentally affected. Co-purification of contaminants was not a significant problem, however, elution of the protein of interest during wash steps was minimised by ensuring a low stringency wash with 4 mM imidazole buffer. A step gradient of imidazole

concentration for optimal elution indicated the greatest yield of purified protein could be achieved with a 400 mM imidazole buffer.

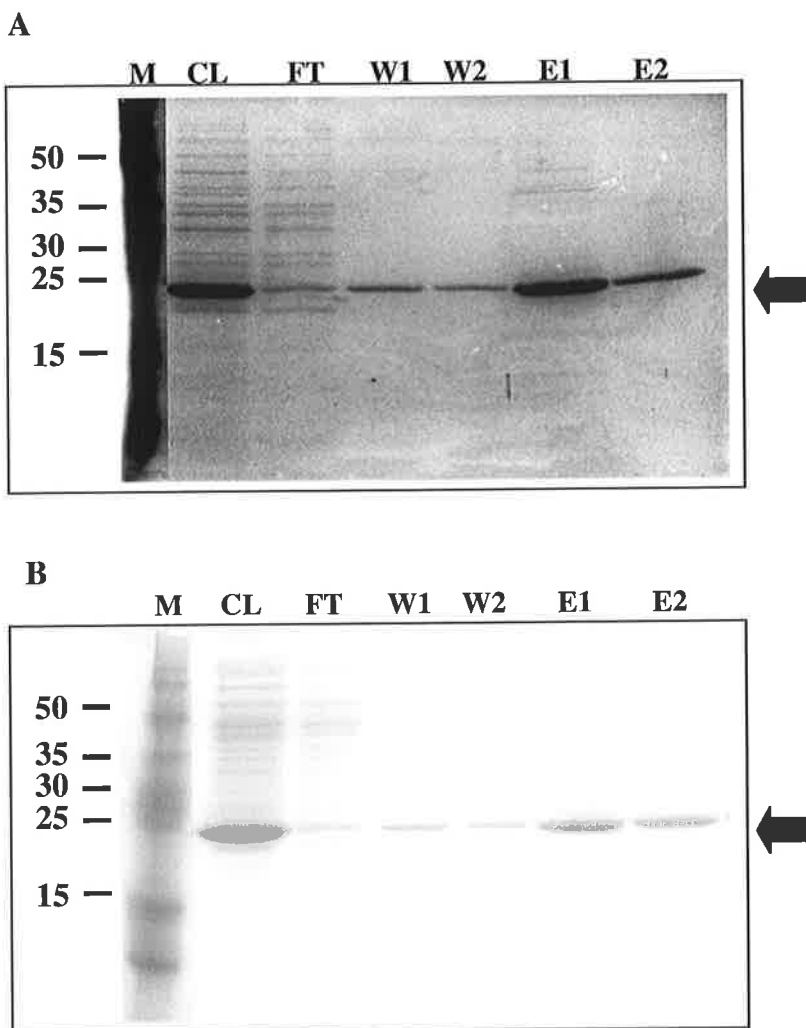


**Figure 7.18 Optimisation of purification of His-Linker-Bfl-1 and Bfl-1-Linker-His under native conditions.**

Recombinant protein purification of His-Linker-Bfl-1 (A) and Bfl-1-Linker-His (B) under native conditions using Ni-NTA resin. M: Marker (Amersham), CL: Cleared cell lysate, FT: Flow through, W1 and W2: Wash with 4 mM imidazole buffer, E1-2: Elution with 400 mM imidazole buffer. The molecular weight markers are indicated on the left and black arrowheads designate the location of recombinant Bfl-1.

In contrast to His-tagged Bfl-1 expressed from pQE30 and pQE60, the equivalent recombinant proteins were readily purifiable by IMAC when expressed from pGSLink-

NBfl-1 and pGSLink-C-Bfl-1 (compare Figure 7.19A and B). These results directly implicated the presence of the peptide linker as being key to enabling successful purification.

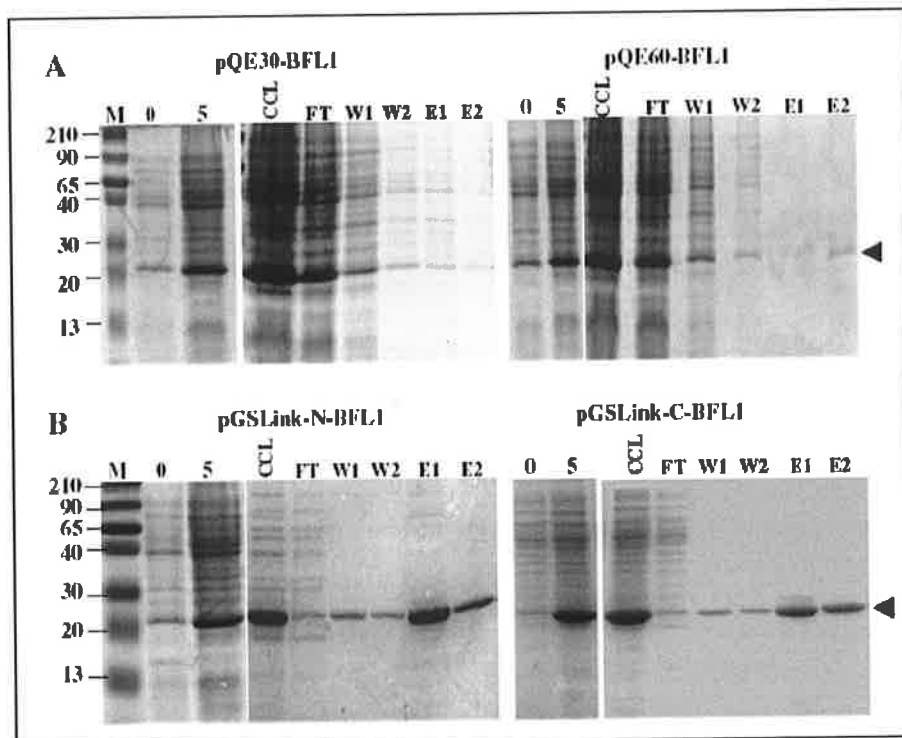


**Figure 7.19 Expression and purification of recombinant His-tagged Bfl-1 in *E. coli***

(A and B) Total *E. coli* proteins were prepared from recombinant clones following IPTG induction. Cells were lysed in native lysis buffer and purification of His-tagged proteins was carried out using a batch column procedure under native conditions. Samples from purification stages were analyzed by SDS-PAGE (15 % separating gel, 5 % stacking gel) followed by staining with Coomassie blue. Lanes: M, markers (indicated on the left in kDa); 0 and 5, hs post induction with 0.1 mM IPTG; CCL, cleared cell lysate; FT, flow through; W1 and W2, washes 1 and 2; E1 and E2, elutions 1 and 2. The location of recombinant Bfl-1 is indicated with black arrowheads.

### 7.2.10 Antigen Preparation

Optimised purification conditions were then used to prepare protein from large-scale expression cultures (Section 2.8.4). The resulting eluates were pooled and applied to an Amicon™ ultra-filter (Section 2.8.5) with a 10 kDa cut-off to allow for protein concentration and buffer exchange to PBS (Appendix), the desired buffer for immunisation. The concentration of the resultant protein solution in PBS (analysed by SDS-PAGE in Figure 7.20) was determined to be ~0.8 mg/ml by measuring absorbance at 280 nm using a Nanodrop™ spectrophotometer and was based on the protein molecular weight and extinction co-efficient (Table 7-1) predicted in Section 7.2.7.

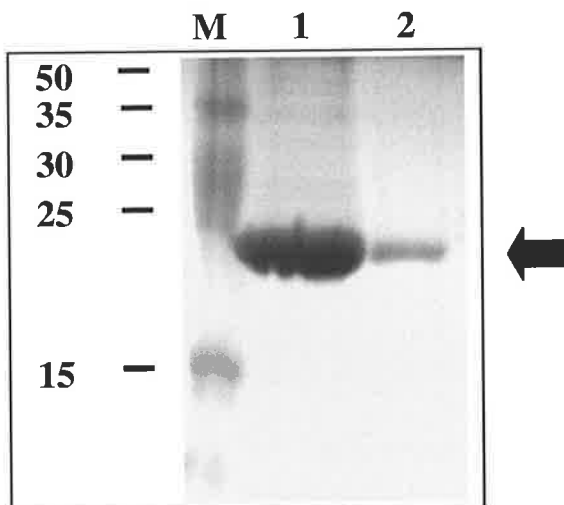


**Figure 7.20 Purified concentrated Bfl-1 recombinant protein**

Pooled eluates from preparative purification were concentrated using an Amicon™ ultrafilter and the solvent buffer was simultaneously exchanged to PBS. The concentration of the resultant protein preparation in PBS was determined to be ~0.8 mg/ml and the integrity of same was monitored by SDS-PAGE. Lanes; M, Marker (Amersham), Lane 1/2, concentrated protein preparation: neat/1/10 dilution. The molecular weight markers are indicated on the left and black arrowheads designate the location of recombinant Bfl-1.

### 7.2.11 Antibody preparation and analysis by ELISA and western blotting

Prepared antigen was subsequently used to immunise a rabbit in order to generate polyclonal antibodies directed against Bfl-1. Custom Hybridoma laboratories (The Netherlands) carried out immunisation and maintenance of the rabbit followed by blood collection and sera recovery. The presence of antibodies in the rabbit serum specific for the His-tagged Bfl-1 antigen was confirmed by ELISA (Figure 7.21; performed by Custom Hybridoma laboratories).

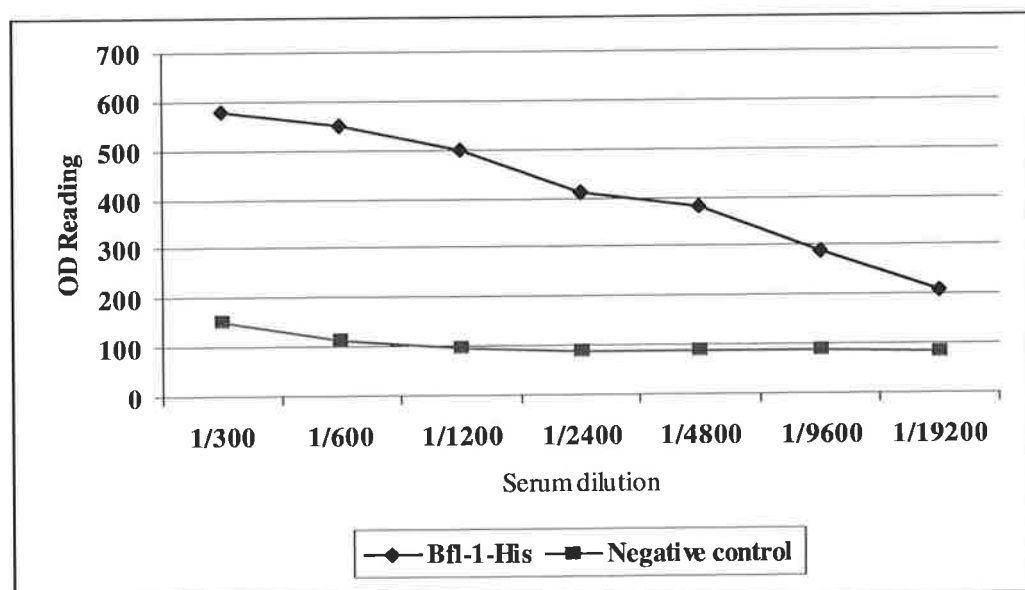
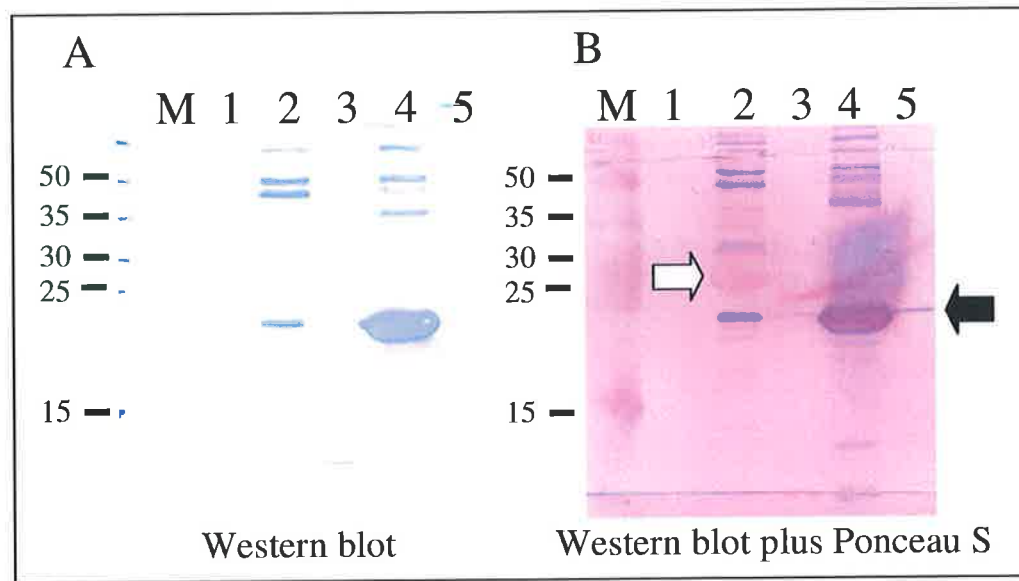


Figure 7.21 ELISA to detect BFL-1-His in immune serum

The Bfl-1-His antigen was attached to polysorb plates. Rabbit serum was applied in the respective dilution for 2 h at room temperature. Specific IgGs were detected using Gamma-chain specific anti-rabbit IgG-HPRO conjugate. Data presented as averages OD readings for the respective wells. (1 OD = 1000). Reaction is stopped by reaching 1000.

The presence of Bfl-1-specific antibodies in the rabbit serum was confirmed by western blot analysis (Section 2.7.4) of expression lysates. Nitrocellulose membrane with transferred electrophoresed proteins from expression lysates was blocked with 5 % marvel and probed with rabbit serum diluted in 5 % marvel (range of dilutions; 1/50, 1/150, 1/500 and 1/1000). An anti-rabbit antibody conjugated to alkaline phosphatase

(AP) was used to detect primary antibody binding. Chromogenic detection of AP was achieved by application of AP substrate, BCIP, to the membrane.



**Figure 7.22 Western blot using rabbit anti-sera**

(A) Immunoreactivity of rabbit anti-sera (diluted 1/1000 in 5 % marvel) with expression lysates of *E. coli* RosettaBlue™ harbouring pGSLink-N-Bfl-1 (Lane 4) or *E. coli* strain harbouring plasmid expressing unrelated His-tagged recombinant protein (Lane 2). His-Linker-Bfl-1 (Lane 4) protein was detected at predicted molecular weight of ~23 kDa. The molecular weight markers (Lane M (Amersham)) are indicated on the left and black arrowheads designate the location of recombinant Bfl-1. (B) Developed western blot membrane overlaid with Ponceau S protein stain to highlight the position of the unrelated overexpressed His-tagged protein in Lane 2 at ~29 kDa, designated by a white arrow.

The antisera produced in response to the supplied antigen (Bfl-1 protein separated from His tag by GS linker) had no cross-reactivity with the unrelated His-tagged recombinant protein procured from the Applied Biochemistry group at DCU, revealed in lane 2 of Figure 7.22B (indicated by white arrow). This overexpressed unrelated His-tagged protein was exposed when the developed western blot was overlaid with Ponceau S to stain for total protein. The lack of signal in Figure 7.22A at the molecular weight of this unrelated overexpressed tagged protein (~29 kDa) indicated that the antibodies produced were specific for the Bfl-1 fusion partner and not directed against the His tag portion of the recombinant antigen (Figure 7.22A; lane 4). The anti-sera also detected some non-specific proteins in the *E. coli* lysate including one resolving at the same

molecular weight as the Bfl-1 recombinant protein (Figure 7.22A; lane 2), these are most likely due to the presence of low-level contaminant *E. coli* proteins in the antigen preparation. The anti-sera detected the Bfl-1 recombinant protein over the range of dilutions tested (1/50, 1/150, 1/500 and 1/1000) by western blotting.

### 7.3 Discussion

The polyhistidine-tag, which utilises IMAC to purify recombinant proteins containing a short affinity-tag consisting of polyhistidine residues is a small tag and is not as immunogenic as large tags (such as glutathione s-transferase or maltose-binding protein) and can be used directly as an antigen in antibody production, without the need for tag cleavage.

Many authors have cited the need for good quality anti-Bfl-1 antibody preparations in recent years. In this study it was chosen to prepare His-tagged recombinant Bfl-1 protein for rabbit immunisation and production of anti-Bfl-1 polyclonal antibodies. The generation of N- or C-terminal His-tagged Bfl-1 using the expression vectors pQE60 and pQE30 is described. These vectors were chosen for this purpose as they permit the high-level and regulatable expression of His-tagged recombinant proteins. Initial efforts to express recombinant His-tagged Bfl-1 using pQE30-Bfl-1 and pQE60-Bfl-1 were unsuccessful. The use of an *E. coli* strain engineered to supply tRNAs rarely expressed in *E. coli* enabled protein expression by overcoming a codon bias.

The subsequent failure to purify His-Bfl-1 and Bfl-1-His proteins by IMAC presented another challenge in this study. To overcome this barrier, a modified expression vector was constructed using the pQE60 vector as backbone. In addition to the features offered by the pQE60 vector, the modified vector (pGSLink) allows expression of the protein of interest linked to a His-tag by a flexible GS linker. It was reasoned that insertion of a spacer or linker peptide between the two moieties of the fusion protein would enhance the flexibility of the His-tag to adopt a range of conformations and maximise the opportunity for interaction with resin binding sites during IMAC.

The modified vector pGSLink permits the positioning of a 6xHis-tag linked to any protein of interest by a 21-amino acid (Gly<sub>4</sub>Ser)<sub>4</sub>Gly linker. The rationale for using a linker with this particular sequence was that (i) the serine residues would enhance the hydrophilicity of the peptide backbone to allow hydrogen bonding to solvent molecules,

(ii) the glycine residues would provide the linker with flexibility to adopt a range of conformations and maximise the opportunity for interaction with resin binding sites during IMAC (Argos, 1990), (iii) these properties could also serve to prevent interaction of the linker peptide with hydrophobic interfaces on protein domains, and (iv) the linker peptide would be poorly immunogenic, a particular advantage when the recombinant protein is to be used directly as an immunogen (the His-tag itself is small and does not need to be removed prior to immunisations). In another study, the plasmid pKW32 was generated so as to permit the expression of recombinant proteins with His-tagged bacterial hemoglobin (VHb; 15.7 kDa) as an N-terminal fusion partner (Kwon *et al.*, 2005), with a requirement for subsequent enzymatic removal of the VHb domain. In an effort to resolve IMAC purification difficulties associated with some proteins, that vector was recently modified to include a short glycine-rich sequence distal to the N-terminal VHb domain/His-tag. Here, however, in addition to the difference in linker peptide design, pGSLink distinguishes itself as a tool for similar purposes in that it offers the possibility of generating both N- and C-terminal glycine/serine linker-separated His-tagged fusion proteins from one vector, as demonstrated here using the human *bfl-1* ORF, or double N- and C-terminal His-tagged proteins simultaneously, depending on the cloning sites used, and does not necessitate cleavage and repurification steps post-IMAC.

In order to determine if the presence of the linker could detrimentally affect protein folding and/or functionality, the horse radish peroxidase (HRP) ORF was cloned into *NcoI* and *XmaI* sites of the pGSLink construct by Mr. Barry Ryan at DCU. The HRP-Linker-His protein was expressed and purified under denaturing conditions and subsequently refolded. The His-linked-HRP protein was subsequently assayed for HRP enzymatic activity using a chromogenic assay and was found to be active. The presence of the Linker therefore did not interfere with protein folding or function.

Our strategy could also be applied to enhance the purification of His-tagged proteins made from yeast, mammalian cells and baculovirus-infected insect cell systems. As a tool, His-tagging is increasingly being used in peptide/protein chip design, high-throughput purification, peptide/protein libraries, large-scale production systems, and drug delivery strategies. This modified vector and particular linker design may be of general use in assisting to overcome problems associated with the purification of recombinant proteins.

The pGSLink vector was instrumental in obtaining purified antigen by IMAC in this project. The presence of the linker moiety facilitated purification of recombinant tagged Bfl-1 protein, which was then used for rabbit immunisation. The antisera produced in response to the antigen (Bfl-1 protein separated from His tag by GS linker) detected recombinant Bfl-1 by ELISA and at the predicted molecular weight by western blotting over a range of tested dilutions. The anti-sera had no cross-reactivity with an unrelated His-tagged recombinant protein indicating that the His tag did not illicit an immune response in the animal. The anti-sera is currently being tested for its ability to detect endogenous Bfl-1 protein in human cell lines by western blotting. Once optimised, this reagent will serve as a valuable tool for monitoring Bfl-1 expression at the protein level in related studies in our laboratory.

Mechanistic studies of the contribution of *bfl-1* to cell survival will provide important information about both normal B cell development and potential routes to B cell malignancy and the need to correlate mRNA expression with the protein level is increasingly imperative.

## **CHAPTER 8 General Discussion**

The development, maintenance, and progression of malignant lymphomas depend mechanistically on a deregulation of cellular pathways that control differentiation, proliferation, or apoptosis in lymphocytes (Jost and Ruland, 2007). Impaired apoptosis is both critical in cancer development and a major barrier to effective treatment, and the Bcl-2 family of apoptosis-regulating proteins is a recognised source of potential targets for molecular cancer therapy (reviewed in Adams and Cory, 2007; Letai, 2005; Kirkin *et al.*, 2004). Bcl-2 family members are essential regulators of the intrinsic apoptotic pathway, the physiological result of a pro-apoptotic decision beginning with permeabilisation of the mitochondrial outer membrane. The commitment to apoptosis involves complex interactions among pro- and anti-apoptotic Bcl-2 family proteins. Anti-apoptotic members share sequence homology in four  $\alpha$ -helical Bcl-2-homology (BH) domains, BH1-BH4 [Bcl-xL, Bcl-w, Bfl-1 (A1) and Mcl-1], whereas others which possess only BH1-3 domains (Bax and Bak) promote death. The balance is displaced in favour of death by BH3 only proteins (including Bim, Bad, Bid, Nbk/Bik, Bmf, Hrk, Puma and Noxa), which interact with Bcl-2-like proteins and inactivate their function (reviewed in Willis and Adams, 2005). Deregulation of Bcl-2 family function or expression contributes to the oncogenic transformation of normal cells (reviewed in Kirkin *et al.*, 2004).

Bcl-2 family proteins have been linked to many chronic degenerative diseases of excessive cell death through gain of pro-apoptotic or loss of anti-apoptotic Bcl-2 family members (reviewed in Letai, 2005). Cancer, one of the most common diseases known to man, with more than 10 million people diagnosed every year throughout the world (World Health Organisation, 2004), is a disease characterised by deficient cell death. Infact, Bcl-2 was initially identified and cloned from the breakpoint of the t(14;18) chromosomal translocation found in the vast majority of patients with follicular lymphoma, an indolent B-cell NHL (Tsujimoto *et al.*, 1985; Cleary and Sklar, 1985; Bakhshi *et al.*, 1985). Aberrant expression of several of the Bcl-2 family members in neoplastic disease has now been reported and implicated in tumourigenesis (reviewed in Heiser *et al.*, 2004).

Anti-apoptotic Bcl-2 family member, Bfl-1, originally identified as a hematopoietic specific early response gene by Choi *et al.*, in 1995, has been reported to be expressed in several epithelial and hematopoietic malignancies. In B cell chronic lymphocytic leukaemia, high expression of *bfl-1* contributes to the apoptosis resistant phenotype (Morales *et al.*, 2005) and engagement of surface IgM elicits a survival programme that is associated with upregulation of Bcl-2, Mcl-1 and Bfl-1 anti-apoptotic proteins

(Bernal *et al.*, 2001). Elsewhere, overexpression of the murine homologue of Bfl-1, A1, protects murine B lymphoma cells from anti-IgM-induced apoptosis (Craxton *et al.*, 2000). Also, in mantle cell lymphomas, inhibition of constitutively activated NF-κB pathway leads to tumour cell apoptosis in association with the down-regulation of *bfl-1* expression (Pham *et al.*, 2003). *Bfl-1* has been identified in molecular profiling experiments of large B cell lymphomas (Feuerhake *et al.*, 2005; Monti *et al.*, 2005) and recently, Brien and coworkers demonstrated that Bfl-1 silencing in two cell lines of diffuse large B-cell lymphoma potently induced apoptosis and sensitised these cell lines to apoptosis induced by chemotherapeutic molecules (Brien *et al.*, 2007).

*Bfl-1* is preferentially expressed in hematopoietic and endothelial cells (Choi *et al.*, 1995), and its expression is controlled by inflammatory stimuli such as TNF and IL-1. Bfl-1 suppresses p53-mediated apoptosis and can inhibit the pro-apoptotic activities of other Bcl-2 members (D'Sa Eipper and Chinnadurai, 1998; D'Sa Eipper *et al.*, 1996; Werner *et al.*, 2002; Zhang *et al.*, 2000). *Bfl-1* is a direct transcriptional target of NF-κB (Grumont *et al.*, 1999; Wang *et al.*, 1999; Zong *et al.*, 1999; D'Souza *et al.*, 2004) and its induction through a CD40/NF-κB pathway is associated with increased resistance to BCR-mediated cell death in B cell lines and mature B cells (Grumont *et al.*, 1999; Kuss *et al.*, 1999; Lee *et al.*, 1999; Wang *et al.*, 1999; Zong *et al.*, 1999). It was previously shown in our laboratory that *bfl-1* is upregulated by the EBV proteins, LMP1 (D'Souza *et al.*, 2004) and EBNA2 (Pegman *et al.*, 2006), and that it confers protection from apoptosis induced by growth factor withdrawal when expressed ectopically in an EBV-negative Burkitt's lymphoma-derived cell line (D'Souza *et al.*, 2000).

H/RS cells of HL represent clonal progeny of GC B-cells that contain nonfunctional IgG suggesting that they are derived from GC cells that should have been negatively selected but instead evaded apoptosis. The H/RS cell expression patterns of Bcl-2 family members, Bad, Bim, Bid, Bcl-2, Bcl-x, Bcl-x<sub>L</sub>, Mcl-1, Bax, and Bak have all been reported to date. One study reported the absence of Bcl-2 and Bcl-xL expression in a significant proportion of cHL cases (56.5 % and 32.8 % respectively), observations that suggest a role for other anti-apoptotic proteins in ensuring the survival of EBV+ H/RS cells (Kim *et al.*, 2004). Despite many extensive studies, information on the status of *bfl-1* expression is limited to an observation in Hinz *et al.*, (2002), that *bfl-1* mRNA expression was downregulated in a H/RS cell line following NF-κB inhibition by microarray analysis. It was an aim in this study to further the current understanding of

the molecular mechanisms that cause the H/RS cell to survive by elucidating the expression status and role of the *bfl-1* gene in HL.

NF-κB signaling is a tightly regulated cascade that mediates development, activation, and survival of normal T- and B-lymphocytes for regulated immune responses. However, aberrant NF-κB activation can promote continuous lymphocyte proliferation and survival and has recently been recognised as a hallmark of several lymphoid malignancies. Constitutive activity of NF-κB has been detected in primary H/RS cells (Bargou *et al.*, 1996 and 1997) (reviewed in detail in Chapter 1). Multiple defects in the homeostatic regulation of NF-κB have been uncovered in all cultured H/RS cells tested so far, such as the aberrant activation of IKKs or the failure to express functional IκBα proteins, thereby giving a survival advantage to the tumour cell (Krappman *et al.*, 1999; Jungnickel *et al.*, 2000).

As *bfl-1* expression can be driven by NF-κB, it was reasoned that *bfl-1* was therefore a candidate gene that might play an important anti-apoptotic role in HL. Indeed, one study identified *bfl-1* by DNA microarray analysis as part of a network of genes whose expression was transcriptionally down-regulated in a HL-derived cell line upon transduction with a recombinant adenovirus expressing the super-repressor IκBαDN (Hinz *et al.*, 2001). As yet however, there are no reports of *bfl-1* expression in primary H/RS cells *in vivo*, or any investigation into a role for this anti-apoptotic gene in HL.

Here, evidence is presented in Chapter 3 that *bfl-1* is expressed in both primary H/RS cells from HL tumour biopsies and H/RS-derived cell lines irrespective of their EBV status. The detection of *bfl-1* mRNA in bystander/reactive cells of HL biopsies was not surprising. Cytokines produced by H/RS cells are thought to contribute to the pathogenesis of this disease both by acting as autocrine (affecting the H/RS cell itself) and paracrine growth factors by initiating and sustaining the reactive infiltrate (Skinnider and Mak, 2002) and may be responsible for the expression of *bfl-1* in neighbouring cells by activation of various signalling pathways (discussed in detail in Section 3.3). Similarly, cytokines produced by surrounding reactive cells may be contributing to H/RS cell proliferation and survival.

The lack of expression of the *bik* gene in cultured H/RS cells (Chapter 3) is a subject that merits further investigation which is ongoing in the laboratory, but for the purpose of this study was not pursued any further.

NF-κB modulation is a therapeutic endeavour of increasing interest, in particular concerning hematologic malignancies (reviewed in Panwalkar *et al.*, 2004). Inhibition of NF-κB by exogenous expression of a super-repressor IκBα has shown that NF-κB activity is required for proliferation and the raised threshold of resistance to apoptosis seen in H/RS cells (Bargou *et al.*, 1997; Hinz *et al.*, 2001). Inhibition of NF-κB by arsenic trioxide has also been shown to sensitise HL cells to apoptosis indicating that pharmacological blockade of NF-κB might be a powerful treatment option for HL (Mathas *et al.*, 2003). Mathas *et al.*, (2003), demonstrated in *in vivo* experiments with xenotransplanted H/RS cell lines in nonobese diabetic severe combined immunodeficient (NOD/Scid) mice, a substantial reduction of the tumour volume in arsenite-treated animals compared with controls. This reduction was directly associated with decreased NF-κB activity in isolated tumor cells, indicating that strategies to inhibit the NF-κB pathway should be developed as therapies for HL. The findings presented here in Chapter 4 with BAY 11 and sodium arsenite support these studies, again demonstrating that constitutive NF-κB is required for resistance to apoptosis in H/RS cells.

Loss of *bfl-1* mRNA expression was observed upon NF-κB inhibition in H/RS-derived cell lines in Chapter 4, indicating that *bfl-1* is an important NF-κB target gene in this cell context. In order to test if ectopic expression of Bfl-1 could protect these cells from NF-κB-inhibitor-induced apoptosis, it was essential to have a system in which *bfl-1* could be expressed as the sole protein independently of other NF-κB target proteins. For this reason, a vector capable of inducible expression (by addition of tetracycline) of Bfl-1 protein fused to the hemagglutinin tag was constructed and employed. In cells induced to express exogenous Bfl-1 however, apoptotic death was almost completely inhibited at the same inhibitor concentrations used in the controls. In this dual expression system, the amount of GFP in a given cell was proportional to the level of exogenous Bfl-1, and it is clearly to be seen in these experiments that even those cells expressing the lowest levels of GFP were rescued from apoptosis induced using the NF-κB inhibitors. Together, these results indicate that *bfl-1* is a key NF-κB target gene in H/RS cells and show for the first time that ectopic expression of Bfl-1 protects H/RS cells from apoptosis induced by chemotoxic NF-κB inhibitors.

As discussed in Chapter 4, ectopic expression of Bcl-2 family members has been shown previously to protect malignant cells from apoptosis. Wagner *et al.*, (1993), showed that Bcl-2 effectively inhibited Myc-induced apoptosis in serum-deprived Rat 1a fibroblasts

without blocking entry into the cell cycle. Elsewhere, high-level expression of an exogenous *bcl-2* gene, introduced into IL-6-dependent B9 myeloma cells via retroviral or bovine papilloma virus-based vectors, was shown to suppress apoptotic death following cytokine deprivation (Schwarze and Hawley, 1995). Alam *et al.*, (1997), demonstrated that overexpression of Bcl-xL or Bcl-2, protected the BL cell line, Ramos, from apoptosis induction in response to calcium ionophore, anti-Ig and macromolecular synthesis inhibition. However, in contrast to Bcl-2 in that study, ectopic overexpression of Bcl-xL did not rescue Ramos cells from Fas-mediated apoptosis. In H/RS cell context, infection of the L428 cell line with a recombinant adenoviral vector expressing the super-repressor I $\kappa$ B $\alpha$ DN, which inhibits NF- $\kappa$ B activation, induced an apoptotic response that was rescued by ectopic expression of Bcl-xL (Hinz *et al.*, 2001).

Elevated levels of several anti-apoptotic proteins would increase the range of apoptotic stimuli against which the host cell can protect itself, since the overlap in the range of apoptotic stimuli to which different anti-apoptotic proteins can respond is not always complete. For instance, although Bcl-2 and A20 can independently protect cells against a number of different apoptotic stimuli, Bcl-2 but not A20 is effective against glucocorticoid-induced apoptosis (Oripipari *et al.*, 1992). In addition to protecting against p53-mediated apoptosis, Bfl-1 protects against apoptosis induced by serum deprivation and TNF- $\alpha$ -induced cytotoxicity and it exhibits cell proliferation and transforming activities *in vitro* (Karsan *et al.*, 1996a; D'Souza *et al.*, 2000; D'Sa Eipper *et al.*, 1996; D'Sa Eipper and Chinnadurai, 1998). Furthermore, functional dissection of the protein suggests that its anti-apoptotic and transforming activities may be linked (D'Sa Eipper 1998).

There is evidence that anti-apoptotic Bcl-2 proteins such as Bcl-x<sub>L</sub>, Bcl-w, Bcl-2, and Mcl-1 have anti-proliferative effects in *in vitro* systems (O'Reilly *et al.*, 1996; Huang *et al.*, 1997; Rathmell *et al.*, 2000; Craig, 2002; Gil-Gomez *et al.*, 1998; Fujise *et al.*, 2000). For example, bcl-x<sub>L</sub> and bcl-2 enhance G0 arrest and delay G0- to G1 transition in fibroblasts (Janumyan *et al.*, 2003). Furthermore, Bcl-2 protein expression correlates with lower proliferative activity (S-phase fraction measured by flow cytometry) in intermediate and high-grade non-HL (Winter *et al.*, 1998). Unlike other anti-apoptotic Bcl-2 proteins, Bfl-1 has been shown to facilitate proliferation of rat kidney epithelial cells (D'Sa-Eipper and Chinnadurai, 1996; D'Sa-Eipper *et al.*, 1998). Here, ectopic expression of Bfl-1 had no anti-proliferative effect in L428 cells in agreement with

previously reported data relating to overexpression of A1, the mouse homolog of Bfl-1 in primary T cells.

Direct down-regulation of *bfl-1* expression was next used to evaluate its contribution as a pro-survival NF-κB target gene in HL. In transfection experiments with L428, two out of three anti-*bfl-1* siRNAs significantly inhibited *bfl-1* expression as reflected in decreased *bfl-1* mRNA levels, whereas control siRNA did not. siRNA transfected cells were then left untreated or treated with suboptimal levels of Bay 11-7082 or sodium arsenite. Knockdown of *bfl-1* expression significantly potentiated the pro-apoptotic effect of both inhibitors to an extent commensurate with the degree of knockdown achieved with each siRNA. Since knockdown of *bfl-1* potentiated the chemotherapeutic effect of these agents, a crucial role for Bfl-1 in setting the elevated threshold of resistance of these malignant cells to apoptosis is implied. In view of the fact that downregulation served to greatly increase the sensitivity of cells to chemotoxic agent-induced apoptosis, silencing of Bfl-1 in this cell context might be of considerable interest for the future treatment of HL in tandem with low-dose polychemotherapy.

The findings detailed in Chapter 6 further demonstrate that *bfl-1* is an NF-κB target gene and show that *bfl-1* promoter regulation is effected through a consensus p65-binding DNA element located in the upstream transcriptional regulatory region. The major loss of *bfl-1* promoter activity seen upon mutation of -52 NF-κB-binding site is in contrast to previous observations in our laboratory in EBV-driven lymphoblastoid cell lines (LCLs) wherein this mutation only has a modest effect (D'Souza *et al.*, 2004; and data not shown). This result highlights the importance of the -52/-43 element as a site through which *trans*-activation of *bfl-1* is effected by activated NF-κB in H/RS cells.

It is now clear that HL cell proliferation and survival is maintained by cytokine signaling. The principal signaling pathway induced by cytokines is the JAK–STAT pathway (Kisseleva, 2002) and constitutive STAT3 and 6 activation has been reported in HL-derived cell lines (Kube *et al.*, 2001; Skinnider, 2002) suggesting that this aberrant STAT activity may in part contribute to the deregulation of cell homeostasis in the HL. Interestingly, *bfl-1* has recently been shown to be one of a number of target genes of STAT proteins, and inhibition of constitutive STAT activation led to apoptosis in HL-derived cell lines (Cochet *et al.*, 2006).

The effectiveness of current radiation and chemotherapies are presumed to be mediated by apoptosis, and it was set out in this study to investigate a potential molecular mechanism that causes the H/RS to survive. It is shown here, that *bfl-1* is expressed in H/RS cells *in vivo* and that its expression is regulated by NF- $\kappa$ B. It is observed that exogenous Bfl-1 protected H/RS cells from apoptosis-inducing doses of the NF- $\kappa$ B inhibitors Bay-11 and sodium arsenite. Furthermore, knockdown of *bfl-1* expression significantly increased the chemosensitivity of cultured H/RS cells to these inhibitors, implying that it is a crucial anti-apoptotic NF- $\kappa$ B target gene in this context. An important issue for the development of NF- $\kappa$ B inhibitors as chemotherapeutic agents is the impact of such modulation on normal cells. Bortezomib (PS-341), is a reversible inhibitor of the 26S proteasome which interferes with the degradation of a variety of proteins including I $\kappa$ B $\alpha$ , leading to less NF- $\kappa$ B and increased apoptosis and is one of a novel class of chemotherapeutic agents that has been FDA-approved for the treatment of multiple myeloma in adults (Voorhees *et al.*, 2003). However, in a Phase I study of Bortezomib in patients with advanced hematologic malignancies, dose-limiting toxicities included thrombocytopenia, hyponatremia, fatigue, malaise and peripheral neuropathy (Voorhees *et al.*, 2003). Specific targeting of the phenotypic effector genes could prove more effective than transcription factor targeting. Here, the potential of Bfl-1 as a rational therapeutic target in HL is highlighted. Targeting of Bfl-1 in H/RS cells by means of its functional blockade or inhibition of its expression could possibly restore the apoptotic machinery in these cells and sensitise HL tumours to chemo- and radiotherapies. Pharmacological manipulation of Bcl-2 family members to control cell death is a promising area of research into novel anti-cancer therapies (reviewed in Cory and Adams, 2007). This study suggests that the downregulation of Bfl-1 may be used to enhance apoptosis of tumour cells of cHD treated with chemotoxic agents. Silencing Bfl-1 may permit the use of lower amounts of drug to achieve the same effect, thereby avoiding undesirable side effects and late toxicities described in Section 1.3.2.

A recent study showed that Bfl-1 silencing sensitises large B cell lymphoma-derived cell lines to apoptosis in response to anti-CD20 (Rituximab), doxorubicin and cisplatin (Brien *et al.*, 2007). Jazirehi *et al.*, (2004), showed that the chimeric anti-CD20 antibody, Rituximab, widely used in the clinical treatment of patients with NHL, inhibited the ERK1/2 pathway and sensitised NHL cells to drug-induced apoptosis. A subsequent study by this group (Jazirehi *et al.*, 2005), showed that Rituximab

significantly up-regulated Raf-1 kinase inhibitor protein expression and interrupted the NF-κB signaling pathway resulting in Bcl-xL and Bfl-1/A1 down-regulation.

Normally, B cells with self reactive or low affinity antibody die by Fas-mediated apoptosis, whereas cells that express Ig with increased affinity for the corresponding antigen are stimulated to proliferate and exit the GC as memory B cells or plasma cells (Rajewsky, 1996). H/RS cells have been shown to be resistant to cell death-induction via Fas activation *in vitro* (Re *et al.*, 2000), evidence that the Fas death-signaling pathway must be interrupted in H/RS cells. In Jurkat T cells, oxidative stress induces the expression of Bfl-1 via NF-κB activation and this early response gene protects cells from Fas-mediated apoptosis (Kim *et al.*, 2005). Also, *Bfl-1* induction through the CD40/NF-κB pathway is associated with an increased resistance to BCR-mediated cell death in B cell lines and mature B cells (Grumont *et al.*, 1999; Kuss *et al.*, 1999; Lee *et al.*, 1999). Whether Bfl-1 is involved in the evasion of Fas-mediated apoptosis in H/RS cells by inhibiting the mitochondrial apoptotic pathway is a matter warranting further investigation.

It has been estimated that 25-50 % of all HL cases contain EBV DNA in the H/RS cells (reviewed in Keegan *et al.*, 2005). The EBV LMP1, a TNFR superfamily member that constitutively drives NF-κB activation in the absence of ligand, was recently shown to be expressed in 21 % of H/RS cells of 124/577 HL patients, with significantly more frequent detection in the mixed cellularity than the nodular sclerosis subtype (Herling *et al.*, 2003). EBV LMP2A has been shown to increase the expression of genes associated with cell cycle induction and inhibition of apoptosis in H/RS cells (Portis *et al.*, 2003). The question remains as to whether EBV LMP1 and LMP2A have a role in regulating the expression of the *bfl-1* gene in HL and would prove an interesting investigation.

Chapter 7 describes how due to the unavailability of robust anti-Bfl-1 antibody preparations, the *bfl-1* gene was cloned into an expression vector, expression and purification from a compatible expression host was achieved and purified recombinant protein was used as antigen to generate polyclonal antibodies specific for Bfl-1. Several challenges were overcome, most significantly to surmount the failure to purify recombinant protein, a novel vector (pGSLink) was designed and constructed to permit high-level expression of a protein linked at the N- or C-terminal to a His-tag by a flexible, poorly immunogenic linker peptide of 21 Glycine and Serine amino acids;

(Gly<sub>4</sub>Ser)<sub>4</sub>Gly. This novel vector permitted the expression and purification of His-Linker-Bfl-1 and Bfl-1-Linker-His fusion proteins using IMAC. Purified recombinant Bfl-1 was then used to immunise a rabbit (Custom Hybridoma Laboratories) and polyclonal antisera was produced in response to the tagged Bfl-1 protein antigen. This modified vector and particular linker design may be of general use in assisting to overcome problems associated with the purification of recombinant proteins and has been published in Analytical Biochemistry (Loughran *et al.*, 2006). It is hoped that generated anti-sera will serve as a valuable tool for correlating Bfl-1 expression at the protein level in related studies in B cell malignancies in our laboratory.

Finally, in the future, the success of cancer therapeutics will depend on their ability to interfere with distinct pathways leading to apoptosis. Considering the ability of Bfl-1 to protect H/RS cells from chemotoxic agent-induced apoptosis and in light of the evidence presented here on Bfl-1 silencing leading to decreased apoptotic threshold, development and testing of inhibitors of this anti-apoptotic protein for use as a therapeutic agent would be valuable.

## **CHAPTER 9 Bibliography**

- Aagaard-Tillery, K.M. and Jelinek, D.F. (1996). Phosphatidylinositol 3-kinase activation in normal human B lymphocytes. *J. Immunol.*, 156, 4543-4554.
- Abrahante, J.E., Daul, A.L., Li, M., Volk, M.L., Tennessen, J.M., Miller, E.A. and Rougvie, A.E. (2003). The *Caenorhabditis elegans* hunchback-like gene lin-57/hbl-1 controls developmental time and is regulated by microRNAs. *Dev. Cell.*, 4, 625-637.
- Adams, J.M. and Cory, S. (2007). The Bcl-2 apoptotic switch in cancer development and therapy. *Oncogene.*, 26, 1324-1337.
- Adams, J.M. and Cory, S. (2002). Apoptosomes: engines for caspase activation. *Curr. Opin. Cell Biol.*, 14, 715-720.
- Adams, J.M. and Cory, S. (1998). The Bcl-2 protein family: arbiters of cell survival. *Science.*, 281, 1322-1326.
- Aggarwal, S., Ichikawa, H., Takada, Y., Sandur, S.K., Shishodia, S. and Aggarwal, B.B. (2006). Curcumin (diferuloylmethane) down-regulates expression of cell proliferation and antiapoptotic and metastatic gene products through suppression of IkappaBalpha kinase and Akt activation. *Mol. Pharmacol.*, 69, 195-206.
- Akgul, C., Moulding, D.A. and Edwards, S.W. (2004). Alternative splicing of Bcl-2-related genes: functional consequences and potential therapeutic applications. *Cell Mol. Life Sci.*, 61, 2189-2199.
- Alam, M.K., Davison, S., Siddiqui, N., Norton, J.D. and Murphy, J.J. (1997). Ectopic expression of Bcl-2, but not Bcl-xL rescues Ramos B cells from Fas-mediated apoptosis. *Eur. J. Immunol.*, 27, 3485-3491.
- Al-Shamkhani, A. (2004). The role of CD30 in the pathogenesis of haematopoietic malignancies. *Curr. Opin. Pharmacol.*, 4, 355-359.
- Andersson, M.L., Stam, N.J., Klein, G., Ploegh, H.L. and Masucci, M.G. (1991). Aberrant expression of HLA class-I antigens in Burkitt lymphoma cells. *Int. J. Cancer.*, 47, 544-550.
- Andjelic, S., Hsia, C., Suzuki, H., Kadokami, T., Koyasu, S. and Liou, H.C. (2000). Phosphatidylinositol 3-kinase and NF-kappa B/Rel are at the divergence of CD40-mediated proliferation and survival pathways. *J. Immunol.*, 165, 3860-3867.
- Annunziata, C.M., Safiran, Y.J., Irving, S.G., Kasid, U.N. and Cossman, J. (2000). Hodgkin disease: pharmacologic intervention of the CD40-NF kappa B pathway by a protease inhibitor. *Blood.*, 96, 2841-2848.
- Ansell, S.M. (2003). Adding cytokines to monoclonal antibody therapy: does the concurrent administration of interleukin-12 add to the efficacy of rituximab in B-cell non-hodgkin lymphoma?. *Leuk. Lymphoma.*, 44, 1309-1315.

- Antonsson, B., Montessuit, S., Sanchez, B. and Martinou, J.C. (2001). Bax is present as a high molecular weight oligomer/complex in the mitochondrial membrane of apoptotic cells. *J. Biol. Chem.*, 276, 11615-11623.
- Argos, P. (1990). An investigation of oligopeptides linking domains in protein tertiary structures and possible candidates for general gene fusion. *J. Mol. Biol.*, 211, 943-958.
- Axdorph, U., Porwit-MacDonald, A., Sjoberg, J., Grimfors, G., Ekman, M., Wang, W., Biberfeld, P. and Bjorkholm, M. (1999). Epstein-Barr virus expression in Hodgkin's disease in relation to patient characteristics, serum factors and blood lymphocyte function. *Br. J. Cancer.*, 81, 1182-1187.
- Bai, M., Panoulas, V., Papoudou-Bai, A., Horianopoulos, N., Kitsoulis, P., Stefanaki, K., Rontogianni, D., Agnantis, N.J. and Kanavaros, P. (2006). B-cell differentiation immunophenotypes in classical Hodgkin lymphomas. *Leuk. Lymphoma*, 47, 495-501.
- Bakhshi, A., Jensen, J.P., Goldman, P., Wright, J.J., McBride, O.W., Epstein, A.L. and Korsmeyer, S.J. (1985). Cloning the chromosomal breakpoint of t(14;18) human lymphomas: clustering around JH on chromosome 14 and near a transcriptional unit on 18. *Cell*, 41, 899-906.
- Baldwin, A.S., Jr. (1996). The NF-kappa B and I kappa B proteins: new discoveries and insights. *Annu. Rev. Immunol.*, 14, 649-683.
- Balzarotti, M., Magagnoli, M. and Santoro, A. (2003). Early restaging positron emission tomography with 18F-fluorodeoxyglucose in aggressive non-Hodgkin's lymphomas: is it too easy to be true?. *Ann. Oncol.*, 14, 1155-1156.
- Barberis, A., Widenhorn, K., Vitelli, L. and Busslinger, M. (1990). A novel B-cell lineage-specific transcription factor present at early but not late stages of differentiation. *Genes Dev.*, 4, 849-859.
- Bargou, R.C., Emmerich, F., Krappmann, D., Bommert, K., Mapara, M.Y., Arnold, W., Royer, H.D., Grinstein, E., Greiner, A., Scheidereit, C. and Dorken, B. (1997). Constitutive nuclear factor-kappaB-RelA activation is required for proliferation and survival of Hodgkin's disease tumor cells. *J. Clin. Invest.*, 100, 2961-2969.
- Bargou, R.C., Leng, C., Krappmann, D., Emmerich, F., Mapara, M.Y., Bommert, K., Royer, H.D., Scheidereit, C. and Dorken, B. (1996). High-level nuclear NF-kappa B and Oct-2 is a common feature of cultured Hodgkin/Reed-Sternberg cells. *Blood*, 87, 4340-4347.
- Bartlett, N.L., Rosenberg, S.A., Hoppe, R.T., Hancock, S.L. and Horning, S.J. (1995). Brief chemotherapy, Stanford V, and adjuvant radiotherapy for bulky or advanced-stage Hodgkin's disease: a preliminary report. *J. Clin. Oncol.*, 13, 1080-1088.

- Bash, J., Zong, W.X., Banga, S., Rivera, A., Ballard, D.W., Ron, Y. and Gelinas, C. (1999). Rel/NF-kappaB can trigger the Notch signaling pathway by inducing the expression of Jagged1, a ligand for Notch receptors. *EMBO J.*, 18, 2803-2811.
- Baumforth, K.R.N., Flavell, J.R., Reynolds, G.M., Davies, G., Pettit, T.R., Wei, W., Morgan, S., Stankovic, T., Kishi, Y., Arai, H., Nowakova, M., Pratt, G., Aoki, J., Wakelam, M.J.O., Young, L.S. and Murray, P.G. (2005). Induction of autotaxin by the Epstein-Barr virus promotes the growth and survival of Hodgkin lymphoma cells. *Blood.*, 106, 2138-2146.
- Bechtel, D., Kurth, J., Unkel, C. and Kuppers, R. (2005). Transformation of BCR-deficient germinal-center B cells by EBV supports a major role of the virus in the pathogenesis of Hodgkin and posttransplantation lymphomas. *Blood.*, 106, 4345-4350.
- Beck, A., Pazolt, D., Grabenbauer, G.G., Nicholls, J.M., Herbst, H., Young, L.S. and Niedobitek, G. (2001). Expression of cytokine and chemokine genes in Epstein-Barr virus-associated nasopharyngeal carcinoma: comparison with Hodgkin's disease. *J. Pathol.*, 194, 145-151.
- Beg, A.A., Sha, W.C., Bronson, R.T. and Baltimore, D. (1995a). Constitutive NF-kappa B activation, enhanced granulopoiesis, and neonatal lethality in I kappa B alpha-deficient mice. *Genes Dev.*, 9, 2736-2746.
- Beg, A.A., Sha, W.C., Bronson, R.T., Ghosh, S. and Baltimore, D. (1995b). Embryonic lethality and liver degeneration in mice lacking the RelA component of NF-kappa B. *Nature.*, 376, 167-170.
- Bellavia, D., Campese, A.F., Alesse, E., Vacca, A., Felli, M.P., Balestri, A., Stoppacciaro, A., Tiveron, C., Tatangelo, L., Giovarelli, M., Gaetano, C., Ruco, L., Hoffman, E.S., Hayday, A.C., Lendahl, U., Frati, L., Gulino, A. and Scarpanti, I. (2000). Constitutive activation of NF-kappaB and T-cell leukemia/lymphoma in Notch3 transgenic mice. *EMBO J.*, 19, 3337-3348.
- Ben-Bassat, H., Goldblum, N., Mitrani, S., Goldblum, T., Yoffey, J.M., Cohen, M.M., Bentwich, Z., Ramot, B., Klein, E. and Klein, G. (1977). Establishment in continuous culture of a new type of lymphocyte from a "Burkitt like" malignant lymphoma (line D.G.-75). *Int. J. Cancer.*, 19, 27-33.
- Benharroch, D., Prinsloo, I., Apte, R.N., Yermiah, T., Geffen, D.B., Yanai-Inbar, I. and Gopas, J. (1996). Interleukin-1 and tumor necrosis factor-alpha in the Reed-Sternberg cells of Hodgkin's disease. Correlation with clinical and morphological "inflammatory" features. *Eur. Cytokine Netw.*, 7, 51-57.
- Benharroch, D., Shemer-Avni, Y., Myint, Y.Y., Levy, A., Mejirovsky, E., Suprun, I., Shandler, Y., Prinsloo, I., Ariad, S., Rager-Zisman, B., Sacks, M. and Gopas, J. (2004). Measles virus: evidence of an association with Hodgkin's disease. *Br. J. Cancer.*, 91, 572-579.
- Bernal, A., Pastore, R.D., Asgary, Z., Keller, S.A., Cesarman, E., Liou, H.C. and Schattner, E.J. (2001). Survival of leukemic B cells promoted by engagement of the antigen receptor. *Blood.*, 98, 3050-3057.

- Bernstein, E., Caudy, A.A., Hammond, S.M. and Hannon, G.J. (2001a). Role for a bidentate ribonuclease in the initiation step of RNA interference. *Nature.*, 409, 363-366.
- Bernstein, E., Denli, A.M. and Hannon, G.J. (2001b). The rest is silence. *RNA.*, 7, 1509-1521.
- Berridge, M.V. and Tan, A.S. (1993). Characterization of the cellular reduction of 3-(4,5-dimethylthiazol-2-yl)-2,5-diphenyltetrazolium bromide (MTT): subcellular localization, substrate dependence, and involvement of mitochondrial electron transport in MTT reduction. *Arch. Biochem. Biophys.*, 303, 474-482.
- Bertrand, F.E., Eckfeldt, C.E., Lysholm, A.S. and LeBien, T.W. (2000). Notch-1 and Notch-2 exhibit unique patterns of expression in human B-lineage cells. *Leukemia.*, 14, 2095-2102.
- Bianchini, R., Nocentini, G., Krausz, L.T., Fettucciari, K., Coaccioli, S., Ronchetti, S. and Riccardi, C. (2006). Modulation of Pro- and Antiapoptotic Molecules in Double-Positive (CD4+CD8+) Thymocytes following Dexamethasone Treatment. *J Pharmacol Exp Ther.*, 319, 887-897.
- Bogoyevitch, M.A. and Court, N.W. (2004). Counting on mitogen-activated protein kinases--ERKs 3, 4, 5, 6, 7 and 8. *Cell. Signal.*, 16, 1345-1354.
- Boise, L.H., Gonzalez-Garcia, M., Postema, C.E., Ding, L., Lindsten, T., Turka, L.A., Mao, X., Nunez, G. and Thompson, C.B. (1993). Bcl-X, a Bcl-2-Related Gene that Functions as a Dominant Regulator of Apoptotic Cell Death. *Cell.*, 74, 597-608.
- Bonadonna, G. (1982). Chemotherapy strategies to improve the control of Hodgkin's disease: the Richard and Hinda Rosenthal Foundation Award Lecture. *Cancer Res.*, 42, 4309-4320.
- Borchmann, P., Treml, J.F., Hansen, H., Gottstein, C., Schnell, R., Staak, O., Zhang, H.F., Davis, T., Keler, T., Diehl, V., Graziano, R.F. and Engert, A. (2003). The human anti-CD30 antibody 5F11 shows in vitro and in vivo activity against malignant lymphoma. *Blood.*, 102, 3737-3742.
- Borner, C. (2003). The Bcl-2 protein family: sensors and checkpoints for life-or-death decisions. *Mol. Immunol.*, 39, 615-647.
- Bornkamm, G.W., Berens, C., Kuklik-Roos, C., Bechet, J.M., Laux, G., Bachl, J., Korndoerfer, M., Schlee, M., Holzel, M., Malamoussi, A., Chapman, R.D., Nimmerjahn, F., Mautner, J., Hillen, W., Bujard, H. and Feuillard, J. (2005). Stringent doxycycline-dependent control of gene activities using an episomal one-vector system. *Nucleic Acids Res.*, 33, e137.
- Boulton, T.G., Yancopoulos, G.D., Gregory, J.S., Slaughter, C., Moomaw, C., Hsu, J. and Cobb, M.H. (1990). An insulin-stimulated protein kinase similar to yeast kinases involved in cell cycle control. *Science.*, 249, 64-67.

- Braeuninger, A., Kuppers, R., Strickler, J.G., Wacker, H.H., Rajewsky, K. and Hansmann, M.L. (1997). Hodgkin and Reed-Sternberg cells in lymphocyte predominant Hodgkin disease represent clonal populations of germinal center-derived tumor B cells. *Proc. Natl. Acad. Sci. U. S. A.*, 94, 9337-9342.
- Brattsand, G., Cantrell, D.A., Ward, S., Ivars, F. and Gullberg, M. (1990). Signal transduction through the T cell receptor-CD3 complex. Evidence for heterogeneity in receptor coupling. *J. Immunol.*, 144, 3651-3658.
- Brauninger, A., Schmitz, R., Bechtel, D., Renne, C., Hansmann, M.L. and Kuppers, R. (2006). Molecular biology of Hodgkin's and Reed/Sternberg cells in Hodgkin's lymphoma. *Int. J. Cancer.*, 118, 1853-1861.
- Bray, S.J. (2006). Notch signalling: a simple pathway becomes complex. *Nat. Rev. Mol. Cell Biol.*, 7, 678-689.
- Brennan, P., Babbage, J.W., Burgener, B.M., Groner, B., Reif, K. and Cantrell, D.A. (1997). Phosphatidylinositol 3-kinase couples the interleukin-2 receptor to the cell cycle regulator E2F. *Immunity.*, 7, 679-689.
- Brennecke, J., Hipfner, D.R., Stark, A., Russell, R.B. and Cohen, S.M. (2003). bantam encodes a developmentally regulated microRNA that controls cell proliferation and regulates the proapoptotic gene hid in Drosophila. *Cell.*, 113, 25-36.
- Brice, P. (1998). Staging of Hodgkin's disease. *Rev. Prat.*, 48, 1070-1074.
- Brice, P., Divine, M., Simon, D., Coiffier, B., Leblond, V., Simon, M., Voilat, L., Devidas, A., Morschhauser, F., Rohrlich, P., Andre, M., Lepage, E. and Ferme, C. (1999). Feasibility of tandem autologous stem-cell transplantation (ASCT) in induction failure or very unfavorable (UF) relapse from Hodgkin's disease (HD). SFGM/GELA Study Group. *Ann. Oncol.*, 10, 1485-1488.
- Brien, G., Trescol-Biemont, M.C. and Bonnefoy-Berard, N. (2007). Downregulation of Bfl-1 protein expression sensitizes malignant B cells to apoptosis. *Oncogene.*
- Brink, A.A., Oudejans, J.J., van den Brule, A.J., Kluin, P.M., Horstman, A., Ossenkoppele, G.J., van Heerde, P., Jiwa, M. and Meijer, C.J. (1998). Low p53 and high bcl-2 expression in Reed-Sternberg cells predicts poor clinical outcome for Hodgkin's disease: involvement of apoptosis resistance?. *Mod. Pathol.*, 11, 376-383.
- Brummelkamp, T.R., Bernards, R. and Agami, R. (2002). Stable suppression of tumorigenicity by virus-mediated RNA interference. *Cancer Cell.*, 2, 243-247.
- Cabannes, E., Khan, G., Aillet, F., Jarrett, R.F. and Hay, R.T. (1999). Mutations in the IkBa gene in Hodgkin's disease suggest a tumour suppressor role for IkappaBalph. *Oncogene.*, 18, 3063-3070.

- Caldwell, R.G., Brown, R.C. and Longnecker, R. (2000). Epstein-Barr virus LMP2A-induced B-cell survival in two unique classes of EmuLMP2A transgenic mice. *J. Virol.*, 74, 1101-1113.
- Caldwell, R.G., Wilson, J.B., Anderson, S.J. and Longnecker, R. (1998). Epstein-Barr virus LMP2A drives B cell development and survival in the absence of normal B cell receptor signals. *Immunity.*, 9, 405-411.
- Calender, A., Billaud, M., Aubry, J.P., Banchereau, J., Vuillaume, M. and Lenoir, G.M. (1987). Epstein-Barr virus (EBV) induces expression of B-cell activation markers on in vitro infection of EBV-negative B-lymphoma cells. *Proc. Natl. Acad. Sci. U. S. A.*, 84, 8060-8064.
- Campos, A.H., Wang, W., Pollman, M.J. and Gibbons, G.H. (2002). Determinants of Notch-3 receptor expression and signaling in vascular smooth muscle cells: implications in cell-cycle regulation. *Circ. Res.*, 91, 999-1006.
- Canellos, G.P. (1998). Treatment of relapsed Hodgkin's disease: strategies and prognostic factors. *Ann. Oncol.*, 9 Suppl 5, S91-6.
- Carbone, A., Gloghini, A., Aldinucci, D., Gattei, V., Dalla-Favera, R. and Gaidano, G. (2002). Expression pattern of MUM1/IRF4 in the spectrum of pathology of Hodgkin's disease. *Br. J. Haematol.*, 117, 366-372.
- Carbone, A., Gloghini, A., Gattei, V., Aldinucci, D., Degan, M., De Paoli, P., Zagonel, V. and Pinto, A. (1995). Expression of functional CD40 antigen on Reed-Sternberg cells and Hodgkin's disease cell lines. *Blood.*, 85, 780-789.
- Carbone, A., Gloghini, A., Gattei, V., Degan, M., Improta, S., Aldinucci, D., Canzonieri, V., Perin, T., Volpe, R., Gaidano, G., Zagonel, V. and Pinto, A. (1997). Reed-Sternberg cells of classical Hodgkin's disease react with the plasma cell-specific monoclonal antibody B-B4 and express human syndecan-1. *Blood.*, 89, 3787-3794.
- Carbone, A., Gloghini, A., Gruss, H.J. and Pinto, A. (1995). CD40 antigen expression on Reed-Sternberg cells. A reliable diagnostic tool for Hodgkin's disease. *Am. J. Pathol.*, 146, 780-781.
- Carbone, P.P., Kaplan, H.S., Musshoff, K., Smithers, D.W. and Tubiana, M. (1971). Report of the Committee on Hodgkin's Disease Staging Classification. *Cancer Res.*, 31, 1860-1861.
- Carey, G.B. and Scott, D.W. (2001). Role of phosphatidylinositol 3-kinase in anti-IgM- and anti-IgD-induced apoptosis in B cell lymphomas. *J. Immunol.*, 166, 1618-1626.
- Carrio, R., Lopez-Hoyos, M., Jimeno, J., Benedict, M.A., Merino, R., Benito, A., Fernandez-Luna, J.L., Nunez, G., Garcia-Porrero, J.A. and Merino, J. (1996). A1 demonstrates restricted tissue distribution during embryonic development and functions to protect against cell death. *Am. J. Pathol.*, 149, 2133-2142.

- Casola, S., Otipoby, K.L., Alimzhanov, M., Humme, S., Uyttersprot, N., Kutok, J.L., Carroll, M.C. and Rajewsky, K. (2004). B cell receptor signal strength determines B cell fate. *Nat. Immunol.*, 5, 317-327.
- Certo, M., Del Gaizo Moore, V., Nishino, M., Wei, G., Korsmeyer, S., Armstrong, S.A. and Letai, A. (2006). Mitochondria primed by death signals determine cellular addiction to antiapoptotic BCL-2 family members. *Cancer. Cell.*, 9, 351-365.
- Cerveny, C.G., Law, C.L., McCormick, R.S., Lenox, J.S., Hamblett, K.J., Westendorf, L.E., Yamane, A.K., Petroziello, J.M., Francisco, J.A. and Wahl, A.F. (2005). Signaling via the anti-CD30 mAb SGN-30 sensitizes Hodgkin's disease cells to conventional chemotherapeutics. *Leukemia.*, 19, 1648-1655.
- Chang, F., Steelman, L.S., Lee, J.T., Shelton, J.G., Navolanic, P.M., Blalock, W.L., Franklin, R.A. and McCubrey, J.A. (2003). Signal transduction mediated by the Ras/Raf/MEK/ERK pathway from cytokine receptors to transcription factors: potential targeting for therapeutic intervention. *Leukemia.*, 17, 1263-1293.
- Chen, F., Demers, L.M., Vallyathan, V., Lu, Y., Castranova, V. and Shi, X. (1999). Involvement of 5'-flanking kappaB-like sites within bcl-x gene in silica-induced Bcl-x expression. *J. Biol. Chem.*, 274, 35591-35595.
- Chen, F.E. and Ghosh, G. (1999). Regulation of DNA binding by Rel/NF-kappaB transcription factors: structural views. *Oncogene.*, 18, 6845-6852.
- Chen, L., Willis, S.N., Wei, A., Smith, B.J., Fletcher, J.I., Hinds, M.G., Colman, P.M., Day, C.L., Adams, J.M. and Huang, D.C. (2005). Differential targeting of prosurvival Bcl-2 proteins by their BH3-only ligands allows complementary apoptotic function. *Mol. Cell.*, 17, 393-403.
- Cheng, P., Zlobin, A., Volgina, V., Gottipati, S., Osborne, B., Simel, E.J., Miele, L. and Gabrilovich, D.I. (2001). Notch-1 regulates NF-kappaB activity in hemopoietic progenitor cells. *J. Immunol.*, 167, 4458-4467.
- Cheng, Q., Lee, H.H., Li, Y., Parks, T.P. and Cheng, G. (2000). Upregulation of Bcl-x and Bfl-1 as a potential mechanism of chemoresistance, which can be overcome by NF-kappaB inhibition. *Oncogene.*, 19, 4936-4940.
- Choi, S.S., Park, I.C., Yun, J.W., Sung, Y.C., Hong, S.I. and Shin, H.S. (1995). A novel Bcl-2 related gene, Bfl-1, is overexpressed in stomach cancer and preferentially expressed in bone marrow. *Oncogene.*, 11, 1693-1698.
- Choi, S.S., Park, S.H., Kim, U.J. and Shin, H.S. (1997). Bfl-1, a Bcl-2-related gene, is the human homolog of the murine A1, and maps to chromosome 15q24.3. *Mamm. Genome.*, 8, 781-782.
- Chou, J.J., Li, H., Salvesen, G.S., Yuan, J. and Wagner, G. (1999). Solution structure of BID, an intracellular amplifier of apoptotic signaling. *Cell.*, 96, 615-624.

- Choudhury, A. and Kiessling, R. (2004). Her-2/neu as a paradigm of a tumor-specific target for therapy. *Breast Dis.*, 20, 25-31.
- Chuang, P.I., Yee, E., Karsan, A., Winn, R.K. and Harlan, J.M. (1998). A1 is a constitutive and inducible Bcl-2 homologue in mature human neutrophils. *Biochem. Biophys. Res. Commun.*, 249, 361-365.
- Chung, C.N., Hamaguchi, Y., Honjo, T. and Kawaichi, M. (1994). Site-directed mutagenesis study on DNA binding regions of the mouse homologue of Suppressor of Hairless, RBP-J kappa. *Nucleic Acids Res.*, 22, 2938-2944.
- Cioca, D.P., Aoki, Y. and Kiyosawa, K. (2003). RNA interference is a functional pathway with therapeutic potential in human myeloid leukemia cell lines. *Cancer Gene Ther.*, 10, 125-133.
- Civil, A., Bakker, A., Rensink, I., Doerre, S., Aarden, L.A. and Verweij, C.L. (1996). Nuclear appearance of a factor that binds the CD28 response element within the interleukin-2 enhancer correlates with interleukin-2 production. *J. Biol. Chem.*, 271, 8321-8327.
- Civil, A., Rensink, I., Aarden, L.A. and Verweij, C.L. (1999). Functional disparity of distinct CD28 response elements toward mitogenic responses. *J. Biol. Chem.*, 274, 34369-34374.
- Clark, S.T., Radford, J.A., Crowther, D., Swindell, R. and Shalet, S.M. (1995). Gonadal function following chemotherapy for Hodgkin's disease: a comparative study of MVPP and a seven-drug hybrid regimen. *J. Clin. Oncol.*, 13, 134-139.
- Cleary, M.L. and Sklar, J. (1985). Nucleotide sequence of a t(14;18) chromosomal breakpoint in follicular lymphoma and demonstration of a breakpoint-cluster region near a transcriptionally active locus on chromosome 18. *Proc. Natl. Acad. Sci. U. S. A.*, 82, 7439-7443.
- Cochet, O., Frelin, C., Peyron, J.F. and Imbert, V. (2006). Constitutive activation of STAT proteins in the HDLM-2 and L540 Hodgkin lymphoma-derived cell lines supports cell survival. *Cell. Signal.*, 18, 449-455.
- Cory, S. and Adams, J.M. (2002). The Bcl2 family: regulators of the cellular life-or-death switch. *Nat. Rev. Cancer.*, 2, 647-656.
- Cossman, J., Annunziata, C.M., Barash, S., Staudt, L., Dillon, P., He, W.W., Ricciardi-Castagnoli, P., Rosen, C.A. and Carter, K.C. (1999). Reed-Sternberg cell genome expression supports a B-cell lineage. *Blood.*, 94, 411-416.
- Craddock, B.L., Orchiston, E.A., Hinton, H.J. and Welham, M.J. (1999). Dissociation of apoptosis from proliferation, protein kinase B activation, and BAD phosphorylation in interleukin-3-mediated phosphoinositide 3-kinase signaling. *J. Biol. Chem.*, 274, 10633-10640.

- Craig, R.W. (2002). MCL1 provides a window on the role of the BCL2 family in cell proliferation, differentiation and tumorigenesis. *Leukemia.*, 16, 444-454.
- Crawford, D.H. (2001). Biology and disease associations of Epstein-Barr virus. *Philos. Trans. R. Soc. Lond. B. Biol. Sci.*, 356, 461-473.
- Craxton, A., Chuang, P.I., Shu, G., Harlan, J.M. and Clark, E.A. (2000). The CD40-inducible Bcl-2 family member A1 protects B cells from antigen receptor-mediated apoptosis. *Cell. Immunol.*, 200, 56-62.
- Crump, M., Smith, A.M., Brandwein, J., Couture, F., Sherret, H., Sutton, D.M., Scott, J.G., McCrae, J., Murray, C. and Pantalony, D. (1993). High-dose etoposide and melphalan, and autologous bone marrow transplantation for patients with advanced Hodgkin's disease: importance of disease status at transplant. *J. Clin. Oncol.*, 11, 704-711.
- Danial, N.N. and Korsmeyer, S.J. (2004). Cell death: critical control points. *Cell.*, 116, 205-219.
- Davis, R.J. (2000). Signal transduction by the JNK group of MAP kinases. *Cell.*, 103, 239-252.
- Delabie, J., Shipman, R., Bruggen, J., De Strooper, B., van Leuven, F., Tarcsay, L., Cerletti, N., Odink, K., Diehl, V. and Bilbe, G. (1992). Expression of the novel intermediate filament-associated protein restin in Hodgkin's disease and anaplastic large-cell lymphoma. *Blood.*, 80, 2891-2896.
- Delibrias, C.C., Floettmann, J.E., Rowe, M. and Fearon, D.T. (1997). Downregulated expression of SHP-1 in Burkitt lymphomas and germinal center B lymphocytes. *J. Exp. Med.*, 186, 1575-1583.
- Dent, P. and Grant, S. (2001). Pharmacologic interruption of the mitogen-activated extracellular-regulated kinase/mitogen-activated protein kinase signal transduction pathway: potential role in promoting cytotoxic drug action. *Clin. Cancer Res.*, 7, 775-783.
- Devita, V.T., Jr, Serpick, A.A. and Carbone, P.P. (1970). Combination chemotherapy in the treatment of advanced Hodgkin's disease. *Ann. Intern. Med.*, 73, 881-895.
- Diehl, V., Franklin, J., Hasenclever, D., Tesch, H., Pfreundschuh, M., Lathan, B., Paulus, U., Sieber, M., Ruffer, J.U., Sextro, M., Engert, A., Wolf, J., Hermann, R., Holmer, L., Stappert-Jahn, U., Winnerlein-Trump, E., Wulf, G., Krause, S., Glunz, A., von Kalle, K., Bischoff, H., Haedicke, C., Duhamke, E., Georgii, A. and Loeffler, M. (1998). BEACOPP: a new regimen for advanced Hodgkin's disease. German Hodgkin's Lymphoma Study Group. *Ann. Oncol.*, 9 Suppl 5, S67-71.
- Diehl, V., Franklin, J., Pfreundschuh, M., Lathan, B., Paulus, U., Hasenclever, D., Tesch, H., Herrmann, R., Dorken, B., Muller-Hermelink, H.K., Duhamke, E., Loeffler, M. and German Hodgkin's Lymphoma Study Group. (2003). Standard and increased-dose BEACOPP chemotherapy compared with COPP-ABVD for advanced Hodgkin's disease. *N. Engl. J. Med.*, 348, 2386-2395.

- Diehl, V., Kirchner, H.H., Burrichter, H., Stein, H., Fonatsch, C., Gerdes, J., Schaadt, M., Heit, W., Uchanska-Ziegler, B., Ziegler, A., Heintz, F. and Sueno, K. (1982). Characteristics of Hodgkin's disease-derived cell lines. *Cancer Treat. Rep.*, 66, 615-632.
- Diehl, V., Thomas, R.K. and Re, D. (2004/1). Part II: Hodgkin's lymphoma—diagnosis and treatment. *The Lancet Oncology.*, 5, 19-26.
- Dong, H., Nilsson, L. and Kurland, C.G. (1996). Co-variation of tRNA abundance and codon usage in *Escherichia coli* at different growth rates. *J. Mol. Biol.*, 260, 649-663.
- D'Sa-Eipper, C. and Chinnadurai, G. (1998). Functional dissection of Bfl-1, a Bcl-2 homolog: anti-apoptosis, oncogene-cooperation and cell proliferation activities. *Oncogene.*, 16, 3105-3114.
- D'Sa-Eipper, C., Subramanian, T. and Chinnadurai, G. (1996). bfl-1, a bcl-2 homologue, suppresses p53-induced apoptosis and exhibits potent cooperative transforming activity. *Cancer Res.*, 56, 3879-3882.
- D'Souza, B., Rowe, M. and Walls, D. (2000). The bfl-1 gene is transcriptionally upregulated by the Epstein-Barr virus LMP1, and its expression promotes the survival of a Burkitt's lymphoma cell line. *J. Virol.*, 74, 6652-6658.
- D'Souza, B.N., Edelstein, L.C., Pegman, P.M., Smith, S.M., Loughran, S.T., Clarke, A., Mehl, A., Rowe, M., Gelinas, C. and Walls, D. (2004). Nuclear factor kappa B-dependent activation of the antiapoptotic bfl-1 gene by the Epstein-Barr virus latent membrane protein 1 and activated CD40 receptor. *J. Virol.*, 78, 1800-1816.
- Dukers, D.F., Meijer, C.J., ten Berge, R.L., Vos, W., Ossenkoppele, G.J. and Oudejans, J.J. (2002). High numbers of active caspase 3-positive Reed-Sternberg cells in pretreatment biopsy specimens of patients with Hodgkin disease predict favorable clinical outcome. *Blood.*, 100, 36-42.
- Duriez, P.J., Wong, F., Dorovini-Zis, K., Shahidi, R. and Karsan, A. (2000). A1 functions at the mitochondria to delay endothelial apoptosis in response to tumor necrosis factor. *J. Biol. Chem.*, 275, 18099-18107.
- Dutton, A., O'Neil, J.D., Milner, A.E., Reynolds, G.M., Starczynski, J., Crocker, J., Young, L.S. and Murray, P.G. (2004). Expression of the cellular FLICE-inhibitory protein (c-FLIP) protects Hodgkin's lymphoma cells from autonomous Fas-mediated death. *Proc. Natl. Acad. Sci. U. S. A.*, 101, 6611-6616.
- Dutton, A., Reynolds, G.M., Dawson, C.W., Young, L.S. and Murray, P.G. (2005). Constitutive activation of phosphatidyl-inositide 3 kinase contributes to the survival of Hodgkin's lymphoma cells through a mechanism involving Akt kinase and mTOR. *J. Pathol.*, 205, 498-506.
- Edelstein, L.C., Lagos, L., Simmons, M., Tirumalai, H. and Gelinas, C. (2003). NF-kappa B-dependent assembly of an enhanceosome-like complex on the promoter region of apoptosis inhibitor Bfl-1/A1. *Mol. Cell. Biol.*, 23, 2749-2761.

Elbashir, S.M., Harborth, J., Weber, K. and Tuschl, T. (2002). Analysis of gene function in somatic mammalian cells using small interfering RNAs. *Methods.*, 26, 199-213.

Eliopoulos, A.G., Dawson, C.W., Mosialos, G., Floettmann, J.E., Rowe, M., Armitage, R.J., Dawson, J., Zapata, J.M., Kerr, D.J., Wakelam, M.J., Reed, J.C., Kieff, E. and Young, L.S. (1996). CD40-induced growth inhibition in epithelial cells is mimicked by Epstein-Barr Virus-encoded LMP1: involvement of TRAF3 as a common mediator. *Oncogene.*, 13, 2243-2254.

Eliopoulos, A.G. and Young, L.S. (2001). LMP1 structure and signal transduction. *Semin. Cancer Biol.*, 11, 435-444.

Ellisen, L.W., Bird, J., West, D.C., Soreng, A.L., Reynolds, T.C., Smith, S.D. and Sklar, J. (1991). TAN-1, the human homolog of the Drosophila notch gene, is broken by chromosomal translocations in T lymphoblastic neoplasms. *Cell.*, 66, 649-661.

Emmerich, F., Meiser, M., Hummel, M., Demel, G., Foss, H.D., Jundt, F., Mathas, S., Krappmann, D., Scheidereit, C., Stein, H. and Dorken, B. (1999). Overexpression of I kappa B alpha without inhibition of NF-kappaB activity and mutations in the I kappa B alpha gene in Reed-Sternberg cells. *Blood.*, 94, 3129-3134.

Emmerich, F., Theurich, S., Hummel, M., Haeffker, A., Vry, M.S., Dohner, K., Bommert, K., Stein, H. and Dorken, B. (2003). Inactivating I kappa B epsilon mutations in Hodgkin/Reed-Sternberg cells. *J. Pathol.*, 201, 413-420.

Engert, A., Diehl, V., Schnell, R., Radszuhn, A., Hatwig, M.T., Drillich, S., Schon, G., Bohlen, H., Tesch, H., Hansmann, M.L., Barth, S., Schindler, J., Ghiette, V., Uhr, J. and Vitetta, E. (1997). A phase-I study of an anti-CD25 ricin A-chain immunotoxin (RFT5-SMPT-dgA) in patients with refractory Hodgkin's lymphoma. *Blood.*, 89, 403-410.

Feldman, G.M., Rosenthal, L.A., Liu, X., Hayes, M.P., Wynshaw-Boris, A., Leonard, W.J., Hennighausen, L. and Finbloom, D.S. (1997). STAT5A-deficient mice demonstrate a defect in granulocyte-macrophage colony-stimulating factor-induced proliferation and gene expression. *Blood.*, 90, 1768-1776.

Fend, F. and Raffeld, M. (2000). Laser capture microdissection in pathology. *J. Clin. Pathol.*, 53, 666-672.

Feuerhake, F., Kutok, J.L., Monti, S., Chen, W., LaCasce, A.S., Cattoretti, G., Kurtin, P., Pinkus, G.S., de Leval, L., Harris, N.L., Savage, K.J., Neuberg, D., Habermann, T.M., Dalla-Favera, R., Golub, T.R., Aster, J.C. and Shipp, M.A. (2005). NFkappaB activity, function, and target-gene signatures in primary mediastinal large B-cell lymphoma and diffuse large B-cell lymphoma subtypes. *Blood.*, 106, 1392-1399.

- Fiumara, P., Snell, V., Li, Y., Mukhopadhyay, A., Younes, M., Gillenwater, A.M., Cabanillas, F., Aggarwal, B.B. and Younes, A. (2001). Functional expression of receptor activator of nuclear factor kappaB in Hodgkin disease cell lines. *Blood.*, 98, 2784-2790.
- Floettmann, J.E., Eliopoulos, A.G., Jones, M., Young, L.S. and Rowe, M. (1998). Epstein-Barr virus latent membrane protein-1 (LMP1) signalling is distinct from CD40 and involves physical cooperation of its two C-terminus functional regions. *Oncogene.*, 17, 2383-2392.
- Floettmann, J.E. and Rowe, M. (1997). Epstein-Barr virus latent membrane protein-1 (LMP1) C-terminus activation region 2 (CTAR2) maps to the far C-terminus and requires oligomerisation for NF-kappaB activation. *Oncogene.*, 15, 1851-1858.
- Floettmann, J.E., Ward, K., Rickinson, A.B. and Rowe, M. (1996). Cytostatic effect of Epstein-Barr virus latent membrane protein-1 analyzed using tetracycline-regulated expression in B cell lines. *Virology.*, 223, 29-40.
- Foo, S.Y. and Nolan, G.P. (1999). NF-kappaB to the rescue: RELs, apoptosis and cellular transformation. *Trends Genet.*, 15, 229-235.
- Förster, V.T. (1948). Zwischenmolekulare Energiewanderung und Fluorescence. *Annals of Physics (Leipzig)*.
- Fortini, M.E. (2002). Gamma-secretase-mediated proteolysis in cell-surface-receptor signalling. *Nat. Rev. Mol. Cell Biol.*, 3, 673-684.
- Foss, H.D., Herbst, H., Gottstein, S., Demel, G., Araujo, I. and Stein, H. (1996). Interleukin-8 in Hodgkin's disease. Preferential expression by reactive cells and association with neutrophil density. *Am. J. Pathol.*, 148, 1229-1236.
- Foss, H.D., Herbst, H., Oelmann, E., Samol, J., Grebe, M., Blankenstein, T., Matthes, J., Qin, Z.H., Falini, B. and Pileri, S. (1993). Lymphotoxin, tumour necrosis factor and interleukin-6 gene transcripts are present in Hodgkin and Reed-Sternberg cells of most Hodgkin's disease cases. *Br. J. Haematol.*, 84, 627-635.
- Foss, H.D., Reusch, R., Demel, G., Lenz, G., Anagnostopoulos, I., Hummel, M. and Stein, H. (1999). Frequent expression of the B-cell-specific activator protein in Reed-Sternberg cells of classical Hodgkin's disease provides further evidence for its B-cell origin. *Blood.*, 94, 3108-3113.
- Fu, G.F., Lin, X.H., Han, Q.W., Fan, Y.R., Xu, Y.F., Guo, D., Xu, G.X. and Hou, Y.Y. (2005). RNA interference remarkably suppresses bcl-2 gene expression in cancer cells in vitro and in vivo. *Cancer. Biol. Ther.*, 4, 822-829.
- Fujise, K., Zhang, D., Liu, J. and Yeh, E.T. (2000). Regulation of apoptosis and cell cycle progression by MCL1. Differential role of proliferating cell nuclear antigen. *J. Biol. Chem.*, 275, 39458-39465.

- Gandhi, M.K., Tellam, J.T. and Khanna, R. (2004). Epstein-Barr virus-associated Hodgkin's lymphoma. *Br. J. Haematol.*, 125, 267-281.
- Georgakis, G.V., Li, Y., Rassidakis, G.Z., Medeiros, L.J., Mills, G.B. and Younes, A. (2006). Inhibition of the phosphatidylinositol-3 kinase/Akt promotes G1 cell cycle arrest and apoptosis in Hodgkin lymphoma. *Br. J. Haematol.*, 132, 503-511.
- Gerber, H.P., Dixit, V. and Ferrara, N. (1998). Vascular endothelial growth factor induces expression of the antiapoptotic proteins Bcl-2 and A1 in vascular endothelial cells. *J. Biol. Chem.*, 273, 13313-13316.
- Ghosh, P., Tan, T.H., Rice, N.R., Sica, A. and Young, H.A. (1993). The interleukin 2 CD28-responsive complex contains at least three members of the NF kappa B family: c-Rel, p50, and p65. *Proc. Natl. Acad. Sci. U. S. A.*, 90, 1696-1700.
- Gil-Gomez, G., Berns, A. and Brady, H.J. (1998). A link between cell cycle and cell death: Bax and Bcl-2 modulate Cdk2 activation during thymocyte apoptosis. *EMBO J.*, 17, 7209-7218.
- Gires, O., Kohlhuber, F., Kilger, E., Baumann, M., Kieser, A., Kaiser, C., Zeidler, R., Scheffer, B., Ueffing, M. and Hammerschmidt, W. (1999). Latent membrane protein 1 of Epstein-Barr virus interacts with JAK3 and activates STAT proteins. *EMBO J.*, 18, 3064-3073.
- Gires, O., Zimber-Strobl, U., Gonnella, R., Ueffing, M., Marschall, G., Zeidler, R., Pich, D. and Hammerschmidt, W. (1997). Latent membrane protein 1 of Epstein-Barr virus mimics a constitutively active receptor molecule. *EMBO J.*, 16, 6131-6140.
- Giri, D.K. and Aggarwal, B.B. (1998). Constitutive activation of NF-kappaB causes resistance to apoptosis in human cutaneous T cell lymphoma HuT-78 cells. Autocrine role of tumor necrosis factor and reactive oxygen intermediates. *J. Biol. Chem.*, 273, 14008-14014.
- Gonzalez, J., Orlofsky, A. and Prystowsky, M.B. (2003). A1 is a growth-permissive antiapoptotic factor mediating postactivation survival in T cells. *Blood.*, 101, 2679-2685.
- Goormachtigh, G., Ouk, T.S., Mougel, A., Tranchand-Bunel, D., Masy, E., Le Clorennec, C., Feuillard, J., Bornkamm, G.W., Auriault, C., Manet, E., Fafeur, V., Adriaenssens, E. and Coll, J. (2006). Autoactivation of the Epstein-Barr virus oncogenic protein LMP1 during type II latency through opposite roles of the NF-kappaB and JNK signaling pathways. *J. Virol.*, 80, 7382-7393.
- Gossen, M. and Bujard, H. (2002). Studying gene function in eukaryotes by conditional gene inactivation. *Annu. Rev. Genet.*, 36, 153-173.
- Grantham, R., Gautier, C., Gouy, M., Mercier, R. and Pave, A. (1980). Codon catalog usage and the genome hypothesis. *Nucleic Acids Res.*, 8, r49-r62.

Greene, F.L., Page, D.L., Fleming, I.D., Fritz, A.G., Balch, C.M., Haller, D.G. and *et al.* (2002). AJCC Cancer Staging Manual 6th Edition. New York, NY: Springer-Verlag, 2002.

Gregory, C.D., Rowe, M. and Rickinson, A.B. (1990). Different Epstein-Barr virus-B cell interactions in phenotypically distinct clones of a Burkitt's lymphoma cell line. *J. Gen. Virol.*, 71 (Pt 7), 1481-1495.

Griffin, J.B. and Zempleni, J. (2005/2). Biotin deficiency stimulates survival pathways in human lymphoma cells exposed to antineoplastic drugs. *The Journal of Nutritional Biochemistry.*, 16, 96-103.

Grosjean, H. and Fiers, W. (1982). Preferential codon usage in prokaryotic genes: the optimal codon-anticodon interaction energy and the selective codon usage in efficiently expressed genes. *Gene.*, 18, 199-209.

Gross, A., McDonnell, J.M. and Korsmeyer, S.J. (1999). BCL-2 family members and the mitochondria in apoptosis. *Genes Dev.*, 13, 1899-1911.

Gross, A., Terraza, A., Ouahrani-Bettache, S., Liautard, J.P. and Dornand, J. (2000). In vitro Brucella suis infection prevents the programmed cell death of human monocytic cells. *Infect. Immun.*, 68, 342-351.

Grossman, S.R., Johannsen, E., Tong, X., Yalamanchili, R. and Kieff, E. (1994). The Epstein-Barr virus nuclear antigen 2 transactivator is directed to response elements by the J kappa recombination signal binding protein. *Proc. Natl. Acad. Sci. U. S. A.*, 91, 7568-7572.

Grumont, R.J., Rourke, I.J. and Gerondakis, S. (1999). Rel-dependent induction of A1 transcription is required to protect B cells from antigen receptor ligation-induced apoptosis. *Genes Dev.*, 13, 400-411.

Gruss, H.J., Brach, M.A., Drexler, H.G., Bonifer, R., Mertelsmann, R.H. and Herrmann, F. (1992). Expression of cytokine genes, cytokine receptor genes, and transcription factors in cultured Hodgkin and Reed-Sternberg cells. *Cancer Res.*, 52, 3353-3360.

Gruss, H.J., Herrmann, F., Gattei, V., Gloghini, A., Pinto, A. and Carbone, A. (1997). CD40/CD40 ligand interactions in normal, reactive and malignant lympho-hematopoietic tissues. *Leuk. Lymphoma.*, 24, 393-422.

Gruss, H.J., Hirschstein, D., Wright, B., Ulrich, D., Caligiuri, M.A., Barcos, M., Strockbine, L., Armitage, R.J. and Dower, S.K. (1994). Expression and function of CD40 on Hodgkin and Reed-Sternberg cells and the possible relevance for Hodgkin's disease. *Blood.*, 84, 2305-2314.

Guan, E., Wang, J., Laborda, J., Norcross, M., Baeuerle, P.A. and Hoffman, T. (1996). T cell leukemia-associated human Notch/translocation-associated Notch homologue has I kappa B-like activity and physically interacts with nuclear factor-kappa B proteins in T cells. *J. Exp. Med.*, 183, 2025-2032.

- Guo, L., Wang, J., Qian, S., Yan, X., Chen, R. and Meng, G. (2000). Construction and structural modeling of a single-chain Fv-asparaginase fusion protein resistant to proteolysis. *Biotechnol. Bioeng.*, 70, 456-463.
- Gupta, S. (2003). Molecular signaling in death receptor and mitochondrial pathways of apoptosis (Review). *Int. J. Oncol.*, 22, 15-20.
- Guthridge, M.A., Barry, E.F., Felquer, F.A., McClure, B.J., Stomski, F.C., Ramshaw, H. and Lopez, A.F. (2004). The phosphoserine-585-dependent pathway of the GM-CSF/IL-3/IL-5 receptors mediates hematopoietic cell survival through activation of NF-kappaB and induction of bcl-2. *Blood.*, 103, 820-827.
- Gutman, G.A. and Hatfield, G.W. (1989). Nonrandom utilization of codon pairs in Escherichia coli. *Proc. Natl. Acad. Sci. U. S. A.*, 86, 3699-3703.
- Hammerschmidt, W. and Sugden, B. (2004). Epstein-Barr virus sustains Burkitt's lymphomas and Hodgkin's disease. *Trends Mol. Med.*, 10, 331-336.
- Hanahan, D. (1985) In: DNA Cloning, Volume 1, D. Glover, ed., IRL Press, Ltd., London, 109.
- Hanissian, S.H. and Geha, R.S. (1997). Jak3 is associated with CD40 and is critical for CD40 induction of gene expression in B cells. *Immunity.*, 6, 379-387.
- Harris, N., Jaffe, E., Stein, H., Banks, P., Chan, J., Cleary, M., Delsol, G., De Wolf-Peeters, C., Falini, B. and Gatter, K. (1994). A revised European-American classification of lymphoid neoplasms: a proposal from the International Lymphoma Study Group. *Blood.*, 84, 1361-1392.
- Hartmann, F., Renner, C., Jung, W., Deisting, C., Juwana, M., Eichentopf, B., Kloft, M. and Pfreundschuh, M. (1997). Treatment of refractory Hodgkin's disease with an anti-CD16/CD30 bispecific antibody. *Blood.*, 89, 2042-2047.
- Hatakeyama, S., Hamasaki, A., Negishi, I., Loh, D.Y., Sendo, F., Nakayama, K. and Nakayama, K. (1998). Multiple gene duplication and expression of mouse bcl-2-related genes, A1. *Int. Immunol.*, 10, 631-637.
- Hawkins, D. (2005). Biomeasurement; understanding, analysing and communicating data in the biosciences. Oxford Press, London.
- Hayden, M.S. and Ghosh, S. (2004). Signaling to NF-kappaB. *Genes Dev.*, 18, 2195-2224.
- He, C.H., Waxman, A.B., Lee, C.G., Link, H., Rabach, M.E., Ma, B., Chen, Q., Zhu, Z., Zhong, M., Nakayama, K., Nakayama, K.I., Homer, R. and Elias, J.A. (2005). Bcl-2-related protein A1 is an endogenous and cytokine-stimulated mediator of cytoprotection in hyperoxic acute lung injury. *J. Clin. Invest.*, 115, 1039-1048.

- He, Y. and Pear, W.S. (2003). Notch signalling in B cells. *Semin. Cell Dev. Biol.*, 14, 135-142.
- Hedvat, C.V., Jaffe, E.S., Qin, J., Filippa, D.A., Cordon-Cardo, C., Tosato, G., Nimer, S.D. and Teruya-Feldstein, J. (2001). Macrophage-derived chemokine expression in classical Hodgkin's lymphoma: application of tissue microarrays. *Mod. Pathol.*, 14, 1270-1276.
- Heiser, D., Labi, V., Erlacher, M. and Villunger, A. (2004). The Bcl-2 protein family and its role in the development of neoplastic disease. *Exp. Gerontol.*, 39, 1125-1135.
- Hell, K., Lorenzen, J., Fischer, R. and Hansmann, M.L. (1995). Hodgkin cells accumulate mRNA for bcl-2. *Lab. Invest.*, 73, 492-496.
- Henderson, S.T., Gao, D., Lambie, E.J. and Kimble, J. (1994). lag-2 may encode a signaling ligand for the GLP-1 and LIN-12 receptors of *C. elegans*. *Development.*, 120, 2913-2924.
- Hengartner, M.O. (2000). The biochemistry of apoptosis. *Nature.*, 407, 770-776.
- Henkel, T., Ling, P.D., Hayward, S.D. and Peterson, M.G. (1994). Mediation of Epstein-Barr virus EBNA2 transactivation by recombination signal-binding protein J kappa. *Science.*, 265, 92-95.
- Herbst, H. (1996). Epstein-Barr virus in Hodgkin's disease. *Semin. Cancer Biol.*, 7, 183-189.
- Herbst, H., Samol, J., Foss, H.D., Raff, T. and Niedobitek, G. (1997). Modulation of interleukin-6 expression in Hodgkin and Reed-Sternberg cells by Epstein-Barr virus. *J. Pathol.*, 182, 299-306.
- Herling, M., Rassidakis, G.Z., Medeiros, L.J., Vassilakopoulos, T.P., Kliche, K.O., Nadali, G., Viviani, S., Bonfante, V., Giardini, R., Chilos, M., Kittas, C., Gianni, A.M., Bonadonna, G., Pizzolo, G., Pangalis, G.A., Cabanillas, F. and Sarris, A.H. (2003). Expression of Epstein-Barr virus latent membrane protein-1 in Hodgkin and Reed-Sternberg cells of classical Hodgkin's lymphoma: associations with presenting features, serum interleukin 10 levels, and clinical outcome. *Clin. Cancer Res.*, 9, 2114-2120.
- Heslop, H.E., Ng, C.Y., Li, C., Smith, C.A., Loftin, S.K., Krance, R.A., Brenner, M.K. and Rooney, C.M. (1996). Long-term restoration of immunity against Epstein-Barr virus infection by adoptive transfer of gene-modified virus-specific T lymphocytes. *Nat. Med.*, 2, 551-555.
- Heuck, F., Ellermann, J., Borchmann, P., Rothe, A., Hansen, H., Engert, A. and von Strandmann, E.P. (2004). Combination of the human anti-CD30 antibody 5F11 with cytostatic drugs enhances its antitumor activity against Hodgkin and anaplastic large cell lymphoma cell lines. *J. Immunother.* (1997), 27, 347-353.
- Hinz, M., Lemke, P., Anagnostopoulos, I., Hacker, C., Krappmann, D., Mathas, S., Dorken, B., Zenke, M., Stein, H. and Scheidereit, C. (2002). Nuclear factor kappaB-dependent gene expression profiling of Hodgkin's disease tumor cells, pathogenetic significance, and link to constitutive signal transducer and activator of transcription 5a activity. *J. Exp. Med.*, 196, 605-617.

- Hinz, M., Loser, P., Mathas, S., Krappmann, D., Dorken, B. and Scheidereit, C. (2001). Constitutive NF-kappaB maintains high expression of a characteristic gene network, including CD40, CD86, and a set of antiapoptotic genes in Hodgkin/Reed-Sternberg cells. *Blood.*, 97, 2798-2807.
- Hochuli, E. (1989). Genetically designed affinity chromatography using a novel metal chelate absorbent. *Biologically Active Molecules.*, 217-239.
- Hochuli, E., Dobeli, H. and Schacher, A. (1987). New metal chelate adsorbent selective for proteins and peptides containing neighbouring histidine residues. *J. Chromatogr.*, 411, 177-184.
- Hockenberry, D., Nunez, G., Milliman, C., Schreiber, R.D. and Korsmeyer, S.J. (1990). Bcl-2 is an inner mitochondrial membrane protein that blocks programmed cell death. *Nature.*, 348, 334-336.
- Hodgkin, T. (1832) On some morbid experiences of the absorbant glands and spleen. *Med Chir Trans.*, 17, 68-114.
- Hofelmayr, H., Strobl, L.J., Stein, C., Laux, G., Marschall, G., Bornkamm, G.W. and Zimber-Strobl, U. (1999). Activated mouse Notch1 transactivates Epstein-Barr virus nuclear antigen 2-regulated viral promoters. *J. Virol.*, 73, 2770-2780.
- Hong, T., Shimada, Y., Kano, M., Kaganai, J., Uchida, S., Komoto, I., Yamabe, H. and Imamura, M. (2000). The Epstein-Barr virus is rarely associated with esophageal cancer. *Int. J. Mol. Med.*, 5, 363-368.
- Horie, R., Watanabe, T., Ito, K., Morisita, Y., Watanabe, M., Ishida, T., Higashihara, M., Kadin, M. and Watanabe, T. (2002a). Cytoplasmic aggregation of TRAF2 and TRAF5 proteins in the Hodgkin-Reed-Sternberg cells. *Am. J. Pathol.*, 160, 1647-1654.
- Horie, R., Watanabe, T., Morishita, Y., Ito, K., Ishida, T., Kanegae, Y., Saito, I., Higashihara, M., Mori, S., Kadin, M.E. and Watanabe, T. (2002b). Ligand-independent signaling by overexpressed CD30 drives NF-kappaB activation in Hodgkin-Reed-Sternberg cells. *Oncogene.*, 21, 2493-2503.
- Horning, S.J., Hoppe, R.T., Breslin, S., Bartlett, N.L., Brown, B.W. and Rosenberg, S.A. (2002). Stanford V and radiotherapy for locally extensive and advanced Hodgkin's disease: mature results of a prospective clinical trial. *J. Clin. Oncol.*, 20, 630-637.
- Hsieh, J.J., Henkel, T., Salmon, P., Robey, E., Peterson, M.G. and Hayward, S.D. (1996). Truncated mammalian Notch1 activates CBF1/RBPJ $\kappa$ -repressed genes by a mechanism resembling that of Epstein-Barr virus EBNA2. *Mol. Cell. Biol.*, 16, 952-959.
- Hsu, J.L. and Glaser, S.L. (2000). Epstein-barr virus-associated malignancies: epidemiologic patterns and etiologic implications. *Crit. Rev. Oncol. Hematol.*, 34, 27-53.

- Hsu, S.M., Xie, S.S., el-Okda, M.O. and Hsu, P.L. (1992a). Correlation of c-fos/c-jun expression with histiocytic differentiation in Hodgkin's Reed-Sternberg cells. Examination in HDLM-1 subclones with spontaneous differentiation. *Am. J. Pathol.*, 140, 155-165.
- Hsu, S.M., Xie, S.S., Hsu, P.L. and Waldron, J.A., Jr. (1992b). Interleukin-6, but not interleukin-4, is expressed by Reed-Sternberg cells in Hodgkin's disease with or without histologic features of Castleman's disease. *Am. J. Pathol.*, 141, 129-138.
- Hu, X., Yee, E., Harlan, J.M., Wong, F. and Karsan, A. (1998). Lipopolysaccharide induces the antiapoptotic molecules, A1 and A20, in microvascular endothelial cells. *Blood.*, 92, 2759-2765.
- Huang, D.C., O'Reilly, L.A., Strasser, A. and Cory, S. (1997). The anti-apoptosis function of Bcl-2 can be genetically separated from its inhibitory effect on cell cycle entry. *EMBO J.*, 16, 4628-4638.
- Huang, D.C. and Strasser, A. (2000). BH3-Only proteins-essential initiators of apoptotic cell death. *Cell.*, 103, 839-842.
- Hubmann, R., Schwarzmeier, J.D., Shehata, M., Hilgarth, M., Duechler, M., Dettke, M. and Berger, R. (2002). Notch2 is involved in the overexpression of CD23 in B-cell chronic lymphocytic leukemia. *Blood.*, 99, 3742-3747.
- Hutvagner, G. and Zamore, P.D. (2002). RNAi: nature abhors a double-strand. *Curr. Opin. Genet. Dev.*, 12, 225-232.
- Ichikawa, H., Takada, Y., Shishodia, S., Jayaprakasam, B., Nair, M.G. and Aggarwal, B.B. (2006). Withanolides potentiate apoptosis, inhibit invasion, and abolish osteoclastogenesis through suppression of nuclear factor- $\kappa$ B (NF- $\kappa$ B) activation and NF- $\kappa$ B-regulated gene expression. *Mol Cancer Ther.*, 5, 1434-1445.
- Ikemura, T. (1981). Correlation between the abundance of Escherichia coli transfer RNAs and the occurrence of the respective codons in its protein genes: a proposal for a synonymous codon choice that is optimal for the E. coli translational system. *J. Mol. Biol.*, 151, 389-409.
- Ip, Y.T. and Davis, R.J. (1998). Signal transduction by the c-Jun N-terminal kinase (JNK)--from inflammation to development. *Curr. Opin. Cell Biol.*, 10, 205-219.
- James, J.A., Smith, M.A., Court, E.L., Yip, C., Ching, Y., Willson, C. and Smith, J.G. (2003). An investigation of the effects of the MEK inhibitor U0126 on apoptosis in acute leukemia. *Hematol. J.*, 4, 427-432.
- Jang, M.S., Miao, H., Carlesso, N., Shelly, L., Zlobin, A., Darack, N., Qin, J.Z., Nickoloff, B.J. and Miele, L. (2004). Notch-1 regulates cell death independently of differentiation in murine erythroleukemia cells through multiple apoptosis and cell cycle pathways. *J. Cell. Physiol.*, 199, 418-433.

Janumyan, Y.M., Sansam, C.G., Chattopadhyay, A., Cheng, N., Soucie, E.L., Penn, L.Z., Andrews, D., Knudson, C.M. and Yang, E. (2003). Bcl-xL/Bcl-2 coordinately regulates apoptosis, cell cycle arrest and cell cycle entry. *EMBO J.*, 22, 5459-5470.

Janz, M., Dorken, B. and Mathas, S. (2006a). Reprogramming of B lymphoid cells in human lymphoma pathogenesis. *Cell. Cycle.*, 5, 1057-1061.

Janz, M., Hummel, M., Truss, M., Wollert-Wulf, B., Mathas, S., Johrens, K., Hagemeier, C., Bommert, K., Stein, H., Dorken, B. and Bargou, R.C. (2006b). Classical Hodgkin lymphoma is characterized by high constitutive expression of activating transcription factor 3 (ATF3), which promotes viability of Hodgkin/Reed-Sternberg cells. *Blood.*, 107, 2536-2539.

Jazirehi, A.R., Huerta-Yepez, S., Cheng, G. and Bonavida, B. (2005). Rituximab (Chimeric Anti-CD20 Monoclonal Antibody) Inhibits the Constitutive Nuclear Factor-{kappa}B Signaling Pathway in Non-Hodgkin's Lymphoma B-Cell Lines: Role in Sensitization to Chemotherapeutic Drug-induced Apoptosis. *Cancer Res.*, 65, 264-276.

Jazirehi, A.R., Vega, M.I., Chatterjee, D., Goodlick, L. and Bonavida, B. (2004). Inhibition of the Raf-MEK1/2-ERK1/2 Signaling Pathway, Bcl-xL Down-Regulation, and Chemosensitization of Non-Hodgkin's Lymphoma B Cells by Rituximab. *Cancer Res.*, 64, 7117-7126.

Johansen, L.M., Deppmann, C.D., Erickson, K.D., Coffin, W.F., Thornton, T.M., Humphrey, S.E., Martin, J.M. and Taparowsky, E.J. (2003). EBNA2 and activated Notch induce expression of BATF. *J. Virol.*, 77, 6029-6040.

Johnson, G.L., Dohlman, H.G. and Graves, L.M. (2005). MAPK kinase kinases (MKKs) as a target class for small-molecule inhibition to modulate signaling networks and gene expression. *Curr. Opin. Chem. Biol.*, 9, 325-331.

Jones, M.D., Foster, L., Sheedy, T. and Griffin, B.E. (1984). The EB virus genome in Daudi Burkitt's lymphoma cells has a deletion similar to that observed in a non-transforming strain (P3HR-1) of the virus. *EMBO J.*, 3, 813-821.

Joos, S., Kupper, M., Ohl, S., von Bonin, F., Mechtersheimer, G., Bentz, M., Marynen, P., Moller, P., Pfreundschuh, M., Trumper, L. and Lichter, P. (2000). Genomic imbalances including amplification of the tyrosine kinase gene JAK2 in CD30+ Hodgkin cells. *Cancer Res.*, 60, 549-552.

Joos, S., Menz, C.K., Wrobel, G., Siebert, R., Gesk, S., Ohl, S., Mechtersheimer, G., Trumper, L., Moller, P., Lichter, P. and Barth, T.F. (2002). Classical Hodgkin lymphoma is characterized by recurrent copy number gains of the short arm of chromosome 2. *Blood.*, 99, 1381-1387.

Jost, P.J. and Ruland, J. (2007). Aberrant NF-kappaB signaling in lymphoma: mechanisms, consequences, and therapeutic implications. *Blood.*, 109, 2700-2707.

- Josting, A., Katay, I., Rueffer, U., Winter, S., Tesch, H., Engert, A., Diehl, V. and Wickramanayake, P.D. (1998). Favorable outcome of patients with relapsed or refractory Hodgkin's disease treated with high-dose chemotherapy and stem cell rescue at the time of maximal response to conventional salvage therapy (Dex-BEAM). *Ann. Oncol.*, 9, 289-295.
- Jucker, M., Abts, H., Li, W., Schindler, R., Merz, H., Gunther, A., von Kalle, C., Schaadt, M., Diamantstein, T. and Feller, A.C. (1991). Expression of interleukin-6 and interleukin-6 receptor in Hodgkin's disease. *Blood.*, 77, 2413-2418.
- Jundt, F., Probsting, K.S., Anagnostopoulos, I., Muehlinghaus, G., Chatterjee, M., Mathas, S., Bargou, R.C., Manz, R., Stein, H. and Dorken, B. (2004). Jagged1-induced Notch signaling drives proliferation of multiple myeloma cells. *Blood.*, 103, 3511-3515.
- Jundt, F., Raetzel, N., Muller, C., Calkhoven, C.F., Kley, K., Mathas, S., Lietz, A., Leutz, A. and Dorken, B. (2005). A rapamycin derivative (everolimus) controls proliferation through down-regulation of truncated CCAAT enhancer binding protein {beta} and NF-{kappa}B activity in Hodgkin and anaplastic large cell lymphomas. *Blood.*, 106, 1801-1807.
- Jundt, F., Anagnostopoulos, I., Forster, R., Mathas, S., Stein, H. and Dorken, B. (2002). Activated Notch1 signaling promotes tumor cell proliferation and survival in Hodgkin and anaplastic large cell lymphoma. *Blood.*, 99, 3398-3403.
- Jung-Ha, H., Kim, D., Lee, S.B., Hong, S.I., Park, S.Y., Huh, J., Kim, C.W., Kim, S.S., Lee, Y., Choi, S.S. and Shin, H.S. (1998). Expression of Bfl-1 in normal and tumor tissues: Bfl-1 overexpression in cancer is attributable to its preferential expression in infiltrating inflammatory cells. *Hum. Pathol.*, 29, 723-728.
- Jungnickel, B., Staratschek-Jox, A., Brauninger, A., Spieker, T., Wolf, J., Diehl, V., Hansmann, M.L., Rajewsky, K. and Kuppers, R. (2000). Clonal deleterious mutations in the IkappaBalphagene in the malignant cells in Hodgkin's lymphoma. *J. Exp. Med.*, 191, 395-402.
- Kamakura, S., Oishi, K., Yoshimatsu, T., Nakafuku, M., Masuyama, N. and Gotoh, Y. (2004). Hes binding to STAT3 mediates crosstalk between Notch and JAK-STAT signalling. *Nat. Cell Biol.*, 6, 547-554.
- Kamesaki, H., Fukuwara, S., Tatsumi, E., Uchino, H., Yamabe, H., Miwa, H., Shirakawa, S., Hatanaka, M. and Honjo, T. (1986). Cytochemical, immunologic, chromosomal, and molecular genetic analysis of a novel cell line derived from Hodgkin's disease. *Blood.*, 68, 285-292.
- Kanavaros, P., Stefanaki, K., Vlachonikolis, J., Eliopoulos, G., Kakolyris, S., Rontogianni, D., Gorgoulis, V. and Georgoulias, V. (2000). Expression of p53, p21/waf1, bcl-2, bax, Rb and Ki67 proteins in Hodgkin's lymphomas. *Histol. Histopathol.*, 15, 445-453.

- Kane, J.F. (1995). Effects of rare codon clusters on high-level expression of heterologous proteins in *Escherichia coli*. *Curr. Opin. Biotechnol.*, 6, 494-500.
- Kanzler, H., Kuppers, R., Hansmann, M.L. and Rajewsky, K. (1996). Hodgkin and Reed-Sternberg cells in Hodgkin's disease represent the outgrowth of a dominant tumor clone derived from (crippled) germinal center B cells. *J. Exp. Med.*, 184, 1495-1505.
- Kapahi, P., Takahashi, T., Natoli, G., Adams, S.R., Chen, Y., Tsien, R.Y. and Karin, M. (2000). Inhibition of NF-kappa B activation by arsenite through reaction with a critical cysteine in the activation loop of Ikappa B kinase. *J. Biol. Chem.*, 275, 36062-36066.
- Kaplan, H.S. (1980). Essentials of staging and management of the malignant lymphomas. *Semin. Roentgenol.*, 15, 219-226.
- Kapp, U., Yeh, W.C., Patterson, B., Elia, A.J., Kagi, D., Ho, A., Hessel, A., Tipsword, M., Williams, A., Mirtsos, C., Itie, A., Moyle, M. and Mak, T.W. (1999). Interleukin 13 is secreted by and stimulates the growth of Hodgkin and Reed-Sternberg cells. *J. Exp. Med.*, 189, 1939-1946.
- Karin, M. and Ben-Neriah, Y. (2000). Phosphorylation meets ubiquitination: the control of NF-[kappa]B activity. *Annu. Rev. Immunol.*, 18, 621-663.
- Karin, M., Liu, Z. and Zandi, E. (1997). AP-1 function and regulation. *Curr. Opin. Cell Biol.*, 9, 240-246.
- Karsan, A., Yee, E. and Harlan, J.M. (1996a). Endothelial cell death induced by tumor necrosis factor-alpha is inhibited by the Bcl-2 family member, A1. *J. Biol. Chem.*, 271, 27201-27204.
- Karsan, A., Yee, E., Kaushansky, K. and Harlan, J.M. (1996b). Cloning of human Bcl-2 homologue: inflammatory cytokines induce human A1 in cultured endothelial cells. *Blood.*, 87, 3089-3096.
- Kashkar, H., Haefs, C., Shin, H., Hamilton-Dutoit, S.J., Salvesen, G.S., Kronke, M. and Jurgensmeier, J.M. (2003). XIAP-mediated caspase inhibition in Hodgkin's lymphoma-derived B cells. *J. Exp. Med.*, 198, 341-347.
- Kashkar, H., Kronke, M. and Jurgensmeier, J.M. (2002). Defective Bax activation in Hodgkin B-cell lines confers resistance to staurosporine-induced apoptosis. *Cell Death Differ.*, 9, 750-757.
- Kato, H., Sakai, T., Tamura, K., Minoguchi, S., Shirayoshi, Y., Hamada, Y., Tsujimoto, Y. and Honjo, T. (1996). Functional conservation of mouse Notch receptor family members. *FEBS Lett.*, 395, 221-224.
- Kato, H., Taniguchi, Y., Kurooka, H., Minoguchi, S., Sakai, T., Nomura-Okazaki, S., Tamura, K. and Honjo, T. (1997). Involvement of RBP-J in biological functions of mouse Notch1 and its derivatives. *Development.*, 124, 4133-4141.

- Keegan, T.H., Glaser, S.L., Clarke, C.A., Gulley, M.L., Craig, F.E., Digiuseppe, J.A., Dorfman, R.F., Mann, R.B. and Ambinder, R.F. (2005). Epstein-Barr virus as a marker of survival after Hodgkin's lymphoma: a population-based study. *J. Clin. Oncol.*, 23, 7604-7613.
- Keller, S.A., Schattner, E.J. and Cesarman, E. (2000). Inhibition of NF-kappaB induces apoptosis of KSHV-infected primary effusion lymphoma cells. *Blood.*, 96, 2537-2542.
- Kelly, G., Bell, A. and Rickinson, A. (2002). Epstein-Barr virus-associated Burkitt lymphomagenesis selects for downregulation of the nuclear antigen EBNA2. *Nat. Med.*, 8, 1098-1104.
- Kenny, J.J., Knobloch, T.J., Augustus, M., Carter, K.C., Rosen, C.A. and Lang, J.C. (1997). GRS, a novel member of the Bcl-2 gene family, is highly expressed in multiple cancer cell lines and in normal leukocytes. *Oncogene.*, 14, 997-1001.
- Kerkela, R. and Force, T. (2006/8/1). p38 Mitogen-Activated Protein Kinase: A Future Target for Heart Failure Therapy?. *Journal of the American College of Cardiology.*, 48, 556-558.
- Kerr, A.H., James, J.A., Smith, M.A., Willson, C., Court, E.L. and Smith, J.G. (2003). An investigation of the MEK/ERK inhibitor U0126 in acute myeloid leukemia. *Ann. N. Y. Acad. Sci.*, 1010, 86-89.
- Kim, H., Kim, Y.N., Kim, H. and Kim, C.W. (2005). Oxidative stress attenuates Fas-mediated apoptosis in Jurkat T cell line through Bfl-1 induction. *Oncogene.*, 24, 1252-1261.
- Kim, J.K., Kim, K.D., Lee, E., Lim, J.S., Cho, H.J., Yoon, H.K., Cho, M.Y., Baek, K.E., Park, Y.P., Paik, S.G., Choe, Y.K. and Lee, H.G. (2004). Up-regulation of Bfl-1/A1 via NF-kappaB activation in cisplatin-resistant human bladder cancer cell line. *Cancer Lett.*, 212, 61-70.
- Kirkin, V., Joos, S. and Zornig, M. (2004). The role of Bcl-2 family members in tumorigenesis. *Biochim. Biophys. Acta.*, 1644, 229-249.
- Klein, E., Klein, G., Nadkarni, J.S., Nadkarni, J.J., Wigzell, H. and Clifford, P. (1968). Surface IgM-k specificity on a Burkitt's lymphoma cell *in vivo* and in derived culture lines. *Cancer Res.*, 28, 1300-1310.
- Klein, S., Jucker, M., Diehl, V. and Tesch, H. (1992). Production of multiple cytokines by Hodgkin's disease derived cell lines. *Hematol. Oncol.*, 10, 319-329.
- Knecht, H., Berger, C., McQuain, C., Rothenberger, S., Bachmann, E., Martin, J., Esslinger, C., Drexler, H.G., Cai, Y.C., Quesenberry, P.J. and Odermatt, B.F. (1999). Latent membrane protein 1 associated signaling pathways are important in tumor cells of Epstein-Barr virus negative Hodgkin's disease. *Oncogene.*, 18, 7161-7167.
- Ko, J.K., Choi, K.H., Kim, H.J., Choi, H.Y., Yeo, D.J., Park, S.O., Yang, W.S., Kim, Y.N. and Kim, C.W. (2003a). Conversion of Bfl-1, an anti-apoptotic Bcl-2 family protein, to a potent pro-apoptotic protein by fusion with green fluorescent protein (GFP). *FEBS Lett.*, 551, 29-36.

- Ko, J.K., Lee, M.J., Cho, S.H., Cho, J.A., Lee, B.Y., Koh, J.S., Lee, S.S., Shim, Y.H. and Kim, C.W. (2003b). Bfl-1S, a novel alternative splice variant of Bfl-1, localizes in the nucleus via its C-terminus and prevents cell death. *Oncogene.*, 22, 2457-2465.
- Korsmeyer, S.J., Wei, M.C., Saito, M., Weiler, S., Oh, K.J. and Schlesinger, P.H. (2000). Pro-apoptotic cascade activates BID, which oligomerizes BAK or BAX into pores that result in the release of cytochrome c. *Cell Death Differ.*, 7, 1166-1173.
- Koul, D., Takada, Y., Shen, R., Aggarwal, B.B. and Yung, W.K.A. (2006). PTEN enhances TNF-induced apoptosis through modulation of nuclear factor-[kappa]B signaling pathway in human glioma cells. *Biochemical and Biophysical Research Communications.*, 350, 463-471.
- Krajewski, S., Krajewska, M. and Reed, J.C. (1996). Immunohistochemical analysis of in vivo patterns of Bak expression, a proapoptotic member of the Bcl-2 protein family. *Cancer Res.*, 56, 2849-2855.
- Krajewski, S., Krajewska, M., Shabaik, A., Miyashita, T., Wang, H.G. and Reed, J.C. (1994). Immunohistochemical determination of in vivo distribution of Bax, a dominant inhibitor of Bcl-2. *Am. J. Pathol.*, 145, 1323-1336.
- Krappmann, D., Emmerich, F., Kordes, U., Scharschmidt, E., Dorken, B. and Scheidereit, C. (1999). Molecular mechanisms of constitutive NF-kappaB/Rel activation in Hodgkin/Reed-Sternberg cells. *Oncogene.*, 18, 943-953.
- Krappmann, D., Hatada, E.N., Tegethoff, S., Li, J., Klippel, A., Giese, K., Baeuerle, P.A. and Scheidereit, C. (2000). The I kappa B kinase (IKK) complex is tripartite and contains IKK gamma but not IKAP as a regular component. *J. Biol. Chem.*, 275, 29779-29787.
- Krens, S.F., Spaink, H.P. and Snaar-Jagalska, B.E. (2006). Functions of the MAPK family in vertebrate-development. *FEBS Lett.*, 580, 4984-4990.
- Kretschmer, C., Jones, D.B., Morrison, K., Schluter, C., Feist, W., Ulmer, A.J., Arnoldi, J., Matthes, J., Diamantstein, T. and Flad, H.D. (1990). Tumor necrosis factor alpha and lymphotoxin production in Hodgkin's disease. *Am. J. Pathol.*, 137, 341-351.
- Kreuz, S., Siegmund, D., Scheurich, P. and Wajant, H. (2001). NF-kappaB inducers upregulate cFLIP, a cycloheximide-sensitive inhibitor of death receptor signaling. *Mol. Cell. Biol.*, 21, 3964-3973.
- Kube, D., Holtick, U., Vockerodt, M., Ahmadi, T., Haier, B., Behrmann, I., Heinrich, P.C., Diehl, V. and Tesch, H. (2001). STAT3 is constitutively activated in Hodgkin cell lines. *Blood.*, 98, 762-770.
- Kuppers, R., Rajewsky, K., Zhao, M., Simons, G., Laumann, R., Fischer, R. and Hansmann, M. (1994). Hodgkin Disease: Hodgkin and Reed-Sternberg Cells Picked from Histological Sections Show Clonal Immunoglobulin Gene Rearrangements and Appear to be Derived from B Cells at Various Stages of Development. *PNAS.*, 91, 10962-10966.

- Kuss, A.W., Knodel, M., Berberich-Siebelt, F., Lindemann, D., Schimpl, A. and Berberich, I. (1999). A1 expression is stimulated by CD40 in B cells and rescues WEHI 231 cells from anti-IgM-induced cell death. *Eur. J. Immunol.*, 29, 3077-3088.
- Kuwana, T., Mackey, M.R., Perkins, G., Ellisman, M.H., Latterich, M., Schneiter, R., Green, D.R. and Newmeyer, D.D. (2002). Bid, Bax, and lipids cooperate to form supramolecular openings in the outer mitochondrial membrane. *Cell.*, 111, 331-342.
- Kwon, S.Y., Choi, Y.J., Kang, T.H., Lee, K.H., Cha, S.S., Kim, G.H., Lee, H.S., Kim, K.T. and Kim, K.J. (2005). Highly efficient protein expression and purification using bacterial hemoglobin fusion vector. *Plasmid.*, 53, 274-282.
- Lai, E.C. (2002). Keeping a good pathway down: transcriptional repression of Notch pathway target genes by CSL proteins. *EMBO Rep.*, 3, 840-845.
- Lakowicz, J.R. (1983). Energy transfer. In: *Principles of Fluorescent Spectroscopy*, New York: Plenum Press, pp. 303-339.
- Laux, G., Adam, B., Strobl, L.J. and Moreau-Gachelin, F. (1994a). The Spi-1/PU.1 and Spi-B ets family transcription factors and the recombination signal binding protein RBP-J kappa interact with an Epstein-Barr virus nuclear antigen 2 responsive cis-element. *EMBO J.*, 13, 5624-5632.
- Laux, G., Dugrillon, F., Eckert, C., Adam, B., Zimber-Strobl, U. and Bornkamm, G.W. (1994b). Identification and characterization of an Epstein-Barr virus nuclear antigen 2-responsive cis element in the bidirectional promoter region of latent membrane protein and terminal protein 2 genes. *J. Virol.*, 68, 6947-6958.
- Lee, H.H., Dadgostar, H., Cheng, Q., Shu, J. and Cheng, G. (1999). NF-kappaB-mediated up-regulation of Bcl-x and Bfl-1/A1 is required for CD40 survival signaling in B lymphocytes. *Proc. Natl. Acad. Sci. U. S. A.*, 96, 9136-9141.
- Lee, J.H., Hwang, B.Y., Kim, K.S., Nam, J.B., Hong, Y.S. and Lee, J.J. (2003). Suppression of RelA/p65 transactivation activity by a lignoid manassantin isolated from Saururus chinensis. *Biochem. Pharmacol.*, 66, 1925-1933.
- Lee, J.H., Koo, T.H., Yoon, H., Jung, H.S., Jin, H.Z., Lee, K., Hong, Y.S. and Lee, J.J. (2006). Inhibition of NF-kappa B activation through targeting I kappa B kinase by celastrol, a quinone methide triterpenoid. *Biochem. Pharmacol.*, 72, 1311-1321.
- Lenoir, G.M., Vuillaume, M. and Bonnardel, C. (1985). The use of lymphomatous and lymphoblastoid cell lines in the study of Burkitt's lymphoma. *IARC Sci. Publ.*, (60), 309-318.
- Leonard, W.J. and O'Shea, J.J. (1998). Jaks and STATs: biological implications. *Annu. Rev. Immunol.*, 16, 293-322.

- Leppa, S. and Bohmann, D. (1999). Diverse functions of JNK signaling and c-Jun in stress response and apoptosis. *Oncogene*, 18, 6158-6162.
- Letai, A. (2005). Pharmacological manipulation of Bcl-2 family members to control cell death. *J. Clin. Invest.*, 115, 2648-2655.
- Li, H., Zhu, H., Xu, C.J. and Yuan, J. (1998). Cleavage of BID by caspase 8 mediates the mitochondrial damage in the Fas pathway of apoptosis. *Cell*, 94, 491-501.
- Liljeholm, S., Hughes, K., Grundstrom, T. and Brodin, P. (1998). NF-kappaB only partially mediates Epstein-Barr virus latent membrane protein 1 activation of B cells. *J. Gen. Virol.*, 79 (Pt 9), 2117-2125.
- Lima, R.T., Martins, L.M., Guimaraes, J.E., Sambade, C. and Vasconcelos, M.H. (2004). Specific downregulation of bcl-2 and xIAP by RNAi enhances the effects of chemotherapeutic agents in MCF-7 human breast cancer cells. *Cancer Gene Ther.*, 11, 309-316.
- Lin, E.Y., Orlofsky, A., Berger, M.S. and Prystowsky, M.B. (1993). Characterization of A1, a novel hemopoietic-specific early-response gene with sequence similarity to bcl-2. *J. Immunol.*, 151, 1979-1988.
- Lin, M., Juan, C., Chang, K., Chen, W. and Kuo, M. (2001). IL-6 inhibits apoptosis and retains oxidative DNA lesions in human gastric cancer AGS cells through up-regulation of anti-apoptotic gene mcl-1. *Carcinogenesis*, 22, 1947-1953.
- Ling, P.D., Hsieh, J.J., Ruf, I.K., Rawlins, D.R. and Hayward, S.D. (1994). EBNA-2 upregulation of Epstein-Barr virus latency promoters and the cellular CD23 promoter utilizes a common targeting intermediate, CBF1. *J. Virol.*, 68, 5375-5383.
- Liu, Y., Denlinger, C.E., Rundall, B.K., Smith, P.W. and Jones, D.R. (2006a). Suberoylanilide Hydroxamic Acid Induces Akt-mediated Phosphorylation of p300, Which Promotes Acetylation and Transcriptional Activation of RelA/p65. *J. Biol. Chem.*, 281, 31359-31368.
- Liu, Y., Smith, P.W. and Jones, D.R. (2006b). Breast Cancer Metastasis Suppressor 1 Functions as a Corepressor by Enhancing Histone Deacetylase 1-Mediated Deacetylation of RelA/p65 and Promoting Apoptosis. *Mol. Cell. Biol.*, 26, 8683-8696.
- Livak, K.J. and Schmittgen, T.D. (2001). Analysis of relative gene expression data using real-time quantitative PCR and the 2(-Delta Delta C(T)) Method. *Methods*, 25, 402-408.
- Loughran, S.T., Loughran, N.B., Ryan, B.J., D'Souza, B.N. and Walls, D. (2006/8/1). Modified His-tag fusion vector for enhanced protein purification by immobilized metal affinity chromatography. *Analytical Biochemistry*, 355, 148-150.

- Luo, X., Budihardjo, I., Zou, H., Slaughter, C. and Wang, X. (1998). Bid, a Bcl2 interacting protein, mediates cytochrome c release from mitochondria in response to activation of cell surface death receptors. *Cell.*, 94, 481-490.
- MacLennan, I.C., Liu, Y.L. and Ling, N.R. (1988). B cell proliferation in follicles, germinal centre formation and the site of neoplastic transformation in Burkitt's lymphoma. *Curr. Top. Microbiol. Immunol.*, 141, 138-148.
- Maggio, E.M., Van Den Berg, A., de Jong, D., Diepstra, A. and Poppema, S. (2003). Low frequency of FAS mutations in Reed-Sternberg cells of Hodgkin's lymphoma. *Am. J. Pathol.*, 162, 29-35.
- Maier, S., Santak, M., Mantik, A., Grabusic, K., Kremmer, E., Hammerschmidt, W. and Kempkes, B. (2005). A somatic knockout of CBF1 in a human B-cell line reveals that induction of CD21 and CCR7 by EBNA-2 is strictly CBF1 dependent and that downregulation of immunoglobulin M is partially CBF1 independent. *J. Virol.*, 79, 8784-8792.
- Malisan, F., Briere, F., Bridon, J.M., Harindranath, N., Mills, F.C., Max, E.E., Banchereau, J. and Martinez-Valdez, H. (1996). Interleukin-10 induces immunoglobulin G isotype switch recombination in human CD40-activated naive B lymphocytes. *J. Exp. Med.*, 183, 937-947.
- Maniatis, T. (1999). A ubiquitin ligase complex essential for the NF-kappaB, Wnt/Wingless, and Hedgehog signaling pathways. *Genes Dev.*, 13, 505-510.
- Marafioti, T., Hummel, M., Anagnostopoulos, I., Foss, H.D., Falini, B., Delsol, G., Isaacson, P.G., Pileri, S. and Stein, H. (1997). Origin of nodular lymphocyte-predominant Hodgkin's disease from a clonal expansion of highly mutated germinal-center B cells. *N. Engl. J. Med.*, 337, 453-458.
- Marafioti, T., Hummel, M., Foss, H.D., Laumen, H., Korbjuhn, P., Anagnostopoulos, I., Lammert, H., Demel, G., Theil, J., Wirth, T. and Stein, H. (2000). Hodgkin and reed-sternberg cells represent an expansion of a single clone originating from a germinal center B-cell with functional immunoglobulin gene rearrangements but defective immunoglobulin transcription. *Blood.*, 95, 1443-1450.
- Martinez, L.A., Naguibneva, I., Lehrmann, H., Vervisch, A., Tchenio, T., Lozano, G. and Harel-Bellan, A. (2002). Synthetic small inhibiting RNAs: efficient tools to inactivate oncogenic mutations and restore p53 pathways. *Proc. Natl. Acad. Sci. U. S. A.*, 99, 14849-14854.
- Martinez-Valdez, H., Guret, C., de Bouteiller, O., Fugier, I., Banchereau, J. and Liu, Y.J. (1996). Human germinal center B cells express the apoptosis-inducing genes Fas, c-myc, P53, and Bax but not the survival gene bcl-2. *J. Exp. Med.*, 183, 971-977.
- Martin-Sabero, J.I., Gesk, S., Harder, L., Sonoki, T., Tucker, P.W., Schlegelberger, B., Grote, W., Novo, F.J., Calasanz, M.J., Hansmann, M.L., Dyer, M.J. and Siebert, R. (2002). Recurrent involvement of the REL and BCL11A loci in classical Hodgkin lymphoma. *Blood.*, 99, 1474-1477.

- Mathas, S., Hinz, M., Anagnostopoulos, I., Krappmann, D., Lietz, A., Jundt, F., Bommert, K., Mechta-Grigoriou, F., Stein, H., Dorken, B. and Scheidereit, C. (2002). Aberrantly expressed c-Jun and JunB are a hallmark of Hodgkin lymphoma cells, stimulate proliferation and synergize with NF-kappa B. *EMBO J.*, 21, 4104-4113.
- Mathas, S., Janz, M., Hummel, F., Hummel, M., Wollert-Wulf, B., Lusatis, S., Anagnostopoulos, I., Lietz, A., Sigvardsson, M., Jundt, F., Johrens, K., Bommert, K., Stein, H. and Dorken, B. (2006). Intrinsic inhibition of transcription factor E2A by HLH proteins ABF-1 and Id2 mediates reprogramming of neoplastic B cells in Hodgkin lymphoma. *Nat. Immunol.*, 7, 207-215.
- Mathas, S., Johrens, K., Joos, S., Lietz, A., Hummel, F., Janz, M., Jundt, F., Anagnostopoulos, I., Bommert, K., Lichter, P., Stein, H., Scheidereit, C. and Dorken, B. (2005). Elevated NF-kappaB p50 complex formation and Bcl-3 expression in classical Hodgkin, anaplastic large-cell, and other peripheral T-cell lymphomas. *Blood.*, 106, 4287-4293.
- Mathas, S., Lietz, A., Anagnostopoulos, I., Hummel, F., Wiesner, B., Janz, M., Jundt, F., Hirsch, B., Johrens-Leder, K., Vornlocher, H.P., Bommert, K., Stein, H. and Dorken, B. (2004). c-FLIP mediates resistance of Hodgkin/Reed-Sternberg cells to death receptor-induced apoptosis. *J. Exp. Med.*, 199, 1041-1052.
- Mathas, S., Lietz, A., Janz, M., Hinz, M., Jundt, F., Scheidereit, C., Bommert, K. and Dorken, B. (2003). Inhibition of NF-kappaB essentially contributes to arsenic-induced apoptosis. *Blood.*, 102, 1028-1034.
- Matsukura, S., Jones, P.A. and Takai, D. (2003). Establishment of conditional vectors for hairpin siRNA knockdowns. *Nucleic Acids Res.*, 31, e77.
- McDonnell, J.M., Fushman, D., Milliman, C.L., Korsmeyer, S.J. and Cowburn, D. (1999). Solution structure of the proapoptotic molecule BID: a structural basis for apoptotic agonists and antagonists. *Cell.*, 96, 625-634.
- McMahon, K.J., Minihan, D., Campion, E.M., Loughran, S.T., Allan, G., McNeilly, F. and Walls, D. (2006/8/25). Infection of pigs in Ireland with lymphotropic [gamma]-herpesviruses and relationship to postweaning multisystemic wasting syndrome. *Veterinary Microbiology.*, 116, 60-68.
- Mello, C.C., Draper, B.W. and Priess, J.R. (1994). The maternal genes *apx-1* and *glp-1* and establishment of dorsal-ventral polarity in the early *C. elegans* embryo. *Cell.*, 77, 95-106.
- Mercurio, F., Zhu, H., Murray, B.W., Shevchenko, A., Bennett, B.L., Li, J., Young, D.B., Barbosa, M., Mann, M., Manning, A. and Rao, A. (1997). IKK-1 and IKK-2: cytokine-activated IkappaB kinases essential for NF-kappaB activation. *Science.*, 278, 860-866.
- Merz, H., Houssiau, F.A., Orschescheck, K., Renauld, J.C., Fliedner, A., Herin, M., Noel, H., Kadin, M., Mueller-Hermelink, H.K. and Van Snick, J. (1991). Interleukin-9 expression in human malignant

lymphomas: unique association with Hodgkin's disease and large cell anaplastic lymphoma. *Blood*, 78, 1311-1317.

Messineo, C., Jamerson, M.H., Hunter, E., Braziel, R., Bagg, A., Irving, S.G. and Cossman, J. (1998). Gene expression by single Reed-Sternberg cells: pathways of apoptosis and activation. *Blood*, 91, 2443-2451.

Miele, L. (2006). Notch Signaling. *Clin Cancer Res.*, 12, 1074-1079.

Mikhailov, V., Mikhailova, M., Pulkrabek, D.J., Dong, Z., Venkatachalam, M.A. and Saikumar, P. (2001). Bcl-2 prevents Bax oligomerization in the mitochondrial outer membrane. *J. Biol. Chem.*, 276, 18361-18374.

Minoguchi, S., Taniguchi, Y., Kato, H., Okazaki, T., Strobl, L.J., Zimber-Strobl, U., Bornkamm, G.W. and Honjo, T. (1997). RBP-L, a transcription factor related to RBP-Jkappa. *Mol. Cell. Biol.*, 17, 2679-2687.

Molin, D., Fischer, M., Xiang, Z., Larsson, U., Harvima, I., Venge, P., Nilsson, K., Sundstrom, C., Enblad, G. and Nilsson, G. (2001). Mast cells express functional CD30 ligand and are the predominant CD30L-positive cells in Hodgkin's disease. *Br. J. Haematol.*, 114, 616-623.

Montalban, C., Garcia, J.F., Abraira, V., Gonzalez-Camacho, L., Morente, M.M., Bello, J.L., Conde, E., Cruz, M.A., Garcia-Sanz, R., Garcia-Larana, J., Grande, C., Llanos, M., Martinez, R., Flores, E., Mendez, M., Ponderos, C., Rayon, C., Sanchez-Godoy, P., Zamora, J., Piris, M.A. and Spanish Hodgkin's Lymphoma Study Group. (2004). Influence of biologic markers on the outcome of Hodgkin's lymphoma: a study by the Spanish Hodgkin's Lymphoma Study Group. *J. Clin. Oncol.*, 22, 1664-1673.

Monti, S., Savage, K.J., Kutok, J.L., Feuerhake, F., Kurtin, P., Mihm, M., Wu, B., Pasqualucci, L., Neuberg, D., Aguiar, R.C., Dal Cin, P., Ladd, C., Pinkus, G.S., Salles, G., Harris, N.L., Dalla-Favera, R., Habermann, T.M., Aster, J.C., Golub, T.R. and Shipp, M.A. (2005). Molecular profiling of diffuse large B-cell lymphoma identifies robust subtypes including one characterized by host inflammatory response. *Blood*, 105, 1851-1861.

Morales, A.A., Olsson, A., Celsing, F., Osterborg, A., Jondal, M. and Osorio, L.M. (2005). High expression of bfl-1 contributes to the apoptosis resistant phenotype in B-cell chronic lymphocytic leukemia. *Int. J. Cancer*, 113, 730-737.

Moreb, J.S. and Schweder, M. (1997). Human A1, a Bcl-2-related gene, is induced in leukemic cells by cytokines as well as differentiating factors. *Leukemia*, 11, 998-1004.

Moreb, J.S. and Zucali, J. (2001). Human A1 expression in acute myeloid leukemia and its relationship to Bcl-2 expression. *Blood*, 97, 578-579.

- Morgan, R.K., Costello, R.W., Durcan, N., Kingham, P.J., Gleich, G.J., McLean, W.G. and Walsh, M. (2005). Diverse Effects of Eosinophil Cationic Granule Proteins on IMR-32 Nerve Cell Signaling and Survival. *Am. J. Respir. Cell Mol. Biol.*, 33, 169-177.
- Morimura, T., Miyatani, S., Kitamura, D. and Goitsuka, R. (2001). Notch signaling suppresses IgH gene expression in chicken B cells: implication in spatially restricted expression of Serrate2/Notch1 in the bursa of Fabricius. *J. Immunol.*, 166, 3277-3283.
- Mumm, J.S. and Kopan, R. (2000). Notch signaling: from the outside in. *Dev. Biol.*, 228, 151-165.
- Murray, P.G., Oates, J., Reynolds, G.M., Crocker, J. and Young, L.S. (1995). Expression of B7 (CD80) and CD40 antigens and the CD40 ligand in Hodgkin's disease is independent of latent Epstein-Barr virus infection. *Clin. Mol. Pathol.*, 48, M105-M108.
- Murray, P.G. and Young, L.S. (2001). Epstein-Barr virus infection: basis of malignancy and potential for therapy. *Expert Rev. Mol. Med.*, 2001, 1-20.
- Muschen, M., Rajewsky, K., Brauninger, A., Baur, A.S., Oudejans, J.J., Roers, A., Hansmann, M.L. and Kuppers, R. (2000). Rare occurrence of classical Hodgkin's disease as a T cell lymphoma. *J. Exp. Med.*, 191, 387-394.
- Nakshatri, H., Bhat-Nakshatri, P., Martin, D.A., Goulet, R.J., Jr and Sledge, G.W., Jr. (1997). Constitutive activation of NF-kappaB during progression of breast cancer to hormone-independent growth. *Mol. Cell. Biol.*, 17, 3629-3639.
- Nefedova, Y., Cheng, P., Alsina, M., Dalton, W.S. and Gabrilovich, D.I. (2004). Involvement of Notch-1 signaling in bone marrow stroma-mediated de novo drug resistance of myeloma and other malignant lymphoid cell lines. *Blood.*, 103, 3503-3510.
- Nilsson, K. and Ponten, J. (1975). Classification and biological nature of established human hematopoietic cell lines. *Int. J. Cancer.*, 15, 321-341.
- Novy, R., Drott, D., Yaeger, K., Mierendorf, R. (2001). Overcoming the codon bias of *E. coli* for enhanced protein expression. *Innovations.*, 12, 1-3.
- Nutt, S.L., Thevenin, C. and Busslinger, M. (1997). Essential functions of Pax-5 (BSAP) in pro-B cell development. *Immunobiology.*, 198, 227-235.
- Oakley, F., Mann, J., Ruddell, R.G., Pickford, J., Weinmaster, G. and Mann, D.A. (2003). Basal expression of IkappaBalphai is controlled by the mammalian transcriptional repressor RBP-J (CBF1) and its activator Notch1. *J. Biol. Chem.*, 278, 24359-24370.
- O'Grady, J.T., Stewart, S., Lowrey, J., Howie, S.E. and Krajewski, A.S. (1994). CD40 expression in Hodgkin's disease. *Am. J. Pathol.*, 144, 21-26.

- Ohshima, K., Akaiwa, M., Umehita, R., Suzumiya, J., Izuohara, K. and Kikuchi, M. (2001). Interleukin-13 and interleukin-13 receptor in Hodgkin's disease: possible autocrine mechanism and involvement in fibrosis. *Histopathology*, 38, 368-375.
- Okamoto, S., Mukaida, N., Yasumoto, K., Rice, N., Ishikawa, Y., Horiguchi, H., Murakami, S. and Matsushima, K. (1994). The interleukin-8 AP-1 and kappa B-like sites are genetic end targets of FK506-sensitive pathway accompanied by calcium mobilization. *J. Biol. Chem.*, 269, 8582-8589.
- Opipari, A.W., Hu, H.M., Yabkowitz, R., Dixit, V. (1992). The A20 zinc finger protein protects cells from tumour necrosis factor cytotoxicity. *J Biol Chem.*, 267:12424-12427.
- O'Reilly, L.A., Huang, D.C. and Strasser, A. (1996). The cell death inhibitor Bcl-2 and its homologues influence control of cell cycle entry. *EMBO J.*, 15, 6979-6990.
- Orkin, S.H. (1992). GATA-binding transcription factors in hematopoietic cells. *Blood*, 80, 575-581.
- Orlofsky, A., Somogyi, R.D., Weiss, L.M. and Prystowsky, M.B. (1999). The murine antiapoptotic protein A1 is induced in inflammatory macrophages and constitutively expressed in neutrophils. *J. Immunol.*, 163, 412-419.
- Oswald, F., Liptay, S., Adler, G. and Schmid, R.M. (1998). NF-kappaB2 is a putative target gene of activated Notch-1 via RBP-Jkappa. *Mol. Cell. Biol.*, 18, 2077-2088.
- Oswald, F., Winkler, M., Cao, Y., Astrahantseff, K., Bourteel, S., Knochel, W. and Borggrefe, T. (2005). RBP-Jkappa/SHARP recruits CtIP/CtBP corepressors to silence Notch target genes. *Mol. Cell. Biol.*, 25, 10379-10390.
- Pagliari, L.J., Perlman, H., Liu, H. and Pope, R.M. (2000). Macrophages require constitutive NF-kappaB activation to maintain A1 expression and mitochondrial homeostasis. *Mol. Cell. Biol.*, 20, 8855-8865.
- Pahl, H.L. (1999). Activators and target genes of Rel/NF-kappaB transcription factors. *Oncogene*, 18, 6853-6866.
- Pajor, L., Kajtar, B., Jakso, P., Lacza, Laszlo, R., Radvanyi, G., Morocz, I., Toth, A. and Varga, G. (2006). Epstein-Barr virus-induced B-cell proliferation of Hodgkin's and Reed-Sternberg cell pheno- and genotype may develop in peripheral T-cell lymphomas. *Histopathology*, 49, 553-557.
- Pang, X.P., Hershman, J.M. and Karsan, A. (1997). TNF-alpha induction of A1 expression in human cancer cells. *Oncol. Res.*, 9, 623-627.
- Panwalkar, A., Verstovsek, S. and Giles, F. (2004). Nuclear factor-kappaB modulation as a therapeutic approach in hematologic malignancies. *Cancer*, 100, 1578-1589.

- Park, I.C., Lee, S.H., Whang, D.Y., Hong, W.S., Choi, S.S., Shin, H.S., Choe, T.B. and Hong, S.I. (1997). Expression of a novel Bcl-2 related gene, Bfl-1, in various human cancers and cancer cell lines. *Anticancer Res.*, 17, 4619-4622.
- Pegman, P.M., Smith, S.M., D'Souza, B.N., Loughran, S.T., Maier, S., Kempkes, B., Cahill, P.A., Simmons, M.J., Gelinas, C. and Walls, D. (2006). Epstein-Barr Virus Nuclear Antigen 2 trans-Activates the Cellular Antiapoptotic bfl-1 Gene by a CBF1/RBPJ $\kappa$ -Dependent Pathway. *J. Virol.*, 80, 8133-8144.
- Peh, S.C., Kim, L.H. and Poppema, S. (2001). TARC, a CC chemokine, is frequently expressed in classic Hodgkin's lymphoma but not in NLP Hodgkin's lymphoma, T-cell-rich B-cell lymphoma, and most cases of anaplastic large cell lymphoma. *Am. J. Surg. Pathol.*, 25, 925-929.
- Perkins, N.D., Schmid, R.M., Duckett, C.S., Leung, K., Rice, N.R. and Nabel, G.J. (1992). Distinct combinations of NF- $\kappa$ B subunits determine the specificity of transcriptional activation. *Proc. Natl. Acad. Sci. U. S. A.*, 89, 1529-1533.
- Petros, A.M., Olejniczak, E.T. and Fesik, S.W. (2004). Structural biology of the Bcl-2 family of proteins. *Biochimica et Biophysica Acta (BBA) - Molecular Cell Research.*, 1644, 83-94.
- Pham, L.V., Tamayo, A.T., Yoshimura, L.C., Lo, P. and Ford, R.J. (2003). Inhibition of constitutive NF- $\kappa$ B activation in mantle cell lymphoma B cells leads to induction of cell cycle arrest and apoptosis. *J. Immunol.*, 171, 88-95.
- Pierce, J.W., Schoenleber, R., Jesmok, G., Best, J., Moore, S.A., Collins, T. and Gerritsen, M.E. (1997). Novel inhibitors of cytokine-induced IkappaBalph phosphorylation and endothelial cell adhesion molecule expression show anti-inflammatory effects in vivo. *J. Biol. Chem.*, 272, 21096-21103.
- Pileri, S.A., Ascani, S., Leoncini, L., Sabattini, E., Zinzani, P.L., Piccaluga, P.P., Pileri, A., Jr, Giunti, M., Falini, B., Bolis, G.B. and Stein, H. (2002). Hodgkin's lymphoma: the pathologist's viewpoint. *J Clin Pathol.*, 55, 162-176.
- Pinkus, G.S., Pinkus, J.L., Langhoff, E., Matsumura, F., Yamashiro, S., Mosialos, G. and Said, J.W. (1997). Fascin, a sensitive new marker for Reed-Sternberg cells of hodgkin's disease. Evidence for a dendritic or B cell derivation?. *Am. J. Pathol.*, 150, 543-562.
- Pinto, A., Aldinucci, D., Gloghini, A., Zagonel, V., Degan, M., Impronta, S., Juzbasic, S., Todesco, M., Perin, V., Gattei, V., Herrmann, F., Gruss, H.J. and Carbone, A. (1996). Human eosinophils express functional CD30 ligand and stimulate proliferation of a Hodgkin's disease cell line. *Blood.*, 88, 3299-3305.
- Pinto, A., Gattei, V., Zagonel, V., Aldinucci, D., Degan, M., De Iuliis, A., Rossi, F.M., Tassan Mazzocco, F., Godeas, C., Rupolo, M., Poletto, D., Gloghini, A., Carbone, A. and Gruss, H.J. (1998). Hodgkin's disease: a disorder of dysregulated cellular cross-talk. *Biotherapy.*, 10, 309-320.

Pogue, S.L., Kurosaki, T., Bolen, J. and Herbst, R. (2000). B cell antigen receptor-induced activation of Akt promotes B cell survival and is dependent on Syk kinase. *J. Immunol.*, 165, 1300-1306.

Ponzielli, R., Katz, S., Barsyte-Lovejoy, D. and Penn, L.Z. (2005). Cancer therapeutics: targeting the dark side of Myc. *Eur. J. Cancer.*, 41, 2485-2501.

Poppema, S. and van den Berg, A. (2000). Interaction between host T cells and Reed-Sternberg cells in Hodgkin lymphomas. *Semin. Cancer Biol.*, 10, 345-350.

Porath, J., Carlsson, J., Olsson, I. and Belfrage, G. (1975). Metal chelate affinity chromatography, a new approach to protein fractionation. *Nature.*, 258, 598-599.

Portis, T., Cooper, L., Dennis, P. and Longnecker, R. (2002). The LMP2A signalosome--a therapeutic target for Epstein-Barr virus latency and associated disease. *Front. Biosci.*, 7, 414-26.

QIAexpressionist Manual, 2003

[http://www1.qiagen.com/literature/handbooks/PDF/Protein/Expression/QXP\\_QIAexpressionist/1024473\\_QXPHB\\_0603.pdf](http://www1.qiagen.com/literature/handbooks/PDF/Protein/Expression/QXP_QIAexpressionist/1024473_QXPHB_0603.pdf)

QIAGEN Plasmid Purification Handbook, 2005

[http://www1.qiagen.com/literature/handbooks/PDF/PlasmidDNAPurification/PLS\\_Plasmid/1034637\\_HB\\_QIAGENPlasmid\\_112005.pdf](http://www1.qiagen.com/literature/handbooks/PDF/PlasmidDNAPurification/PLS_Plasmid/1034637_HB_QIAGENPlasmid_112005.pdf)

QIAGEN OneStep RT-PCR Handbook, 2002

<http://www1.qiagen.com/literature/handbooks/literature.aspx?id=1000223>

QIAGEN RNeasy Handbook, 2006

[http://www1.qiagen.com/literature/handbooks/PDF/RNAStabilizationAndPurification/FromAnimalAndPlantTissuesBacteriaYeastAndFungi/RNY\\_Mini/1035969\\_HB\\_BenchProtocol.pdf](http://www1.qiagen.com/literature/handbooks/PDF/RNAStabilizationAndPurification/FromAnimalAndPlantTissuesBacteriaYeastAndFungi/RNY_Mini/1035969_HB_BenchProtocol.pdf)

Radford, J.A., Rohatiner, A.Z., Ryder, W.D., Deakin, D.P., Barbui, T., Lucie, N.P., Rossi, A., Dunlop, D.J., Cowan, R.A., Wilkinson, P.M., Gupta, R.K., James, R.D., Shamash, J., Chang, J., Crowther, D. and Lister, T.A. (2002). ChlVPP/EVA hybrid versus the weekly VAPEC-B regimen for previously untreated Hodgkin's disease. *J. Clin. Oncol.*, 20, 2988-2994.

Radtke, F. and Raj, K. (2003). The role of Notch in tumorigenesis: oncogene or tumour suppressor?. *Nat. Rev. Cancer.*, 3, 756-767.

Rajewsky, K. (1996). Clonal selection and learning in the antibody system. *Nature.*, 381, 751-758.

Ramachandran, G.N. and Sasisekharan, V. (1968). Conformation of polypeptides and proteins. *Adv. Protein Chem.*, 23, 283-438.

- Rangarajan, A., Syal, R., Selvarajah, S., Chakrabarti, O., Sarin, A. and Krishna, S. (2001). Activated Notch1 signaling cooperates with papillomavirus oncogenes in transformation and generates resistance to apoptosis on matrix withdrawal through PKB/Akt. *Virology.*, 286, 23-30.
- Rassidakis, G.Z., Lai, R., McDonnell, T.J., Cabanillas, F., Sarris, A.H. and Medeiros, L.J. (2002). Overexpression of Mcl-1 in anaplastic large cell lymphoma cell lines and tumors. *Am. J. Pathol.*, 160, 2309-2310.
- Rassidakis, G.Z., Medeiros, L.J., McDonnell, T.J., Viviani, S., Bonfante, V., Nadali, G., Vassilakopoulos, T.P., Giardini, R., Chilos, M., Kittas, C., Gianni, A.M., Bonadonna, G., Pizzolo, G., Pangalis, G.A., Cabanillas, F. and Sarris, A.H. (2002). BAX expression in Hodgkin and Reed-Sternberg cells of Hodgkin's disease: correlation with clinical outcome. *Clin. Cancer Res.*, 8, 488-493.
- Rassidakis, G.Z., Medeiros, L.J., Vassilakopoulos, T.P., Viviani, S., Bonfante, V., Nadali, G., Herling, M., Angelopoulou, M.K., Giardini, R., Chilos, M., Kittas, C., McDonnell, T.J., Bonadonna, G., Gianni, A.M., Pizzolo, G., Pangalis, G.A., Cabanillas, F. and Sarris, A.H. (2002). BCL-2 expression in Hodgkin and Reed-Sternberg cells of classical Hodgkin disease predicts a poorer prognosis in patients treated with ABVD or equivalent regimens. *Blood.*, 100, 3935-3941.
- Rathmell, J.C., Vander Heiden, M.G., Harris, M.H., Frauwirth, K.A. and Thompson, C.B. (2000). In the absence of extrinsic signals, nutrient utilization by lymphocytes is insufficient to maintain either cell size or viability. *Mol. Cell.*, 6, 683-692.
- Ravi, R. and Bedi, A. (2004). NF-kappaB in cancer--a friend turned foe. *Drug Resist Updat.*, 7, 53-67.
- Re, D., Hofmann, A., Wolf, J., Diehl, V. and Staratschek-Jox, A. (2000). Cultivated H-RS cells are resistant to CD95L-mediated apoptosis despite expression of wild-type CD95. *Exp. Hematol.*, 28, 348.
- Re, D., Muschen, M., Ahmadi, T., Wickenhauser, C., Staratschek-Jox, A., Holtick, U., Diehl, V. and Wolf, J. (2001a). Oct-2 and Bob-1 deficiency in Hodgkin and Reed Sternberg cells. *Cancer Res.*, 61, 2080-2084.
- Re, D., Staratschek-Jox, A., Holtick, U., Diehl, V. and Wolf, J. (2001b). Dereulation of immunoglobulin gene transcription in the Hodgkin-Reed Sternberg cell line L1236. *Br. J. Haematol.*, 115, 326-328.
- Re, D., Starostik, P., Massoudi, N., Staratschek-Jox, A., Dries, V., Thomas, R.K., Diehl, V. and Wolf, J. (2003). Allelic losses on chromosome 6q25 in Hodgkin and Reed Sternberg cells. *Cancer Res.*, 63, 2606-2609.
- Re, D., Kuppers, R. and Diehl, V. (2005). Molecular Pathogenesis of Hodgkin's Lymphoma. *J Clin Oncol.*, 23, 6379-6386.
- Reed, D.M. (1902). On the pathological changes in Hodgkin disease, with especial reference to its relation to tuberculosis. *Johns Hopkins Hospital Reports.*, 10, 133.

- Reed, J.C. (1998). Bcl-2 family proteins. *Oncogene.*, 17, 3225-3236.
- Rehman, A.O. and Wang, C. (2006/6). Notch signaling in the regulation of tumor angiogenesis. *Trends in Cell Biology.*, 16, 293-300.
- Renne, C., Willenbrock, K., Kuppers, R., Hansmann, M.L. and Brauninger, A. (2005). Autocrine- and paracrine-activated receptor tyrosine kinases in classic Hodgkin lymphoma. *Blood.*, 105, 4051-4059.
- Renoize, C., Biola, A., Pallardy, M. and Breard, J. (1998). Apoptosis: identification of dying cells. *Cell Biol. Toxicol.*, 14, 111-120.
- Robinson, C.R. and Sauer, R.T. (1998). Optimizing the stability of single-chain proteins by linker length and composition mutagenesis. *Proc. Natl. Acad. Sci. U. S. A.*, 95, 5929-5934.
- Rodig, S.J., Savage, K.J., Nguyen, V., Pinkus, G.S., Shipp, M.A., Aster, J.C. and Kutok, J.L. (2005). TRAF1 expression and c-Rel activation are useful adjuncts in distinguishing classical Hodgkin lymphoma from a subset of morphologically or immunophenotypically similar lymphomas. *Am. J. Surg. Pathol.*, 29, 196-203.
- Ross, D.T., Scherf, U., Eisen, M.B., Perou, C.M., Rees, C., Spellman, P., Iyer, V., Jeffrey, S.S., Van de Rijn, M., Waltham, M., Pergamenschikov, A., Lee, J.C., Lashkari, D., Shalon, D., Myers, T.G., Weinstein, J.N., Botstein, D. and Brown, P.O. (2000). Systematic variation in gene expression patterns in human cancer cell lines. *Nat. Genet.*, 24, 227-235.
- Roux, P.P. and Blenis, J. (2004). ERK and p38 MAPK-activated protein kinases: a family of protein kinases with diverse biological functions. *Microbiol. Mol. Biol. Rev.*, 68, 320-344.
- Ruco, L.P., Pomponi, D., Pigott, R., Stoppacciaro, A., Monardo, F., Uccini, S., Boraschi, D., Tagliabue, A., Santoni, A. and Dejana, E. (1990). Cytokine production (IL-1 alpha, IL-1 beta, and TNF alpha) and endothelial cell activation (ELAM-1 and HLA-DR) in reactive lymphadenitis, Hodgkin's disease, and in non-Hodgkin's lymphomas. An immunocytochemical study. *Am. J. Pathol.*, 137, 1163-1171.
- Ryffel, B., Brockhaus, M., Durmuller, U. and Gudat, F. (1991a). Tumor necrosis factor receptors in lymphoid tissues and lymphomas. Source and site of action of tumor necrosis factor alpha. *Am. J. Pathol.*, 139, 7-15.
- Ryffel, B., Brockhaus, M., Greiner, B., Mihatsch, M.J. and Gudat, F. (1991b). Tumour necrosis factor receptor distribution in human lymphoid tissue. *Immunology.*, 74, 446-452.
- Sade, H., Krishna, S. and Sarin, A. (2004). The anti-apoptotic effect of Notch-1 requires p56lck-dependent, Akt/PKB-mediated signaling in T cells. *J. Biol. Chem.*, 279, 2937-2944.
- Sambrook, J., Fritsch, E.F., Maniatis, T. (1989). Molecular cloning: a laboratory manual, 2<sup>nd</sup> ed. Cold Spring Harbour Laboratory Press, Cold Spring Harbour, N.Y.

- Samoszuk, M. and Nansen, L. (1990). Detection of interleukin-5 messenger RNA in Reed-Sternberg cells of Hodgkin's disease with eosinophilia. *Blood.*, 75, 13-16.
- Sandur, S.K., Ichikawa, H., Sethi, G., Ahn, K.S. and Aggarwal, B.B. (2006). Plumbagin (5-Hydroxy-2-methyl-1,4-naphthoquinone) Suppresses NF-{kappa}B Activation and NF-{kappa}B-regulated Gene Products Through Modulation of p65 and I{kappa}B{alpha} Kinase Activation, Leading to Potentiation of Apoptosis Induced by Cytokine and Chemotherapeutic Agents. *J. Biol. Chem.*, 281, 17023-17033.
- Santoro, M.G., Rossi, A. and Amici, C. (2003). NF-kappaB and virus infection: who controls whom. *EMBO J.*, 22, 2552-2560.
- Sanz, L., Garcia-Marcos, J.A., Casanova, B., de la Fuente, Maria Teresa, Garcia-Gila, M., Garcia-Pardo, A. and Silva, A. (2004/3/12). Bcl-2 family gene modulation during spontaneous apoptosis of B-chronic lymphocytic leukemia cells. *Biochemical and Biophysical Research Communications.*, 315, 562-567.
- Schaadt, M., Fonatsch, C., Kirchner, H. and Diehl, V. (1979). Establishment of a malignant, Epstein-Barr-virus (EBV)-negative cell-line from the pleura effusion of a patient with Hodgkin's disease. *Blut.*, 38, 185-190.
- Scherr, M., Battmer, K., Winkler, T., Heidenreich, O., Ganser, A. and Eder, M. (2003). Specific inhibition of bcr-abl gene expression by small interfering RNA. *Blood.*, 101, 1566-1569.
- Schlaifer, D., Krajewski, S., Rigal-Huguet, F., Laurent, G., Pris, J., Delsol, G., Reed, J.C. and Brousset, P. (1996). Bcl-x gene expression in Hodgkin's disease. *Leuk. Lymphoma.*, 23, 143-146.
- Schlesinger, P.H., Gross, A., Yin, X.M., Yamamoto, K., Saito, M., Waksman, G. and Korsmeyer, S.J. (1997). Comparison of the ion channel characteristics of proapoptotic BAX and antiapoptotic BCL-2. *Proc. Natl. Acad. Sci. U. S. A.*, 94, 11357-11362.
- Schlessinger, J. (2000). Cell signaling by receptor tyrosine kinases. *Cell.*, 103, 211-225.
- Schneider, E.M., Torlakovic, E., Stuhler, A., Diehl, V., Tesch, H. and Giebel, B. (2004). The early transcription factor GATA-2 is expressed in classical Hodgkin's lymphoma. *J. Pathol.*, 204, 538-545.
- Schwarz, E., Scherrer, G., Hobom, G., and Kössel, H. (1978). Nucleotide sequence of cro, cII and part of the O gene in phage lambda DNA. *Nature.*, 272, 410-414.
- Schwarze, M.M. and Hawley, R.G. (1995). Prevention of myeloma cell apoptosis by ectopic bcl-2 expression or interleukin 6-mediated up-regulation of bcl-xL. *Cancer Res.*, 55, 2262-2265.
- Schwering, I., Brauninger, A., Klein, U., Jungnickel, B., Tingueley, M., Diehl, V., Hansmann, M.L., Dalla-Favera, R., Rajewsky, K. and Kuppers, R. (2003). Loss of the B-lineage-specific gene expression program in Hodgkin and Reed-Sternberg cells of Hodgkin lymphoma. *Blood.*, 101, 1505-1512.

- Sedlak, T.W., Oltvai, Z.N., Yang, E., Wang, K., Boise, L.H., Thompson, C.B. and Korsmeyer, S.J. (1995). Multiple Bcl-2 family members demonstrate selective dimerizations with Bax. *Proc. Natl. Acad. Sci. U. S. A.*, 92, 7834-7838.
- Seitz, V., Hummel, M., Marafioti, T., Anagnostopoulos, I., Assaf, C. and Stein, H. (2000). Detection of clonal T-cell receptor gamma-chain gene rearrangements in Reed-Sternberg cells of classic Hodgkin disease. *Blood*, 95, 3020-3024.
- Selkoe, D. and Kopan, R. (2003). Notch and Presenilin: regulated intramembrane proteolysis links development and degeneration. *Annu. Rev. Neurosci.*, 26, 565-597.
- Shaulian, E. and Karin, M. (2002). AP-1 as a regulator of cell life and death. *Nat. Cell Biol.*, 4, E131-6.
- Shi, B., Triebe, D., Kajiji, S., Iwata, K.K., Bruskin, A. and Mahajna, J. (1999). Identification and characterization of baxepsilon, a novel bax variant missing the BH2 and the transmembrane domains. *Biochem. Biophys. Res. Commun.*, 254, 779-785.
- Shi, Y. (2003). Mammalian RNAi for the masses. *Trends Genet.*, 19, 9-12.
- Shishodia, S. and Aggarwal, B.B. (2006). Diosgenin inhibits osteoclastogenesis, invasion, and proliferation through the downregulation of Akt, I $\kappa$ B kinase activation and NF- $\kappa$ B-regulated gene expression. *Oncogene*, 25, 1463-1473.
- Silverman, N. and Maniatis, T. (2001). NF- $\kappa$ B signaling pathways in mammalian and insect innate immunity. *Genes Dev.*, 15, 2321-2342.
- Skinnider, B.F., Elia, A.J., Gascoyne, R.D., Patterson, B., Trumper, L., Kapp, U. and Mak, T.W. (2002a). Signal transducer and activator of transcription 6 is frequently activated in Hodgkin and Reed-Sternberg cells of Hodgkin lymphoma. *Blood*, 99, 618-626.
- Skinnider, B.F., Kapp, U. and Mak, T.W. (2002b). The role of interleukin 13 in classical Hodgkin lymphoma. *Leuk. Lymphoma*, 43, 1203-1210.
- Skinnider, B.F. and Mak, T.W. (2002). The role of cytokines in classical Hodgkin lymphoma. *Blood*, 99, 4283-4297.
- Smith, S.M. (2005). Epstein-Barr virus latent proteins regulate expression of the anti-apoptotic cellular *bfl-1* gene. PhD Thesis, Dublin City University, Ireland.
- Sorensen, M.A., Kurland, C.G. and Pedersen, S. (1989). Codon usage determines translation rate in Escherichia coli. *J. Mol. Biol.*, 207, 365-377.
- Sorenson, C.M. (2004). Bcl-2 family members and disease. *Biochim. Biophys. Acta*, 1644, 169-177.

- Staber, P.B., Linkesch, W., Zauner, D., Beham-Schmid, C., Guelly, C., Schauer, S., Sill, H. and Hoefler, G. (2004). Common alterations in gene expression and increased proliferation in recurrent acute myeloid leukemia. *Oncogene.*, 23, 894-904.
- Stark, G.L., Wood, K.M., Jack, F., Angus, B., Proctor, S.J., Taylor, P.R. and Northern Region Lymphoma Group. (2002). Hodgkin's disease in the elderly: a population-based study. *Br. J. Haematol.*, 119, 432-440.
- Staudt, L.M. (2000). The molecular and cellular origins of Hodgkin's disease. *J. Exp. Med.*, 191, 207-212.
- Stein, H., Delsol, G., Pileri, S., et al. (2001a). Classical Hodgkin lymphoma. In: Jaffe, E.S., Harris, N.L., Stein, H., et al., eds. World Health Organisation classification of tumours. *Pathology and genetics of tumours of haematopoietic and lymphoid tissues*. Lyon: IARC Press, 2001:244-253.
- Stein, H., Marafioti, T., Foss, H.D., Laumen, H., Hummel, M., Anagnostopoulos, I., Wirth, T., Demel, G. and Falini, B. (2001b). Down-regulation of BOB.1/OBF.1 and Oct2 in classical Hodgkin disease but not in lymphocyte predominant Hodgkin disease correlates with immunoglobulin transcription. *Blood.*, 97, 496-501.
- Stetler-Stevenson, M., Crush-Stanton, S. and Cossman, J. (1990). Involvement of the bcl-2 gene in Hodgkin's disease. *J. Natl. Cancer Inst.*, 82, 855-858.
- Straus, S.E., Jaffe, E.S., Puck, J.M., Dale, J.K., Elkorn, K.B., Rosen-Wolff, A., Peters, A.M., Sneller, M.C., Hallahan, C.W., Wang, J., Fischer, R.E., Jackson, C.M., Lin, A.Y., Baumler, C., Siegert, E., Marx, A., Vaishnav, A.K., Grodzicky, T., Fleisher, T.A. and Lenardo, M.J. (2001). The development of lymphomas in families with autoimmune lymphoproliferative syndrome with germline Fas mutations and defective lymphocyte apoptosis. *Blood.*, 98, 194-200.
- Sternberg, C. (1898). Über eine eigenartige unter dem bilde der pseudoleukämie verlaufende tuberkulose des lymphatischen apparatus. *Z Heilkunde.*, 19, 21-90.
- Strobl, L.J., Hofelmayr, H., Marschall, G., Brielmeier, M., Bornkamm, G.W. and Zimber-Strobl, U. (2000). Activated Notch1 modulates gene expression in B cells similarly to Epstein-Barr viral nuclear antigen 2. *J. Virol.*, 74, 1727-1735.
- Sumbayev, V.V. and Yasinska, I.M. (2006). Role of MAP Kinase-Dependent Apoptotic Pathway in Innate Immune Responses and Viral Infection. *Scand. J. Immunol.*, 63, 391-400.
- Sweetenham, J.W., Taghipour, G., Milligan, D., Blystad, A.K., Caballero, D., Fassas, A. and Goldstone, A.H. (1997). High-dose therapy and autologous stem cell rescue for patients with Hodgkin's disease in first relapse after chemotherapy: results from the EBMT Lymphoma Working Party of the European Group for Blood and Marrow Transplantation. *Bone Marrow Transplant.*, 20, 745-752.

- Takada, Y., Fang, X., Jamaluddin, M.S., Boyd, D.D. and Aggarwal, B.B. (2004). Genetic Deletion of Glycogen Synthase Kinase-3 $\beta$  Abrogates Activation of I $\kappa$ B $\alpha$  Kinase, JNK, Akt, and p44/p42 MAPK but Potentiates Apoptosis Induced by Tumor Necrosis Factor. *J. Biol. Chem.*, 279, 39541-39554.
- Tarte, K., Jourdan, M., Veyrune, J.L., Berberich, I., Fiol, G., Redal, N., Shaughnessy, J., Jr and Klein, B. (2004). The Bcl-2 family member Bfl-1/A1 is strongly repressed in normal and malignant plasma cells but is a potent anti-apoptotic factor for myeloma cells. *Br. J. Haematol.*, 125, 373-382.
- Tax, F.E., Yeargers, J.J. and Thomas, J.H. (1994). Sequence of *C. elegans* lag-2 reveals a cell-signalling domain shared with Delta and Serrate of *Drosophila*. *Nature*, 368, 150-154.
- Taylor, C.R. and Riley, C.R. (2001). Molecular morphology of Hodgkin lymphoma. *Appl. Immunohistochem. Mol. Morphol.*, 9, 187-202.
- Terpe, K. (2003). Overview of tag protein fusions: from molecular and biochemical fundamentals to commercial systems. *Appl. Microbiol. Biotechnol.*, 60, 523-533.
- Thomas, R.K., Kallenborn, A., Wickenhauser, C., Schultze, J.L., Draube, A., Vockerodt, M., Re, D., Diehl, V. and Wolf, J. (2002a). Constitutive expression of c-FLIP in Hodgkin and Reed-Sternberg cells. *Am. J. Pathol.*, 160, 1521-1528.
- Thomas, R.K., Re, D., Wolf, J. and Diehl, V. (2004a). Part I: Hodgkin's lymphoma--molecular biology of Hodgkin and Reed-Sternberg cells. *Lancet Oncol.*, 5, 11-18.
- Thomas, R.K., Re, D., Zander, T., Wolf, J. and Diehl, V. (2002b). Epidemiology and etiology of Hodgkin's lymphoma. *Ann. Oncol.*, 13 Suppl 4, 147-152.
- Thomas, R.K., Wickenhauser, C., Kube, D., Tesch, H., Diehl, V., Wolf, J. and Vockerodt, M. (2004b). Repeated clonal relapses in classical Hodgkin's lymphoma and the occurrence of a clonally unrelated diffuse large B cell non-Hodgkin lymphoma in the same patient. *Leuk. Lymphoma*, 45, 1065-1069.
- Thorley-Lawson, D.A. and Gross, A. (2004). Persistence of the Epstein-Barr virus and the origins of associated lymphomas. *N. Engl. J. Med.*, 350, 1328-1337.
- Tohda, S. and Nara, N. (2001). Expression of Notch1 and Jagged1 proteins in acute myeloid leukemia cells. *Leuk. Lymphoma*, 42, 467-472.
- Torii, S., Yamamoto, T., Tsuchiya, Y. and Nishida, E. (2006). ERK MAP kinase in G1 cell cycle progression and cancer. *Cancer Science*, 97, 697-702.
- Torlakovic, E., Tierens, A., Dang, H.D. and Delabie, J. (2001). The transcription factor PU.1, necessary for B-cell development is expressed in lymphocyte predominance, but not classical Hodgkin's disease. *Am. J. Pathol.*, 159, 1807-1814.

- Torlakovic, E., Torlakovic, G., Nguyen, P.L., Brunning, R.D. and Delabie, J. (2002). The value of anti-pax-5 immunostaining in routinely fixed and paraffin-embedded sections: a novel pan pre-B and B-cell marker. *Am. J. Surg. Pathol.*, 26, 1343-1350.
- Tournier, C., Dong, C., Turner, T.K., Jones, S.N., Flavell, R.A. and Davis, R.J. (2001). MKK7 is an essential component of the JNK signal transduction pathway activated by proinflammatory cytokines. *Genes Dev.*, 15, 1419-1426.
- Trinh, R., Gurbaxani, B., Morrison, S.L. and Seyfzadeh, M. (2004). Optimization of codon pair use within the (GGGGS)3 linker sequence results in enhanced protein expression. *Mol. Immunol.*, 40, 717-722.
- Tsang, R.W., Hodgson, D.C. and Crump, M. (2006/0). Hodgkin's Lymphoma. *Current Problems in Cancer.*, 30, 107-158.
- Tsujimoto, Y., Jaffe, E., Cossman, J., Gorham, J., Nowell, P.C. and Croce, C.M. (1985). Clustering of breakpoints on chromosome 11 in human B-cell neoplasms with the t(11;14) chromosome translocation. *Nature.*, 315, 340-343.
- Tsujimoto, Y. and Shimizu, S. (2000). Bcl-2 family: life-or-death switch. *FEBS Lett.*, 466, 6-10.
- Tun, T., Hamaguchi, Y., Matsunami, N., Furukawa, T., Honjo, T. and Kawaichi, M. (1994). Recognition sequence of a highly conserved DNA binding protein RBP-J kappa. *Nucleic Acids Res.*, 22, 965-971.
- Tuschl, T., Zamore, P.D., Lehmann, R., Bartel, D.P. and Sharp, P.A. (1999). Targeted mRNA degradation by double-stranded RNA in vitro. *Genes Dev.*, 13, 3191-3197.
- UICC-International Union Against Cancer. TNM Classification of Malignant Tumours, 6th Edition. New York, NY: Wiley-Liss, 2002.
- van de Wetering, M., Oving, I., Muncan, V., Pon Fong, M.T., Brantjes, H., van Leenen, D., Holstege, F.C., Brummelkamp, T.R., Agami, R. and Clevers, H. (2003). Specific inhibition of gene expression using a stably integrated, inducible small-interfering-RNA vector. *EMBO Rep.*, 4, 609-615.
- van den Berg, A., Visser, L. and Poppema, S. (1999). High expression of the CC chemokine TARC in Reed-Sternberg cells. A possible explanation for the characteristic T-cell infiltrate in Hodgkin's lymphoma. *Am. J. Pathol.*, 154, 1685-1691.
- Vanhaezebroeck, B. and Alessi, D.R. (2000). The PI3K-PDK1 connection: more than just a road to PKB. *Biochem. J.*, 346 Pt 3, 561-576.
- Vara, J.A.F., Casado, E., de Castro, J., Cejas, P., Belda-Iniesta, C. and Gonzalez-Baron, M. (2004/4). PI3K/Akt signalling pathway and cancer. *Cancer Treatment Reviews.*, 30, 193-204.

Verweij, C.L., Geerts, M. and Aarden, L.A. (1991). Activation of interleukin-2 gene transcription via the T-cell surface molecule CD28 is mediated through an NF- $\kappa$ B-like response element. *J. Biol. Chem.*, 266, 14179-14182.

Vockerodt, M., Haier, B., Buttgereit, P., Tesch, H. and Kube, D. (2001/2/15). The Epstein-Barr Virus Latent Membrane Protein 1 Induces Interleukin-10 in Burkitt's Lymphoma Cells but Not in Hodgkin's Cells Involving the p38/SAPK2 Pathway. *Virology*, 280, 183-198.

Voorhees, P.M., Dees, E.C., O'Neil, B. and Orlowski, R.Z. (2003). The proteasome as a target for cancer therapy. *Clin. Cancer Res.*, 9, 6316-6325.

Wagner, A.J., Small, M.B. and Hay, N. (1993). Myc-mediated apoptosis is blocked by ectopic expression of Bcl-2. *Mol. Cell. Biol.*, 13, 2432-2440.

Wagner, E.F. (2001). AP-1-Introductory remarks. *Oncogene*, 20, 2334-2335.

Wahl, A.F., Klussman, K., Thompson, J.D., Chen, J.H., Francisco, L.V., Risdon, G., Chace, D.F., Siegall, C.B. and Francisco, J.A. (2002). The anti-CD30 monoclonal antibody SGN-30 promotes growth arrest and DNA fragmentation in vitro and affects antitumor activity in models of Hodgkin's disease. *Cancer Res.*, 62, 3736-3742.

Waltzer, L., Bourillot, P.Y., Sergeant, A. and Manet, E. (1995). RBP-J kappa repression activity is mediated by a co-repressor and antagonized by the Epstein-Barr virus transcription factor EBNA2. *Nucleic Acids Res.*, 23, 4939-4945.

Waltzer, L., Logeat, F., Brou, C., Israel, A., Sergeant, A. and Manet, E. (1994). The human J kappa recombination signal sequence binding protein (RBP-J kappa) targets the Epstein-Barr virus EBNA2 protein to its DNA responsive elements. *EMBO J.*, 13, 5633-5638.

Wang, C.Y., Guttridge, D.C., Mayo, M.W. and Baldwin, A.S., Jr. (1999). NF- $\kappa$ B induces expression of the Bcl-2 homologue A1/Bfl-1 to preferentially suppress chemotherapy-induced apoptosis. *Mol. Cell. Biol.*, 19, 5923-5929.

Wang, J., Shelly, L., Miele, L., Boykins, R., Norcross, M.A. and Guan, E. (2001). Human Notch-1 inhibits NF- $\kappa$ B activity in the nucleus through a direct interaction involving a novel domain. *J. Immunol.*, 167, 289-295.

Watanabe, M., Ogawa, Y., Ito, K., Higashihara, M., Kadin, M.E., Abraham, L.J., Watanabe, T. and Horie, R. (2003). AP-1 Mediated Relief of Repressive Activity of the CD30 Promoter Microsatellite in Hodgkin and Reed-Sternberg Cells. *Am J Pathol.*, 163, 633-641.

Watanabe, M., Sasaki, M., Itoh, K., Higashihara, M., Umezawa, K., Kadin, M.E., Abraham, L.J., Watanabe, T. and Horie, R. (2005). JunB Induced by Constitutive CD30-Extracellular Signal-Regulated

Kinase 1/2 Mitogen-Activated Protein Kinase Signaling Activates the CD30 Promoter in Anaplastic Large Cell Lymphoma and Reed-Sternberg Cells of Hodgkin Lymphoma. *Cancer Res.*, 65, 7628-7634.

Waugh, D.S. (2005/6). Making the most of affinity tags. *Trends in Biotechnology*, 23, 316-320.

Wei, M.C., Lindsten, T., Mootha, V.K., Weiler, S., Gross, A., Ashiya, M., Thompson, C.B. and Korsmeyer, S.J. (2000). tBID, a membrane-targeted death ligand, oligomerizes BAK to release cytochrome c. *Genes Dev.*, 14, 2060-2071.

Wei, M.C., Zong, W.X., Cheng, E.H., Lindsten, T., Panoutsakopoulou, V., Ross, A.J., Roth, K.A., MacGregor, G.R., Thompson, C.B. and Korsmeyer, S.J. (2001). Proapoptotic BAX and BAK: a requisite gateway to mitochondrial dysfunction and death. *Science*, 292, 727-730.

Weiss, M.J. and Orkin, S.H. (1995). Transcription factor GATA-1 permits survival and maturation of erythroid precursors by preventing apoptosis. *Proc. Natl. Acad. Sci. U. S. A.*, 92, 9623-9627.

Wensing, B. and Farrell, P.J. (2000). Regulation of cell growth and death by Epstein-Barr virus. *Microbes Infect.*, 2, 77-84.

Werner, A.B., de Vries, E., Tait, S.W., Bontjer, I. and Borst, J. (2002). Bcl-2 family member Bfl-1/A1 sequesters truncated bid to inhibit its collaboration with pro-apoptotic Bak or Bax. *J. Biol. Chem.*, 277, 22781-22788.

Weston, C.R. and Davis, R.J. (2002). The JNK signal transduction pathway. *Curr. Opin. Genet. Dev.*, 12, 14-21.

Willis, S.N. and Adams, J.M. (2005). Life in the balance: how BH3-only proteins induce apoptosis. *Curr. Opin. Cell Biol.*, 17, 617-625.

Wilson, G. and Miller, G. (1979). Recovery of Epstein-Barr virus from nonproducer neonatal human lymphoid cell transformants. *Virology*, 95, 351-358.

Winter, J.N., Andersen, J., Reed, J.C., Krajewski, S., Variakojis, D., Bauer, K.D., Fisher, R.I., Gordon, L.I., Oken, M.M., Jiang, S., Jeffries, D. and Domer, P. (1998). BCL-2 expression correlates with lower proliferative activity in the intermediate- and high-grade non-Hodgkin's lymphomas: an Eastern Cooperative Oncology Group and Southwest Oncology Group cooperative laboratory study. *Blood*, 91, 1391-1398.

Wolf, J., Kapp, U., Bohlen, H., Kornacker, M., Schoch, C., Stahl, B., Mucke, S., von Kalle, C., Fonatsch, C., Schaefer, H.E., Hansmann, M.L. and Diehl, V. (1996). Peripheral blood mononuclear cells of a patient with advanced Hodgkin's lymphoma give rise to permanently growing Hodgkin-Reed Sternberg cells. *Blood*, 87, 3418-3428.

- Wurster, A.L., Tanaka, T. and Grusby, M.J. (2000). The biology of Stat4 and Stat6. *Oncogene.*, 19, 2577-2584.
- Xerri, L., Birg, F., Guigou, V., Bouabdallah, R., Poizot-Martin, I. and Hassoun, J. (1992). In situ expression of the IL-1-alpha and TNF-alpha genes by Reed-Sternberg cells in Hodgkin's disease. *Int. J. Cancer.*, 50, 689-693.
- Xerri, L., Carbuccia, N., Parc, P., Hassoun, J. and Birg, F. (1995). Frequent expression of FAS/APO-1 in Hodgkin's disease and anaplastic large cell lymphomas. *Histopathology.*, 27, 235-241.
- Xia, L., Wurmback, E., Waxman, S. and Jing, Y. (2006). Upregulation of Bfl-1/A1 in leukemia cells undergoing differentiation by all-trans retinoic acid treatment attenuates chemotherapeutic agent-induced apoptosis. *Leukemia.*, 20, 1009-1016.
- Xiang, Z., Moller, C. and Nilsson, G. (2006). IgE-receptor activation induces survival and Bfl-1 expression in human mast cells but not basophils. *Allergy.*, 61, 1040-1046.
- Yamamoto, Y. and Gaynor, R.B. (2001). Role of the NF-kappaB pathway in the pathogenesis of human disease states. *Curr. Mol. Med.*, 1, 287-296.
- Yang, J.L., Yong, G., Zijian, C., Jinke, H., Jianyi, D., Li, L., Warren, C., Zhijian, L., Zheng-gang and Su, B. (2001). The essential role of MEKK3 in TNF-induced NF-[kappa]B activation. *Nature Immunology.*, 2, 620-624.
- Yoon, H.S., Hong, S.H., Kang, H.J., Ko, B.K., Ahn, S.H. and Huh, J.R. (2003). Bfl-1 gene expression in breast cancer: its relationship with other prognostic factors. *J. Korean Med. Sci.*, 18, 225-230.
- Young, L.S. and Rickinson, A.B. (2004). Epstein-Barr virus: 40 years on. *Nat. Rev. Cancer.*, 4, 757-768.
- Zamzami, N. and Kroemer, G. (2001). The mitochondrion in apoptosis: how Pandora's box opens. *Nat. Rev. Mol. Cell Biol.*, 2, 67-71.
- Zha, J., Weiler, S., Oh, K.J., Wei, M.C. and Korsmeyer, S.J. (2000). Posttranslational N-myristoylation of BID as a molecular switch for targeting mitochondria and apoptosis. *Science.*, 290, 1761-1765.
- Zhang, H., Cowan-Jacob, S.W., Simonen, M., Greenhalf, W., Heim, J. and Meyhack, B. (2000). Structural basis of BFL-1 for its interaction with BAX and its anti-apoptotic action in mammalian and yeast cells. *J. Biol. Chem.*, 275, 11092-11099.
- Zhao, Q. and Lee, F.S. (1999). Mitogen-activated protein kinase/ERK kinase kinases 2 and 3 activate nuclear factor-kappaB through IkappaB kinase-alpha and IkappaB kinase-beta. *J. Biol. Chem.*, 274, 8355-8358.

- Zheng, B., Fiumara, P., Li, Y.V., Georgakis, G., Snell, V., Younes, M., Vauthey, J.N., Carbone, A. and Younes, A. (2003). MEK/ERK pathway is aberrantly active in Hodgkin disease: a signaling pathway shared by CD30, CD40, and RANK that regulates cell proliferation and survival. *Blood.*, 102, 1019-1027.
- Zimber-Strobl, U., Strobl, L., Hofelmayr, H., Kempkes, B., Staeghe, M.S., Laux, G., Christoph, B., Polack, A. and Bornkamm, G.W. (1999). EBNA2 and c-myc in B cell immortalization by Epstein-Barr virus and in the pathogenesis of Burkitt's lymphoma. *Curr. Top. Microbiol. Immunol.*, 246, 315-20; discussion 321.
- Zimber-Strobl, U. and Strobl, L.J. (2001). EBNA2 and Notch signalling in Epstein-Barr virus mediated immortalization of B lymphocytes. *Semin. Cancer Biol.*, 11, 423-434.
- Zimber-Strobl, U., Strobl, L.J., Meitinger, C., Hinrichs, R., Sakai, T., Furukawa, T., Honjo, T. and Bornkamm, G.W. (1994). Epstein-Barr virus nuclear antigen 2 exerts its transactivating function through interaction with recombination signal binding protein RBP-J kappa, the homologue of Drosophila Suppressor of Hairless. *EMBO J.*, 13, 4973-4982.
- Zong, W.X., Edelstein, L.C., Chen, C., Bash, J. and Gelinas, C. (1999). The prosurvival Bcl-2 homolog Bfl-1/A1 is a direct transcriptional target of NF-kappaB that blocks TNFalpha-induced apoptosis. *Genes Dev.*, 13, 382-387.
- Zong, W.X., Lindsten, T., Ross, A.J., MacGregor, G.R. and Thompson, C.B. (2001). BH3-only proteins that bind pro-survival Bcl-2 family members fail to induce apoptosis in the absence of Bax and Bak. *Genes Dev.*, 15, 1481-1486.
- zur Hausen, H. and de Villiers, E.M. (2005). Virus target cell conditioning model to explain some epidemiologic characteristics of childhood leukemias and lymphomas. *Int. J. Cancer.*, 115, 1-5.
- Zurawski, G. and de Vries, J.E. (1994). Interleukin 13, an interleukin 4-like cytokine that acts on monocytes and B cells, but not on T cells. *Immunol. Today.*, 15, 19-26.

## **CHAPTER 10 APPENDIX**

a

## **10.1 Solutions for DNA Manipulation**

### **10.1.1 Storage of DNA**

#### **0.5 M EDTA (pH 8.0)**

186.1 g	EDTA
800 ml	dH <sub>2</sub> O

The pH was adjusted to 8.0 by addition of NaOH pellets and the volume adjusted to 1 L with dH<sub>2</sub>O. The solution was sterilised by autoclaving and stored at RT.

#### **TE buffer (pH 8.0)**

10 mM	Tris-Cl (pH 8.0)
1 mM	EDTA (pH 8.0)

### **10.1.2 Solution for Bacterial Growth Media**

#### **Ampicillin stock solution**

A stock solution of ampicillin was made up to a concentration of 100 mg/ml in dH<sub>2</sub>O. The stock solution was filter sterilised and stored at -20°C.

#### **Tetracycline stock solution**

A stock solution of tetracycline was made up to a concentration of 5 mg/ml in 70 % ethanol (v/v). The stock solution was filter sterilised and stored at -20°C.

#### **Chloramphenicol stock solution**

A stock solution of chloramphenicol was made up to a concentration of 50 mg/ml in 100 % ethanol (v/v). The stock solution was filter sterilised and stored at -20°C.

### **LB broth**

5 g	tryptone
2.5 g	yeast extract
5g	NaCl

The volume was adjusted to 500 ml, followed by autoclaving for 20 minutes at 15 lb/sq. and storage at 4°C.

### **LB broth with antibiotics**

Antibiotics were added to autoclaved LB broth to a final concentration of 100 µg/ml (Ampicillin), 12.5 µg/ml (Tetracycline) and 34 µg/ml (Chloramphenicol) and stored at 4°C.

### **LB agar**

5 g	tryptone
2.5 g	yeast extract
5 g	NaCl
7.5 g	agar

The volume was adjusted to 500 ml with dH<sub>2</sub>O, followed by autoclaving and agar plates were stored at 4°C.

### **LB agar with antibiotics**

Antibiotics were added to autoclaved LB broth to a final concentration of 100 µg/ml (Ampicillin), 12.5 µg/ml (Tetracycline) and 34 µg/ml (Chloramphenicol) after cooling the LB agar to ~50°C. Plates were stored at 4°C.

### **SOB medium**

10 g	tryptone
2.5 g	yeast extract
0.025 g	NaCl
5 ml	KCl (250 mM)

The pH was adjusted to 7.0 with 5 M NaOH.

The volume was adjusted to 500 ml with dH<sub>2</sub>O and the medium autoclaved.

2.5 ml of 2 M MgCl<sub>2</sub> was added after cooling the broth to 5°C and the medium was stored at 4°C.

### **SOC medium**

98 ml	SOB medium
2 ml	1 M glucose (filter sterilised)

Stored at 4°C.

### **10.1.3 Solutions for Preparation of Competent Cells**

#### **1M MgSO<sub>4</sub>**

24.65 g	MgSO <sub>4</sub> .7H <sub>2</sub> O
100 ml	dH <sub>2</sub> O

Sterilised by filtering and stored at RT.

**TFB1**

30 mM	potassium acetate
10 mM	CaCl <sub>2</sub>
50 mM	MnCl <sub>2</sub>
100 mM	RbCl
15 %	glycerol

The pH was adjusted to 5.8 with 1 M acetic acid, and the solution filter sterilised and stored at RT.

**TFB2**

100 mM	MOPS (pH 6.5)
75 mM	CaCl <sub>2</sub>
10 mM	RbCl
15 %	glycerol

The pH was adjusted to 6.5 with 1 M KOH, and the solution filter sterilised and stored at RT.

#### **10.1.4 Solutions for DNA preparations**

**Buffer P1 (Re-suspension buffer)**

50 mM	Tris-Cl (pH 8.0)
10 mM	EDTA (pH8.0)
100 µg/ml	RNase A

Stored at 4°C following addition of RNase A.

### **DNase-free RNase**

RNase A (1 mg/ml) in upH<sub>2</sub>O.  
Heated to 100°C for 30 minutes.  
Cooled slowly and stored at -20°C.

### **Buffer P2 (Lysis buffer)**

200 mM	NaOH
1 % (w/v)	SDS

Stored at RT.

### **Buffer P3 (Neutralization buffer; (3 M potassium acetate)**

29.6 g	potassium acetate
50 ml	dH <sub>2</sub> O
11.5 ml	glacial acetic acid

Adjust volume to 100 ml with dH<sub>2</sub>O.

The resulting solution is 3 M with respect to potassium and 5 M with respect to acetate.

Stored at RT.

### **Buffer QBT (Equilibration buffer)**

750 mM	NaCl
50 mM	MOPS (pH 7.0)
15 % (v/v)	isopropanol
0.15 % (v/v)	Triton-X 100

Stored at RT.

**Buffer QC (Wash buffer)**

1 M	NaCl
50 mM	MOPS (pH 7.0)
15 % (v/v)	isopropanol

Stored at RT.

**Buffer QF (Elution buffer)**

1.25 M	NaCl
50 mM	Tris-Cl (pH 8.5)
15 %	isopropanol

Stored at RT.

**50 % (v/v) Glycerol**

25 ml	glycerol
25 ml	dH <sub>2</sub> O

The solution was autoclaved and stored at RT.

**Annealing buffer**

100 mM	Potassium acetate
30 mM	Hepes-KOH, pH 7.4
2 mM	Magnesium acetate

Stored at 4 – 8 °C.

### **10.1.5 Solutions for Agarose Gel Electrophoresis**

#### **50 X TAE (Tris-acetate/EDTA electrophoresis buffer)**

242 g	Tris base
57.1 ml	glacial acetic acid
100 ml	0.5 M EDTA (pH 8.0)

The volume was adjusted to 1 L with dH<sub>2</sub>O and the buffer was stored at RT.

#### **1 X TAE (Working solution)**

20 ml	50 X TAE
980 ml	dH <sub>2</sub> O

Stored at RT.

#### **Agarose gel loading dye**

40 % (w/v)	sucrose
0.25 % (w/v)	bromophenol blue

Stored at RT.

#### **Ethidium bromide**

10 mg	ethidium bromide
1 ml	dH <sub>2</sub> O

The solution was stored in the dark at 4 °C. 100 µl of stock solution was added to 1 L of dH<sub>2</sub>O for TAE gel staining.

## **10.2 Solutions for Cell Culture**

### **10.2.1 Media and Supplements**

#### **Supplemented RPMI 1640 (200 ml)**

176 ml	RPMI 1640
20 ml	foetal bovine serum (decomplemented at 50°C for 30 minutes)
2 ml	200 mM L-glutamine
2 ml	penicillin/streptomycin (10 mg/ml)

#### **Estrogen ( $\beta$ -Estradiol)**

A 20 mM solution was prepared in 100 % ethanol and stored at -20°C.

#### **Tetracycline**

A 5 mg/ml stock was prepared in 100 % ethanol and stored at -20°C.

#### **Phosphate buffered saline (PBS)**

5 tablets were dissolved in 500 ml dH<sub>2</sub>O to give a 1 X working concentration of PBS, and the solution was sterilised by autoclaving.

## **10.2.2 Solutions for DEAE-Dextran Tranfections Protocol**

### **Tris buffered saline (TBS)**

25 mM	Tris-Cl (pH 7.4)
137 mM	NaCl
5 mM	KCl
0.7 mM	CaCl <sub>2</sub>
0.5 mM	MgCl <sub>2</sub>
0.6 mM	Na <sub>2</sub> HPO <sub>4</sub>

To make 200 ml TBS:

5 ml	1 M Tris-Cl (pH 7.4)
5.48 ml	5 M NaCl
0.5 ml	2 M KCl
1.4 ml	100 mM CaCl <sub>2</sub>
0.1 ml	1 M MgCl <sub>2</sub>
0.2 ml	0.6 M Na <sub>2</sub> HPO <sub>4</sub>
187.32 ml	upH <sub>2</sub> O

TBS was prepared from autoclaved stocks, aliquoted and filter sterilised before use.

### **DEAE dextran**

DEAE dextran was prepared at a concentration of 1 mg/ml in TBS on the day of use and filter sterilised.

## **10.2.3 $\beta$ -Galactosidase Assay**

### **100 X Mg solution**

0.1 M	MgCl <sub>2</sub>
4.5 M	2-mercaptoethanol

Stored at -20°C.

### **0.1 M sodium phosphate buffer**

41 ml	0.2 M Na <sub>2</sub> HPO <sub>4</sub> .2H <sub>2</sub> O
9 ml	0.2 M NaH <sub>2</sub> PO <sub>4</sub> .2H <sub>2</sub> O
50 ml	dH <sub>2</sub> O

### **1 X ONPG substrate**

ONPG was prepared at a concentration of 4 mg/ml in 0.1 M sodium phosphate buffer (pH 7.5) and stored at -20°C.

### **1 M sodium carbonate**

10.59 g	Sodium Carbonate
100 ml	dH <sub>2</sub> O

Stored at room temperature.

### **Acridine orange/ethidium bromide stain**

50 µg/ml	Acridine orange (Sigma)
50 µg/ml	Ethidium bromide (Sigma)
1000 µl	PBS

Store up to 6 months at 4°C.

## **10.3 Solutions for Tumour Tissue Methods**

### **4 % Paraformaldehyde**

4 g	Paraformaldehyde
100 ml	Phosphate Buffered Saline (PBS)

Stored at room temperature

### **20 X SSC**

3 M	NaCl
0.3 M	Sodium citrate pH 7

Stored at room temperature

## **10.4 Solutions for RNA Analysis**

### **DEPC-treated H<sub>2</sub>O**

1 ml	DEPC
1000 ml	dH <sub>2</sub> O

The mixture was left in a fume cupboard overnight, followed by autoclaving.

### **RNA loading buffer**

50 %	glycerol
1 mM	EDTA (pH 8.0)
0.25 %	bromophenol blue
0.25 %	xylene cyanol FF
1 µg/ul	ethidium bromide

## **10.5 Solutions for Protein Analysis**

### **10.5.1 Solutions for Protein Isolation**

#### **Suspension buffer**

0.1 M	NaCl
0.01 M	Tris-Cl (pH 7.6)
0.001 M	EDTA (pH 8.0)
1 µg/ml	leupeptin
1 µg/ml	aprotinin
100 µg/ml	PMSF

Stored at 4°C

#### **Leupeptin**

A stock solution of leupeptin was made to a concentration 2 mg/ml in dH<sub>2</sub>O and stored at -20°C.

#### **Aprotinin**

0.1 M stock solution of aprotinin was made up in dH<sub>2</sub>O and stored at -20°C.

#### **PMSF**

A stock solution of PMSF was made up in isopropanol and stored at -20°C in the dark.

## **2 X SDS loading buffer**

100 mM	Tris-Cl (pH 7.6)
4 % (w/v)	SDS
20 % (w/v)	glycerol
10 % (v/v)	2-mercaptoethanol
0.2 %	bromophenol blue
Stored at RT.	

## **10.5.2 Solutions for SDS-PAGE/ Western Blotting**

**Table 10-1 10 % (v/v) resolving gels and 5 % (v/v) stacking polyacrylamide gels**

Component	10 % Resolving Gel (ml)	5 % Stacking Gel (ml)
Acrylagel	3.33	0.42
Bis-Acrylagel	1.35	0.168
1.5 M Tris (pH 8.8)	2.5	0
1 M Tris (pH 6.8)	0	0.312
dH <sub>2</sub> O	2.61	1.5475
10 % (v/v) SDS	0.10	0.025
10 % (v/v) APS	0.10	0.025
TEMED	0.01	0.0025
Total	10 ml	2.5 ml

## **5 X Tris-glycine running buffer**

15.1 g	Tris base
95.4 g	glycine (pH 8.3)
50 ml	10 % (w/v) SDS

Made up to 1 L with dH<sub>2</sub>O and stored at RT.

### **1 X Tris-glycine running buffer**

200 ml	5 X Tris-glycine running buffer
800 ml	dH <sub>2</sub> O

### **Destain**

450 ml	methanol
450 ml	dH <sub>2</sub> O
100 ml	glacial acetic acid

Store at RT.

### **Coomassie blue stain**

0.25 g	Coomassie Brilliant Blue R250
100 ml	destain

Store at RT.

### **Transfer buffer**

750 ml	dH <sub>2</sub> O
2.9 g	glycine
5.8 g	Tris base
3.7 ml	10 % (w/v) SDS
200 ml	methanol

Adjusted volume to 1 L with dH<sub>2</sub>O and stored at 4°C.

**1X Tris buffered saline (TBS)**

6.1 g	Tris base
8.8 g	NaCl
800 ml	dH <sub>2</sub> O

The pH was adjusted to 7.5 with HCl and the volume adjusted to 1 L. Stored at RT.

**TBS-T**

1 L	1 X TBS
1 ml	Tween 20

Stored at RT.

**Blocking Buffer**

5 g	non fat dry milk powder
100 ml	TBS-T

Stored at 4°C.

## **10.6 Solutions for Expression and Purification of Recombinant Proteins**

### **10.6.1 Denaturing solutions**

#### **Lysis buffers**

##### **Buffer B (1 liter):**

100 mM NaH <sub>2</sub> PO <sub>4</sub>	13.8 g NaH <sub>2</sub> PO <sub>4</sub> ·H <sub>2</sub> O (MW 137.99 g/mol)
10 mM Tris·Cl	1.2 g Tris base (MW 121.1 g/mol)
8 M urea	480.5 g (MW 60.06 g/mol)

Adjust pH to 8.0 using NaOH.

#### **Wash buffer**

##### **Buffer C (1 liter):**

100 mM NaH <sub>2</sub> PO <sub>4</sub>	13.8 g NaH <sub>2</sub> PO <sub>4</sub> ·H <sub>2</sub> O (MW 137.99 g/mol)
10 mM Tris·Cl	1.2 g Tris base (MW 121.1 g/mol)
8 M urea	480.5 g (MW 60.06 g/mol)

Adjust pH to 6.3 using HCl.

#### **Elution buffers**

##### **Buffer D (1 liter):**

100 mM NaH <sub>2</sub> PO <sub>4</sub>	13.8 g NaH <sub>2</sub> PO <sub>4</sub> ·H <sub>2</sub> O (MW 137.99 g/mol)
10 mM Tris·Cl	1.2 g Tris base (MW 121.1 g/mol)
8 M urea	480.5 g (MW 60.06 g/mol)

Adjust pH to 5.9 using HCl.

**Buffer E (1 liter):**

100 mM NaH <sub>2</sub> PO <sub>4</sub>	13.8 g NaH <sub>2</sub> PO <sub>4</sub> ·H <sub>2</sub> O (MW 137.99 g/mol)
10 mM Tris·Cl	1.2 g Tris base (MW 121.1 g/mol)
8 M urea	480.5 g (MW 60.06 g/mol)

Adjust pH to 4.5 using HCl.

**10.6.2 Native solutions****Lysis buffer (1 liter):**

50 mM NaH <sub>2</sub> PO <sub>4</sub>	6.90 g NaH <sub>2</sub> PO <sub>4</sub> ·H <sub>2</sub> O (MW 137.99 g/mol)
300 mM NaCl	17.54 g NaCl (MW 58.44 g/mol)
2 mM imidazole	0.68 g imidazole (MW 68.08 g/mol)

Adjust pH to 8.0 using NaOH.

**Wash buffer (1 liter):**

50 mM NaH <sub>2</sub> PO <sub>4</sub>	6.90 g NaH <sub>2</sub> PO <sub>4</sub> ·H <sub>2</sub> O (MW 137.99 g/mol)
300 mM NaCl	17.54 g NaCl (MW 58.44 g/mol)
4 mM imidazole	1.36 g imidazole (MW 68.08 g/mol)

Adjust pH to 8.0 using NaOH.

**Elution buffer (1 liter):**

50 mM NaH <sub>2</sub> PO <sub>4</sub>	6.90 g NaH <sub>2</sub> PO <sub>4</sub> ·H <sub>2</sub> O (MW 137.99 g/mol)
300 mM NaCl	17.54 g NaCl (MW 58.44 g/mol)
400 mM imidazole	17.00 g imidazole (MW 68.08 g/mol)

Adjust pH to 8.0 using NaOH.